AN INVESTIGATION INTO COLUMN FLOTATION OF SOUTH AFRICAN COALS

A thesis submitted to the
UNIVERSITY OF CAPE TOWN
in fulfillment of the requirements
for the degree of
MASTER OF SCIENCE IN ENGINEERING

by
SEAN THOMAS VON HOLT B.Sc. (Chem. Eng.) (Cape Town)

Department of Chemical Engineering
University of Cape Town
Rondebosch, 7700
South Africa

April 1992

SYNOPSIS

The high efficiency of separation of fine (typically the -150 μm fraction) particles achievable with column flotation technology is well established. The principal aim of this thesis is to investigate whether column flotation can be used to recover saleable, particularly low-ash quality, coal from South African coal fines which are presently discarded.

Samples of thickener underflow fines from the Durnacol, Kleinkopje and Greenside Collieries were used in laboratory column testwork. In addition, on-line column trials were performed at the Kleinkopje Colliery. The effects of column operating parameters were established using both one-variable-at-a-time testing and fractional factorial design experiments. An investigation into coal slurry conditioning using oil and oil-water dispersions was also undertaken.

The results of laboratory and plant column testwork showed that it was possible to recover the desired quality products from all three of the coal fines samples investigated. For all the coals tested, better grades were obtained at any given yield from column cell flotation than with conventional (batch) froth flotation.

The test results also demonstrated that the column cell is best suited to recovering and upgrading the finer (< 75 μm) size fractions. Column performance was found to be strongly affected by the petrographic composition of the coal fines feed, i.e. by coal TYPE. Coals with high vitrinite and, conversely, low inertinite contents were found to be the most easily floatable. Depending on the coal TYPE, the rate of mass transport in either the pulp or froth phase was found to be rate limiting; this in turn dictated which operating parameters affected product yields and grades.

Existing methods of conditioning coal slurries were found to be inadequate. Considerable scope for improvement in coal conditioning lies in better choice of collector and "promotor" reagents as well as in designing more energetically efficient conditioning vessels.

ACKNOWLEDGEMENTS

The author would like to extend his thanks to the following people who assisted with this study :

Prof. J-P. Franzidis for the guidance he provided and interest he showed during the testwork and write-up phase of this study.

My colleague Ashli Breed who helped in running the pilot column during the plant trials and who provided constructive advice on many aspects related to this thesis.

Helen Divey, Denise Moody and Lorna Wall for their assistance in preparation of the samples generated during the laboratory tests and for performing ash and float and sink analyses on these samples.

The staff at the Kleinkopje Colliery, particularly Messrs Paul Henry, Brian Hartzenburg and Dave Power. Their advice and co-operation during the plant trials was much appreciated.

Lindsey McNeill of the UCT Statistics Department for running the fractional design data on the GENSTAT package.

The staff of the mechanical and electronic workshops who provided and maintained the equipment and facilities used during this thesis.

Colleagues and Staff in the Chemical Engineering Department for their interest and willingness to be of assistance whenever this was sought.

CONTENTS

LIST OF TABLES

Page

Page

LIST OF FIGURES

Page

Page

Page

Page

NOMENCLATURE

(S.I. Units have been used)

a	= number of levels of factor x_1
A_c	= column cross-sectional area
AF	= volumetric flowrate (@ 1 atm); l/min
A_{H^+}, A_{OH^-}	= activity of H^+, OH^- ions in bulk solution
$A_{H^+}^*$, $A_{OH^-}^*$	= activity of H^+, OH^- ions in bulk solution at the point of zero charge (PZC)
α_i	= effect of factor x_1 at level i
α_{ij}	= effect of factor i at level j
$\alpha\beta_{ij}$	= effect of factor interaction x_1x_2 at level ij
b	= number of levels of factor x_2
c	= number of levels of factor x_3
C	= constant
C_a	= carrying capacity; t/hr.m^2
C_b	= bulk frother concentration
C_j	= contrast coefficient for response y_j
C_p	= concentration of floatable particles
C_p	= rate of solids production in concentrate; t/hr.m^2
CC	= collector dosage; g/t
CH	= collection zone height; m
CFeed	= calculated feed % ash
CS	= coefficient of separation
γ	= interfacial tension (surface free energy)
γ_{sg}	= interfacial tension at solid-gas interface
γ_{sl}	= interfacial tension at solid-liquid interface
γ_{lg}	= interfacial tension at liquid-gas interface
γ_s	= work of spreading at oil-solid interface
Γ	= adsorption density per unit area at a interface
d_b	= bubble diameter
d_c	= capillary diameter
d_i	= impeller diameter
d_j	= droplet diameter in j'th interval
d_o	= oil droplet diameter
d_{oc}	= oil droplet diameter

d_p = particle diameter
d_{bf} = bubble diameter at overflow
d_{bi} = bubble diameter at pulp-froth interface
d_{80} = 80 % passing size
d_{95} = 95 % passing size
d.a.f. = dry ash free coal
D = dispersion coefficient
D_c = column diameter
δ = thickness
δ_c = critical film thickness
δ_f = water film thickness
δ_s = thickness of stable film
E_c = collision efficiency
E_a = attachment efficiency
E_k = collection efficiency
$e = S - y$ = difference between expected and observed response
e_{ijk} = random error component
$E = \Sigma e^2$ = cumulative error function
E_{yld} = effect on product yield
E_{Rec} = effect on product recovery
E_{Ash} = effect of product ash content
ϵ_g = fractional gas holdup, slurry phase
ϵ_f = mean gas holdup in froth phase
ϵ = rate of energy dissipation
ϵ_d = rate of energy dissipation within impeller dicharge zone
$\epsilon_{avg} = P/V$ = power supplied per unit volume of pulp
f = predicted response value
F = Faraday constant
F_a = solids feedrate,; $t/hr.m^2$
FC = frother concentration; $\mu l/l$, g/t
FCWW = supply water frother concentration; $\mu l/l$
FCT = frother concentration in slurry feed tank,; $\mu l/l$
FH = froth height; m
FC_d = total rate of frother addition; $\mu l/min$
ζ_o = oil droplet zeta potential

ζ_p = particle zeta potential

ΔG_{flot} = net change in Gibb's free energy due to formation of contact angle at gas-solid-liquid interface

η = empirical fudge factor

H = collection zone height

θ = static contact angle at point of bubble-solid-liquid contact

θ_e = static/equilibrium contact angle

J_g = superficial gas velocity (@ 1 atm); cm/s

J_l = superficial net downward liquid velocity; cm/s

J_f = superficial slurry feedrate; cm/s

J_t = superficial velocity of tails slurry; cm/s

$J_{tf} = J_t - J_f$ = net difference between slurry and tails superficial velocities

J_{ts} = volumetric flowrate of tails solids per unit column cross-sectional area

J_w = superficial wash water velocity; cm/s

K = flotation efficiency parameter

k = overall flotation rate constant

k_p = first order rate constant

k_s = "slow" flotation rate constant

k_f = "fast" flotation rate constant

L = column, impeller diameter

LC = level control measurement

l_{x1} = contrast for factor x_1

μ = overall mean

μ_{ij} = average response of factor i at level j

μ_l = liquid viscosity

m = slope of covariate parameter

$MSe = s_e^2$ = mean square of the error

MFeed = measured feed % ash

n = slope

N = valency of potential determining ion

N = impeller speed

N = total number of tests

N = total number of samples

N_p = vessel dispersion number
ξ = zeta potential
P = power supplied to impeller; W
P = pressure; bar, atm
PI = proportional integral controller
P_a = probability of particle-bubble attachment
P_c = probability of particle-bubble collision
P_c = absolute pressure at concentrate overflow
P_d = probability of detachment
P_d = disjoining pressure in liquid film
p_d = dynamic pressure
P_f = probability of flotation
P_g = gauge pressure; bar, atm
P_t = absolute pressure at bottom of column
$P_{electrical}$ = electrical component of disjoining pressure
$P_{hydration}$ = hydration component of disjoining pressure
$P_{van\ der\ Waals}$ = van der Waals component of disjoining pressure
PZC = point-of-zero-charge
P.D. = pulp density; mass/volume (% m/v) basis
Q = volumetric flowrate
Q_t = volumetric tailings flowrate
Q_g = volumetric gas flowrate]
QF = slurry volumetric feedrate; l/min
ρ_c = continuous phase density; g/cm^3, kg/m^3
ρ_l = liquid density; g/cm^3, kg/m^3
ρ_p = particle density; g/cm^3, kg/m^3
r = number of repeat tests
σ = oil-water surface tension
r_c = critical radius
σ_e = population standard error
σ_e^2 = population variance
r_p = particle radius
σ_s = surface charge
R = universal gas constant
R = regression coefficient
R = repeatability within a pulp batch

R_f = recovery in froth zone
R_g = gangue recovery
R_p = recovery in pulp zone
R_T = total recovery
R_w = water recovery
RB = reproducibility between pulp batches
Re = bubble Reynolds number
R_{A1} = recovery of valuable component in concentrate
R_{B2} = removal of gangue from tails
s = sample standard deviation
s_e = standard error
s_e^2 = error mean square
S_f = solids feedrate; $t/hr.m^2$
S = pulp solids content
S = expected value of response (covariate parameter included)
ST = sparger type
SW = rate of "USBM" sparger water addition; l/min
τ = mean residence time; minutes
τ_f = mean froth residence time; minutes
τ_l = mean liquid residence time in pulp; minutes
τ_n = nominal slurry residence time; minutes
τ_p = mean particle residence time in pulp; minutes
t_c = contact time
t_i = induction time
T = absolute temperature
U_b = bubble rise velocity; cm/s, m/s
U_b = bubble electromobility
U_l = interstitial liquid velocity; cm/s
U_o = oil droplet electromobility
U_p = particle settling velocity; cm/s
U_p = particle electromobility
ϕ, ϕ_d = volume fraction of dispersed phase
V = volume of mixing tank (pulp)
VS = variable speed pump
V_c = collection zone volume

V_R = repulsion potential energy

WW = wash water rate; l/min

ψ_δ = potential at Stern plane

ψ_o = potential of solid surface with respect to bulk solution

x_c = covariate parameter

X_{avg} = average ash content

y_j = response of trial (test) j

y_{ijkl} = observed response value

y_T = overall system mean

z = froth bed depth; cm, m

CHAPTER 1

INTRODUCTION

1.1 BACKGROUND

1.1.1 South African Coal Fines and Ultrafines

Approximately 20 % of the total run-of-mine (ROM) production (224 Mt in 1988; DMEA Report, 1989) of South African collieries is discarded annually. The energy value of these discards amounts to approximately 10 % of the total energy content of the ROM coal (Grobbelaar, 1988). Two factors are responsible for this rather high discard figure. Firstly, the continuing trend towards higher levels of mechanisation has resulted in less selective mining as lower quality material is mined together with the coal seam. Secondly, a consequence of high market demand (both local and international) for premium quality, size-specific thermal (≈ 13.0-14.0 % ash) and low-ash (≈7.0-7.5 % ash) coal is that between 30-40 % of the coal feed to washing plants is discarded as an undesired byproduct.

The discard material itself varies tremendously in quality and size. Generally, because of improved liberation of the mineral components from the carbonaceous matter, the unit energy value is highest in the fines (nominally -0.5 mm) fraction. The most recent discard (and duff) inventory survey was carried out in 1985 (DMEA Report, 1987). It was estimated that the total discard production in 1985 was 44.2 Mt of which 4.1 Mt consisted of bituminous and anthracitic slurry fines. The mean calorific value of this fines discard was estimated as between 23 and 26 MJ/kg. The calorific value specification of export power station coal is approximately 28 MJ/kg while ESKOM burns coal with calorific values as low as 16 MJ/kg.

There are economic and environmental incentives for recovering at least some valuable (i.e. saleable) product from the discard material that is currently dumped. In 1985 (DMEA Report, 1987) reclamation and dumping/stockpiling costs were estimated to vary from R1.32 to R8.75 per

ton. An increased product recovery would simultaneously increase sales revenues and reduce disposal costs; although in an overall economic analysis the cost of the technology used to process the discard would also have to be considered (Harris, 1988). The fines fraction, in particular, should be relatively amenable to further processing as it contains the better liberated, higher energy content material. Consequently, separation of predominantly carbonaceous material from minéral containing matter should be easier (and hence cheaper) in the fines than for coarser sizes.

The negative environmental impact of dumping coal discards also has to be considered. Grobbelaar (1988) points out that "discard dumps present significant health, safety and enviromental hazards ... are a constant source of acid water pollution and, if burning, emit noxious or toxic fumes ... and ... lower the value of adjacent land." As it is generally expected (e.g. CSIR Report, 1991) that "green" issues will become an increasingly important political factor within the next decade, pressures to improve upon current waste disposal practices are likely to arise.

Indeed, the period since 1984 has seen a proliferation in the use of spiral concentrators to treat the -0.5+0.1 mm coal fines fraction. There are now seventeen spiral plants installed on South African collieries with an estimated combined production capacity of 5 Mtpa (Franzidis, 1991). The spirals produce a steam quality (≈28 MJ/kg) product only: their separating efficiency is relatively poor, which precludes the generation of "low-ash" product from South African coals with their typically high in situ ash contents. However, their mechanical simplicity endows spiral concentrators with the dual advantages of low capital and operating costs (Burt and Mills, 1984).

As particle size decreases, bulk density based solid-solid separations become rapidly ineffectual; Horsfall and Franzidis (1988) have proposed that for South African coals the exploitation of surface property differences is a more appropiate process route for the beneficiation of -0.15 mm "ultrafines". Candidate surface-property based technologies include froth flotation, oil agglomeration and selective flocculation. Of the three, froth flotation is considered the most commercially viable (Aplan, 1987).

However, despite its widespread application in the processing of mineral ore fines, the use of flotation in the (North American and European) coal industry is comparatively limited. Aplan (1987) has cited a number of reasons for this; they include the inability of conventional cells to make clean separations at finer sizes (particularly for slurries containing a high proportions of clays), high dewatering costs and the relatively low unit value of coal.

In South Africa the use of froth flotation to treat coal fines is even more restricted. There are only six froth flotation plants processing coal fines in the entire country, only one of these treating non-coking quality coal (Franzidis, 1991).

South African coals, in common with the other Gondwanaland deposits of India, South America and Australia, are difficult to float compared with the Laurasian coals of the Northern Hemisphere. The reason for this is that the two have fundamentally different chemical and physical structures (manifested in their petrographic properties) as well as dissimilar modes of mineral deposition within the coal matrix (Falcon, 1977, 1978a). In general, South African coals are low in vitrinite and exinite content and contain large amounts of syngenetic minerals and hence a high proportion of "middlings" material. Vitrinite content crudely correlates with ease of floatability (Klimpel and Hansen, 1987) and the presence of substantial quantities of "middlings" makes it difficult to produce low-ash quality coals.

Because of these (especially the last-mentioned) factors, the most important coalfield in the country, namely the Witbank coalfield, has no froth flotation plants.

1.1.2 Column Flotation

The advent of column flotation cells has been one of the most significant advances in froth flotation technology in the last decade. These units, in a single separation step, produce a product recovery and quality (grade) equivalent to that generally achieved by multistage flotation in conventional cells. As they are significantly cheaper to

build and operate than mechanically agitated cells, their use in cleaning and other applications in the processing of fine mineral ores is now widespread (Yianatos, 1989; Moon and Sirois, 1988).

However, with the exception of one commercial scale operation (Groppo and Parekh, 1990), the use of column cells within the coal industry is still largely at the development stage; the low bulk commercial value of coal has discouraged capital expenditure. There has nevertheless been considerable Research and Development effort, largely conducted in the U.S.A., Australia and India, which has invariably demonstrated that column cells are extremely efficient in performing fine particle separations. For example, Misra and Harris (1988) report that gangue separations are possible at particle sizes down to 10 μm.

It is the potential for achieving better particle separation efficiencies than has hitherto been possible in single stage conventional cells that has provided the stimulus for continuing research into the column flotation of coal fines.

1.2 THESIS AIMS AND SCOPE

The principal aims of this thesis are to investigate whether column flotation technology can be suitably applied for recovering saleable, particularly low-ash, quality coal from South African coal fines which are presently discarded; and to determine what the important, or dominant, operating parameters are for this process.

The thesis begins with a brief review of coal properties. Characteristic features of the flotation process, particularly as they pertain to treating coal fines are then discussed. Column flotation technology and the parameters affecting column flotation of coal are also reviewed. Finally, given the rather large number of process variables involved, and the necessity to resolve the key factors dictating column performance in comparatively few tests, some aspects of multi-variable experimental design are examined.

The experimental work itself is divided into three sections. Four samples were used in the column testwork, namely thickener underflow fines from the Durnacol, Kleinkopje Collieries; and both "as is" and

milled (95 % passing 45 μm) thickener underflow fines from the Greenside Colliery. In Chapter 3 hydrodynamic aspects of two-phase bubble columns and the effect of surfactant dosage are examined. In addition, difficulties experienced in conditioning the Kleinkopje fines prompted an investigation into coal slurry conditioning using oil and oil-water dispersions. Samples of thickener underflow from the Goedehoop and Zululand Anthracite Collieries was also used in these comparative oil conditioning tests.

Chapter 4 describes how column operating parameter effects were studied and quantified using a fractional factorial design technique; the coal used was a sample of Durnacol Colliery thickener underflow fines. In addition, column performance was compared with the ideal flotation separation curve, the characteristic washability curve and the results of a series of batch flotation tests. Laboratory column tests were also performed on samples of thickener underflow from the Kleinkopje and Greenside Collieries. Finally, column flotation tests were performed on milled samples of Greenside thickener underflow; the primary objective being to determine the extent to which improved liberation of gangue mineral from the coal matrix increased the yield of low-ash coal.

In Chapter 5 the results of on-line plant trials conducted at the Kleinkopje Colliery are reported. The primary objective of these tests was to produce a steam quality ($\approx$27.6 MJ/kg) concentrate product from the thickener underflow fines. Key operating parameters were again identified; these are compared with those found to be significant in the laboratory trials; and the extent to which the column was able to meet the objective of producing steam quality coal is evaluated.

In Chapter 6 the conclusions drawn from the thesis are summarised and recommendations are made for future work.

CHAPTER 2

LITERATURE REVIEW

2.1 COAL CHARACTERISATION

The diversity of the original plant materials and the degree of coalification which has occurred are the two major reasons for the variety in the physical and chemical behaviour of coal (Falcon, 1978a). As this heterogeneity has a direct impact on coal mining, beneficiation, coking and conversion processes, some understanding of coal behaviour is advisable. The emphasis of the review presented here is directed in particular towards examining those coal properties which are relevant to flotation behaviour.

2.1.1 The Process of Coal Formation

Coal development occurred in two distinct phases. Initially the plant vegetation died and decayed via innumerable biochemical pathways. The degradation products which formed and the reactions which occurred depended both on the initial flora species present and on the "reacting" environment, e.g. pH, temperature, etc. However, the dominant factor dictating degradation of the plant matter was accessibility to oxygen, i.e. system redox (Eh) potential. The proportions and chemical composition of the organic constituents formed during the peatification stage are the precursors of the macerals which impart to the fossilised coal its characteristic organic composition (TYPE). This is known as the **diagenetic** phase of coal formation.

Gradually the decayed plant material was buried under inorganic sediments and biological activity ceased. However, the organic matter continued to undergo chemical and physical transformation, the driving force for these now abiotic processes being geothermal heat and pressure. This stage is known as the **metamorphic** stage of coal development. On a chemical level metamorphic development or coalification represents an enrichment of the organic matter in carbon

content, principally at the expense of hydrogen and oxygen loss. The carbon contents of coal can be arranged in ascending order to form a "coal series" often putatively written as

peat → lignite → subbituminous → bituminous → anthracite

The level which the coal has reached in the coalification series is termed its RANK.

Falcon (1977) has presented data indicating how the elemental carbon, hydrogen and oxygen contents of coal change with rank. These are reproduced in Table 2.1. It appears that the hydrogen content (in absolute terms) remains rather static and that enrichment in carbon is attained primarily through loss of oxygen.

Table 2.1 : Elemental composition as a function of metamorphic development, modified from Falcon (1977)

Material	% Carbon	% Hydrogen	% Oxygen
Wood	50	6	43
Peat	57.5	5.5	35
Lignite	70	5	23
Low rank coal	81	5.1	11.6
Steam coal	92.4	4.0	1.3
Anthracite	94.4	2.9	0.9

On a molecular level, coal is considered to consist of condensed polynuclear aromatic systems (molecular aggregates) with various substituted components such as short-chain alkyls and cyclic groups attached to the aromatic skeleton. These substituted components constitute the "volatile matter" content of a coal. The fraction of aromatic carbon ranges from about 0.72 in subbituminous coals to 1.0 in anthracites.

Maturation of the coal is associated with the elimination of the substituent groups and a slow but progressive increase in spatial order

of the molecular aggregates and an increase in aromatisation as coals develop towards anthracites.

The number of condensed aromatic rings which form the core structure of the molecular aggregates changes with rank, from about 2 in lignitic coals, between 3 and 5 in bituminuous coals, to about 40 in anthracitic coals with carbon contents greater than 95 %.

The inorganic mineral sediments which are intermixed with a coal patently represent a contaminant. The ease with which they may be removed from the coal is dependent on the extent and manner in which the minerals were deposited in the coal seam. The proportion of mineral matter present in a coal is termed its GRADE.

The forms in which mineral matter is present in coal may be split into two categories, viz, intrinsic inorganic matter which was present in the original living plant vegetation and extrinsic matter which was incorporated into the coal mass during the diagenetic and/or metamorphic stages. **Extrinsic deposition** is the more important of the two mineral formation mechanisms.

The inorganic material which was carried into the decaying debris by wind and water during the diagenetic stage is termed primary or syngenetic matter. **Syngenetic** minerals are typically colloidally dispersed through the coal matrix. Mineral matter which deposited during the metamorphic stage by percolation of mineral waters into fissures, cavities and pores within the coal seam are termed **epigenetic** minerals. These minerals are present as more or less distinct veins in the coal seam.

Liberation of mineral matter from coal is achieved by size reduction (typically a primary crushing stage at a Coal Washing Plant). It is evident from the preceding discussion that coals containing predominantly **epigenetic** minerals are more **readily liberated** than coals which have high syngenetic mineral contents.

The mechanisms of coal development are discussed by numerous authors including Berkowitz (1979, 1985), Falcon (1977), Horsfall (1983), Tsai (1982) and Ward (1984a).

2.1.2 Coal Petrography

Coal petrography is defined as the study of the microscopic organic and inorganic materials that make up coal (Falcon, 1978a). The importance of coal petrography lies in the increasing recognition that a coal's physical, chemical and technological properties (e.g. coking ability) are determined not only by classical rank determining parameters but also by the maceral components and mineral matter present. Thus petrographic characterisation complements rank parameters in defining coal behaviour (Falcon, 1978b; Falcon and Snyman, 1986) :

i.e. coal behaviour = function(RANK, TYPE, GRADE)

Coal macerals are organic analogues of minerals in rocks, and range in size from 1 - 50 μm. They originate from the precursor masses formed in the diagenetic phase of coal development and are detectable from characteristic structural morphology, colour and light reflectance properties.

Based on plant origin or mode of degradation, similar macerals are associated into sets of maceral groups. In humic coals there are three maceral groups : vitrinite, exinite and inertinite. Each maceral group has specific rank-dependent chemical, physical and technological properties. Some of these are summarised in Table 2.2.

Combinations of maceral groups in turn form distinctive microlithotypes. Finally sets of microlithotype are associated as macroscopic lithotypes. These lithotypes fall under two classes, namely, those belonging to either humic or sapropelic coals. A feature of humic (especially bituminuous) coals is that the lithotypes which constitute the coal body are often visible as "banded components". Stopes (1919) proposed that the four such "bands" visible in humic coals be named vitrain, clarain, durain and fusain respectively.

The structure outlined above forms the basis for petrographic classification of coal (Falcon and Snyman, 1986) and its principal advantage is that maceral groups and microlithotypes are recognisable in all coals other than anthracites.

Table 2.2 : A Summary of the Major Characteristics of the Three Maceral Groups in Hard Coal (modified from Falcon, 1986)

Maceral Group	Plant Origin	Reflectance			Chemical Properties			Technological Characteristics						
		Description	Rank	% Reflected Light	Characteristic Element	Typical Products on Heating		Combustion			Pyrolysis		Hydrogenation and Liquefaction	
								Ignition	Burn Out	Smoke	Coke	Liquors		
VITRINITE	woody trunks, branches, stems, bark, leaf tissue, shoots and detrital organic matter gelified/vitrinitized in aquatic reducing conditions.	Dark to medium grey	Low rank to Medium rank Bituminous	0.5-1.1	Intermediate hydrogen content	Light hydrocarbons	Intermediate volatiles decreasing rank	###	###	**	**	***	##	###
				1.1-1.6				##	##	*	****	(*)	#	##
		Pale grey	High rank Bituminous	1.6-2.0	-	-		#	#	(*)	(*)		(#)	(#)
		White	Anthracite	2.0-10.0	-	-		#	#	-	-	-		
EXINITE	cuticles, spores, resin, algae accumulating in sub-aquatic conditions.	Black-brown	Low rank	0.0-0.5	Hydrogen rich	Early methane gas	Volatile-rich decreasing with rank	####	####	****	*	****	####	##
		Dark grey	Bituminous	-0.5-0.9				###	###	***	*	**	###	###
				-0.9-1.1		Oil		#	#	**	*	*	#	#
		Pale grey	Medium rank Bituminous	-1.1-1.6		Condensates wet gases decreasing		(#)	(#)	(*)	(*)	(*)	-	
		Pale grey (-vitrinite) to white shadows	High rank Bituminous to Anthracite	-1.6-10.0	-	-	-	-	-	-	-	-	-	
INERTINITE	As for vitrinite, but fusinitised in aerobic oxidising conditions.	Medium grey	Low rank Bituminous	0.7-1.6	Hydrogen poor	-	Low volatiles in all ranks	#	#	*	-	-	-	-
		Pale grey to white and yellow-white	Medium rank Bituminous to Anthracite	-1.6-1.8				#	#	(*)	-	-	-	-
				-1.8-10.0	-	-		(#)	(#)	-	-	-	-	

KEY	
#	: Capacity or rate
####	: Fast
#	: Slow
	: Zero
*	: Proportion
****	: High
*	: Low
-	: Absent

The biochemical conditions under which the aforementioned maceral groups were formed have been discussed by Falcon (1978a) and Falcon and Snyman (1986). Vitrinization or gelification of the plant matter occurred under conditions where oxygen supply was restricted due to partial submergence in water or burial beneath sediment. Inertinites originate from similar plant material to vitrinite; however, here decay took place in comparatively dry, well aerated (i.e. positive redox potential) environments and consequently far greater plant decomposition occurred. Also, because the plant material was relatively exposed, mineral matter tended to be deposited syngenetically. Exinites are relatively sparse in humic bituminous coals but are abundant in sapropelic coals (coals formed under completely anaerobic conditions where plant degradation occurred by fermentation).

The maceral groups also have different densities. In general the density sequence is given by (Falcon and Snyman, 1986) :

ρ inertinite > ρ vitrinite > ρ exinite

Exinite is the lightest maceral group ranging in density from 1.18 to 1.25 g/cm^3 with increasing rank of the coal. The inertinite group macerals range in density from 1.35 to 1.70 g/cm^3; however, very little change with rank occurs. Vitrinite density changes with rank, from 1.3 g/cm^3 in high volatile bituminous coal, to a minimum of 1.27 g/cm^3 in the medium volatile bituminous range, to 1.8 g/cm^3 in anthracites.

2.1.3 Molecular Structural Features of the Maceral Groups

By the use of spectrographic and analytical techniques it is possible to determine certain molecular structural components within the group macerals (Falcon and Snyman, 1986; Berkowitz, 1985; Tsai, 1982).

The vitrinite component of lower rank coals consists of molecular aggregates of low molecular weight substituted groups (OH, COOH, CH_3) attached to an anthracenic, phenanthrenic type aromatic nucleus. These molecular aggregates are randomly orientated and so lower rank coals tend to be structurally amorphous and relatively porous. As the rank

increases, the substituted groups are removed by aromatisation reactions, the aromatic skeleton becomes larger and more planar and the aromaticity and carbon content increase.

Exinite in low rank coals contains fewer and smaller aromatic groups than vitrinite. The substituted functional groups are aliphatic compounds, as evidenced by high carbon to hydrogen ratios. The aliphatic groups are therefore responsible for the high volatile matter content of exinites.

Inertinite is much more aromatic than either vitrinite or exinite in lower rank coals. In addition, however, it is characterised by rather high oxygen and low hydrogen contents. This maceral group also shows very little change in physical or chemical properties with rank. It is the high oxygen content of inertinite which chiefly distinguishes it from vitrinite and exinite. This oxygen may be present in the form of alcoholic or phenolic groups (OH), carboxyl groups (COOH), carbonyls (C=O) or etheric groups ($-OCH_3$) which act as bridges between adjacent molecular aggregates.

2.1.4 Parameters Defining Rank

Rank is not directly measurable and is usually defined by reference to sets of empirical parameters, usually proximate and ultimate analyses. Proximate analyses include moisture, volatile matter and fixed carbon content. Ultimate analysis gives elemental compositions of carbon, hydrogen, sulphur, nitrogen and oxygen.

Correlation of the above parameters with rank is generally database dependent and extrapolation to coals which were not included in the original analysis is unreliable. Thus, for example, rank classification criteria developed for North American and European coals are often not applicable to South African and other Gondwanaland coals. There are fundamental reasons for this which are discussed below.

Because proximate and ultimate analyses are often inadequate rank indicators, it is now common practice to rank coal on the basis of light reflectance from the vitrinite surface of a polished cross-section of a

representative coal sample - the higher the carbon content, the higher the reflectance (Falcon and Snyman, 1986). Standard coal classification systems are described by Osborne (1988).

2.1.5 Mineral Matter in Coal

It is possible to identify the mineral components in a coal by spectroscopic X-ray diffraction and infrared methods (Tsai, 1982) as well as optical petrographic techniques (Falcon and Snyman, 1986).

The major mineral matter constituents of South African coals are clays (mostly illite and kaolinite aluminosilicates), carbonates, sulphides (pryites and marcasites) and quartz. Between 60-70 % of the clay minerals are present as syngenetic material. Iron sulphides also occur syngenetically. Sulphur contents of South African coals are, however, comparatively low. Falcon (1978a) reports a maximum sulphur content of 2.5 %. Quartz occurs epigenetically. Phosphorous-bearing heavy minerals are also present in significant quantities.

At this point it is appropiate to recognise the difference between mineral matter and ash. Ash is the product of inorganic dehydration, decomposition and oxidation reactions which occur when the coal mass is combusted in a furnace. Thus, the chemical composition and properties of mineral matter and ash are quite different. The mass of mineral matter may be related to ash content by using Parr's formula (Tsai, 1982), although the mass change due to ashing is fairly small (approximately 0.05 times the ash content).

2.1.6 Characteristic Features of South African Coals

South African coals, which are part of the Gondwanaland coal series, were formed in the final stages of the Permian ice age (≈200 million years ago). They are, in general, characterised by high proportions of inertinites and syngentic silica-alumina clays (Falcon, 1978a). There are of course local variations in coal composition. For example, the Witbank coalfield contains inertinite rich bituminous coals whilst the

deposits of Northern Natal are typically bright banded coals abundant in vitrinite (Ward, 1984b).

The high inertinite and syngenetic minerals content of many South African coals are responsible for their poor washability chararteristics (Falcon, 1978a). These coals contain high proportions of intermediate (R.D. 1.35-1.60) density material, the so-called "middlings" fraction. Production of low-ash quality coals from this fraction is problematic as syngenetic minerals are not removable by physical beneficiation methods unless the coal is ground to the mineral grain size, an impracticality in the case of clays as they approach colloidal sizes (1-2 μm). Also, the low-ash fractions (R.D < 1.3) contain predominately vitrinite (Falcon, 1986).

By contrast, the Laurasian coals of the Carboniferous era (circa 250 million years ago) contain mostly vitrinites. Mineral deposition in these coals tends to be *epigenetic*. These features make physical separations comparatively easy and thus the Laurasian coals are intrinsically more amenable to washing at the preparation plant than typical Gondwanaland coals.

Falcon (1977) has summarised differences in petrographic properties between Northern and Southern Hemisphere coals. These are reproduced below.

Table 2.3 - Average maceral proportions of three coal source regions in the world (Falcon, 1977).

Maceral Group	Carboniferous coals, Germany	Permian S.Africa	Permian, Tertiary N. America
Vitrinite	70	40	82
Exinite	15	0	8
Inertinite	15	60	10

2.1.7 Summary of Coal Properties

The technological properties of a given coal are determined by its characteristic rank, petrographic composition and the extent and mode of mineral deposition within the coal matrix. Inertinite macerals have more oxygen, less hydrogen and are more aromatic than vitrinites. In both macerals oxygen is present in the form of polar functional groups. The oxygen content of coals decreases with increasing rank.

In contrast with North American and European coals which are rich in vitrinite, South African coals have high inertinite and low vitrinite contents.

Mineral matter in South African coals tends to be syngenetically deposited, unlike North American and European coals where mineral deposition is typically epigenetic. Because of this, liberation of mineral matter from the coal matrix is intrinsically more difficult for South African coals than for the Northern Hemisphere coals.

2.2. BASIC PRINCIPLES OF FLOTATION

As the flotation process is based on selective utilisation of surface phenomena at phase-phase interfaces, it is expedient to briefly review some general theories of interfacial chemistry, particularly those which apply to mineral-water and mineral-air-water interfaces.

The fundamentals of flotation interfacial chemistry have been extensively researched and numerous texts on the subject are available. The material presented here was derived from the following sources : Fuerstenau and Raghavan (1976a), Fuerstenau and Urbina (1988), Somasundaran (1975), and Sutherland and Wark (1955).

2.2.1 The Electrical Double Layer at a Mineral-Water Interface

Upon submergence in an aqueous solution a mineral surface develops an electrical potential with respect to the bulk solution. This potential arises from charged species transferring across the interface between

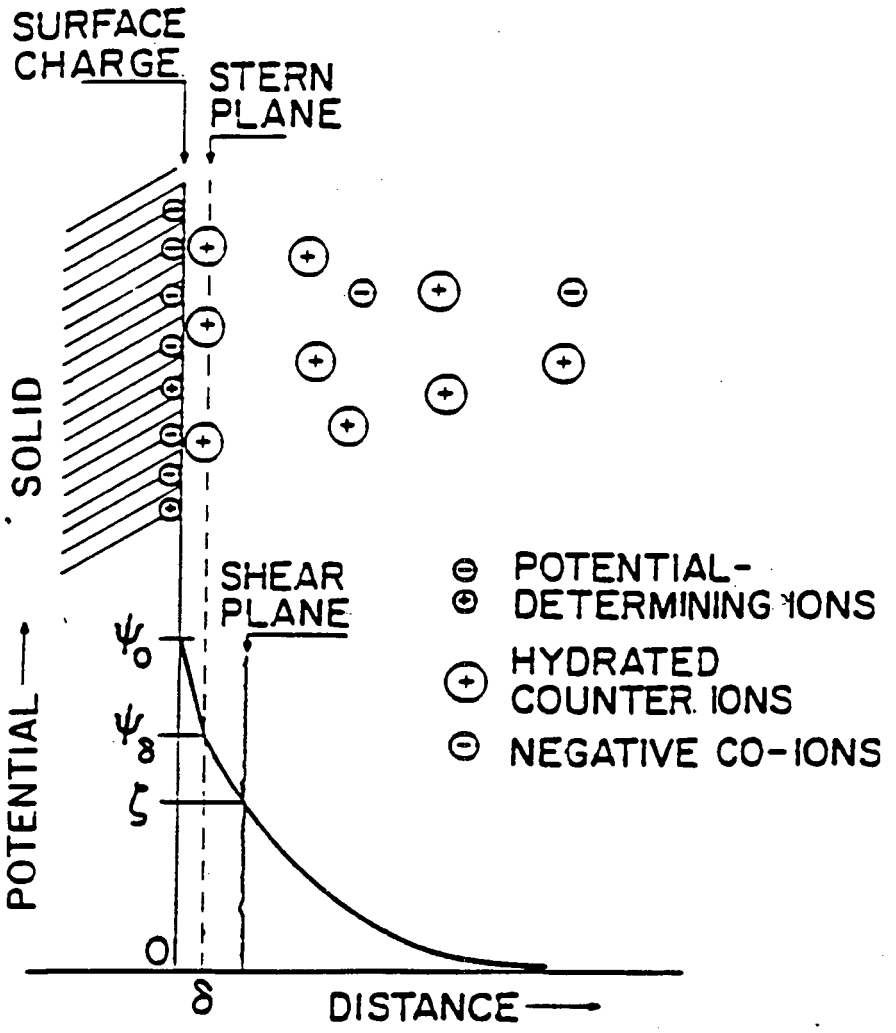

Figure 2.1 : Schematic representation of double layer according to Stern's model.

the solid and liquid phases. Mass transfer to and from the solid surface can be initiated by a number of mechanisms including chemisorption from solution, preferential dissolution of surface ions, and mineral lattice substitution.

The Stern electrical double layer model is considered to represent adequately surface charge characteristics at a mineral/water interface. A schematic of this model is displayed in Figure 2.1.

Ions which establish the surface charge are known as potential determining ions. The surface charge, σ_s, is the nett difference between positive and negative charged surface species. For oxide type minerals which are the most important class of non-metallic minerals (hydrophilic sites on coal surfaces are analagous to oxide mineral surfaces), the H^+ and OH^- ions are potential determining and the surface reactions are (Somasundaran, 1975) :

$$M(H_2O)+_{surface} \underset{H^+}{\rightleftharpoons} --MOH_{surface} \overset{OH^-}{\rightleftharpoons} — MO^-surface + H_2O \qquad (2.1)$$

The surface charge is given by

$$\sigma_s = F\ (\Gamma_{H+} - \Gamma_{OH-}) \qquad (2.2)$$

F = Faraday constant

Γ = adsorption density on solid surface

In order to maintain overall system electroneutrality, counterions co-adsorb at the mineral surface. In a typical mineral flotation pulp, counterions would include inorganic anions, cations and collector ions. Adsorption can occur by chemisorption, physisorption or by a combination of both mechanisms. Physisorption occurs predominantly through electrostatic (coulombic) attraction, but other attractive forces such as dispersion and solvation effects occasionally manifest themselves.

The layer of counterions immediately adjacent to the surface is known as the Stern layer, the thickness of which depends on the size of the ionic radius, δ. Beyond the Stern plane, there is a diffuse double layer of counterions, known as the Gouy layer, which balances the residual fixed double layer charge.

The charge at a surface is indicated by the potential which exists between the surface and the bulk solution, i.e. ψ_o. The condition for which the mineral surface charge is equal to zero is known as the point of zero charge (PZC). It is usually assumed that the charge across the double layer is also zero when a surface is at its PZC.

For oxide type minerals the surface potential, ψ_o, can be related to the bulk solution activities of the potential determining ions H^+, OH^- :

$$\psi_o = R\ T\ /\ N\ F\ *\ \ln\ \{\ A_{H^+}\ /\ A_{H^+}{}^*\} \qquad (2.3)$$

or

$$\psi_o = R\ T\ /\ N\ F\ *\ \ln\ \{\ A_{OH^-}\ /\ A_{OH^-}{}^*\} \qquad (2.4)$$

N = valency of potential determining ion
A_{H^+}, A_{OH^-} = activity of H^+, OH^- ions in bulk solution
$A_{H^+}{}^*$, $A_{OH^-}{}^*$ = activity of H^+, OH^- ions in bulk solution at PZC

In dilute solutions activities and concentrations are equivalent. If the pH of a mineral oxide solution is below the PZC, the solid surface charge, ψ_o, will be positive. The converse will apply at solution pH's above the PZC.

Surface potentials are usually inferred from electrokinetic measurements. Basically two electrodes are placed into a solution containing solid particles and relative motion between the particles and solution is induced by an applied voltage. As a result of the bulk motion, a shear plane develops close to the boundary between the Stern and Gouy layers. The potential at the shear plane, known as the electrokinetic or zeta potential, can be related to the applied voltage and relative particle velocity.

From Figure 2.1 it is apparent that a zeta potential measurement, ξ, provides a measure of the surface potential, ψ_o. The point at which the zeta potential, ξ, becomes zero is known as the isoelectric point (IEP). The shear and Stern planes are commonly assumed to be coincident, since the difference between the zeta and Stern potentials, i.e. $\xi - \psi_\delta$, will be small compared to the surface charge ψ_o. The surface potential can

be related to the Stern (zeta) potential by employing the Gouy-Chapman charge distribution function (Fuerstenau, 1982).

In conventional flotation applications, mineral surface charges are adjusted by adding appropriate types and dosages of soluble (usually ionic) collectors. It is the adsorption of these molecular species at the mineral-water interface that induces the hydrophobicity necessary for the flotation step. Coal flotation is, however, a bulk flotation process where typically a fuel oil is added to condition the pulp. The oil is dispersed into droplets by the action of a mechanical impeller; the dispersed droplets subsequently distribute through the pulp and collide with and adsorb onto the suspended coal particles. Consequently one would expect that the intrinsic charge properties of the coal surfaces would have a strong influence on the extent of oil adsorption, i.e. on the efficiency of coal pulp conditioning. This is in fact the case and is further discussed in section 3.4 below.

2.2.2 Thermodynamics of Wetting Solid Surfaces

Ore beneficiation by the froth flotation process is based on differences in wettabilities exhibited by the surfaces of the various solid species in the pulp. Solids which have non-polar groups on the surface can only bond with adjacent water molecules by van der Waals dispersion forces, which are weak compared with the intermolecular hydrogen bonding forces linking the water molecules. Such solids are hydrophobic and in an aerated pulp will preferentially attach to rising air bubbles. Conversely, minerals which have ionic or polar surface functional groups are attracted to water molecules by solvation forces; these solids are hydrophilic and remain in solution.

Three interfacial surfaces are involved in flotation, namely the solid-water (SL), the solid-air (SG) and the air-water (LG) interfaces. On a macro-level the energy state at each interface is characterised by a surface tension (surface free-energy) value, γ.

Contact angle measurements are commonly used to assess the floatability of a mineral. The technique involves contacting an air bubble with a

smooth planar solid surface submerged in a liquid (typically water). The process is schematically illustrated in Figure 2.2.

The thermodynamic principle of minimum potential energy dictates that a change in system state will occur only if the total potential energy of the system is reduced. Applying this principle here requires that the energy state of the air-solid interfacial area created is less than the sum of the energy states of the mineral-water and water-air interfacial areas which existed prior to bubble contact, i.e.

$$\gamma_{SG} < \gamma_{SL} + \gamma_{LG} \qquad (2.5)$$

Equivalently one can write

$$\Delta G_{flot} = \gamma_{SG} - \gamma_{SL} - \gamma_{LG} < 0 \qquad (2.6)$$

For flotation to occur the net free-energy change must be negative, $\Delta G_{flot} < 0$. Solid interfacial tensions are not directly measurable; however, by employing the Young-Dupre relation, γ_{SG} and γ_{SL} can be eliminated from equation 2.6 :

$$(\gamma_{SG} - \gamma_{SL})/\gamma_{LG} = \cos \theta \qquad (2.7)$$

where the contact angle, θ, is defined as the angle measured across the liquid at the point of bubble-solid-water contact. Substitution of (2.7) into (2.6) gives

$$\Delta G_{flot} = \gamma_{LG} (\cos \theta - 1) \qquad (2.8)$$

Thus for flotation to be thermodynamically feasible a finite contact angle, θ, must be formed, i.e. $0^o < \theta < 180^o$. The magnitude of the contact angle, θ, is clearly a measure of the ease of floatability : as the contact angle increases, the more floatable is the solid.

While this statement is qualitatively correct there is no simple relationship between contact angle measurements and collection of particles by bubbles in flotation pulps; the reason lies in the limitations of contact angle measurements.

Firstly, only if the particle diameter, d_p, in a flotation pulp is at least an order of magnitude smaller than the bubble diameter, d_b, i.e. $d_p << d_b$, will the particle-bubble geometry in actual flotation pulps resemble that of contact angle experiments. Also the effects of hysteresis due to solids loading on bubbles, surface roughness and contamination are neglected. Secondly and more importantly, contact angle measurements are static equilibrium measurements whereas flotation pulps are dynamic systems in which a bubble and particle are only in contact for a limited time, i.e. nonequlibrium conditions exist.

2.2.3 Dynamic Bubble-Particle Interactions

Particle capture in a flotation pulp is viewed as a stochastic event in which the probability of particle capture by a bubble is the product of three terms (Kitchener, 1984) :

$$P_f = P_c * P_a * (1 - P_d) \qquad (2.9)$$

where
P_f = probability of flotation
P_c = probability of particle-bubble collision
P_a = probability of attachment
P_d = probability of detachment

The probability of collision is obviously controlled by the hydrodynamic state of the pulp. The probability of detachment, P_d, is a function of particle size. Larger particles detach more readily than do finer particles because the inertia of heavy particles causes them to lag behind the accelerating bubble with consequent straining of the bubble skin. King (1982) reports that the maximum floatable particle size, d_{pmax}, ranges between 400 and 1000 μm.

Hydrodynamic theories of particle-bubble collisions have been developed by various workers including Flint and Howarth (1971) and Reay and Ratcliffe (1973). The models apply to rather idealised systems, namely dilute suspensions of monodisperse spherical bubbles. In addition they

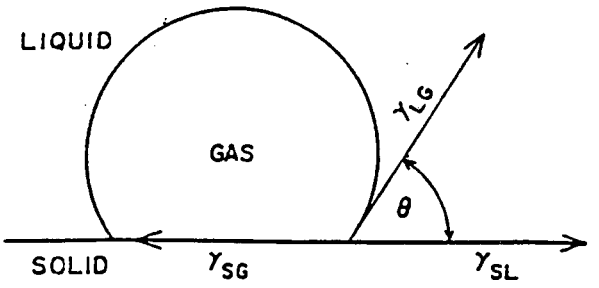

Figure 2.2 : Schematic representation of the equilibrium contact angle between an air bubble and a solid immersed in a liquid.

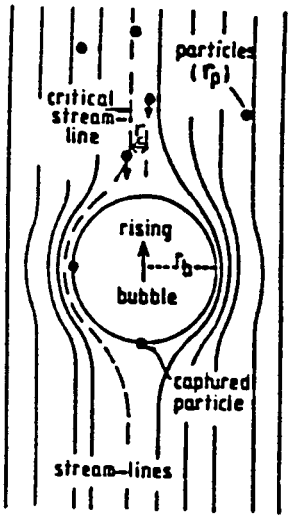

Figure 2.3 : Trajectories of small spherical particles sedimenting near a rising bubble at low Reynolds numbers.

ignore the possibility that particle-bubble trajectories are influenced by their electric fields (Collins and Jameson, 1976).

The central idea of the hydrodynamic theory is that particles will follow the streamlines around the bubble (Figure 2.3). Inertial effects are usually neglected. Consequently only particles situated within a critical radius, r_c, can actually collide with the bubble. Thus collision efficiency, E_c, is defined as the fraction of particles in the path of the bubble which actually collide with it. The radius, r_c, can be calculated from the rate of rise of the bubble and the rate of settling of the particle. Particles sedimenting beyond r_c pass around the bubble without touching, those within r_c may bounce off or slide around.

Jameson et al (1977) have reviewed both results obtained from experiments and proposed theories of particle-bubble collisions. They report that the influence of inertial forces compared with viscous forces (evaluated from Stoke's Law) can be represented by a parameter, K, where

$$K = 2\rho_p r_p 2U_b / 9\mu r_b \qquad (2.10)$$

The bubble rise velocity, U_b, is defined as terminal velocity of a bubble rising freely in water (Jameson, 1984).

When $K \approx 1$ particles are large and collision efficiencies are dependent on inertial forces; conversely for fine particles, where $K \approx 0.1$ or less, viscous forces predominate.

The magnitude of the parameter K determines how collision efficiency is affected by bubble size. When $\underline{K}$ is *greater* than $\underline{1}$ E_c *increases* as bubble size, d_b, *increases* whereas when $\underline{K \approx 0.1}$ E_c *increases* with *decreasing* bubble size, d_b. This principle explains why bubble flotation columns have been successful in floating extremely coarse ($d_p \approx 1$ mm) particles or very fine ($d_p < 45$ μm) particle sizes (see section 2.3). Jameson et al (1977) concluded that for most cases encountered in flotation inertial effects can be ignored (i.e. $K < 0.1$).

The flotation rate constant, k, is a function of the particle and bubble Reynolds numbers. For bubble sizes between 800 μm and 1500 μm, where the Reynolds number is of the order of 100, streamlines around the bubble can be found by potential flow theory. Under these circumstances the flotation rate constant dependence on particle and bubble sizes is given by (Jameson et al, 1977) :

$$k \propto E_c/d_b \propto d_p^2 \,/\, d_b^{2.67} \approx d_p^2/d_b^3 \qquad (2.11)$$

where d_p lies between 10 to 50 μm; d_b between 600 and 1000 μm; K≈0.1

In an actual flotation system where a range of bubble and particle sizes exists, a distribution of particle-bubble capture rates will arise. Jameson et al (1977) observed that under these circumstances "distributed" rate constants which are particle-size dependent may be appropriate for describing flotation rates. Also, given the strong influence of bubble size, d_b, on the rate constant, k, it was recommended that control over bubble size distributions generated be attempted through the development of improved sparging systems.

As a result of the collision stage a thin film, $\delta \approx 1$ μm (Jameson et al, 1977) is formed between the particle and bubble. Continued thinning and eventual rupture of the film, i.e. establishment of particle-bubble adhesion, depends on the molecular surface forces of attraction and repulsion existing between the gas-liquid and solid-liquid interfaces. This step is the *rate determining step* for the *pulp* phase of the flotation process (Fuerstenau and Raghavan, 1976b).

Rao (1974) has reviewed the surface forces involved in flotation. He lists three types of interaction forces as important in flotation. These are (a) van der Waals forces of attraction, (b) electrical forces arising from overlapping double layers in the liquid around the particles and bubbles, and (c) hydration forces between hydrophilic groups on particle surfaces and adjacent water molecules.

These forces have been related to the stability of thin liquid films by Derjaguin (1957, 1961) who introduced the concept of disjoining pressure. Disjoining pressure accounts for all three components of the surface forces :

$$P_d = P_{\text{van der Waals}} + P_{\text{electrical}} + P_{\text{hydration}} \qquad (2.12)$$

P_d = disjoining pressure within the liquid film

Derjaguin showed that if the disjoining pressure, P_d, is positive then the thin (multi-layer) film is stable. This stability arises from attractive hydration forces and repulsive electrical double layer forces. Conversely for *hydrophobic* surfaces the *disjoining pressure* is *negative*. This negative disjoining force overcomes the attractive force holding the wetting film on the surface and as a result causes the wetting film to become unstable. The unstable film thins and eventually ruptures thereby establishing air-solid adhesion. In other words for bubble-particle attachment to occur P_d must decrease as the film thins; if this happens, the film will rupture once a critical film thickness δ_c has been reached, specifically at the point where P_d becomes negative. Otherwise if the solid is hydrophilic, P_d will become increasingly positive as the film thins and a stable film of thickness δ_s will develop.

Rao (1974) emphasised the importance of the electrical component, $P_{\text{electrical}}$, in contributing to film stability. This is always repulsive in flotation systems and consequently if a mineral is surrounded by a charged electrical double layer away from the PZC the surface of the mineral will be hydrophilic, i.e. *floatability* requires that the mineral surface be *near* its **PZC**.

The time taken between particle contact with the bubble surface and the rupture of the wetting film is known as the induction time. Once rupture has occurred the liquid around the point of rupture draws back and forms a stable contact angle with the solid. It is highly unlikely that the initial contact angle is the static equilibrium angle and consequently this dynamic contact angle will continue to move until the equilibrium configuration has been attained (Jameson, 1977). Also, King (1982) has pointed out that during the induction period, t_i, the particle is swept along the bubble surface towards the bubble rear; the time taken for this process to occur is known as the contact time, t_c. If the induction time is longer than the contact time, bubble-particle adhesion will *not* take place.

Dobby and Finch (1987) have developed a single bubble-particle collision model. At a bubble Reynolds number of 100 a theoretical relationship between the efficiency of attachment (E_a), induction time (t_i), and particle size (d_p), was developed. At a constant induction time, attachment efficiency was shown to increase with decreasing particle size, although for very small particles (d_p<10 μm) attachment efficiencies were similar. A collection efficiency (E_k) dependence with particle size (d_p), was also derived where E_k was defined as the product of collision and attachment efficiencies, i.e. $E_k = E_c.E_a$. A peak in collection efficiency with particle size was found to occur; this arises because although larger particles collide more easily with bubbles, their contact times are relatively short.

There is abundant experimental evidence to support this hypothesis (Trahar and Warren, 1976; Trahar, 1981). Laboratory and plant data has shown that depending on the particular ore characteristics, particle sizes between around 20-100 μm are the most floatable. At sizes finer than 20 μm recoveries drop off because of low collision probabilities. At coarse sizes low recoveries are obtained because the particles are insufficiently hydrophobic. Trahar (1981) concluded that the minimum degree of hydrophobicity required for floatability is a function of particle size; coarser particles require a relatively higher degree of hydrophobicity (manifested say in contact angle measurements) for particle flotation than do finer sizes.

2.2.4 Froth Phase Effects

Ultimately the recovery and grade achieved in a flotation cell is determined by the mass transport processes occurring in the froth phase.

The froth performs two basic functions. Firstly, it serves as the medium which enables hydrophobic particles recovered by air bubbles in the pulp to be removed from the flotation cell. Secondly, it upgrades the recovered material by returning entrained gangue and less hydrophobic solid particles to the pulp phase.

The efficiency of these processes is determined by the froth's stability. Froth stability is fixed by the rate of drainage of the water films (lamellae) surrounding the bubbles: stable froths are those where froth drainage (and eventual bubble coalescence) is resisted.

In general the main factors determining the stability of 3-phase froths are surfactant chemical structure and concentration; viscosity of the aqueous lamellae surrounding the bubbles; and particle properties such as size, shape and hydrophobicity (Subrahmanyan and Forssberg, 1988).

Typical frothers are hetero-polar organic molecules with a non-polar hydrocarbon chain and an alcoholic (-OH), carboxylic (COOH) or etheric (OCH_3) polar functional group. Adsorption at the (pulp phase) bubble surfaces lowers the air-water interfacial tension and reduces bubble size. The relationship between surface adsorption, extent of adsorption, bulk frother concentration, C_b, and change in surface tension, $d\gamma$, is described by the Gibbs adsorption equation (Harris, 1982) :

$$\Gamma = -C_b/RT.d\gamma/dC_b \qquad (2.13)$$

where

Γ is the adsorption density per unit area at the interface

γ is the surface tension

T is the absolute temperature

C_b is the bulk frother concentration

Water solubility and froth stability are influenced by the size of the non-polar portion of the molecule; Harris (1982) reports that for carbon chain lengths greater than eight $d\gamma/dC_b$ becomes so large that the froth becomes excessively stable.

The froth structure is a function of the thickness of the interbubble lamellae, δ. In conventional flotation froths, the bubbles immediately above the pulp-froth interface are spherical; but as they rise through the froth, water drains out of the lamellae and the bubbles assume a polyhedral structure. Thus as Kugelschaum or spherical foams have thicker lamellae than Polyschaum or polyhedral foams, they are the more stable. In conventional froths this leads to poorer concentrate grades as the recovery of gangue (hydrophilic -10 μm solids) in the froth is

directly proportional to the pulp water recovery, i.e. $R_g \propto R_w$ (Subrahmanyam and Forssberg, 1988). In column flotation cells (section 2.3 below) a water sprinkle is added to the top of the froth producing a Kugelschaum foam below the water distributor: however, provided the net downward flow of water permeates evenly through the froth bed, entrained feed water is completely washed back into the pulp.

Froth characteristics are greatly changed by the presence of hydrophobic solids. Harris (1982) reports that hydrophobic fine particles can stabilise a froth if they form a packed monolayer in the lamellae between adjacent bubbles. The solid particles "hold" the water in the lamellae thus retarding froth drainage. However, particle hydrophobicity should not be excessive; if the contact angle θ exceeds 90^o the froth film will rupture if two adjacent bubbles come into contact with such a particle, since each bubble will attempt to form its own equilibrium contact angle with the particle surface. Also, according to Harris, large particles or particles with angular edges can destabilise a froth even if their contact angles are less than 90^o. Hemmings (1981) states that high solids concentrations also contribute to froth stability.

Flynn and Woodburn (1987) have used the concept of disjoining pressure to explain the stabilising effect of hydrophobic particles. They postulate that a thin water film, δ_f, approximately 1 μm in thickness exists between the air-water and water-solid interfaces; this film is stabilised by mutual repulsion forces arising from the presence of adsorbed surfactant at both interfaces.

Further aspects of froth behaviour are discussed in sections 2.3 and 2.5 below.

2.2.5 Summary of Flotation Fundamentals

A surface potential, ψ_o, arises at a mineral-water interface as a result of the exchange of charged molecular species (known as potential determining ions) between a solid surface and the bulk solution. Hydration forces between a solid surface and adjacent water molecules cause minerals which exhibit large surface potentials to be hydrophilic.

The surfaces of hydrophobic (floatable) solids are mostly non-polar and consequently have virtually neutral surface charges. Hydrophobicity is usually achieved by adding appropriate chemical reagents, which adsorb on the solid surface, prior to the flotation step.

From a thermodynamic viewpoint, the floatability of a mineral is determined by its equilibrium contact angle, θ. For flotation to occur a finite contact angle must be formed, i.e. $0^o < \theta < 180^o$.

A flotation pulp is a dynamic system where air bubbles and solid particles are in simultaneous motion; the air bubbles rise towards the pulp-froth interface and the solids settle in the pulp. The rate of particle collection by the air bubbles is determined both by the probability (distribution) of particle-bubble collision, P_c; and the probability (distribution) of particle-bubble adhesion, P_a. The latter factor is determined by the surface chemical forces which arise as the air-water and solid-water interfaces approach each other.

Collision probability is chiefly affected by particle, d_p, and bubble, d_b, sizes. It has been shown that the rate of flotation, k, is proportional to the square of the particle diameter (d_p^2) and inversely proportional to the cube of the bubble diameter ($1/d_b^3$). As a result of particle-bubble collision a thin film (thickness $\delta \approx 1$ μm) forms between the solid and bubble surfaces. For particle-bubble adhesion to occur this aqueous film must continue to thin and eventually rupture, thus creating a solid-air interface. Film stability is determined by the characteristic disjoining pressure, P_d, in the thin film. For hydrophobic solids the disjoining pressure is negative, i.e. $P_d < 0$. Film thinning is considered as the rate determining step which controls pulp phase flotation kinetics.

The time frame within which particle-bubble collision and adhesion events occur must also be considered. Successful particle-bubble attachment requires that the time taken for film thinning, known as the induction time, t_i; be less than the time, t_c, for which the particle and bubble are in contact. Large particles have favourable collision probabilities, however, the induction times required are longer. The converse applies to fine particles. Because of this a maximum in recovery versus particle size is often observed experimentally.

The stability of the froth ultimately dictates what recoveries and grades are achieved in a flotation cell. Stable froths are those in which drainage of the water films (lamellae) surrounding the bubbles is resisted. High surfactant dosages and the presence of fine, hydrophobic particles enhance froth stability. The higher the froth stability, the greater the proportion of particles collected in the pulp which are removed in the concentrate overflow. The drawback to this, however, is that because of reduced drainage of entrained pulp water back into the pulp, there is an increase in the recovery of gangue mineral in the concentrate product. Column flotation cells have the unique feature of a water sprinkle which is added near the top of the froth bed. This washwater effectively rinses back the entrained pulp water. Consequently a zero pulp water recovery in the concentrate overflow is attainable, which is why column cells have a superior cleaning action compared with conventional flotation cells. This is further discussed in sections 2.3 and 2.5 below.

2.3 THE COLUMN FLOTATION CELL

Column flotation technology has been one of the most important innovations in minerals processing in the last decade. Column flotation, unlike conventional flotation, does not use mechanical agitation to disperse air or suspend the pulp. It is the mechanical simplicity of column cells which gives them the advantages of lower capital, operating and maintenance costs compared with conventional cells. However, more than any other factor, it is the high particle-gangue separating efficiency, particularly at fine sizes, achievable with column cells which has made them an accepted technology for the flotation of metallic minerals, where they are used almost exclusively in cleaner applications (Yianatos, 1989; Moon and Sirois, 1988).

2.3.1 General Description of Column Cell

Although there are a variety of designs currently available (Miller, 1988), the column cell most commonly used is based on a design developed by the Canadians Boutin and Tremblay in the mid-1960's.

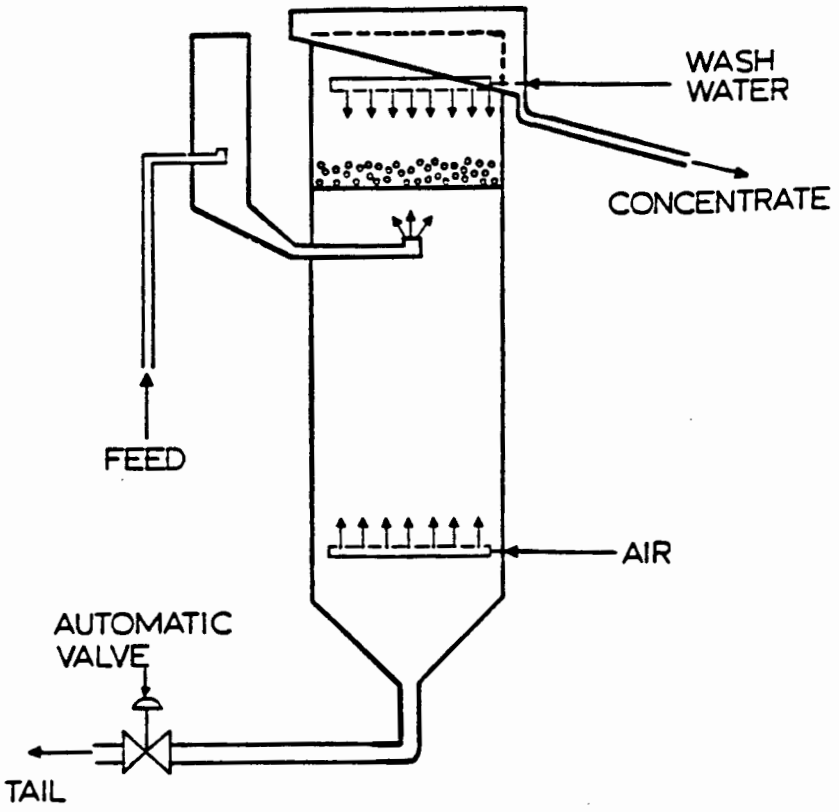

Figure 2.4 : Schematic diagram of the Canadian type column cell.

A schematic representation of the Canadian type column cell is shown in Figure 2.4. A feed slurry (in this case coal) is introduced about 3/4 of the way up the column. Air bubbles are generated by a gas sparger positioned at the bottom of the column.

The slurry flows down the column countercurrent to the swarm of rising air bubbles. Collisions occur and the hydrophobic particles attach themselves to the surfaces of the air bubbles. This region, which extends from the air sparger to the feed point, is termed the collection/recovery zone. The recovered particles are transported through an intermediate pulp zone to the pulp-froth interface.

The froth zone is a packed bubble bed to which wash water is usually added at the top of the column via a sprinkler type distributor. A conventional froth develops above the distributor as the water content of interbubble lamellae is reduced through drainage. The intermediate pulp zone and the froth bed together constitute the cleaning zone.

Column cells operate at a tailings withdrawal rate slightly greater than the column feed rate. The resultant net downward water flow in the column, termed positive bias, is very effective in preventing entrained gangue from reaching the concentrate. This gangue suppressment action of the cleaning zone is one of the principal advantages of column cells over conventional cells. The washwater also reduces bubble coalescence and promotes a stable froth.

In summary, column cells can be considered as consisting of two regimes, a collection zone where particle recovery occurs and a cleaning zone where mineral upgrading takes place.

2.3.2 Flotation Column Flow Regimes

The flotation column is really a particular application of a bubble column reactor. The bubble dynamics and flow regimes characteristic of these units have been reviewed by Shah et al (1982). For comparative scale-up purposes, volumetric flowrates are converted to superficial

velocities which are obtained by dividing the volumetric flowrate by the column cross-sectional area.

Operating parameters of interest include superficial gas velocity, J_g, bubble rise velocity, U_b, superficial net downward liquid velocity, J_l, superficial washwater addition rate, J_w, superficial slurry feed rate, J_f, and fractional volume air holdup, ϵ_g.

The three flow regimes associated with bubble columns are shown in Figure 2.5. Column flotation cells operate countercurrently in the bubbly flow regime. Shah et al (1982) report that for superficial gas velocities $J_g < 0.05$ m/s and bubble rise velocities, U_b, of between 0.03-0.20 m/s, bubbly flow exists in aqueous systems. The average superficial air rate can be corrected for hydrostatic head by using the following relationship (Yianatos, 1989) :

$$J_g = P_c.J_g^*.\ln(P_t/P_c)/(P_t - P_c) \qquad (2.14)$$

where
J_g^* is the superficial velocity at atmospheric (standard) conditions
P_c is the absolute pressure at the overflow
P_t is the absolute pressure at the bottom of the column.

Typical column flotation air velocites are J_g = 1-3 cm/s (Yianatos, 1989). This corresponds to a maximum bubble Reynolds number, Re, of about 500 and a maximum bubble diameter of around 2 mm (Yianatos et al, 1988a). The bubble Reynolds number is defined as

$$Re = d_b.U_b.\rho_l / \mu_l \qquad (2.15)$$

Bubbles smaller than 1 mm in diameter are spherical and rise with a steady rectilinear motion (Jameson, 1984). Bubbles larger than 2 mm become ellipsoidal in shape and rise in helical paths (Yianatos et al, 1988a). The rise velocity, U_b, is a function of bubble size, d_b: small bubbles have low rise velocities. Yianatos et al (1988a) have used the hindered settling equations orginally derived by Masliyah (1979) to relate terminal rise velocity, U_{bavg}, downward liquid velocity, J_l and holdup, ϵ_g, to the mean bubble size, d_{bavg}, in a bubble swarm. Jameson (1984) has reported data which show that the relationship between bubble

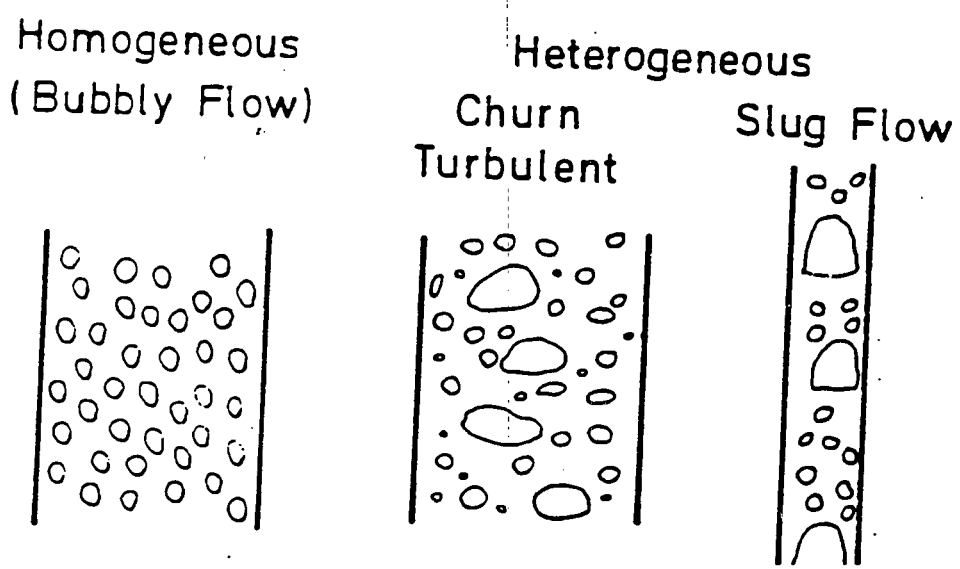

Figure 2.5 : Flow regimes in bubble columns.

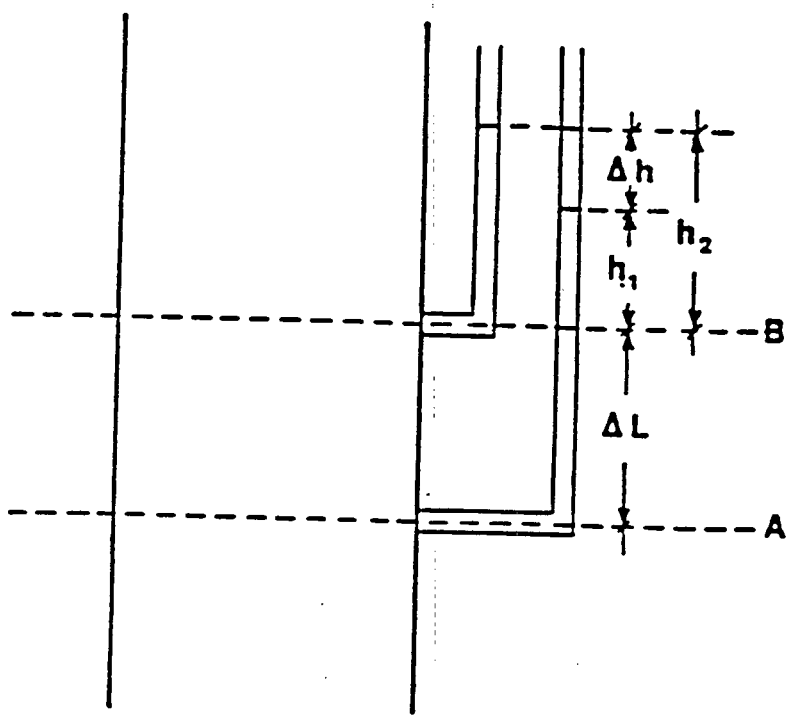

Figure 2.6 : Manometric measurements in flotation column.

rise velocity and bubble size is strongly influenced by the presence of adsorbed surfactants at air-water interfaces, i.e. frothers do not change U_b merely by reducing bubble size.

Shah et al (1982) reported the following relationship between fractional holdup and superficial gas velocity

$$\epsilon_g \propto J_g^n \qquad (2.16)$$

For bubbly flow n varies between 0.7 and 2.0.

The pulp zone of a flotation column is a 3-phase system where some of the solid species are transferring between the slurry and gaseous phases. The presence of solids can increase the gas holdup, typically by about 15 %, to between 20-25 % (Yianatos, 1989). This is because rise velocities are reduced as solids attach to the bubble surfaces. The viscosity of the slurry also has a weak effect (Yianatos et al, 1988a). Average gas holdup in the froth zone lies between 60-80 % (Finch and Dobby, 1990a).

Pulp phase fractional holdups can be determined experimentally by static head measurements (Figure 2.6). The change in kinetic energies between points A and B is assumed neglible, consequently Δh (ϵ_g) can be calculated from Bernoulli's equation.

Collection zone kinetics and gas holdup are interrelated. Large values of ϵ_g reduce particle residence times; however, they may also reflect high solids loading on bubble surfaces.

The superficial bias rate, J_b is defined as

$$J_b = J_l - J_f \qquad (2.17)$$

Positive bias rates, $J_b > 0$, are necessary for preventing pulp feed water from reporting to the concentrate. Positive bias is provided by the addition of washwater, J_w.

Yianatos has provided a summary of typical operating conditions for pilot and industrial flotation columns. These are reproduced below.

Table 2.4 : Typical flotation column operating parameter values, from (Yianatos, 1989)

Operating parameter	Value
Superficial gas rate, J_g	1-3 cm/s
Superficial slurry rate, J_f	1-2 cm/s
Superficial wash water rate, J_w	0.3-0.5 cm/s
Superficial bias rate, J_b	0.1-0.2 cm/s
Average bubble size, d_{bavg}	0.5-2 mm
Height/Diameter ratio	> 10:1

2.3.3 Column Modelling and Scale-Up

The scale-up methodology that has been developed for column flotation is based on modelling the rate of particle collection in the pulp zone. Froth phase effects are confined to predicting solid efflux from the concentrate overflow.

The methodology developed by Dobby and Finch (1986a) forms the basis for column scale-up. Key features of this methodology are described here.

The rate of particle collection in the pulp phase is determined by the kinetics of particle-bubble collision and attachment, the residence time of the particles in the pulp and pulp mixing characteristics.

The rate of particle recovery is considered to obey first order kinetics

$$dC_p/dt = - (1.5\ J_g\ E_k\ /\ d_b)\ C_p = -\ k\ C_p \qquad (2.18)$$

$$E_k = E_c . E_a \qquad (2.19)$$

J_g is the superficial gas velocity
E_k is the particle collection efficiency, E_c and E_a were defined in section 2.2.3
d_b is the average bubble diameter

C_p is the concentration of floatable species
k is the first order rate constant

Only particles collected by bubbles are considered in the model. It is assumed that the packed bubble bed froth completely suppresses recovery by entrainment.

The rate at which the particles are collected depends mainly on bubble and particle size distributions was well as particle hydrophobicities (section 2.2.3). The dependence of k on gas rate and bubble size has been investigated by Dobby and Finch (1986b). Rate constants are determined from laboratory or pilot scale column studies. As size dependent criteria are not readily elicited from experimental data, the determination of distributed rate constants is usually confined to partitioning the collected solids into "fast" and "slow" floating classes of material, k_s and k_f, according to the method described by Kelsall (1961).

Although slurry and air bubbles flow countercurrently in a column flotation cell, some deviation from ideal plug-flow behaviour occurs, especially at relatively large column diameters (L $\approx$ 1 m). The extent of axial dispersion is quantified by the vessel dispersion number, N_p, where

$$N_p = D / [(U_l+U_p).H] \qquad (2.20)$$

$$U_l = J_l / (1-\epsilon_g) \qquad (2.21)$$

U_p is the particle settling velocity
D is the dispersion coefficient
U_l is the interstitial liquid velocity
H is the height of the collection zone

Dobby and Finch (1985) found that dispersion coefficients of the liquid and solid particles were the same, i.e. $D_p = D_l$. Laplante et al (1988) related D to column diameter, L, superficial gas rate, J_g, and pulp solids content, S, as follows :

$$D = 2.98 * L^{1.31} * J_g \exp(-0.025S) \qquad (2.22)$$

where L is the column diameter.

Mills and O'Connor (1990) have questioned whether the assumption of equivalent liquid and solid dispersion coefficients applies for all operating conditions encountered in column flotation, and have also postulated that a tanks-in-series model might be more suitable than the axial dispersion model for scaling mixing effects. In addition they report that bubble size, d_b, substantially affects mixing, a factor not explicitly accounted for in equation (2.22).

In classical chemical engineering kinetics fractional conversion, x, is a function of the intrinsic reaction rate, mixing characteristics and the residence time of the reacting materials in the reactor system, i.e. $x = f(k, N_p, \tau)$.

Dobby and Finch have used the Dispersion Model for first order kinetics described in standard Chemical Engineering texts (e.g. Smith, 1981) to predict the fractional mass recovery of floatable material in the pulp, i.e. $R_p = f(k, N_p, \tau_p)$. It should be noted that the Dispersion Model was developed for homogeneous kinetics. The residence time used in the conversion (assuming no changes in fluid density) function is

$$\tau = V_c / Q \qquad (2.23)$$

where
Q is the volumetric flowrate
V_c the volume within which chemical reaction occurs

A flotation column is a heterogeneous 3-phase system and it has been questioned (Jameson et al, 1977) whether the chemical reaction analogy is particularly apt for flotation systems. In any case, the solids residence time, τ_p, is a function of particle settling velocity, U_p, and the interstitial liquid velocity, U_l. U_p, which is a function of particle density, ρ_p, and size, d_p, can be determined from the hindered settling equation of Masliyah (1979). Thus

$$\tau_p/\tau_l = U_l / (U_l + U_p) \qquad (2.24)$$

The mean slurry residence time, τ_l, is defined as

$$\tau_l = A_c.H.(1-\epsilon_g) \; / \; Q_t \qquad (2.25)$$

where Q_t is the tailings flowrate

H can be defined as the distance from the sparger to the pulp-froth interface, or more conservatively, as the distance to the slurry feed port. In the absence of gas holdup data, as is most commonly the case, the *nominal slurry residence time*, τ_n, is a useful parameter :

$$\tau_n = A_c.H \; / \; Q_t \qquad (2.26)$$

Clearly, the solids have shorter residence times than the liquid; however, as ultrafine sizes ($\approx$ 38 μm) are approached $U_p \rightarrow 0$ and $\tau_p \rightarrow \tau_l$ (Dobby and Finch, 1985).

The total column recovery is given by (Dobby and Finch 1986a)

$$R_T = R_p R_f \; / \; (R_p R_f + (1-R_p)) \qquad (2.27)$$

R_f is the fractional recovery of collected material in the froth zone.

Dobby and Finch assumed a 100 % recovery in the froth zone. Subsequent studies conducted by Falutsu and Dobby (1989) showed that fractional recovery in the froth zone, R_f, was less than 60 %. Falutsu and Dobby attributed mechanical shock resulting from sudden deceleration at the pulp-froth interface as the reason for drop back of collected particles into the pulp. Yianatos (1989) recommends that rate constants be experimentally determined from overall recoveries, R_T, citing a method described by Espinosa et al (1988).

As stated earlier, modelling of the transport processes occurring in the froth bed has been confined to predicting rates of solid efflux based on bubble surface area in the concentrate overflow. In particular the models developed calculate the *maximum solids loading* level, known as the froth *carrying capacity*. Yianatos (1989) reports the following semi-theoretical relationship for carrying capacity :

$$C_a = 60.\eta.d_p.\rho_p.J_g \,/\, d_{bf} \qquad (2.28)$$

η is an empirical fudge factor, typically $\eta \approx 0.6$ (Yianatos, 1989)
d_p is the characteristic particle diameter of the concentrate solids
d_{bf} is the bubble diameter (assumed spherical) at concentrate overflow

Espinosa-Gomez et al (1988a) have developed an empirical correlation for carrying capacity based on pilot and plant data taken from columns treating Cu, Zn, Pb and silica ores :

$$C_a = 0.0682 * d_{80} * \rho_p \qquad (2.29)$$

C_a is the carrying capacity in $t/hr.m^2$
d_{80} is the 80 % passing size of the concentrate solids

Luttrell et al (1990) have reported that this relationship also applies to coal columns. Thus, the carrying capacities, C_a, of column flotation cells treating coal fines is low because their bulk densities, ρ_p, are low compared to mineral ores. Espinosa-Gomez et al (1988b) have found that C_a is a weak function of the volumetric gas rate Q_g.

It is apparent from equation (2.29) that the solids production rate achievable with a column is severely limited by the fineness of the feed. Also, it has been found (Murdock and Wyslouzil, 1991) that for large (D_c=2-3 m) commercial columns, the carrying capacity is no longer independent of column diameter. Amelunxen (1990) proposed that lip loading capacity, defined as the carrying capacity divided by the cross-section perimeter, be used to account for reduced solid loadings in large column cells.

Investigations into froth phase mixing characteristics have received scant attention. Goodall and O'Connor (1989) have measured solids residence time distributions in a column froth using isotopically labelled gold present in a pyritic ore as a tracer. A plug-flow model with recycle, where the recycle ratio R varied between 1.2 and 3.4, was found to best describe solids mixing behaviour in the froth bed. Interestingly, the mean residence times, τ_f, in the froth bed were found to be approximately the same as that of the pulp, i.e. $\tau_p \approx \tau_f$. Yianatos et al (1988b) have used a plug-flow model to describe the flow

of collected and entrained solids through the froth as a function of froth bed depth, z. The model was found to agree reasonably with grade and solid profile measurements taken from two flotation columns in a MoS_2 cleaning circuit.

Excessive froth mixing is undesirable since it allows pulp feed water to short-circuit into the concentrate, thereby reducing product grade. Yianatos et al (1988b) have reported that unlike deep froths (> 1m) which exhibit upgrading of the recovered mineral with increasing distance from the pulp-froth interface, shallow froths (< 50 cm) have flat grade-froth bed depth profiles. This difference between deep and shallow froths was attributed to mixing.

2.3.4 Summary of Column Flotation Features

The flotation column is a bubble column reactor in which rising air bubbles and settling solid particles flow countercurrently. A washwater sprinkle added near the top of the froth bed produces a net downward water flow (the volumetric tails rate is larger than the slurry feedrate) in the column. This condition, known as positive bias, effectively prevents entrained gangue from reaching the concentrate. Postive bias imparts to the column its superior cleaning action compared with conventional flotation cells.

Column cells operate in the bubbly flow regime (Reynolds number Re_b < 500). Air bubbles are spherical and usually 1 mm to 2 mm in diameter. Fractional gas holdups in the pulp phase, ϵ_g, lie between 15 % and 25 %; whereas in the froth bubble bed average holdups, ϵ_f, are between 60 % and 80 %.

Average superficial gas, J_g, washwater, J_w; slurry feed, J_f; and bias, J_b, velocities are approximately 2.0 cm/s, 0.4 cm/s, 1.5 cm/s and 0.15 cm/s respectively.

The rate of particle collection in the pulp phase is first order with respect to particle concentration. Fractional recovery of particles from the pulp is a function of the first order rate constant, k, particle residence time, τ, and the mixing characteristics (defined by the vessel dispersion number, N_p) of the pulp phase. Only about 60 % of

the particles collected in the pulp phase are retained in and recovered from the froth.

The maximum rate of solids removal in the concentrate overflow is termed the column carrying capacity, C_a. Carrying capacity is proportional to the product of the d_{80} and bulk density, ρ_p, of the collected solids. Thus, relatively light, fine solids severely limit the solids throughput which a column is capable of processing.

Shallow froths (froth bed depth < 50 cm) are generally more mixed than deeper (> 1 m) froth beds; thus unless cleaning is very efficient, poorer grade concentrates will be produced in the former.

2.4 FACTORS AFFECTING THE FLOTATION OF COAL

2.4.1 Coal Surface Chemical Properties

On a macroscopic level the floatability of coal is directly related to its rank. Broadly speaking, the hydrophobicity of the coal surface increases with rank, with low volatile bituminous type coals being the most floatable.

This has been confirmed experimentally by various workers including Ye et al (1989) who measured induction times, contact angles and zeta potentials over a range of coal ranks and subsequently related this to flotation recovery. The measurement results are plotted in Figures 2.7-2.9. It can be seen from Figure 2.7 that induction times were at a minimum when the pH ranged between 4 and 6; this was also the pH range for which the zeta potential was nearest to zero (Figure 2.8). The lignite coal was distinctly different from the others since it had the longest induction times and the most negative zeta potentials. It is also apparent that at typical flotation pH's (usually pH≈7) coal surfaces are invariably negatively charged. Measured contact angles, which are plotted in Figure 2.9, increased with from 0^o for low rank linites to a maximum of $\approx 50^o$ for the medium-volatile and low-volatile bituminous coals. The flotation test results which were performed in the absence of a collector, are plotted in Figure 2.10. Lignite coal, which had the lowest contact angle ($\theta \approx 0^o$), was the least floatable

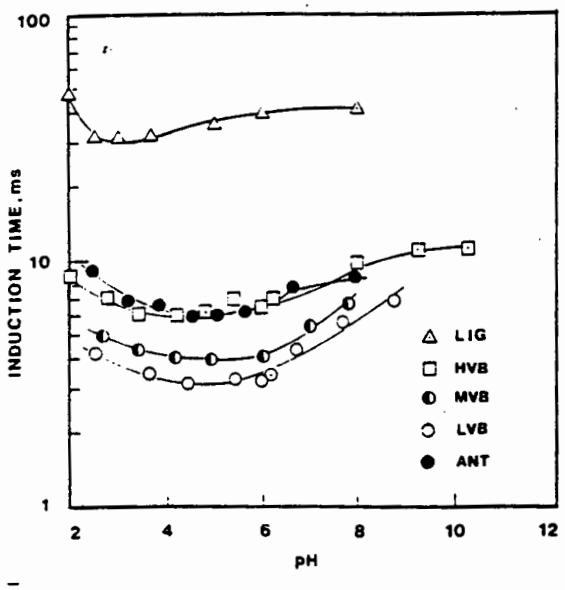

Figure 2.7 : Measured induction times for coals of different rank as a function of pH (Ye et al, 1989).

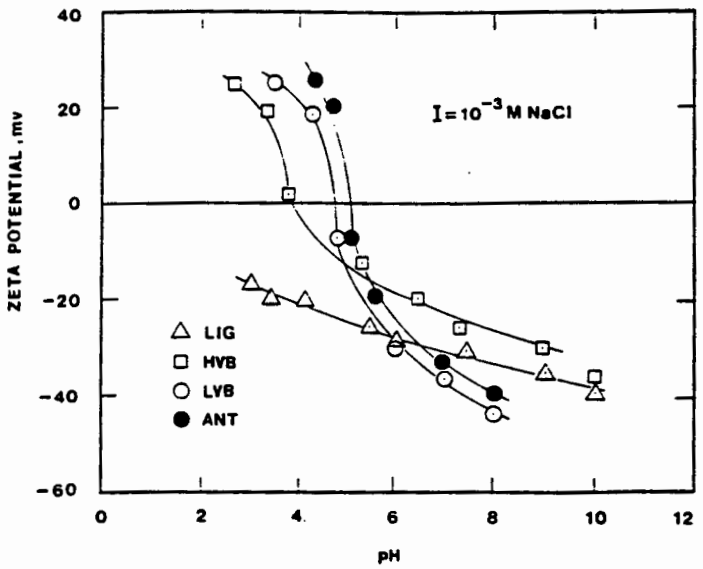

Figure 2.8 : Measured zeta potentials for coals of different rank as a function of pH (Ye et al, 1989).

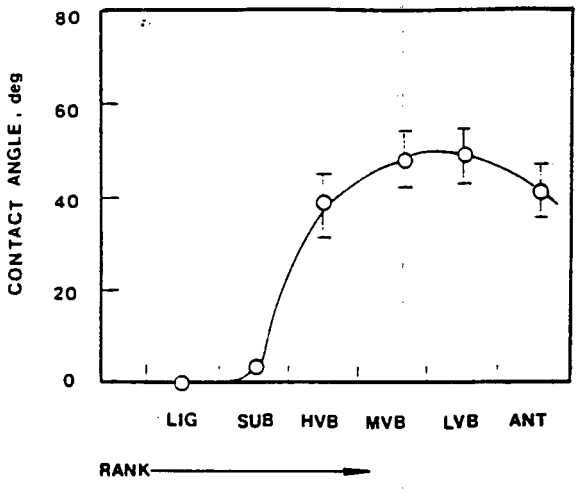

Figure 2.9 : Measured contact angles for coals of different rank. pH = 6.0 (Ye et al, 1989).

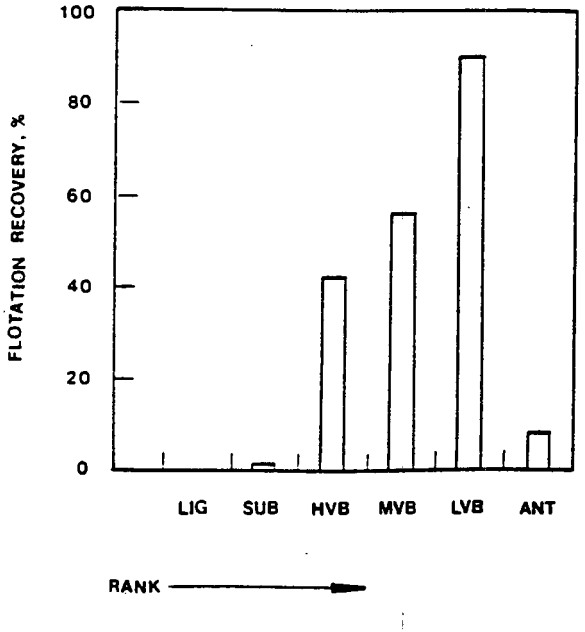

Figure 2.10 : Maximum reagentless Hallimond tube recovery at pH = 6.0 for coals of different rank (Ye et al, 1989).

with a virtually zero recovery being obtained while the largest recovery ($\approx$ 80 %) was obtained with the low volatile bituminous coal ($\theta \approx 50^{o}$). The highest ranking anthracitic coal also produced a rather poor ($\approx$ 10 %) recovery, indicating that an optimum floatability with respect to rank exists.

In a recent review paper Aplan (1988) has reported similar tests where static (i.e. equilibrium) contact angle measurements were obtained as a function of fixed carbon content and vitrinite rank parameters. The results corroborate the work of Ye et al (1989). Coals of rank lower than high volatile bituminous did not attach to the static bubble ($\theta_e \approx 0^{o}$) whereas medium, low volatile and the anthracitic coals attached at the largest contact angles ($\theta_e \approx 45 - 65^{o}$).

Sun (1954) developed a theory which explains coal floatability in terms of surface components present. He theorised that a coal consists of both floatable and non-floatable components. Floatable components are defined as oil-avid and water repellent whereas non-floatable components are water avid and oil repellent. The relative proportions of these components present in the coal can be inferred from floatability indexes based on ultimate analyses of carbon, hydrogen, oxygen, sulphur, nitrogen and moisture contents. It is assumed that the bulk floatable/non-floatable component split also applies at the coal surface.

On a more fundamental level, the hydrophobicity of a coal is related to the chemical functional groups existing on the coal surface. Some molecular structural features of coals were discussed in section 2.1 above, where it was noted that these are a function of rank and petrographic composition.

It has been proposed that there are three types of sites on the surface of coal (Aplan, 1988) :

1. strongly hydrophobic sites
2. weakly hydrophobic sites
3. hydrophilic sites

Hydrophobic surface sites occur where non-polar or slightly polar molecular groups are present. Coal can be considered to exhibit a skeleton "macromolecular" type of structure (see section 2.1). As the number of aromatic ring groups in these "macromolecules" is increased, i.e. as the rank increases, fewer substituted functional groups are present. Since aromatic rings are only weakly polar, one can expect the hydrophobicity to increase. This agrees with the observed improvement in coal floatability with rank.

Hydrophilic sites arise because of the presence of trace minerals or oxygen functional groups on the surface. These form polar covalent or ionic bonds in solution. Oxygen functional groups are present mostly as carboxylic (COOH) and phenolic groups (OH). Such groups hydrolyse and dissociate in water in a manner analagous to mineral oxides (Mishra, 1987). Thus for coal slurries H^+ (or H_3O^+) and OH^- are the potential determining ions; hence surface charge is determined by the pulp pH.

Lower rank coals have higher proportions of oxygen functional groups (Aplan, 1988) and are consequently more hydrophilic than higher rank coals. Heavily oxdised coals behave analogously to low rank coals (Aplan, 1988).

Similar arguments can be advanced to explain why petrographic composition affects floatability. In section 2.1 it was noted that inertinites have high oxygen and (syngenetic) mineral contents compared with vitrinites. Thus inertinite rich coals can be expected to be intrinsically less amenable to flotation than coals which contain predominantly vitrinite.

2.4.2 Porosity and Moisture Content Properties

Aplan (1988) and Mishra (1987) report that porosity and moisture content are strongly rank dependent. The pores of low rank lignitic coals (< 75 % carbon) are macropores (300-3000 A°) whereas higher rank bituminous coals have a microporous structure (4-12 A°). Porosities of 40-50 % are typical of lignites, 25-30 % for subbituminous coals and 1-3 % for bituminous coals. Porosity increases again to about 10 % in anthracitic coals.

Mishra reports variations in moisture contents ranging from 1-5% for medium volatile bituminous coals to 30-40 % in liginitic coals. Aplan states that the surface moisture of the -250 μm fines fraction can be as high as 20 %. High moisture contents contribute to reducing the already poor hydrophobicity of lower rank coals.

2.4.3 Wetting of Coals Using Oily Collectors

Brown et al (1958) investigated the spreading of oil on polished coal surfaces, using static contact angle measurements. They reported that oils do not spread spontaneously over any coal surface, regardless of its rank and that an energy input to the system, termed the work of spreading, γ_s, is required for the oil to spread.

The energy of spreading, γ_s, is a strong function of both coal rank and oil molecular structure and composition. Brown et al reported that oils spread more easily (i.e. lower γ_s required) over high rank coals than over low rank coals. Furthermore, commercial grade oils containing surfactant impurities were the best collectors since they caused the largest reduction in the work of spreading γ_s. Burkin and Bramley (1963) reached a similar conclusion; the addition of surface-active reagents to an oil improved spreading at coal-water interfaces. However, both studies showed that there was no simple relationship between spreading ability and flotation performance. Poorer flotation recoveries were obtained when coals were conditioned with pure aromatic oils than when less readily spreading pure aliphatic oils were used. It was postulated that this occurred because (pure) oils which spread well over a coal surface spread more easily over an air bubble; such oil films detach from the coal surface and preferentially adsorb onto the air bubbles in an aerated pulp. The surfactant molecules in impure (commercial) oils on the other hand tend to accumulate as a monolayer at the oil surface. This surface layer lowers the oil-water surface tension thus retarding the tendency of oil to spread at air-water interfaces.

Anderson (1988) investigated the adsorption of hydrocarbon collectors on washed and unwashed coals. He concluded that aromatic oils adsorb more

readily on coal surfaces than do aliphatic oils; however, this did not necessarily translate into improved flotation recoveries being attained with the use of aromatic oils.

Klimpel and Hansen (1987) have described some techniques that may be used to enhance adsorption of hydrocarbon oils on difficult-to-float coals. These included blending the oil with nonionic surfactants, the addition of water soluble "promotors" such as long-chain amines and the use of carboxylate-containing materials such as fatty acid amides.

Researchers in the USSR (Antipenko et al, 1986) have reported that primary alcohol (70-90 %)/aldehyde (10-30 %) mixtures selectively adsorb on medium rank coals and carbominerites with concomittant improvements in flotation recoveries.

Aplan (1988) has reported point of zero charge (PZC) data (Table 2.5) of coals conditioned with oily collector. These were compared with the PZC's of the same coals obtained in the absence of an oily collector. It was found that the presence of oily collector did not significantly alter the PZC. This has interesting implications for flotation, since as stated earlier in section 2.2, optimum floatability usually occurs at or near the PZC, consequently one would infer that if the PZC remains unaltered so has the ease of floatability of the coal.

Table 2.5 : The PZC of Coal in the Presence of Collectors (modified from Aplan, 1988)

Coal Rank	No Reagent	No. 2 Fuel Oil
mvb	7.6	6.7
hvAb	5.8	7.6
hvBb	5.7	5.8
(oxidised)	2.3	2.3
sub-B	2.5	2.4
(oxidised)	2.1	3.5
sub-C	2.1	
lig	2.1	

Brown et al (1958) found that penetration of oil into pores, even those of low rank coals, was negligible. This is largely because the oils are unable to displace the strongly adsorbed water molecules from the interior pore surfaces. Thus oil depletion on coal surfaces due to absorption can probably be neglected as a factor retarding floatability.

2.4.4 Kinetics of Conditioning in Mechanically Stirred Tanks

Conditioning is, in essence, a mass transfer operation in which oil is transferred from an aqueous pulp phase to a solid phase. Contacting of the coal slurry and oily collector is usually performed in a mechanically stirred tank. Conditioning may be conceptually categorised as consisting of 4 major sub-processes, viz :

1. Breakup of the oil into droplets. This occurs at the impeller.
2. Dispersion of the droplets throughout the pulp by bulk turbulence.
3. Contacting/collision of oil droplets and coal particles.
4. Adsorption/spreading of dispersed droplets onto coal particle surfaces.

The division outlined above is somewhat arbitrary, since all four steps occur simultaneously. Nevertheless it is a useful conceptual approach since it recognises that the flow dynamics involved in sub-processes 1-3 play a major role in determining the efficiency of the conditioning process.

The oil droplet sizes and size distribution generated in step 1. are functions of nominal volumetric fraction of the dispersed oil phase, ϕ_d, fluid turbulence within the impeller discharge zone, ϵ_d, and the size, shape and rotational speed of the impeller.

The surfaces of oil droplets are generally negatively charged (since the smaller H^+ ions move across the oil-water interface more easily than the larger OH^- ions) and therefore affected by pH, i.e. OH^- and H_3O^+ are often the potential determining ions (Burkin and Bramley, 1961; Ng, 1982). However, by blending an oil with a cationic surfactant, positively charged droplets can be produced (Klimpel and Hansen, 1987).

The principles of turbulence and scale-up of fluid flow in stirred tanks have been described by Davies (1972), Calderbank (1967) and Treybal (1982a).

Cutter (1966) has examined variations of local energy dissipation rates, ϵ, with position in a V=20 l capacity perspex tank fitted with a 4" diameter 6-bladed turbine impeller. He found that 70 % of the total power consumption, P, was dissipated within the impeller discharge stream whose distance from the impeller ranged from 20-40 mm. In this region turbulence was isotropic, i.e. $\epsilon_d \neq$ f(position), and the turbulence intensity was nearly two orders of magnitude higher than the nominal tank average, $\epsilon_d/\epsilon_{avg} \approx 70$ (ϵ_{avg} = P/V). Outside the discharge zone turbulence intensities decayed exponentially to around $\epsilon/\epsilon_{avg} \approx$ 0.25 in the bulk fluid.

Droplet breakup in oil-water mixtures is considered to occur only within the impeller discharge zone where turbulence is isotropic (Sprow, 1967). Dynamic pressure fluctuations, p_d, over the droplet surfaces promoting rupture are resisted by surface tension forces. For dilute oil-water dispersions ($\phi_d < 0.005$) the equilibrium mean droplet size and size distributions can be calculated from various correlations (e.g. Calbrese et al, 1986a) which are based on Kolmogoroff's theory of isotropic turbulence (Davies, 1972a). These correlations are invariably developed in mixer systems fitted with turbine impellers.

$$d_o \propto \sigma^{0.6} / \rho_c . \epsilon^{0.4} \qquad (2.30)$$

d_o = maximum droplet diameter
ρ_c = continuous phase density
σ = oil-water interfacial tension

Most correlations use ϵ_{avg} to represent the energy term (Clark, 1988) although, as was pointed out earlier, droplet breakup occurs in a region where energy dissipation rates, ϵ_d, are two orders of magnitude greater than the mean.

Assuming V $\propto$ L3, where L is the impeller diameter, equation (2.30) can be rewritten

$$d_o \propto (\sigma/\rho_c)^{0.6}.N^{-1.2}.L^{-0.8} \qquad (2.31)$$

N = impeller speed rpm

The value of the proportionality constant is a function of tank and impeller geometry.

On a volume basis droplet sizes are normally distributed. It can be shown that 68 % of the area of the dispersed oil phase is associated with droplets within ±23 % (or 1 standard deviation) of d_o. However, if one considers conditioning sub-process 3. it is evident that conditioning efficiency is dependent on the *number* of droplets, i.e droplet frequencies, not the droplet interfacial area.

Using a Coulter Counter sizing technique, Anderson (1988a) experimentally determined droplet size distributions of dilute oil-water dispersions (ϕ = 0.0002). One of the oils investigated was Shellsol AB, a commercial grade aromatic oil (95 % aromatic content) similar to Shellsol A, the standard oil collector used in this thesis. The volume mean droplet size, d_o, was found to be 22.17 μm and the standard deviation σ = 9.57 μm and the droplet dispersion was found to be normally distributed. Anderson's data indicated that 95 % of the volume of the oil was present in droplets 3.4 μm $\leq d_j \leq$ 41.0 μm.

More significant, however, was the finding that volume-based size distributions can be misleading since they create the impression that most droplets are of the order of the mean droplet size. In fact on a frequency basis, the vast majority of droplets sizes are typically an order of magnitude smaller than the mean droplet diameter, d_o.

Based on droplet number (frequency) distributions Anderson (1988) found that for the Shellsol AB-water dispersion just mentioned, of the order of 10^5 droplets of size 1-5 μm were present per millilitre of dispersion, whereas for droplets close to the mean size, $d_o \approx 20$ μm, about 10^4 droplets were present per millilitre of dispersion. Droplets of colloidal size (< 1 μm) dominated the dispersion on a frequency basis although their cumulative volume was insignificant.

Anderson also investigated the effect of impeller speed and found that the total number of droplets increased by an order of magnitude when the impeller speed was increased from 800 to 1600 rpm. This is in qualitative agreement with equation (2.31) which predicts that droplet size decreases (and thus for a fixed oil volume the number of droplets in the system increases) as the impeller speed is raised.

In fact, it can be shown (see Appendix F1) that at the collector dosages typically used for conditioning coal pulps, the majority of the coal particles are conditioned by droplets approaching ultrafine and colloidal sizes (i.e. $d_o < 5$ μm).

Under the turbulent conditions necessary to produce fine droplets, it is reasonable to assume that the oil-containing slurry is well mixed if the tank is adequately baffled. It is interesting to note, however, that there are conflicting requirements for pulp suspension and oil dispersion (Davies, 1972b) :

$$Q / p_d \propto d_i / N \qquad (2.32)$$

where Q is the volumetric circulation rate at constant ϵ_{avg}

Solids suspension is best achieved with pitched blade impellers operating at low speeds whereas good dispersion requires turbine type impellers and high rotational speeds.

Collins and Jameson (1977) investigated the effects of particle and bubble charge on the collection of ultrafine polystyrene particles (d_p 4-20 μm) by fine air bubbles ($d_{bavg} \approx 50$ μm). Both the particles and bubbles carried positive charges and the solution potential was controlled by the level of sodium sulphate addition. It was found that the flotation rate constant, k_p, was strongly dependent on the magnitude of bubble and particle charges; raising the solution potential from 30 to 60 mV decreased k_p by an order of magnitude, i.e.

$$-\ln(k_p/d_p^{1.5}) = 3.9 + 0.116\ U_p.U_b \qquad (2.33)$$

d_p is the particle size
U_p, U_b are the electromobilities of the particle and bubble respectively

The tests were conducted in the Stokes flow regime (Re ≈ 1) and indicate that although particle size (i.e. collision hydrodynamics) plays a role in determining the flotation rate, electrical double layer repulsion effects can quite easily predominate in systems where the interacting species are both very fine.

Conditioning sub-processes 3. and 4. can be evaluated in a manner analogous to that just described, as they also involve contacting a solid and hydrophobic phase; also the dimensions involved are similar. Thus one can consider an adsorption rate constant, k_a, which is proportional to the product of oil droplet-coal particle collision efficiency, E_c, and the efficiency of oil adsorption, E_a, i.e.

$$k_a \propto E_c.E_a \propto U_p.U_o \qquad (2.34)$$

Mishra (1987) states that oil droplet-coal particle interactions can be analysed on the basis of DLVO (Derjaguin, Landau, Verwey and Overbeek) theory for particle-particle interactions, namely

$$V_R \propto \zeta_p.\zeta_o \text{ (i.e. } \propto U_p.U_o) \qquad (2.35)$$

V_R is the repulsion potential energy
ζ_p, ζ_o are the coal particle and oil droplet zeta potentials

Equations (2.34) and (2.35) apply to virtually quiescent systems; in an agitated tank kinetic energy of stirring can be expected to contribute to overcoming V_R. An order of magnitude relationship between particle size and relevant system energies, reproduced from Sivamohan (1990), is depicted in Figure 2.11. Van der Waals attractive forces arise from long-range steric forces of attraction between large non-polar functional groups. The strong influence of electrostatic repulsion forces at very fine sizes, despite agitation energy inputs and Van der Waals dispersion forces, is clearly evident.

In summary, there are both kinetic and thermodynamic barriers to conditioning coals with oily collectors and these are, to a large extent, determined by the rank, petrographic and mineral compostion of the coal. Low rank coals, coals containing predominantly inertinite and

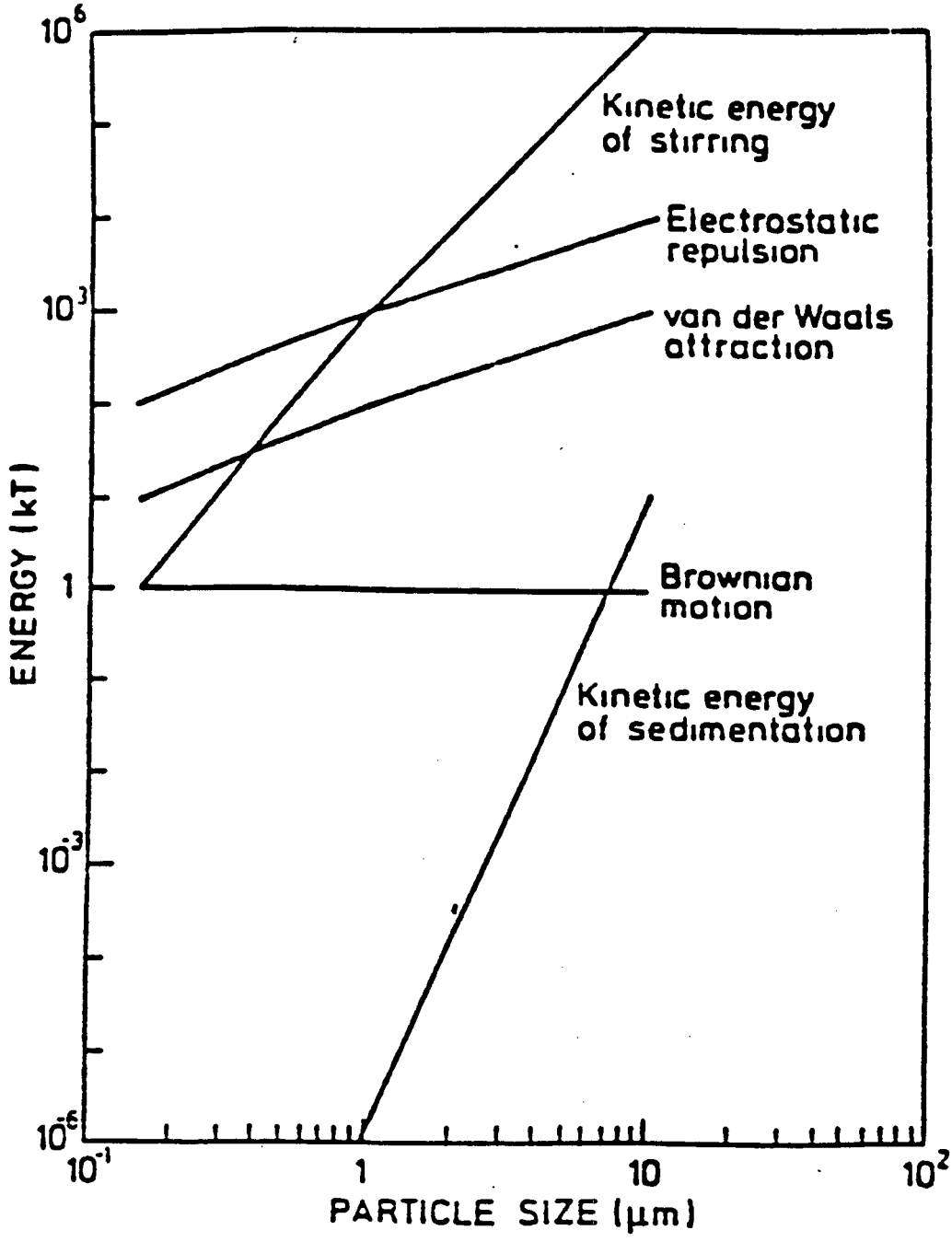

Figure 2.11 : Relative orders of magnitude of energies of interaction of and between particles in suspension (Sivamohan, 1990).

coals with high proportions of surface minerals are intrinsically difficult to condition. However, it is also apparent that through alteration of the electrolytic environment or the use of water soluble "activator" reagents, oil-surfactant blending, etc. there is considerable scope for manipulation of droplet and coal particle surface properties. In addition, it is evident that conditioning and flotation are not necessarily independent, consequently optimal oil adsorption onto coal does not necessarily translate into improved flotation recoveries.

2.4.5 pH and Temperature Effects

Aplan (1976) states, that over a range of 3-50°C, temperature has no significant effect on the rate of coal flotation.

Aplan (1976) and Zimmerman (1968) report that optimal recoveries in coal flotation occur at or near neutral pH conditions (between pH 6-7.5). In section 2.4.1 it was noted that at neutral pH's coal surfaces are usually negatively charged. More importantly, PZC data of oil-wetted coals, presented in Table 2.5, appeared to indicate that oil adsorption on a coal surface did not substantially alter the coal's PZC. The discrepancy between the experimentally observed range of optimal flotability and the acidic range indicated by zeta potential studies probably arises because the effect of solution pH on bubble charge and, by induction, on bubble-particle adhesion are neglected. The influence of bubble and particle charges on the rate of flotation has been demonstrated by Collins and Jameson (1976, 1977).

2.4.6 Summary of Factors Determining the Floatability of Coal

At typical coal flotation pH's of between 6 and 8, coals invariably carry a negative surface charge, i.e. $\psi_o < 0$. This surface charge arises largely from the presence of carboxylic (COOH) and phenolic (OH) functional groups, as well as mineral ions, on the coal surface. The floatability of coals increases with rank since higher rank coals contain less oxygen than do low rank coals. Similarly, coals rich in vitrinite can be expected to be intrinsically more floatable than coals

containing predominantly inertinite. Also, mineral rich coals can be expected to be poorly floatable.

Conditioning of coals using oily collectors is also strongly dependent on coal surface properties. From a thermodynamic viewpoint, the spreading of an oil film on a coal surface requires an energy input, termed the work of spreading, γ_s. Oils spread more easily (i.e. lower γ_s required) over high rank coals than over low rank coals. In addition, the structure and composition of the oil plays a role; aromatic oils containing surfactant impurities generally spread the most readily, however, enhanced oil spreading does not necessarily improve flotation recoveries.

Conditioning of coal slurries is typically carried out in a mechanically stirred tank. Droplet breakup occurs at the impeller. At the dilute oil concentrations (dispersed phase volume fraction, $\phi_d < 0.005$) used in coal conditioning, the size distribution of the dispersion generated is a function of power input to the mixer per unit volume of pulp, ϵ_{avg}; and impeller shape and rotational speed. The oil droplets conditioning the coal particles approach colloidal ($\approx$1 μm) sizes, consequently molecular surface forces rather than hydrodynamic forces are predominant. Oil droplets are invariably negatively charged and hence repulsion potentials, V_R, between the coal-water and oil-water interfaces can significantly retard contacting between oil droplets and coal particles, especially where intrinsically poorly floatable coals are concerned. The kinetic energy of stirring and Van der Waals forces provide the countering attractive forces necessary for oil adsorption on the coal particles.

Pulp temperature has a negligible effect on the rate of flotation over a range of between 3-50 ^{o}C.

2.5 COLUMN FLOTATION OF COAL - OPERATING PARAMETER EFFECTS

The Canadian type column cell is illustrated in Figure 2.4 above. The principal operating (input) parameters of interest include feed particle size, volumetric slurry feedrate, solids content of the feed slurry, height of the collection zone, type of sparger system installed,

volumetric air flowrate, rate of surfactant addition, rate of washwater addition, and depth of the froth bed. Some of these factors were discussed briefly in section 2.3; this section is directed specifically towards assessing how these input variables affect the column flotation of coal.

2.5.1 Particle Size

Ye et al (1989) have reported tests where a single captive bubble is contacted on a coal particle bed for a series of time intervals. After contact the particles which attached to the bubble surface were counted under a microscope. Repeated observations were taken at each time interval. A distribution of particle attachments with contact time was derived. Ye et al defined the induction time, t_{is}, as the contact time for which attachment occurred for 50 % of the observations.†

The measurements were taken for coals of varying rank and particle size; the results are shown in Figure 2.12. It is apparent that there is an order of magnitude dependence of induction time, t_{is}, on particle size. The influence of rank was small in comparision.

Misra and Harris (1988) compared particle collection and coal-mineral separation efficiencies of column and conventional flotation cells, as a function of particle size. Their results are indicated in Figure 2.13. The coefficient of separation is defined as

$$CS = R_{A1} + R_{B2} - 1 \qquad (2.36)$$

where
CS is the coefficient of separation
R_{A1} is the recovery of valuable component in the concentrate
R_{B2} is the removal of gangue in the tails

It is apparent from Figure 2.13 that for particle sizes finer than 80 μm column flotation cells are better suited to upgrading coal fines than are conventional cells.

---

† Although this measurement is not the same as the induction time in an aerated pulp where the particle slides over the bubble surface, it is evidently an improved measure of floatability compared with contact angle determinations.

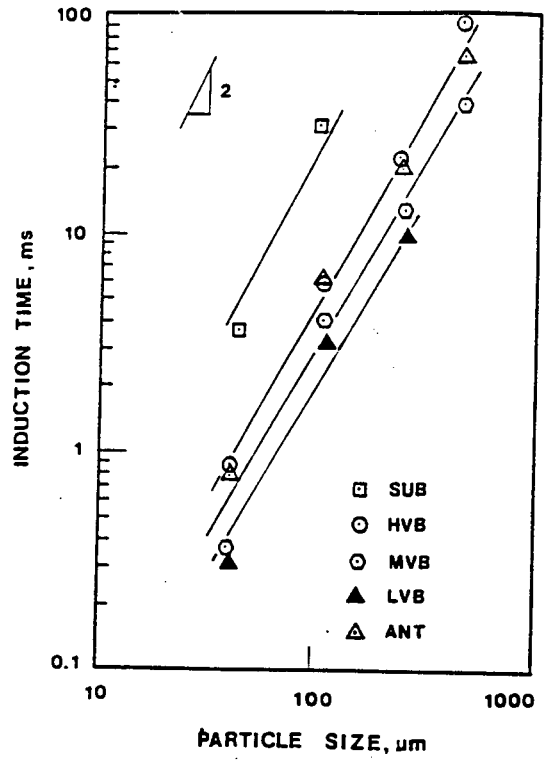

Figure 2.12 : Effect of particle size and coal rank on induction time (Ye et al, 1989).

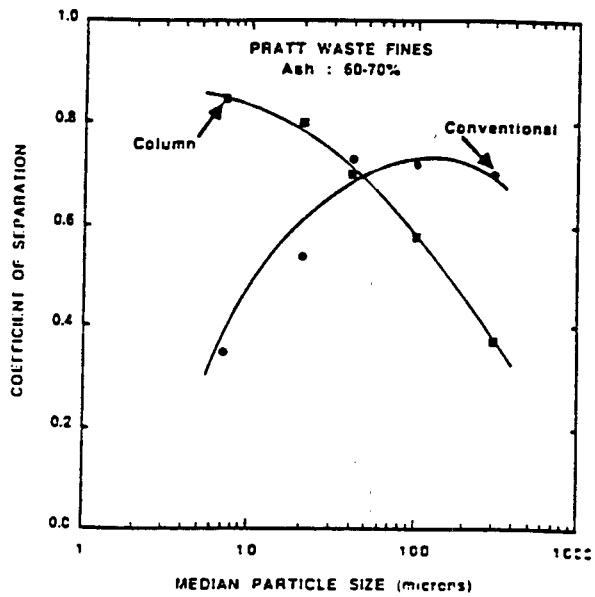

Figure 2.13 : Effect of particle size on the coefficient of separation (Misra and Harris, 1989).

The disparities in performance between the two classes of flotation machines arises from two sources, namely, differences in particle-bubble collision efficiencies in the pulp phase and the extent of fines entrainment in the froth phase (Kawatra and Eisele, 1987). The aerated pulp in a conventional flotation cell is highly turbulent, thus both the particles and bubbles have large velocities. However, because flow direction is dictated by impeller motion both the air bubbles and particles move in the same direction. Relative particle-bubble velocity and hence collision efficiency is therefore low. Conversely, the countercurrent approach of bubbles and particles, and the relatively quiescent flow characteristic of a column cell, ensures that particle-bubble collision efficiencies are quite high. In addition, bubble formation in a conventional cell occurs (in a manner analagous to oil formation of oil dispersions) at the impeller discharge zone of mechanical impellers. It is known that coalescence takes place in this region (van't Riet and Smith, 1973); the bubbles produced are coarser than those generated by the sparger devices used in column cells (Kawatra and Eisele, 1987). The influence of bubble size on the flotation rate constant was emphasised in sections 2.2.3 and 2.3.3. The ability of column cells to suppress recovery by entrainment has already been remarked on (see section 2.3 above).

A review of pilot scale column flotation tests conducted at a few South African collieries by Franzidis and Harris (1989) corroborates the findings of Misra and Harris (1988). Franzidis and Harris reported that column cells efficiently recovered the -75 μm fractions, however, recovery of coarser (+75 μm) size fractions was poor.

The discussion thus far has been (implicitly) confined to pulp phase effects. In section 2.2.4 the contribution of fine hydrophobic particles to stabilising a froth bed was noted. Engel and Smitham (1988) have investigated the effects of rank and particle size (of selected washed coal samples taken from some Australian collieries) on froth stability. In the absence of an oily collector froth stability was found to increase by an order of magnitude as the particle size decreased from 75 μm to 20 μm. The effect of coal rank on stability was also discernible. The addition of an oily collector masked rank effects but an order of magnitude dependence of froth stability on particle size was still observed.

Hemmings (1981) has measured film thicknesses of 3-phase froths in Australian coal beneficiation plants. He found that for (conventional) coal froths the lamellae thickness, δ, varied between 280-830 μm. Woodburn et al (1989) reported similar results for the limiting lamellae thickness of coal froths, froths drained to a thickness, δ^*, approximately the same size as the d_{95} of the concentrate solids.

2.5.2 Slurry Feedrate and Solids Content

Typical feed slurry velocities were reported in Table 2.4 above. For a given size (diameter) column, the permissible range of volumetric feedrates is governed by two factors, namely the pulp residence time necessary to obtain a desired recovery and, secondly, the rate of solids removal as concentrate overflow per unit cross-sectional area; this should not exceed the column carrying capacity.

Parekh et al (1988) reported that residence times of between 3-8 minutes were sufficient to ensure a 90 % coal recovery. The coal tested was a refuse sample from the Kentucky coalfield of North America. Australian investigators (Nicol et al, 1988) have described similar results. Tests performed with a pilot-scale (D_c = 100 mm) column on a sample of -100 μm fines taken from the BHP-Utah Riverside Mine in Queensland showed that a residence time of about 3 minutes was sufficient to produce a 70 to 80 % recovery of combustible matter. Durney (1990) has reported a residence time of approximately 12 minutes for an industrial scale (D_c=2.4 m) Deister Flotaire column cell installed on a preparation plant in Virginia, U.S.A.

It was shown in section 2.3.3 that the solids loading capacity of a column is severely limited by the fineness of the feed solids. Reddy et al (1988) reported figures which indicate that typical solid throughputs for coal columns range between 1.4-2.5 t/hr.m^2. In addition, they conducted tests on a -0.5 mm sample of coal fines using three columns with respective diameters of 80 mm, 100 mm and 200 mm. A production rate, C_p, of around 1.2 t/hr.m^2 was found to be the optimum. The feed solids throughput of the industrial Flotaire column just mentioned has been reported as $F_a \approx 2$ t/hr.m^2 (Durney, 1990). Solids feedrates as high

as 4 t/hr.m^2 have been used (Parekh et al, 1986), although large bubble surface areas, i.e. fine bubbles in the concentrate overflow, are achieved at the expense of high concentrate water contents. This reduces grade as it reflects less efficient washing of the froth bubble bed (Misra and Harris, 1988).

Crowding effects, with subsequent loss of selectivity at high solids concentrations, especially near carrying capacity, is another factor to be considered. Misra and Harris (1988) report that coal columns can operate at pulp densities of up to 16 % without any impairment in grade and recovery performance; however, dilute (< 10 %) pulp feeds are more common (Luttrell et al, 1990).

2.5.3 Column (Pulp Zone) Height

The selection of an appropriate column height is, like the volumetric feedrate, QF, determined by pulp residence time considerations. Column heights of up to 8 m have been used for laboratory-scale testwork (Parekh et al, 1988). The Deister Flotaire column described by Durney (1990) is 26 ft in height. Nicol et al (1988), using data from the pilot scale column described above, installed a 1.7 m diameter, 8.5 m high column at the BHP-Utah Riverside Mine in Queensland. In general, height to diameter ratios, H/D_c, decrease from approximately 10-15:1 in laboratory columns to around 5:1 for industrial size units.

Ynchautsi et al (1988) have measured grade and recovery profiles in both the pulp and froth zones of a 2.5" diameter Plexiglass flotation column. They recommend that since negligible recovery occurs in the pulp zone between the feed inlet port and the pulp-froth interface, the collection zone height, H, be defined as the distance from the sparger to the feed inlet port. Grade profile data normalised with respect to feed mineral composition showed that the intermediate pulp zone between the feed port and the pulp-froth interface functions as an efficient cleaner, achieving a relative upgrading in feed composition of approximately 30 %.

The location of the feed point relative to the pulp-froth interface is a factor influencing performance only insofar as it affects the volume of

the collection zone; if this is lowered, retention time and hence recovery is reduced (Ynchautsi et al, 1988).

2.5.4 Sparger Design

In section 2.2.3 it was shown that the flotation rate constant, k, theoretically follows an inverse cubic dependence on the bubble diameter, d_b. Indeed, the industrial experience of column flotation has been that bubble size is, in many cases, critical to recovery and grade performance (McKay and Foot, 1990). It is unsurprising therefore that considerable attention has been paid to the development of improved bubble generation devices.

Spargers used in column cells fall into two classes, namely porous media spargers and the so-called "external bubble generator" systems.

Typical porous media materials include rubber (pierced with micron-sized holes), filter cloth fabrics, fritted glass and porous metals (Flint et al, 1986). Pores range from approximately 25 to 100 μm in size (Perry, 1973). Although porous media spargers are widely used in laboratory size columns they are increasingly disfavoured in industrial applications (McKay and Foot, 1990). They are prone to pore blockage owing to solids deposition on the sparger surface; this reduces their operating lifespan. Also, because the surfactant is typically added to the feed slurry (and sometimes the washwater stream), the air bubbles adsorb surfactant as they rise through the pulp. Thus a frother concentration profile develops in the column and local rates of adsorption at the air-water interface do not occur at steady state (Jameson, 1984).

External bubble generation systems for column cells were first developed by McKay et al (1988) at the U.S. Bureau of Mines. Bubble generation is based on the principle of pressure dissolution; a water/frother solution and air are mixed under pressure (between 20-100 psig) and pass into a perforated tube with orifices 0.2-2 mm in diameter. McKay et al identified orifice diameter as the most critical parameter determining bubble size. A diameter of $\approx$ 1mm was found to be optimal. In addition, they showed that the control over bubble size, d_b, achievable with an

external bubble generator was far superior to that obtained with conventional porous media spargers. Flint et al (1986) hypothesised that the reason for this is that in external bubble generator systems, unlike porous spargers where adsorption occurs from the bulk solution, surfactant is present at the orifices where creation of air-water interface occurs. From an operating viewpoint external spargers are more desirable since commercial designs are available which make on-line maintenance possible (Murdock, 1991).

Finally, another important area where external spargers have an advantage over porous media spargers is in scaling air flowrates from laboratory or pilot size columns to large industrial units. Nicol et al (1988) and Parekh et (1988) found that air velocities were not linearly scaleable. It was concluded that this occurred because the ratio of (porous) sparger surface area to column cross-section was lower for commercial scale columns than for test size units. As the number of tubes and the number of nozzles on each tube can be adjusted, uniform air distributions across a column are more readily attainable with external bubble generators.

2.5.5 Air Flowrate

The (pulp phase) rate of flotation is directly proportional to the superficial gas velocity, J_g (equation. 2.18). Increasing the volumetric air flowrate, AF, should therefore increase recovery. In fact, a peak in gas rate vs recovery is generally observed experimentally (Dobby and Finch, 1986b); this occurs because bubble size increases with air rate. Carrying capacity is also theoretically a function of air rate (Equation 2.28); however, in practice only a weak dependence is observed (Espinosa-Gomez et al, 1988b).

Published testwork on column flotation of coal fines indicates that both product recovery and ash content increase with increasing air rate (Luttrell et al, 1990; Misra and Harris, 1988; Parekh et al, 1986; Parekh et al, 1988). Increase in ash content occurs due to the recovery of less well liberated material and also possibly as a result of increased entrainment in the froth bubble bed. Air flowrate is a major

factor contributing to hydraulic entrainment into the froth bubble bed. This is further discussed in section 2.5.8 below.

2.5.6 Frother Dosage

At a fixed volumetric gas rate raising surfactant dosages levels reduces bubble size and increases the number of bubbles, both of which contribute to an increased rate of flotation. Froth bed stability is obviously also dependent on surfactant concentration (section 2.2.4). Excessive frother dosages (equivalently small bubbles) reduces bias which can result in poorer grade concentrates (Finch and Dobby, 1990a). Harris (1982) reports that frothing power and stability increase dramatically beyond (pulp phase) frother concentrations of ≈ 20 ppm. Aplan (1976) states that typical surfactant dosages used in coal flotation range between 0.1 to 0.5 lb/ton.

A possibility not discussed thus far is that the presence of a frother alters the rate of flotation through adsorption on the surfaces of (oil coated) coal particles. Collector-frother synergism is a well documented phenomenon in mineral and coal flotation systems (Fuersteneau and Urbina, 1988; Hansen and Klimpel, 1987). However, since with the exception of the plant trials (Chapter 5) and the laboratory tests on ultrafines (section 4.6), only one oily collector (ShellsolA) and one frother (tri-ethoxybutane) were used, reagent synergism can be neglected as a factor to be considered in this thesis.

2.5.7 Washwater Addition and Bias

The concept of adding a water sprinkle near the top of the froth bed to reduce or eliminate recovery of pulp feed water was introduced in section 2.3.1. It has been shown that this addition of washwater increases froth stability and allows the development of deep (≈ 1m) froth beds (Ynchausti et al, 1988), although Parekh et al (1986) found that its effect on coal recovery and grade was less significant than the input variables frother concentration, air flowrate and column height. From a design viewpoint, the washwater sparger should distribute water evenly across the column cross-section. Also the sparger should be

capable of maintaining a sprinkle and not produce a jet over the range of washwater rates employed (Yianatos, 1989). The position of the washwater distributor is also important (see section 2.5.8 below).

Yianatos (1989) lists superficial washwater velocities, J_w, of between 0.3-0.5 cm/s as suitable. Luttrell et al (1990) recommend that for coal flotation a minimum washwater velocity, J_w, of 0.25 cm/s be used, the reason being that below this value washing of the froth is erratic due to the relatively high proportion of washwater which short-circuits into the concentrate product. However, excessive superficial washwater velocities are also undesirable as this increases channeling and recirculation (i.e. mixing) within the froth bubble bed (section 2.3.3).

It is the washwater which provides the net downward water flow in a column cell. Based on this definition bias rate is given by (Finch and Dobby, 1990b)

$$J_b = J_{tf} = J_t - J_f \qquad (2.37)$$

where
J_{tf} is the difference in slurry flowrate between tailings and feed
J_t is the tails slurry superficial velocity
J_f is the feed slurry superficial velocity

Postive bias ($J_b > 0$) is required for suppression of entrainment; however, large bias rates ($J_b > 0.4$ cm/s) increase mixing and reduce mean slurry residence time (Yianatos, 1989).

Strictly speaking the solids flowrate should also be accounted for (Finch and Dobby, 1990b). Then

$$J_b = J_{tf} - J_{ts} \qquad (2.38)$$

where J_{ts} is the volumetric flowrate of solids reporting to the tails per unit area.

Finch and Dobby (1990b) state that for pulp densities greater than 12 % by volume, J_{cs} approaches 0.1 cm/s.

2.5.8 Froth Height

Typically froth bed depths in columns range from 0.5-1.5 m (Yianatos, 1989). At moderate gas rates (J_g < 1.5 cm/s) hydraulic entrainment can be eliminated with shallow (≈ 0.5 m) froths. Finch and Dobby (1990a) state that under these conditions recovery of pulp feed water in the froth phase is eliminated within 10 cm of the pulp-froth interface. Two phase tracer studies conducted by Yianatos et al (1987) showed that at high superficial gas velocities (J_g > 2cm/s) feed water penetration into the froth bed increased near (< 30 cm) the pulp-froth interface but remained insignificant for froth depths greater than 70 cm. If selectivity between floated species is required than froth depths of ≈ 1m or more are required (Yianatos et al, 1988).

Parekh et al (1988) reported that increasing froth bed height from 0.6 to 1.2 m reduced the concentrate ash content of a Kentucky coal fines sample from 8 % ash to 5 % ash whilst the recovery remained constant at 95 %. They also found that the position of the washwater distributor relative to the overflow lip affected concentrate grade. As stated in section 2.2.4, a conventional froth exists above, and a bubble foam bed below, the washwater distributor. Parekh et al termed this conventional froth region a froth drainage zone and found that increasing its length from 0.15 to 0.45 m reduced product ash contents of the aforementioned Kentucky coal fines sample from 9.6 to 4.7 % ash whilst maintaining a combustible recovery of 95 %.

Although it has been reported that froth bed depth often has no significant effect on either recovery or grade over a wide range of operating conditions (Yianatos, 1989; Finch and Dobby, 1990a), it is apparent that the flow conditions in the froth zone are influenced by the combination of parameter values, principally air flowrate, froth bed height and washwater rates, selected. Thus, the degree to which any of the above parameters influences column performance depends on what parameter levels are chosen for the other two variables.

2.5.9 Summary of Column Parameter Effects

A comparison of coal recovery and coal-mineral separation efficiencies between column and conventional flotation cells indicated that column cells are better at recovering and cleaning finer size fractions (80 μm or less) than conventional cells. Results from column trials conducted at South African coal collieries corroborate this finding.

For a given size (diameter) column, pulp residence time and solids content of the slurry dictate what range of slurry volumetric feedrates are selected. Coals generally have fast flotation kinetics; residence times, τ, required are short, typically ranging between 3 and 12 minutes. Carrying capacities of coal columns range between 1.4 to 2.5 t/hr.m^2.

Column height, like slurry feedrate, is determined by the residence time required to attain a desired recovery. Column height to diameter ratios decrease from $\approx$ 10-15:1 in laboratory column cells (D_c < 10 cm) to around 5:1 in larger commercial size (D_c > 1 m) units. The collection zone height, where particle collection occurs, is defined as the distance between the feed and sparger ports.

The bubble generation device used is often of critical importance. Types of porous media spargers used include filter cloth, glass frits and rubber sleeves pierced with micron-sized holes. So-called "external bubble generators" are spargers where air-water/surfactant mixtures pass through a perforated tube. Bubble formation occurs at an orifice(s) typically $\approx$ 1 mm in diameter. Advantages exhibited by the latter over porous media spargers include better control over bubble size and distribution; easier scale-up of air distribution per unit column cross-section; lower susceptibility to solids blockage; and on-line maintenance capability. Consequently "external spargers" are favoured in industrial applications.

Increasing air flowrate raises both the recovery and ash content of coal concentrates. Whilst high frother dosages ($\approx$ 20 ppm) dramatically improve froth stability (and hence recovery) they also retard froth drainage which lowers product grade. Elimination of entrainment into the froth product necessitates that a column operate in positive bias,

i.e. $J_b > 0$. This requires the addition of washwater at the top of the froth. Column flotation of coal requires a minimum superficial washwater addition velocity, J_w, of $\approx$ 0.25 cm/s, however, if the washwater rates are excessive ($J_b > 0.4$ cm/s) increased mixing and channeling in the froth bed reduces product grade. The mechanical design of the washwater distributor is also important; an even water sprinkle over the froth bubble bed is required.

At moderate air flowrates ($J_g < 1.5$ cm/s) shallow froth beds ($\approx$ 0.5 m) are sufficient. If air velocities exceed 2 cm/s feed water penetration increases near (< 30 cm) the pulp-froth interface. Consequently deeper froth beds (> 0.7 m) are necessary.

2.6 STATISTICALLY DESIGNED EXPERIMENTS

2.6.1 Motivation

A characteristic feature of systems encountered in the Engineering and Applied Science disciplines is that several (system input) variables affect the process responses (outputs). A block diagram of an arbitrary process is represented in Figure 2.14. The x variables represent n independent inputs and the y variables m independent process outputs. As both the individual variables (factors) and sometimes specific combinations of input variables (factor interactions) influence the process response(s), the behaviour of these systems is rather complex.

In particular, under the latter circumstances, the classical testing one-factor-at-a-time approach to experimentation is inefficient, requiring a separate set of observations for each variable and using each variable just once. Also, since no factors are varied simultaneously, it is incapable of detecting whether input variable interactions are present.

Consider as an example the system represented in Figure 2.15. Here two independent variables, residence time (x_1) and pressure (x_2) both influence the reaction yield response (y). The system behaviour can be seen to be characterised by a family of contour responses, collectively known as the response surface; it is apparent that the process responds

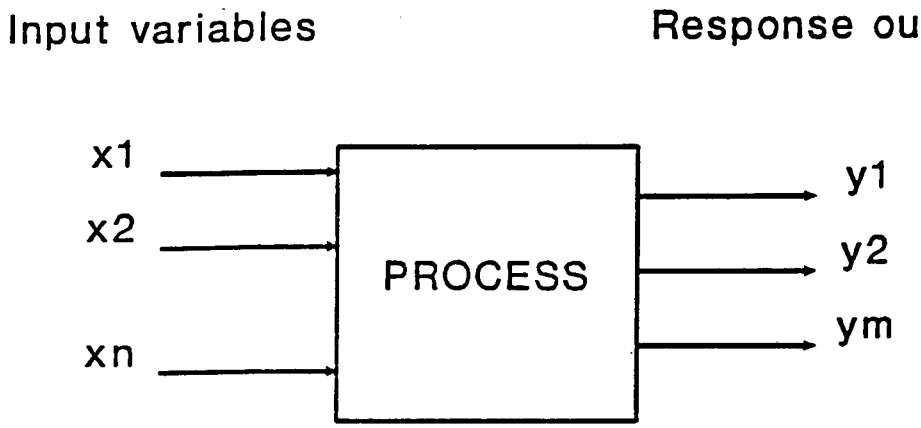

Figure 2.14 : Schematic of an arbitrary physical process.

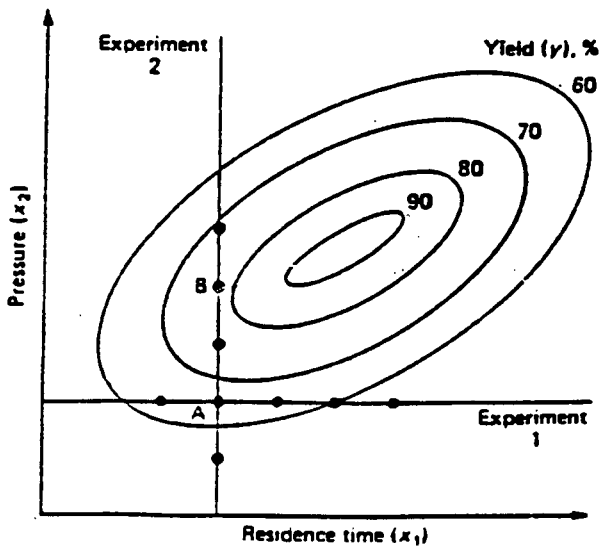

Figure 2.15 : Effect of residence time and pressure on the % yield response of an arbitrary process reaction.

in a highly non-linear manner to changes in the input variables. Mathematically the yield response, y, can be represented by

$$y = f(x_1 , x_2) \qquad (2.39)$$

The classical one-variable-at-a-time approach implicitly assumes that additive function properties exist, i.e.

$$y = f(x_1 , x_2) = f_1(x_1) + f_2(x_2) \qquad (2.40)$$

Consequently, if one wants to maximise y, one proceeds as follows : Vary x_1 over a suitable range of values to obtain f_{1opt} (point A). Once this has been achieved hold x_1 constant at $x_1 = x_{1opt}$ and vary x_2 over a range of values until y_{opt} (= $f_{1opt} + f_{2opt}$) has been reached (point B).

Unfortunately, as Figure 2.15 indicates, the yield at **point B** ($70 < y < 80$ %) is **not** the **optimum** (maximum) **yield** which can be achieved; the maximum yield achievable being greater than 90 %. Now consider what happens if equation (2.40) is rewritten as

$$y = f(x_1 , x_2) = f_1(x_1) + f_2(x_2) + g(x_1 , x_2) \qquad (2.41)$$

where the function g denotes a joint x_1, x_2 factor effect (interaction).

Under equation (2.41) f_{1opt}, f_{2opt} at $x_1 = x_{1opt}$, $x_2 = x_{2opt}$ does not necessarily represent the best operating conditions as g is not necessarily optimal at x_{1opt}, x_{2opt} [$g_{opt} \neq g(x_{1opt} , x_{2opt})$].

Refer again to Figure 2.15. Aside from the issue of optimality, the 9 one-variable-at-a-time experiments performed cover a relatively narrow portion of the response surface; there is only information about the effect of varying residence time (x_1) on yield (y) at one fixed pressure and, conversely, information about the effect of varying system pressure (x_2) on yield at only one fixed residence time. As in many practical situations the experimenter would like to "map" changes in yield due to varying residence times as a function of pressure or vice versa, the limitations of the classical type of experiment become apparent.

A better experimental approach would be to vary x_1 and x_2 simultaneously. This can be done in several ways, of which the most

efficient, in terms of runs required, is typically a factorial experiment.

2.6.2 Factorial Designs

As implied above, factorial experiments have, in principle, a twofold advantage over one-variable-at-a-time testing; firstly, they allow the experimenter to detect factor interactions and, secondly, for a given number of trial runs, they cover a broader spectrum of the response surface, thereby better defining the system's behaviour than do classical experimental methods.

The details of construction and analysis of factorial designs are discussed in Appendices A1 and A2; only key conceptual features underlying the subject are presented here. The statistical texts consulted include Das and Giri (1979), Mason et al (1989), Miller (1986), Murphy (1977), Montgomery (1984) and Scheffe (1959).

The most widely used class of factorial experiments are the 2^n series of designs. Here each of the n input variables (factors) presented in Figure 2.14 is tested at two levels, arbitrarily designated low (-) and high (+). For convenience, suppose only a single response output, y, is of interest. A single replicate (i.e. no factor-level combination is tested more than once) of a full factorial design then has $N = 2^n$ responses $y_1, y_2, \ldots y_N$. Also, there are evidently $2^n - 1$ degrees of freedom associated with such a design.

Now any input factor, say x_1, is tested 2^{n-1} times at the low (-) level and 2^{n-1} times at the high level. Therefore, one way of defining the effect, E, of factor x_1 is to subtract the average of the responses at the low (-) level from that at the high (+) level. Mathematically one can write

$$E = 2 \left[- \Sigma_{j(-)} y_j + \Sigma_{j(+)} y_j \right] / N \qquad (2.42)$$

One can re-formulate the above expression as

$$E = 2 \Sigma_j C_j * y_j / N \qquad (2.43)$$
$$= 2\, l / N$$

where

l = linear combination of responses y_j

C_j = coefficient of response y_j

C_j = -1 for j(-)

C_j = +1 for j(+)

Also, it is evident that

$$\Sigma_j C_j = 0 \qquad (2.44)$$

Any linear combination, l, of responses, y_j, which obeys the constraint equation (2.44) is known as a **contrast**. The contrast defined above has 2^n elements; however, one can select any number of elements to form a contrast provided (2.44) is obeyed. The elements of a contrast can be transposed to form a column vector, $\mathbf{lv}$. For a 2^n *full factorial* experimental design, the effect of every input variable (factor) and input variable combination (a total of $2^n - 1$ factor/interaction effects) is defined by a unique contrast (or contrast vector) consisting of 2^n elements. Mathematically this is equivalent to stating that for a 2^n factorial design there are $2^n - 1$ *independent* (mutually orthogonal) vectors, $\mathbf{lv}_k$, one defining every factor effect.

The advantage of using equation (2.42) to define factor effects is that it utilises the underlying symmetry of 2^n designs to account for non-linearity in system response behaviour.

Consider, for example, the effect, E, of the input variable x_1. At each level of x_1 there are N/2 combinations of x_1 with the other input variables $x_2, \ldots x_n$. Furthermore, aside from the x_1 factor, the test run combinations at each test level (-) and (+) are mirror images of each other. Therefore under a null hypothesis that the input variable x_1 exerts no influence on the process response, y, the *sum* (or average) of *responses* at *each level* will be the same (neglecting random error), i.e. $E \approx 0$. Conversely, if the level of factor x_1 does affect system behaviour this will be reflected in the value of the response effect E.

Two-level factorial designs are basically used only to detect and quantify statistically significant factor and factor-interaction effects. Although response surface methodology can be used to model system response as a linear function of the input variables, more elaborate model functions which account for response curvature require investigation of at least three factor levels.

The major drawback of full factorial experiments is that, even for a moderate number of input variables, the number of test runs required for the design (e.g. for n = 6, N = 64) rapidly becomes impractical either because the resources and time available in which to perform the experiment is limited or because it is not possible to run the entire experiment under homogeneous conditions.

Consequently it is common practice to run only a subset (**fraction**) of 2^a test runs from the full 2^n factorial design. The contrasts defining the factor effects are given by

$$l^* = \sum_{j=1}^{m} C_j * y_j \qquad (2.45)$$

$$m = 2^a$$

and the constraint equation (2.44) still holds, i.e. $\Sigma_j C_j = 0$.

Now $2^a < 2^n$ and therefore $(2^a-1) < (2^n-1)$, i.e. only (2^a-1) independent contrasts exist and since there *remain* (2^n-2^a) factor effects, *different factor effects* are defined by the *same contrast*. In statistical terminology this is known as **confounding**. Factor effects which are confounded are called **aliases**.

Clearly the *factor aliases* which arise from a fractional experiment depend on which *test runs* are *selected*.

Recall that for the two-factor system example discussed above, the function $g(x_1, x_2)$ was introduced to account for the effect of simultaneous x_1x_2 level combinations on the process yield response; it is apparent that g represents a 2-factor interaction. As the definition

of the function g was arbitrary it can be extended to account for k-factor interactions $g(x_1, x_2, \ldots x_k)$.

In the majority of physical systems simultaneous interactions of 3 or more input variables (factors) influencing a process response are rarely encountered, i.e.

$$g(x_1 \ldots x_k) \approx 0 \text{ for } k \geq 3 \qquad (2.46)$$

The latter remark provides the clue to reducing the number of test runs required to investigate n input variables, each at two levels.

Suppose an arbitrary contrast, L^*, is chosen which defines both the effect of an input variable, x_1, (also known as a main effect) and the effect of a five-factor interaction, $x_1x_2x_3x_4x_5$. In fact L^* represents the algebraic sum of the x_1 and $x_1x_2x_3x_4x_5$ effects, i.e.

$$L^* = l_{x1} \pm l_{x1x2x3x4x5} \approx l_{x1} \qquad (2.47)$$

if $l_{x1x2x3x4x5} \approx 0$

Two-factor interactions often exert a strong influence on a process response, therefore one would avoid confounding main effects and two-factor interactions as far as possible [see equation(2.46)] since one cannot necessarily assume that a two-factor interaction effect is neglible (i.e. $l_{x1x2} \neq 0$).

In fractional factorial design terminology, the concept of *design resolution* is employed to describe how main effects and interactions are confounded. Basically the higher the design resolution, the greater the size of the interaction term which the lower order factor effects (typically main and two-factor interactions) are confounded with.

Methods of constructing fractional factorial designs as well as further discussion on the subject of design resolution are presented in Appendix A1.3. An authoritative discourse on the construction, features and areas of application of fractional designs is presented by Box and Hunter (1961a, 1961b).

Fractional factorial designs are widely used as *screening* designs in the initial stages of an experimental programme; their major purpose is to *identify* a *small* number of *dominant factors* from a fairly large number of input variables.

2.6.3 Analysis of Fractional Factorial Designs

The detection of statistically significant factor and factor-interaction effects can be accomplished using the Analysis of Variance (ANOVA) technique.

The ANOVA method requires a linear model of the form indicated in equation (2.41) but extended to include k input variables (factors). For example if there are 3 input variables (k = 3) then

$$y_{ijkl} = \mu + \alpha_i + \beta_j + \gamma_k + \alpha\beta_{ij} + \alpha\gamma_{ik} + \beta\gamma_{jk} + \alpha\beta\gamma_{ijk} + e_{ijkl} \qquad (2.48)$$
$$= f(x_1, x_2, x_3) + e_{ijkl}$$

y_{ijkl} = observed response value
f = predicted response value
μ = overall mean
α_i = effect of factor x_1 at level i
$\alpha\beta_{ij}$ = effect of factor-interaction x_1x_2 at level ij, etc.
e_{ijk} = random error component

As discussed previously, in a fractional factorial design some of the model functional terms are lumped together or assumed neglible, the grouping being dependent on the design resolution.

The above model is a **fixed** effects **model** because it is taken that the input variables can each be set at a specified level for each test run. The system response is, however, random because the error component is a continuous variable. Models where the input variables vary within a range of values are known as random effects models.

The basis of the ANOVA technique is that the overall system variability is partitioned into a random error component as well as components corresponding to the particular factor and factor-interaction effects.

The latter components can be individually compared to the random error variability; if these are large enough it can be concluded that they affect the response behaviour of the system under investigation.

For a 3 factor design the overall system response average is given by

$$y_T = \Sigma_i\Sigma_j\Sigma_k\Sigma_l\ y_{ijkl} / N \qquad (2.49)$$

y_T = overall system mean
N = abcr = total number of test runs performed
a = number of levels of factor x_1
b = number of levels of factor x_2
c = number of levels of factor x_3
r = number of repeat tests

For convenience the design presented here is *balanced*, i.e. there are no test runs for which data is missing and every test run has an equal number of repeat tests. It is not always possible to statistically analyse unbalanced designs, especially where the design has multiple input variables. Chun Li (1982) has reviewed some of the principles involved in analysing unbalanced data. In addition, error estimates can be obtained from unreplicated fractional designs; one decides a priori to obtain estimates of some parameter values, for example main effects and certain two-factor interactions, from model fits executed on computer software packages. The residual degrees of freedom (i.e. those not used to estimate parameter values) account for higher order (interaction) terms, as these are invariably negligible they provide an estimate of the sample error (Box and Meyer, 1986).

Now the overall system variability is expressed by the relationship

$$SS_T = \Sigma_i\Sigma_j\Sigma_k\Sigma_l\ (y_{ijkl} - y_T)^2 \qquad (2.50)$$
$$= SS_{x1} + SS_{x2} + SS_{x3} + SS_{x1x2} + \ldots + SS_e$$

$SS_{x1} = bcr\ \Sigma_i\ \alpha_i^2$
$SS_{x1x2} = cr\ \Sigma_i\Sigma_j\ \alpha\beta_{ij}^2$ etc

Every sum of squares term is divided by its number of degrees-of-freedom to obtain a normalised unit variance called a mean square. A one-tailed

F test can then be used to check whether the ratio of the mean square of a factor effect to that of the random error is sufficiently large to be regarded as statistically significant. A sum of squares term, say SS_{x1}, can be **related** to the **square** of the **contrast**, l_{x1}^2, defining the **overall effect** of the input variable x_1 on the process response, y. Details of the procedure are discussed in Appendix A2.

In many physical experiments, the situation is encountered where some additional variable, aside from the designated input variables, which is either supposed constant or cannot be controlled, affects the process response, y. Such an ancillary variable which is really an additional input variable is known as a **covariate**. A covariate factor can be incorporated in the model to account for its effect on the process response. The statistical model (2.48) can be reformulated as

$$y_{ijkl} = f(x_1, x_2, x_3) + m.x_c + e_{ijkl} \qquad (2.51)$$
$$= S + e_{ijkl}$$

x_c = covariate parameter
m = slope

If a linear relationship between the covariate and the response parameter cannot be assumed, a more elaborate functional relationship must be chosen.

The **individual** model **terms** α_i, β_j, m etc can be calculated using **multiple variable regression** techniques. These take the form

$$e = y - S \qquad (2.52)$$

$$E = \Sigma (y - S)^2 \qquad (2.53)$$

The estimates of the constants α_i etc are obtained by minimisation of the cumulative error function, E; one sets the normal partial derivatives equal to zero :

$\partial E/\partial \mu = 0$; $\partial E/\partial \alpha_i = 0$ (i = 1 to a) etc

To obtain a unique solution set, one requires additional constraint equations $\Sigma \alpha_i = 0$ etc. Details of multiple regression techniques are

available in Mason et al (1989) as well as a host of texts dealing with multivariate data analysis (e.g. Hochberg and Tanhane, 1987). Model fits are computationally intensive and consequently only performed on computers. At UCT the statistical software available on a VAX 6000-330 system is the GENSTAT package.

2.6.4 ANOVA Assumptions

Conclusions based on modelled data are obviously only reliable if the assumptions underpinning the model are satisfied or at least not seriously violated in the physical system which the model is attempting to describe.

Key assumptions underlying ANOVA methods are

(i) factor effects are additive, i.e. process responses can be modelled as the sum of separate component functions as represented in equation (2.41) and derived forms such as equations (2.48) and (2.50).

(ii) The error components are *normally distributed* across *all factor-levels* with a **common** population variance $\sigma_e 2$. Error normalities can be checked by residual plots on semi-logarithmic paper.

As indicated earlier, the *numerical values* of the *model terms* α_i, $(\alpha\beta)_{ij}$, $\Sigma_i\ \alpha_i^2$ etc are derived from *data* generated in the designed experiment. Thus, in effect, the numerical values of the response component functions, e.g. $f(x_1)_{x1=x11} = \alpha_1$, where x_{11} is an aribtrary value of the input variable x_1, etc are estimated *without* specifying the *form* these *functions* have taken. Consequently, without being mathematically rigorous, one would expect that sets of component functions exist, which although they are unknown, satisfy the additivity assumption inherent to linear models.

Rao and Sedransk (1984) in a review of the contributions of an eminent American Statistician W.G. Cochran to the theory and practice of statistics, reported Cochran's assessment of the assumptions underlying the ANOVA technique. Cochran (1947) stated that where multiplicative rather than additive component functions better define the effect of

input variables on system response, F ratios decrease and consequently the additive model becomes incapable of detecting factor effects which affect the system behaviour, i.e. the linear model suffers from a loss of power. Rao and Sedransk also cited a 1-degree-of-freedom test for non-additivity proposed by Tukey (1949).

Cochran regarded nonnormality as the least important deviation from assumptions in ANOVA. In any case, error normalities can be easily checked by the Kolmogorov/Smirnov test.

Finally Cochran emphasised that the principle of performing tests in random order should be adhered to as far as possible.

One only needs to select specific functional relationships between the response and the input variables if one wishes to construct a theoretical model predicting the process response as a function of the input variables. Such empirical statistical models fall under the realm of Response Surface Methodology and are not further considered here. An introductory text on the subject by Box and Draper (1987) is listed in the attached bibliography.

CHAPTER 3

PRELIMINARY TESTWORK

3.1 INTRODUCTION

The experimental programme for this thesis comprised a number of phases, namely batch and column laboratory flotation tests, plant trials conducted at a Witbank colliery, and bubble size and conditioning testwork. This chapter describes the characterisation of the samples used throughout the experimental programme and sets out the results of preliminary testwork which were concerned with the measurement of bubble size distributions and the determination of the effect of conditioning on coal flotation. Specifically, the effect of air flowrate, frother type and concentration on bubble size was investigated, as were the effects of various methods of dispersing oil in coal pulps and the size of the vessel used for the conditioning step.

3.2 SAMPLE CHARACTERISATION

Samples of thickener underflow fines from five collieries were used in this investigation. They included samples from three Witbank collieries, namely Kleinkopje, Greenside and Goedehoop Collieries, as well as two Natal coals; a coking coal from the Durnacol Colliery and an anthracitic coal from Zululand Anthracite Colliery (ZAC).

Characterisation tests performed on these coals included petrographic and proximate analyses, elemental sulphur analysis, size and ash-by-size determinations, float/sink analyses and differential flotation tests (which approximate the ideal flotation separation curve). Petrographic analyses were carried out by Falcon Research Laboratories in Johannesburg. Proximate analyses and sulphur determinations were carried out by RICHLAB which is also located in Johannesburg. These analyses were performed on all five samples; the results are presented in Tables 3.1 and 3.2. Characteristic washability data for the Durnacol, Kleinkopje, Greenside and ZAC samples are plotted in Figure 3.1. Differential flotation tests were performed on the Durnacol,

Kleinkopje and ZAC samples; the yield versus grade data obtained are plotted in Figure 3.2.

Table 3.1 : Maceral analysis (% by vol) of the five thickener underflow fines samples.

Sample	Vitrinite	Exinite	Inertinite
Durnacol	85.0	4.0	11.0
ZAC bit.	71.0	2.7	26.3
ZAC Anthr.	45.0	0.0	55.0
Kleinkopje	27.3	1.7	71.0
Goedehoop	41.3	2.7	56.0
Greenside	40.1	2.0	57.9

Table 3.2 : Proximate and sulphur analyses of the five thickener underflow fines samples.

Sample	H_2O %	Volatiles %	Fixed carbon %	CV MJ/kg	Sulphur %	Ash %
Durnacol	1.7	21.0	48.9	23.91	1.39	28.4
ZAC	1.9	13.2	58.7	24.10	1.05	26.2
Kleinkopje	2.3	21.9	52.9	24.10	1.67	22.9
Goedehoop	2.1	28.0	53.9	26.69	1.10	16.0
Greenside	2.6	24.6	53.9	25.50	0.97	18.9

The Greenside float/sink data shown in Figure 3.1 was taken from Buys (1989) who used the same Greenside sample used in this thesis.

Size and ash-by-size analyses, float/sink testing and the differential flotation tests were done at UCT. Ash analyses were carried out according to SABS Standard Method No. 296. Results are reported on an air-dry basis. Details of the tests performed on the individual samples follow.

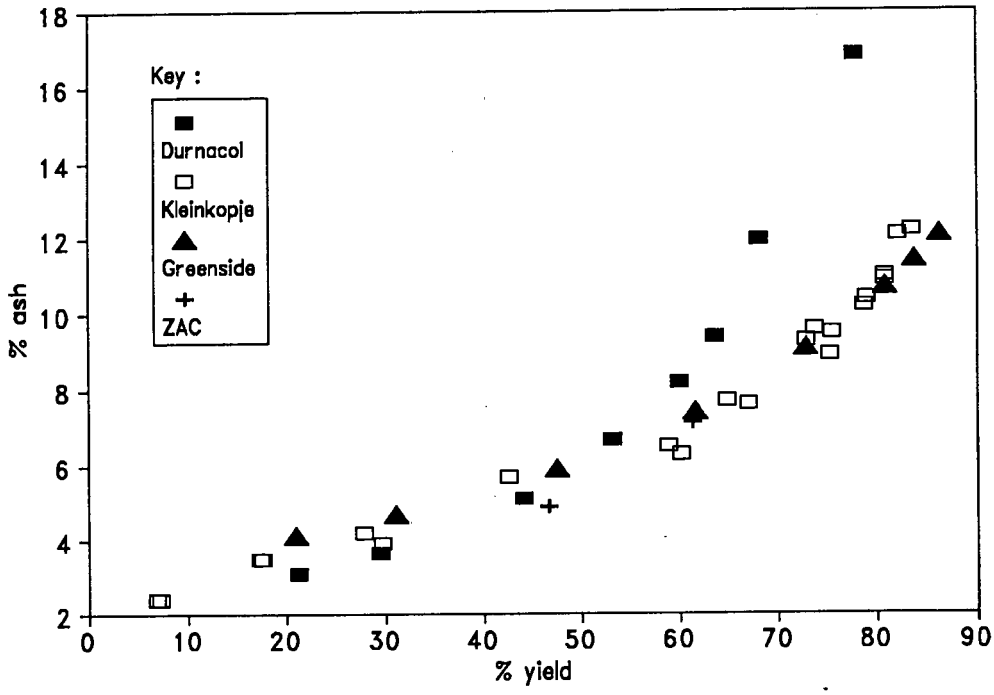

Figure 3.1 : Float-and-sink data for Durnacol, Kleinkopje and Greenside Colliery thickener underflow samples and a fines sample from Zululand Anthracite Colliery.

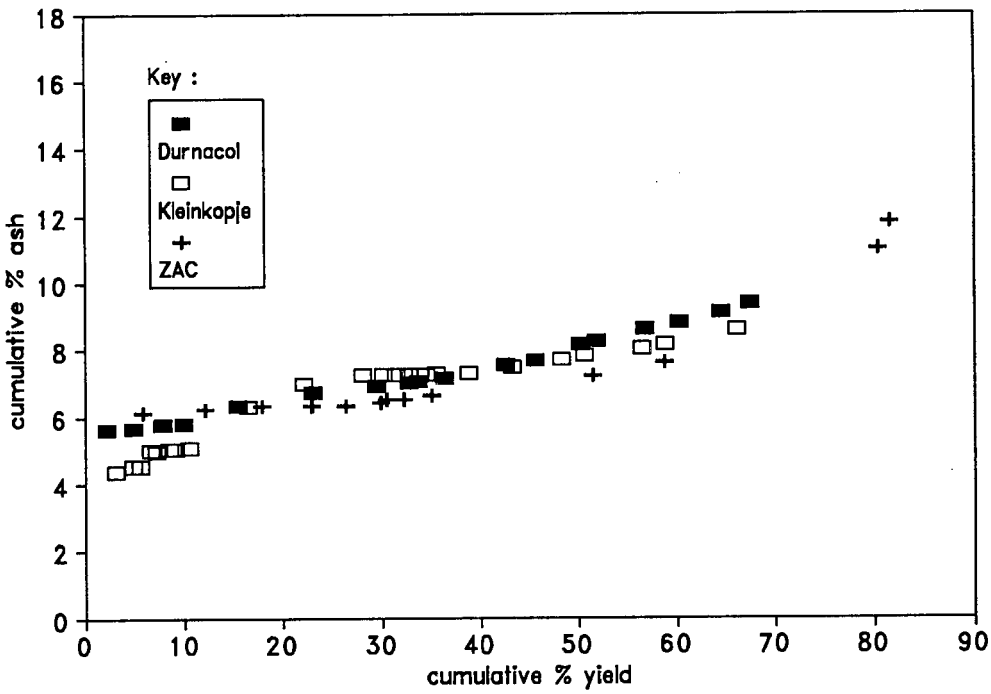

Figure 3.2 : Release flotation data for Durnacol, Kleinkopje and Greenside Colliery thickener underflow samples and a fines sample from Zululand Anthracite Colliery.

3.2.1 Durnacol Thickener Underflow Fines

This coal sample originated from the Durban Navigation Colliery (Durnacol) in Natal. The Colliery beneficiates the raw coal to a coking quality product. A thickener underflow sample was collected at the Colliery and sent to UCT in a sealed 44 gallon drum. Representative sub-samples, used for flotation and float/sinks testwork, were taken from the drum using the fractional shovelling method described by Gy (1982).

The petrographic data presented in Table 3.1 indicate that the Durnacol thickener underflow sample had a vitrinite content of 85.0 %. This is twice as high as the vitrinite contents of the coal samples taken from the Kleinkopje, Goedehoop and Greenside collieries which had vitrinite contents of 27.3 %, 41.3 % and 40.1 % respectively. Consequently, one would expect that the Durnacol sample would be much more floatable than the Witbank coals.

Table 3.2 indicates that this coal sample had an ash content of 28.4 % and a calorific content of 23.91 MJ/kg. The fixed carbon content was 48.9 %. Both the unit calorific value and fixed carbon contents were slightly below those of all the other coal samples.

Size and ash-by-size distribution data are presented in Table 3.3. 17 % of the thickener underflow sample was coarser than 150 μm, 66 % finer than 75 μm and 56 % finer than 53 μm. The ash content of -75 μm fraction increased steadily with decreasing particle size, from a value of 24.8 % ash in the -75+53 μm fraction to 41.6 % ash in the -25 μm fraction.

A float/sinks analysis, laboratory column tests, batch flotation tests and a "release" float test were performed on this coal. The yield/grade results are presented in section 4.3. The laboratory column tests formed the basis for identifying which of the column input parameters discussed in section 2.5 most significantly affected the performance of a laboratory column. In addition, this coal was used for the conditioning tests described in section 3.4 below.

Table 3.3 : Average feed size properties, Durnacol thickener underflow fines.

Feed size fraction i	% mass size i	% ash content
+150 μm	17.38	12.16
+125 - 150 μm	3.13	13.70
+ 75 - 125 μm	12.96	18.24
+ 53 - 75 μm	9.65	24.81
+ 38 - 53 μm	8.13	31.92
+ 25 - 38 μm	11.44	31.92
- 25 μm	37.31	41.57
Total	100.00	29.57

3.2.2 Kleinkopje Thickener Underflow Fines

The Kleinkopje thickener underflow stream is a composite blend of by-product fines from two process streams, one producing low-ash and the other steam coal. As the plant fines stream is a discard stream, no effort is made to regulate its composition; consequently this fluctuates continuously.

Whilst at the Kleinkopje Colliery carrying out on-line column flotation plant trials (the results of which are described in Chapter 5) the author collected a fines sample which was used in subsequent laboratory testwork. Six 44 gallon drums were filled simultaneously with thickener underflow slurry. Once the solids had settled out, the water was decanted. This procedure was repeated daily for a period of one week until each drum contained approximately 150 kg of wet coal.

Representative sub-samples were taken from one of the drums using the fractional shovelling method described by Gy (1982). The sampling method used is described in more detail in section 4.4 below.

The petrographic analysis (Table 3.1) shows that this sample contained 71.0 % inertinite and 27.1 % vitrinite. It is also evident from an

examination of Table 3.1 that the Kleinkopje sample contained the most inertinite and least vitrinite of all the coals listed. Inertinite has a greater oxygen content and is less floatable than vitrinite (see sections 2.1 and 2.4). Consequently one might expect the Kleinkopje thickener underflow fines to be less floatable than the other coals.

Table 3.2 indicates that the Kleinkopje thickener fines sample had an ash content of 22.9 % and a calorific value of 24.1 MJ/kg. The fixed carbon content was 52.9 %. Interestingly, the fixed carbon contents of all the Witbank coals were virtually identical. Also, the Kleinkopje sample had the lowest volatile content of the three Witbank coals. This is consistent with the high inertinite content of the Kleinkopje sample noted above (inertinites are more aromatic and have fewer substituted groups than vitrinites - see section 2.1 above).

Size and ash-by-size properties are presented in Table 3.4. Approximately 37 % of the Kleinkopje sample was coarser than 75 μm, and 20 % coarser than 150 μm. 50 % of the feed was finer than 45 μm; this is also the fraction which contained the most mineral matter (except for the +425 μm material whose mass was negligible). In section 2.5 it was noted that column flotation cells most efficiently recover relatively fine (< 75-80 μm) size fractions.†

Float/sink analyses and differential flotation tests were also performed. The method of Franzidis and Harris (1986) was used for the float/sinks analyses. The differential float approximates the ideal flotation separation ("release") curve; the procedure used is described in Appendix G1. The two separation curves are presented in section 4.4 where they are compared with global batch and laboratory column flotation results. Various methods of conditioning this coal were also tested; these are described in section 3.4.

---

† It was found necessary during the on-line plant trials at the Kleinkopje Colliery to screen out the coarse +200 μm material from the plant feed. Thus the size and ash-by-size data in Table 3.4 refer to the sample used in the laboratory testwork. Size analysis of the column feed samples taken during the on-line plant trials are discussed and reported in section 5.3.1.2 below.

Table 3.4 : Average Feed size properties, Kleinkopje thickener underflow fines

Feed size fraction i	% mass size i	% ash content
+425 μm	2.62	30.30
+212 - 425 μm	9.16	27.58
+150 - 212 μm	8.23	21.99
+106 - 150 μm	8.43	19.75
+ 75 - 106 μm	9.05	18.69
+ 45 - 75 μm	12.67	18.96
- 45 μm	49.85	25.58
Total	100.00	23.75

3.2.3 Greenside Thickener Underflow Fines

The Greenside Colliery is one of South Africa's most important sources of low ash coal for export. In addition, much work has been carried out previously on this coal (Franzidis; 1987, 1988; Buys, 1989). The sample obtained from the Greenside Colliery was a 20 kg thickener underflow sample which was received air dried in a sealed plastic-lined 25 l drum.

The petrographic analysis (Table 3.1) of the thickener underflow from the Greenside Colliery, which like Kleinkopje mines from the Witbank Number 2 seam, showed that this underflow sample contained approximately 40 % vitrinite and 58 % inertinite. The fines were of a slightly better grade than the Kleinkopje sample, having ash and calorific values of 18.9 % and 25.5 MJ/kg respectively. The carbon content was 53.9 %.

Size and ash-by-size data are presented in Table 3.5. The size and ash distributions are generally similar to the Kleinkopje fines; in particular the -45 μm fraction constituted 55 % of the sample and had an ash content of 23.9 %, compared with a 50 % passing 45 μm and a 24.6 % ash content of for the Kleinkopje fraction. In one important aspect the ash-by-size distributions are different, in that for the Greenside sample the ash content *decreased* with increasing particle size, whereas it increased for the Kleinkopje sample (+45 μm fraction).

Table 3.5 : Average feed size properties, Greenside thickener underflow fines

Feed size fraction i	% mass size i	% ash content
+212 μm	8.63	12.97
+150 – 212 μm	7.62	14.52
+106 - 150 μm	9.18	15.90
+75 - 106 μm	9.53	17.32
+45 - 75 μm	9.70	17.43
-45 μm	55.34	23.87
Total	100.00	20.24

Batch and column laboratory flotation tests were performed on this sample. The global results obtained are compared in section 4.5. Also, float/sinks, batch and column laboratory tests were performed on ultrafine (d_{95} = 45 μm) samples of milled thickener underflow. Details of the milling procedure followed and the ultrafine coal size and ash distributions as well as the test results are described in section 4.6.

3.2.4 Zululand Anthracite (ZAC) Colliery Fines

Approximately 30 kg of wet fines was collected from a belt filter during test conducted at the Zululand Anthracite Colliery in 1990 (Harris, 1990). This sample was used in subsequent laboratory tests conducted at UCT.

The petrographic analysis (Table 3.1) indicated that the ZAC fines sample was comprised of a blend of two coal ranks : 41 % Bituminous and 59 % Anthracite. Petrographic analysis of the two coal ranks was performed separately. Table 3.1 shows that the Bituminous portion of the coal blend had a vitrinite content of 71.0 % and the Anthracite contained 45 % vitrinite. Thus the average vitrinite content of the coal blend was 55.7 %. This is higher than the Witbank coals and consequently the ZAC sample can be expected to be more floatable than the former coals.

Proximate analyses indicated that the sample had an ash content of 26.2 % and a calorific value of 24.1 MJ/kg. This coal was also only used in conditioning tests described below in section 3.4.

3.2.5 Goedehoop Thickener Underflow Fines

Samples of thickener underflow slurry were collected by the Goedehoop Colliery personnel and sent to UCT in five sealed 50 l PVC drums. A sub-sample from one of these drums was used for laboratory testwork.

It can be seen from Table 3.1 that the petrographic compositions of this coal is virtually identical to that of the Greenside sample; both have vitrinite and inertinite contents of around 40 % and 57 %, respectively. The proximate analyses indicate that the Goedehoop thickener sample had an ash content of 16.0 % and a calorific value of 26.7 MJ/kg. As the ash content of the Greenside sample was 18.9 % and the calorific value 25.5 MJ/kg, it is evident that the Goedehoop sample was of slightly better quality than the Greenside sample. The similar petrographic characteristics of both coals would lead one to expect that they respond similarly to flotation with the Goedehoop sample possibly being slightly more flotatable. Like the ZAC sample, this coal was only used for a limited series of comparative conditioning tests (see section 3.4 below).

3.2.6 Overall Comparison of the Properties of the Natal Versus Witbank Coal Samples

The Durnacol and (composite) ZAC samples had vitrinite contents of 85.0 % and 55.7 % respectively. This was higher than the Witbank coal samples; the Kleinkopje sample used for laboratory tests contained only 27.3 % vitrinite and the Goedehoop and Greenside samples had vitrinite contents of 41.3 % and 40.1 % respectively. Thus one would expect that the Natal coal samples would be more easily floated than the Witbank coals.

From Figure 3.1 it can be seen that the Kleinkopje and Greenside coal samples have better washability characteristics compared with the Durnacol sample, especially at yields in excess of 70 %. In other words the Durnacol sample was less well liberated than either the Kleinkopje or Goedehoop samples. The approximate release flotation data for the Durnacol and Kleinkopje sample plotted in Figure 3.2 are also virtually coincicident at yields of up to 60 %. Under ideal flotation conditions, i.e. optimum coal hydrophobicities, similar yield/grade results (provided the yield remains below 60 %) can therefore be expected from the latter pair of samples.

From Tables 3.3, 3.4 and 3.5 it can be determined that the Durnacol, Kleinkopje and Greenside samples had roughly similar size distributions, especially in the finer (-75 μm) fraction in which the percentage of material passing 75 μm ranged between 62 % and 67 %. In the ultrafine (-25 μm) fraction there was a noticeable difference between the Durnacol and two Witbank coals; only 37 % of the Durnacol sample was finer than 25 μm compared with 50 % and 55 % for the Kleinkopje and Greenside samples respectively. Also, the ash content of this fraction in the Durnacol sample was 41.6 % compared with an ash content of $\approx$ 25 % for the two Witbank coals. In other words, a lower proportion of ultrafine (-25 μm) material was present in the Durnacol sample and furthermore, this was of a poorer grade than the material present in the Kleinkopje and Greenside ultrafine fractions.

3.3 BUBBLE SIZE TESTWORK

The strong dependence of the flotation kinetic rate constant, k, and pulp phase fractional air holdup, ϵ_g (equivalently residence time, τ), on bubble size, d_b, was emphasised in Chapter 2. It was decided that quantitative information on bubble size distributions at the operating conditions typically encountered in flotation columns would be useful. Consequently tests were undertaken to measure bubble sizes generated in aerated water-frother mixtures in a laboratory scale column cell.

The effect of frother type, frother concentration and air rate on bubble size was investigated. As simultaneous level measurement readings were

taken, it was also possible to obtain fractional gas holdup data for the operating conditions tested.

3.3.1 Experimental Equipment and Operation

The equipment used can be divided into two groups, namely that associated with the operation of the column cell, and that used to perform the bubble sizing task.

The relevant dimensions of the 54 mm inner diameter, 1.5 m long perspex laboratory column are indicated in Figure 3.3. The feed port was 400 mm below the concentrate overflow lip and the sparger inlet port 600 mm below the feed port. A 1" glass tube, used as a water manometer, was attached to a port 400 mm below the sparger. A filter cloth sparger was used for these series of tests. Other items of equipment included an air rotameter calibrated at a gauge pressure of 4 bar, a 30 l perspex vessel fitted with 0.25 kW, 1440 rpm Denver mixer (the air induction holes on the impeller shaft were sealed) and two Watson/Marlow type 503S variable speed peristaltic pumps whose maximum pumping capacities were 2 l/min.

The column air requirement was drawn from the Departmental compressed air utility line; the (gauge) pressure in this line fluctuates between 5 and 6 bar. A needle valve and pressure gauge were fitted beyond the rotameter outlet. The air reaching the filter cloth sparger was maintained at a constant (gauge) pressure of 4 bar by suitable adjustment of this needle valve.

A frother/water solution of the desired strength was made up in the 30 l capacity perspex tank. The solution was agitated by the Denver mixer. The frother/water mixture was pumped via a peristaltic pump to the feed port. The feedrate was maintained at a constant value of 1 l/min throughout the tests.

At each operating condition (test run) the volumetric tails rate, the interface level in the bubble column and the water level in the manometer were measured. The interface level was taken as the distance from the sparger to the froth/water interface. The interface level was

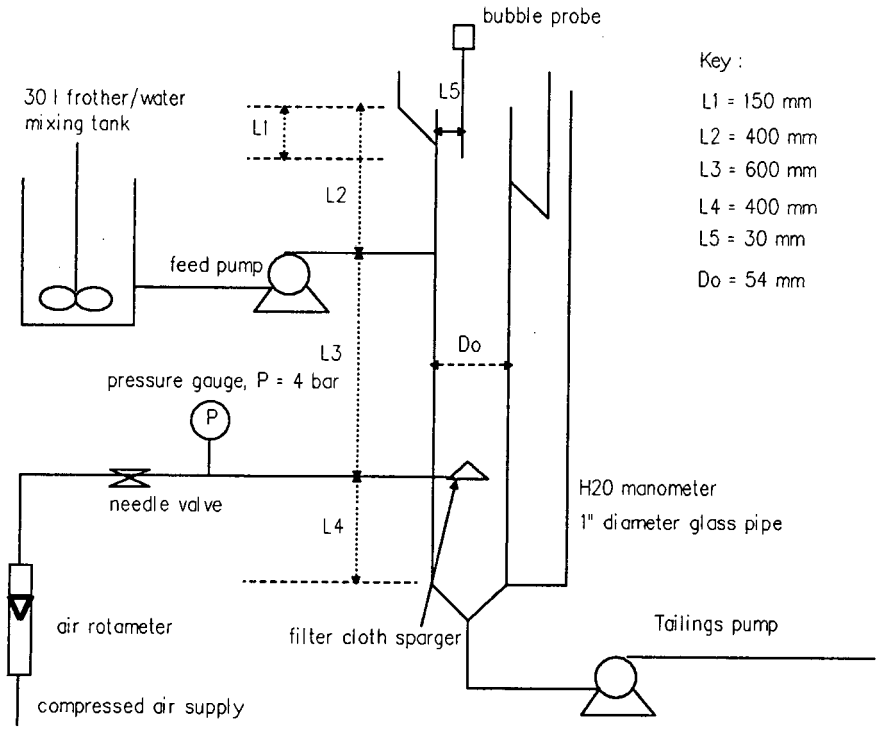

Figure 3.3 : Laboratory bubble column dimensions

maintained by manual adjustment of the variable speed tailings pump. The column was run on a continuous basis and bubbles were sampled under steady state conditions. Every test run was performed at least twice.

Three commercial grade frothers were tested, namely methyl-isobutyl carbinol (MIBC), di-isobutyl ketone (DIBK) and tri-ethoxybutane (HTEB). DIBK and HTEB were used in the laboratory column flotation testwork (Chapter 4).

A schematic of the bubble size apparatus is provided in Figure 3.4. The equipment may be divided into three categories; that used to collect bubbles, the electronics which detect and record the passage of the bubbles, and the software used to read the recorded data and perform the bubble size calculations. The bubble capture equipment consisted of a glass capillary tube, a gas burette, a vacuum pump, a mercury manometer and a glass water reservoir. The electronics system comprised two photo-transistors vertically mounted a distance of 5 mm apart and encased in a brass housing, an amplifier system, and a Motorola 6809

processor. The computer software was written in Borland's Turbo Pascal (Version 4) and was run from a PC. A detailed description of the hardware components and specifics of the detection principle involved have been reported by Randall et al (1988).

The central axis of the capillary tube was positioned 30 mm from the radial centre of the column cell. Two capillary sizes were used : at frother concentrations of 5 μl/l a diameter, d_c, of 1 mm was used; at higher dosage levels a capillary with a diameter of 0.75 mm was used. The bell-shaped end of the capillary tubes, designed to prevent bubble breakage as air bubbles are drawn into the capillary, reached a distance of 150 mm below the concentrate oveflow lip.

A vacuum of between 40-50 cm Hg was used to draw air bubbles into the capillary tube. Air bubbles travelled up the capillary tube, past the pair of photo-transistors, through an open T-Tap and into the (inverted) gas burette. At the commencement of a bubble size run this burette was filled with water to the zero calibration mark. A water line between the burette and vacuum supply prevented air bubbles from being drawn past the burette. When the bubble capture system was under vacuum, water was gravity fed to this line via a reservoir positioned 1 m above the bottom of the burette.

Once sufficient bubbles were collected (see below) the T-Tap above the capillary tube was closed and the vacuum supply shut off. The water reservoir was then detached from its mounting and moved down until the water levels in the burette and reservoir were the same. The distance (air volume) of the water level in the burette below the zero mark was then recorded.

The passage of bubbles through the capillary was detected by the pair of photo-transistors. The basis for bubble detection was the difference in refractive index between air and water. As the front of an air bubble reached the lower pair of photo-transistors an "on" condition was activated and this was repeated when the bubble reached the upper transistors. "Off" conditions were restored when the rear end of the bubble passed each transistor pair. The output voltages were amplified and converted to a square wave form. Thus two timed signals were produced for each bubble, from which velocity and length pulses could be

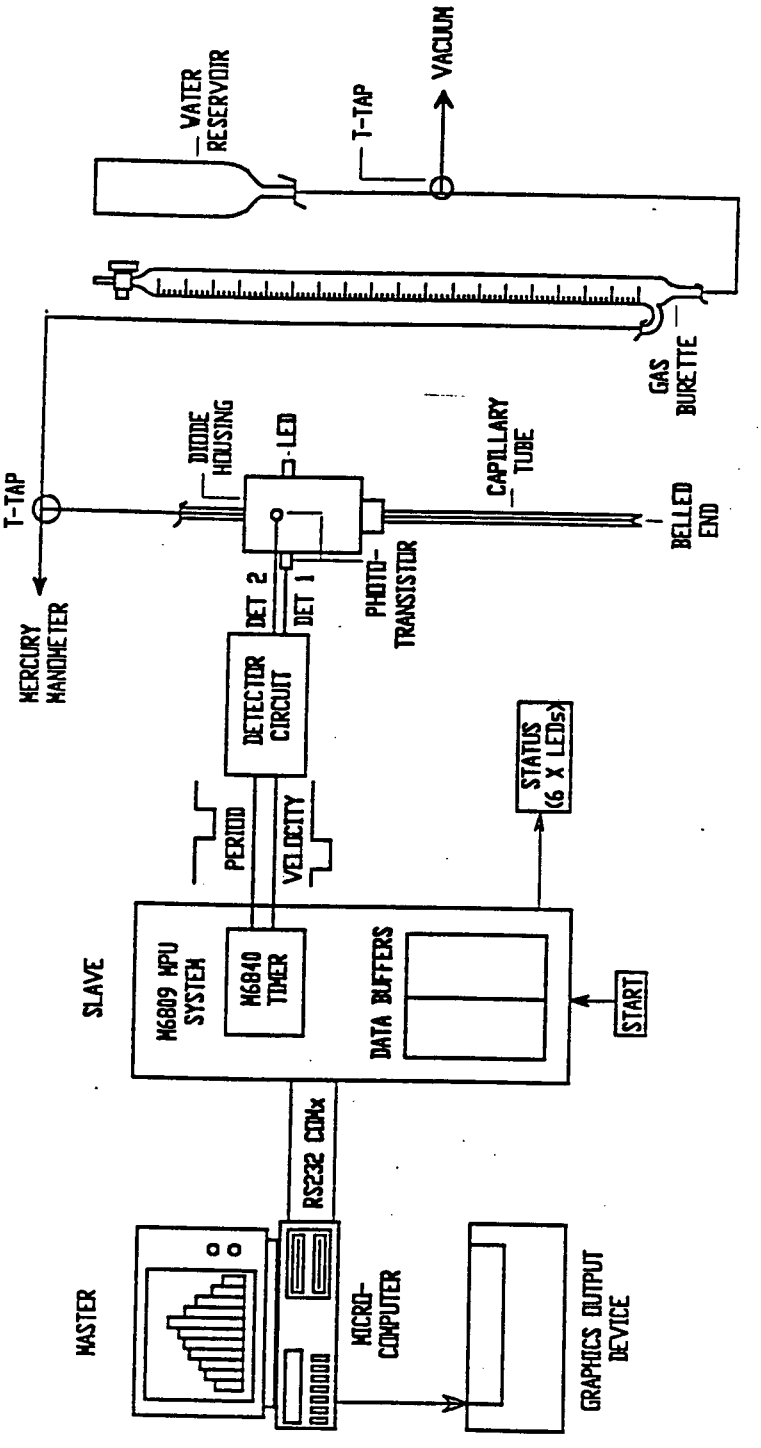

Figure 3.4 : Schematic diagram of bubble sizing apparatus (Randall et al, 1989).

generated. These signals, together with the real time of the event, were stored in a memory "buffer". The data capture system had 56 K of RAM memory which allowed up to 7000 bubbles to be processed in a single sizing run. Bubbles are detected at an approximate rate of 50 bubbles per second, a speed which exceeds typical bubble generation rates of ≈ 20 bubbles per second.

At the end of the measurement cycle the data was transferred to a micro-computer. Software programmes processed the data and calculated bubble volumes from the velocity and length (period) readings. The thickness of the water films (enveloping the bubbles) formed on the capillary wall was dependent on the applied vacuum. Consequently these constituted an unknown variable; however, the applied vacuum remained virtually constant for the duration of a bubble detection run. Consequently the bubble volumes determined could be normalised with respect to the total gas volume collected and the bubble size distribution corrected for water content.

Theoretically both the period and velocity groups measured during a run should have been of the same byte size (if the bubble is travelling at a reasonably constant velocity up the capillary tube); however, when the volume occupied by a bubble is less than the volume between the detectors, period and velocity pulse readings became asynchrous and fewer velocity readings were generated. Discrepancies of 10 % or less between the number of velocity and period (length) readings are considered acceptable. Nonetheless smaller bubbles were better detected using smaller diameter capillaries. Changes in hydrostatic head can be neglected as a factor influencing bubble size since the distance between the sparger and interface level was in all instances less than 1 m.

3.3.2 Testwork Results

A total of 91 test runs were carried out. Typical operating conditions employed in four runs are listed in Table 3.6. The corresponding outputs from the bubble analysis programme are reproduced in Table 3.7. Detailed information on all the bubble size tests conducted are given in Appendix B1.

Table 3.6 : Parameter levels for Table 3.7 examples

File ID	Frother Type and dosage μl/l	Superficial gas velocity J_g cm/s	Net downward liquid velocity J_l cm/s
5HTEB3	HTEB 5	2.5	0.60
5HTEB4	HTEB 5	2.5	0.60
25XHTEB1	HTEB 25	1.7	0.56
25XHTEB9	HTEB 25	1.7	0.58

As may be seen from Tables 3.6. and 3.7, at a surfactant concentration of 5 μl HTEB/l feed water, the mean bubble diameter produced was $\approx$ 2 mm whereas at high frother concentrations (25 μl HTEB /l feed water) the mean bubble diameter was $\approx$ 1 mm. However, in both cases the standard deviation, s, in the diameter was approximately 400 μm.

The bubble size distributions obtained for the runs conducted at 5 μl HTEB / l feed water (Runs 5hteb3 and 5hteb4) are plotted in Figures 3.5a and 3.5b, respectively. The two runs are evidently quite comparable: their respective mean diameters and standard diameter deviations agree within 0.01 cm (100 μm) and the shapes of two distribution curves are very alike, i.e. good reproducibility between individual test runs was achieved.

Similar remarks apply to the test runs conducted at a surfactant concentration of 25 μl/l (Runs 25xhteb1 and 25xhteb9). These are plotted in Figures 3.6a and 3.6b, respectively. However, for this operating condition the distinct "tail" at bubble sizes, d_b, larger than the mean, d_{bavg} = 0.110 cm, reflects that the diameter distributions can no longer be regarded as normal.

Anderson (1988b) measured bubble size distributions of two-phase oil-water, frother-water and oil-frother-water dispersions. Both aromatic and aliphatic oils were used as was MIBC frother. Frother dosages of 6 μl/l and 12 μl/l were used; these levels are similar to the frother dosages used for the tests reported here. The oil dosages used were also typical of coal flotation. He found that all the distributions measured could be fitted to either normal or log-normal distribution

Table 3.7 : Examples of bubble size programme outputs

SUMMARY OF FILE a:5hteb3

Mean bubble volume	0.0050	(ml)
Standard deviation (volume)	0.0035	(ml)
Mean bubble diameter	0.2051	(cm)
Standard deviation (diameter)	0.0367	(cm)
Number of velocity readings	3200	
Number of period readings	3202	
% Discrepancy in readings	0.06	
Average Water Pulse Length	60.9613	
Average Air Pulse Length	6.3719	

SUMMARY OF FILE a:25xhteb1

Mean bubble volume	0.0010	(ml)
Standard deviation (volume)	0.0012	(ml)
Mean bubble diameter	0.1089	(cm)
Standard deviation (diameter)	0.0385	(cm)
Number of velocity readings	3233	
Number of period readings	3331	
% Discrepancy in readings	2.94	
Average Water Pulse Length	1.6511	
Average Air Pulse Length	5.7547	

SUMMARY OF FILE a:5hteb4

Mean bubble volume	0.0053	(ml)
Standard deviation (volume)	0.0042	(ml)
Mean bubble diameter	0.2078	(cm)
Standard deviation (diameter)	0.0400	(cm)
Number of velocity readings	3142	
Number of period readings	3144	
% Discrepancy in readings	0.06	
Average Water Pulse Length	62.6458	
Average Air Pulse Length	6.4306	

SUMMARY OF FILE a:25xhteb9

Mean bubble volume	0.0010	(ml)
Standard deviation (volume)	0.0013	(ml)
Mean bubble diameter	0.1114	(cm)
Standard deviation (diameter)	0.0398	(cm)
Number of velocity readings	3153	
Number of period readings	3276	
% Discrepancy in readings	3.75	
Average Water Pulse Length	2.1487	
Average Air Pulse Length	5.1171	

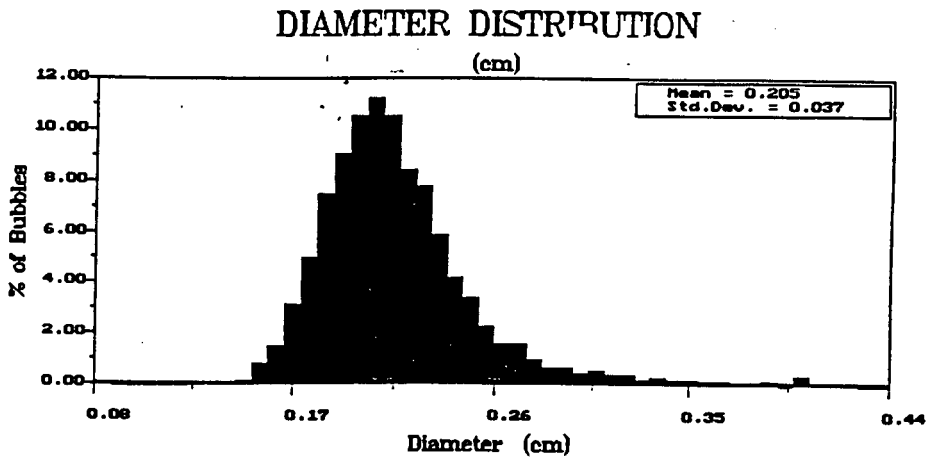

Figure 3.5a : Bubble size distribution - HTEB frother; frother concentration 5 μl/l; air rate, J_g, 2.5 cm/s; net downward liquid velocity, J_l, 0.60 cm/s.

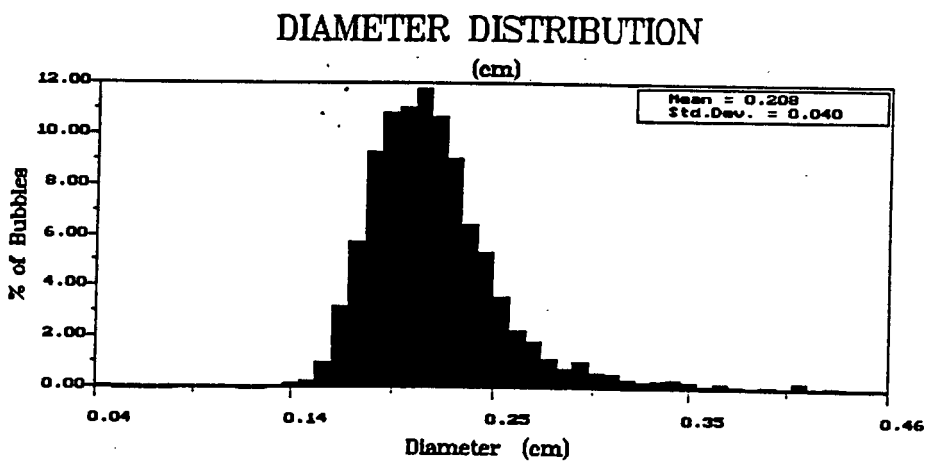

Figure 3.5b : Bubble size distribution - conditions listed in Figure 3.5a above repeated; net downward liquid velocity, J_l, 0.60 cm/s.

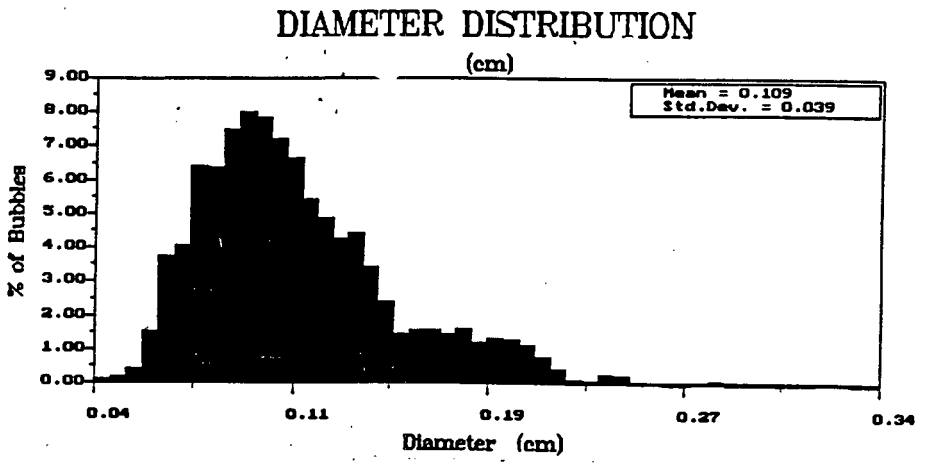

Figure 3.6a : Bubble size distribution - HTEB frother; frother concentration 25 μl/l; air rate, J_g, 1.7 cm/s; net downward liquid velocity, J_l, 0.56 cm/s.

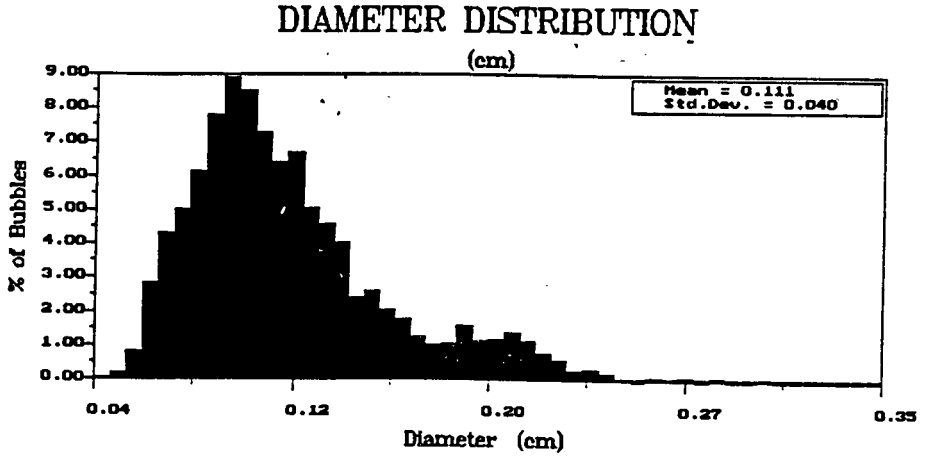

Figure 3.6b : Bubble size distribution - conditions listed in Figure 3.6a above repeated; net downward liquid velocity, J_l, 0.58 cm/s.

functions. Log-normal functions were fitted to distributions which were characterised by relatively few large (> ≈ 1mm) bubbles and an order of magnitude greater quantity of finer (< ≈ 0.5 mm) bubbles. Anderson attributed the presence of the larger bubbles to the occurrence of coalescence between the finer-sized bubbles. It is reasonable to suppose that coalescence also was responsible for the "tails" at bubble diameters larger than the mean observed in Figures 3.6a and 3.6b.

In section 2.3 it was noted that bubble sizes of between 1 and 2 mm are typical of flotation columns. Thus it appears that nominal pulp phase frother concentrations of between 5 and 25 μl/l will produce bubbles of the required size.

The effect of frother type, frother concentration and superficial gas velocity on mean bubble diameter is illustrated in Figures 3.7 to 3.10. At a frother concentration of 5 μl/l (Figure 3.7) bubble size was strongly affected by frother type, with MIBC producing the biggest and DIBK the smallest bubbles. An increase in air flowrate also produced bigger bubbles. It is evident from Figure 3.7 that the mean bubble sizes produced at frother concentrations of 5 μl/l ranged between 1.5 mm and 2.2 mm.

A frother structural influence was still evident at surfactant concentration of 10 μl/l (Figure 3.8): here MIBC produced the smallest bubbles, while bubbles produced from DIBK and HTEB frother/water mixtures were indistinguishable in size. Bubble sizes, d_{bavg}, ranged between 0.9 and 1.7 mm which is slightly smaller than those produced above. Again average bubble size, d_{bavg}, increased with an increase in air flowrate.

At 15 μl frother/l water (Figure 3.9) frother type (structure) effects were not evident. The range of bubble sizes produced narrowed considerably compared with the previous tests; d_{bavg} values were between 1.0 and 1.2 mm. Whether air flowrate affected bubble size was unclear. However, at 25 μl/l (Figure 3.10) an increase in (average) bubble size accompanying an increase in air flowrate was again observed. Also, the bubbles (d_{bavg} between 0.9-1.2 mm) produced were of virtually the same sizes as those generated at 15 μl/l. This suggests that if bubble size measurements had been taken at additional air flowrates at frother

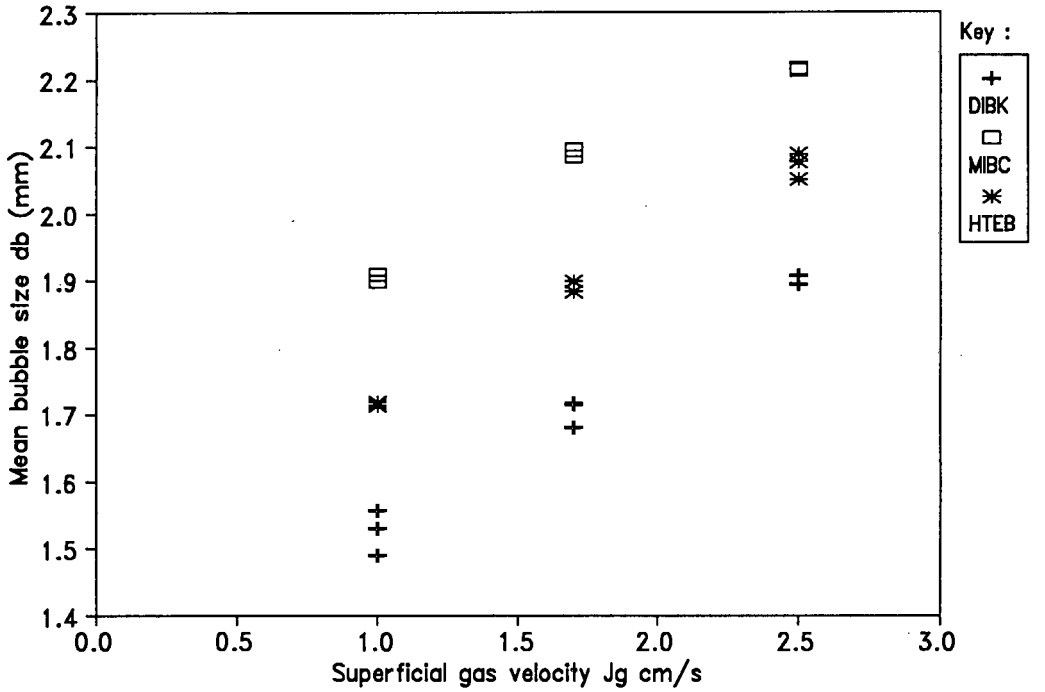

Figure 3.7 : Effect of air flowrate on bubble size, d_b, for three different frothers. Frother dosage 5 μ/l. Downward liquid velocity, J_l = 0.58 - 0.64 cm/s

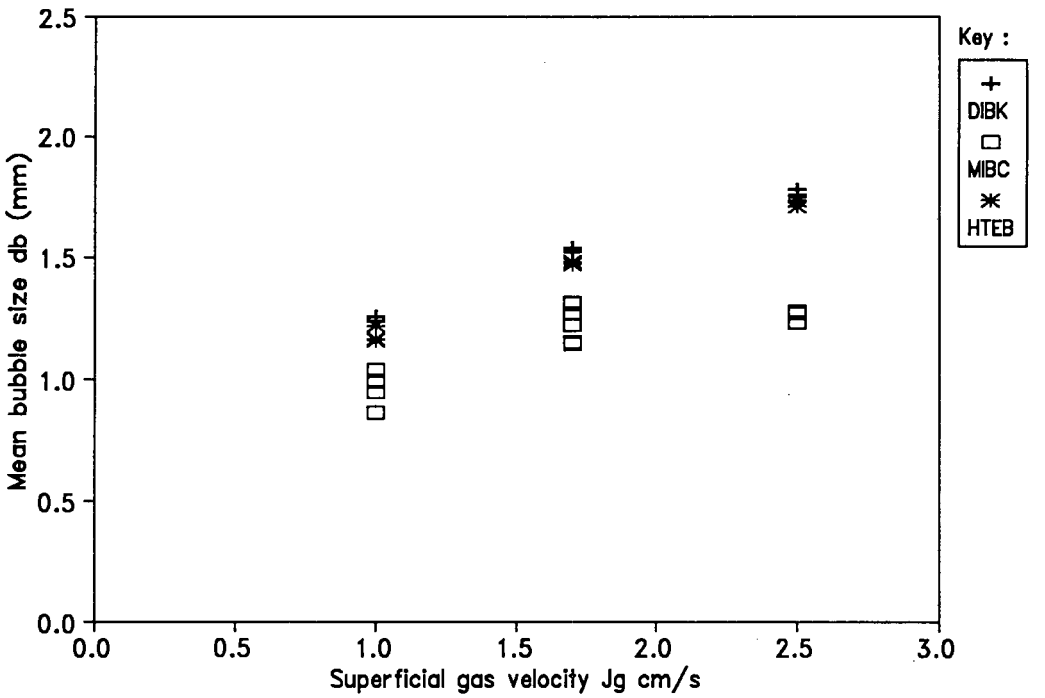

Figure 3.8 : Effect of air flowrate on bubble size, d_b, for three different frothers. Frother dosage 10 μ/l. Downward liquid velocity, J_l = 0.55 - 0.70 cm/s.

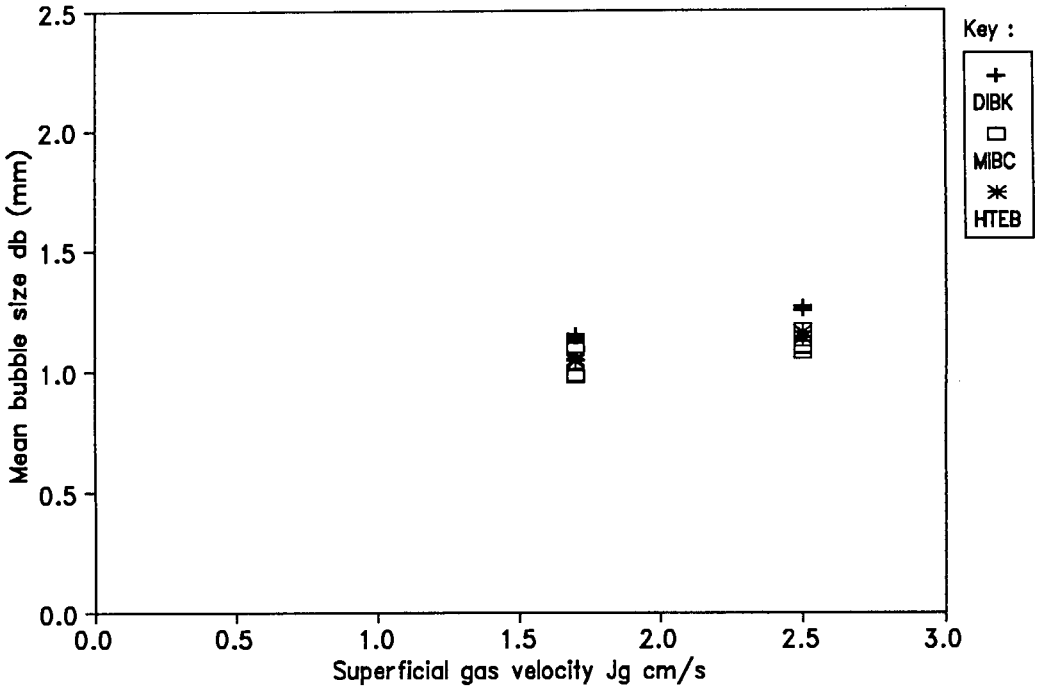

Figure 3.9 : Effect of air flowrate on bubble size, d_b, for three different frothers. Frother dosage 15 μ/l. Downward liquid velocity, J_l = 0.63 - 0.70 cm/s

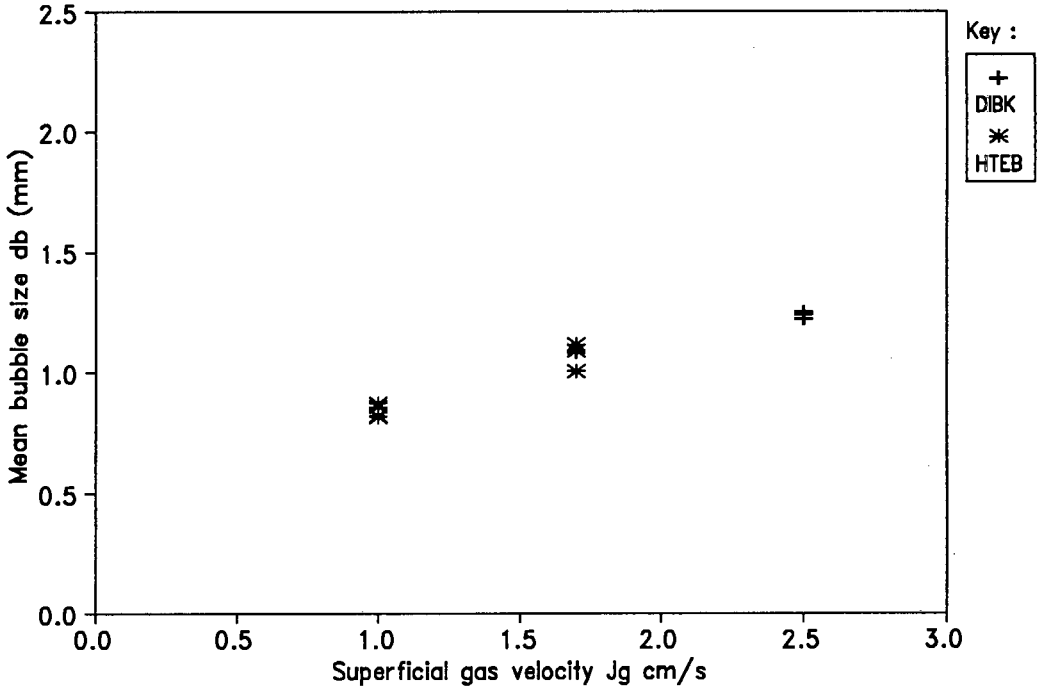

Figure 3.10 : Effect of air flowrate on bubble size, d_b, for two different frothers. Frother dosage 25 μ/l. Downward liquid velocity, J_l = 0.57 - 0.70 cm/s

dosages of 15 μl/l, the expected dependence of bubble size on air flowrate would have been observed.

Overall, the following conclusions may be drawn from the data presented in Figures 3.7 to 3.10 : the mean bubble size decreases with increasing frother dosage; the limit to the efficiency of frother addition appears to be about 15 μl/l (i.e. increasing frother dosage to 25 μl/l hardly had any affect on bubble size); differences in bubble size arising from the type of frother selected are only apparent at low frother dosages; and lastly an increase in air rate invariably causes larger bubbles to be produced.

At the gas velocities employed in column flotation, bubbles produced from porous media spargers should obey the relationship (section 2.5.4)

$$d_b = C.J_g^n \qquad (3.1)$$

where the exponent n varies between 0.2 - 0.4 depending on the sparger material.

The bubble size/gas velocity data plotted in Figures 3.7-3.10 were fitted to Equation (3.1) for each frother type and concentration combination. The exponent values, n, obtained varied between 0.21-0.45, however, no distinctions between respective frother types or frother concentration effects were apparent. A summary of the regression data is presented in Table 3.8 below.

Fractional gas holdup data for HTEB/water mixtures as a function of frother concentration and air velocity are plotted in Figure 3.11. Fractional gas holdup, ϵ_g, is defined as the fractional gas volume between the filter cloth sparger and the water solution/froth interface.

There appears to be a linear relationship between holdup, ϵ_g, and superficial gas velocity, J_g, which is in agreement with holdup/velocity trends reported by Finch and Dobby (1990c). Increases in gas holdup were observed as frother dosage was increased but, overall, air velocity effects predominated. Fractional gas holdup varied from 10 to 14 % at J_g = 1 cm/s to between 20 and 30 % at J_g = 2.5 cm/s.

Table 3.8 : Regression of mean bubble diameter, d_{bavg}, with superficial velocity, J_g.

$$[\ln(d_{bavg}) = \ln(C) + n.\ln(J_g)]$$

Frother Type	Dosage μl/l	Degrees of freedom model	Degrees of freedom error	Slope n	Regression coefficient R	Standard error s_e
HTEB	5	2	5	0.206	0.993	0.010
	10	2	5	0.412	0.995	0.016
	15††	1	9	0.271	0.998	0.009
	25††	1	6	0.446	0.958	0.054
DIBK	5	2	5	0.236	0.985	0.017
	10	2	5	0.373	0.998	0.010
	15††	1	3	0.251	0.994	0.016
	25††	1	4	0.339	0.994	0.019
MIBC	5	2	3	0.166	0.998	0.005
	10	2	11	0.314	0.884	0.053
	15††	1	7	0.205	0.649	0.091

The HTEB frother data presented in Figures 3.7 to 3.10 is replotted in Figure 3.12 in terms of fractional gas holdup, ϵ_g, versus mean bubble diameter, d_{bavg}. The influence of air flowrate on air holdup and bubble size may be inferred by recalling the effects of air rate on bubble size observed in Figures 3.7 to 3.10; an increase in air velocity of about 0.5 cm/s produced an increase fractional holdup of about 10 %. At an air velocity of 1 cm/s, raising frother dosages from 10 μl/l to 25 μl/l also increased the holdup by approximately 10 %.

Similar gas holdup profiles could be reasonably expected for some of the laboratory column testwork conducted, especially where the same internal column diameter, D_c, and comparable operating parameter levels were encountered.

†† at 15 and 25 μl/l readings were taken at only 2 gas velocities, thus the regressions are measures of slope fit only.

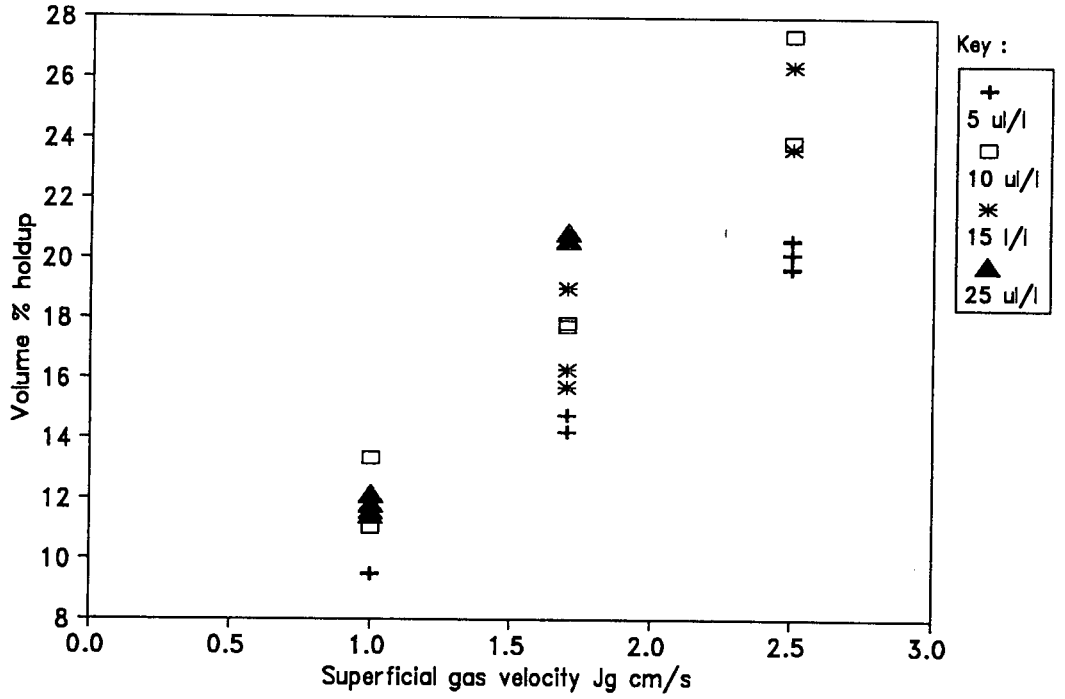

Figure 3.11 : Relationship between gas velocity, J_g, HTEB frother concentration and gas holdup, ϵ_g.

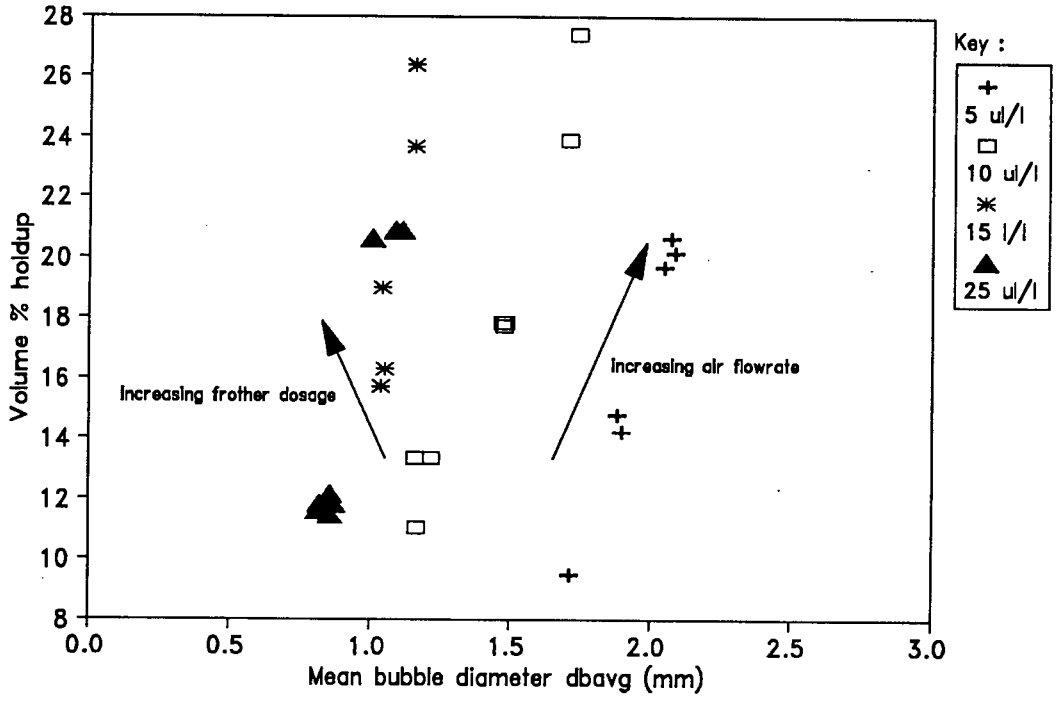

Figure 3.12 : Relationship between mean bubble diameter, d_b, HTEB frother concentration and gas holdup, ϵ_g.

3.3.4 Summary and Conclusions

The effect of frother type, frother dosage and superficial air velocity on mean bubble diameter and size distribution was investigated. For the bubbles sizes typical for column flotation (d_{bavg} 1.0 -2.5 mm) nominal pulp phase frother concentrations of between 5 μl/l and 15 μl/l are sufficient. Increasing frother dosage from 15 μl/l to 25 μl/l had a negligible effect on bubble size. At all the frother dosages used increasing the air rate caused an increase in mean bubble diameter. At superficial air velocities, J_g, of 1 cm/s, fractional air holdups, ϵg, were between 10 % and 14 %; at air velocities of 2.5 cm/s fractional air holdups of between 20 % and 30 % were observed.

3.4 CONDITIONING TESTWORK

3.4.1 Introduction

Both kinetic and thermodynamic aspects of coal wetting by oily collectors were discussed in section 2.4, where it was remarked that coal rank, petrographic composition and oil dispersion properties all play an important role in the process. Furthermore, as conditioning can be considered a mass transfer operation, the mechanical design of the conditioning equipment and its mode of operation also contribute towards determining the efficiency of the conditioning step.

The importance of considering the operational aspects of conditioning becomes apparent when coal flotation testwork is conducted on relatively large, continuously operated types of flotation equipment such as the flotation column and air-sparged hydrocyclone. In particular, problems were encountered during column flotation plant trials conducted at the Kleinkopje Colliery (see Chapter 5), where collector dosages required for acceptable flotation recoveries were excessive ($\approx$ 6000 g/t or higher). This emphasised that adequate chemical preparation of the coal slurry is required for successful operation of large scale flotation equipment, especially where poorly floatable coal fines are to be treated.

Recognition of this prompted an investigation into various conditioning methods, and how they affect the floatabilities of some local coals. Two Witbank and two Natal coals were studied. Five different methods of conditioning the coals were examined. A special effort was made to study the effect of improving the dispersion of oily collector in coal pulps, as this has been variously reported to enhance conditioning efficiency and subsequent flotation performance (Burkin and Bramley, 1963; Misra and Anazia, 1987), presumably because conditioning kinetics are improved by an increase in droplet-particle collision frequencies.

This work and the results obtained are discussed in the sections which follow. Also, based on the material presented in section 2.4, an attempt is made to interpret the result in terms of coal and oil surface properties and equipment design. In particular, as petrographic analyses were performed on these samples (section 3.2), floatability could be directly assessed as a function of maceral composition.

3.4.2 Experimental Apparatus and Method

The conditioning study was carried out using the coal samples obtained from the Kleinkopje and Goedehoop Collieries near Witbank and the Durnacol and ZAC collieries in Natal. Details of these coal samples are given in section 3.2 above.

Five types of conditioning modes were investigated. These were :

1. Bulk addition of oil to a coal pulp suspended in a laboratory batch cell.

2. Bulk addition of pre-dispersed oil-water emulsions to a coal pulp suspended in a laboratory batch cell.

3. Continuous dosing of oil-water emulsions to a continuously flowing pulp suspended in a laboratory mixer cell.

4. Lowering of pulp pH prior to pulp conditioning according to method 2.

5. Bulk addition of oil to a coal pulp suspended in a 240 l capacity mixing tank.

These conditioning methods are described in more detail in the sections which follow. The effectiveness of each of the five conditioning methods was inferred from the yield (mass) of concentrate produced by standard batch flotation of each pulp sample after it had been conditioned. The effect of conditioning method on concentrate grade, i.e. flotation selectivity, was not examined. Ideally microflotation tests should have been carried out instead of batch floats.

The sections below describe the experimental equipment used in the testwork, and the standard procedures employed.

3.4.2.1 Apparatus

Conditioning methods 1., 2. and 4. were performed in a 3 l capacity modified Leeds laboratory flotation cell. This was fitted with a standard 50 mm diameter, 6-bladed turbine impeller, driven by a 0.18 kW variable speed single phase motor. All the flotation tests were also carried out in this cell.

With the exception of two tests, which are described below, conditioning method 3. (continuous conditioning of pulp) was performed in a 4 l capacity Denver flotation cell which was modified to act only as a mixing (and conditioning) tank by sealing the air induction holes on the mixer shaft. The mixer unit was belt driven from a 0.25 kW asynchrous motor. The belt could be run on either of two pulley heads which enabled the impeller to be run at speeds of 1440 or 2700 rpm. Two pulp samples were continuously conditioned in the modified Leeds cell. Peristaltic pumps (Watson/Marlow Type 503S) were used for continuous slurry feed and discharge. The conditioned pulp was transferred to the modified Leeds cell for batch flotation. The 3 l slurry samples required for the flotation tests were collected from the pump line discharging out of the Denver cell.

Conditioning method 5. was performed in the 240 l capacity pulp mixing tank which was used for the column cell plant trials (Chapter 5). The

mixer unit of this tank comprises a 0.37 kW, 1400 rpm single phase motor and a 150 mm diameter, 30 mm wide flat-bladed impeller fitted to a stainless steel shaft. After conditioning, some of the coal pulp was pumped out of the tank using the Watson Marlow pump described above. A 3 l pulp sample collected at the pump discharge was transferred to the modified Leeds cell for batch flotation.

Pre-dispersion of oil-water mixtures was carried out in a well baffled cylindrical PVC vessel, 230 mm in diameter and 320 mm high. A 60 W variable speed direct drive laboratory mixer, fitted with a 50 mm diameter 6-bladed turbine impeller, was used to disperse the mixtures. The ratio of blade height to impeller diameter was 1:8. The clearance between the impeller and the tank bottom was 100 mm, thus the clearance to vessel height ratio was $\approx$ 1:3. The experimental equipment and dimensions were similar to those reported by others (e.g. Sprow, 1967; Calabrese et al, 1986b) investigating dilute oil-water dispersions.

For the continuous conditioning tests (method 3.), the dispersed emulsions were pumped from the PVC vessel to the mixer cell using a Watson/Marlow Type 501U peristaltic pump.

The unconditioned "as is" pulps, from which the samples were drawn for experiment, were suspended either in the 240 l mixing tank described above or in a 400 l capacity polyethylene tank fitted with a 0.25 kW motor and mixer (see section 4.2).

3.4.2.2 Flotation reagents

ShellsolA and high-flash tri-ethoxybutane, HTEB, were the collector and frother reagents used. ShellsolA and HTEB were the standard reagents used in the laboratory and on-line column cell tests (see Chapters 4 and 5 below).

ShellsolA is a commercial grade oil with a 95 % aromatic content. The advantages of using an oily collector containing surfactant impurities (e.g. commercial grade aromatic oil) were discussed in section 2.4.3. The collector dosage was varied depending on the particular coal sample being investigated.

HTEB was chosen as the standard frother as it forms persistent froths and would ensure stable bubble beds with minimum coalescence in the froth. The frother dosage was kept constant at 36 μl for all the flotation tests, apart from those performed on the ZAC fines, where a frother dosage of 108 μl was used.

3.4.2.3 Experimental procedures

Conditioning method 1. served as the standard against which the other methods were evaluated. In this method, a 3 l sample of known pulp density was taken from the "as is" pulp tank‡ and added to the Leeds cell. A predetermined quantity of ShellsolA collector (say x g/t) was then added to the pulp with a micropipette. The pulp was conditioned at an impeller speed of 1200 rpm for 3 minutes after which the required dosage of HTEB frother was added. A further minute was allowed to elapse, subsequent to which a standard float performed. The impeller speed of 1200 rpm was maintained throughout the experiment.

The standard float involved collecting timed concentrates until the froth was barren. Each concentrate was filtered, dried and weighed to determine the yield over the duration of the float. The procedure for this float is described in more detail in Appendix G1.

The oil-water dispersions used for conditioning methods 2. and 3. were produced as follows :

The dispersion vessel was filled with tap water to a volume of 3 l and the agitator turned on. Impeller speed was fixed at 1500 rpm. 35 ml of ShellsolA oil was added after which the tank was filled to 6 l. Thus the volume fraction of the dispersed oil phase, ϕ, was extremely low, ($\phi \approx 0.005$) and hence droplet coalescence could be assumed to be negligible (section 2.4.4). A period of 1 hour was allowed for equilibrium droplet dispersion distribution of the oil phase to be attained.

---

‡ Unless otherwise specified this refers to the 400 l capacity tank.

Conditioning method 2. was very similar manner to method 1. A 3 l pulp sample was taken from the "as is" pulp feed tank. Approximately 2 l of this sample was placed in the laboratory batch cell. Subsequently, a required volume of the emulsion mixture, calculated such that the collector concentration in the 3 l pulp would correspond to x g/t, was added to the suspended slurry. After this, the pulp volume was made up to 3 l and allowed to condition for 3 minutes. Subsequently frother was added, one minute allowed to elapse and the standard batch flotation test performed.

Conditioning method 3. was the method most extensively investigated. A 4 l slurry sample was conditioned (in the continuous mixer cell) according to the same method as described above for conditioning method 2. Impeller speeds of 1440 and 2700 rpm were used when the Denver cell was used as the conditioning vessel. The 3 l Leeds cell was also used as a conditioning vessel for two tests. In these cases impeller speeds of 1200 or 2000 rpm were used. After 3 minutes, the slurry feed and discharge and the emulsion dosage pumps were switched on. The slurry was pumped at rates of either 0.5 or 1.0 l/min through the conditioning vessel. The ShellsolA-water dispersions were dosed into the pulp at rates of between 10 - 30 ml/min. The system was allowed to condition for 3 mean slurry residence times (defined as cell volume/ slurry feedrate) before a 3 l slurry discharge sample was taken. This sample was then placed in the laboratory batch flotation cell (Leeds cell) after which frother was added, one minute allowed to elapse and the pulp subjected to the standard flotation test (at a constant impeller speed of 1200 rpm).

Conditioning method 4 was similar to method 2. except that, prior to batch dosing with dispersed collector oil, dilute sulphuric acid was added to the coal pulp in the laboratory batch cell and the pH lowered to 1.65. Subsequently the standard batch float was performed. In the other conditioning tests the flotation pulp pH was 7.8.

Conditioning mode 5. tests were conducted as follows :

Approximately 100 l of slurry was suspended in the 240 l capacity pulp tank. A predetermined quantity of collector (x g/t), was then added to the pulp tank. After 20 minutes of conditioning a 3 l pulp sample was

taken. This sample was transferred to the batch flotation cell whereupon frother was added and a standard float performed as before.

3.4.3 Results and Discussion

A total of 32 conditioning tests were carried out. The test runs corresponding to the Figures shown below are identified in Appendix B2; the calculated cumulative yield versus time data for each test run may be found in Appendix C3.

Samples of thickener underflow coal fines obtained from the Kleinkopje and Durnacol Collieries were subjected to conditioning methods 1. and 2. The results of these tests are displayed in Figure 3.13-3.16. In each figure, the suffix r indicates a repeat test.

It is apparent from Figure 3.13 that predispersing the collector oil (mode 2.) worsened the conditioning efficiency of the Kleinkopje coal fines compared with the standard method (mode 1.). The rate of flotation was drastically reduced when the collector oil was predispersed before addition. After 2 minutes of flotation following mode 1. conditioning, the cumulative yield was nearly 70 %; following mode 2. conditioning, the cumulative yield after 2 minutes of flotation was only just over 10 %. After 5 minutes of flotation following mode 1. conditioning flotation was complete (the cumulative yield was between 75 and 80 %). Conversely, after 10 minutes of flotation follwing mode 2. conditioning the yield was only 55 % and still rising slowly. As may be seen from the figure, these results are very repeatable.

As noted in Table 3.1 above, the Kleinkopje coal sample had a high inertinite (71 %) and low vitrinite (only 27 %) content. In sections 2.1.3 and 2.4.1 it was noted that inertinite is rich in polar oxygen functional groups. Consequently the Kleinkopje coal fines would have quite strongly negative zeta potential values at typical coal pulp pH's of $\approx$ 6-8 (section 2.4.5). As discussed in section 2.4.4, oil droplets are negatively charged and on a frequency basis approach ultrafine and colloidal sizes ($d_o < 5$ μm). Under these circumstances it is debatable whether the kinetic energies of the extremely fine droplets constituting the dilute oil-water dispersions were sufficiently large to overcome the

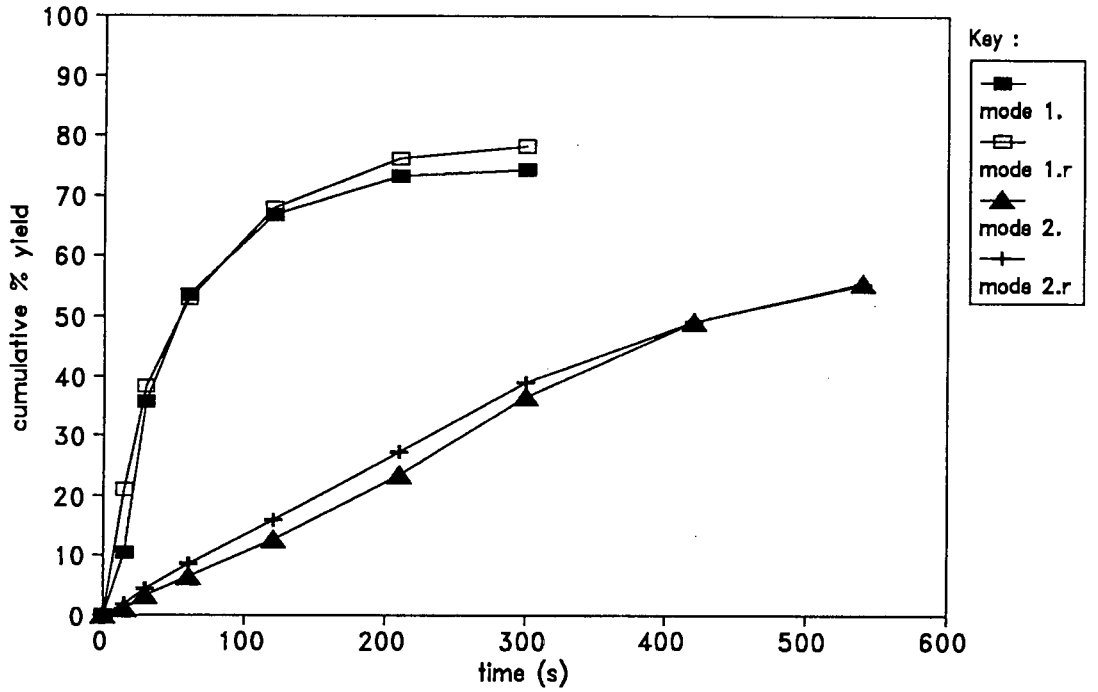

Figure 3.13 : Effect of addition of pre-dispersed oil-water emulsion to pulp batch on flotation yield; sample - Kleinkopje thickener underflow fines; collector - ShellsolA; collector dosage - nominally 1500 g/t; mode 1. = bulk oil addition (standard method), mode 2. = addition of pre-dispersed of oil-water emulsion, r = repeat test.

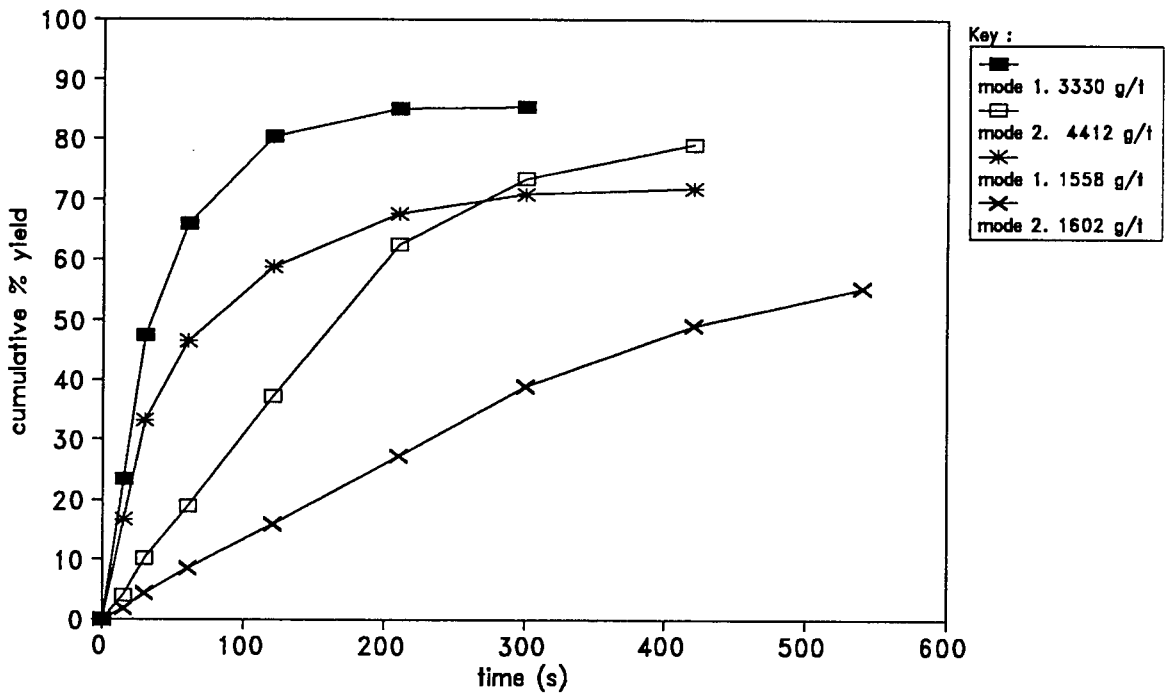

Figure 3.14 : Effect of oil dosage on bulk (mode 1.) and pre-dispersed (mode 2.) conditioning of coal pulp on flotation yield; sample - Kleinkopje thickener underflow fines; collector - ShellsolA; collector dosages - see graph legends.

electrostatic coulombic repulsive forces induced by the negative surface charges of both the oil droplets and coal particles.

It is apparent that whatever the kinetic energy of the predispersed droplets, they would be smaller on average and hence contain less kinetic energy than the larger droplets produced by the bulk addition of collector oil to the agitated pulp. By this reasoning the less well dispersed oil droplets produced by the standard method (mode 1.) would be expected to condition the pulp better than a predispersed oil-water emulsion (mode 2.) since there would be more larger droplets, say of minimum size d_{oc}, capable of contributing to the total kinetic energy state of the oil-water-coal pulp mixture.

Therefore, despite the increase in oil phase surface area and number of (finer) droplets generated, the net result of predispersing the oil in the water would be to lower conditioning efficiency. It was noted in section 2.4.3 that the spontaneous spreading of oils over coal surfaces is thermodynamically unfavourable and that an energy input required to induce spreading. Furthermore, the amount of energy required is determined by the coal's characteristic properties, principal of which is rank.

This argument is well supported by the experimental evidence. Figure 3.14 shows the effect of more than doubling the quantity of predispersed oil (at the same oil/water volume fraction) added to the batch cell. As the size distribution of the oil dispersion theoretically remained unchanged, the number of oil droplets should have increased two and a half fold as the nominal collector dosage was raised from 1600 to 4400 g/t. If the rate of conditioning is dependent on the number of oil droplets present of size d_{oc} or larger, (see section 2.4.4) the rate at which the flotation yield increases with time should rise. Figure 3.14 appears to confirm this; after 2 minutes of flotation following mode 2. conditioning at a collector dosage of 4400 g/t, the cumulative yield was nearly 40 %, double that obtained with a nominal collector dosage of 1600 g/t. Furthermore, Figure 3.14 indicates that after 7 minutes of flotation following mode 2. conditioning (at a collector dosage of 4400 g/t) the cumulative yield was 80 % indicating that flotation was virtually complete. It is also evident from Figure 3.14 that for approximately the first four minutes of flotation, the rate of flotation

(as indicated by the yield at a given flotation time) was lower for the pulp conditioned according to mode 2. at a collector dosage of 4400 g/t than for the pulp conditioned according to mode 1. at a collector dosage of only 1500 g/t. Thus, despite the addition of substantially more (and possibly uneconomical quantities) of collector, the mode 2. conditioning method remained inferior to the standard (mode 1.) technique.

It could be argued that the sole result of varying the conditioning method used is to vary the rate of flotation. Consequently, provided a long enough flotation time was allowed, the same yields would be obtained irrespective of how the coal pulp was conditioned. This argument is in fact spurious: the reason for its apparent validity lies in the manner in which the effectiveness of each conditioning method was inferred. As mentioned above, the impeller speed was kept constant at 1200 rpm during the standard batch floats. The pulp was, in effect in a high state of turbulence, with an average power input/cell volume value, ϵ_{avg}, of 60 W/l. The role of the kinetic energy of stirring in overcoming the coulombic repulsion barrier which exists between the surfaces of the coal particles and oil droplets was discussed above in section 2.4.4. Thus one could argue that the initial flotation rates were dependent on the method by which the coal was conditioned and that the final yields reached arose from the fact that conditioning of the coal pulp continued to occur during the standard batch flotation test. In a larger pilot or industrial size flotation cell, the energy state of the pulp, as represented by ϵ, would be low (see section 3.4.3.2 below) compared with the batch laboratory cell, and in the case of a column cell, negligible (there is no energy of mixing input). Continued conditioning would therefore not occur to the same extent (if at all) during flotation.

It is interesting to contrast these findings with those conducted with the sample from Durnacol, shown in Figure 3.15. Here the difference between the two conditioning methods which were conducted at nominal collector dosages of 1500 g/t, was negligible. This could, however, have been predicted. The Durnacol coal fines have a vitrinite content of 85% and an inertinite content of only 11 %. Therefore the Durnacol coal surface potentials would be less negative and hence the electrostatic barriers to droplet-particle collision would be lower compared with the Kleinkopje coal sample. As mentioned in section 3.2

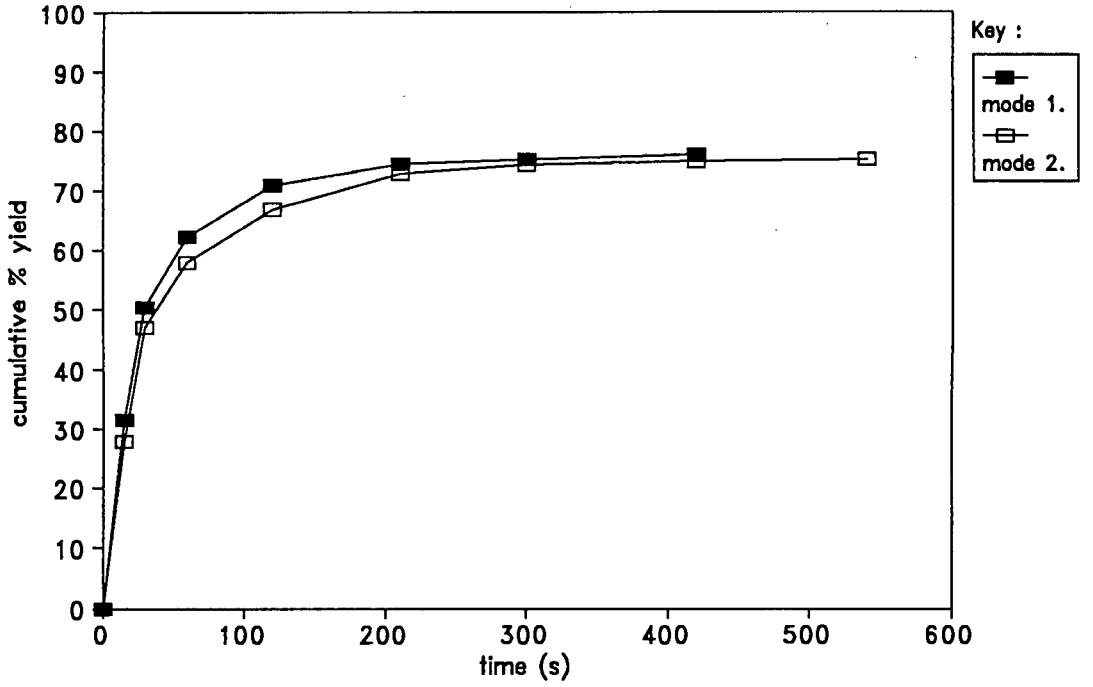

Figure 3.15 : Effect of addition of pre-dispersed oil-water emulsion to pulp batch on flotation yield; sample - Durnacol thickener underflow fines; collector ShellsolA; collector dosage - nominally 1500 g/t; mode 1. = bulk oil addition (standard method), mode 2. = addition of pre-dispersed of oil-water emulsion.

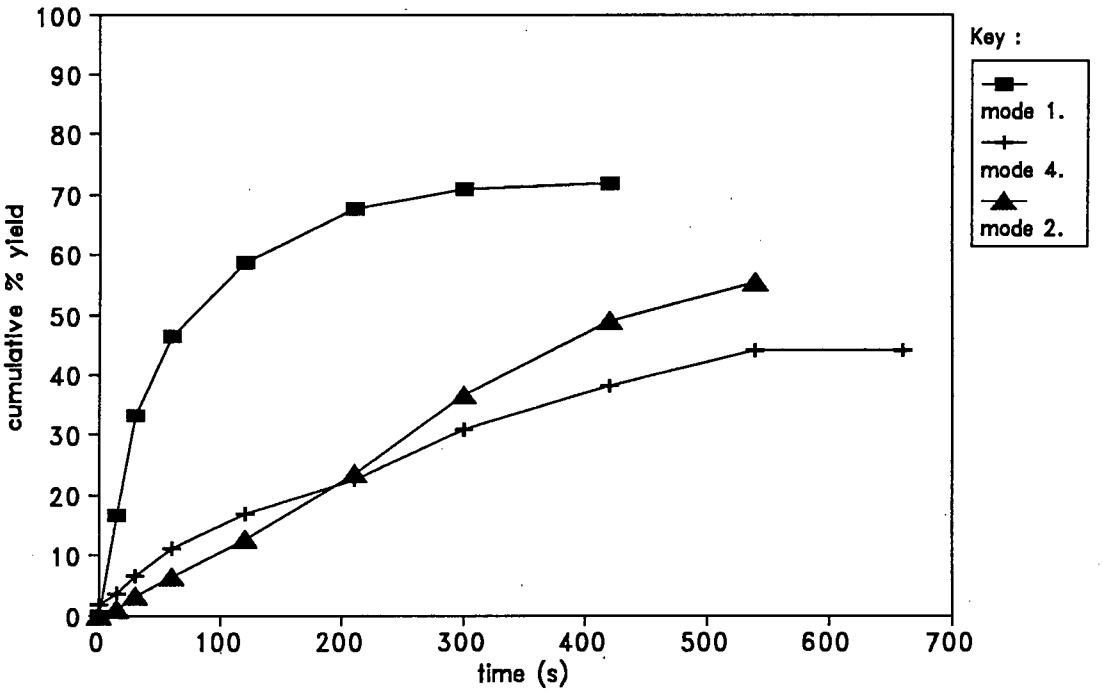

Figure 3.16 : Effect of pH on flotation yield; pulp conditioned by addition of pre-dispersed oil-water emulsion; sample - Kleinkopje thickener underflow fines; collector - ShellsolA; collector dosage - nominally 1500 g/t; mode 1. - bulk oil addition, mode 2. - addition of pre-dispersed oil-water emulsion, mode 4. - addition of pre-dispersed oil-water emulsion at initial pulp pH = 1.65.

above, the size distributions of the Durnacol and Kleinkopje samples were similar.

In an attempt to lower its coulombic repulsion barrier, the pH of a Kleinkopje coal pulp was adjusted to pH = 1.65 (mode 4.) . The pH of the pulp was continuously monitored but no attempt was made to regulate it, and it had risen to 3.45 by the end of the flotation experiment. The recovery rate curve obtained is displayed in Figure 3.16, as are the equivalent standard bulk addition (mode 1.) and predispersed conditioned (mode 2.) floats. It is apparent that no improvement in conditioning performance was obtained by the lowering of pulp pH. This is possibly because electrostatic repulsion forces remained sufficiently large to hinder particle-droplet collisions. Also, the lowering of the pH was observed to affect the froth characteristics (a more watery froth was produced); it is reasonable to infer that the subsequent flotation step sub-processes such as frother adsorption onto air bubbles were also affected by the change in slurry redox potential.

The effect of continuously conditioning (mode 3.) Kleinkopje fines is shown in Figures 3.17-3.19. Slurry ($\approx$ 7 % pulp density, m/v) flowrates entering and leaving the 4 l Denver mixing cell were adjusted to between 0.5 and 0.6 l/min, thus the mean pulp residence time, τ_p, was in the region of 7-8 min. The distribution of oil droplet and coal particle residence times which would arise from a continuous flowing stirred tank reactor would be expected to reduce conditioning efficiency compared with the batch case as short circuiting of material would now occur.

As may be seen from Figure 3.17, continuous conditioning at a nominal collector dosage of 1500 g/t was even less effective than batch pre-dispersed conditioning (mode 2.).

The effects of increased turbulence (i.e. higher kinetic energy inputs) and collector dosage were subsequently examined. Figure 3.18 shows that, irrespective of the collector dosages used, higher impeller speeds in the flow-through conditioning cell did not improve conditioning. However, as was the case with the batch pre-dispersed conditioning tests (mode 2.), raising the collector dosage from around 1500 g/t to above 4000 g/t dramatically improved the rate of flotation.

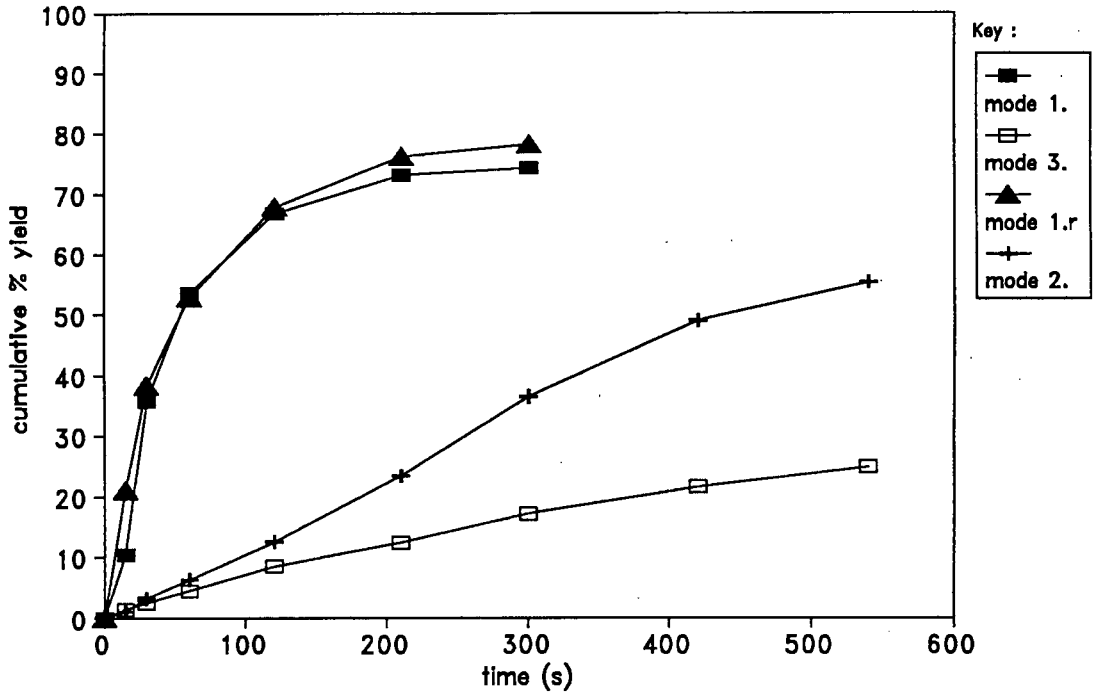

Figure 3.17 : Comparison of batch oil addition (both bulk and pre-dispersed) to coal pulps with continuous dosing of an oil-water dispersion to a continuously flowing pulp; sample - Kleinkopje thickener underflow fines; collector - ShellsolA; collector dosage - nominally 1500 g/t; mode 1. - bulk oil addition; mode 2. - batch addition of oil-water emulsion, mode 3. continuous addition of oil-water emulsion, r - repeat test.

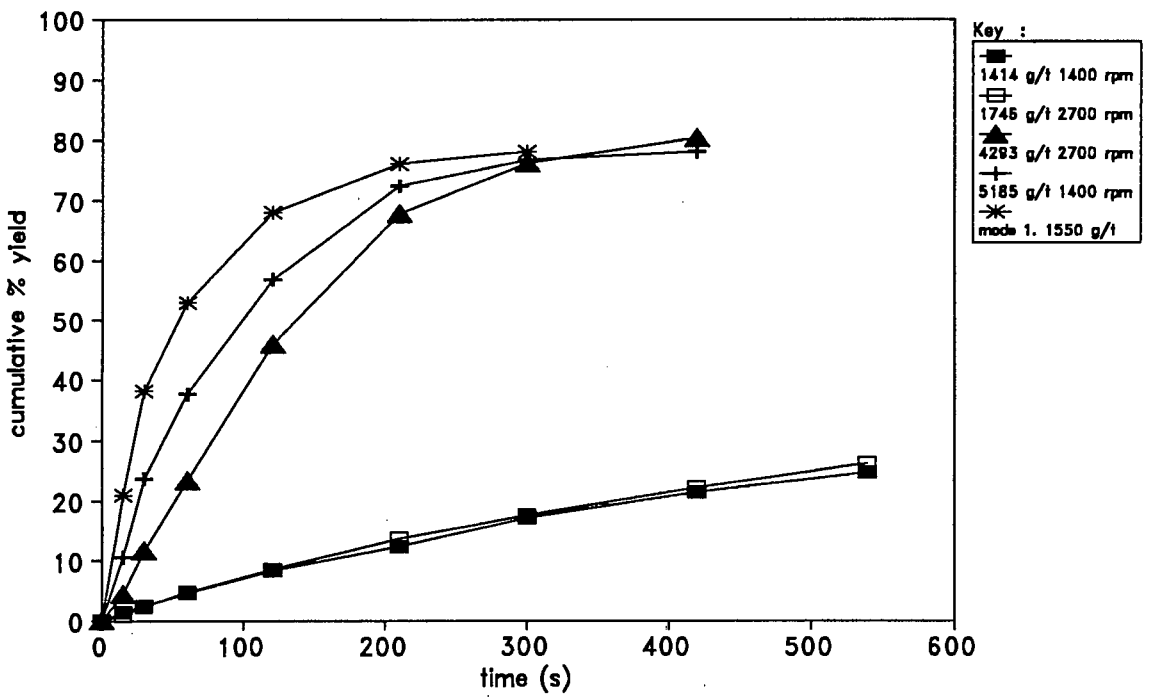

Figure 3.18 : Effect of collector dosage and impeller speed on continuous conditioning (mode 3.); sample - Kleinkopje thickener underflow fines; collector - ShellsolA; collector dosages - see legends; mode 1. - bulk oil addition (for comparison).

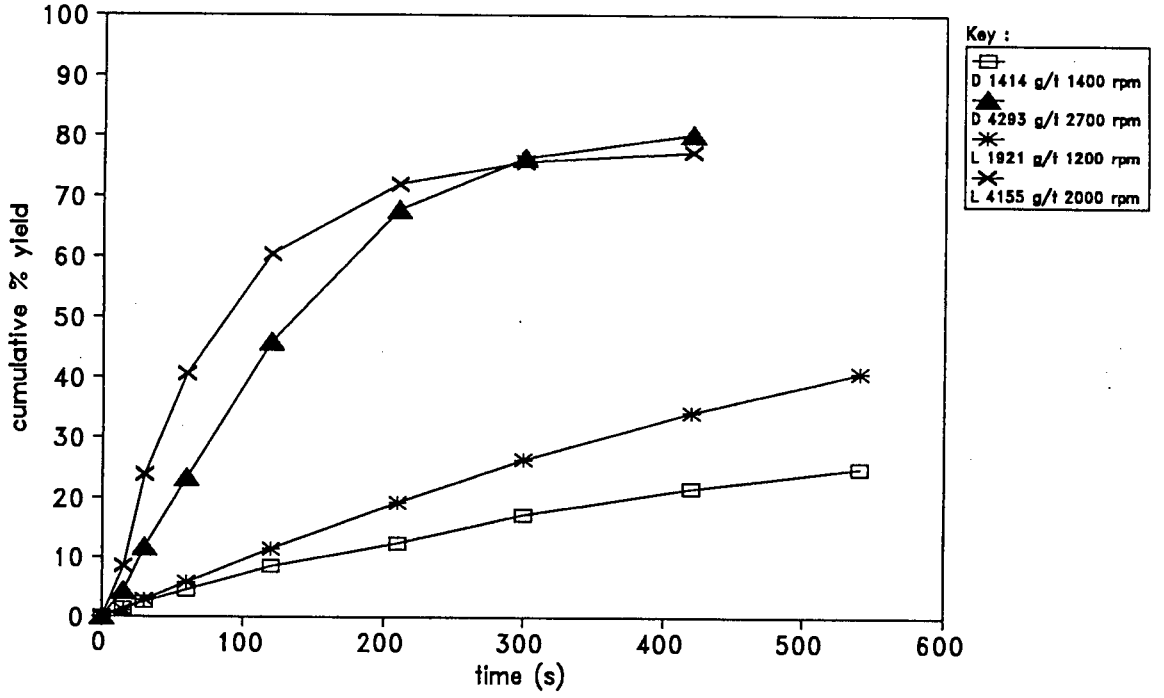

Figure 3.19 : Effect of cell type and impeller speed on continuous conditioning; sample - Kleinkopje thickener underflow; collector - ShellsolA; collector dosage - see legends; mode 3. conditioning; D - Denver cell, L - 3 l modified Leeds cell.

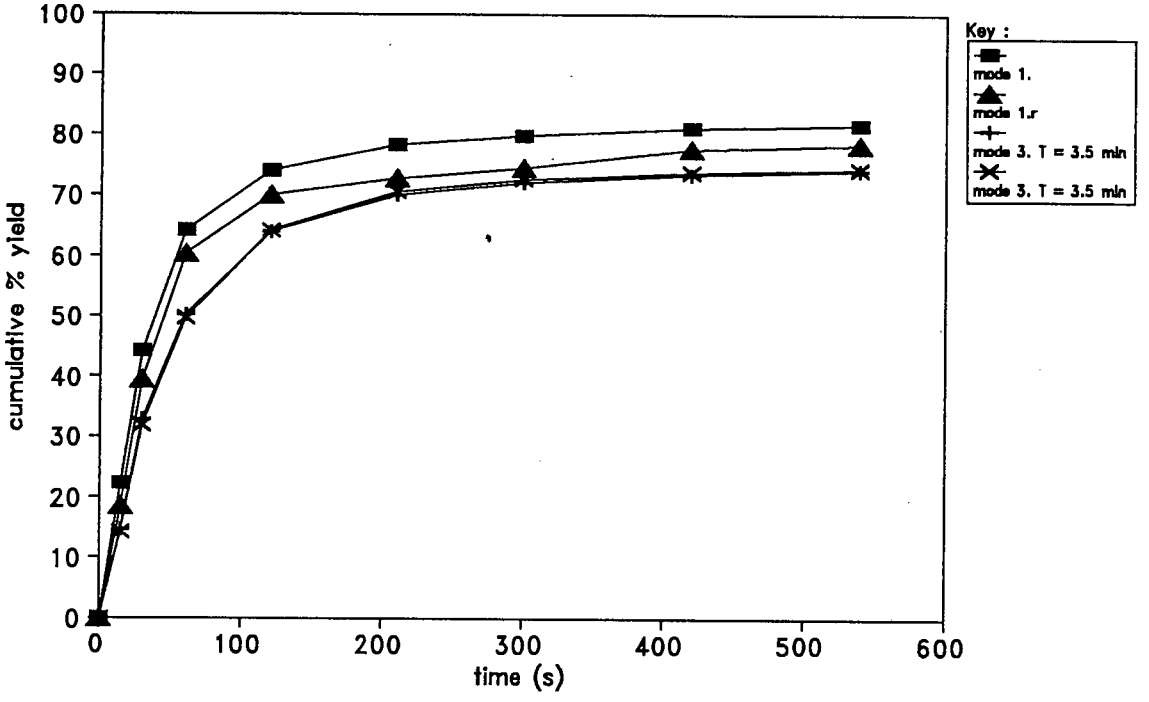

Figure 3.20 : Comparison of batch oil (bulk) addition to coal pulps with continuous dosing of an oil-water dispersion to a continuously flowing pulp; sample - Durnacol thickener underflow fines; collector - ShellsolA; collector dosage - nominally 1500 g/t; mode 1. - bulk oil addition; mode 3. continuous addition of oil-water emulsion, r - repeat test.

The influence of mixing cell design was another factor which was considered. Figure 3.19 indicates that the well baffled Leeds type cell is possibly a better conditioning unit than the Denver cell; however, the improvement was small. Again an improvement in both rate of flotation and yield attained resulted from increasing the collector dosage to above 4000 g/t.

A similar series of tests to those just described were performed on samples of Durnacol fines. The results of these tests are displayed in Figure 3.20. For the two (mode 3.) tests indicated in Figure 3.20 slurry flowrates of ≈ 1-1.2 l/min were used. Thus the slurry mean residence time was reduced to around three and a half minutes. The recovery rate curves which characterise continuous conditioning were only slightly below those of the batch tests, implying that continuous conditioning was a satisfactory technique for treating Durnacol fines. This in fact was the method used for laboratory column flotation tests on Durnacol thickener underflow (see section 4.3 below).

Despite the relatively better performance of the Durnacol compared with the Kleinkopje mode 2. conditioning tests, the fact remains that there was not a single test where predispersing the oil produced a better recovery rate curve than the standard bulk batch addition method. This suggests that predispersing the oil before adding it to the pulp is an intrinsically poor conditioning method where small scale (≈ 3-4 l) mixing vessels are used for oil-pulp contacting.

It has been shown that bulk addition of reagent is an efficient method of conditioning a coal pulp in a laboratory size cell. However, pulp tank volumes required for column testwork are of the order of 100-500 l. The question arises whether this collector dosage technique is adequate for such tank sizes, where there is a far lower degree of turbulence (power per unit volume ϵ_{avg} = P/V ≈ 1-5 W/l pulp) and hence less kinetic energy of mixing compared with the laboratory scale cells (ϵ_{avg} ≈ 60 W/l pulp). Also, droplet sizes are directly related to unit power input (section 2.4.4).

A short series of experiments was conducted to check if this bulk mixing scale-up effect influenced conditioning performance. This corresponds to conditioning method 5. described in section 3.4.2.3 above. Thickener

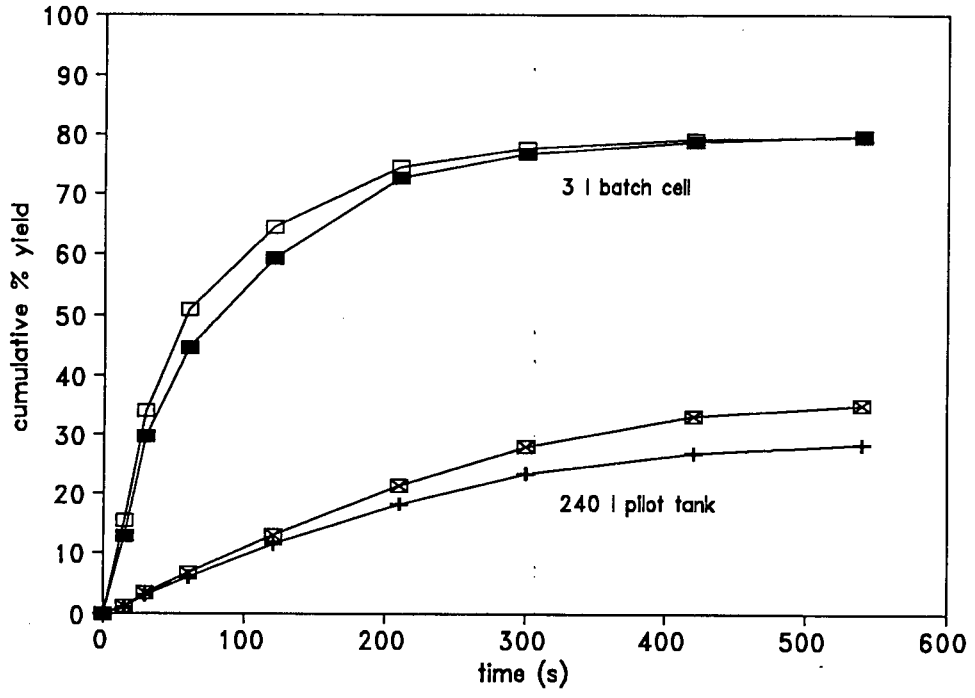

Figure 3.21 : Comparison between bulk addition of oil to a 3 l laboratory Leeds cell (batch cell) and a 240 l capacity pilot rig tank; sample - Kleinkopje thickener underflow fines; collector dosage - nominally 1500 g/t.

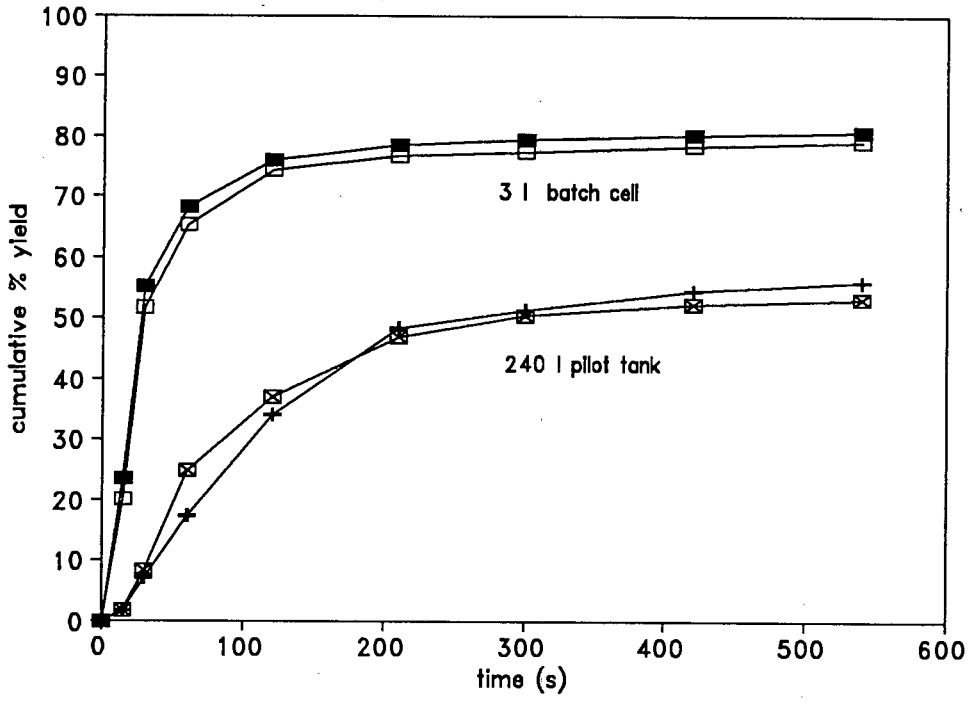

Figure 3.22 : Comparison between bulk addition of oil to a 3 l laboratory Leeds cell (batch cell) and a 240 l capacity pilot rig tank; sample - Goedehoop thickener underflow fines; collector dosage - nominally 1000 g/t.

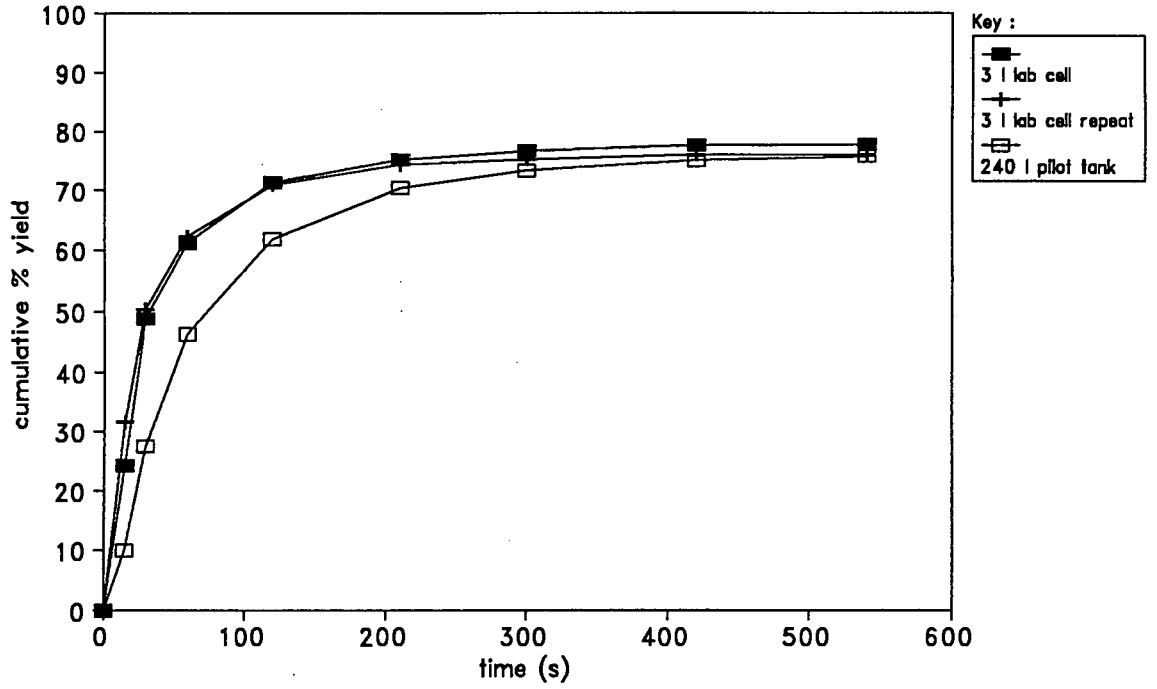

Figure 3.23 : Comparison between bulk addition of oil to a 3 l laboratory Leeds cell (batch cell) and a 240 l capacity pilot rig tank; sample - Durnacol thickener underflow fines; collector dosage - nominally 1000 g/t.

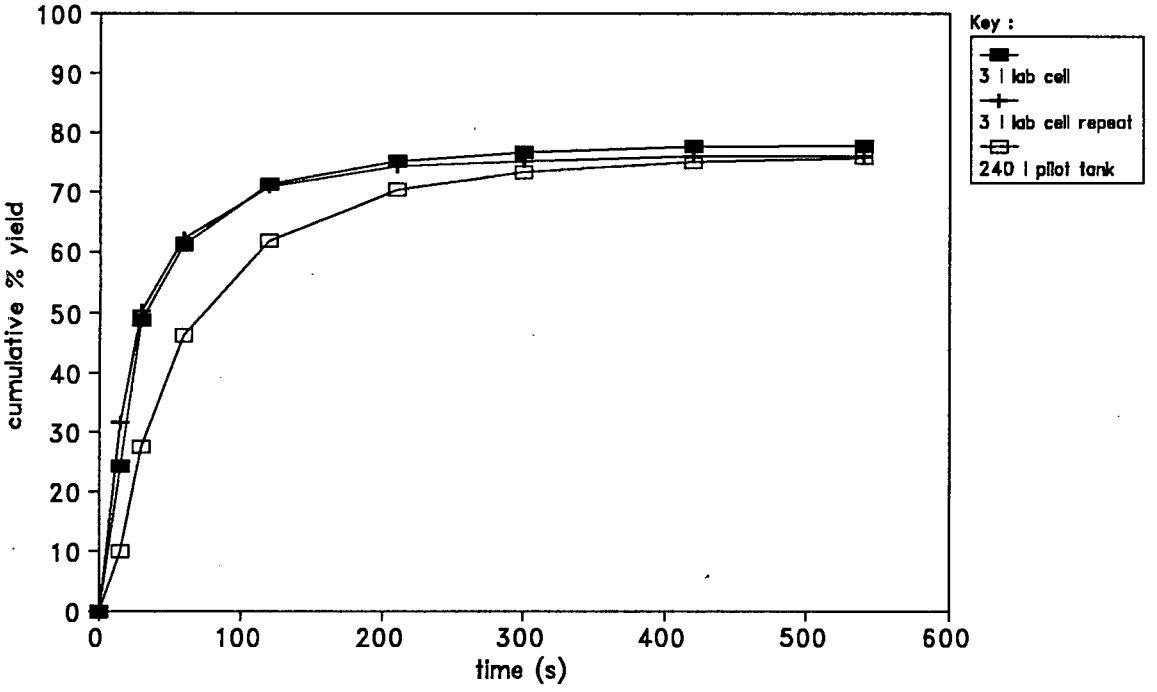

Figure 3.24 : Comparison between bulk addition of oil to a 3 l laboratory Leeds cell (batch cell) and a 240 l capacity pilot rig tank; sample - Zululand Anthracite (ZAC) thickener underflow fines; collector dosage - nominally 1500 g/t.

underflow fines samples from Kleinkopje, Goedehoop, Durnacol and ZAC Collieries were used for these tests. The effects of conditioning mode 5. on flotation yield/time curves are shown in Figures 3.21-3.24. The Kleinkopje and Goedehoop tests were performed in duplicate as was the Durnacol mode 1. conditioned float.

As may be seen from Figures 3.21 and 3.22 (for the two Witbank coals), the conditioning efficiency obtained in a large (≈ 240 l) tank was clearly inferior to that achieved in the batch flotation cell. The Goedehoop coal was less susceptible to the scale-up effect than the Kleinkopje coal, indicating that it floated more readily than did the former. The petrographic analysis of the Goedehoop coal (Table 3.1) showed that this sample had a vitrinite content of 40 % compared with only 27 % for the Kleinkopje coal. A better flotation response would therefore be expected from the Goedehoop sample.

The Natal coals were not nearly as severely affected by poor conditioning in the pulp tank (Figures 3.23 and 3.24) as the Witbank coals. The Durnacol and composite ZAC samples had vitrinite contents of 85 % and 55 % respectively (section 3.2) and thus could be expected to float better than the Witbank coals.

However, it remains debatable whether bulk addition of oil to the pulp is really a suitable method of conditioning large capacity pulp tanks, even if vitrinite-rich coals are treated. A laboratory column, 50 mm in diameter and 2 m high, would, depending on the specific flotation kinetics, take anywhere between 5 - 10 hours to process a 400 l batch of pulp. Under such circumstances, the possibility of the oil desorbing from the coal surfaces and returning to the suspended pulp while the column is operating cannot be discounted.

Thus, in practice no real alternative to continuous conditioning (mode 3.) exists when performing laboratory column tests. Consequently, unsatisfactory results obtained from column tests could be a result of poor conditioning and not of deficiencies in the column flotation process itself. This is discussed in section 4.3.2 and Chapter 5 below.

3.4.4 Summary and Conclusions

This limited test programme has clearly demonstrated that existing conditioning techniques for laboratory or plant-scale column flotation tests are inadequate. Although this is partially due to poor mechanical design of conditioning units, the surface chemistry of oil-coal adsorption is more critical; this has been shown to be highly dependent on coal petrographic composition. Coals with high inertinite contents (equivalently low vitrinite contents) can be expected to respond poorly to flotation.

Bulk addition of oil to the coal pulp is suitable for conditioning small volumes of pulp ($V_p \approx 3$ l) which in a laboratory flotation mixer cell are subjected to quite energetic mixing ($\epsilon_{avg} \approx 60$ W/l). However, bulk reagent addition is unsuitable for pulp volumes of the order of 100 l or greater required for pilot and laboratory column testwork. Although, in laboratory mixer cells, continuous dosing of a coal pulp in an intermediate mixing vessel was found to be less efficient than bulk oil addition, the former method (mode 2.) is more appropriate for conditioning the pulp volumes required column testwork since at least with this the entire pulp volume is subjected to the same mixing intensity (i.e. $P/V \approx$ constant) and mean residence time in the conditioning vessel.

However, because of the different efficiencies associated with the various conditioning techniques, the quantities of oil required to obtain a desired flotation response differ. In particular, the tests conducted on the Kleinkopje sample showed that for laboratory batch tests (mode 1.) collector dosages of approximately 1500 g/t were sufficient, whereas adding oil-water dispersions in either a batch (mode 2.) or continuous (mode 3.) required collector dosages in excess of 4000 g/t.

CHAPTER 4

LABORATORY COLUMN FLOTATION TESTWORK

4.1 INTRODUCTION

As stated in section 1.2 above, the principal aim of this thesis is to investigate whether column flotation technology can be used to recover saleable quality coal from fines presently discarded by South African collieries. A preliminary evaluation of whether this objective can be satisfied is most readily inferred from small-scale column tests conducted under laboratory conditions, where the quantities of material processed are manageable and operating parameters (foremost of which is the maintenance of a consistent feed composition) may be readily controlled.

This Chapter describes the results of column tests performed on four coal samples. The effect of operating parameters (e.g. air flowrate, solids throughput) is investigated and discussed. The results obtained from column cell flotation are compared with conventional batch flotation, ideal ("release") flotation separations and float/sink washability data.

The four coal samples used for the laboratory column tests were :

(i) Durnacol thickener underflow
(ii) Kleinkopje thickener underflow
(iii) Greenside thickener underflow
(iv) Greenside thickener underflow milled to ultrafine sizes.

Tests on sample (iv) were performed in a column with an internal diameter, D_c, of 90 mm; column flotation of all the other coals was carried out in a 54 mm internal diameter column cell.

This chapter begins with a description of the equipment and sampling methods used and the column operating procedures followed.

Subsequently, the results of the tests performed on each of the coal samples are reported and discussed.

4.2 LABORATORY COLUMN CELL RIGS

Two column cells were used for the laboratory testwork; flotation of the raw thickener underflow samples was performed in a 54 mm diameter column whilst flotation of the ultrafine sample was conducted in a 90 mm diameter column. These units and their operation are described separately in the sections below.

4.2.1 54 mm Diameter Column Cell - Rig Description and Operation

A schematic of the 54 mm diameter laboratory column cell and the accompanying equipment is shown in Figure 4.1. This rig was used, with minor variations, for the tests conducted on samples of Durnacol, Kleinkopje and Greenside thickener underflow. Details of the method of column operation and specific equipment used can be found under the individual sections dealing with the column flotation of each sample.

The column was constructed from detachable sections of 54 mm ID PVC piping. The topmost section, fitted with a launder box, was made from clear PVC. The position of the pulp-froth interface could therefore be visually distinguished during column operation. The feed port was situated 1.25 m below the upper column lip. The distance from the feed port to the sparger port, termed the collection zone, could be adjusted (see sections 4.3 - 4.5) by adding or removing PVC pipe sections. The sparger port was positioned 75 cm above the column base.

Two types of spargers were used viz, a filter cloth sparger and an external bubble generator type ("USBM") of sparger. Column cell sparger design was discussed in section 2.5.4. The "USBM" sparger used here consisted a 25 cm long 1" inner diameter PVC pipe containing 1 mm glass beads connected to a copper tube (inside the column) with two 1 mm holes positioned 45 degrees below the horizontal plane. A centrifugal pressure pump capable of pumping at pressures of between 4-5 bar gauge was used to deliver water to the "USBM" sparger. The water was supplied from a 120 l polypropylene tank.

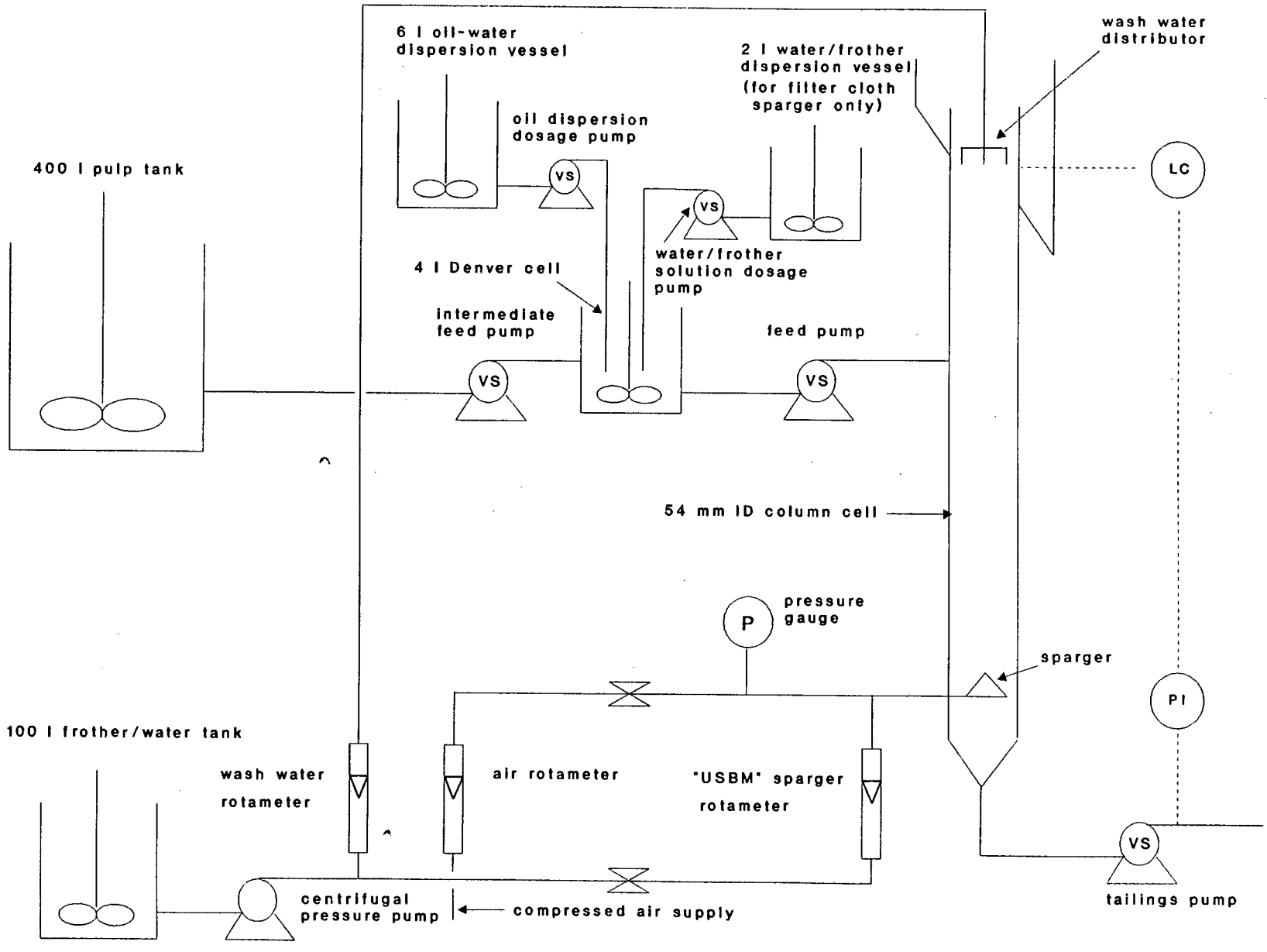

Figure 4.1 : Schematic of laboratory column rig

The air requirement was drawn from the Departmental compressed air utility line; the (gauge) pressure in this line fluctuates between 5 and 6 bar. The column air supply line was fitted with a rotameter and, beyond the rotameter outlet, a needle valve and pressure gauge. The air reaching the spargers was maintained at a constant (gauge) pressure of 4 bar by adjustment of this needle valve.

The washwater distributor was constructed from 6 mm outer diameter copper tubing. From a vertical perspective the distributor appears cross-shaped, consisting of 4 branches each 20 mm long. The total length of either pair of co-axially joined branches was 45 mm. Three 1 mm equally spaced holes were drilled in the bottom face of each branch.

Water was supplied to the washwater distributor via a variable speed Watson/Marlow peristaltic pump capable of delivering flowrates up to 2 l/min. The water source was a water/frother mixture contained in a 120 l tank which also served as a water supply for the USBM sparger when this was in operation. At the frother concentrations used ($\approx$ 5-25 ppm, see sections 4.3 - 4.5 below) HTEB frother is water soluble.

Differences in the electrical conductivities of the pulp (strong electrolyte) and froth (weak electrolyte) phases formed the basis for pulp level measurement. Two 1.0 m long parallel chrome/nickel wires, part of the pulp-level control system, ran down the inside walls of the clear PVC section. A voltage was applied between the two electrodes. The resultant voltage drop depended on the amount of current flowing between the electrodes and this essentially occurred only in the pulp phase. Consequently the measured voltage drop was a function of the position of the pulp along the chrome/nickel electrodes. An electronic controller received the measured voltage signal and, executing a PI control algorithm, varied the tailings pump speed in order to maintain the desired pump level. A variable speed Masterflex peristaltic pump capable of delivering flowrates up to 10 l/min was used as a tailings pump.

A 400 l capacity cylindrical polyethylene tank used to suspend the "as is" coal pulp had a diameter and height of 0.9 m. The mixer unit comprised a 0.25 kW, 1440 rpm single phase motor and a 150 mm by 40 mm

pitched impeller fitted to a stainless steel shaft. The clearance between the impeller and the tank bottom was 100 mm.

A 4 l capacity Denver flotation cell was modified to act only as a mixing (and conditioning) tank by sealing the air induction holes on the mixer shaft. The mixer unit was belt driven from a 0.25 kW asynchrous motor and run at a speed of 1440 rpm. Watson/Marlow Type 503S peristaltic pumps were used to provide feed slurry to the Denver cell and to discharge conditioned coal slurry into the column cell.

When the filter cloth sparger was used it was necessary to dose a water/frother solution into the Denver cell in a similar manner to that described for collector reagent addition in section 3.4. A 2 l water/frother dispersion, agitated by a 30 W laboratory mixer, was pumped into the Denver cell using a Watson/Marlow 502S variable speed peristaltic pump.

4.2.2 90 mm Diameter Column Cell - Rig Description and Operation

Column testwork on the ultrafine Greenside sample was carried out in a perspex column cell whose characteristic dimensions are listed in Table 4.1 below.

Table 4.1 : Column cell description

Dimension	Length
internal diameter	90.4 mm
total column height	3.5 m
feed port position (below overflow lip)	1.5 m
collection zone height	2.0 m
froth bed depth	1.0 m

The column and collection zone heights are taken relative to four glass frit spargers equispaced in a common plane at the column base. The

collection zone height is defined as the distance from the spargers to the feed inlet port.

The washwater distributor was constructed from 6 mm diameter copper tubing. The distributor consisted of three concentric pipes all joined to a common horizontal feed pipe centrally positioned and in the same horizontal plane as the branched ring pipes. Fifty-six 1 mm holes evenly distributed across the centre pipe and its branches effectively covered the column cross-section.

Calibrated rotameters were used to regulate air and washwater volumetric flowrates. The air supply was drawn from the Departmental compressed air utility line. Washwater was supplied via a rotameter directly from the building tapwater supply line. Two variable speed Masterflex peristaltic pumps were used as feed and tailings pumps respectively.

A baffled 120 l PVC tank fitted with a mechanical impeller was used as a column feed reservoir. Pulp suspension was maintained by a pitched paddle impeller rotating at a speed of 100 rpm.

4.3 FACTORIAL DESIGN INVESTIGATION - DURNACOL COAL

4.3.1 Introduction

The Durnacol thickener underflow sample was shown (section 3.4) to be the most floatable of the coals tested in this thesis. This coal is therefore most suited to satisfying the preliminary objectives of the laboratory test programme, namely identifying which operating parameters most affect column performance, and establishing a region of suitable column operating parameter values.

A fractional factorial design technique was used to establish systematically which operating parameters most critically affected column performance when treating Durnacol coal. The design chosen was a $1/8\ 2^{7-3}_{IV}$ fractional factorial design, a summary layout of which is presented in section 4.3.5 below. The complete design construction is given in Appendix A1.5.

Basically the effects of 7 input variables were investigated at two levels (high (+) and low (-)) in 16 tests (trials). The parameter permutations within and between each trial were chosen such that the effects on column performance of main (i.e. parameter) and two factor (i.e. parameter-parameter) interactions were quantifiable. It was assumed that three factor and higher interactions had a negligible influence on column operation. As emphasised earlier, in section 2.6.2; *fractional factorial* designs usually form only the preliminary (*screening*) phase of an investigation programme and optimal sets of operating conditions are typically obtained by further experimentation. For the Durnacol laboratory tests, not enough sample was available to proceed with a further series of optimisation orientated tests once the screening factorial experiments were completed. The effects of this limitation on the absolute recovery/grade performances achieved with the laboratory column cell are discussed below.

4.3.2 Characterisation of Durnacol Laboratory Sample

Proximate analyses and the size distribution characteristics of the Durnacol thickener underflow were reported in section 3.2 above. Average ash contents of feed samples taken from column flotation tests, batch flotation tests, release floats and float/sink analyses are listed in Table 4.2 below.

Table 4.2 : Durnacol bulk feed ash properties

Sample Type	Number N	Average X_{avg}	Sample deviation s
Column	15	29.52	2.56
Batch†	7	29.11	2.26
Release float	2	29.92	0.26
Float/Sink††	8	28.34	0.54

† based on reconstituted feeds.

†† based on reconstituted feeds of float/sinks conducted at relative densities ranging from S.G. = 1.3 to S.G. = 1.7 at intervals of 0.5.

As may be seen, the mean ash contents of samples used for the respective tests are in good agreement; however, the standard deviations, s, of the column and batch feed samples are quite high. This may be attributed to the manner in which these samples were taken. Both sets of (slurry) samples were taken from mechanical mixer tanks.

Samples for the batch flotation tests (see section 3.4 above) were taken from a 240 l capacity tank. Samples for the column flotation tests were taken from the 400 l tank. In the case of the column flotation tests, the comparatively low energy input P/V ≈ 0.6 W/l pulp, which resulted in erratic solids mixing in the pulp feed tank, was attributed as the cause of the large standard variability observed. A normal probability plot did, however, show that the measured column feed ash data were normally distributed. Solids mixing in the 400 l tank is further discussed in section 4.3.3.1 below; details of the statistical tests performed on the column feed data may be found in Appendix A3.3.

The effect of variability in feed composition on column performance is discussed in section 4.3.5 below.

4.3.3 Laboratory Column Cell Experimental Procedure

4.3.3.1 Column rig operation, sampling and analysis

The laboratory column rig was described in section 4.2.1 above. A schematic of the laboratory column cell rig was shown in Figure 4.1.

"As is" coal slurry was pumped from the 400 l mixing tank to an intermediate 4 l capacity Denver flotation cell. The slurry was pumped at rates of either ≈0.5 or ≈1.0 l/min. Oil-water dispersions (dispersed oil phase volumetric concentration $\phi \approx 0.005$) were dosed into the Denver cell at either ≈10 or ≈25 ml/min depending on the slurry flowrate.

When the filter cloth sparger was used it was necessary to dose a water/frother solution into the Denver cell in a similar manner to that described for collector reagent addition (section 3.4). The water/frother dispersion was pumped into the Denver cell at a rate of 35 ml/min. Depending on the total frother dosage rate required (see next

section on selection of column operating parameter levels) the dispersed phase frother concentration was either 120 or 750 μl/l H_2O.

The time required to reach a steady state condition in the column was estimated as 3 times the nominal collection zone volume of either 6.3 or 12.0 litres (including air voidage), divided by the measured tails rate.

It was theoretically possible to test eight different steady state conditions with each 400 l pulp batch, although in practice 3 batches were required to conduct 16 tests because of extraneous occurrences such as bursting of peristaltic tubing, etc. Statistical comparision tests (Appendix A3.3) indicated that the variabilities in ash content between and within batches were indistinguishable, the latter variability arising from poor solids mixing in the slurry holding tank, as discussed in section 4.3.2 above.

Concentrate and tails samples were taken simultaneously at steady state. Tails samples were taken over 1 minute, but the concentrate sample time varied between 1 and 5 minutes, depending on the rate at which solids were being removed in the concentrate overflow. Sixteen different steady state conditions were tested. For all but four of these a second pair of concentrate and tails samples were taken 5 minutes after the first set of samples. After the latter sampling was completed, the slurry line into the column was disconnected and a timed volumetric feed sample was taken. The superficial bias rate was calculated as the difference between the tailings and feed flowrates divided by the column cross-section (see section 2.5 above). When the USBM sparger was used, the sparger water addition rate was subtracted from the tails rate.

All samples were dried, weighed and analysed for bulk ash content. Results are reported on an air-dry basis.

4.3.3.2 Flotation reagents

ShellsolA, a 95 % aromatic oil, was selected as the standard collector for the testwork. Tri-ethoxybutane, HTEB, was chosen as the standard frother.

4.3.3.3 Pulp and frother dispersion pH

Both the pulp and water/frother volumes were made up using Cape Town tap water which has a pH of 7.8.

4.3.4. Selection of Operating Conditions for Durnacol Laboratory Column Testwork

Parameters which were not varied or otherwise not controlled during the test programme are listed in Table 4.3.

Table 4.3 : Constant and uncontrolled operating parameters

Parameter	Value
Pulp density, P.D.	nominally 8 % m/v
Collector dosage, CC	nominally 1500 g/t
Sparger water (USBM), SW	1.2 l/min
Inner column diameter	5.4 cm
Feed point distance below top overflow lip	1.25 m
Distance of water distributor below overflow lip	5 cm

The feed inlet port was situated 1.25 m below the upper column lip, thus the minimum distance between the feed port and the pulp-froth interface, which constitutes the pulp cleaning zone, was 50 cm.

Water addition rate to the USBM sparger was maintained at 1.2 l/min. A water pressure regulator was used to set the water pressure at 4 bar gauge. No attempt was made to vary the operating performance of this sparger.

Pulp density varied between 6.5 - 10 % solids on a mass/volume basis. To account for the effect of feed property fluctuations, feed ash

content was considered as a covariate parameter when analyses of column performance were undertaken (this subject is addressed in the following sub-section). Collector was continuously added as an oil/water emulsion, the nominal dosage used was ≈ 1500 g/t.

The input variables selected for investigation were

1. Froth height, FH
2. Frother concentration, FC
3. Air flowrate, AF
4. Slurry feedrate, QF
5. Washwater addition rate, WW
6. Sparger type, ST
7. Collection zone height, CH

The low (-) and high (+) factor levels chosen are listed in Table 4.4 below.

Froth height is defined here as the distance from the pulp-froth interface to the upper column lip.

The surfactant dosage variable, FC, was based on the rate of frother addition to the column. A concentration basis, for example grams reagent per ton of solid feed, was not used since it has the disadvantage of being coupled with the slurry feedrate parameter, QF.

The method of frother addition used depended on which sparger was in operation (see section 4.2.1). The higher slurry feedrate was chosen as the basis for selecting the two frother dosage rate levels. Even at a fixed dosage level there was some fluctuation in the total dosage rate because the washwater, to which frother was added, was varied independently of the frother concentration. However, this effect was comparatively minor, resulting in changes of ± 1 μl/min at FC(-) and ± 4 μl/min at FC(+).

The frother dosage rates and superficial air velocities used were selected to cover the range of bubble sizes typical to column flotation. The results of bubble size measurements in frother/water mixtures were reported in section 3.4.; at the air flowrates and dosage levels

indicated in Table 4.4 the mean bubble sizes in the aqueous phase of HTEB/water mixtures were approximately $d_b \approx 2$ mm at a frother dosage FC = 5 μl/l feed H_2O and $d_b \approx 1$ mm at FC = 25 μl/l feed H_2O. O' Connor et al (1990) reported that, for a pyrite flotation system, increases in particle size and pulp density produced slight increases in the (average) size of bubbles measured. However, it is the froth phase properties which are usually most dramatically affected by the presence of solids; fine, moderately hydrophobic particles enhance froth stability (sections 2.2.4, 2.5).

Table 4.4 : Column operating parameters, Durnacol laboratory tests

Parameter	Symbol	Low (-)	High (+)
Froth height	FH	0.35 m	0.75 m
Total Frother dosage rate	FC	5-7 μl/min 50-150 g/t	+30 μl/min 350 - 650 g/t
Water tank frother concentration	FCWW	5 μl/l	20 μl/l
Air flowrate	AF J_g	2.06 l/min 1.5 cm/s	3.44 l/min 2.5 cm/s
Slurry feedrate	QF J_f	0.5-0.6 l/min $\approx$ 0.40 cm/s	1.0-1.2 l/min $\approx$ 0.80 cm/s
Washwater rate	WW J_w	0.40 l/min 0.29 cm/s	0.60 l/min 0.44 cm/s
Sparger Type	ST	filter cloth	USBM
Collection height	CH	2.75 m	5.25 m

The superficial air velocities indicated in Table 4.4 are quoted at standard (1 atm) pressure; the supply air pressure to filter cloth or USBM sparger nozzle was set at a gauge pressure, P_g, of 4 bar.

The column height/slurry feedrate combinations were selected to cover a broad spectrum of particle residence times. On a basis of CH = 2.75 m,

QF = 1.2 l/min, net washwater rate = 0.4 l/min, a minimum slurry nominal residence time of $\tau_{min} \approx 4$ minutes could be expected. Conversely, operating conditions of zero bias, $J_b = 0$, CH = 5.25 m and QF = 0.5 l/min would impart a maximum nominal slurry residence time of $\tau_{max} \approx 24$ minutes. The high (+) level solids feedrate corresponded to $F_a \approx 2.5$ t/hr.m^2.

The minimum washwater addition rate selected was $J_w = 0.29$ cm/s (WW = 0.4 l/min). Luttrell et al (1990) recommend a minimum superficial washwater rate of $J_w = 0.25$ cm/s for column flotation of coal fines. Below this value cleaning is erratic as separation efficiency becomes sensitive to changes in the characteristics of the froth phase.

4.3.5 Experimental Design Layout, Results and Statistical Analysis

The input variable combinations used in each of the 16 test runs are presented in Table 4.5. Also shown is the sequence in which the runs were conducted. With the exceptions of Runs 1, 2, 4 and 6 (for which no repeat samples are available) the product yields, recoveries and grades quoted in the Table are *averages* of two repeat sample sets taken within 5 minutes of each other (see section 4.3.3.1). The individual run data values are listed in Appendix A3.3.

Two approaches to analysing the column performance data were adopted. *Initially* F-tests were performed on the (average) contrast effects defining the input factors and factor-interactions. Yield, recovery and concentrate grade response errors were estimated from the available duplicate run data (Appendix 3.1). As these represent *repeat samples* taken at a run operating condition, not repeats of the test runs themselves, the residuals obtained underestimate the overall process response errors. However, for preliminary data analysis purposes, it was assumed that the sub-sample residuals and overall residuals were approximately equal.

A *second*, more accurate approach involved the use of a multivariable linear regression procedure run on the GENSTAT statistical package. Using this method it was possible to obtain an estimate of both the overall and sub-sample response errors; the overall errors were used for

F-tests. Also, the covariate factor, bulk feed composition, could be incorporated into the statistical model. In the remainder of this section the results obtained from the two approaches are evaluated from a statistical viewpoint. Physical interpretation of the test data and rationalisation of the selection of significant two-factor interactions are discussed in section 4.3.6 below.

Table 4.5 : Durnacol laboratory tests - 2^{7-3}_{IV} Class Experimental Design

Test No	Run ID‡	FH	FC	AF	QF	WW	ST	CH	% Yield	% Recovery	% Ash
1	15	-	-	-	+	+	+	-	5.90	7.86	8.45
2	14	+	-	-	-	-	+	+	22.97	30.58	8.05
3	7	-	+	-	-	+	-	+	81.63	92.39	19.96
4	4	+	+	-	+	-	-	-	58.34	70.94	12.14
5	2	-	-	+	+	-	-	+	16.42	22.24	8.65
6	3	+	-	+	-	+	-	-	35.77	42.68	11.86
7	5	-	+	+	-	-	+	-	81.41	93.53	15.97
8	6	+	+	+	+	+	+	+	74.63	90.31	13.14
9	8	+	+	+	-	-	-	+	81.21	94.03	17.36
10	9	-	+	+	+	+	-	-	78.44	92.14	16.66
11	10	+	-	+	+	-	+	-	32.57	42.74	9.37
12	12	-	-	+	-	+	+	+	24.22	31.04	10.27
13	11	+	+	-	-	+	+	-	81.88	94.73	18.83
14	13	-	+	-	+	-	+	+	67.39	81.82	15.55
15	16	+	-	-	+	+	-	+	17.99	22.94	6.97
16	1	-	-	-	-	-	-	-	15.66	20.24	10.05

4.3.5.1 Statistical analysis using average contrast effects

The average contrast effects calculated for the results of the 16 runs are listed in Tables 4.6a and 4.6b below. Contrast effects are defined in section 2.6.2. and Appendix A1.2. Briefly, an *input variable* effect (e.g. effect of AF on recovery) is obtained by adding and subtracting the 16 property results according to the input variable sign permutations displayed in Table 4.5. This net effect, known as a

‡ The Run ID number indicates the sequence in which the trials were conducted.

contrast, is then divided by 8 to get an average net effect (contrast effect, l_i). Interaction effects are obtained in a similar manner, except that one major change is made; the sign coefficients from Test No's 9-16 are multiplied by -1 before the addition and subtraction operations on the response data are performed.

Table 4.6a : Input variable (main) contrast effects

		Net response changes		
		% Yield	% Recovery	% Ash
Symbol	Parameter	E_{Yld}	E_{Rec}	E_{Ash}
A	FH	4.29	5.96	-0.98
B	FC	54.18	61.20	6.99
C	AF	9.11	10.91	0.41
D	QF	-9.13	-8.53	-2.68
E	WW	3.06	2.24	1.12
F	ST	0.69	1.88	-0.50
G	CH	-0.44	0.06	-0.42

Examination of Table 4.6a indicates that frother concentration was the dominant factor dictating column performance. The *average* increase in yield and recovery arising from a change in frother dosage levels was of the order of 50 %. Unfortunately the penalty for this dramatic improvement in product recovery was an average increase in concentrate grade of ≈ 7 % ash.

An increase in slurry volumetric feedrate appears to have caused a reduction in yield, recovery and concentrate grade whilst higher air flowrates improved yields and recoveries. The effect of the other factors was small in comparison; estimates of the standard errors associated with the yield, recovery and grade response parameters are provided in Tables 4.7a and 4.10a below.

Aliased groups of two-factor interactions and their associated average response changes are listed in Table 4.6b. Alongside the alias groups are the individual interactions selected for the multivariable linear regression programme. It is assumed that the remaining interactions in each group (see Appendix A1.5) were neglible. The interaction which

appears to have exerted some effect on yield and recovery is the FH.FC interaction.

Table 4.6b : 2-factor interaction contrast effects

		Net response changes		
		% Yield	% Recovery	% Ash
Symbol	Parameter	E_{Yld}	E_{Rec}	E_{Ash}
BD+CE+FG	QF.FC	-2.70	-1.34	-0.98
AD+CF+EG		-0.44	-0.25	-0.94
AE+BF+DG	QF.CH	0.73	0.84	-0.15
AB+CG+EF	FH.FC	-7.49	-8.43	-0.69
AC+BG+DF		1.64	1.74	1.03
BC+AG+DE		-2.50	-3.37	-1.25
CD+BE+AF	AF.QF	4.00	5.07	0.77

Duplicate samples, taken for 12 of the 16 test runs, were used to provide estimates of the yield, recovery and concentrate grade response errors. After the contrast effects listed in Tables 4.6a and 4.6b were converted to mean squares, F-tests were used to statistically verify the qualitative observations inferred from the linearly averaged response data.

The mean squares of the response errors, and F-ratios for the factor and interaction effects are presented in Tables 4.7 a-c respectively. Detailed data workings may be found in Appendix A3.1 and A3.2.

Table 4.7a : Response error mean squares, s_r^2

$F_{(1,12)} = 3.18$ at $\alpha = 10$ % significance level
$F_{(1,12)} = 4.75$ at $\alpha = 5$ % significance level

Response	Mean square, s_r^2
% Yield	8.57
% Recovery	5.78
% Concentrate ash	0.26

Tables 4.7b and 4.7c confirm the inferences drawn from the preceding rudimentary analysis of the individual response contrast effects. At a 95 % confidence level, frother dosage rate (FC) and slurry feedrate (QF) affected all three response parameters whilst air flowrate (AF) only influenced the yield and recovery responses. At a significance level between 90-95 % the FH.FC interaction also appeared to have exerted some influence on yield and recovery.

Table 4.7b : Main effect F-ratios

Symbol	Parameter	Yield	Recovery	% Ash
A	FH	1.07	3.07	1.85
B	FC	171.26	324.00	94.03
C	AF	4.85	10.29	0.32
D	QF	4.87	6.30	13.79
E	WW	0.55	0.44	2.43
F	ST	0.03	0.31	0.49
G	CH	0.01	0.00	0.34

Table 4.7c : Interaction effect F-ratios

Symbol	Parameter	Yield	Recovery	% Ash
BD+CE+FG	QF.FC	0.42	0.15	1.85
AD+CF+EG		0.01	0.01	1.71
AE+BF+DG	QF.CH	0.03	0.06	0.05
AB+CG+EF	FH.FC	3.27	6.14	0.91
AC+BG+DF		0.16	0.26	2.02
BC+AG+DE		0.37	0.98	2.99
CD+BE+AF	AF.QF	0.93	2.22	1.13

4.3.5.2 Statistical analysis based on multivariable linear regression

The aforementioned analyses were performed on the assumption that the feed composition properties remained constant during and between the individual test runs. However, as shown in Table 4.2, the measured

standard deviation of the bulk feed ash composition was s = ±2.56 % ash. It is possible that this large fluctuation in bulk composition, which reflects an underlying variability in feed particle size and grade-by-size distributions, influenced the yield, recovery and concentrate grade response values. Thus the feed composition can be considered a covariate parameter (see section 2.6 above).

Accordingly, the statistical analysis was repeated using a multivariable linear regression technique which incorporates a covariate parameter. The model fit was performed using the GENSTAT package and run on the UCT VAX 6000-330.

Only main effects and 2-factor interactions were assumed significant. There are 7 main effects and 21 two-factor interactions. Of these, the factor effects, i, investigated on GENSTAT are listed below. They include the 7 main (input variable) effects and 4 two-factor interactions. A complete output listing is provided in Appendix A4.

i = FH, FC, AF, QF, WW, ST, CH, QF.AF, QF.FC, QF.CH, FH.FC

For 16 run combinations there are only 15 degrees of freedom (d.o.f.). Of these, 11 d.o.f. were used to determine the factor-effects listed above, the remaining 4 d.o.f. constitute a residual effect and therefore could be used to estimate *overall* process response *error*.

The GENSTAT programme calculates "best fit" means, μ_{ij}, at each factor and factor/interaction level, i.e.

$$\mu_{ij} = \mu + \alpha_{ij} \qquad (4.1)$$

μ_{ij} = average response of factor i at level j, j = (-) or (+)
μ = overall mean
α_{ij} = effect due to factor i

As the design is a 2 level factorial design, $\alpha_{i(-)} = -\alpha_{i(+)}$. As stated in section 2.6 above, the factor effects α_{ij}, etc. are calculated by a minimisation of least squares procedure. Accordingly, there is a confidence interval and hence a standard variability, s_e, associated with each calculated factor/interaction mean.

The fitted data were subjected to an ANOVA analysis. The numerical values of the F ratios obtained (see Appendix A4) were slightly different to those given in Tables 4.7b and 4.7c since for the fitted data *overall* response *error* estimates were used.

The GENSTAT ANOVA routines were then repeated with feed ash data included to represent a *covariate* effect. A linear relationship between the yield, recovery and concentrate ash responses and the feed ash data was assumed, i.e.

$$y \propto m * \Delta x_c \qquad (4.2)$$

The overall process response then became

$$y = f + e + m.Dx_c \qquad (4.3)$$

y = process response
f = theoretical value
e = error component
Δx_c = % change feed ash bulk composition
m = slope

Now an increase in feed ash composition represents a decrease in the quality of the feed, hence one would expect the yield and recovery responses to drop, as there is less floatable material in the feed to the column cell, i.e.

$m < 0$ for $\Delta x_c > 0$ if y = % yield, % recovery

Concentrate grade should also be affected by fluctuations in feed composition if this reflects changes in the composition of the floatable material available.

The extent to which the inclusion of a covariate factor improved the accuracy of the regression fit can be inferred from Table 4.8.

The numerical values of the covariate slopes and standard errors fall within the confidence intervals associated with the factor means, μ_{ij}. For example, the absolute standard yield error associated with the mean % yield, μ_{Yj} lies between 2.1 % and 3.7 %. The covariate slope, m_{Yld}, is

-1.0, thus a change in feed composition of 2 % ash will change the yield by -1*2 = 2 %. This lies within the standard yield errors listed above. In other words, the inclusion of a covariate parameter did not improve the accuracy of parameter estimation using a regression analysis.

Table 4.8 : Covariate/responses slopes and standard errors

Parameter	Value	Standard error s_e
m_{Yld}	-1.0	1.30
m_{Rec}	-1.4	1.66
m_{ash}	-0.11	0.71
Mean % Yield j, μ_{Yj}		2.1 - 3.7
Mean % Recovery, μ_{Rj}		2.8 - 4.6
Mean % Ash, μ_{Aj}		1.0 - 1.5

Contrast effects calculated from the GENSTAT programme (with the covariate effect included) are listed in Tables 4.9a and 4.9b below.

The effects that input variables exerted on column performance were virtually unchanged by the inclusion of a covariate factor. The same applies to three of the four two-factor interactions tested, although the yield and recovery contrast effects representing the AF.QF interaction doubled in magnitude.

Table 4.9a : Input variable (main) contrast effects (Covariate effect included)

		Net response changes		
		% Yield	% Recovery	% Ash
Symbol	Parameter	E_{Yld}	E_{Rec}	E_{Ash}
A	FH	4.03	5.63	-1.01
B	FC	54.65	61.81	7.04
C	AF	8.81	10.51	0.38
D	QF	-7.75	-6.73	-2.53
E	WW	2.41	1.38	1.06
F	ST	1.34	2.73	-0.43
G	CH	0.31	1.03	-0.35

Table 4.9b : 2-factor interaction contrast effects (Covariate effect included)

Symbol	Parameter	Net response changes % Yield E_{Yld}	% Recovery E_{Rec}	% Ash E_{Ash}
BD+CE+FG	QF.FC	-1.81	-0.18	-0.89
AE+BF+DG	QF.CH	0.15	0.07	0.22
AB+CG+EF	FH.FC	-4.03	-5.62	0.49
CD+BE+AF	AF.QF	4.65	5.92	0.38

The yield, recovery and concentrate ash error mean squares calculated from the residual degrees of freedom are given in Table 4.10a. They are an order of magnitude greater than the sample errors indicated in Table 4.7a and, in the case of the grade variability, two orders of magnitude larger. A standard variability of 6 - 8 % is acceptable for yield and recovery responses, however, a standard deviation of $s \approx \pm 3.3$ % for the concentrate grade parameter reflects that froth conditions were poorly reproducible. This was not due to unsteady state conditions, since the repeat sample variability s_r, was only $\approx$ 0.5 % ash. It rather reflects that inconsistent cleaning occurred in the froth bubble bed between the individual test runs. This aspect of column performance is better addressed in the following section where physical interpretations of column performance are discussed.

Table 4.10a : Response error mean squares - calculated from residual two-factor interactions

$F_{(1,4)} = 6.39$ at $\alpha = 5$ % significance level
$F_{(1,4)} = 4.54$ at $\alpha = 10$ % significance level
$F_{(1,4)} = 4.06$ at $\alpha = 13.7$ % significance level
$F_{(1,4)} = 3.08$ at $\alpha = 17.7$ % significance level

Response	Mean square, s_e^2
% Yield	37.17
% Recovery	60.45
% Concentrate ash	11.18

On a purely statistical level, the probability exists that the response error terms are inflated somewhat since only 4 d.o.f. are used to estimate these errors.

Tables 4.10b and 4.10c lead to practically the same conclusions regarding which parameters affected column performance as those deduced earlier from Tables 4.7b and 4.7c. There are a few minor changes : QF no longer affects grade or recovery at a 5 % significance level, neither does the FH.FC interaction have any influence at a significance level below 10 %.

Table 4.10b : Main effect F-ratios

Symbol	Parameter	Yield	Recovery	% Ash
A	FH	3.42	4.10	0.71
B	FC	598.56	470.88	33.04
C	AF	16.21	14.17	0.10
D	QF	7.85	3.63	2.78
E	WW	1.09	0.22	0.70
F	ST	0.34	0.86	0.12
G	CH	0.02	0.12	0.07

Table 4.10c : Interaction effect F-ratios

Symbol	Parameter	Yield	Recovery	% Ash
BD+CE+FG	QF.FC	0.56	0.00	0.44
AE+BF+DG	QF.CH	0.00	0.00	0.03
AB+CG+EF	FH.FC	3.08	2.14	0.08
CD+BE+AF	AF.QF	4.06	4.06	0.44

4.3.6 Interpretation of Column Performance

4.3.6.1 Global results

The overall results obtained from the factorial design experiments carried out on the Durnacol sample in the 54 mm inner diameter laboratory column cell are plotted in Figure 4.2. For comparative purposes the results of batch flotation experiments, two release flotation experiments, and data obtained from float/sink analysis are also shown. The differential batch floats approximate the ideal flotation separation "release" curve by obtaining incremental concentrate samples at minimal collector and frother dosages. These conditions minimise gangue entrainment into the concentrate product and produce an "ideal" limit to separation achievable by flotation. The float/sink and batch run data are presented in Appendix C; the column run data are presented in Appendix D. Batch and "release" flotation procedures are described in Appendix G1.

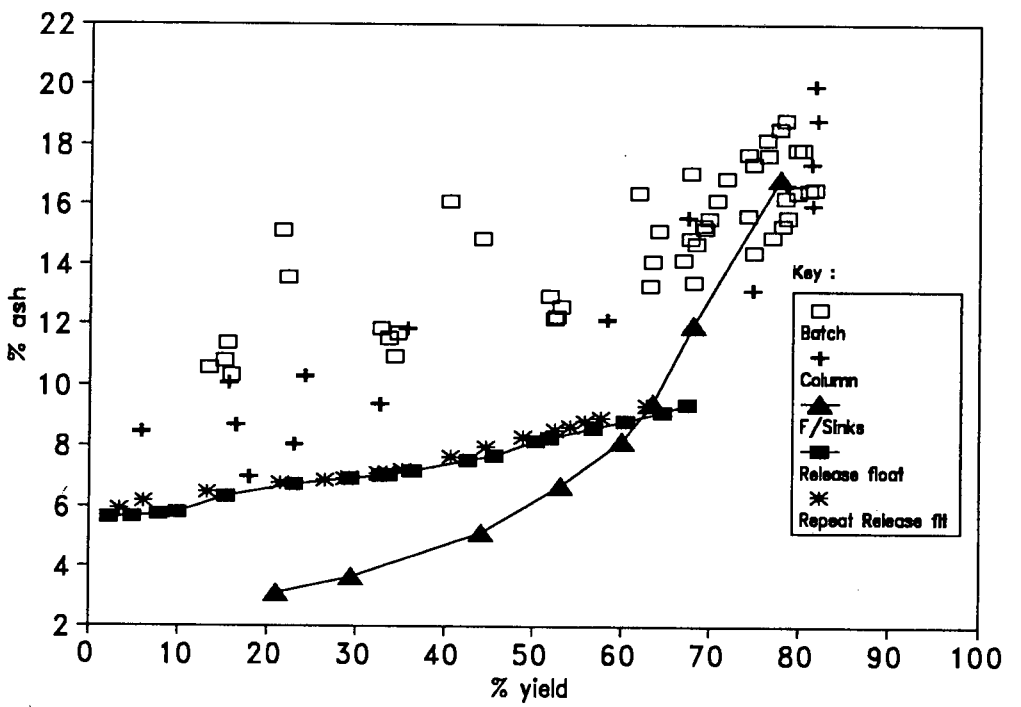

Figure 4.2 : Global results : Durnacol thickener underflow fines.

Considered as a whole, the results indicate that, at a given yield, the column cell was mostly able to produce better grade concentrates than

floats. However, except at very high mass recoveries (yields Y > 70 %), these grades were invariably poorer than those indicated by the two differential "release" floats. This reflects that entrained gangue was present in most of the column concentrates. The best results obtained were a 12 % ash product at a 60 % yield and a 13 % ash concentrate at a 75 % yield. Botha (1980) states that to produce a coking coal the maximum ash content should be approximately 12 %.

It is also apparent that the float/sink (ideal density separation curve) and flotation release curve (ideal flotation separation curve) are not coincident. This difference between the washability and floatability curves arises from the high percentage of middlings (mineral syngenetically intermixed with the carbonaceous matter) present in the Durnacol sample, a feature which is characteristic of South African coals. Furthermore, the existence of a difference between the two separation curves is consistent with results reported by Botha (1980) who also performed laboratory float/sink and flotation tests on a sample of screened Durnacol fines.

Actually, on a global level, the column test data merely emphasises that preliminary experiments rarely produce optimal results, but can be sufficiently encouraging (column concentrate grades were invariably better than the batch grades) to warrant further investigation.

4.3.5.3 Parameter effects

Increases in flotation yield and recovery arising from changes in operating parameters can be attributed to

(i) improved (pulp phase) flotation kinetics
(ii) higher solids loading of the froth bubble bed, i.e. froth phase kinetics

At steady state the rate of particle collection by bubbles in the pulp phase, r_P, and the rate of solids efflux in the concentrate overflow, r_F, are equal. One of these transport steps is usually rate limiting : consequently, changes in operating parameters will predominately affect the kinetics of the rate limiting phase. A knowledge of how the

operating parameters influence the kinetics of each phase, coupled with relevant parameter-recovery test results, should make it possible to identify the rate limiting phase.

Prior to attempting to interpret the factorial design test results from a kinetic viewpoint, it is important to bear in mind that each of the 16 column runs performed is characterised by a unique rate of solids transport, i.e. it has unique kinetics. In each run, depending on the input parameter levels selected, either the pulp phase or the froth phase was rate limiting. *Contrast* effects and *F ratios* define *average* response parameter *changes* taken over the entire 16 column runs. Thus the inferences drawn regarding kinetic effects describe the *overall mean result* : it is possible that the rate determining step of some of the individual runs differs from that of the mean.

In section 4.3.5, the input variables and input variable combinations which significantly ($\alpha \approx 10$ % or less) affected column performance parameters were identified as frother concentration, FC; air flowrate, AF; slurry feedrate, QF; and possibly the FH.FC and AF.QF interactions. This information (which is contained in Tables 4.7 - 4.10) is presented graphically in Figures 4.3, 4.4 and 4.5.

The effect of frother dosage on yield and product grade may be seen in Figure 4.3. The factorial design results are clearly grouped into two distinct data clusters, each cluster corresponding to a frother dosage level. The difference between the average yield response of the pair of clusters, which is represented by the contrast effect l_{FC}, is about 50 %. In other words, irrespective of the levels chosen for the other factors, yield increased by an average of 50 % when the frother concentration was raised from the low (-) to the high (+) level. Simultaneously, the grade (ash content) increased by an average of 7 %.

The effect of air flowrate on column performance is plotted in Figure 4.4. Here, the dominant effect due to frother dosage is clearly apparent; but, within each cluster, on average better yields were obtained at the higher air flowrate.

A similar analysis may be made of Figure 4.5 in which the effect of slurry feedrate on yield is presented. In this case, yields decreased

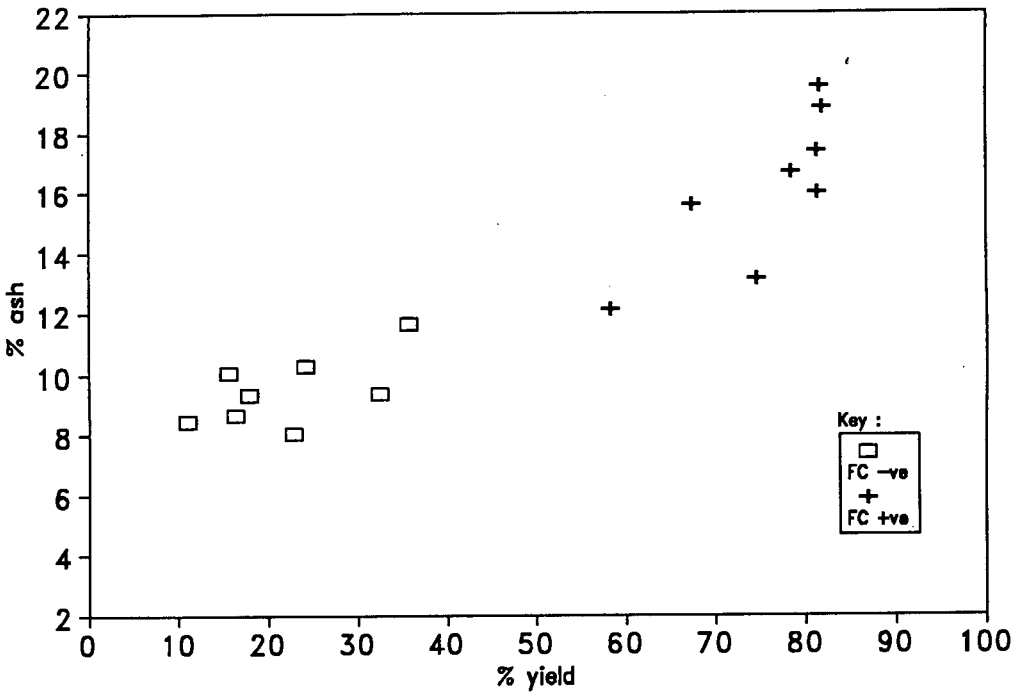

Figure 4.3 : Effect of frother concentration on column flotation of Durnacol thickener underflow fines.

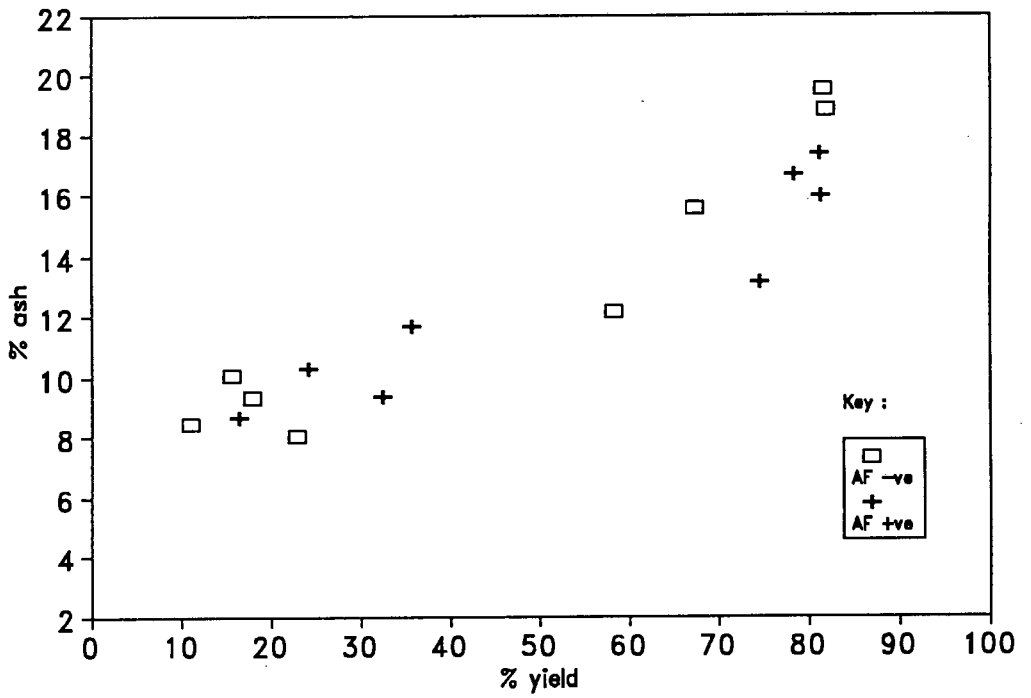

Figure 4.4 : Effect of air flowrate on column flotation of Durnacol thickener underflow fines.

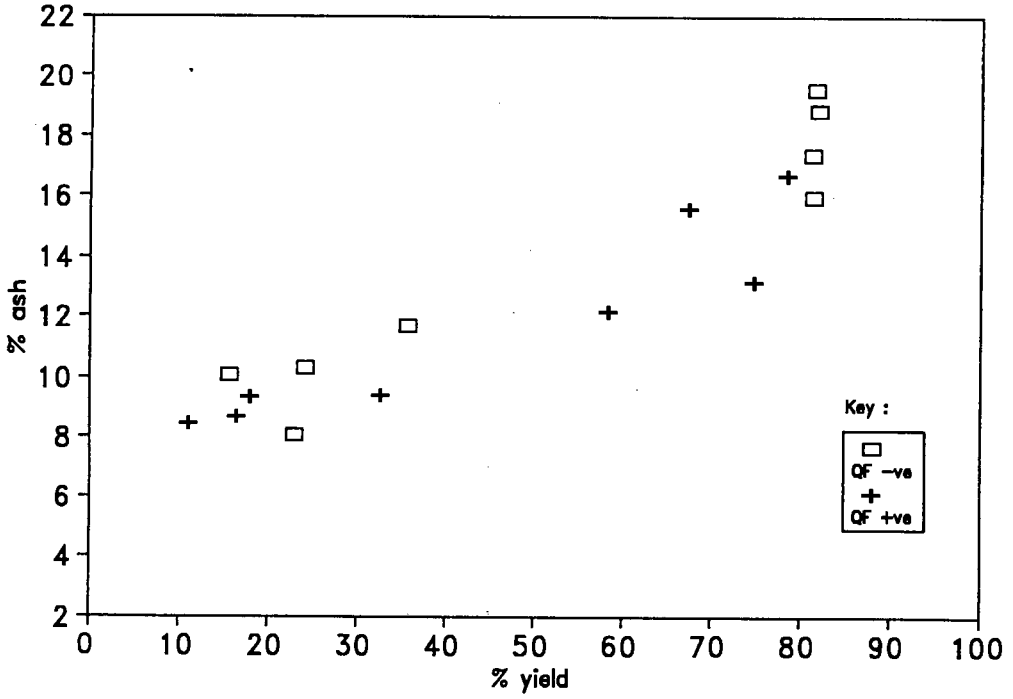

Figure 4.5 : Effect of slurry feedrate on column flotation of Durnacol thickener underflow fines.

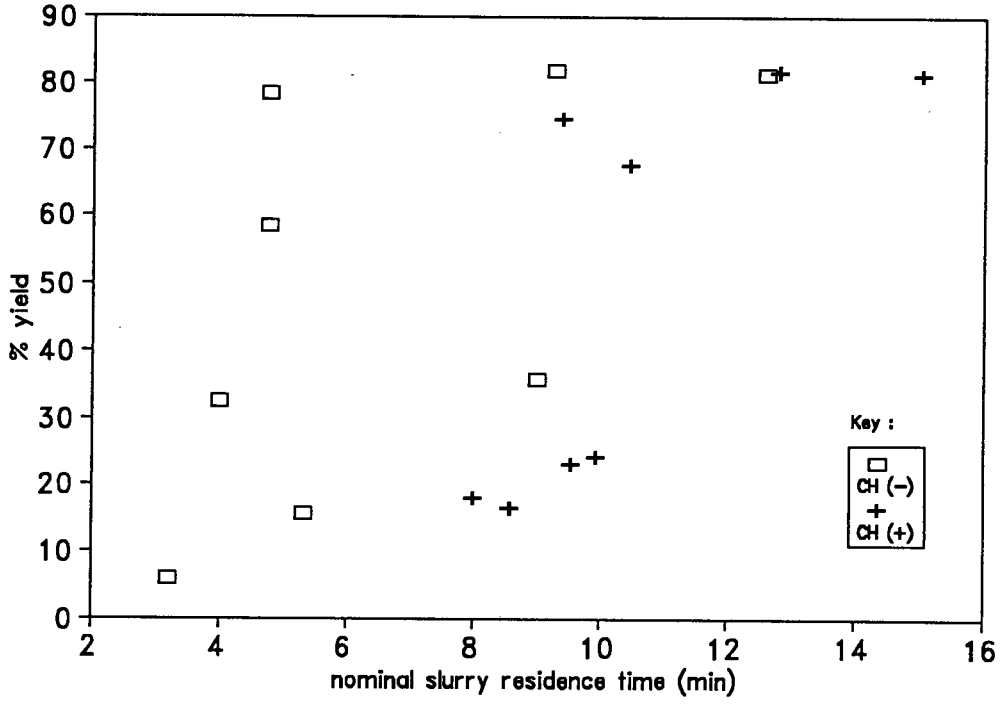

Figure 4.6 : Effect of column height (CH) and nominal mean slurry residence time on column flotation of Durnacol thickener underflow fines.

slightly at the higher slurry feedrates. Statistical F-tests (Appendix A3.4) indicate that slurry feedrate only significantly affected yield at the high frother dosage level (FC+).

The relationship between column height, nominal mean slurry residence time and yield is illustrated in Figure 4.6. The data are grouped into two distinct clusters, which again correspond to the high (FC+) and low (FC-) frother dosage levels. As confirmed by the statistical analysis (Tables 4.6a and 4.9a above) increasing the collection zone height from 2.75 to 5.25 m produced no improvement in yield and recovery at either frother dosage level. As expected, statistical analysis (Appendix A3.4) confirmed that, at each frother dosage level, an increase in collection zone height resulted in an increase in mean nominal residence time; however, as this had no effect on yield and recovery it can be concluded that average column performance was not determined by pulp zone collection kinetics.

In other words, for the Durnacol column tests, *froth phase solid loading* determined concentrate yield and recovery. In fact, the negligible values of the column height, yield and recovery contrasts (l_{CH}'s $\approx$ 0 in Tables 4.6a and 4.9a) make it extremely unlikely that pulp kinetics were rate limiting in any of the column runs performed. The relationship between frother dosage, concentrate solids production rate and yield is plotted in Figure 4.7; the effect on concentrate grade is shown in Figure 4.8. As may be seen, froth solids loading was dramatically improved by increasing frother dosage (Figure 4.7), increasing on average from $\approx$ 0.5 t/hr.m^2 at FC(-) to $\approx$ 1.5 t.hr.m^2 at FC(+), although this occurred at the expense of concentrate grade (Figure 4.8).

At this stage it is appropriate to question whether a solids loading (i.e. carrying capacity) limit was actually reached in any of the column trials. The slurry feedrate contrast effect value, l_{QF}, and the data plotted in Figure 4.5, establish that, on average, concentrate yield and recovery decreased at the high (QF+) slurry feedrates. As pulp kinetic effects cannot be invoked to explain these observed effects, one can only conclude that in some of column runs conducted at solids feedrates corresponding to QF+, the carrying capacity of the column was exceeded*.

* remembering that slurry feedrate only significantly affected yield at the high frother dosage (FC+) level.

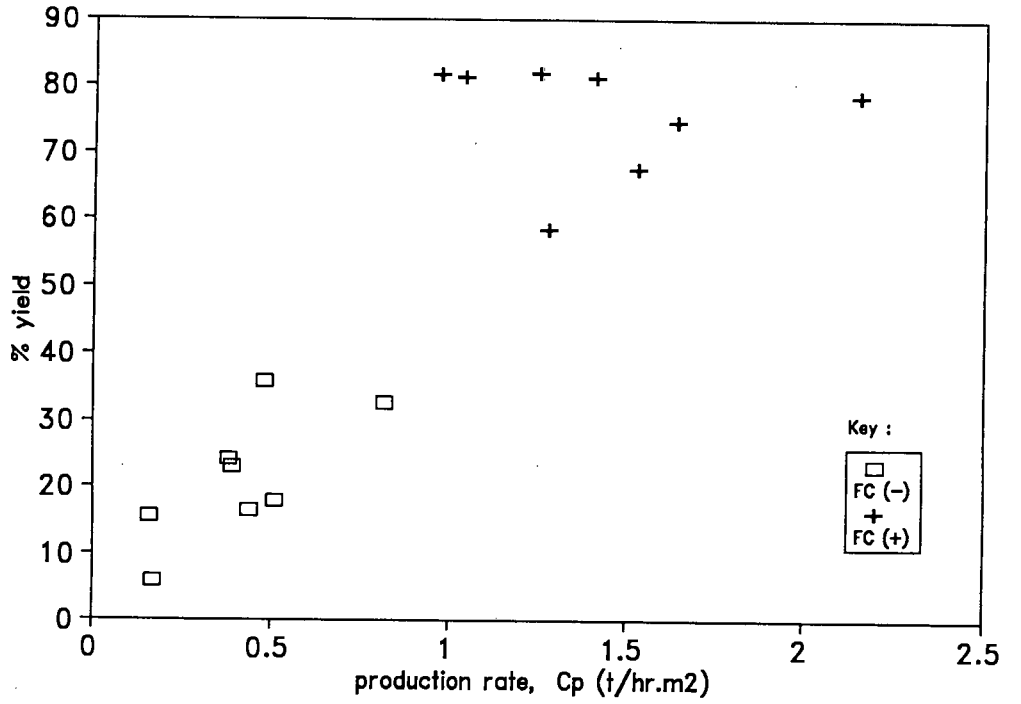

Figure 4.7 : Relationship between solids production rate, C_p, and flotation yield for column flotation of Durnacol thickener underflow fines (FC = frother concentration).

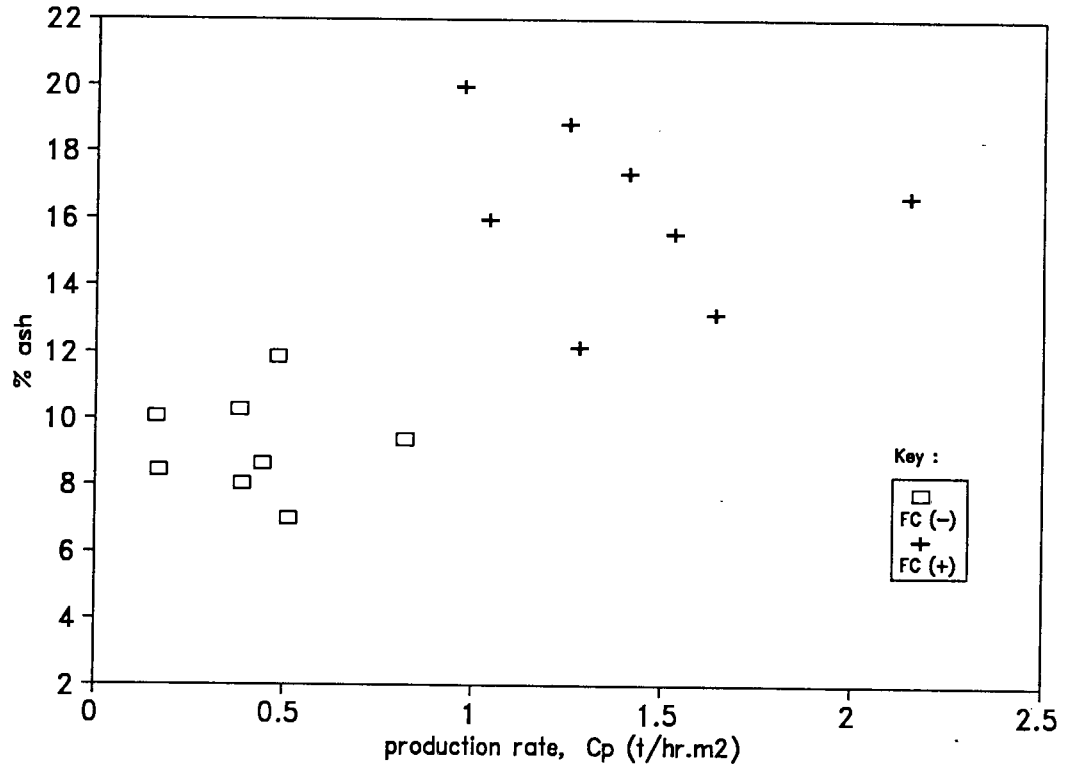

Figure 4.8 : Relationship between solids production rate, C_p, and concentrate grade for column flotation of Durnacol thickener underflow fines (FC = frother concentration).

Furthermore, since carrying capacity is a weak function of air rate (section 2.5.5), an increase in air rate, AF, from 1.5 to 2.5 cm/s should produce a slight improvement in concentrate yield and recovery. This in fact was observed in Figure 4.4 above. Contrast effect and F ratio analyses of the AF.QF interaction also tend to corroborate this interpretation. Table 4.10c demonstrates that this interaction affects yield and recovery at a significance level of $\alpha \approx 14$ %, which corresponds to an average increase in yield and recovery of ≈ 5 % (Table 4.9b).

As the FH and the FH.FC interaction yield and recovery contrast effects and F ratios are only slightly smaller than those of the AF.QF parameter, one might also be tempted to consider them as having some tenuous impact on column performance. Unfortunately, an increase in yield and recovery with an increase in froth depth conflicts with the physical interpretation of this factor effect. Bubble coalescence, which increases (or at best remains constant) as froth bubble bed depth is increased, reduces solids loading of the bubbles, hence it should lower yield and recovery. Therefore, any apparent improvement in yield and recovery with the froth height parameter, FH, can only be ascribed to experimental error. This apparent increase in yield and recovery with FH is also responsible for the sign and size of the FH.FC interaction effect; consequently, any effect ostensibly caused by this factor interaction should also be considered spurious.

The factor interaction groups QF.FC and QF.CH were selected for investigation on GENSTAT for independent reasons. Firstly ShellsolA collector is known to have slight frothing properties (Anderson, 1988).

Thus, an increase in slurry feedrate to the Denver cell, which effectively lowers conditioning time, could result in an increased collector concentration in the aqueous phase of the slurry due to reduced oil-coal adsorption kinetics. This might slightly improve frothing characteristics and/or reduce pulp phase bubble size at low (-) frother dosages. Secondly, particle recovery in the pulp phase can be modelled as a non-linear function of solids concentration, mean residence time, axial mixing and the flotation first order rate constant, k (section 2.3). If pulp phase kinetics are rate limiting, the difference in yield, $\Delta y_{(-)}$, arising from changing the slurry

feedrates at CH (-) will differ from the $\Delta y_{(+)}$ obtained at CH (+). The negligible value of the QF.CH contrast effect and F ratio provides further evidence that under the operating conditions tested, mass transport was predominantly limited by the kinetics of the froth phase.

In section 4.3.5 above, it was commented that the concentrate ash contents were, on average, 7 % greater at FC (+) than at FC (-). The relationship between frother dosage level, concentrate grade and bias rate, J_b, is depicted in Figure 4.9. At the high FC (+) dosage level the column trials were, with one exception, run at virtually zero (and in some cases even negative) bias rates. Conversely, the column runs performed at low frother dosage levels invariably had bias rates in the region of 0.3 cm/s. Bias rate is a bulk parameter which describes the net downward water flowrate in the column cell; it does not provide any information about local hydraulic flow patterns in either the froth bubble bed or pulp collection zones. Consequently positive bias is a necessary but insufficient condition for ensuring optimal cleaning of the coal concentrate. This observation is supported by examination of Figure 4.10 which shows the results of experiments conducted at high and low frother dosage levels as well as the release flotation and float/sinks curves. Although the concentrate grades at the low frother dosage level were better than those at the high level, this is largely because lower yields were obtained. The difference between a concentrate grade obtained from a column trial run and the grade indicated by the "release" curve at the same yield can be considered as a measure of column cleaning efficiency. If this criterion is applied it is apparent that cleaning efficiencies were not enhanced by increases in bias rates.

The corollary to this finding is that increasing the levels of the washwater, WW, and froth height, FH, parameters from low (-) to high (+) values should produce no improvements in concentrate grades. This is in agreement with the summary statistics reported in Tables 4.9a and 4.9b.

These results more or less corroborate those reported in sections 2.5.7 and 2.5.8 where it was noted that effectiveness of adding washwater to the froth bubble bed depends on the flow conditions existing in the froth bubble bed; excessive mixing negates the rinsing effect of wash water. In particular it is likely that it is the design of the

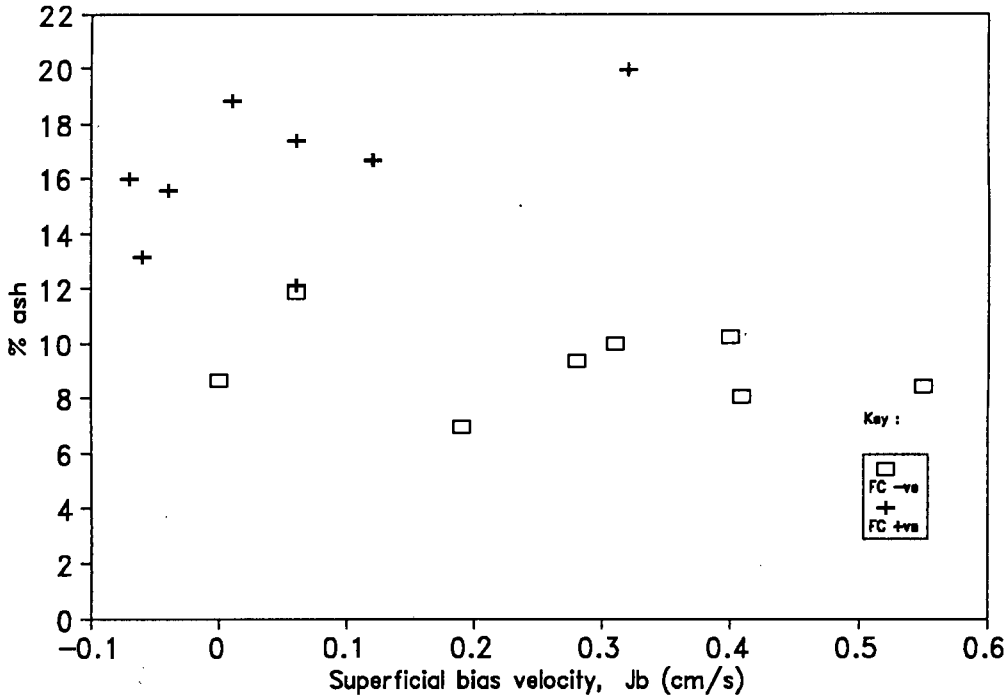

Figure 4.9 : Effect of superficial bias rate, J_b, on concentrate grade for column flotation of Durnacol thickener underflow fines (FC = frother concentration).

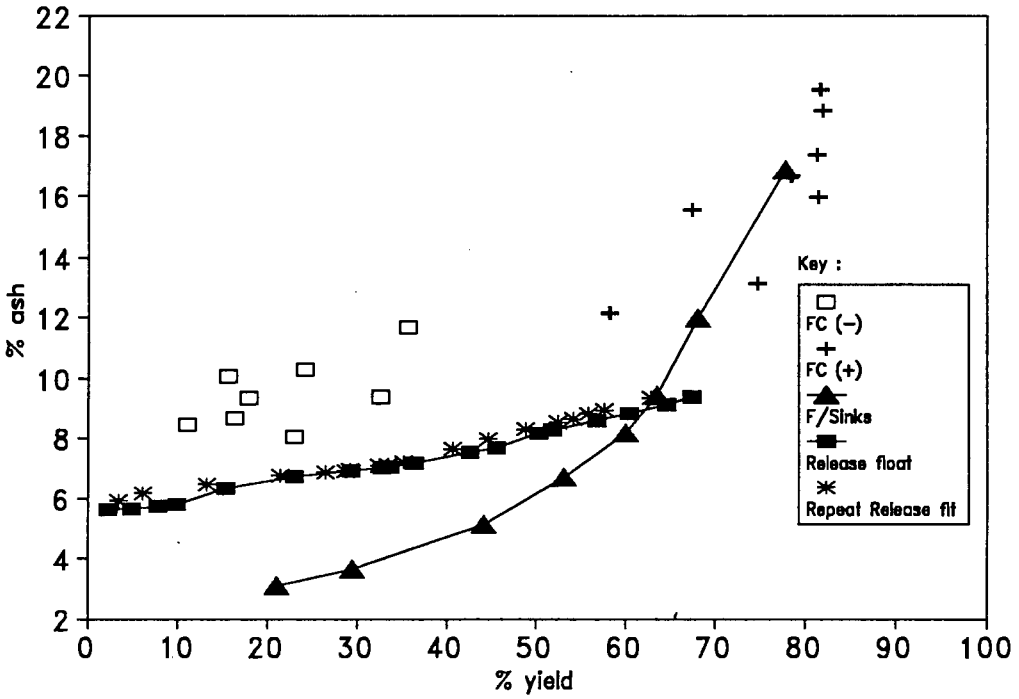

Figure 4.10 : Comparison of column flotation results with ideal ("release") flotation and density separation curves. Durnacol thickener underflow fines.

washwater distributor rather than the rates (provided $J_w > 0.25$ cm/s) which dictate the washing efficiency in the froth bubble bed. It is probable that due to the cross-shaped mechanical design and relatively few number (12) of distributor holes, the washwater distributor sprinkled water over the froth bubble bed unevenly. Also, at the air rate levels chosen, the froth bed depths used were probably too shallow; this resulted in a more mixed froth bed than is desirable. Consequently removal of gangue from the coal fines occurred predominantly in the pulp-froth interfacial zone. Furthermore, high pulp water recoveries are associated with the small bubbles produced at higher frother concentrations ($d_{bi} \approx 1$ mm were observed at the pulp-froth interface at FC (+); as noted in section 2.2.4 recovery by entrainment is directly related to recovery of pulp water in the froth.

In summary, it appears that the hydrodynamic characteristics of a froth bubble bed are a strong function of what combinations of washwater addition rate, surfactant dosage, air rate and froth height are selected. Consequently the efficiency of cleaning will vary as these parameter levels are changed (analagous to changes in particle recovery in the collection zone when mixing characteristics and mean retention times are altered). This phenomenon explains the poor product grade reproducibilty (MSe $\approx$ 11 % absolute ash content) recorded in Table 4.10a.

Another interesting feature of the experimental results is the insignificant impact of sparger design on column performance. It was expected that this variable might play a major role in dictating recovery (section 2.5.4). As Durnacol coking coal is inherently hydrophobic, one might postulate that in this case attachment efficiency, or the film thinning step, (section 2.2.4) rather than collision probability, determined the rate of particle collection in the pulp phase. Sparger design comparisons were also performed during the plant trial testwork; this is discussed in Chapter 5.

4.3.6 Effectiveness of the 2^{7-3}_{IV} Factorial Experiment

Considering that only 16 tests were conducted, the information yielded by the fractional factorial design was considerable. Not only were 7 input variables investigated and key parameters dictating column performance identified, but it was also possible to apply physical interpretations to the results observed. Moreover, the determination of two-factor interaction parameter effects provided corroborative information for rate and grade mechanisms proposed.

4.3.7 Summary of Durnacol Laboratory Column Testwork

The stated objective of identifying which operating parameters dictated column flotation performance for an easily floating (i.e. hydrophobic) coal was achieved. Frother concentration was found to be the most influential variable. Increasing frother dosages from approximately 150 g/t to around 500 g/t raised the flotation yield by an average of 50 %; however, the ash content of the concentrates increased on average by 7 %. Increasing the superficial air velocity from 1.5 cm/s to 2.5 cm/s produced an average increase in yield of $\approx$ 10 %. Conversely increasing the slurry (and solids feedrate) from $F_a \approx 0.5$ t/hr.m^2 to ≈ 1.5 t/hr.m^2 reduced yields by about 10 %. Based on the yield results of the fractional factorial design it was deduced that the rate of solids transport through the froth bubble bed was the rate limiting transportation step.

Washwater and froth bed height were found to exert no effect on concentrate grade. In fact, it was postulated that washwater distributor design and the combination of air flowrate, froth bed selected control the washing efficiency in the froth bed.

Sparger design was found to have no influence on column performance.

In the sections below these findings and conclusions are compared with those obtained from less easily floating coals.

4.4 LABORATORY COLUMN FLOTATION OF KLEINKOPJE THICKENER UNDERFLOW SAMPLE

4.4.1 Introduction

On-line column flotation trials were conducted on the thickener underflow stream of the Kleinkopje Colliery near Witbank for a two month period during April and May of 1990. The aim of the pilot tests was to produce a steam quality (≈ 27.6 MJ/kg) product from the discard thickener underflow stream. These tests are reported in Chapter 5 below.

The plant trials were a mixed success. The product specification of 27.6 MJ/kg was achieved at yields of up to 70 % : however, collector dosages required were invariably in excess of 6000 g/t. The fines feed composition fluctuated daily, between a minimum bulk ash content of 19.5 % ash and a maximum value of 27.5 % ash. The reason for this was that the thickener fines are a blend of by-product fines from two process streams which treat different sections of the No. 2 seam; one stream produces low ash ("select") coal and the other steam ("non-select") coal.

Because of the ambivalent outcome of the plant trials, it was decided to perform some additional tests under laboratory conditions. A composite sample which was a blend of the "select" and "non-select" process streams was collected whilst at the plant (section 3.2). A series of laboratory column flotation tests were performed on this sample. The same laboratory column cell was used as for the Durnacol sample. For comparative purposes, batch flotation tests, a "release" float and a float/sink analysis were also performed.

The objectives of the laboratory testwork were threefold: firstly, to establish whether under controlled laboratory conditions, a consistent feed composition would permit the reduction of collector dosage compared with that used on the plant trials; secondly, to compare the yield/grade performances attained under laboratory conditions with the results from the plant trials; and, thirdly, to further investigate operating parameter effects.

Although the work was performed chronologically after the plant trials reported in Chapter 5, the results are discussed and described in this Chapter, for consistency.

4.4.2 Characterisation and Preparation of the Laboratory Sample

The characterisation of the Kleinkopje thickener underflow sample used in the laboratory testwork was described in section 3.2 above. Proximate analysis and size distribution characteristics of the sample were reported.

The manner in which equivalent samples were collected in six 44 gallon drums whilst at the Kleinkopje Colliery was described in section 3.2. One of these drums was used for the laboratory testwork. The sample was reduced into representative smaller sub-samples following the fractional shovelling method of Gy (1982).

Average ash contents and corresponding standard deviations of feed samples taken from laboratory and plant column flotation tests, batch flotation tests, a "release" float and a float/sink analysis are presented in Table 4.11 below. The mean and sample deviation of ash determinations performed on a wet 1 kg sub-sample obtained by Gy's (1982) fractional shovelling method are also listed.

It is apparent from Table 4.11 that the feed ash contents of all the laboratory flotation samples (A, C and D) were the same. The composite sub-sample, the float/sink samples and the averaged plant feed (F, E and B repsectively) also had the same average ash content. However, a statistical t-test shows that, at a 95 % confidence level, the (average) feed ash contents of samples (A) and (B) were different; the former being lower than the latter. Thus, a sample bias exists between the ash contents of the samples used for the laboratory and plant column flotation tests.

As stated in section 3.2 above, fractional shovelling was shown to be a satisfactory (i.e. unbiased) sub-sampling technique. This assertion is corroborated by a comparison of the average ash contents of the composite sub-sample (F) and the average ash content of the column

slurry feed over the period of the plant trials (B); they are evidently the same. Therefore, the wet solids charged to the laboratory mixer tanks can be considered as representative samples. Thus the origin of the sample bias lay in the manner in which sample was removed from the the 240 l and 400 l mixer tanks for ash determinations.

Table 4.11 : Kleinkopje Laboratory and Plant sample properties

Sample Type	Number N	Average Xavg	Sample deviation s
Laboratory column (A)	9	20.16	1.09
Plant column (B)	71	23.06	2.06
Laboratory batch† (C)	2	19.70	0.54
Laboratory release float† (D)	1	19.13	
Laboratory float/sinks†† (E)	10	23.06	0.39
1 kg wet composite sub-sample (F)	15	23.65	0.60

† based on reconstituted feeds

†† based on reconstituted feeds of floats/sinks conducted at relative densities ranging from S.G = 1.3 to S.G = 1.8 at intervals of 0.5.

A suspension sample calculation (Appendix F2) indicates that the supplied (to the impeller) power of 250 W should be sufficient to fully suspend a 400 l, 10 % m/v pulp density coal slurry, up to particle size of ≈ 0.4 mm. A similar calculation shows that the power (370 W) supplied to the 240 l tank was also sufficient to fully suspend the coal solids.

As mentioned in section 3.4 this latter tank was used as the pulp feed tank during the plant trials. Coal slurry was pumped from the 240 l tank at rates of between 2 to 3 l/min during the plant testwork. Conversely for the conditioning tests, slurry feedrates of approximately 0.5 l/min were used. The slurry sample pipes were positioned near (≈ 150 mm) the bottom of the mixer tanks, consequently the rise in head between the sample pipe and pump inlets was approximately 1 m. Thus it appears that pumping the suspended slurry out of the 240 l mixing tank, and not the suspension conditions in the tank, caused the sample biases observed.

This argument can also be applied to explain the sample bias observed in the 400 l mixing tank. The effects of this bias on the results obtained in the laboratory column compared with the plant trials are discussed in Chapter 5.

4.4.3 Description of Laboratory Column Rig and Operation and Slurry Sampling Methods

The laboratory column rig used was the same as that used for the Durnacol laboratory column testwork and was described in section 4.2.1. The 400 l capacity tank was used a slurry feed tank. ShellsolA and HTEB were used as the respective collector and frother reagents. Pulps were adjusted to the desired strengths by the addition of Cape Town tap water.

As described in section 4.3.3.1 above, laboratory column feed slurry samples were taken from the feed pump discharge line. The batch flotation tests performed on Kleinkopje fines were reported in section 3.4 where it was noted that samples for these tests were taken from a 240 l capacity tank. The "release" flotation sample was taken in the same manner.

4.4.4 Selection of Operating Parameters

The following parameters were varied during the test programme : collector dosage, CC, and method of conditioning (mode 1. or mode 3., see section 3.4); frother dosage rate (FC_d); column height (CH); slurry feedrate (QF); air flowrate (AF); wash water rate (WW); sparger type (ST) and froth height (FH).

A total of 17 runs were performed. Three pulp batches were charged to the 400 l pulp tank. Details of the parameter levels chosen are presented in Tables 4.12 and 4.13. The division of the column tests into two distinct groupings is based on the mode of collector addition used. The runs listed in the Table 4.12 were those for which the oily collector was added in bulk to the feed pulp tank (mode 1.), whereas for

those listed in Table 4.13 a continuous mode of collector addition (mode 3.) was used. The method of continuous conditioning used has been variously described in sections 3.4 and 4.3,; suffice to say that three oil-water dispersion concentrations were utilised, namely 5.83, 8.33 and 16.67 ml ShellsolA/l water. The parameter-level selections were initially based on a 2^{7-4}_{III} fractional factorial design. However, as the runs progressed, the yields obtained tended to depend predominantly on collector dosage and consequently the factorial design combinations were abandoned. Because of the low kinetic energy of the tank mixer system, which was at least partially responsible for the poor conditioning of the coal pulp, it was decided to switch to the continuous conditioning mode when the feed tank was charged with second and third batches of fresh coal fines.

The dosages indicated under the acronym CC in Table 4.12 are calculated on the basis of a pulp volume of 400 l, a bulk oil addition of 45 ml and the measured pulp densities of feed slurry samples taken for individual column runs. The first two runs, identified as KKLC1 and KKLC2, were performed using a filter cloth sparger. The remaining tests (KKLC3-KKLC6) reported in Table 4.12 were done with the "USBM" sparger system.

The filter cloth sparger was also used for the runs KKLC12, KKLC13 and KKLC14 listed in Table 4.13.

4.4.5 Flotation Results

The overall results of the laboratory column testwork are plotted in Figure 4.11. The results of batch flotation experiments, the "release" float and the float/sink analysis are also shown. The data for the latter set of tests is tabulated in Appendix C.

Barring two column trials, namely those runs for which product grades of 8 % and 18 % were obtained at respective yields of 2% and 87%, the column test results coincided with either the flotation release curve, or, at higher (greater than 70 %) yields, with the float/sink curve. In other words, especially when contrasted with the batch flotation data, virtually optimal yield/grade performances were attained in the laboratory column. Coal concentrates with an ash content of less than

10 % were produced at yields in the region of 70-75 %. However, the very good performance achieved in the laboratory column compared with the float/sink curve was at least partially a consequence of sample bias between the float/sink and laboratory samples noted above.

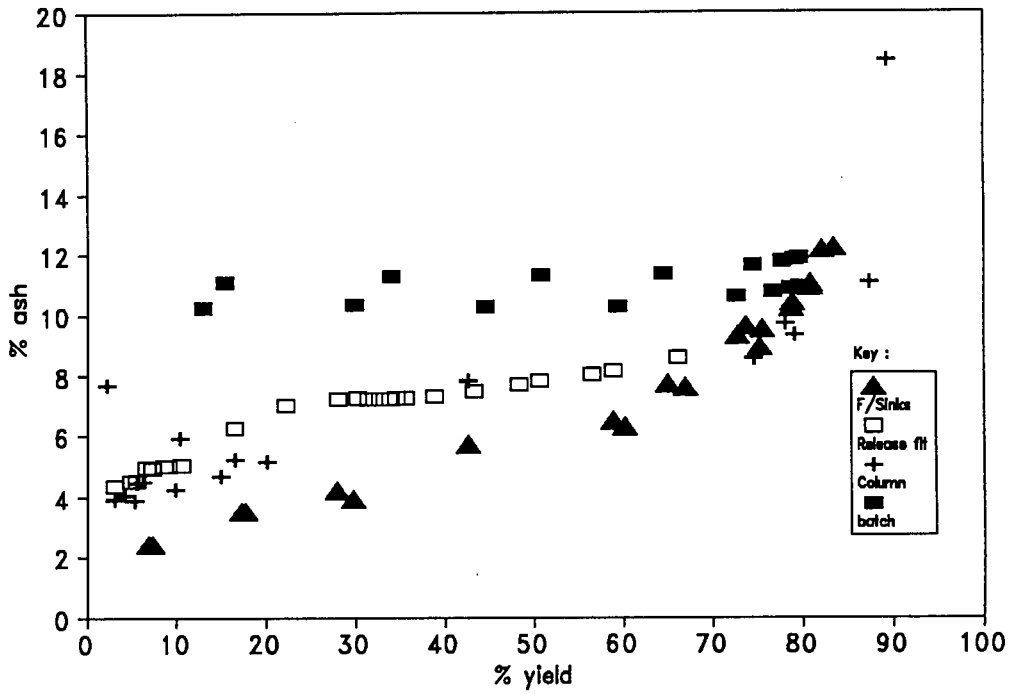

Figure 4.11 : Global results : Kleinkopje laboratory thickener underflow fines.

It is also apparent that, with one exception, the column data are clustered into two groups corresponding to yields of less than 20 % or above 70 %. As is the case with the plant trials (see Chapter 5), these groupings are determined by collector addition levels.

It is evident from Table 4.12 that a collector dosage of ≈1000 g/t produced low-ash (< 7.5 % ash) quality concentrates, but the yields attained were poor; the highest yield was only 16 %. Table 4.13 shows that collector dosages of 5000 g/t or higher were needed to obtain yields of 70 % or higher. Thus the collector dosage levels required were not lower than those used during the plant trials (≈ 6000 g/t).

A petrographic analysis of the Kleinkopje thickener underflow sample used for the laboratory tests was presented in section 3.2. 71 % of the Kleinkopje sample consisted of the maceral group inertinite; only 27 %

KK Laboratory sample - Column Testwork

Table 4.12 - Bulk oil addition (mode 1.) to feed pulp tank

Run ID	FCWW ul/l	CC g/t	CH m	FH m	Jf cm/s	Sf t/hr.m2	Jg cm/s	Jw cm/s	SW l/min	% Yield	Conc % ash	MFeed % ash	CFeed % ash	Cp t/hr.m2	% P.D.	FCd ul/min	Jb cm/s	FC g/t
*KKLC1	15		5.25	0.75		1.00	1.69	0.44		5.2	3.9	19.0	18.6	0.05		9.4		245
*KKLC2	25	1049	5.25	0.35	0.36	1.18	2.49	0.29		2.2	7.7	20.0	19.3	0.03	9.04	20.0	0.26	443
KKLC3	15	1123	5.25	0.35	0.24	0.94	1.69	0.29	1.2	16.5	5.3	19.3	18.8	0.15	10.97	22.4	0.72	624
KKLC4	25	1018	5.25	0.75	0.80	2.14	2.49	0.44	1.2	4.2	4.1	19.5	22.4	0.09	7.42	40.9	0.07	501
KKLC5	15	1362	2.75	0.75	0.38	1.04	2.49	0.29	1.2	3.1	3.9	19.6	20.0	0.03	7.65	22.4	1.84	562
KKLC6	25	1048	2.75	0.35	0.40	1.00	1.69	0.44	1.2	9.8	4.3	21.8	19.6	0.10		40.9		1070

Table 4.13 - Continuous oil/water dispersion addition (mode 3.)

Run ID	FCWW ul/l	CC g/t	CH m	FH m	Jf cm/s	Sf t/hr.m2	Jg cm/s	Jw cm/s	SW l/min	% Yield	Conc % ash	MFeed % ash	CFeed % ash	Cp t/hr.m2	% P.D.	FCd ul/min	Jb cm/s	FC g/t
KKLC7	15	3632	2.75	0.75		0.93	2.14	0.29	1.0	6.2	4.5		19.5	0.06		20.1		569
KKLC8	25	4280	2.75	0.35	0.33	0.89	1.59	0.44	1.0	14.9	4.7	20.4	18.6	0.13	7.41	38.5	0.03	1130
KKLC9	15	4957	2.75	0.75		1.19	2.14	0.29	1.0	78.2	9.7		22.3	0.93		21.0		463
KKLC10	25	7581	2.75	0.35	0.31	0.75	1.59	0.44	1.0	79.1	9.3	19.8	20.1	0.59	6.80	40.0	-0.01	1400
KKLC11	5	7235	2.75	0.75	0.36	0.84	2.14	0.29	1.0	20.1	5.2		20.5	0.17	6.45	7.0		217
*KKLC12	5	7182	2.75	0.35		1.70	2.14	0.44		10.4	7.8		21.6	0.72		9.0	0.38	138
*KKLC13	15	7159	2.75	0.75	0.61	1.71	1.59	0.29		42.6	6.0	22.1	22.0	0.18	7.76	23.3	0.58	357
*KKLC14	5	12230	5.25	0.75	0.28	0.51	1.59	0.44		74.6	8.6		19.6	0.38	5.11	8.1	0.45	417
KKLC15	15	7458	5.25	0.35		1.76	1.59	0.29	1.0	87.4	11.1		18.9	1.54		21.0		313
KKLC16	15	9330	5.25	0.75	0.51	1.40	2.14	0.44	1.0	89.4	18.4		19.5	1.25	7.66	24.0	0.19	448
KKLC17	5	4150	5.25	0.35	0.52	1.58	1.59	0.29	1.0	5.5	4.5		26.8	0.09	8.37	7.0		116

* performed using filter cloth sparger, other runs "USBM" sparger used

of the maceral group vitrinite was present. It was reported in section 2.1 that inertinite is characterised by a high oxygen content compared with vitrinite and, in section 2.4, it was noted that the presence of oxygen functional groups on coal surface retards floatability. The conditioning tests conducted, which were reported in section 3.4, confirmed that the Kleinkopje sample was poorly floatable compared with the other coals tested (Durnacol, ZAC and Goedehoop) which had higher vitrinite (at least 40 %) contents than did the Kleinkopje coal sample. As discussed in section 3.4, the conditioning techniques used in the column cell testwork were not well suited to enhancing the floatability of coals which were already intrinsically poorly hydrophobic. Consequently, large quantities of oily collector were required.

It is also evident from Table 4.12 that at low collector dosages, the addition of large amounts of frother (in excess of 500 g/t) did not improve flotation yield. Conversely Table 4.13 shows that if the collector dosage was greater than ≈5000 g/t, raising frother dosages from below 200 g/t to above 300 g/t increased yields by at least 20 % (e.g. runs KKLC17 and KKLC15). Thus collector and frother dosage levels played a major role in determining the yields obtained in the laboratory column cell. Reagent effects are evaluated further below when the individual column results are analysed.

An interesting concentrate grade/parameter level combination effect was noticed in the early runs listed in Table 4.12. For column trial *KKLC1* a 5 % product yield was obtained at a grade of 3.9 % ash. A comparatively *deep froth* bubble *bed*, FH = 0.75 m, a *moderate gas* flowrate, J_g = 1.7 cm/s and a superficial washwater velocity, J_w, of 0.44 cm/s, were used. For column run *KKLC2* a *shallow froth* bed, FH = 0.35 m, a *high gas rate*, J_g = 2.5 cm/s, and a *lower washwater* rate, J_w = 0.29 cm/s, were used; the effect on product grade was remarkable : the *ash content* of the *KKLC2* concentrate *doubled*, rising in value from 3.9 % ash to 7.7 % ash.

The only difference between column runs KKLC7 and KKLC9 was the amount of collector that was added (to the intermediate Denver conditioning cell), which in the former case corresponds to ≈3500 g/t and in the latter instance ≈5000 g/t. These values are based on the measured oil-water dispersion addition rates divided by the (calculated) solids

feedrates. The difference in yields between the two runs (≈6 % for KKLC7 and ≈78 % for KKLC9) can thus be attributed solely to the quantity of oil used to condition the coal fines pulp. Collector and frother addition were increased and the solids feedrate was reduced for run KKLC10 : suprisingly, this did not improve the yield, but interestingly did not affect the grade of the coal concentrate either. A further examination of the run parameters reveals that although a shallow froth bed was used, FH = 0.35 m, the gas rate was quite moderate, J_g = 1.6 cm/s, which suggests that gas rate has a dominant influence on concentrate grades. In run KKLC11 the frother dosage rate was dropped from a value of $FC_d \approx 40$ μl/min (≡ 1400 g/t) to $FC_d \approx 7$ μl/min (≡ 217 g/t); this lowered the yield from 79 % to 20 %.

The sparger system was changed to a filter cloth for runs KKLC12-KKLC14. Frother was added to the pulp in the Denver conditioning cell as a frother water dispersion (as described in section 4.2.1). Two surfactant water concentrations were used, viz. 200 and 575 μl HTEB/l water; the corresponding frother dosage rates, FC_d, are indicated in Table 4.13.

The high solids throughputs (F_s = 1.7 t/hr.m^2) used for runs KKLC12 and KKLC13 were achieved by increasing the volumetric slurry feedrates, thus effectively shortening the solids residence times in the pulp phase. Reduced pulp phase kinetics were therefore responsible for the lower yields obtained compared with earlier runs. Carrying capacity limitations were unlikely to have been an influencing factor since in a prior run (KKLC9) a solids production rate , C_p, of ≈ 1 t/hr.m^2 had been attained. The increase in yield between runs KKLC12 and KKLC13 can probably be attributed to raising the frother dosage rate from 9 μl/min (138 g/t) to 23 μl/min (357 g/t).

The surfactant dosage rate was reset to ≈ 8 μl/min for run KKLC14. The collection zone height was increased from 2.75 to 5.25 m and the solids feedrate lowered to 0.5 t/hr.m^2. The product yield of 74 % obtained suggests that the longer pulp residence time was responsible for the improvement in mass recovery compared with run KKLC11, where at a similar surfactant addition rate, only a 20 % yield was obtained. Although the absolute frother addition rate was only 8 μl/min, because the slurry feed velocity and solids feedrate were half those of the

other tests, the frother concentration was large on a g/t (≈ 400) basis. In addition, the substantially higher collector dosage (≈ 12000 g/t) used for run KKLC14 compared with that used for run KKLC11 (≈ 7000 g/t) might also have improved the yield. Despite these confounding factors, the result of column trial KKLC14, when considered in conjunction with the observed affect of volumetric slurry feedrate on yield noted above, suggests that the kinetics of particle collection in the pulp phase strongly influenced the overall rate of flotation.

The solids feedrate, F_s, was again raised to 1.7 t/hr.m^2 for column trial KKLC15. An 11 % ash coal concentrate was obtained at a yield of 87% and, moreover, the concentrate solids production rate was 1.5 t/hr.m^2. In run KKLC16 the air rate was increased to 2.1 cm/s. This caused the ash content of the coal concentrate to increase from 11 % ash to 18 % ash despite a deeper froth bed, FH=0.75 m and a higher washwater addition rate, J_w=0.44 cm/s, than was used in KKLC15. Interestingly, as was the case for run pairs KKLC1 and KKLC2, an increase in air rate did not improve product yield. Also, a washwater velocity of 0.44 cm/s is comparatively high (see section 2.5 above), consequently one might postulate that this caused channeling (mixing) in the froth bed. As a result, the washwater failed to suppress gangue entrainment adequately.

The final column run, KKLC17, was conducted at low frother and collector dosage rates but at a high solids feedrate, F_s = 1.6 t/hr.m^2. The low solids production rate, C_p = 0.1 t/hr.m^2, and the poor yield (≈ 5 %) obtained suggests that slow pulp phase kinetics was the cause of this result. The solids loading capacity of the froth bed must also be considered. For runs KKLC9 to KKLC17 the lowest yields (with the exception of run KKLC12 noted above) were obtained when the frother dosages were between 100 and 300 g/t. Conversely, only at levels above 400 g/t were high yields (≈ 70 %) attained.

4.4.6 Summary of Kleinkopje Laboratory Column Testwork

Column flotation of Kleinkopje thickener underflow produced coal concentrates at grades approaching the ideal flotation ("release") and float/sink separation curves. In particular, it was possible to obtain

a 10 % ash coal product at yields of between 70 to 75 %. This was achieved at concentrate production rates, C_p, of up to 1.0-1.5 t/hr.m^2.

The high inertinite content (71 %) of the composite Kleinkopje sample rendered them poorly floatable. Collector dosages in excess of 5000 g/t were required to achieve the 70-75 % product yields mentioned above. This is comparable to the collector dosages used during the plant trials (CC $\approx$ 6000 g/t). In other words, the use of a consistent feed composition did not lower the dosages of collector required.

Increasing air flowrate from 1.6 cm/s to 2.1 cm/s was found to increase the ash content of the concentrate by between 3 % and 7 % ash.

Increases in frother dosage (above 300 g/t) improved mass recovery only when the collector dosage was in excess of 5000 g/t, i.e. increase in yield were obtained only when the feed to the column was adequately floatable.

As increasing the volumetric slurry feedrate was observed to reduce the yield and conversely, lengthening the collection zone from 2.75 m to 5.25 m, was found to improve mass recovery, it was deduced that the overall rate of flotation was influenced predominantly by pulp phase kinetics.

4.5 LABORATORY COLUMN FLOTATION OF GREENSIDE THICKENER UNDERFLOW SAMPLE

4.5.1 Introduction

The collector dosages used (in excess of 5000 g/t) for the column flotation tests conducted on Kleinkopje underflow samples (section 4.4 above and Chapter 5 below) approach uneconomical levels. As stated in Chapter 1, the Witbank coalfield is the most commercially important in South Africa. Consequently it was decided to attempt column flotation on another coal sample mined from the Witbank No 2. seam. A sample of thickener underflow fines from the Greenside Colliery was chosen since this coal has been used extensively in flotation studies conducted within the UCT Chemical Engineering Department (Fickling, 1985;

Franzidis; 1987, 1988) and is known to be floatable at acceptable (≈ 1000 g/t) collector dosage levels.

As was the case with the Kleinkopje column testwork, the primary objective of these tests was to determine what grade of concentrates could be produced in a column cell compared with other separation methods. Hence, the results obtained from the column cell were compared with conventional batch flotation tests. Operating parameter effects were also investigated; a Resolution III, 2^{7-4} two-level fractional factorial design was used. Significant parameters were identified and compared with the findings of the laboratory column tests performed on the Durnacol and Kleinkopje thickener underflow samples. These points are elaborated further in the sections which follow.

4.5.2 Sample Characterisation

The petrographic composition, proximate analysis and size distribution characterising this underflow sample were presented in section 3.2. Bulk feed ashes of the samples used for batch and column flotation tests are tabulated below.

The column and batch feed ash contents can be seen to be in good agreement.

Table 4.14 : Greenside thickener underflow feed sample properties

Sample Type	Number N	Average X_{avg}	Sample deviation s
Column	9	20.64	1.65
Batch†	2	20.90	0.90

† based on reconstituted feeds

4.5.3 Description of Laboratory Column Rig and Operation

The experimental rig was that used for the Durnacol laboratory tests, i.e. a 54 mm internal PVC laboratory column cell and all its accompanying equipment (see section 4.2.1). A similar mode of column operation was applied, except that collector was not continuously dosed as an oil/water emulsion but added in bulk to the 400 l feed pulp tank immediately prior to column startup, i.e. mode 1. conditioning was used. A conditioning period of half an hour was allowed before coal slurry was pumped from the pulp tank directly to the column. ShellsolA and HTEB were again used as the collector and frother reagents, respectively.

4.5.4 Selection of Operating Parameters

A total of 15 runs were performed. Two batches of coal slurry were used. Parameters varied included collector dosage, CC; column height, (CH); froth height, (FH); slurry feedrate, (QF $\equiv J_f$); pulp density, (PD, m/v basis); air flowrate, (AF $\equiv J_g$); washwater rate, (WW $\equiv J_w$); sparger type, (ST); and "USBM" sparger water addition rate, (SW).

Initial runs were conducted at a low feed pulp solids content ($\approx$3 % m/v) which corresponded to solids feedrates, F_s of between 0.5 - 1.0 t/hr.m^2. The operating parameters selected are summarised in Table 4.15.

Subsequently, tests were conducted (with a fresh batch of coal fines) at a feed slurry density of 8 % m/v. The particulars of these tests are listed in Table 4.16. The basis for parameter combination selection was a 2^{7-4}_{III} fractional factorial design. The parameters investigated were all those listed above, excluding collector dosage, (CC); pulp density, (PD); and "USBM"sparger water addition rate, (SW).

4.5.5 Flotation Results

The overall results of the column flotation tests are shown in Figure 4.12. Batch flotation results are included for comparision. The batch tests were conducted at a pulp density of approximately 8 % m/v. Details of the batch flotation testwork are available in Appendix C3.

Laboratory column testwork - Greenside thickener underflow sample

Table 4.15 - Summary of column operating parameters, 3 % feed pulp density

Run ID	FC ul/l	CC g/t	CH	FH	Jf cm/s	SF t/hr.m2	Jg cm/s	Jw cm/s	SW l/min	% Yield	Conc % ash	MFeed % ash	CFeed % ash	Cp t/hr.m2	P.D.
GRNSLC1	30	97	3.50	0.7	0.57	0.672	1.34	0.15	0.94	17.25	5.32	21.08	24.46	0.116	3.29
GRNSLC2	30	97	3.50	0.7		0.996	1.34	0.15	0.94	18.45	5.66		20.98	0.184	
GRNSLC3	30	97	3.50	0.7		0.734	1.34	0.21	0.94	26.23	6.04	22.11	22.23	0.193	
GRNSLC4	30	97	3.50	0.7		0.745	1.34	0.21	0.94	28.36	6.07		23.35	0.211	
GRNSLC5	30	670	3.50	0.7	0.45	0.455	1.34	0.21	0.94	44.48	6.99	19.27	21.24	0.202	2.80
GRNSLC6	30	670	3.50	0.7	0.47	0.506	1.34	0.21	0.94	48.33	7.58	19.59	21.98	0.245	2.97

Table 4.16 - Summary of column operating parameters, 8 % feed pulp density

Run ID	FC ul/l	CC g/t	CH	FH	Jf cm/s	SF t/hr.m2	Jg cm/s	Jw cm/s	SW l/min	% Yield	Conc % ash	MFeed % ash	CFeed % ash	Cp t/hr.m2	P.D.
GRNSLC7	25	1015	2.75	0.25	0.44	1.20	2.73	0.21	1.20	77.32	12.04	21.38	18.32	0.929	7.52
GRNSLC8	25	1114	2.75	0.25	0.48	1.23	2.73	0.21	1.20	78.14	12.71	19.59	19.35	0.963	7.12
GRNSLC9	15	1092	2.75	0.50	1.11	2.87	1.75	0.21	1.20	3.93	5.84	20.73	20.15	0.113	7.21
GRNSLC10	15	1073	3.50	0.50	0.47	1.30	2.73	0.15	1.20	16.25	7.38	19.90	17.38	0.211	7.76
GRNSLC11	25	983	3.50	0.25	0.96	2.82	1.75	0.15	1.20	3.36	5.76	19.71	19.89	0.095	8.16
*GRNSLC12	15		3.50	0.25	0.92	2.50	2.73	0.21		4.97	8.16	22.16	20.55	0.124	7.58
*GRNSLC13	25		3.50	0.50	0.54	1.70	1.75	0.21		14.09	8.36	21.17	19.37	0.240	8.79
*GRNSLC14	15	1180	2.75	0.25	0.41	0.99	1.75	0.15		16.19	6.81	17.74	17.71	0.160	6.74
*GRNSLC15	25	1076	2.75	0.50	0.87	2.61	2.73	0.15		16.66	9.55	23.40	21.03	0.435	8.30

Note : CH is the distance between feed and sparger ports

Mfeed refers to measured feed ash

Cfeed refers to calculated feed ash

* indicates filter cloth sparger used, other tests "USBM" sparger used

For the column tests performed at the 3 % m/v pulp density, LAC (≈ 7.5 % ash) was produced at a maximum yield of approximately 45 %. However, the corresponding concentrate solids rate, C_p, was only 0.25 t/hr.m^2. Poorer grades and recoveries were obtained from the higher (8 % m/v) pulp density column runs; the best result achieved was a 12 % ash concentrate at a 78 % yield. The corresponding solids production rate, C_p, was 1.0 t/hr.m^2 which was comparable to that attained in the Durnacol and Kleinkopje column flotation trials.

Yield and grade contrast effects for the input parameters investigated are given in Table 4.17. The fractional design is only of Resolution III, hence main effects and two-factor interactions are confounded. Nonetheless, it appears that the yield and recovery responses were influenced by air flowrate, AF, frother dosage, FC, slurry feedrate, QF, and column height, CH, input parameters. The results broadly agree with the Durnacol factorial design experiment (section 4.3.5 above) where frother concentration, air flowrate and slurry feedrate were found to be the dominant parameters affecting yield and recovery.

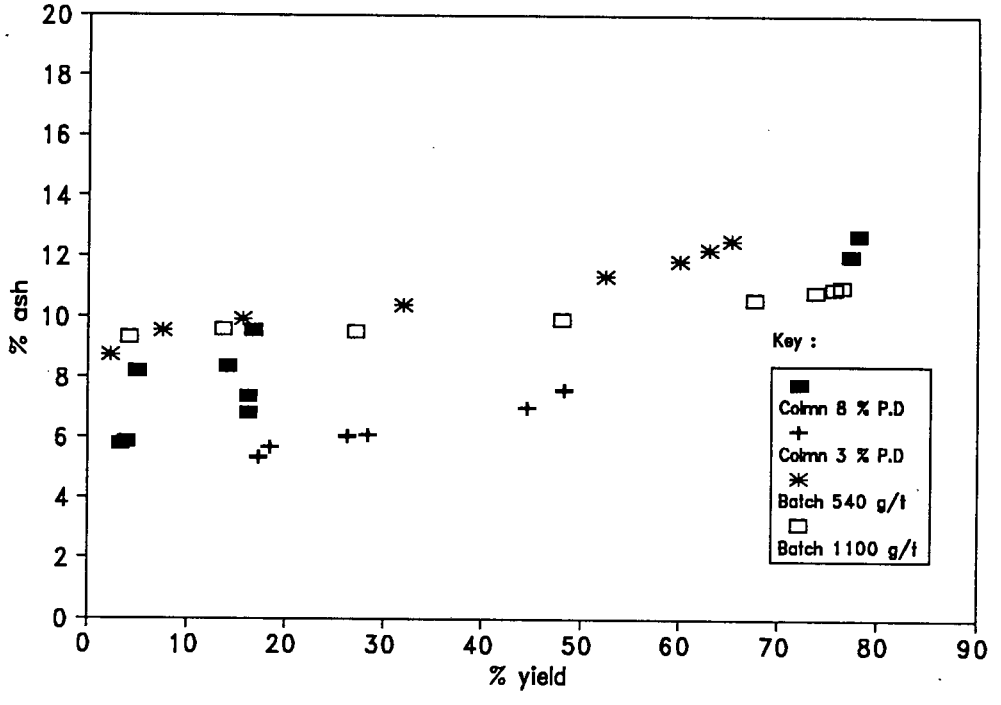

Figure 4.12 : Global results : Greenside thickener underflow fines.

Table 4.17 : Input variable (main) contrast effects

Parameter	Symbol	Net Response changes % Yield E_{Yld}	% Recovery E_{Rec}	% Ash E_{Ash}
air flowrate	AF	19.61	21.20	1.91
frother dosage	FC	17.73	19.15	1.19
sparger type	ST	12.44	13.08	0.22
column height	CH	-19.06	-20.65	-0.46
slurry rate	QF	-23.94	-25.96	-2.01
froth heigh	FH	-12.93	-13.65	-1.10
washwater rate	WW	12.17	12.81	1.91

The Durnacol fines sample was of coking quality and contained 85 % vitrinite. In contrast, the Greenside thickener underflow fines were bituminous with a 40 % vitrinite content (section 3.2). Hence the (pulp phase) flotation kinetics would be slower than for the Durnacol coal fines. This explains why collection zone height had an effect on coal yield and recovery. This finding is in agreement with the results of the Kleinkopje column testwork where it was also concluded that the kinetics of particle collection in the pulp phase affected the rate of flotation.

Unlike the Durnacol factorial experiment where the concentrate ash content increased by an average of 7 % ash between the low (-) and high (+) frother dosage levels, no single parameter had a significant overall (average) effect on the grade of Greenside thickener underflow concentrates.

A further examination of Tables 4.15 and 4.16 reveals some interesting features regarding combinations of operating parameter levels. Firstly the washwater addition rates used were low (J_w = 0.15, 0.21 cm/s) compared with those used in Durnacol column runs. The air rate used for the 3 % feed pulp density column runs, viz. J_g = 1.3 cm/s, was rather lower than the superficial gas velocities of 1.7 and 2.7 cm/s used for the column runs performed at feed pulp densities of ≈ 8 % m/v.

Size and ash-by-size analyses were performed on run GRNSLC 8 (Table 4.16). The results of these size analyses are reported in Table 4.18.

Some explanation of the terms used in the Table is appropriate. For convenience the feed is considered to consist of two components, viz. mineral-free carbonaceous matter (dry-ash-free coal) and gangue mineral. The assumption is made that the mass of ash is equal to the mass of uncombusted mineral. As stated in section 2.1 the difference between the mass of the ash product compared with the uncombusted mineral matter can reasonably be assumed negligible.

As may be seen from Table 4.18, two-thirds of the feed "coal" was finer than 75 μm. This size fraction also contained most of the "ash" material (14.90/20.24 $\approx$ 74 % of the total gangue material present per 100 g feed). More than half ($\approx$ 55 %) of the feed sample was finer than 45 μm.

Table 4.18 : Average d.a.f. Coal in Feed and Concentrate by Size Fraction

Column Yield = 78.14 % ; % coal Recovery = 84.58
Basis - 100 g Feed

Screen size	Feed		Concentrate		% coal Recovery
	g coal	g ash	g coal	g ash	size i
+150 μm	14.03	2.23	3.30	0.28	23.51
-150+105 μm	7.72	1.46	5.97	0.68	77.34
-105+75 μm	7.88	1.65	7.34	0.99	93.19
- 75+45 μm	8.01	1.69	9.83	1.36	100*
- 45 μm	42.13	13.21	41.73	6.66	99.05
Total	79.76	20.24	68.17	9.97	

* calculated recovery exceeds 100 %, $\approx$ 50 g sample used for screening which implies only $\approx$ 4 g present in -75+45 μm fraction

An examination of the concentrate size and grade-by-size data reveals that virtually all the d.a.f. coal present in feed size fractions below

105 μm was recovered in the concentrate product. Also, the coarser +105 μm size fractions were not as readily floated as the finer sizes. This is consistent with the particle size / floatability effects discussed in sections 2.2.3 and 2.5.1 where it was noted that an optimum size range for flotation exists and that induction times required for coal particle-bubble attachment follow an order of magnitude relationship with respect to particle size (where $d_p \approx 50$ - 1000 μm). The ash content of -105 μm size fractions was reduced from 16.55 g ash to 9.01 g (per 100 g feed), a reduction in ash content of over 50 %. However, the overall yield/grade result (see Figure 4.12) lies in the region of the batch float data which indicates that some entrained material still remained in the concentrate product.

4.5.6 Summary and Conclusions

It was found that using a column cell it was possible to produce LAC coal (≈ 7.5 % ash) at yields of up to 45 % from flotation of Greenside thickener underflow. However, this was only achieved at dilute feed pulp densities (3 % m/v) and relatively low production rates (C_p , 0.25 t/hr.m^2). At higher feed pulp densities (8 % m/v) the best result obtained was a 70 % yield of a 12 % ash coal concentrate. The corresponding solids production rate, C_p, of 1 t/hr.m^2 was similar to the rates obtained from column tests conducted on samples of Durnacol and Kleinkopje thickener underflow.

Analysis of the 2^{7-4}_{III} fractional factorial design indicated that air flowrate, AF; frother dosage, FC, slurry feedrate, QF; and column height, CH; were the operating parameters which most affected yield and recovery. The first three parameters listed above were also found to be significant in the Durnacol laboratory column testwork. It is proposed that column (collection zone) height, which had no influence on column flotation of the Durnacol sample, affected column yield and recovery of Greenside thickener underflow because this coal is bituminous and slower floating than Durnacol; hence pulp phase kinetics are important. This conclusion is corroborated by the findings of the Kleinkopje column testwork. Yields and recoveries of this coal, which was shown to be poorly floatable (section 3.4), were also affected by changes in column height (and slurry feedrate).

No parameter effects on concentrate grade were distinguishable.

Size analysis of a feed and concentrate sample showed that particle sizes, d_p, below 105 μm were the most readily recovered. This is in agreement with the coal particle size versus recovery relationships reported in section 2.6.1 where it was noted that sizes of $d_p \approx 80$ μm or less (down to ≈ 10 μm) are optimal for column flotation of coal fines.

4.6 COLUMN FLOTATION OF MILLED GREENSIDE ULTRAFINES

4.6.1 Introduction

The column flotation tests conducted on the sample of Greenside thickener underflow (section 4.5 above) indicated that it was possible to produce LAC ($\approx$ 7.4 % ash) concentrates at yields of up to 45 %. It is probable that the yield of LAC produced from column cell flotation of Greenside thickener underflow would increase if there was better liberation of the mineral gangue from the coal matrix. A reduction in particle sizes would improve the liberation characteristics of the Greenside sample. This can be achieved by milling the thickener underflow sample.

Previous liberation studies conducted on Witbank No.2 seam coals (Harris, 1987; Buys, 1989) indicated that unless grinds finer than 25 μm are produced, communition does not substantially improve liberation of mineral gangue from coal macerals, a result which is largely attributable to the syngenetic nature of mineral deposition within Gondwanaland coals. Thus if physical separation processes are to produce significant quantities of low ash or super-low ash coals, they require finely ground material.

Separation of ultrafine species by conventional froth flotation is traditionally considered problematic because of the difficulty of suppressing unselective particle recovery through hydraulic entrainment. As noted in Chapter 1 and section 2.5 column flotation cells are widely used in cleaning applications because of their ability to achieve better particle separation efficiencies (i.e. reduced entrainment) compared

with single stage conventional flotation cells. In this phase of experimentation the objective was to evaluate the use of a column cell in producing low-ash quality coal from a sample of Greenside thickener underflow milled to ultrafine sizes and to compare the results with column flotation of the "as is" thickener underflow sample. The results could also be compared with conventional froth flotation of the milled sample and the characteristic washability curve of the milled sample.

The coal sample preparation procedure followed and the manner in which the column and batch floats were performed are described below.

4.6.2 Sample Preparation and Characterisation

The ultrafine coal sample was produced from a dry sample of "as is" Greenside thickener underflow. A 1 kg sub-sample of the "as is" thickener underflow was mixed with 3 l of Cape Town tap water. The slurry was then placed in a 31.6 cm diameter stainless rod mill containing 20 rods, and milled for 65 minutes at a rotational speed of approximately 70 rpm.

The size distribution of the milled product is given in Table 4.19. The ultrafine feed sample was 95 % finer than 45 μm and 80 % finer than 25 μm. Averages of bulk ash contents of ultrafine feed samples taken from column flotation tests, batch flotation tests and a float/sinks analysis (section 3.2 above) are reported in Table 4.20.

Table 4.19 : Greenside ultrafines size distribution properties

Size fraction	% Passing
-150+75 μm	1.5
- 75+45 μm	4.0
- 45+25 μm	13.7
- 25 lm	80.8
Total	100.0

Table 4.20 : Greenside ultrafines bulk feed ash properties

Sample type	Number N	Average Xavg	Sample deviation s
Column	6	19.07	0.33
batch	2	18.90	0.24
F/sinks†	1	19.57	
Total	8	19.09	0.34

† ash content of 100 % floats at S.G. = 1.7

Buys (1989) performed a size analysis on a sample of the -25 μm fraction of Greenside thickener underflow milled as described above. The size analysis was done on a Malvern 2600/3600 Particle Sizer. The results of this analysis are reported in Table 4.21. The difference between the proportions of -25 μm material reported in Tables 4.19 and 4.21 can be ascribed to experimental error. Grinding to ultrafine sizes did not generate much sub 5 micron material.

Table 4.21 : Greenside ultrafines, -25 μm size distribution properties

Size fraction	% Passing
+23.5 μm	12.87
- 23.5+10.5 μm	33.03
- 10.5+5.0 μm	23.75
- 5.0+1.2 μm	13.28
-1.2 μm	0.17
Total	83.00

4.6.3 Experimental Procedure

4.6.3.1 Equipment description and operation

The column testwork was carried out in the 90 mm diameter perspex column cell which was described in section 4.2.2. A baffled 120 l PVC tank

fitted with a mechanical impeller was used as a column feed reservoir. Pulp suspension was maintained by a pitched paddle impeller rotating at a speed of 100 rpm.

Depending on the pulp density required, between two and four batches of milled sample were mixed with tapwater in the 120 l PVC tank to make up a total pulp volume of 100 l. The required volume of collector was added to the coal pulp via a syringe inserted below the pulp surface. After 10 minutes of conditioning, frother was added to the pulp in a similar manner and conditioning continued for a further 3 minutes. Two variable speed peristaltic pumps were used to deliver slurry feed and remove tailings discharge. The pulp-froth interface was controlled by manually adjusting the tailings flowrate.

Once steady state had been reached, simultaneous concentrate and tails samples were taken. Sample times of 2 minutes and 1 minutes were allowed for the concentrate and tails samples respectively. It was possible to run at two or three column steady state conditions with each pulp batch. A slurry sample was taken from the feed tank after the final steady state condition was reached.

4.6.3.2 Flotation reagents

ShellsolA was the collector used for this series of tests. Ethyl hexanol was used as a frother in two of the runs while di-iso-butylketone (DIBK) was used as the standard frothing agent for the remainder of the tests.

4.6.3.3 Comparative tests

As noted in section 3.2 above, the method of Franzidis and Harris (1986) was used for float/sink analyses.

Two batch floats were performed in a 3 l bottom driven modified Leeds cell. The standard flotation procedure described in Appendix G1 was followed, except for the following two minor modifications :

(a) The distance from the pulp-froth interface to the concentrate overflow lip (i.e. froth bed depth) was increased to 27 cm by superimposing square perspex sections on the cell base.

(b) Laboratory grade 2-ethylhexanol was added to the coal pulp at a dosage level of 150 μl/l. In order to prevent coagulation of the ultrafines, 165 mg of a dispersant, sodium hexametaphosphate [$Na_6(HPO_3)_6$], was also added to the pulp.

4.6.4 Testwork Results

A summary of the operating parameters investigated during the testwork and the results obtained are presented in Table 4.22. The yield/grade results are plotted in Figure 4.13, as are the results of column flotation tests conducted on the "as is" thickener underflow, and the batch flotation tests and float/sinks analysis performed on the milled sample. The batch flotation and float/sinks data are presented in Appendix C.

It is evident that, for the parameter levels tested, virtually ideal separation of the liberated mineral gangue from the coal-mineral matrix was achieved from column flotation of the ultrafine coal. As the mineral clay impurities in the coal matrix are $\approx$ 1-2 μm in size, complete liberation of the mineral from the coal macerals was not achievable. It was, however, possible to produce low ash quality coal concentrates at yields of up to 70 %. As stated in the introduction to this section, the highest yield of LAC obtained from column flotation of the "as is" thickener undeflow was 45 %, therefore milling the coal to a d_{80} of 25 μm increased the yield of LAC by 25 %. In fact, concentrate grades of between 4-5 % ash were produced. This is directly attributable to the characteristic features of the column cell discussed in Chapter 2, namely high particle-bubble collision efficiencies and suppression of entrainment attainable with a countercurrent flotation column. Conversely, in conventional cells pulp water is required to create a deep froth bed. Some entrainment of gangue into the coal product is, at least in the preliminary stages of batch flotation, inevitable; this explains the relatively poor inital grades produced under deep froth flotation.

Table 4.22 : : Summary of Greenside ultrafines column run conditions and yield/grade results

Key :

CC = Collector dosage
FT = Frother type, (i) 2-ethylhexanol (ii) DIBK
FC = Frother dosage in feed pulp tank
Jf = superficial feed slurry velocity
Sf = solids feedrate
P.D = pulp density
Jg = superficial air velocity (@ 1 atm)
Jw = superficial washwater addition rate

Run ID	CC g/t	FT	FC ul/l	Jf cm/s	Sf t/hr.m2	P.D % m/v	Jg cm/s	Jw cm/s	% Yield	% Rec	Conc % ash	Meas Feed % ash
1-1	0	(i)	150	0.27	0.39	4.0	2.3	0.78	32.48	38.08	6.00	
1-2	0	(i)	150	0.27	0.39	4.0	2.3	0.78	34.47	40.08	5.89	18.98
2-1	500	(ii)	80	0.25	0.26	3.0	2.3	0.78	58.62	67.55	7.13	
2-2	500	(ii)	80	0.25	0.28	3.0	2.3	0.78	51.62	60.56	6.71	19.48
3-1	500	(ii)	80	0.37	0.26	2.0	2.5	0.78	68.27	77.50	7.38	
3-2	500	(ii)	80	0.39	0.28	2.0	2.5	0.78	63.20	73.49	7.40	
3-3	500	(ii)	80	0.39	0.26	2.0	2.5	0.78	66.44	76.12	7.40	19.38
4-1	1000	(ii)	80	0.20	0.14	2.0	2.5	0.78	68.74	78.44	6.94	
4-2	1000	(ii)	80	0.20	0.14	2.0	2.5	0.78	69.25	78.83	6.79	
4-3	1000	(ii)	80	0.19	0.14	2.0	2.5	0.78	64.47	74.43	6.79	19.10
5-1	100	(ii)	80	0.37	0.26	2.0	2.3	0.78	56.36	64.59	6.80	
5-2	100	(ii)	80	0.40	0.28	2.0	1.8	0.78	33.73	39.58	5.32	18.59
6-1	100	(ii)	80	0.40	0.26	2.0	1.8	0.78	37.60	44.09	5.67	
6-2	100	(ii)	80	0.40	0.26	2.0	1.6	0.22	23.19	27.40	4.56	18.89

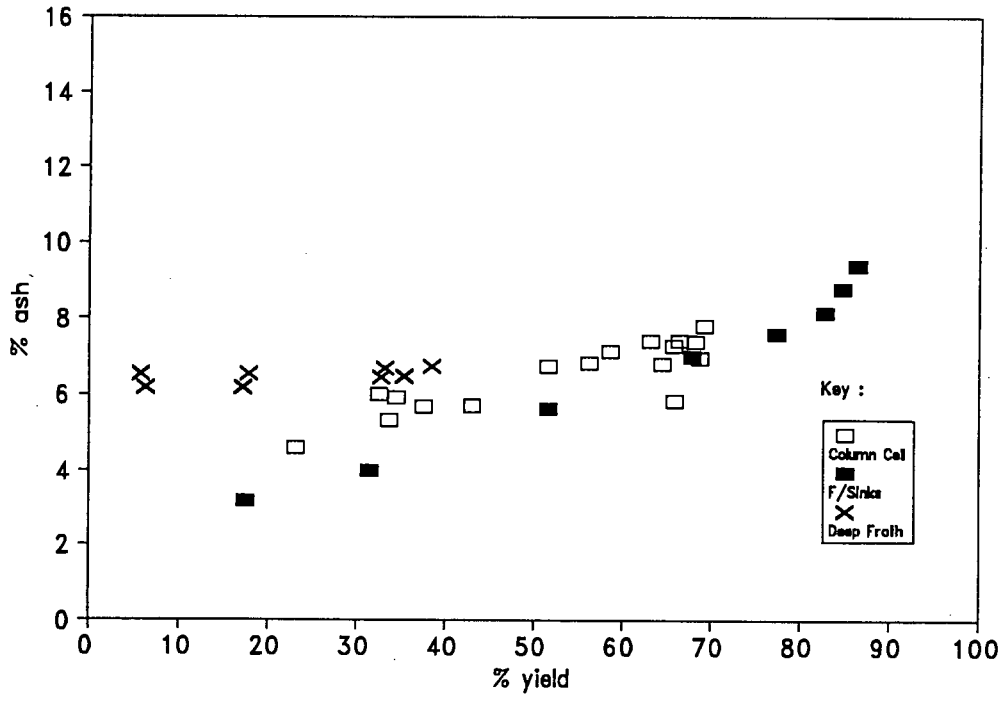

Figure 4.13 : Global results : milled (95 % -45 μm) Greenside thickener underflow fines.

Aside from runs 5-1, 5-2 and 6-1, 6-2 where the air and washwater flowrate levels were changed, all the samples taken within a single pulp batch represent repeat tests at each operating condition.

At a zero collector addition level a 5.9 % ash coal concentrate was obtained at a yield of 33 % (run 1-1 and 1-2). Raising the collector dosage to 100 g/t increased the yield to 56 %, and the ash content of the concentrate to 6.8 % (run 5-1). Reducing the air rate from 2.3 cm/s (run 5-1) to 1.8 cm/s (run 5-2) lowered the yield/grade result to that obtained on runs 1-1 and 1-2 (i.e. a 5.3 % ash concentrate at a 34 % yield).

The d_{80} of the feed was 25 μm thus the solids loading capability of the froth was probably the factor limiting mass recovery. A reduction in the washwater addition rate from J_w = 0.78 cm/s to Jw = 0.22 cm/s (runs 6-1 and 6-2) also caused the yield to drop. The former rate is rather higher than those normally used (section 2.5 above). Increased coalesecence in the froth bubble bed, which again reduces froth solids loading (at the overflow lip the bubble diameter was visually estimated to increase from ≈ 2 mm to ≈ 5 mm when the washwater rate was lowered), was the factor responsible for this phenomenom.

Raising the collector dosage to 500 g/t (runs 2-1 and 2-2) did not increase product yield compared with run 5-1. However, increasing the air rate slightly from 2.3 cm/s to 2.5 cm/s (runs 3-1 to 3-3) raised product yields by about 10 % to an average of 65 %. A further increase in collector dosage to a level of 1000 g/t also did not improve yields (runs 4-1 to 4-3).

The solids production rates attained can be inferred from the solids feedrate and yield data listed in Table 4.22. The maximum coal solids production rate, C_p, achieved was $\approx$ 0.2 t/hr.m^2. Similar values of C_p were recorded for the column tests on the "as is" thickener underflow from which LAC coal concentrates (section 4.5.5) were produced.

4.6.5 Summary and Conclusions

It has been shown that it is possible to obtain an LAC yield of up to 70 % from column flotation of a milled ultrafine (d_{80} = 25 μm) sample of Greenside thickener underflow. This compares favourably with the maxium LAC yield of 45 % attained from column flotation of a sample of the "as is" thickener underflow.

Also, these tests have demonstrated that in using column flotation, it is possible to completely suppress the entrainment of fine material into the concentrate (yield/grade results falling on the float/sinks release curve were obtained).

Collector (ShellsolA) dosages of 100 g/t were found to be sufficient for column flotation of Greenside ultrafines. In fact, air rate had a far stronger influence on yield than did collector dosages beyond 100 g/t; increases in yield of up to 20 % were attained upon raising air rate. Lowering the washwater rate to J_w = 0.22 cm/s caused coalescence in the froth bubble bed and reduced yield by about 10 %. Extremely fine feeds severely limit production capacities (see section 2.3 above) which was why the solids throughputs used ($S_f \approx$ 0.14-0.39 t/hr.m^2) were lower than those conventionally used for coal columns ($S_f \approx$ 1.4-2.5 t/hr.m^2, see section 2.5 above).

4.7 OVERALL EVALUATION OF LABORATORY COLUMN TESTWORK

Laboratory column tests have shown that it is possible to produce coal concentrates at recovery/grade efficiencies approaching the ideal flotation and washability curves.

Column tests on the Durnacol thickener underflow sample produced the poorest results in terms of flotation performance (efficiency) : recovery/grade data points generally fell above the release flotation and washability curves, although they remained below those obtained from standard batch flotation tests. The best column results obtained were a 60 % product yield at 12 % ash; and a 75 % yield at 13 % ash (coking quality coal should have an ash content of less than 12 %). Corresponding concentrate production rates, C_p, were 1.3 and 1.6 t/hr.m^2 respectively. However, the Durnacol laboratory column tests were based on a 2-level (high (+) and low (-)) fractional factorial design (see section 4.2.5) and were not aimed at optimising flotation performance. Fractional factorial designs are used as screening designs in the preliminary phases of an experimental programme; their major purpose is to identify input parameters which most significantly affect a process rather than obtaining optimal results. Typically, once the key variables affecting a process have been identified from a screening design, further experiments are performed with the objective of obtaining values of the key parameters which give optimal process performance. In the case of the Durnacol laboratory column testwork insufficient sample was available for proceeding with further experiments once the screening design was completed. Consequently, it is likely that if a further series of optimisation experiments had been performed better results would have been obtained.

The recovery/grade results obtained from column flotation tests on the composite sample of Kleinkopje fines fell, with two exceptions, on the flotation release or washability curves. The flat shape of these curves, however, indicated that the liberation characteristics of the coal sample were rather poor. For example, for product grades of between 7 and 8 % ash, release float yields ranged from approximately 30 % to 60 %. Concentrates with ash contents of below 10 % were produced at yields of up to 80 % and at production rates, C_p, of between 0.4-0.9

t/hr.m^2. The high inertinite content (70 %) rendered the Kleinkopje fines poorly floatable; consequently ShellsolA collector dosages in excess of 5000 g/t were required to obtain product yields much above 20%.

It is interesting to note that although the Kleinkopje fines were difficult to float, coal recoveries and grades attained in the laboratory column cell were better than those of the readily floatable Durnacol sample. This is because of the different liberation characteristics of the two coals. The float/sinks washability curves characterising Durnacol thickener underflow fines (Figure 4.2) lies above that of Kleinkopje (Figure 4.11) sample when the yield exceeds 60 %. However, the collector dosages required for column flotation of the Durnacol fines were only ≈ 1500 g/t compared with the dosages of 5000 g/t or greater required for flotation of the Kleinkopje fines.

Low-ash (7.4 % ash) coal concentrates were obtained from the milled ultrafine (d_{80} = 25 μm) Greenside sample (average bulk feed ash content 19.0 %) at yields of up to 70 %. However, this was achieved only at low solids throughputs; concentrate solids production rates, C_p, were between 0.07-0.15 t/hr.m^2. At dilute (≈ 3 % m/v) pulp densities, low ash coal was also produced from unmilled Greenside thickener underflow at yields and concentrate production rates of up to 45 % and 0.20 t/hr.m^2 respectively. Size analysis showed that 55 % of the unmilled thickener underflow sample was finer than 45 μm and 15 % coarser than 150 μm. At a maximum overall yield of 78 %, only one quarter of the +150 μm feed fraction was recovered, a result consistent with size/recovery effects discussed in section 2.5.1 above. The influence of particle size on flotation recovery is further evaluated in Chapter 5.

Given that flotation performance is evaluated chiefly on the basis of grade rather than throughput, the column tests indicate that optimal solids production rates lie below the actual carrying capacity of the froth bed. This was evident particularly from the column tests performed on the Durnacol and Greenside thickener underflow samples where, although concentrate solids rates of up to 1.0-2.0 t/hr.m^2 were attained, in agreement with values reported in literature (e.g. Reddy et

al, 1988), the grades were generally above the float/sinks or release flotation curves.

Air flowrate, AF, was found to affect coal recovery and yield for the (both milled and "as is") Greenside and Durnacol samples; an increase in air flowrate raised recovery and yield (and vice versa). However, air flowrate had no effect on the column flotation of Kleinkopje fines. The effect of air flowrate on grade is discussed below. The column tests conducted on the milled sample of Greenside thickener underflow indicated that for the ultrafine feed ($d_{80} \approx 25$ μm) air rate strongly affected yield. This suggests that mass recovery from the froth bubble bed is limited by the rate of generation of bubble surface area; or equivalently, carrying capacity is strongly sensitive to air rate when the column feed is very fine.

Particle collection in the pulp phase was found to be strongly influenced by the petrographic composition of the feed. For the Durnacol sample, which had a vitrinite content of 85 %, pulp phase kinetics had a negligible effect on recovery. Conversely, for the Greenside and Kleinkopje coals, which had vitrinite contents of 40 % and 27 % respectively, increasing column height, CH, or reducing volumetric slurry feedrate, QF, did improve recoveries. Slurry feedrate, QF, was found to be a significant variable for the Durnacol column tests because the change in solids content which occurred as the level of QF was changed (tank pulp density was approximately constant at 8 % m/v) affected the solids loading kinetics of the froth bubble bed.

The fractional factorial design performed on the Durnacol fines showed that frother dosage was the dominant variable determining coal recovery and ash content. Coal recovery (and yield) both increased on average by 50 % when the frother dosage level was raised from 50-150 g/t to 350-650 g/t. Product ash content increased on average by 7.0 %. An increase in flotation recovery and a reduction in the washing (drainage) of the froth bed both contributed to poorer product grades at the high (+) frother concentration level. An increase in frother dosage from 15 to 25 μl/min increased the average column yield of Greenside thickener underflow by 17 %. For the Kleinkopje tests, higher frother dosages only improved mass recovery when the collector dosage was above 5000 g/t.

In general, the cleaning performance of the froth bed was found to be erratic. Air flowrate was found to be the most important parameter affecting grade : if this was low (J_g < 1.5 cm/s) shallow froth beds and low washwater rates were sufficient. Washwater rate did not appear to influence yield or grade for the column runs conducted in the 2" column. Parekh et al (1986), who also investigated the flotation of coal using a 2" diameter column, found that washwater rate had less of an effect on column performance than did frother concentration, air flowrate and column height. In the larger 90 mm diameter column lowering the washwater rate was observed to reduce yield by 10 %.

It is interesting to note that the best grade/recovery results were obtained on the ultrafine feed sample. The washwater distributor for the column (D_c = 90 mm) in which these tests were conducted had fifty-six holes, 1 mm in diameter, covering a column cross-sectional area of 78 cm^2 whereas the 54 mm (2") ID laboratory column in which the other column tests were conducted (on the thickener underflow fines) had a washwater distributor which had only 12 holes, also 1 mm in diameter, covering an area of 20 cm^2. Thus washwater distributor design (and size) appears to play a role in determining the cleaning efficiency in the froth bed.

Column flotation of the Durnacol fines was not affected by sparger design. However, for this coal overall flotation kinetics were controlled by the froth, not pulp phase. Consequently, it is possible that coal fines where pulp phase kinetics are rate limiting, sparger design is an important parameter. In fact, comparative sparger design tests were performed during the plant trial testwork. This is discussed in Chapter 5.

CHAPTER 5

COLUMN FLOTATION TRIALS AT KLEINKOPJE COLLIERY

5.1 INTRODUCTION

On-site column flotation trials were conducted at Kleinkopje Colliery during April and May of 1990. Coal fines from the thickener underflow streams constituted the feed to the column. These fines are generated as a by-product in the Preparation Plant. The Colliery mines both the upper and lower areas of the Witbank number 2 seam and consequently produces both a steam quality coal (from the upper seam) and low ash coal (from the lower parts of the seam). The thickener fines are a blend of the two coal types.

The aim of the on-site trials was to produce a 27.6 MJ/kg (i.e. steam) coal at maximum yield from a feed of approximately 22 - 24 MJ/kg. In this Chapter, the testwork results are discussed in two essentially independent parts. Firstly, the plant trial runs are evaluated in terms of overall performance criteria like yield, concentrate grade, floatability of different feed size fractions, upgrading within these sizes, etc. The success/failure of the column flotation trials can be inferred from this alone. Subsequently, the effects of column parameter selection are considered, and the results of the on-line plant trials compared with the laboratory column tests.

5.2 PILOT COLUMN LAYOUT AND OPERATION

5.2.1 Pilot Rig Description

A schematic diagram of the column rig is shown in Figure 5.1. During the on-site plant trials at the Kleinkopje Colliery, the column unit was located in the pump house adjacent to the plant thickeners.

The column consisted of four 1.5 m long, 100 mm ID sections of PVC piping. The topmost section, fitted with a launder box, was made from

clear PVC. The position of the pulp-froth interface could therefore be visually distinguished during column operation. The feed port was situated 1.0 m below the overflow lip. The distance from the feed port to the sparger port, i.e. the collection zone, was 4.5 m.

Two sparger types were used during the testwork viz, a filter cloth sparger and an "USBM" sparger. The "USBM" sparger consisted of a 25 cm long 1" inner diameter PVC pipe containing 1 mm glass beads, located outside the column, connected to a copper tube with two 1 mm holes each positioned 45 degrees below the horizontal plane, located inside the column.

Two Masterflex peristaltic pumps, each capable of delivering a flowrate of approximately 10 l/min, were used as feed and tailings pumps. A portable compressor supplied air to the column at a gauge pressure P_g = 4 bar. A centrifugal pressure pump capable of pumping at pressures of between 4 - 5 bar gauge was used to deliver water to the washwater distributor and "USBM" sparger. The water required by the pressure pump was supplied from a 200 l polypropylene tank. Three rotameters, affixed to a portable control panel, were used for controlling addition rates of air, washwater and "USBM" sparger water.

The washwater distributor used was that described in section 4.2.2 above. The distributor was constructed from 6 mm outer diameter copper tubing and consisted of three concentric rings attached to a common, centrally positioned distribution pipe. Fifty-six 1 mm holes were evenly distributed across the centre pipe and its ring branches.

Potable water was used in the "USBM" sparger and the washwater distributor, since plant process water generally contained unacceptable levels of fines which could abrade and block the distributor frits and "USBM" nozzles.

Pulp level was controlled by the method of conductivity measurement described in section 4.2.1. Two 0.9 m long parallel chrome/nickel wires, part of the pulp level control system, ran down the inside walls of the clear PVC section. An electronic controller received the measured voltage signal and, executing a PI control algorithm, varied the tailings pump speed in order to maintain the desired pulp level.

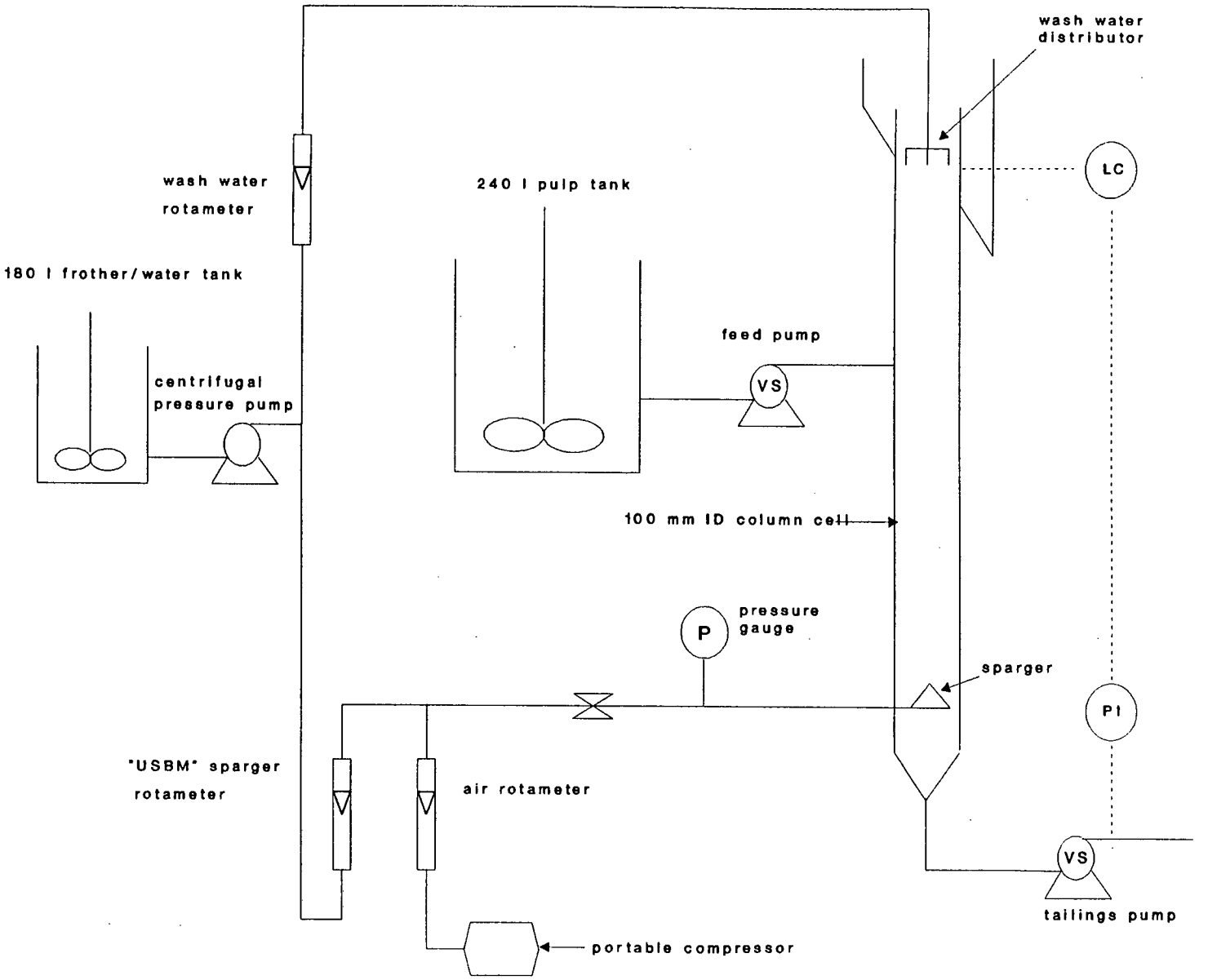

Figure 5.1 : Schematic of pilot column rig.

The pulp feed tank had a capacity of 240 l. The mixer unit comprised a 0.37 kW, 1400 rpm single phase motor and a 150 mm diameter, 30 mm wide flat-bladed type impeller fitted to a stainless steel shaft. This tank was also used for the conditioning testwork described in section 3.4 above.

The ultrafine underflow component from the thickeners constituted the feed to the column. A Delkor linear screen was used to separate the ultrafine fraction, nominally - 150 μm, from coarser oversize material which was discarded.

5.2.2 Column Operation and Sampling

All tests were conducted in a semi-continuous mode. Coal slurry from the linear screen underflow was added to the feed tank and the pulp density adjusted to the desired level, usually about 8 % m/v solids (R.D. 1.020). Collector was then added to the tank. After conditioning the pulp for 10 minutes, the feed pump was switched on.

The time required to reach a steady state condition was estimated as 3 times the nominal collection zone volume of 35 l (including air voidage) divided by the measured tails rate. It was possible to take samples at 2 steady state conditions with each 240 l pulp batch i, designated i.1 and i.2 respectively.

Timed volumetric tails and feed rates were measured at steady state, using a 2 l measuring cylinder, and concentrate and tails samples were taken simultaneously. The feed pump was equipped with a double head; consequently a representative sample of the feed to the flotation column could be obtained directly. Sample times of either 1 or 2 minutes were used.

Ash content, CV and size analyses of samples were performed by AMCOAL's Witbank coal laboratory and by the RICHLAB laboratory in Johannesburg. Results are reported on an air-dry basis.

5.2.3 Flotation Reagents

ShellsolA, a 95 % aromatic oil, was selected as the standard collector for the testwork. This was also used for the laboratory column tests described in section 4.4. Paraffin was, however, used for some of the plant tests. Numerous studies by the UCT Coal Research Group have demonstrated that aromatic oils generally float coal at yields superior to those obtained with aliphatic collectors. The oil was added below the pulp surface and dispersed largely via bulk turbulence. The effectiveness of this dispersion method was discussed in section 3.4.

Tri-ethoxybutane, HTEB, supplied by NCP Mining Chemicals, was chosen as the standard frother. HTEB forms a highly persistent froth and was selected to ensure that stable bubble beds with minimum coalescence could be generated. Limited tests were performed using DIBK and MIBC frothers. Frother was added to the 200 l water tank. If the filter cloth sparger was used then frother was also added to the pulp tank. HTEB is water soluble at the low concentrations (ppm levels) used.

5.2.4 Parameters Investigated

It has already been stated that the primary objective of the testwork was to produce a steam (27.6 MJ/kg) coal at maximum yields. A region of stable and efficient column performance arising from selection of appropriate sets of operating parameters thus had to be determined. Naturally, many suitable parameter values could be chosen on the basis of prior experience or from literature design criteria. However, actual testwork is invariably required to establish parameter effects reliably.

Parameters investigated during the Kleinkopje trials included collector type, (CT); collector dosage, (CC); frother type, (FT); frother dosage, (FC); pulp density, (PD); slurry feedrate, (QF); air flowrate, (AF); washwater rate, (WW); froth height, (FH); and sparger type, (ST).

The range of each parameter investigated is given in section 5.3.2 below. Details of parameter values selected for the individual column runs are given in Tables E8 and E9 in Appendix E.

5.3 TEST RESULTS

5.3.1 Feed Characterisation

5.3.1.1 Feed composition

Underflow from the Plant thickeners essentially constituted the feed to the column. As stated in section 5.1 above, a "select" and "non-select" coal product are produced at the Preparation Plant. These are processed in two essentially independent process streams operating in parallel. The "select" coal, which is a low ash quality coal, is exported and the "non-select" coal, which is a steam quality product, is sold to local power stations. The fines generated as a by-product from the mechanical cleaning units of these two streams are mixed when they enter the thickener underflow streams.

Intermittent production of low ash and steam coal and daily equipment shutdowns occurred during the period over which the column testwork was conducted. Consequently, the composition of the waste fines stream (i.e. the column feed) fluctuated constantly.

During the period of the on-line trials, 71 feed samples were analysed for ash content. The results are plotted as a frequency distribution in Figure 5.2. As may be seen, the distribution is distinctly bi-modal with two distinct peaks, one at 21.5 % ash, the other at 25.5 % ash. The double peak indicates a shifting feed composition split between "select" and "non-select" type coal. No such trend can be obviously distinguished from the feed calorific value data plotted in Figure 5.3, which suggests that calorific content is not as sensitive to coal type as bulk ash content.

Kolmogorov-Smirnov statistical tests for normality were applied to both the feed ash and calorific value (CV) data (Appendix F3). At a 95 % confidence level (i.e. 5 % significance level) the feed CV data could be fitted to a normal distribution function. This indicates that the apparent CV peak at 25 MJ/kg indicated in Figure 5.3 is due to the large size of the CV intervals chosen and would disappear from the frequency distribution histogram if smaller interval sizes were selected. However, the feed ash data failed the normality tests (only fits normal

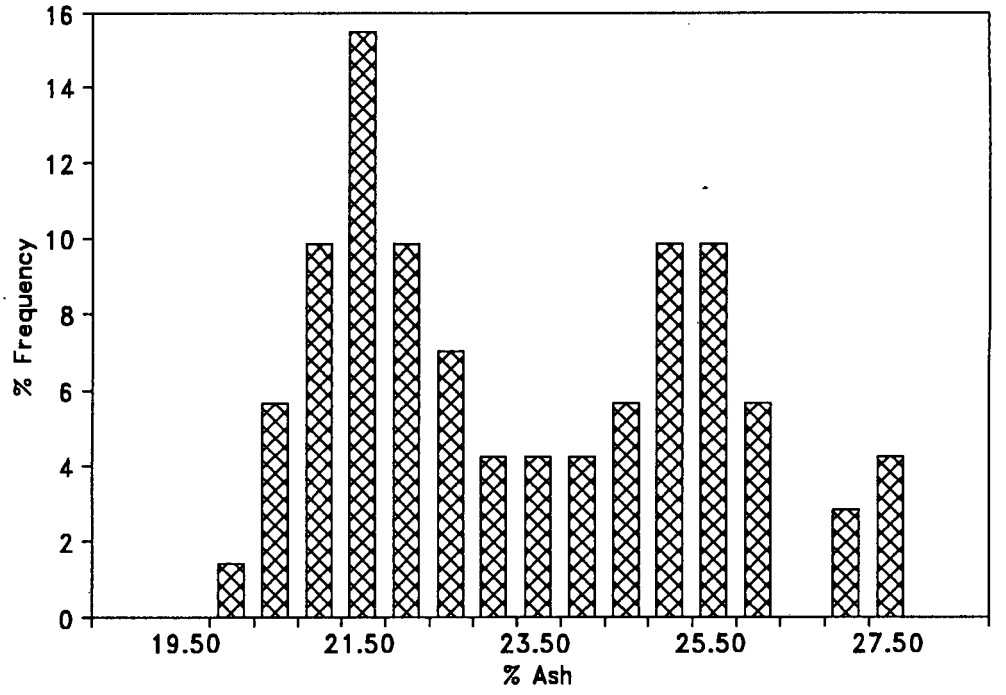

Figure 5.2 : Ash content frequency distribution for pilot column feed samples; number of feed samples, N, equals 71.

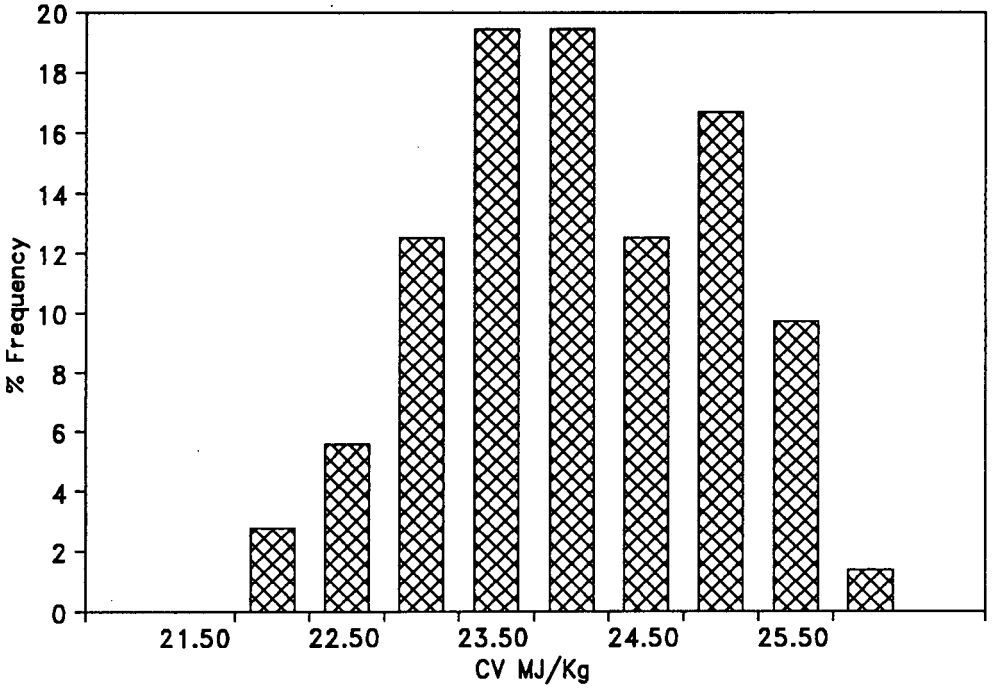

Figure 5.3 : Calorific value frequency distribution for pilot column feed samples; number of feed samples, N, equals 72.

curve at 0.1 % significance level) and therefore the double peaks indicated in Figure 5.2 are in fact representative of the true feed ash distribution properties of the column feed coal fines.

It is reasonable to suppose that fluctuating bulk ash and calorific contents also reflect changes in petrographic composition. It was shown above, for the coals (including the Kleinkopje composite sample) used in this thesis, that petrographic composition, specifically vitrinite content, is a good indicator of floatability (see section 3.4). Thus, an erratic feed composition can be expected to adversely affect flotation of the Kleinkopje coal fines.

5.3.1.2 Feed size characteristics

A linear screen supplied by Delkor was used to remove coarse oversize material (nominally > 150 μm) from the thickener fines. It was necessary to screen the feed since the column feed and tailings slurry lines blocked on every occasion that unscreened underflow was used.

Size analyses were carried out on approximately half the feed samples taken over the test period. These are plotted in chronological order in Figure 5.4. The data are also listed in Table E1 of Appendix E. It is evident that approximately 70 % of the feed was finer than 75 μm and almost half the feed was present in the ultrafines fraction, i.e. finer than 45 μm. Also, the proportion of -75 μm material in the feed increased in the latter half of the testwork. Average feed size properties are presented in Table 5.1.

Table 5.1 : Kleinkopje Feed Average Size Distribution Data

Screen size	Average Cum % passing
150 μm	93.34
106 μm	82.40
75 μm	68.29
45 μm	45.45

The feed fractions represented are satisfactory for coal flotation with columns. In fact, the distributions are typical of feed sizes tested on

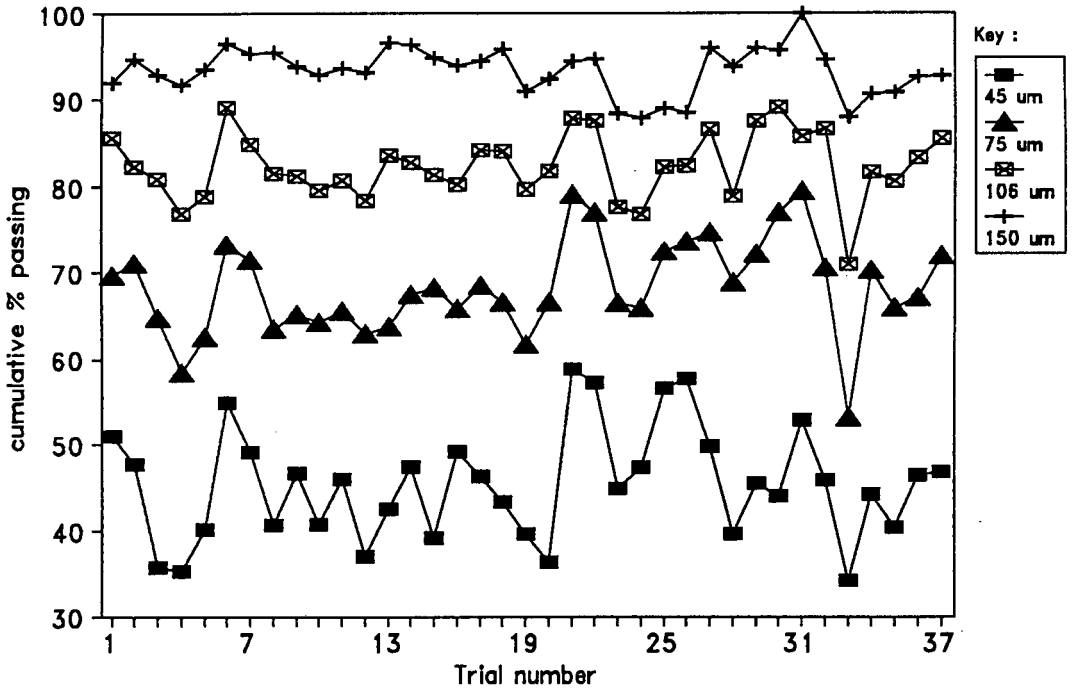

Figure 5.4 : Size fraction distribution data; pilot column feed samples.

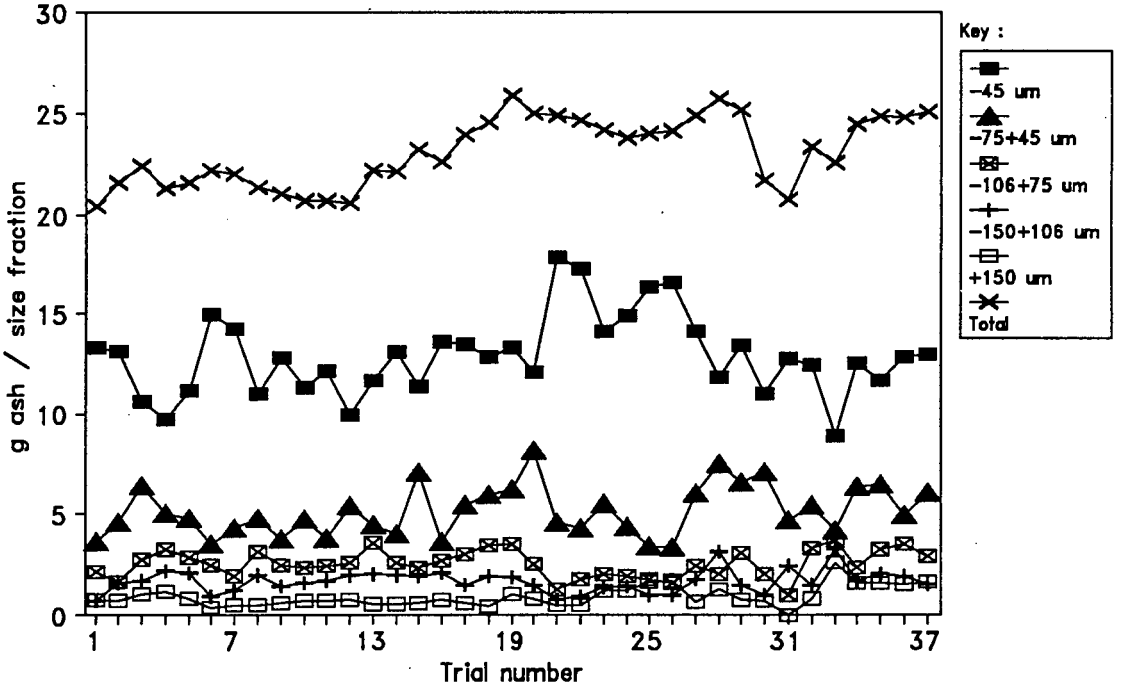

Figure 5.5 : Absolute ash content distribution by size fraction for pilot column feed samples.
Basis : 100 g of coal feed

experimental coal columns in the U.S.A. and Australia (Parekh et al, 1988; Nicol et al, 1988; Durney, 1990).

5.3.1.3 Feed ash content and CV distribution

Ash content determinations were carried out on some of the individual feed size fractions mentioned in section 5.3.1.2 above. Table E2 in Appendix E can be consulted for detailed information.

Figure 5.5 shows the *mass* of ash present in each size fraction and in the total sample based on 100 g feed. The total ash is equal to the sum of the ash masses present in the individual size fractions. The simplifying assumption is made that the mass of ash is equal to the uncombusted mineral mass (section 2.1 above). For example, consider 100 g feed sample for trial N =1 . This sample contained 20.4 % ash by mass or 20.4 g ash / 100 g feed. 13.3 g of this ash was present in the ultrafines fraction below 45 μm, 3.6 g in the fraction -75 + 45 μm fraction, 2 g in -105 + 75 μm fraction and 0.7 g in each of the - 150 + 105 μm and + 150 μm fractions respectively.

The graph clearly indicates that the size fractions finer than 75 μm contained about 3/4 of the total feed gangue component. This is logical since this fraction also contained most of the feed. Clearly, the success of the testwork rested on the ability of the column cell to upgrade the -75 μm size fractions efficiently.

Figure 5.6 shows the calorific value (in MJ) in each size fraction and the corresponding total (MJ/kg) for the feed sample, based on 1 kg of feed. The data are plotted in chronological order. Detailed information is listed in Table E3 of Appendix E.

The absolute calorific values (CV MJ/kg) of the feed size fractions are plotted in Figure 5.7. The -45 μm ultrafines fraction averaged approximately 22 MJ/kg, while the -75 +45 μm material had roughly the same calorific value as the bulk feed, i.e. average of 24 MJ/kg. Therefore the -45 μm fraction needed to be upgraded by an average of 6 MJ/kg in order to meet the product specification of 27.6 MJ/kg, while the coarser sizes, particularly the +106 μm fractions, required minimal

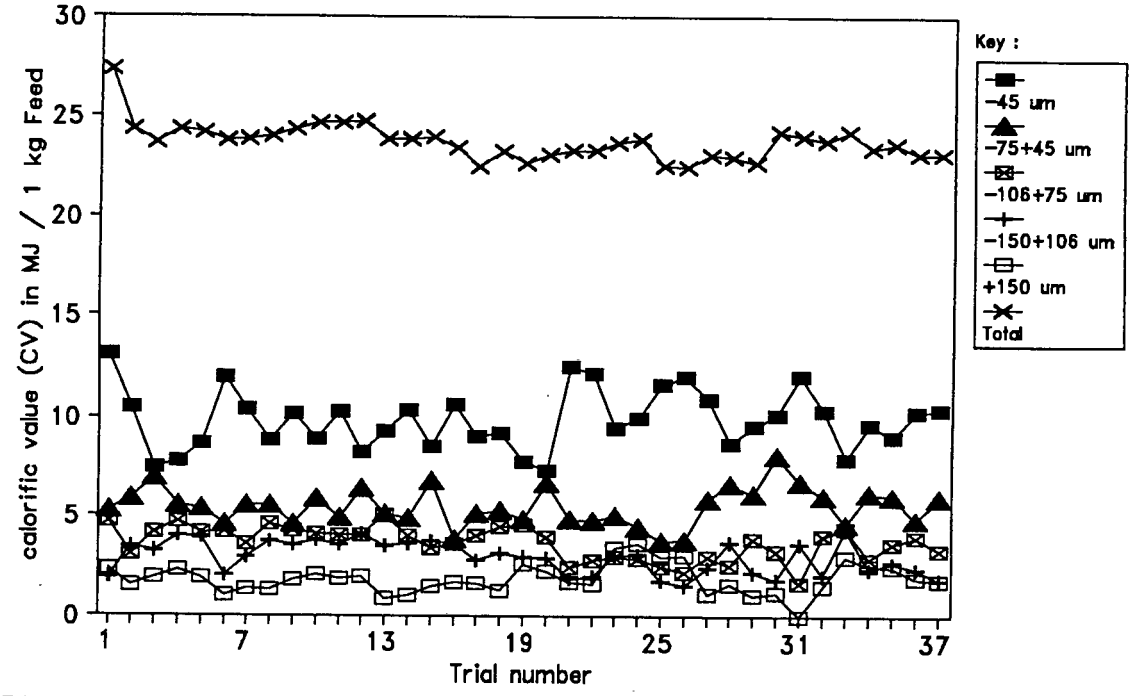

Figure 5.6 : Calorific value distribution by size fraction for pilot column feed samples. Basis : 1 kg of coal feed (i.e. total CV in MJ/kg).

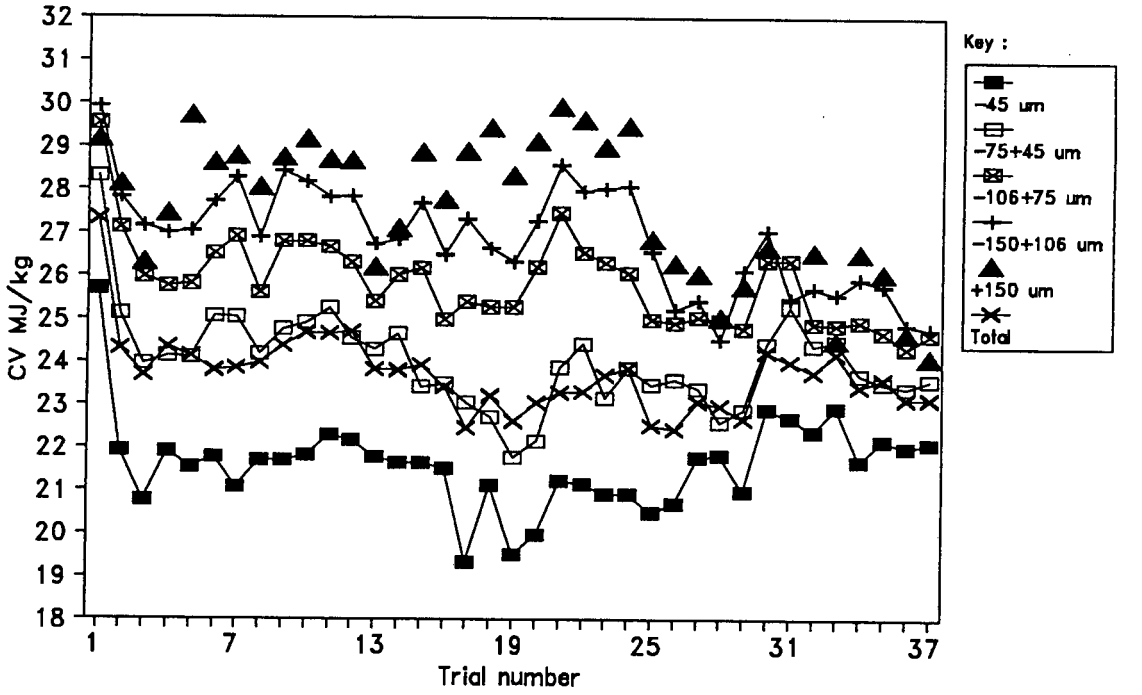

Figure 5.7 : Absolute calorific value distribution by size fraction for pilot column feed samples.

upgrading since for many of the column trials the calorific content of this material already exceeded the product quality requirement.

In other words the column was required to *recover and upgrade* the *fine* (-75 μm) feed material but basically only had to *recover* the *coarser* sizes. Consequently, given the intrinsically efficient cleaning action of the column, one could possibly expect a reasonably consistent quality concentrate irrespective of the yields achieved.

A summarised version of the data discussed above appears in Table 5.2 below.

Table 5.2 : Kleinkopje Feed Average Ash, CV by Size Distribution Data

Screen size	g Ash/100 g feed	CV MJ/1 kg feed	CV MJ/kg
+150 μm	0.89	1.81	27.62
-150+105 μm	1.66	2.94	26.89
-105+ 75 μm	2.52	3.64	25.85
- 75 μm	18.01	15.29	22.41
- 75+ 45 μm	5.13	5.47	24.02
- 45 μm	12.88	9.82	21.61
Total (average)	23.08	23.69	23.71

5.3.2 Column Flotation Testwork

A summary of the operating parameters selected during the testwork is presented below.

INNER COLUMN DIAMETER	100 mm
TOTAL COLUMN HEIGHT	6.0 m
FEED POINT (from top of column)	1.0 m
COLLECTOR TYPE	ShellsolA
COLLECTOR DOSAGE	≈ 2000, 4000, 8000 g/t
FROTHER TYPE	HTEB
FROTHER DOSAGE (water tank)	15, 20, 25 μl/l
% SOLIDS	≈ 8, 15 % m/v
SLURRY FEEDRATE	0.6, 1.0, 1.4, 1.8, 3.0 l/min
equivalently	0.13, 0.21, 0.30, 0.38, 0.64 cm/s

AIR RATE	6.5, 9.2, 11.0, 13.2 l/min
(Air pressure = 0.82 atm)	
equivalently	1.4, 2.0, 2.3, 2.8 cm/s
SPARGER TYPE	USBM, filter cloth
WASHWATER RATE	1.10, 1.40, 1.74, 2.00 l/min
equivalently	0.23, 0.30, 0.37, 0.42 cm/s
FROTH HEIGHT	0.25, 0.50, 0.75 m

Limited tests were also conducted using paraffin as a collector and MIBC and DIBK frothers.

5.3.2.1 Overall results

A total of 73 column runs were performed at the Kleinkopje Colliery. Details of the operating parameter values selected for each test run, and the results obtained, are given in Tables E8 and E9 in Appendix E.

Global concentrate ash content, calorific value and yield data are plotted in Figures 5.8 - 5.10. As can be seen from Figure 5.9, the product specification of 27.6 MJ/kg was achieved in a majority of the trials, demonstrating that the column was capable of cleaning the thickener fines to a steam quality product.

Some overall trends in the relationships between product yields, grades and calorific values are apparent. For example, it can be seen from an examination of Figure 5.8 that, on average, the concentrate ash content increased as the product yield increased, from ash contents of approximately 8 % at at yields of between 15-20 % to ash contents of ≈ 15 % at yields in the region of 80 %. A similar, if weaker, trend is distinguishable in Figure 5.9 in which concentrate calorific values (dry basis) are plotted against product yield; the calorific values of the concentrates decreased as the product yields increased. The calorific values of the coal concentrates are plotted against their corresponding ash contents in Figure 5.10. A strong relationship between the two product properties is discernible : calorific value decreased linearly with increasing ash content.

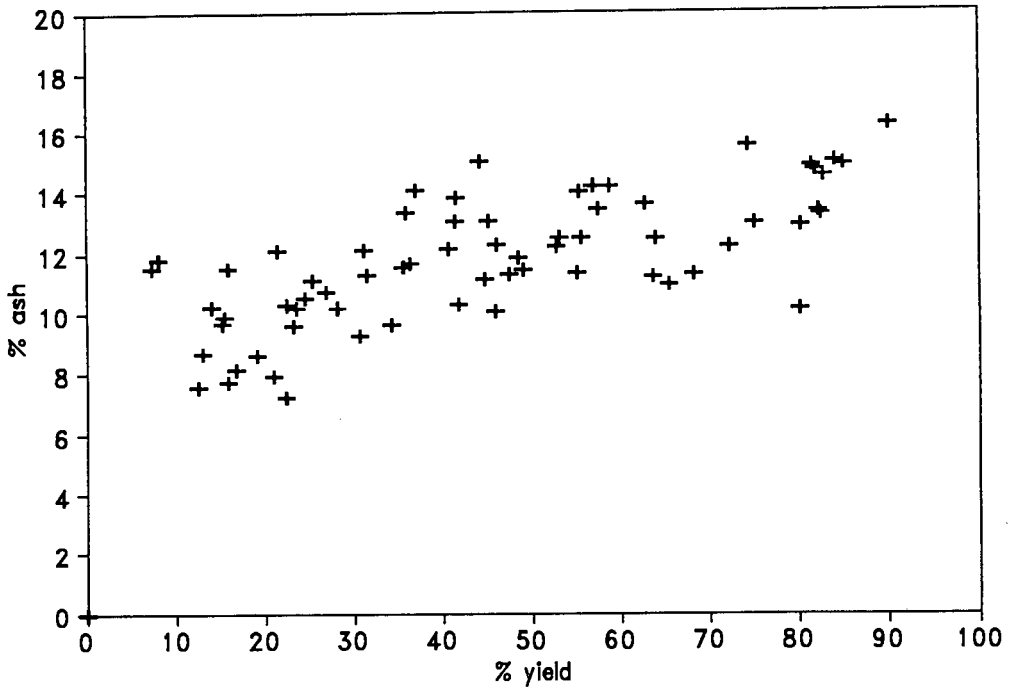

Figure 5.8 : Global yield versus product grade results for on-site Kleinkopje trials performed using pilot column.

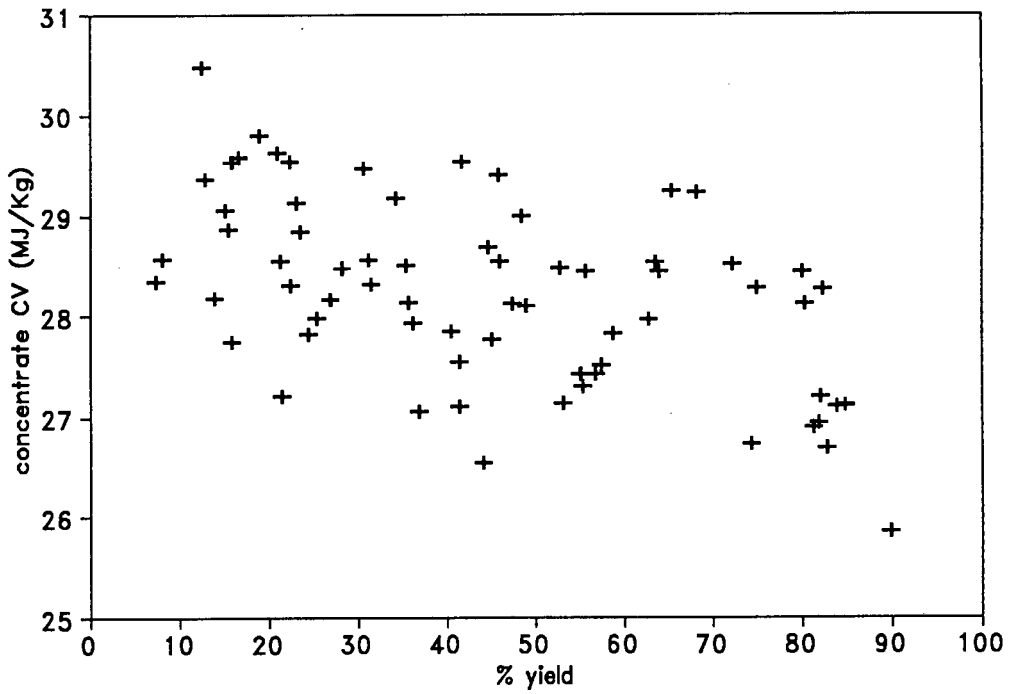

Figure 5.9 : Global yield versus calorific value results for on-site Kleinkopje plant trials performed using pilot column.

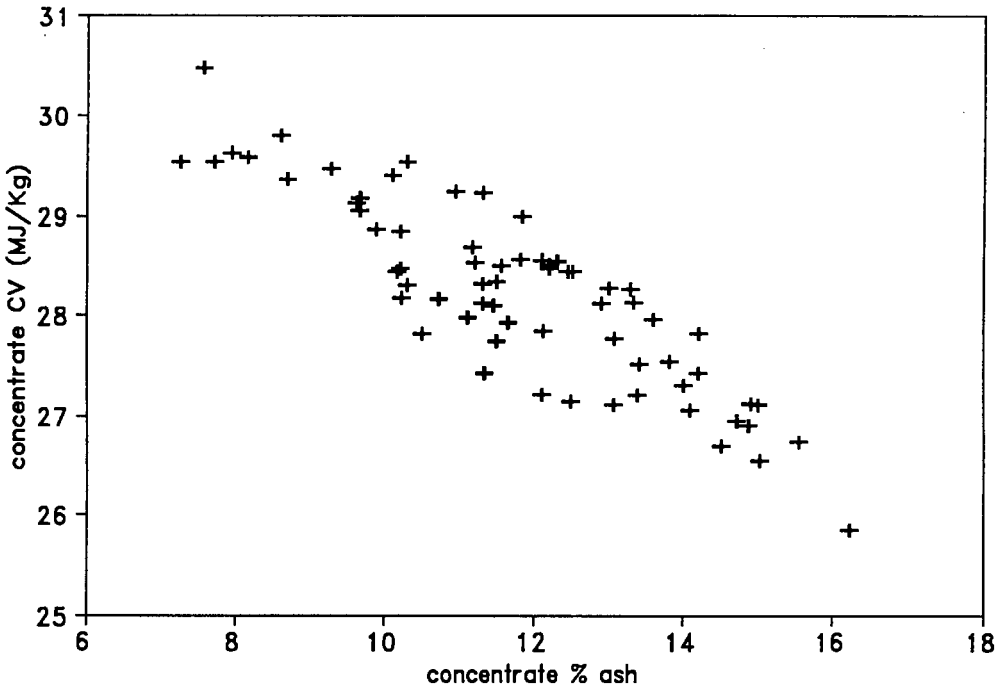

Figure 5.10 : Global column results; concentrate calorific values versus corresponding ash contents.

The trends observed above would be expected. As mass recovery of the column feed into the concentrate increases, less well liberated material with a higher ash content and, conversely, lower calorific value, would be recovered. As noted in section 2.2, a separation of solid components from a slurry is achieved in flotation; the extent of separation is reflected in the product yield attained. In section 5.3.1.1 above the ash content of the Kleinkopje fines fed to the column was found to be more sensitive to changes in the nature of the coal (i.e. the distribution between "select" and "non-select" material present) than was calorific value. Thus, one might expect that the concentrate ash contents would show a stronger relationship to flotation yield than would concentrate calorific value.

The data scatter evident in all three Figures was partly due to the many sets of operating parameters investigated, but was also due to the underlying ash content and calorific value distribution characteristics within the feed and concentrate size fractions. In particular, the considerable data scatter evident in Figure 5.9 was a result of the product size fractions (whose relative distribution in the concentrate changes with recovery) having similar calorific contents, an eventuality

predicted earlier in section 5.3.1.3. The distribution of ash and calorific contents in concentrate size fractions is discussed in the next section.

5.3.2.2 Recovery by size data

Essentially two factors dictate column flotation performance, namely the inherent floatability of the (conditioned) feed (factor A) and the set of column operating parameters selected (factor B). Equivalently, column performance can be considered as equal to the product of the factor A effect and factor B effect (performance = Ae * Be). Clearly, if the influence of column parameter (factor B) effects on product recovery and grade is to be quantified, then factor A, i.e. the feed floatability, must remain reasonably constant, otherwise the effects of the two factors are, to use statistical terminology, confounded, i.e. their individual contributions to the result attained are indeterminable.

In section 5.3.1 it was found that the feed properties were extremely variable during the testwork period. Consequently, column parameter effects are not readily identifiable and an overall interpretation of results is confined to analysis of product (concentrate) characteristics.†

Bulk concentrate grade, calorific value and yield parameters provide a means of assessing whether desired performance criteria (in this case 27.6 MJ/kg product) have been satisfied, but are insufficient for identifying which feed components have been selectively recovered. Size distribution data of the feed and product streams, coupled with ash and CV analyses of the individual size fractions, can, however, furnish such information.

Column trials for which concentrate size distribution data were obtained are listed in Table E4 of Appendix E. Size analyses were carried out on 36 of the 73 column test runs performed. However, comparisons between feed and concentrate size fractions and their properties are confined to

---

† Actually column parameters can only be compared within the same feed batch (see section 5.3.3).

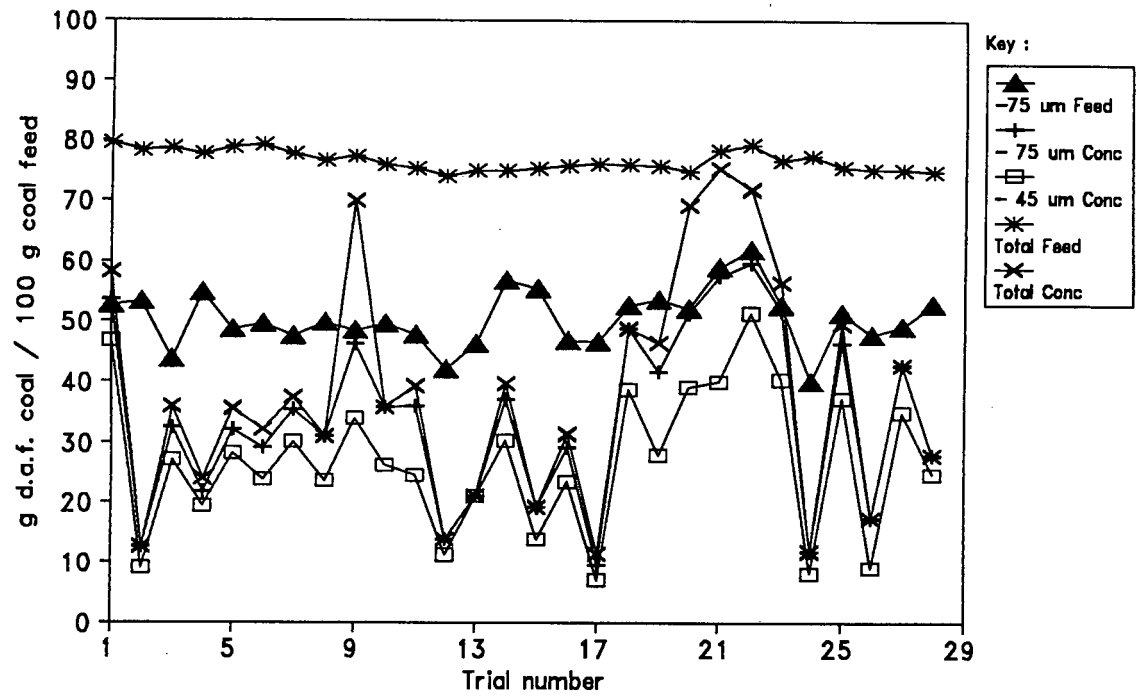

Figure 5.11 : d.a.f. coal contents of -75 μm feed and concentrate size fractions versus total d.a.f. coal present in feed and concentrates. Basis : 100 g of coal feed.

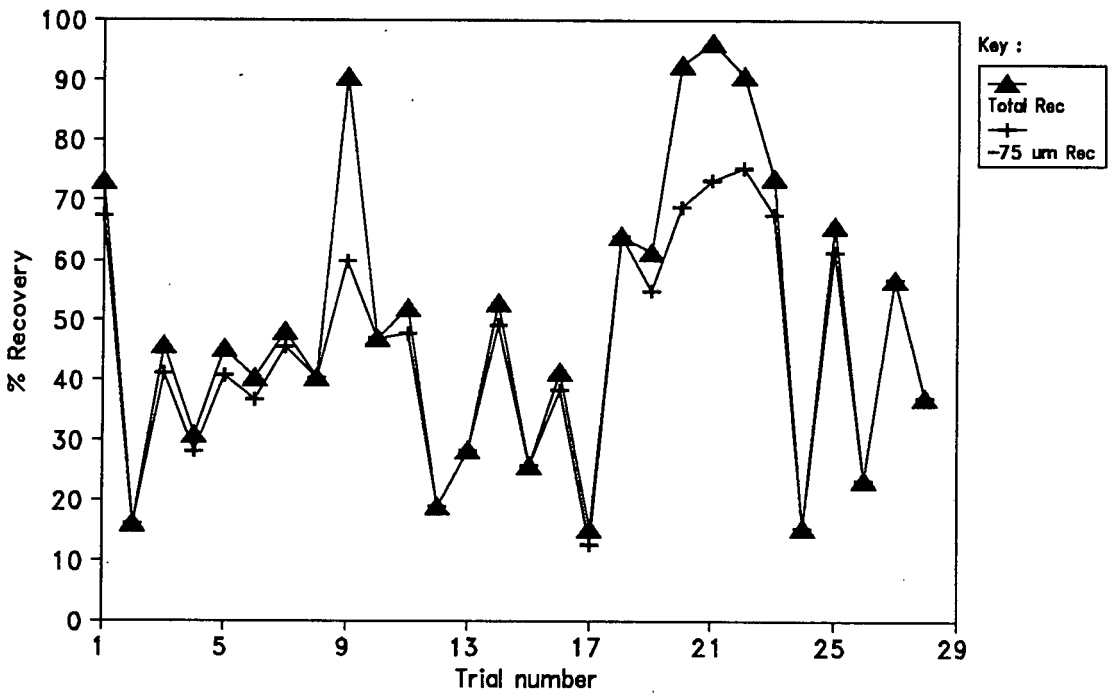

Figure 5.12 : Recovery of d.a.f. coal into -75 μm fraction versus total recovery of d.a.f. coal.

matching pairs of feed and concentrate samples. There are 28 such pairs indicated in Tables E1 - E6 of Appendix E and these are the data which are used for recovery by size analysis. The data from these 28 runs are plotted in Figure 5.11, which depicts the distribution of dry ash free (d.a.f.) coal in feed and concentrate size fractions. The data are plotted in chronological order. A sample calculation illustrating how these values were obtained is given in Appendix H2.

Figure 5.11 plainly demonstrates that coal finer than 75 μm, particularly the -45 μm size fraction, was preferentially floated. In fact, in many trials the concentrate consisted almost entirely of - 75 μm material. This may be seen more clearly in Figure 5.12 which compares the total amounts of coal recovered in each of the 28 runs with the recovery in the -75 μm fraction. For example, consider the first trial N = 1. The total coal recovery was about 73 % and 69 % of the 73 % total was due to recovery from the -75 μm fraction. Also it appears that larger size fractions were floated only when the recovery exceeded about 60 %.‡

The preferential flotation of the -75 μm fraction observed is consistent with the findings of Misra and Harris (1988) and Franzidis and Harris (1989) which were reported in section 2.5. The relationship between particle-bubble collision and attachment efficiencies (Ec, Ea) and particle size was discussed in sections 2.2 and 2.5. Ec is proportional to the square of the particle size; however, the induction time, ti, required to form a stable particle-bubble contact angle, hd, increases by an order of magnitude with increasing (coal) particle size. Clearly particle-bubble attachment cannot occur if the induction time, ti, required is longer than the time, tc, for which the particle and bubble are in contact. Therefore it appears that in the case of the Kleinkopje fines, particles coarser than about 75 μm required too long an induction period for successful flotation.

---

‡ All runs can be identified by consulting Tables E4 - E6 in Appendix E. The corresponding operating parameters are listed in Table E8. It should be noted that the concentrate ash and CV analyses reported in Tables E4 - E6 and Table E8 do not necessarily correspond as some figures quoted in Table E8 are arithmetic averages of bulk and reconstituted values. The data listed in Table E8 do, however, match those in Table E10 where a summary of feed, concentrate and tails properties are presented.

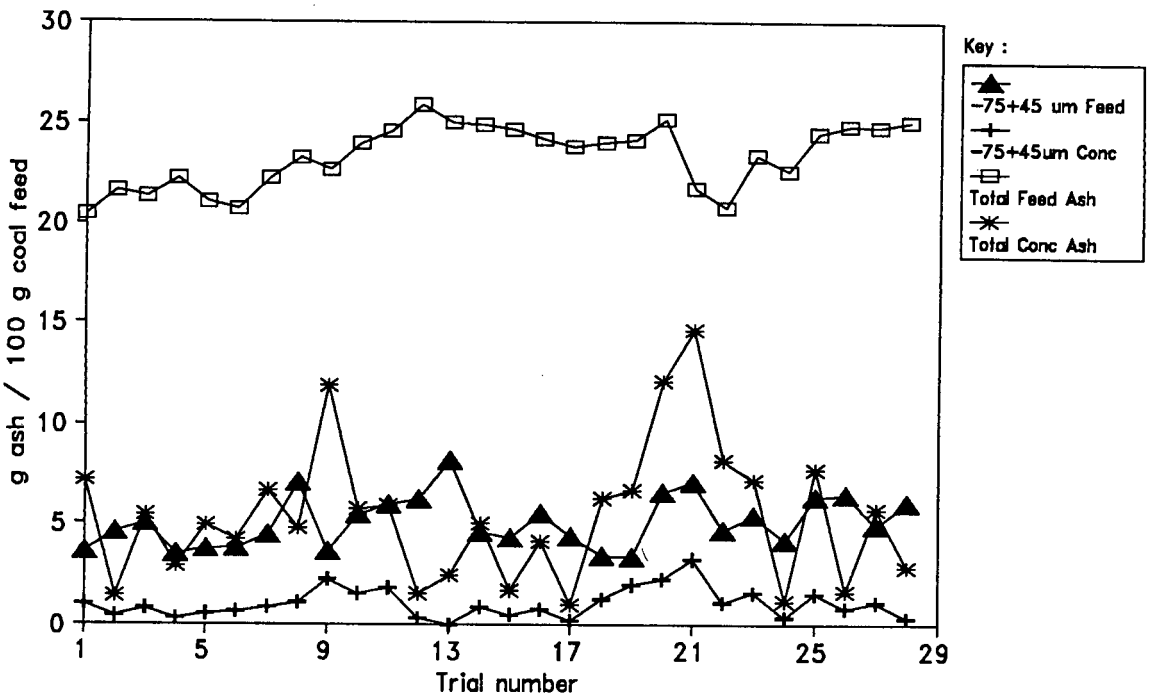

Figure 5.13 : Absolute ash distributions in feed and concentrate -75+45 μm size fractions versus total feed and concentrate ash contents. Basis : 100 g of coal feed.

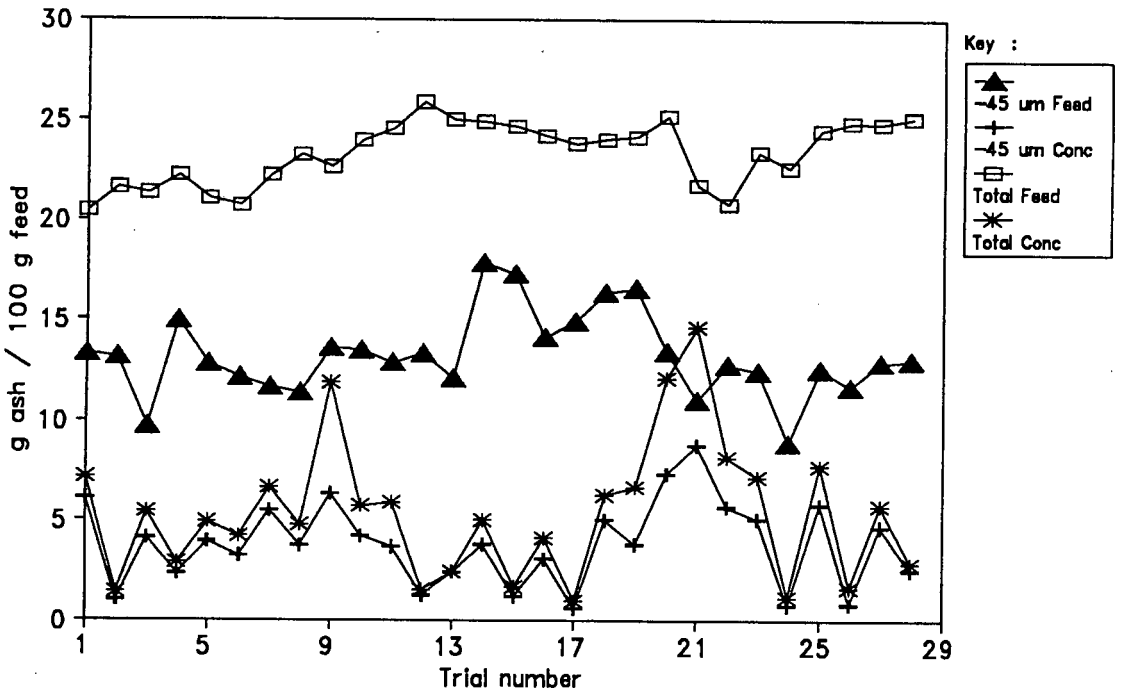

Figure 5.14 : Absolute ash distributions in feed and concentrate -45 μm size fractions versus total feed and concentrate ash contents. Basis : 100 g of coal feed.

The question of the efficiency with which the column upgrades the floated feed fractions can now be addressed.

The mass of ash present in the feed and concentrate size fractions of the 28 matching pairs of samples is plotted in Figures 5.13 and 5.14. Interpretation of the graphs is best illustrated by an example. 100 g of feed is chosen as a basis. For trial N =1 100 g of feed contained 20.4 % ash or equivalently 20.4 g of ash. 3.6 g of the 20.4 g of feed ash was present in the -75+45 μm fraction (Figure 5.13) and 13.3 g was present in the ultrafines (-45 μm) fraction (Figure 5.14), constituting a total of 16.9 g of ash in the -75 μm fraction. 7 g of ash reported to the concentrate, of which 6 g was present in the ultrafines fraction.

Referring back to Figure 5.12, it can be seen that all the d.a.f. coal present in the - 75 μm feed fraction was recovered in the concentrate. 60 % of the ash in the - 75 μm fraction was removed at no penalty to d.a.f. coal recovery in that size fraction, implying that the entrainment of gangue in this size fraction was significantly reduced (possibly completely eliminated) in operation of the column cell. The high particle-particle separation efficiencies achievable with a column cell were remarked on in section 2.5.

The measured ash contents of the feed and concentrate size fractions are plotted in Figure 5.15. As may be seen from the graph, despite having a higher ash content in the feed, the -45 μm fraction was cleaned to the same grade as the -75+45 μm fraction in the concentrate. In fact, in most of the runs reported in Figure 5.15, the ash contents of the -45 μm and -75+45 μm fraction size fractions and the total ash content of the concentrate product were similar, if not identical.

The highest overall coal recoveries were obtained in runs 9 and runs 20-22 (see Figure 5.12). These are also the runs in which the recovery of ash was the highest (see Figure 5.13), although the mass of ash per 100 g feed in run 22 was lower than the others. This is mainly due to the recovery of coarser, less well liberated particles. Indeed, if Tables E4 and E5 of Appendix E are consulted, it can be seen that the concentrates from runs 9, 20 and 21 contained at least 20 % +75 lm material, with an absolute ash content of approximately 11 %. The concentrate from run 22 contained less coarse coal ($\approx$ 17 % +75 μm) and a

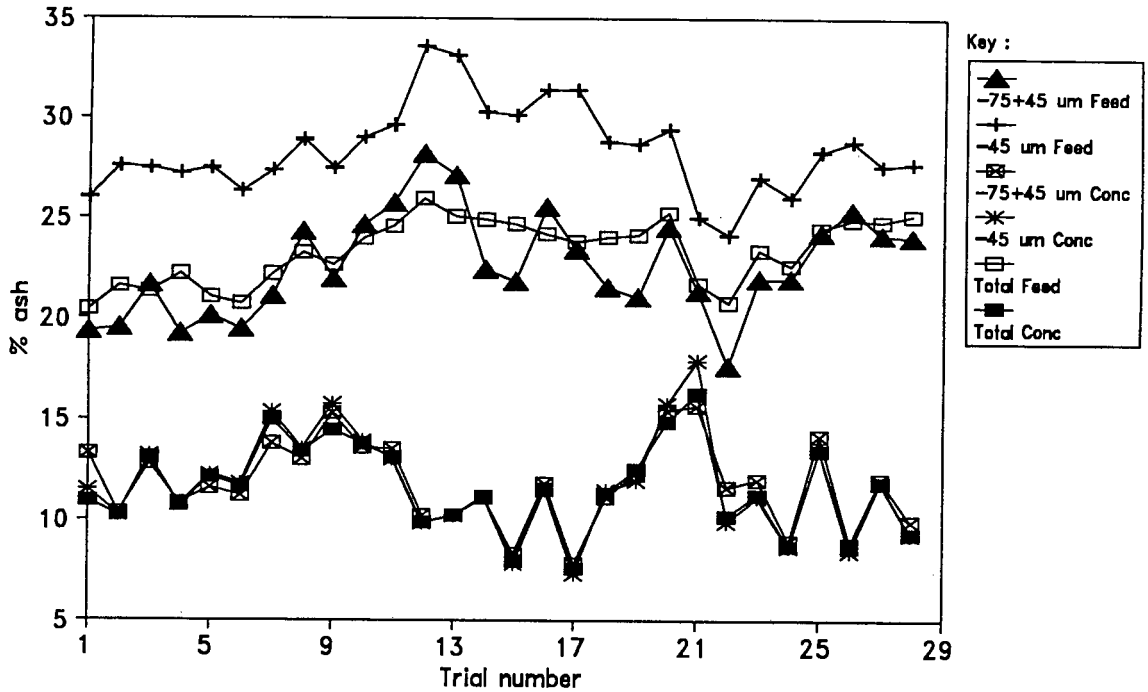

Figure 5.15 : Measured ash contents of feed and concentrate -75 μm size fractions versus total feed and concentrate contents.

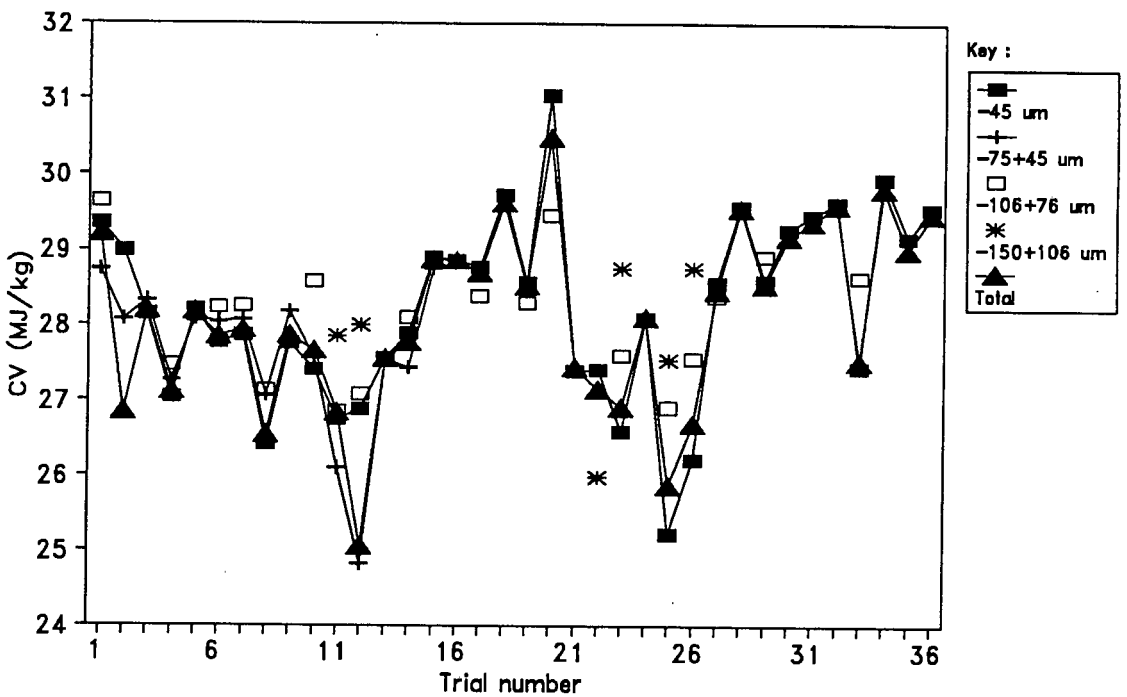

Figure 5.16 : Calorific value (in MJ/kg) distributions of concentrate and concentrate size fractions.

larger proportion of fines (70 % - 45 μm vs ≈ 50 % - 45 μm) compared with runs 9, 20 and 21.

The size fraction properties listed in Tables E1 and E2 indicate that the feed to run 22 had the highest proportion of fines (80 % -75 μm vs ≈ 70 % -75 μm) and the lowest ash content (20.8 % ash vs 22.6, 25.7 and 21.7 % ash for runs 9, 20 and 21 respectively) of the four runs examined. It is also important to note that in runs 9, 20 and 21 (NOT run 22) the ash contents (%) of the -45 μm concentrate fractions were the highest of all the runs for which size analyses were obtained (see Table E5).

This suggests that when the column was operated in a manner such that a substantial portion of the coarse material reported to the concentrate, the ultrafine material was not as well cleaned as in runs where less coarse material was recovered. Thus one can (unsuprisingly) conclude that at maximum recovery levels the performance of the column is sensitive to feed size distribution and liberation characteristics.

A better perception of overall column performance is realised if Table 5.3 is examined. Average d.a.f. coal distributions in the concentrate and feed sizes are listed, as are the calculated recoveries obtained in the respective product fractions. The basis for these calculations are the 28 matched feed and concentrate sample pairs mentioned earlier.

Table 5.3 : Average d.a.f. Coal in Feed and Concentrate by Size Fraction

Size fraction	Feed g coal/100 g Feed	Concentrate g coal/100 g Feed	% Recovery per size i
- 45 μm	33.29	26.89	80.78
- 75+ 45 μm	17.23	7.20	41.79
- 75 μm	50.52	34.09	67.48
-106+ 75 μm	11.41	2.99	26.21
-150+106 μm	8.71	1.05	12.06
+150 μm	6.04	0	0
Total	76.68	38.13	49.73

It is evident that the column was particularly efficient in treating finer sizes, since to recover an average of 80 % of coal in the -45 μm

fraction or 2/3 of the - 75 μm feed coal is a very good performance indeed.

Conversely, it is apparent from Table 5.3 that recovery of the +75 μm fractions achieved by the column was extremely poor. The reasons for this were just discussed above. These sizes are well within the range of floatability using conventional flotation cell technology (since coarser bubbles are generated in these cells - see section 2.5 above).

Specific calorific values (MJ/kg) of all the column concentrate size fraction samples available are depicted in Figure 5.16. Unsurprisingly the calorific values for the -75+45 μm and -45 μm (ultrafines) fractions and the total concentrate are virtually identical for any given trial.

Average concentrate data are summarised in Table 5.4. Again, the basis for the calculations are the 28 matching pairs of feed and concentrate samples.

Table 5.4 : Average Concentrate Ash, CV and Size Distribution Data

Size fraction	% Ash	CV MJ/kg	% size fraction	% Rec size i
- 45 μm	11.63	28.21	71.70	80.78
- 75+ 45 μm	11.77	27.99	20.26	41.79
-106+ 75 μm	11.68	28.08	6.12	26.21
-150+106 μm	10.90	28.18	1.76	12.06
Total	11.49	28.11		49.73

As may be seen, the column concentrates contained on average 90 % -75 μm material, and had a mean calorific value of 28.1 MJ/kg. Also, perhaps more importantly, the poorest grade feed fraction namely the -45 μm ultrafines was the most appreciably upgraded, from a mean feed calorific value of 21.6 MJ/kg (see Table 5.2 above) to an average 28.2 MJ/kg product. Coupled with the high recoveries achieved for the finer sizes, the potential of column flotation for recovering and upgrading the Kleinkopje fine waste fractions is self-evident.

5.3.3 Column Parameter Effects

In this section testwork results are evaluated from an analysis of the various physical and chemical parameters used for column runs. The parameters investigated during the column flotation trials and the range of values selected may be found in section 5.3.2 (page).

Parameter effects are compared only within the same pulp (feed) batch. The reason for the adoption of this approach is explained in section 5.3.3.1 below.

During the on-site trials at Kleinkopje the column was run at two (usually different) steady state conditions with each 240 l feed pulp batch. The parameters varied during the individual column runs are listed in Tables E8 and E9 of Appendix E. Each parameter is assigned a symbol (e.g. effect of air flowrate within a pulp batch or block is designated AF) and the pulp batch for which the particular parameter was tested is given a block number (an exception to this format is the reproducibility attained between batches, a concept described in the following section). This helps in identifying more easily the blocks in which various parameters were tested.

For example, between runs 18/04 R11 and 18/04 R12 the air flowrate was increased from 6.57 to 9.24 l/min (Table E8). In Table E9 this test is identified by the acronym AF1.

5.3.3.1 Reproducibility

The mode of column operation and the sampling method used have been described in section 5.2.2. Basically, two sets of steady state operating conditions were obtained with every 240 l pulp batch, after which the tank was refilled with fresh pulp. The repeatability attainable within a batch (R) and the reproducibility achieved between batches (RB) is consequently of interest.

Repeat samples were taken as if the run operating conditions had been changed, i.e. a period of approximately 3 nominal residence times, $3\tau_n$, was allowed to pass before the second set of concentrate and tails

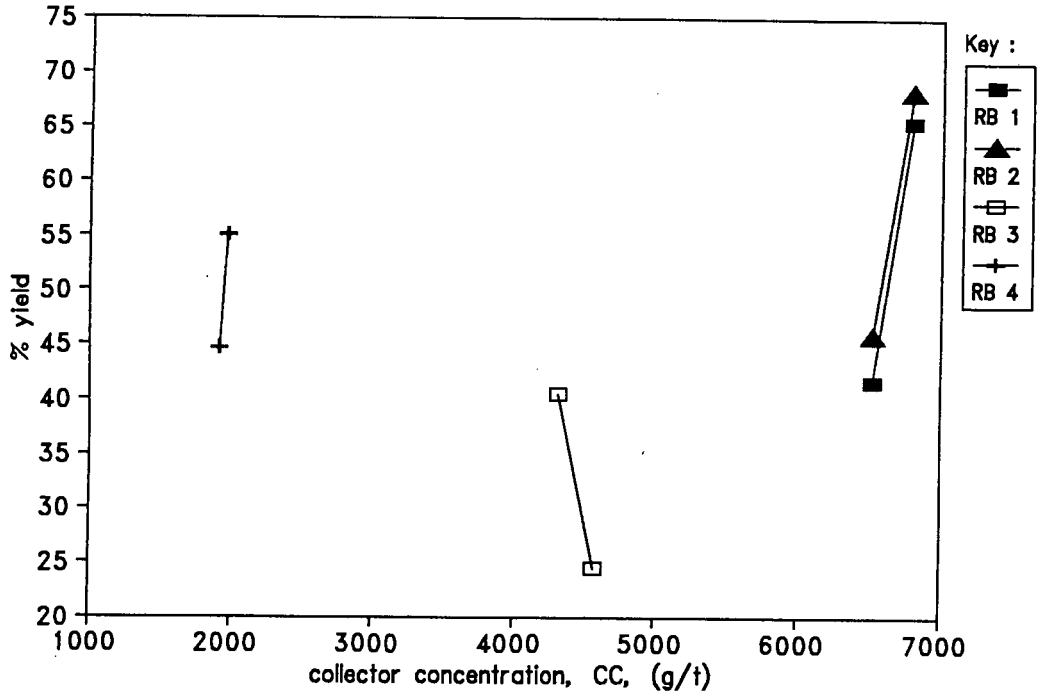

Figure 5.17 : Reproducibility of yields produced between pulp batches in pilot column cell; the acronym RB represents a repeat of run operating conditions between 2 different pulp batches.

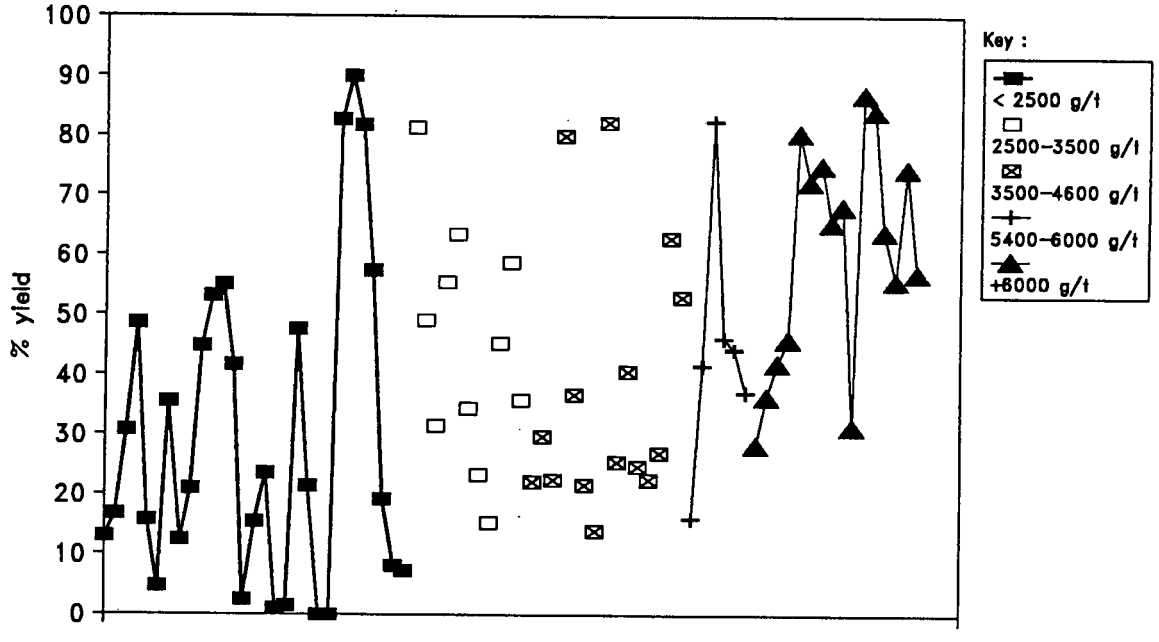

Figure 5.18 : Relationship between collector (ShellsolA) dosage and column flotation yield; number of column runs, N, equals 77.

samples were taken. The standard errors associated with product yield, ash and calorific values are tabulated below. Sample calculations indicating the data sources and statistical procedures used are listed in Appendix F5.

Table 5.5 : Standard error estimates for Kleinkopje column tests

Parameter	Error mean square		Standard error	
	Sample	Population	Sample	Population
	s_e^2	σ_e^2	s_e	σ_e
% Yield	3.76	16.34	1.94	4.04
% Ash	0.34	1.91	0.58	1.38
CV MJ/kg	0.03	0.15	0.16	0.39

The sample standard error values, s_e, obtained correspond well with the duplicate sample errors reported (Table 4.7a) for the Durnacol laboratory testwork. In both cases the error values estimate the extent of fluctuation at steady state and not the variability associated with attempting to reproduce a result obtained at any given set of operating conditions by repeating the test ab initio.

The confidence interval associated with a 95 % confidence level is 2σ, where σ is the population standard error. Therefore the confidence intervals associated with the yield, grade and calorific value errors are approximately 8 %, 2.5 % and 0.8 MJ/kg, respectively. In other words, for changes in the response parameters yield, grade and calorific value to be considered significant, they must be bigger than the values just mentioned.

Some run conditions were repeated between successive pulp batches (RB). The yields obtained from pairs of identical column operating conditions are plotted in Figure 5.17. It is clear that the yield variability (approximately 15 - 20 %) was too large for any useful comparisions between batches (RB) to be reasonably inferred.

As noted in section 5.3.1.1 above, Kleinkopje thickener underflow is a blend of fines generated from "select" and "non-select" production streams. Since column tests were conducted over a period of 5 weeks,

several feed samples were taken when only one of the production streams was on-line. The results from these column trials are presented below.

Table 5.6 : Effect of Coal Type (composition) on Column yield

Sample identification	Coal type	Collector dosage (g/t)	% yield
23/04 R21	select	1922	47.5
23/04 R22	select	1922	21.4
24/04 R21	non-select	2566	1.3
24/04 R22	non-select	2566	1.1
24/04 R31	non-select	2312	0
24/04 R32	non-select	2312	0

The petrographic composition of a composite "select"/"non-select" thickener fines blend was reported in section 3.2 above. This composite sample contained 71 % inertinite and 27 % vitrinite. The data above appears to indicate that vitrinite (the more floatable component, see section 2.4.1) is contained predominately in the "select" fraction. Conversely, the extremely poor floatability of the "non-select" fines indicates that they contain mostly inertinite.

A shifting feed composition split between "select" and "non-select" coals was noted earlier. This factor coupled with the evidently poor floatability of the "non-select" material caused the wide variation in column performance reflected in Figure 5.17. The poor reproducibility observed between successive pulp batches was therefore caused by the fluctuating composition of the coal fines fed to the column. In fact, collector dosages far greater (> 6000 g/t, see section 5.3.3.2 below) than those conventionally considered were required for consistent flotation performance. Consequently, attempts to quantify parameter effects are confined to run pairs within the same feed batch (Block).

5.3.3.2 Collector dosage

The effect of collector dosage on the yields produced during the column trials is summarised in Table 5.7 below. A plot of yield against collector dosage, presented in Figure 5.18, conveys similar information. The variability in yields (between 20 % and 90 %) within similar

collector dosage level ranges (e.g. 2500-3500 g/t) is clearly substantial. Only at dosages of +6000 g/t were acceptable yields (say > 50 %) consistently achieved.

As was discussed in section 5.3.3.1 above, the reason for the substantial variations observed lay in the fluctuating feed composition, specifically the high content of non-floatable inertinites in the coal fines.

Table 5.7 : Effect of Collector Dosage on Yield

Collector dosage (g/t)	min % Yield	max % Yield	Avg % Yield
< 2500	0	89.94	25.39
2500 -3400	15.19	81.36	44.85
3500 - 4600	14.00	82.17	37.58
5400 - 6000	15.90	82.42	44.48
>6000	28.19	86.76	60.38

5.3.3.3 Effect of slurry and solids feedrate

The terms mean pulp residence time, τ, concentrate solids production rate, C_p, and carrying capacity, C_a, which were introduced in section 2.3, are convenient parameters for describing feedrate effects.

Suitable pulp residence times depend greatly on the inherent floatability (hydrophobicity) of the feed material. For instance, high rank Australian and American coal fines typically require nominal residence times τ of 3 - 6 minutes to obtain recoveries of between 80 - 90 % (section 2.5.2). Moderate slurry and solids feedrates were predominantly used for the Kleinkopje trials since the primary goal of the testwork was to obtain an indication of the optimum yield/grade performances attainable with column flotation.

The effect of slurry volumetric feed rate, QF, and corresponding nominal residence time, τ_n, on yield can be seen in Figures 5.19 and 5.20 respectively. Corresponding feed and concentrate solids rates are plotted in Figure 5.21. The nominal residence times, τ_n, varied between 8 and 19 minutes and the product yields obtained were between 10 % and

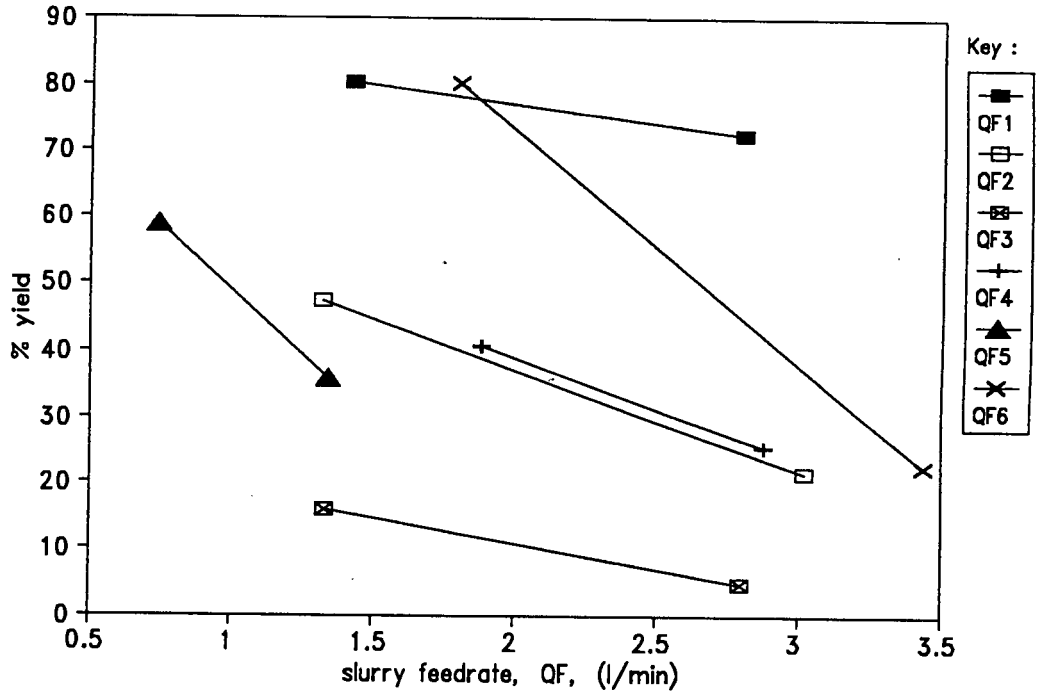

Figure 5.19 : Effect of volumetric slurry feedrate, QF, on column flotation yield. Legend acronyms QF1 etc., indicate which pairs of runs were conducted from the same batch of pulp.

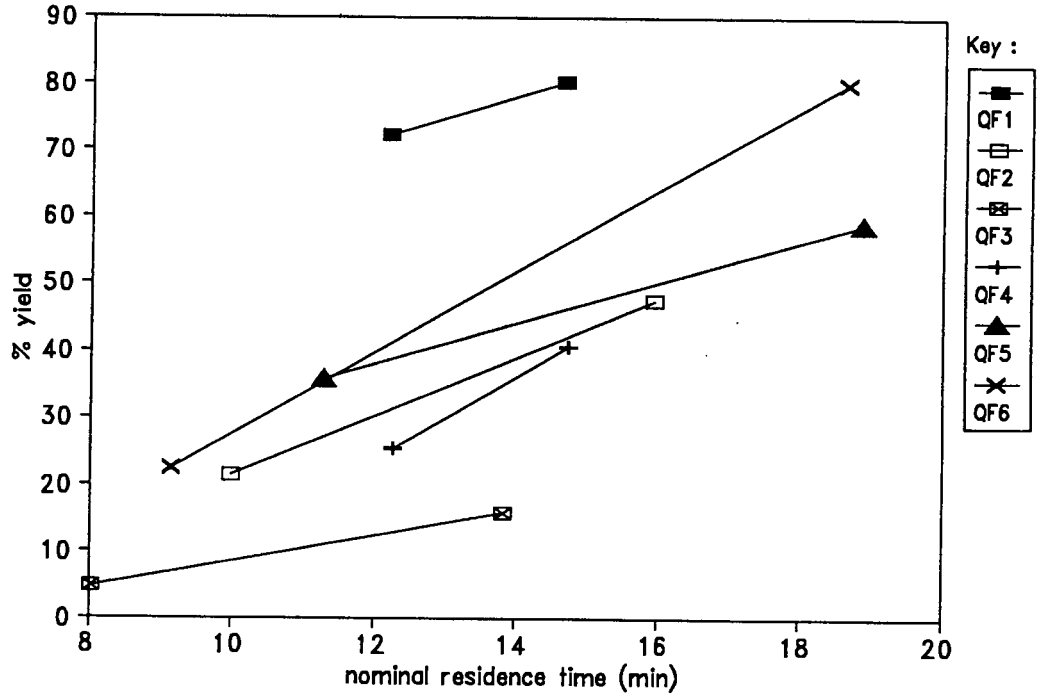

Figure 5.20 : Effect of nominal pulp residence time, τ_n, on column flotation yield. Legend acronyms QF1 etc., indicate which pairs of runs were conducted from the same batch of pulp.

90 %. Despite the fact that comparatively long residence times were allowed (mostly > 10 minutes) the yields dropped substantially upon increasing slurry feed rate. In particular, reducing the residence time from 19 to 9 minutes between run 1 and run 2 of run-block QF6 reduced the yield by 60 %. Particle residence times, τ, influence recovery when the kinetics of particle-bubble collision and adhesion in the pulp phase determine the rate of flotation (see section 2.3.3). As the Kleinkopje coal fines were poorly floatable (i.e. k_s small; see section 2.3.3), and pulp residence times were observed to dramatically affected recovery, one can deduce that the rate of flotation was controlled by the kinetics of particle collection by the bubbles in the pulp zone. This is in agreement with the results of the column laboratory testwork and is further discussed in section 5.3.3.10 below. Furthermore, an improvement in flotation rates (which would be reflected in shorter residence times) would most likely be achieved if the non-floatable "non-select" feed component was removed from the fines fed to the column.

Concentrate production rates from columns treating coal fines are typically between 1-2.5 t/hr.m^2 of solids (section 2.5.2). At yields of 60-80 % these would correspond to solids feedrates of 1.5 - 3.0 t/hr.m^2.

The concentrate solids rates plotted in Figure 5.21 indicate that, with the exception of one run where a production rate, C_p, of 1.3 t/hr.m^2 was attained, all the concentrate production rates lay between 0.2 and 0.8 t/hr.m^2. Concentrate production rates, C_p, of up to 1.0-1.5 t/hr.m^2 were achieved in the laboratory column testwork conducted on a composite Kleinkopje sample (see section 4.4.5.2 above). For the Kleinkopje plant trials, solids feedrates of between 0.5 - 2.0 t/hr.m^2 were used, the lower throughputs being employed during the latter stages of the testwork. Global concentrate solids production rates vs yield are plotted in Figure 5.22. The maximum concentrate production rate, achieved incidentally using a filter cloth sparger, was 1.33 t/hr.m^2 (23/04 R12) at a 72 % yield. Unfortunately, no size data for this trial are available. Overall, it appears that at the conditions selected for the plant trials, the column is operating well below its carrying capacity, i.e. $C_p < C_a$. Production rates achieved in laboratory column flotation tests are compared with those attained during the plant trials in section 5.3.3.10 below.

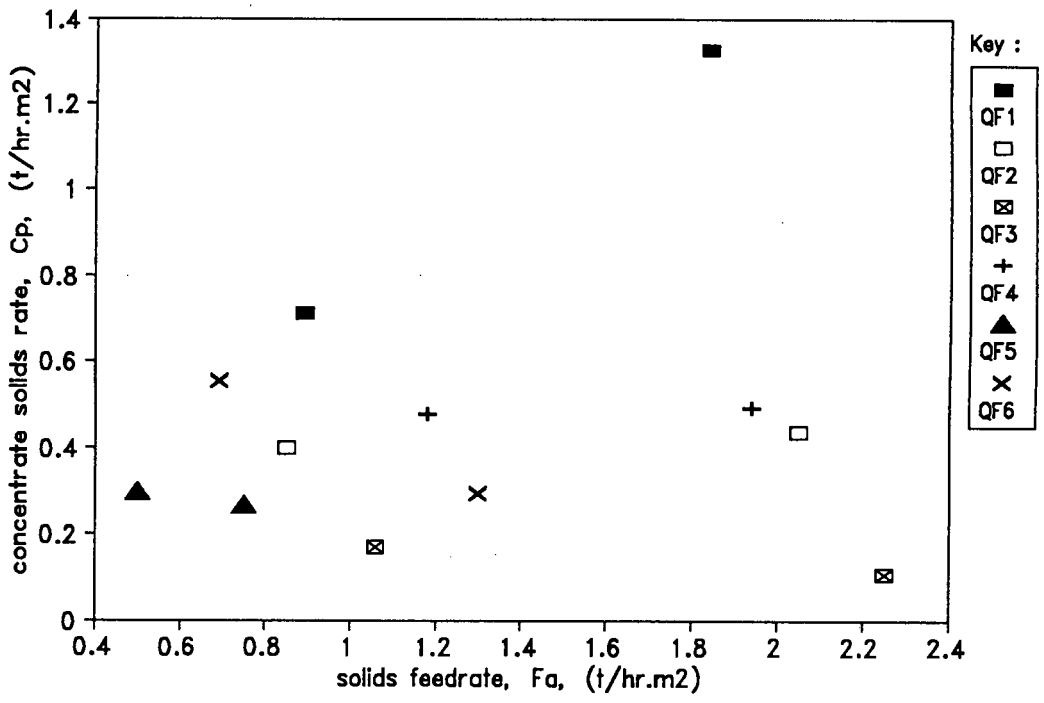

Figure 5.21 : Relationship between solids feedrates, F_a, and rate of production of concentrate solids, C_p, (mass/area basis). Legend acronyms QF1 etc., indicate which pairs of runs were conducted from the same batch of pulp.

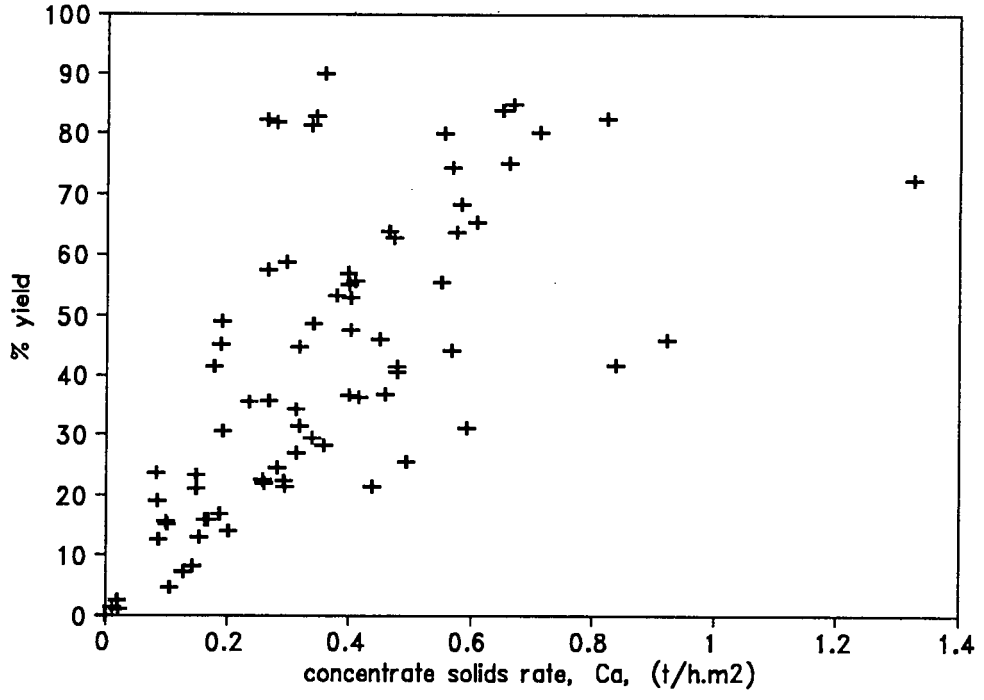

Figure 5.22 : Relationship between rate of production of concentrate solids, C_p, and column flotation yield. Global results; number of column runs, N, equals 77.

5.3.3.4 Effect of air flowrate.

The effect of air flowrate on yield is depicted in Figure 5.23. Equivalent air velocity data are listed in Table E9. The air flowrates tested cover the spectrum of gas superficial velocities used in column cells.

The yield error associated with a result was estimated above as ± 4 %. The largest change in yield achieved as a result of changing air flowrates was only 7 % (AF3 and AF4), consequently one can conclude that the effect of air flowrate on yield was not significant.

The influence of air rates on concentrate grade and calorific value (CV) are illustrated in Figures 5.24 and 5.25 respectively. Recalling that the estimated population standard error associated with an ash result is ± 1.4 % ash, and that associated with calorific value error ± 0.4 MJ/kg, then only differences greater than about 2.8 % ash and 0.8 MJ/kg reflect significant changes in product ash and CV performance. The effect of air rate is again seen to be insignificant.

5.3.3.5 Reagent suite selection

For reasons explained in section 5.2.3 above, ShellsolA, a 95 % aromatic oil, and HTEB, a commercial tri-ethoxybutane derivative, were selected as the standard flotation reagents for the testwork. Paraffin and MIBC are the coal flotation industry standards.

The possibility that unsuitable reagent selection was responsible for the poor column performance at low reagent dosages was considered. Accordingly, several tests were conducted with a paraffin/MIBC reagent suite. The paraffin was obtained from a local oil company (MOBIL) depot and is sold to the public as "Power paraffin". A ShellsolA/DIBK combination was also tested. Detailed information can be found in Tables E8 and E9 of Appendix E. The results of these tests are displayed in Figure 5.26.

It is apparent from Figure 5.26 that at low (≈ 2000 g/t) collector dosages all the collector/frother combinations gave poor (< 50 %)

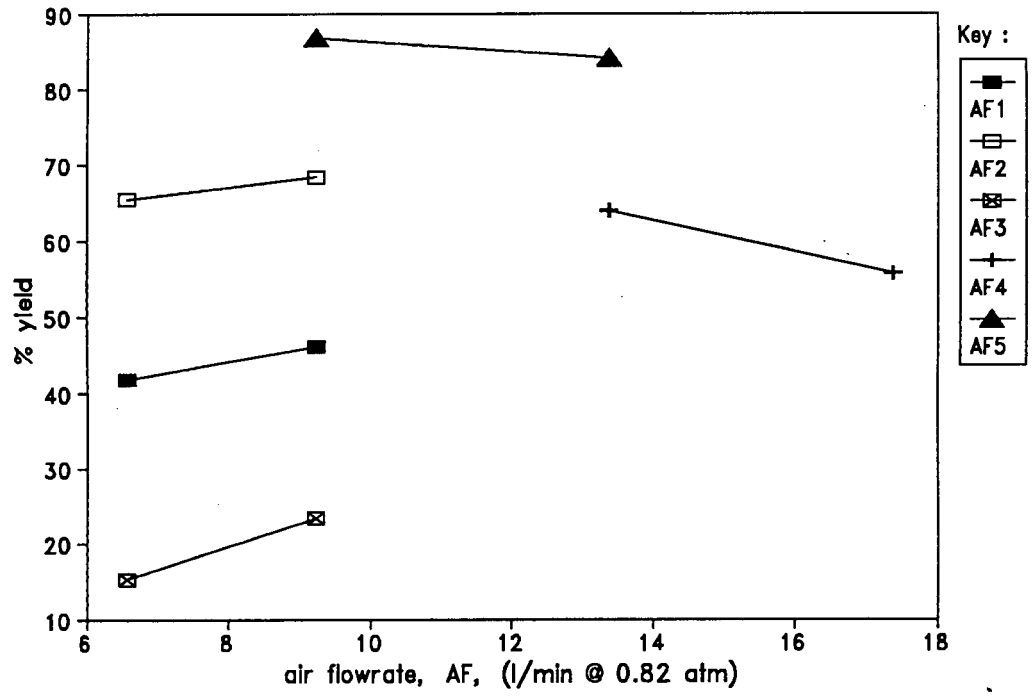

Figure 5.23 : Effect of air flowrate on yield produced in pilot column cell. Legend acronyms AF1 etc., indicate which pairs of runs were conducted from the same batch of pulp.

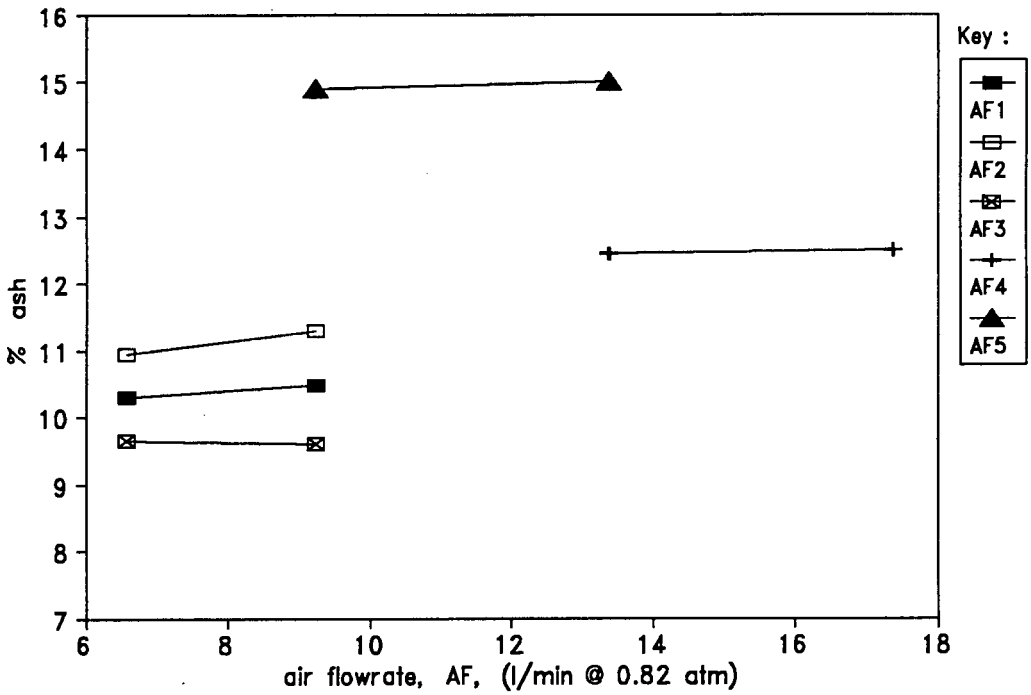

Figure 5.24 : Effect of air flowrate on concentrate grade produced in pilot column cell. Legend acronyms AF1 etc., indicate which pairs of runs were conducted from the same batch of pulp.

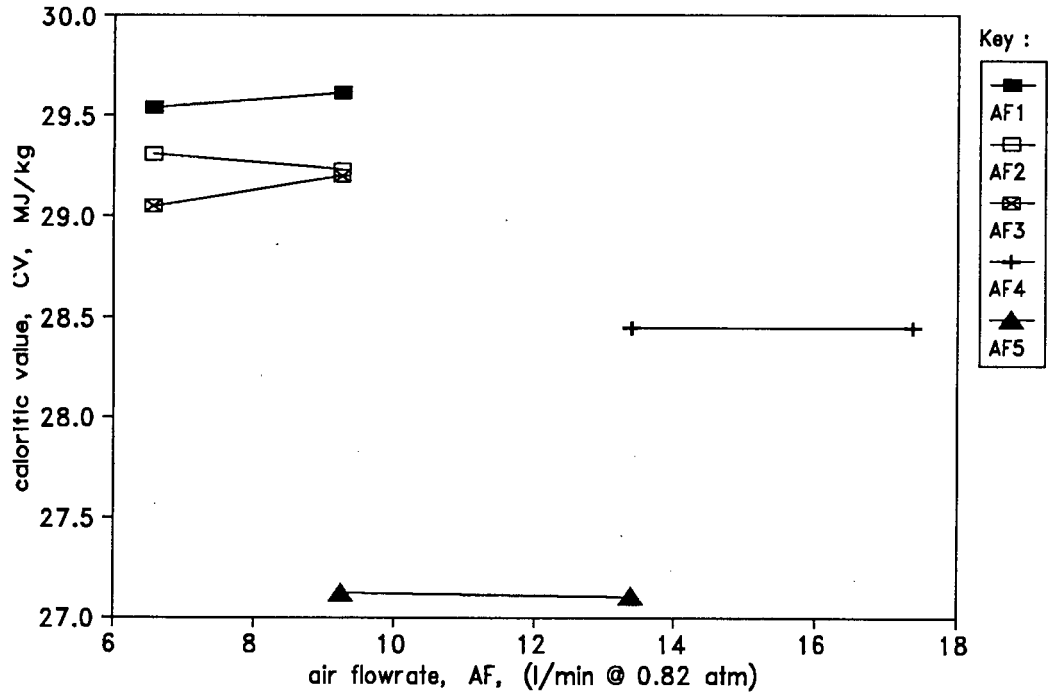

Figure 5.25 : Effect of air flowrate on concentrate calorific values (dry basis) produced in pilot column cell. Legend acronyms AF1 etc., indicate which pairs of runs were conducted from the same batch of pulp.

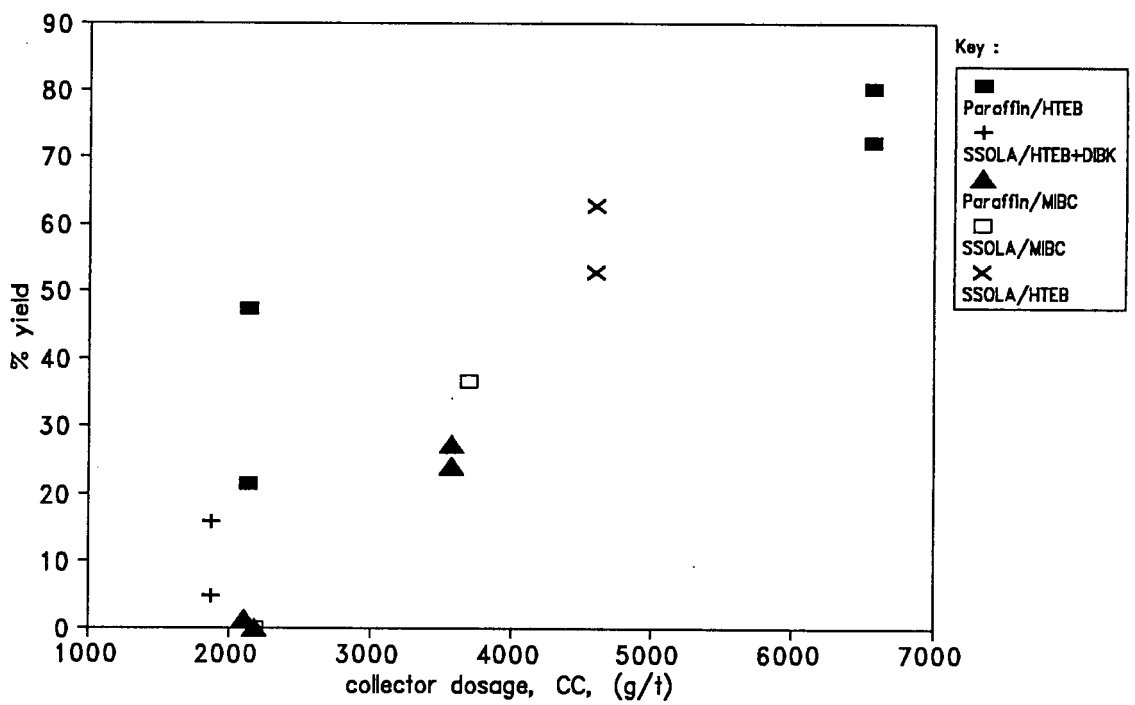

Figure 5.26 : Relationship between reagent suite selection and yields produced in pilot column cell.

flotation yields. Thus, there was no apparent advantage of selecting reagents other than ShellsolA and HTEB and one can conclude that reagent suites were not a primary factor affecting column performance.

5.3.3.6 Effect of wash water addition

The effect of wash water addition rate on concentrate yield, grade and calorific value is illustrated in Figures 5.27, 5.28 and 5.29, respectively. From an examination of Figure 5.27 it is apparent that an optimum region of wash water addition existed, since mass recovery dropped off at low rates (below 1.2 l/min $\equiv$ J_w = 0.25 cm/s) and relatively high rates (above 2 l/min $\equiv$ J_w = 0.42 cm/s). This phenomenon is readily explained by the stabilising effect of wash water on the froth bubble bed; hence the improved recoveries from lower to intermediate water rates. However, once the wash water rate becomes excessive, solid particles detach from the bubble surface, resulting in a drop in yield. In section 2.5 it was noted that washwater rates greater than 0.4 cm/s increase mixing and reduce froth mean residence time.

Concentrate grades and calorific values followed the yield trends indicating that the liberation characteristics of the coal fines was the dominant factor which determined product properties.

5.3.3.7 Effect of froth height

Variation of yield with froth height is shown in Figure 5.30. As the maximum change in yield was only 7.5 % (FH1) it appears that froth height had a negligible affect on column yield. The corresponding concentrate grade and calorific contents are plotted in Figures 5.31 and 5.32, respectively. Recalling that only differences greater than $\pm$ 2.8 % ash and 0.8 MJ/kg are regarded as significant (at a 95 % confidence level), it is evident from these Figures that concentrate grades and calorific values were also unaffected by changes in froth height.

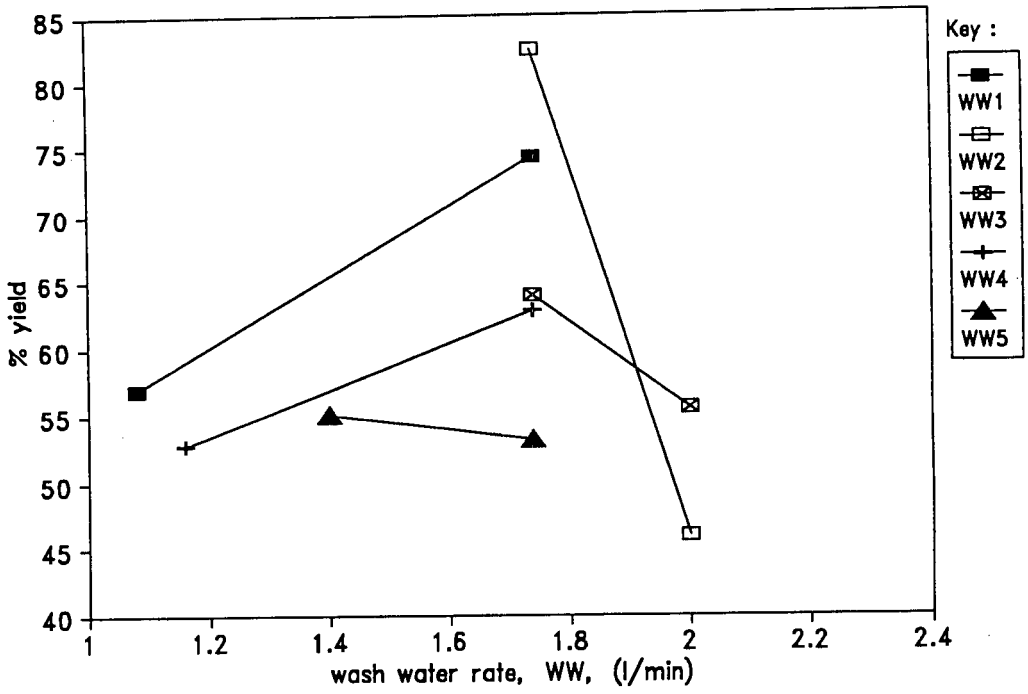

Figure 5.27 : Effect of wash water addition rate on yields produced in pilot column cell. Legend acronyms WW1 etc., indicate which pairs of runs were conducted from the same batch of pulp.

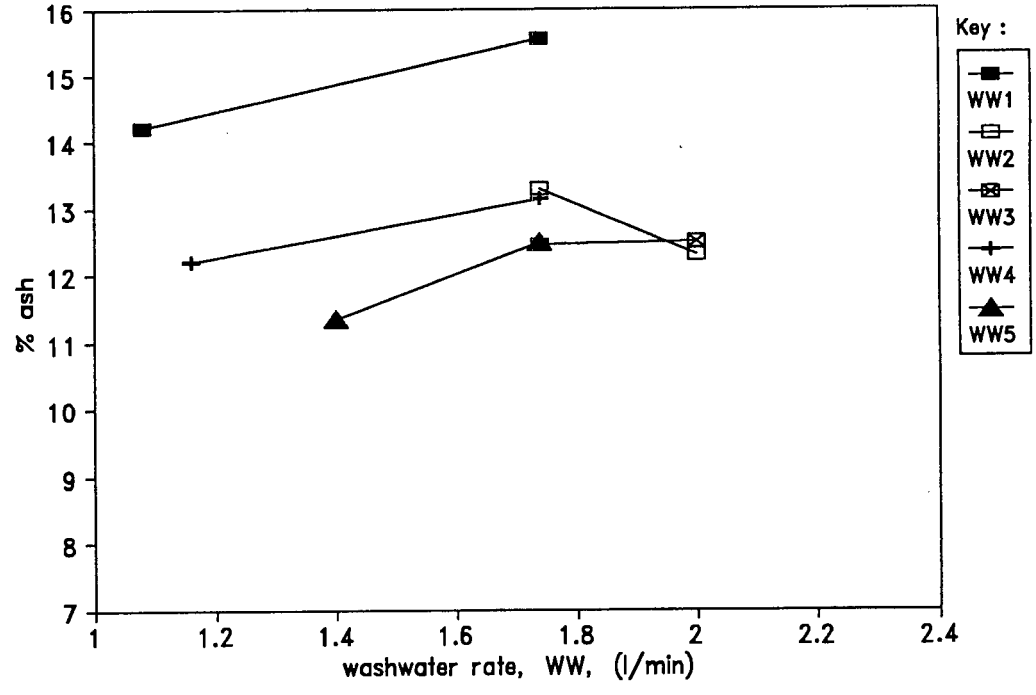

Figure 5.28 : Effect of wash water addition rate on concentrate grades produced in pilot column cell. Legend acronyms WW1 etc., indicate which pairs of runs were conducted from the same batch of pulp.

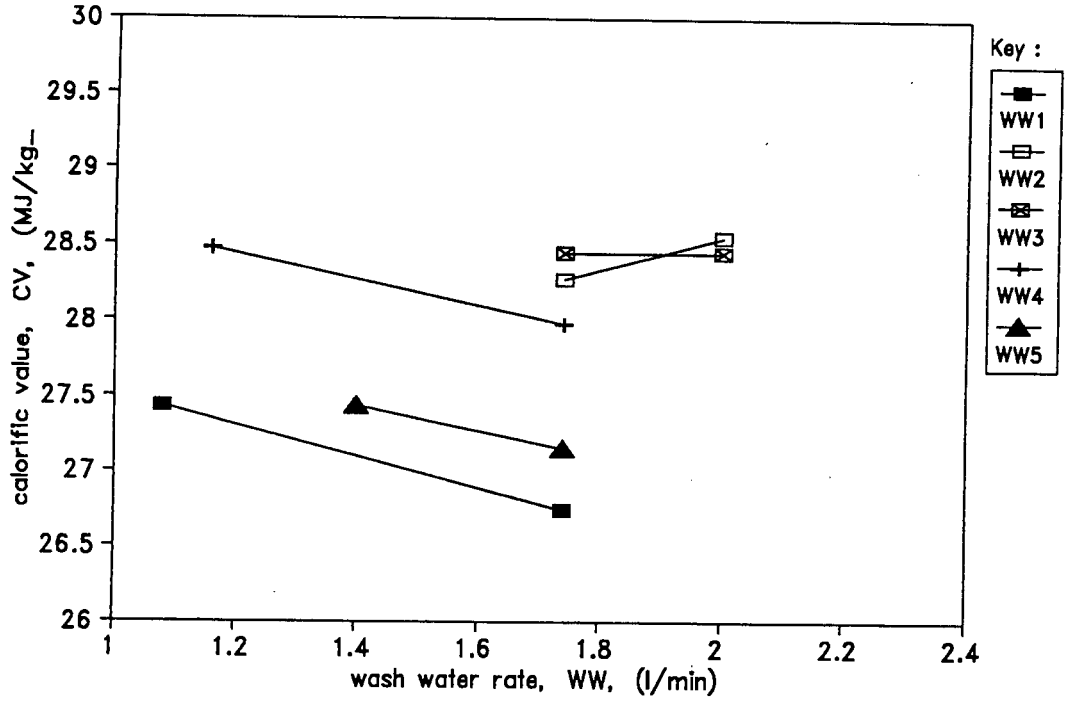

Figure 5.29 : Effect of wash water addition rate on concentrate calorific value (dry basis) produced in pilot column cell. Legend acronyms WW1 etc., indicate which pairs of runs were conducted from the same batch of pulp.

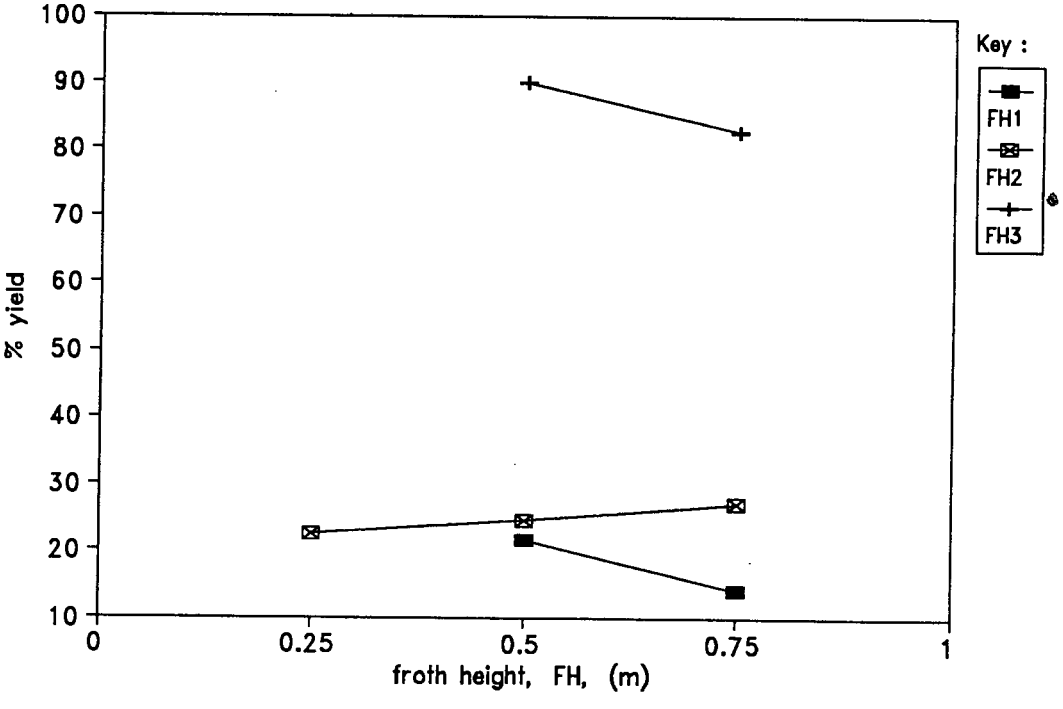

Figure 5.30 : Effect of froth bed height on yields produced in pilot column cell. Legend acronyms FH1 etc., indicate which sets of runs were conducted from the same batch of pulp.

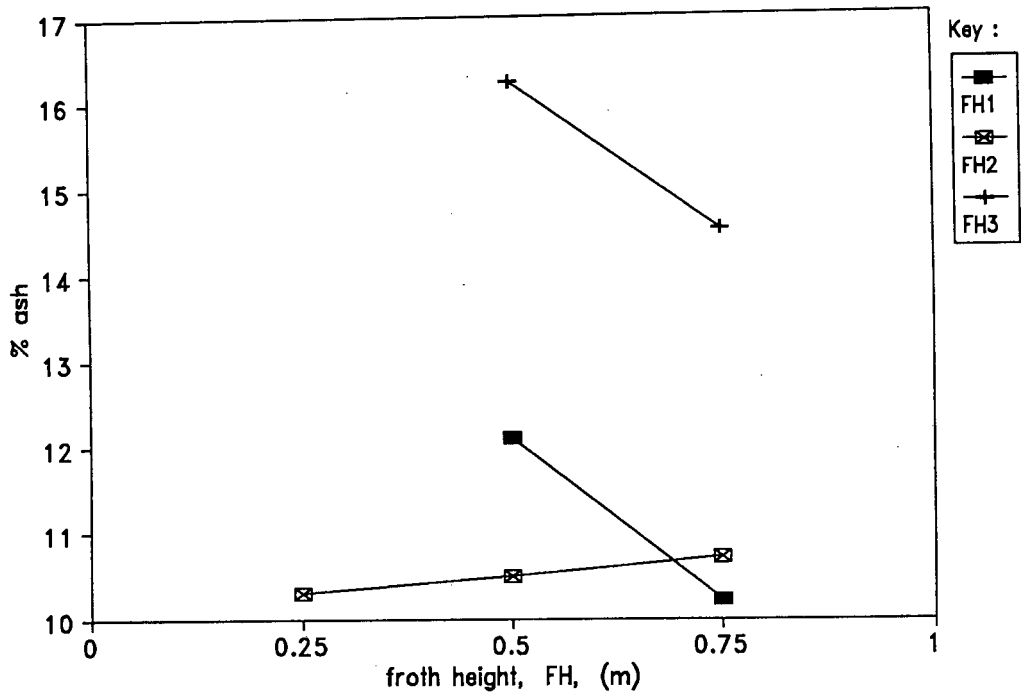

Figure 5.31 : Effect of froth bed height on concentrate grades produced in pilot column cell. Legend acronyms FH1 etc., indicate which sets of runs were conducted from the same batch of pulp.

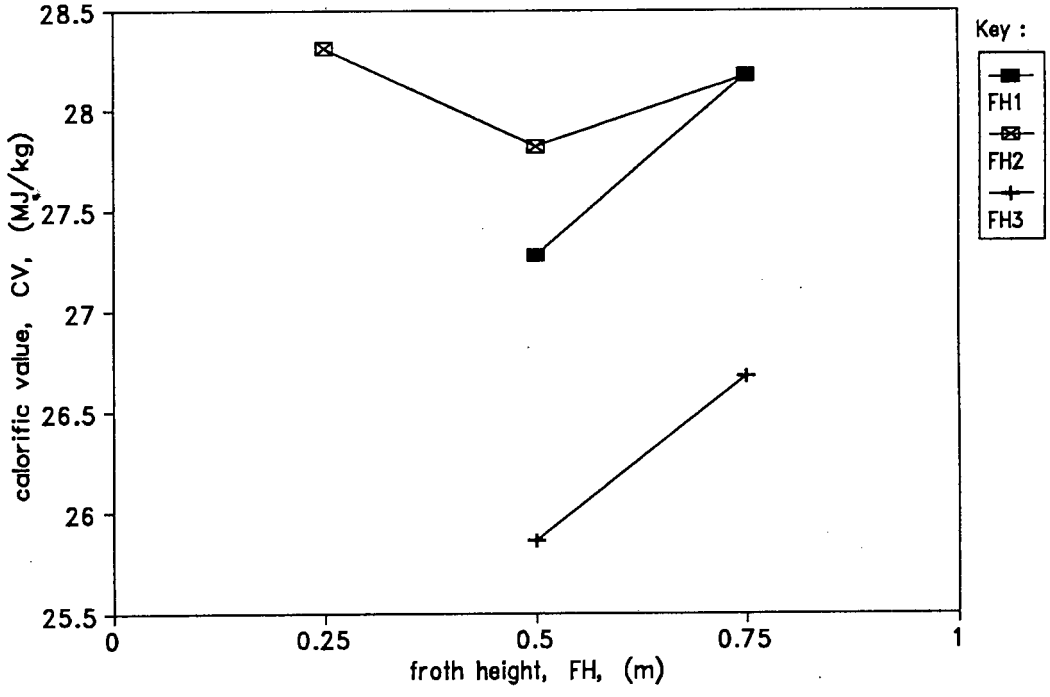

Figure 5.32 : Effect of froth bed height on concentrate calorific value (dry basis) produced in pilot column cell. Legend acronyms FH1 etc., indicate which sets of runs were conducted from the same batch of pulp.

5.3.3.8 Effect of frother concentration

The total frother addition to the column (including frother in the wash water, pulp or sparger water) provides the most convenient basis for investigating the frother concentration effect. The effect of frother addition on column performance was investigated only when the USBM sparger was used; nonetheless, the content of the ensuing discussion also applies to conventional porous spargers such as the filter cloth sparger.

The considerable influence of frother concentration on yield is dramatically illustrated in Figure 5.33. For these runs the sparger water, SW, addition rate was 1 l/min. For run pairs FC1 and FC2 the washwater rate was 1.4 l/min, and for run pair FC3 the washwater rate was 1.7 l/min. Based on reagent consumption per unit feed mass, the frother dosages used ranged between 250 g/t and 500 g/t. Figure 5.33 shows that increases in yield of the order of 30 % were obtained by increasing frother dosage, while all other parameters were kept constant (see also Table E9). Unsurprisingly, the grade and calorific data (Figures 5.34 and 5.35) follow the yield trends; concentrate ash contents increased by an average of 4% and calorific values dropped by an average of 2 MJ/kg.

Improved bubble-particle collection kinetics and enhanced froth bed stability, resulting in higher solids loading levels in the froth bubble bed, can be advanced as explanations for the increases in yields observed (see sections 2.2.3 and 2.2.4 above). Concentrate solids production rate, C_p, is plotted against frother dosage for various levels of collector addition in Figure 5.36. Although the overall trend observed was that concentrate solids production rates, Cp, increased as the frother dosage was raised, it is also evident that, particularly at low collector dosage levels (e.g. CC < 2500 g/t), this was not always the case. The reason for this was discussed in section 5.3.3.3 above, namely that the rate of flotation was determined principally by the composition (i.e. floatability) of the coal fines fed to the column. It was shown in section 5.3.3.2 that collector dosages in excess of 6000 g/t were required to achieve consistent column performance. HTEB belongs to the neutral class of frothers (see section 2.2.4 above) which theoretically do not enhance solids floatability. Thus, unless the

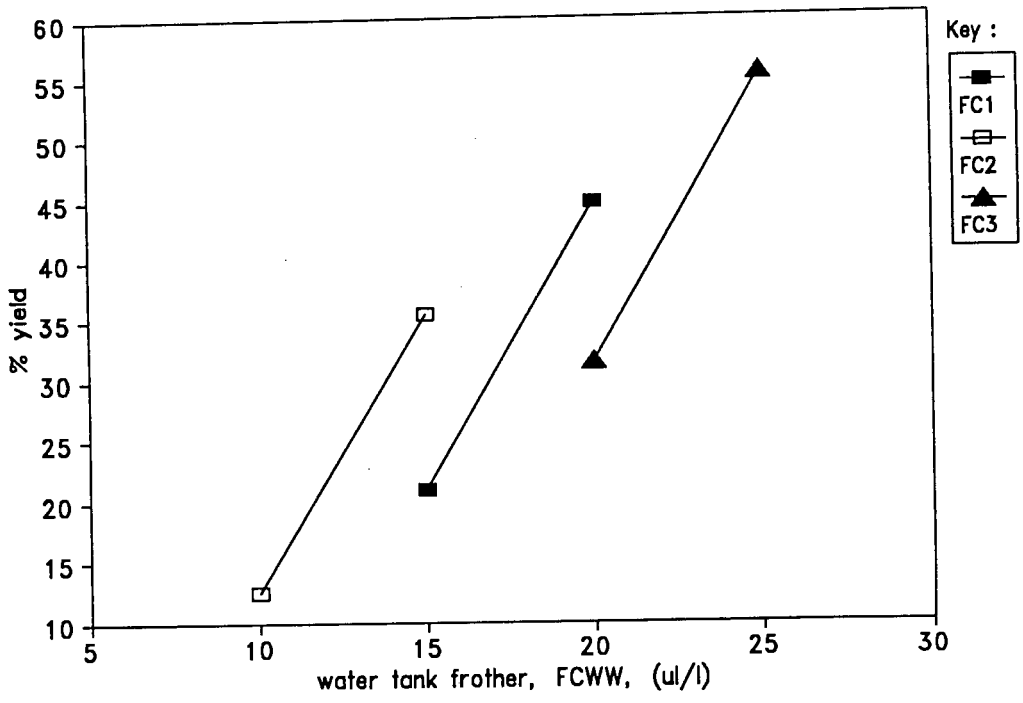

Figure 5.33 : Effect of frother concentration in "USBM" sparger water (μl/l) on yields produced in pilot column cell. Sparger water addition rate, SW, maintained at a constant value of 1.0 l/min. Legend acronyms FC1 etc., indicate which pairs of runs were conducted from the same batch of pulp.

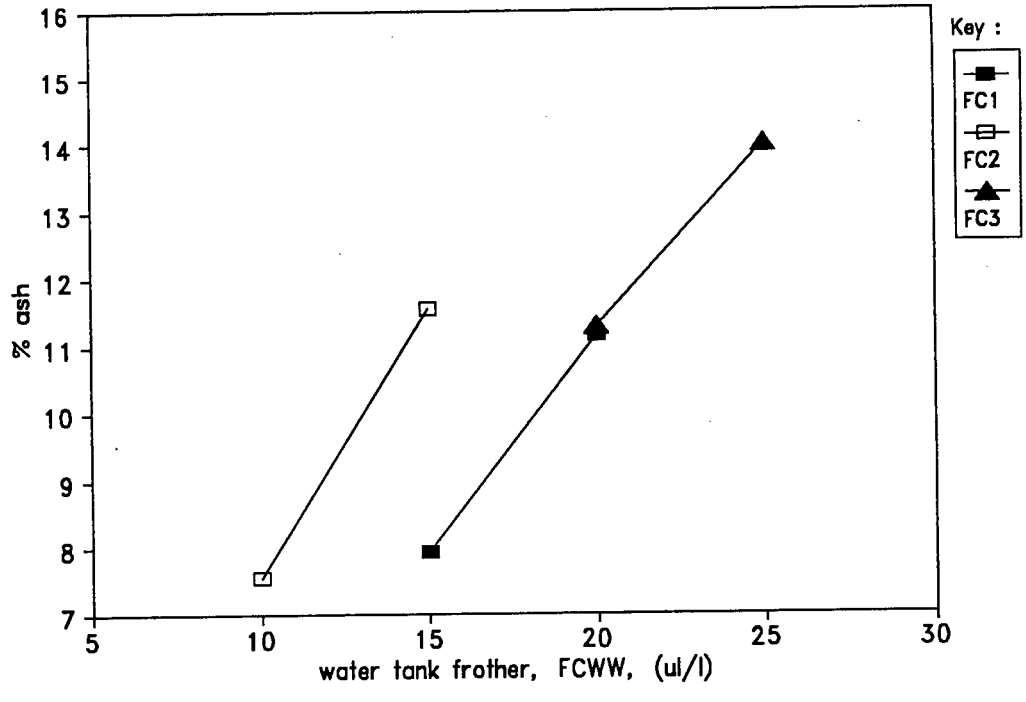

Figure 5.34 : Effect of frother concentration in "USBM" sparger water (μl/l) on concentrate grades produced in pilot column cell. Sparger water addition rate, SW, maintained at a constant value of 1.0 l/min. Legend acronyms FC1 etc., indicate which pairs of runs were conducted from the same batch of pulp.

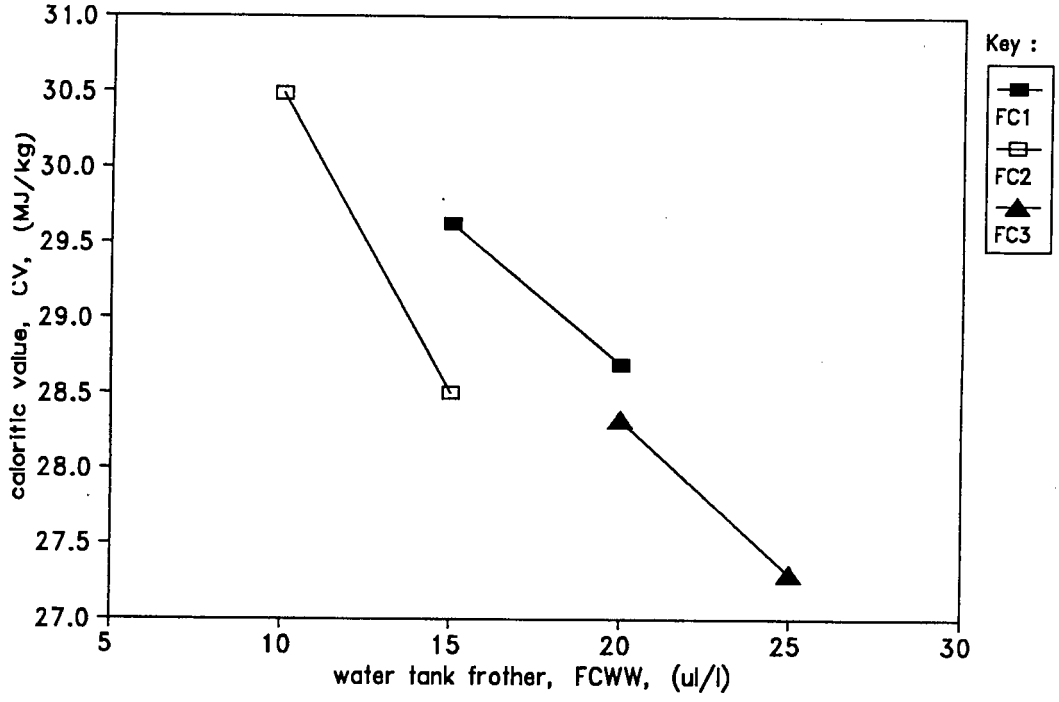

Figure 5.35 : Effect of frother concentration in "USBM" sparger water (μl/l) on concentrate calorific values (dry basis) produced in pilot column cell. Sparger water addition rate, SW, maintained at a constant value of 1.0 l/min. Legend acronyms FC1 etc., indicate which pairs of runs were conducted from the same batch of pulp.

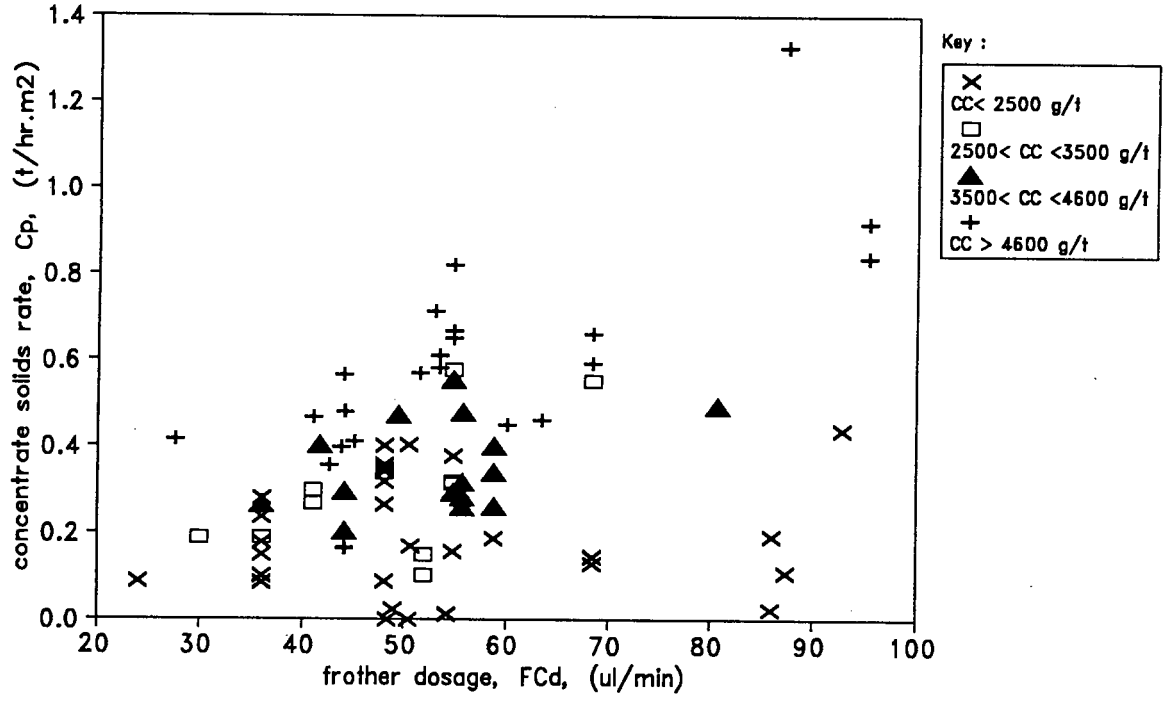

Figure 5.36 : Relationship between rate of production of solids concentrate, C_p, rate of frother addition, FC_d (μl/min), and collector dosage level, CC. Global result; number of column runs, N, equals 77.

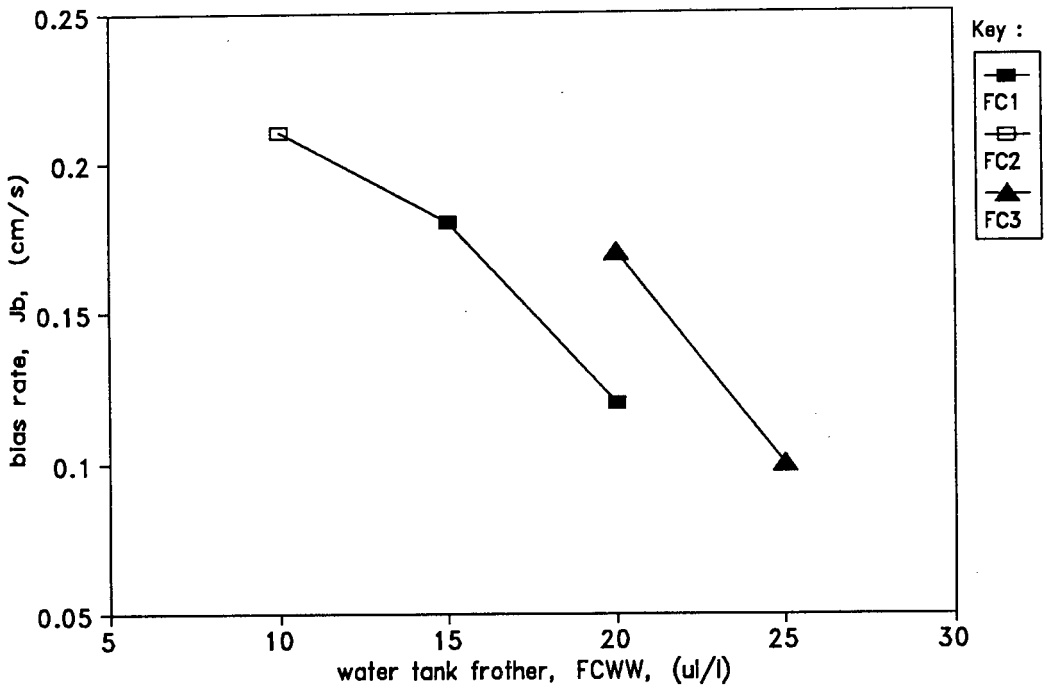

Figure 5.37 : Effect of frother dosage on superficial bias rate, J_b. Same sets of tests as those shown in Figures 5.33-5.35. Sparger water addition rate, SW, maintained at a constant value of 1.0 l/min. Legend acronyms FC1 etc., indicate which pairs of runs were conducted from the same batch of pulp.

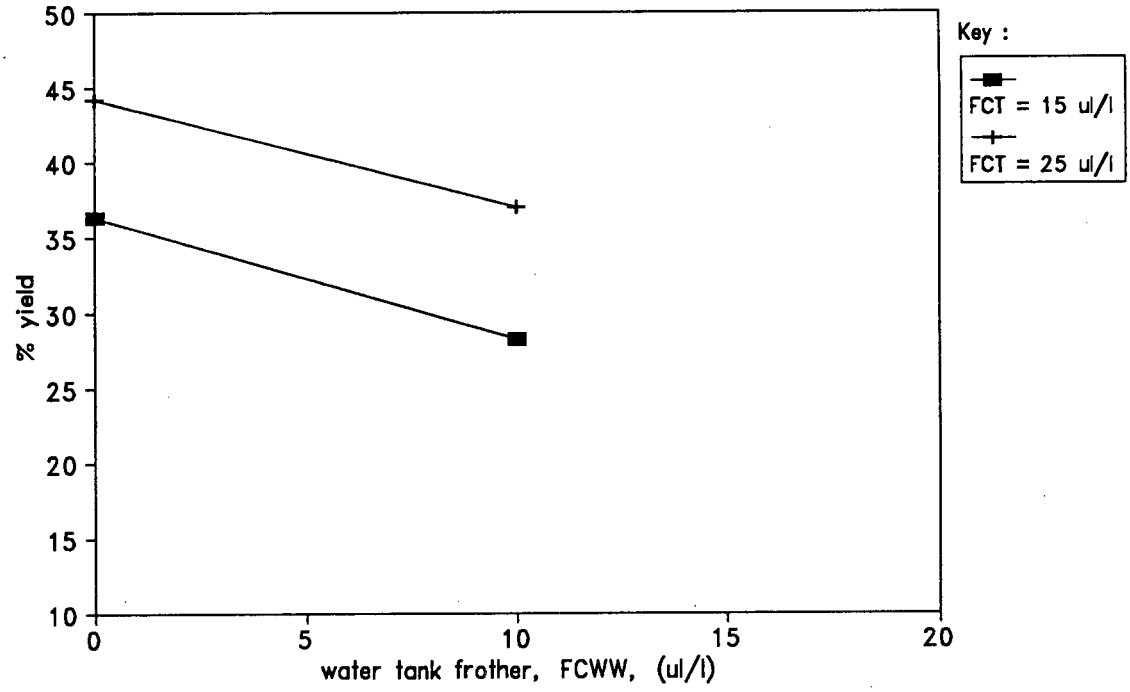

Figure 5.38 : Effect of addition of frother to wash water. "USBM" sparger water and washwater from same supply tank, i.e. same frother concentration, FCWW (μl/l). Filter cloth sparger - frother added to slurry feed pulp tank at a concentration, FCT (μl/l).

column feed was already adequately floatable, increased frother addition did not increase the solids loading of the froth bubble bed.

Excessive frother concentration increases water recovery from the pulp, possibly adversely affecting product grades and calorific contents. This can be partially countered by higher wash water rates. That water recovery in the concentrate increases with frother dosage is clear from Figure 5.37. The bias rate, which is defined as the tails volumetric flow rate subtracted from the feed rate (and sparger water rate if the USBM sparger is used), was reduced as frother dosage increased. Bias rates are listed in Table E9 of Appendix E.

Provided the net downward flow, i.e. bias rate, is sufficiently positive (J_b = 0.1 cm/s is an acceptable minimum, see section 2.3) and the wash water is well distributed, then it is unlikely that entrainment of gangue into the concentrate fraction will occur. Operating at zero or negative bias results in loss of grade. If Table E8 is consulted it can be seen that trials in which the column was operated at zero bias invariably produced concentrate calorific contents below the desired 27.6 MJ/kg specification.

For the majority of column runs (with both the filter and USBM spargers) frother was added to the wash water with the intention of improving froth stability. However, Figure 5.38 appears to indicate that adding frother to the wash water was detrimental to yield performance. Two sets of tests are hardly conclusive : nonetheless, the results belie the assumption that the addition of surfactant necessarily promotes froth stability with concomittant improvements in column performance.

Therefore it is possible that addition of surfactant to the wash water is a superfluous exercise and on an industrial size unit would represent an unnecessary expense.

5.3.3.9 Filter cloth vs USBM sparger

In section 2.5.4 comment was made on the differences between the filter cloth and USBM sparger designs.

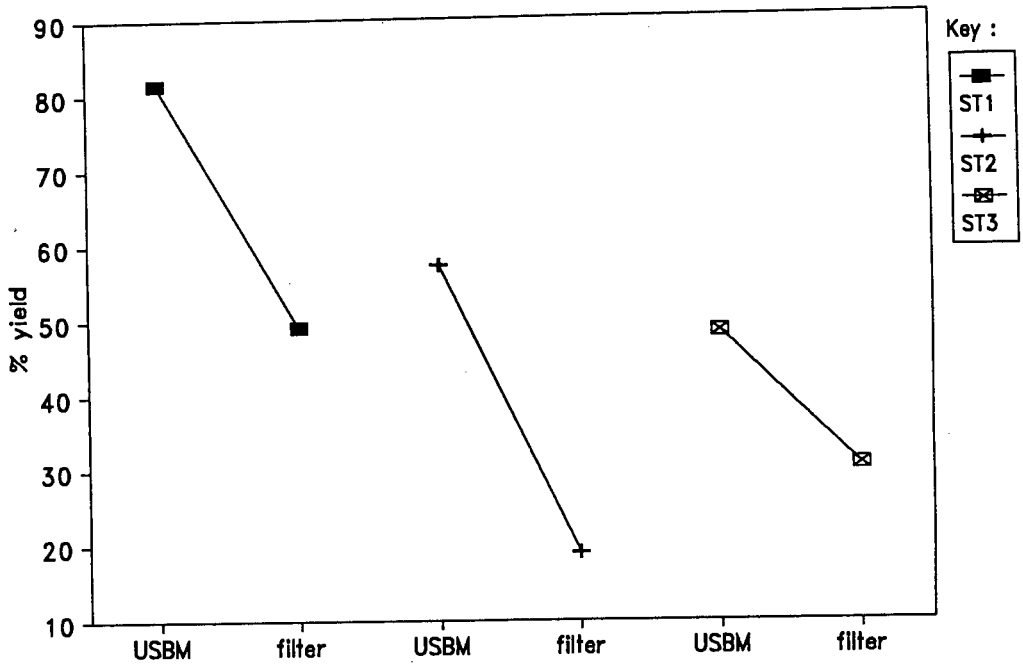

Figure 5.39 : Effect of sparger type on yields produced in pilot column cell. Basis of comparison within blocks - frother dosage rate, FC_d (μl/min) - see Figure 5.40. Legend acronyms ST1 etc., indicate which pairs of runs were conducted from the same batch of pulp.

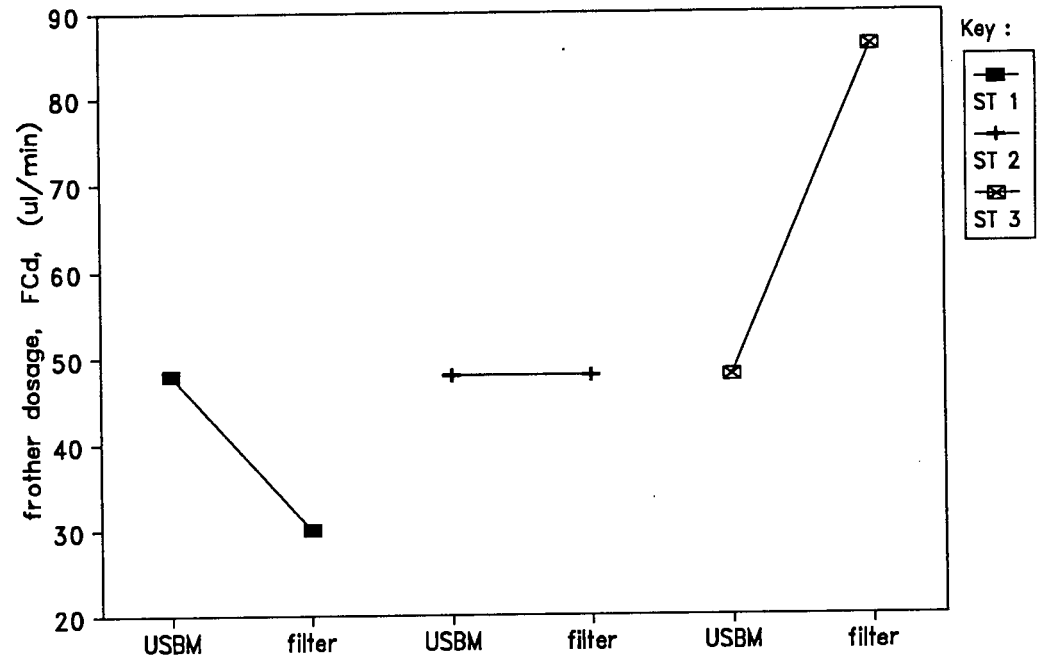

Figure 5.40 : Frother dosage rates of runs plotted in Figure 5.39.

A suitable basis for comparison between the two sparger types is the total rate of frother addition to the column (μl/min). When operating the column with a "USBM" sparger, frother was added to the wash water and sparger water. When the filter cloth sparger was used, frother was added to the wash water and the pulp feed tank.

Figure 5.39 displays the results of tests where the USBM and filter cloth sparger were tested within the same pulp batch. Corresponding frother dosage rates are plotted in Figure 5.40. The sparger trials were conducted at fairly low slurry feedrates (QF = 0.75 to 1.00 l/min). The USBM sparger is clearly superior since, irrespective of the frother dosages used (Figure 5.40), the yields are around 30 % higher than those obtained with the filter cloth (in the same run block). There are inherent drawbacks in adding frother to the pulp tank. Firstly, the surfactant must be adequately dispersed in the pulp tank prior to entering the column with the slurry feed. Also, the hydrodynamics of a column cell are relatively quiescent which is detrimental to efficient mixing.

However, if Figure 5.41 is examined, it is apparent that some good results were achieved with the filter cloth sparger but generally better yields were obtained with the USBM sparger. Tables E8 and E9 of Appendix E can be consulted for details of these tests.

In section 4.3 above, it was found that sparger type had no effect on the flotation of Durnacol thickener underflow fines. The froth phase was found to be rate-determining for this coal. Conversely, for the Kleinkopje thickener fines, both the laboratory (section 4.5) and plant results (section 5.3.3.3) showed that the pulp phase kinetics influenced column yield. Consequently, it appears that sparger type affected column performance on the plant because the kinetics of particle collection in the pulp phase was important.

5.3.3.10 Plant vs laboratory test results

The parameter levels used in the laboratory and plant column tests are compared in Table 5.8 below. Aside from the superficial feed velocities, J_f, and solids feedrates, S_f, which were, on average,

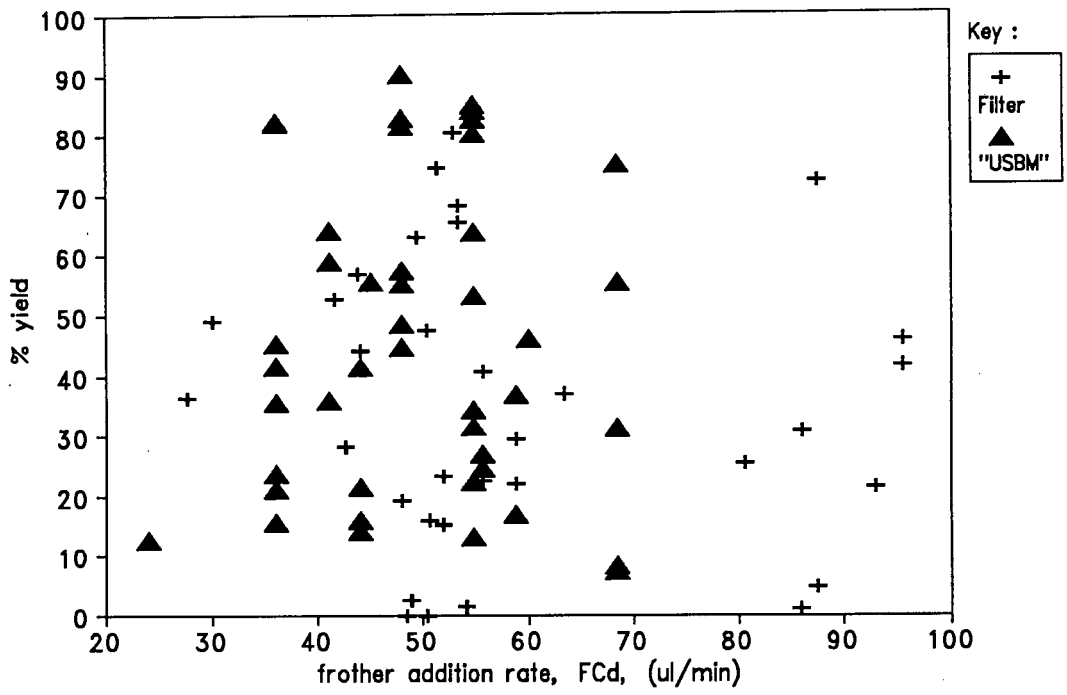

Figure 5.41 : Comparison of yields produced in pilot column cell using "USBM" or filter cloth spargers. Global results; total number of column runs, N, equals 77.

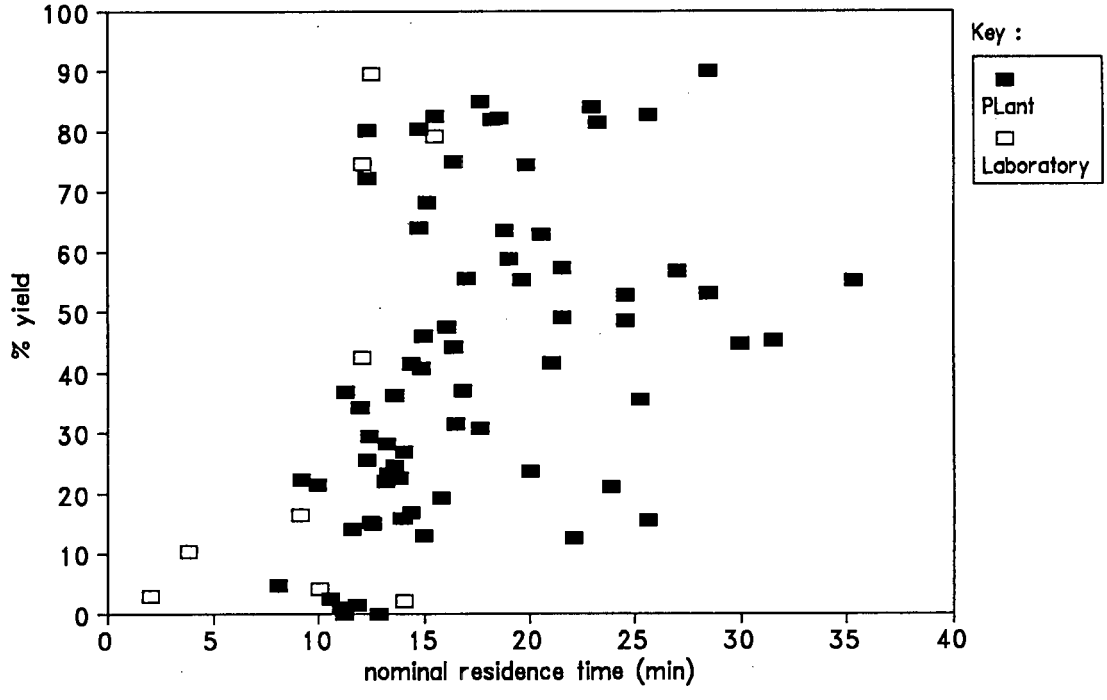

Figure 5.42 : Effect of nominal residence times, τ_n, on flotation yields. Runs conducted in both the 54 mm ID laboratory column cell and the 100 mm ID pilot column cell.

slightly lower for the plant column compared with those used for the laboratory column tests, the operating parameters values were fairly similar. Slurry residence times for the two sets of tests are plotted against yield in Figure 5.42. Nominal slurry residence time, τ_n, was defined in section 2.3.3 above as the volume of the collection zone (between the sparger and feed inlet) divided by the volumetric tails flowrate. Pulp residence times for plant column tests were, on the whole, slightly longer than for those conducted in the laboratory.

Table 5.8 : Summary of operating parameter levels selected for Kleinkopje Laboratory and Plant column tests.

	Plant			Laboratory		
Parameter	Minimum	Maximum	Average	Minimum	Maximum	Average
J_g (cm/s)	1.4	2.8		1.7	2.5	
J_w (cm/s)	0.23	0.42		0.29	0.44	
J_f (cm/s)	0.12	0.73	0.32	0.24	0.80	0.43
S_f ($t/hr.m^2$)	0.32	2.25	0.9	0.51	2.14	1.21
C_p ($t/hr.m^2$)	0.00	1.31	0.35	0.02	1.50	0.38
CC (g/t)	791	7716	3850	1018	12230	4604
FC (g/t)	184	1050	475	116	1400	530
CH (m)			4.5	2.75	5.25	
FH (m)	0.25	0.75	0.50	0.35	0.75	

Global yield/grade results obtained from both the laboratory column tests and the plant trials, together with the float/sinks curve, are plotted in Figure 5.43. It is apparent that the yield/grade performances achieved with the laboratory column were, with one exception, superior to the plant column trials. However, as stated in section 4.4.5.1 above, solids settling in the laboratory feed pulp tank resulted in a sample bias in composition between the laboratory (mean feed ash, X_{avg} = 20.16 %) and average plant (mean feed ash, X_{avg} = 23.06

%) feeds. In the absence of bias, one would therefore expect some overlap between the plant and laboratory yield/grade data.

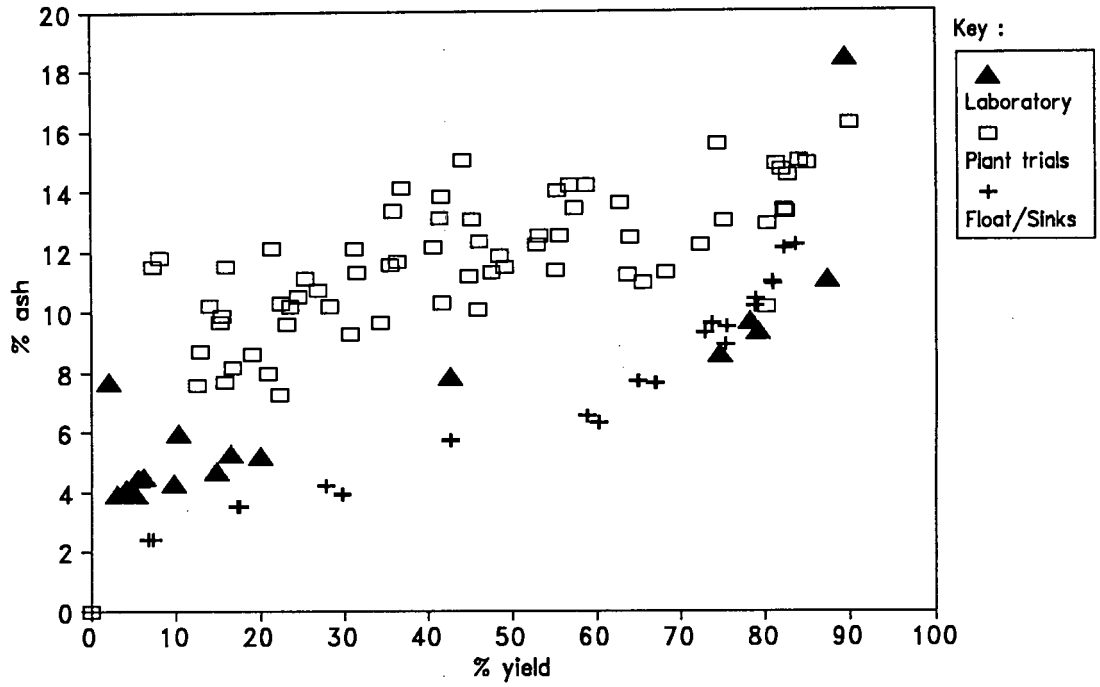

Figure 5.43 : Comparison of global results from laboratory and pilot column tests. Kleinkopje thickener underflow fines.

For both the laboratory and plant column tests, high collector dosages (CC ≈ 6000 g/t) were required to achieve reasonable (say 60 % or higher) yields. As was shown in section 3.4 above, the poor floatabilty of the Kleinkopje fines was directly attributable to the high (70 %) inertinite content of the coal.

The comparison of frother consumption between the pilot and laboratory columns is better made on a g/t rather than addition rate (l/min) basis. Raising frother addition levels to 400 g/t or higher improved yields by about 30 % in the laboratory and pilot columns. However, if insufficient collector was added (see sections 4.4.5.2 and 5.3.3.8 above), raising the frother addition level alone was not sufficient to generate satisfactory yields. Because of improved stability as surfactant dosage was raised, the froth bubble bed was also able to carry more solids. A maximum concentrate production rate, Cp, of 1.5 t/hr.m2 was reached in the laboratory column, whilst during the plant trials the highest production rate was 1.3 t/hr.m2. It is likely that improved pulp phase flotation kinetics (smaller bubbles are produced when surfactant concentrations are increased, as described in section

2.2.3 above) also contributed to the increase in yields observed at high frother concentrations.

Increasing the volumetric slurry feedrate, QF, from 1.6 l/min (J_f = 0.34 cm/s) to 3.5 l/min (J_f = 0.74 cm/s), caused reductions in pilot column yield of up to 60 %. A similar effect was observed in the laboratory column where reductions in yield of 40 % where observed when J_f was increased from 0.3 to 0.6 cm/s. Increasing the collection zone of the laboratory column from 2.75 m to 5.25 m improved yields by up to 40 %. Pulp zone kinetic effects were therefore observed in both the plant and laboratory tests.

Air flowrate did not affect column yields in either the laboratory or plant tests. However, for the laboratory tests, an increase from 1.6 to 2.5 cm/s in superfical air velocity was observed to double concentrate ash content when shallow (FH = 0.35 m) froth beds were used. With, one exception, the plant column trials were conducted at froth bed depths greater than 0.5 m.

Washwater addition rates were observed to affect both the yields and grades obtained during the plant trials. A similar effect was not, however, observed in the laboratory column. It is probable that this reflects that washing of the froth bed was more efficient in the pilot column compared with the laboratory column. In other words a scale effect existed between the wash water distribution through the froth bubble bed in the pilot column compared with that characteristic of the laboratory froth bed. The designs of the laboratory and pilot column washwater distributors have been described in sections 4.2 and 5.2 above. The laboratory column distributor was cross-shaped whilst the pilot rig column distributor was concentric in shape. Thus the latter design covered a bigger fraction of the column cross-sectional area than did the laboratory distributor.

Froth height was not observed to affect yield or grades attained in the pilot column, but for reasons discussed in section 4.4.5.2 above, at high air rates entrainment was noted in shallow (FH = 0.35 m) laboratory column froths. Due to the limited number of laboratory tests conducted, it was not possible to evaluate the influence of sparger design on

laboratory column performance and draw comparisons with the effects noted during the plant trials (section 5.3.3.9 above).

5.4 SUMMARY AND CONCLUSIONS OF PLANT TRIAL TESTWORK

On-site plant trials using a 100 mm ID pilot column showed that column flotation was capable of recovering a steam quality 27.6 MJ/kg product from Kleinkopje thickener fines at yields of up to 70 %. The liberation characteristics of the coal in the various size fractions were such that reasonably consistent grade concentrates (containing 12 - 13 % ash) were produced regardless of the yields obtained.

Problems were experienced with variability in the composition of the column feed (which is a blend of "select" and "non-select" coals); this caused poor flotation reproducibility.

It was found necessary to screen the underflow fractions over a linear screen prior to column flotation. The coal fines were on average 93 % finer than 150 μm and 68 % finer than 75 μm. Column flotation technology is particularly suited to upgrading the finest feed fractions. On average 80 % of the -45 μm fines fraction, which typically constituted nearly 50 % of the feed, was recovered and upgraded from a mean feed ash of 27.9 % ash to an average concentrate grade of 11.63 % ash or equivalently from a mean feed calorific value of 21.6 MJ/kg to a product calorific value of 28.2 MJ/kg.

At dosage levels less than 6000 g/t the yield performance of the pilot column was erratic. This was due to the high inertinite content (on average 70 %) of the Kleinkopje fines.

Frother concentration and slurry feedrate were found to be the pilot column parameters which most significantly affected recovery. The "USBM" sparger, on average, produced better yield results than did the filter cloth. It was postulated that this occurred because of the importance of bubble size when pulp phase kinetics are a factor affecting product recovery.

The maximum production capacity achieved in the pilot column was 1.3 t/hr.m^2 which is comparable to 1.5 t/hr.m2 attained in the laboratory column.

Similar operating parameter effects were observed from the laboratory column and plant trial testwork. Air flowrate was not observed to affect yield, but in the laboratory column was observed to influence grade. This was attributed to poorer washing of the froth bubble bed in the laboratory column compared with the pilot column. The fact that washwater was observed to affect yield and grade in the pilot but not the laboratory column corroborates this.

5.5. RECOMMENDATIONS

Adequate preparation of the Kleinkopje Colliery fines prior to flotation is necessary if column flotation were to be implemented on a commercial scale. Processing steps required would include a size separation to remove overly coarse material (+ 150-200 μm) from the thickener fines, the removal of non-floating "non-select" material so as to ensure a fairly consistent feed composition dominant in vitrinite rich "select" coal fines, and ensuring that the collector added to the pulp conditioned the feed slurry efficiently. The other major problem concerns coal conditioning in large pulp tanks, a technique which has been shown to be intrinsically inefficient. In section 3.4 it was commented that considerable scope for improvement of coal conditioning lies in better choice of collector and "promotor" reagents as well as designing more energetically efficient conditioning vessels. The experience of the Kleinkopje Plant trials makes these remarks all the more pertinent.

CHAPTER 6

SUMMARY AND CONCLUSIONS

The principal aims of this thesis were to investigate whether column flotation technology could be suitably applied for recovering saleable, particularly low-ash, quality coal from South African coal fines which are presently discarded; and to determine what the important, or dominant, operating parameters are for this process.

The results described and discussed in the preceding chapters show that it was possible to recover the desired quality products from all three of the coal fines samples which were subjected to column flotation.

A 12 % coking quality coal was produced at a yield of 60 % from a sample of Durnacol thickener underflow fines.

A maximum low-ash coal yield of ≈ 65 % was attained from column flotation tests performed on a "select"/"non-select" composite sample of thickener underflow from Kleinkopje Colliery. On-line column trials were also conducted at the Kleinkopje Preparation Plant. These tests showed that a steam quality 27.6 MJ/kg product could be recovered from the thickener fines at yields of up to 70 %.

Low-ash (≈ 7.4 % ash) coal at yields of up to 45 % was obtained from column flotation of Greenside thickener underflow fines. Upon milling the Greenside fines to an 80 % passing 25 μm size, the yield of low-ash coal increased to 70%.

For all coals tested, better grades were attained at any given yield from column cell flotation as compared with conventional (batch) froth flotation. In fact, the yield/grade data obtained from column flotation of the milled Greenside thickener underflow coincided with the float/sinks washability curve. Column flotation of Kleinkopje thickener underflow in a laboratory column produced similar results; the yield/grade data coincided with either the "release" flotation or float/sinks curves.

The recovery versus particle size information elicited from the Kleinkopje Colliery trials showed that the column cell is best suited to recovering and upgrading the finer (< 75 μm) size fractions. In particular, it was found that the -45 μm size fraction, which had the highest feed ash content (27.9 % ash), was upgraded to an average concentrate grade of 11.6 % ash. The average recovery of d.a.f. coal in this fraction was 80 %. This finding is consistent with the high particle separation efficiencies known to be achievable in a column cell. Conversely, recovery of size fractions coarser than 75 μm was found to be poor. This result is also in agreement with reported literature on column flotation of coal fines.

It was found that, excluding the milled Greenside fines, the best yield/grade results were obtained at concentrate solids production rates of between 0.5 and 1.0 t/hr.m^2. Above 1.0 t/hr.m^2 relatively poorer grades were achieved; in all probability this was a result of poor drainage and solids crowding effects in the froth bubble bed. As the primary performance criterion for flotation is the product grade attained at a given yield, it may be concluded that optimal solids throughput for a column cell lies below its carrying capacity limit ($C_{popt} < C_a$). The fineness of the column feed is also clearly an influential factor as the largest production throughput achieved with the milled samples (d_{80} = 25 μm) was only $\approx$ 0.15 t/hr.m^2.

Aside from the particle size distribution of the feed, column performance was determined by the floatability of the coal feed and the column operating parameter levels selected.

It was found that the inherent floatability of a coal was strongly influenced by its TYPE. The Durnacol sample which had a vitrinite content of 85 % was the most easily floated coal tested. Conversely, the Kleinkopje composite fines sample which had an inertinite content of 71 % was extremely poorly floatable. In both the laboratory and plant column tests, collector dosages in excess of 6000 g/t were required to obtain yields greater than 50 % from the Kleinkopje thickener underflow fines.

The efficiency of the conditioning step was shown to depend on coal TYPE, the method of oil dispersion used and the size and mechanical design of the conditioning mixing vessel. Adding a pre-dispersed oil-water emulsion to a coal pulp suspended in a 3 l modified Leeds flotation cell lowered the efficiency with which the coal pulp was conditioned compared with the standard method of adding a dose of oily collector below the pulp surface. This effect was most pronounced in the Witbank coals from the Kleinkopje and Goedehoop Collieries; pre-dispersing the oil had a negligible effect on the conditioning (and flotation) of the two Natal coal samples taken from the Durnacol and ZAC Collieries.

However, bulk addition of oil to larger pilot scale ($\approx$ 100 l capacity or greater) mixing vessels was also discovered to be an unsuitable conditioning technique. The pulp turbulence intensity is an order of magnitude lower in a 100 l tank ($\epsilon_{avg} \approx 5$ W/l) compared with the 3 l Leeds cell ($\epsilon_{avg} \approx 60$ W/l); consequently oil dispersion was poorer. As was the case with pre-dispersed oil/water mixtures, this had a negligible impact on the flotation of the Natal coals but seriously reduced the rate of flotation of the Witbank coals, particularly the Kleinkopje fines.

It was postulated that the poor floatability of the inertinite-rich coals arose from their high oxygen contents. Consequently these coal surfaces carried fairly strong negative charges. As oil droplets also exhibit negative surface potentials, the coulombic repulsion energy barrier would be a major impediment to effective collision and spreading of oil-droplets over the coal particle surfaces.

Frother concentration, FC, was found to be the operating parameter which most influenced coal yield and product grade. Raising frother dosage from around 100 g/t to 400 g/t and above increased flotation yields of Durnacol thickener underflow fines by up to 50 %; however, concentrate ash contents increased by between 5 % and 7%. Frother dosage was found to improve the recovery of Kleinkopje fines only if sufficient collector (CC > 5000-6000 g/t) had already been addded. Improved froth bed stability (i.e. reduced bubble coalescence) and, where particle-bubble collision kinetics were important, finer size bubbles in the pulp were

attributed as the reasons for the effects observed. Also, the highest solids production rates were achieved at the higher frother dosages quoted above. A reduction in bias rate was observed to occur when frother dosage was increased, thus poorer cleaning of the froth was probably a factor contributing to lower grades obtained under these conditions.

Air flowrate, AF, was observed to slightly improve product yields from the Greenside and Durnacol thickener underflow fines; no effect was observed in either the plant or laboratory column tests conducted on Kleinkopje thickener underflow fines. However, air rate strongly influenced the yields obtained from the milled Greenside fines samples; lowering the superficial air rate from 2.3 cm/s to 1.8 cm/s resulted in a 20 % drop in yield. This suggests that the rate of generation of bubble surface area limits the recovery of very fine particles. Equivalently, one could say that for ultrafine ($d_{80} \approx 25$ μm) feeds, carrying capacity is a strong function of air rate.

Particle collection in the pulp phase was found to be strongly influenced by the petrographic composition (TYPE) of the coal feed. Pulp phase kinetics had a negligible effect on the recovery of Durnacol coal fines whereas the laboratory column flotation tests performed on the Greenside and Kleinkopje thickener underflow samples showed that increasing collection zone height, CH, or reducing the slurry feedrate, QF, improved mass recoveries. In the case of the plant column trials, the column height was kept constant; however, raising slurry feedrates (or equivalently reducing particle residence times in the pulp phase) reduced yields by up to 60 %. This result was similar to that obtained in the laboratory column tests. Slurry feedrate was found to be significant variable for the Durnacol column tests because the change in solids feedrate which occurred as the level of QF was changed affected the solids loading in the froth bubble bed (when the frother dosage, FC, was at the high (+) level).

The plant trial tests showed that sparger design and mode of operation had influence on column flotation yield whereas the designed experiment conducted on the sample of Durnacol thickener underflow fines indicated no effect. It was postulated that bubble size and distribution is

important when pulp phase kinetics contribute to the overall rate of flotation. Thus the USBM sparger improved the flotation yields obtained from Kleinkopje coal fines but had no impact on the flotation yield of the Durnacol fines because the fast flotation kinetics characteristic of this latter coal resulted in mass transport and recovery in the froth phase controlling the overall rate of flotation.

A scale effect was observed to affect the washing of the froth bubble bed. In the 2" diameter column washwater rate had no effect on yield or grade, however, a combination of high air superficial velocities (> 2 cm/s) and a shallow froth bed (FH < 50 cm) resulted in poor grades which were well above the "release" flotation or washability curves. Conversely, in the larger 90 mm and 100 mm diameter columns the washwater addition rate was found to have a strong influence on yield and grade. It was postulated that the washwater was more evenly distributed (i.e. less channeling along the column wall) through the froth bubble bed in these larger columns than in the 2" column. It was noted that the 2" column had a cross-shaped wash water distributor design and only 12 distributor holes whereas the distributor used for the other columns was concentric in shape with 56 distributor holes evenly distributed over the column cross-section.

Fractional factorial designs were shown to be an effective method for investigating a relatively large number of operating variables (7 in the two cases tested) in a fairly limited number of experiments (8 or 16). These designs are screening, not optimisation designs, i.e. they are intended to identify the most important input variables or input variable interactions from a set of preliminary experiments. It is evident from the above discussion that this goal was achieved using the designed experiments. The factors identified as the most important were in agreement both with physical interpretations of the mass transport processes occurring within the column cell and also confirmed with what was known or expected from the literature consulted. Finally, another useful feature of the factorial design experiments was that they gave an indication of the reproducibility and repeatability associated with column cell operation. It was apparent that for the 2" laboratory column in particular, grade reproducibility was poor, although yield, recovery and grade repeatabilities (i.e. fluctuations as steady state)

were good. The washwater distributor design and inadequate solids suspension in the feed pulp holding tank were attributed as the causes for the comparatively large reproducibility errors observed.

It was concluded (sections 3.4.4. and 5.5) that existing conditioning techniques for laboratory or pilot-scale column tests are inadequate especially in cases where inherently poorly floatable coals, such as coals which consist predominantly of inertinite, are to be conditioned. Scope for improvement in this area lies in better reagent selection and more efficient utilisation of the energy supplied to conditioning vessels.

REFERENCES

Anderson, G.V., "The Role of Hydrocarbon Oils in Coal Flotation : An Investigation into some Pulp-Phase Sub-Processes", PhD Thesis submitted to University of Cape Town, June 1988.

ibid, 1988a, pp 67-85.

Amelunxen, R.L., "Column Flotation : New Carrying Capacity Considerations for Scale-Up", presented at EXPOMINERA '90, Santiago, Chile, May 14-18, 1990.

Antipenko, L.A., Deberdeev, I.Kh. and Nazarenko, V.M., "Coal Flotation Technology and Theoretical Preconditioning of Its Improvement", in Proceedings of 10th International Coal Preparation Congress, Volume 1. Sept 1986, Edmonton, Alberta, Canada, pp 80-89.

Aplan, F.F., "Coal Flotation", in Flotation - A.M. Gaudin Memorial Volume (2) (M.C. Fuersteneau ed.), American Society of Mining Engineers, New York, 1976, pp 1235-1265.

Aplan, F.F., "Fine Coal Preparation - Its Present Status and Future", in Fine Coal Processing - Edited by Mishra, S.K. and Klimpel R.R., Noyes Publications, New Jersey, U.S.A., 1987, pp 12-15.

Aplan, F.F., "How the Nature of Raw Coal Influences its Cleaning", in Industrial Practice of Fine Coal Processing (R.R. Klimpel and P.T. Luckie ed.), Conference Proceedings, Hidden Valley, PA, September 1988, pp 99-111.

Berkowitz, N., "An Introduction to Coal Technnology", Academic Press, New York, 1979, pp 3-20.

Berkowitz, N., "Coal Science and Technology Vol 7 - The Chemistry of Coal", Elsevier Science Publishers B.V., Amsterdam, 1985.

Botha, P.H., "An Investigation of the Flotation of Three South African Coals", Journal of the South African Institute of Mining and Metallurgy, November 1980, pp 395-400.

Box, G.E.P. and Hunter, J.S., "The 2^{k-p} Fractional Factorial Designs : Part I", Journal of the Biometric Society, Vol 17, No 1, March 1961, pp 311 - 351.

Box, G.E.P. and Hunter, J.S., "The 2^{k-p} Fractional Factorial Designs : Part I", Journal of the Biometric Society, Vol 3, No 4, November 1961, pp 449 - 458.

Box, G.E.P. and Meyer, R.D., "Dispersion Effects from Fractional Designs", Technometrics, February 1986, Vol 28, No 1, pp 19 - 27.

Box, G.E.P. and Draper, N.R., "Empirical Model-Building and Response Surfaces", John Wiley and Sons, New York, 1987.

Breed, A.W., Private Communication, Chemical Engineering Department, University of Cape Town, 1992.

Brown, D.J., Gray, V.R. and Jackson, A.W., "The Spreading of Oil on Wet Coal", J. Appl. Chem., 8, 1958, pp 752-759.

Burkin, A.R. and Bramley, J.V., "Flotation with Insoluble Reagents. I. Collision and Spreading Behaviour in the coal-oil-water system", J. Appl. Chem., 11, 1961, pp 300-309.

Burkin, A.R. and Bramley, J.V., "Flotation with Insoluble Reagents. II. Effects of Surface-Active Reagents on the Spreading of Oil at Coal-Water Interfaces", J. Appl. Chem., 1963, pp 417-422.

Burt, R.O. and Mills, C., "Gravity Concentration Technology - Developments in Minerals Processing, Volume 5", Elsevier, New York, 1984, pp 261-287.

Buys, I.E., "A Liberation Study on Ultrafine South African Coals", M.Sc Thesis, University of Cape Town, 1989.

Calabrese, R. V., Wang, C. Y. and Bryner, N. P., "Drop Breakup in Turbulent Stirred-Tank Contactors - Part III: Correlations for Mean Size and Drop Size Distribution", AIChE, Vol 32, No. 4, April 1986a, pp 677-681.

Calabrese, R.V., Chang, T.P.K. and Dang, P.T., "Drop Breakup in Turbulent Stirred-Tank Contactors - Part I: Effect of Dispersed-Phase Viscosity", AIChE Journal, Vol. 32, No. 4, April 1986b, pp 657-666.

Calderbank, P.H., "Chapter 6 - Mass Transfer", in Mixing - Theory and Practice, Volume II, ed. Uhl, V. W. and Gray J. B., Academic Press, New York, 1967.

Chen, H. T. and Middelman S., "Drop Size Distribution in Agitated Liquid-Liquid Systems", AIChE, Vol 13. No 5, pp 989 - 995.

Chun Li, C., "Analysis of Unbalanced Data : a Preprogram Introduction", Cambridge University Press, New York, 1982.

Clark, M. M., "Drop Breakup in a Turbulent Flow - I. Conceptual and Modelling Considerations.", Chemical Engineering Science, Vol 43, 1988, pp 671-679.

Cochran, W.G., "Some Consequences when the Assumptions for the Analysis of Variance are Not Met", Biometrics, 3, 1947, pp 22 -38.

Collins, G.L. and Jameson, G.J., "Experiments on the Flotation of Fine Particles - The Influence of Particle Size and Charge", Chem. Engng. Sci., vol. 31, 1976, pp 985-991.

Collins, G.L. and Jameson, G.J., "Double-Layer Effects in the Flotation of Fine Particles", Chem. Engng. Sci., Vol 32., 1977, pp 239-246.

CSIR Report CPE 1/91, "The Situation of Waste Management and Pollution Control in South Africa. Report to the Department of Environment Affairs by the CSIR Programme for the Environment, Pretoria", pp 358.

Cutter, L. A., "Flow and Turbulence in a Stirred Tank", AIChE Journal, Vol 12., No. 1, 1966, pp 35-45.

Das, M.N., and Giri N.C., "Design and Analysis of Experiments", Halstead Press, John Wiley and Sons, New York, 1979.

Davies, J. T., "TURBULENCE PHENOMENA", Academic Press, New York, 1972.

ibid, 1972a, pp 348-351

ibid, 1972b, pp 62-68

Department of Mineral and Energy Affairs, "South African Discard and Duff Coal - National Inventory 1985", Aurora Printers for Government Printer, Pretoria, 1987.

Department of Mineral and Energy Affairs, "South Africa's Mineral Industry 1988", Minerals Bureau, Johannesburg, 1989.

Derjaguin, B.V. and Zorin, Z.M., "Optical Study of the Adsorption and Surface Condensation of Vapours on a Smooth Surface", 2nd International Congress on Surface Activity 1957, London, Butterworth, vol. 2, 1957, pp 145-152.

Derjaguin, B.V. and Shukakidse, N.D., "Dependence of the flotability of Antimonite on the Value of Zeta Potential", Trans. Instn. Min. Metall., vol. 70, 1960-1961, pp 569-574.

Dobby, G.S. and Finch, J.A., "Mixing Characteristics of Industrial Flotation Columns", Chem. Eng. Sci., Vol. 40, No. 7, 1985, pp 1061-1068.

Dobby, G.S. and Finch, J.A., " Flotation Column Scale-Up and Modelling", CIM Bulletin, Vol. 79, No. 889, May 1986a, pp 89-96.

Dobby, G.S. and Finch, J.A.,"Particle Collection in Columns - Gas Rate and Bubble Size Effects", Canadian Metallurgical Quarterly, Vol. 25, No.1, 1986b, pp 9-13.

Dobby, G.S. and Finch, J.A., "Particle Size Dependence in Flotation Derived from a Fundamental Model of the Capture Process", Int. J. Min. Process, Vol. 21, No. 3-4, Dec 1987, pp 241-260.

Durney, T.E., "Fine Coal Flotation Using the Flotaire Column Flotation Cell", presented at SME Annual Meeting, Salt Lake City, Utah, February 26-March 1, 1990.

Engel, M.D. and Smitham, J.B., "The Relationship between Coal Particle Size and Hydrophobicity in the Formation of Particle-Stabilised Froths", The AusIMM Bulletin and Proceedings, Vol. 293, No. 4, 1988, pp 63-66.

Espinosa, R.G., Finch, J.A. and Johnson, N.W., "Column Flotation of Very Fine Particles", Minerals Engineering, Vol. 1, No. 1, 1988, pp 3-18.

Espinosa-Gomez, R., Finch, J.A., Yianatos, J.B. and Dobby, G.S., "Flotation Column Carrying Capacity - Particle Size and Density Effects", Minerals Engineering, Vol. 1, No. 1, 1988a, pp 77-79.

Espinosa-Gomez, R., Yianatos, J. and Finch, J., "Carrying Capacity Limitations in Flotation Columns", in Column Flotation '88 (K.V.S. Sastri, ed.), SME Annual Meeting, Phoenix, Arizona, U.S.A., January 1988b, pp 143-148.

Falcon, R.M.S., "Coal in South Africa - Part I: The Quality of South African Coal in Relation to its Uses and World Energy Resources", Minerals Sci. Engng, vol. 9, no. 4., Oct., 1977, pp 198-217.

Falcon, R.M.S., "Coal in South Africa, Part II: The Application of Petrography to the Characterisation of Coal", Minerals Science and Engineering, Vol 10, No 1, Jan 1978a, pp 28-52.

Falcon, R.M.S., "Coal in South Africa - Part III: Summary and Proposals-The Fundamental Approach to the Characterisation and Rationalisation of South Africa's Coal", Minerals Sci. Engng, vol 10, no 2, April 1978b, pp 130-153.

Falcon, R.M.S. and Snyman, C.P., "An Introduction to Coal Petrography : Atlas of the constituents of Bituminous Coals of Southern Africa", The Geological Society of South Africa, Review Paper Number 2, February 1986.

Falutsu, M. and Dobby, G.S., "Direct Measurement of Froth Drop Back and Collection Zone Recovery in a Laboratory Flotation Column", Minerals Engineering, Vol. 2, No. 3, 1989, pp 377-386.

Fickling, R.S., "An Investigation into the Froth Flotation of Four South African Coals", M.Sc. Thesis, University of Cape Town, 1985.

Finch, J.A. and Dobby, G.S., "Column Flotation", Pergamon Press, Oxford, U.K., 1990a, pp 75-101.

ibid, 1990b, pp 148-149.

ibid, 1990c, pp 13-15.

Flint, L.R. and Howarth, W.J., "The Collision Efficiency of Small Particles with Air Bubbles", Chemical Engineering Science, Vol. 26, 1971, pp 1155-1168.

Flint, I.M., MacPhail, P. and Dobby, G.S., "Aerosol Addition in Column Flotation", C.I.M. 25'th Annual Conference, Toronto, Ontario, August 17-20, 1986.

Flynn, S.A. and Woodburn, E.T., "A Froth Ultra-Fine Model for the Selective Separation of Coal from Mineral in a Dispersed Air-Flotation Cell", Powder Technology, 49, 1987, pp 127-142.

Franzidis, J-P., "Flotation of South African Coals", CSP Progress Report, Department of Chemical Engineering, University of Cape Town, May, 1987.

Franzidis, J-P., "Flotation of South African Coals", CSP Progress Report, Department of Chemical Engineering, University of Cape Town, August, 1988.

Franzidis, J-P. and Harris, M.C., "A new method for the rapid float/sinks analysis of coal fines", Journal of the South African Institute of Mining and Metallurgy, Vol. 86, No 10, Oct. 1986, pp 409-414

Franzidis, J-P. and Harris, M.C., "Column Flotation of South African Coals", presented at SAIMM Conference, "The Total Utilisation of Coal Resources", Witbank, 30 October - 2 November, 1989.

Franzidis, J-P., "Developments in Fine Coal Beneficiation in South Africa", in press Coal Preparation, 1991.

Fuerstenau, D.W. and Raghavan, S., "Some Aspects of the Thermodynamics of Flotation", in Flotation - A.M. Gaudin Memorial Volume : Volume 1 (M.C. Fuerstenau ed.), American Institute of Mining, Metallurgical and Petroleum Engineers, New York, 1976a, pp 21-65.

ibid., 1976b, pp 29-31.

Fuerstenau, D.W., "Mineral-Water Interfaces and the Electric Double Layer" in in Principles of Flotation (R.P. King ed.), South African Institute of Mining and Metallurgy Monograph Series No. 3, Johannesburg 1982, pp 17-30.

Fuerstenau, D.W. and Urbina, R.H., "Flotation Fundamentals" in Reagents in Mineral Technology (P. Somasunduran and B.M. Moudgil ed.), Marcel Dekker, New York, 1988, pp 1-16.

Goodall, C.M. and O'Connor, C.T., "Residence Time Distribution Studies of the Solid and Liquid Phases in a Laboratory Column Cell", presented at Int. Colloquium Dev. Froth Flotation, S.A.I.M.M., Western Cape Branch, Gordon's Bay, South Africa, 1989.

Grobbelaar, C. J., "Colliery Discards Worldwide with Reference to its Utilisation", S.A. Mining World, October 1988, pp 104-125.

Groppo, J.G. and Parekh. B.K., "Continuous Pilot-Scale Testing of Column Flotation for Recovery of Fine Coal", Mining Engineering, October 1990, pp 1189-1192.

Gy, M., "Sampling of Particulate Solids : Theory and Practice", Elsevier Scientific Publishing, New York, 1982.

Harris, P.J., "Frothing Phenomena and Frothers", in Principles of Flotation (R.P. King ed.), South African Institute of Mining and Metallurgy Monograph Series No. 3, Johannesburg 1982, pp 237-250.

Harris, M.C., "The Liberation Characteristics of Greenside No 2 Seam Coal", M.Sc. Thesis, University of Cape Town, 1987.

Harris, R.C., "Industrial Practice of Fine Coal Processing - The Economics of Fine Coal Preparation", Presented at Proceedings of the AIME Conference at Hidden Valley, Somerset, PA, Sept 1988, pp 29-34.

Hemmings, C.E., "On the Significance of Flotation Froth Liquid Lamella Thickness", Trans. Instn. Min. Metall., 90, September 1981, pp C96-C102.

Hochberg Y., and Tanhane A.C., "Multiple Comparision Procedures", John Wiley and Sons, New York, 1987.

Horsfall, D.W., Ed., "Coal Preparation of Plant Operators", The South African Coal Processing Society, Chamber of Mines, Johannesburg, 1983, pp 1-16.

Horsfall, D.W. and Franzidis, J.-P., "Beneficiation of South African Coal Fines", in Proceedings of the 5th Annual International Pittsburgh Coal Conference, Pittsburgh, PA, September 12-16, 1988, pp 311-325.

Jameson, G.J., Nam, S. and Moo Young, M., "Physical Factors Affecting Recovery Rates in Flotation", Minerals Sci. Engng, vol. 9, no. 3, July 1977, pp 103-118.

Jameson. G.J., "Physics and Hydrodynamics of Bubbles" in The Scientific Basis of Flotation (K.J. Ives ed.), Nato ASI Series E, no. 75, The Hague, 1984, pp 53-77.

Kawatra, S.K. and Eisele, T.C., "Column Flotation of Coal", in Fine Coal Processing (S.K. Mishra and R.R. Klimpel ed.), Noyes Publications, New Jersey, 1987, pp 414-428.

Kelsall, D.F., "Application of Probability Assessment of Flotation Systems", Trans. Instn. of Mining and Metall., Vol. 70, Part 4, No. 650, 1961, pp 161-220.

King, R.P., "Flotation of Fine Particles", in Principles of Flotation (R.P. King ed.), South African Institute of Mining and Metallurgy Monograph Series No. 3, Johannesburg 1982, pp 215-226.

Kitchener, J.A., The Froth Flotation Process : Past, Present and Future - In Brief" in The Scientific Basis of Flotation (K.J. Ives ed.), Nato ASI Series E, no. 75, The Hague, 1984, pp 3-52.

Klimpel, R.R. and Hansen, R.D., "Chemistry of Fine Coal Flotation", in Fine Coal Processing (S.K. Mishra and R.R. Klimpel ed.), Noyes Publications, New Jersey, 1987, pp 78-109.

Koshy, A., Das, T. R. and Kumar, R., "Effects of Surfactants on Drop Breakage in Turbulent Liquid Dispersions", Chemical Engineering Science, Vol. 43., No. 3, 1988, pp 649 - 654.

Laplante, A.R., Yianatos, J. and Finch, J.A., "On the Mixing Characteristics of the Collection Zone in Flotation Columns", in Column Flotation '88 (K.V.S. Sastri, ed.), SME Annual Meeting, Phoenix, Arizona, U.S.A., January 1988, pp 69-79.

Luttrell, G.H., Yan, S., Adel, G.T. and Yoon, R.H., "A Computer-Aided Design Package for Column Flotation", presented at SME Annual Meeting, Salt Lake City, Utah, February 26 - March 1, 1990.

Masliyah, J.H., "Hindered Settling in a Multi-Species Particle System", Chemical Engineering Science, Vol. 34, 1979, pp 1166-1168.

Mason, R.L., Gunst R.F. and Hess J.L., "Statistical Design and Analysis of Experiments - With Applications to Engineering and Science", John Wiley and Sons, New York, 1989.

McKay, J.D., Foot, D.G. and Shirts, M.B., "Column Flotation and Bubble Generation Studies at the Bureau of Mines", in Proceedings - Column Flotation '88, Phoenix, Arizona, January 1988, Chapter 18, pp 173-186.

McKay, J.D. and Foot, D.G., "Recent Column Flotation Advances", Presented at SME Annual Meeting, Salt Lake City,m Utah, February 26-March 1, 1990.

McLean, R.A. and Anderson, V.L., "Applied Factorial and Fractional Designs", Marcel Dekker, New York, 1984.

Miller, R. E., "Experimental Design", Chemical Engineering, June 23, 1986, pp 113 - 117.

Miller, K.J., "Novel Flotation Technology : A Survey of Equipment and Processes", in Industrial Practice of Fine Coal Processing (R.R. Klimpel and P.T. Luckie ed.). Proceedings of Conference at Hidden Valley, Somerset, PA, Sept 1988, pp 347-363.

Mills, P.J.T. and O'Connor, C.T.,"The Modelling of Liquid and Solids Mixing in a Flotation Column", Minerals Engineering, Vol. 3, No. 6, 1990. pp 567-576.

Mishra, S.K., "Improved Recovery of Fine Coal by Flotation Process", in Fine Coal Processing (S.K. Mishra and R.R. Klimpel ed.), Noyes Publications, New Jersey, 1987, pp 110-121.

Misra, M. and Anazia, I., "Ultrafine Coal Flotation by Gas Phase Transport of Atomised Reagents", Minerals and Metallurgical Processing, November 1987, pp 233-236.

Misra, M. and Harris, R., "Column Flotation of Fine Coal from Waste Coal Refuse", Presented at Column Flotation '88 - Proceedings of an International Symposium on Column Flotation, SME Annual Meeting, Phoenix, Arizona, January 1988, pp 235-242.

Montgomery, D.C., "Design and Analysis of Experiments - Second Edition", John Wiley and Sons, New York, 1984.

Moon, K.S. and Sirois, L.L., "Theory and Application of Column Flotation in Canada", in Column Flotation '88 (K.V.S. Sastri, ed.), SME Annual Meeting, Phoenix, Arizona, U.S.A., January 1988, pp 143-148.

Murdock, D.J., "An Overview of Column Flotation", Journal of the South African Institute of Mining and Metallurgy, March 1991, pp i-iii.

Murdock, D.J. and Wyslouzil, H.E., "Large-Diameter Column Flotation Cells take Hold", Engineering and Mining Journal, August 1991, pp 40-42.

Murphy, T.D., "Design and Analysis of Industrial Experiments", Chemical Engineering, June 6, 1977, pp 168 - 182.

Ng, F. L., "Surface phenomena influencing attachment and subsequent transfer of coal particles from an aqueous to a hydrocarbon phase", PhD Thesis submitted to the University of New South Wales, August 1982., p 123

Nicol, S.K., Roberts, T., Bensley, C.N. Kidd, G.W. and Lamb, R., "Column Flotation of Ultrafine Coal : Experience at BHP-Utah Coal Limited's Riverside Mine", Presented at Column Flotation '88 - Proceedings of an International Symposium on Column Flotation, SME Annual Meeting, Phoenix, Arizona, January 1988, Chapter 2, pp 7-11.

O' Connor, C.T., Randall, E.W. and Goodall, C.M., "Measurement of the Effects of Physical and Chemical Variables on Bubble Size", International Journal of Minerals Processing, vol. 28, 1990, pp 139-149.

Osbourne, D.G., "Coal Preparation Technology - Volume One", Graham and Trotman, London, 1988, pp 40-49.

Parekh, B.K., Groppo, J.G. and Bland, A.E., "Optimisation Studies of Column Flotation for Fine Coal Cleaning". Presented at Third Pittsburgh Coal Conference, Pittsburgh, Pennsylvania, September 8-12, 1986.

Parekh, B.K., Groppo, J.G., Stotts, W.F. and Bland, A.E., "Recovery of Fine Coal from Preparation Plant Refuse using Column Flotation", in Proceedings - Column Flotation '88, Phoenix, Arizona, January 1988, Chapter 24, pp 227-233.

Perry, R.H. and Chilton, C.H., ed., "Chemical Engineers Handbook", Fifth Edition, McGraw-Hill International, 1973, pp 18-67 - 18-81.

Raktoe, B.L., Hedayat, A. and Federer, W.T., "Factorial Designs", John Wiley and Sons, New York, 1981.

Rao, S.R., "Surface Forces in Flotation", Minerals Sci. Engng, vol. 6. no. 1, January 1974, pp 45-53.

Rao, P.S.R.S. and Sedransk, J., "W.G. Cochran's Impact on Statistics", John Wiley and Sons, New York, 1984, pp 129 - 140.

Reay, D. and Ratcliffe, G., "Experimental Testing of the Hydrodynamic Model of Fine Particle Flotation", Can. J. Chem. Engng., vol. 51, 1973, pp 178-185.

Reddy, P.S.R., Kumar, S.G., Bhattacharyya, K.K., Sastri, S.R.S. and Narasimhan, K.S., "Flotation Column for Fine Coal Beneficiation", International Journal of Mineral Processing, 24, 1988, pp 161-172.

Sachs, L., "Applied Statistics - A Handbook of Techniques", Springer-Verlag, New York, 1982.

Scheffe, H., "The Analysis of Variance", John Wiley and Sons, New York, 1959.

Shah, Y.T., Kelkar, B.G., Godbole, S.P. and Deckwer, W.D., "Design Parameter Estimations for Bubble Column Reactors", AIChE Journal, Vol. 28, No. 3, 1982, pp 353-380.

Sivamohan, R., "The Problem of Recovering Very Fine Particles in Minerals Processing - A Review", International Journal of Mineral Processing, 28, 1990, pp 247 - 288.

Smith, J.M., "Chemical Engineering Kinetics", Third Edition, McGraw-Hill International, 1981, pp 288-290.

Somasundaran, P., "Interfacial Chemistry of Particulate Flotation", AIChE Symposium Series 150, Volume 71, 1975, pp 1-15.

Sprow, F. B., "Distribution of drop sizes produced in turbulent liquid-liquid dispersion", Chemical Engineering Science, Vol 22, 1967, pp 435 - 442.

Stopes, M.C., "On the Four Visible Ingredients in Banded Bituminous Coals", Proc. R. Soc. Lond., Series B., 90, 1919, pp 470-487.

Subrahmanyam, T.V. and Forssberg, E., "Froth Stability, Particle Entrainment and Drainage in Flotation - A Review", International Journal of Minerals Processing, 23, 1988, pp 33-53.

Sun, S.C., "Hypotheses for Different Floatabilities of Coals, Carbons and Hydrocarbon Minerals", Trans. AIME, vol. 199, 1954, pp 67-75.

Sutherland, K.L. and Wark, I.W., "Principles of Flotation", Australasian Institute of Mining and Metallurgy, Melbourne, 1955, pp 26-37.

Trahar, W.J. and Warren, L.J., "The Flotability of Very Fine Particles - A Review", International Journal of Mineral Processing, Vol. 3, 1976, pp 103-131.

Trahar, W.J., "A Rational Interpretation of the Role of Particle Size in Flotation", International Journal of Minerals Processing, Vol. 8, 1981, pp 289-327.

Treybal, R.E., "Mass-Transfer Operations", Third Edition, McGraw-Hill International, 1982.

ibid, 1982a, pp 146-153.

ibid, 1982b, pp 599-602

Tsai, S.C., "Coal Science and Technology Vol 2 - Fundamentals of Coal Beneficiation and Utilisation", Elsevier Science Publishers B.V., Amsterdam, 1982, pp 1-46.

Tukey, J.W., "One Degree of Freedon for Nonadditivity", Biometrics, 5, 1949, pp 232 - 242.

van't Riet, K. and Smith, J.M., "The behaviour of gas-liquid mixtures near Rushton turbine blades", Chemical Engineering Science, Vol. 28, 1973, pp 1031-1037.

Ward, C.R., ed., "Coal Geology and Coal Technology", Blackwell Scientific Publications, Melbourne, 1984a, pp 151-177.

ibid., 1984b, pp 34-39.

Weisman, J. and Efferding, L.E., "Suspension of Slurries by Mechanical Mixers", A.I.Ch.E. Journal, Vol 6, No. 3, September, 1960, pp 419-426.

Woodburn, E.T., Stockton, J.B. and Robbins, D.J., "Vision-Based Characterisation of 3 Phase Froths", in International Colloquium - Developments in Froth Flotation, The South African Institute of Mining and Metallurgy Western Cape Branch, Gordon's Bay, Cape Town, 3-4 August, Vol. 1, 1989.

Ye, Y., Khandrika, S.M. and Miller, J.D., "Induction-Time Measurements at a Particle Bed", International Journal of Mineral Processing, 25, 1989, pp 221-240.

Yianatos, J.B., Finch, J.A. and Laplante, A.R., "The Cleaning Action in Column Flotation Froths", Trans. Inst. Min. Metall., Section C, vol. 96, December 1987, pp 199-205.

Yianatos, J.B., Finch, J.A., Dobby, G.S. and Manqiu Xu, "Bubble size estimations in a bubble swarm", Journal of Colloid and Interface Science, Vol. 126, No. 1, November 1988a, pp 37-44.

Yianatos, J.B., Finch, J.A. and Laplante, A.R., "Selectivity in Column Flotation Froths", International Journal of Mineral Processing, 23, 1988b, pp 279-292.

Yianatos, J.B., "Column Flotation - Modelling and Technology", presented at Int. Colloquium Dev. Froth Flotation, S.A.I.M.M., Western Cape Branch, Gordon's Bay, South Africa, 1989.

Ynchautsi, R.A., McKay, J.D. and Foot, D.G., "Column Flotation Parameters - Their Effects", in Proceedings - Column Flotation '88, Phoenix, Arizona, January 1988, Chapter 17, pp 157-172.

Zimmerman, R.E., "Flotation Reagents", in Coal Preparation (J.W. Leonard and D.R. Mitchell ed.), Third Edition, The American Institute of Mining, Metallurgical and Petroleum Engineers, New York, 1968, pp 10-73 - 10-79.

APPENDIX A

A1 - CONSTRUCTION OF FACTORIAL DESIGNS

A2 - ANALYSIS OF DESIGNED EXPERIMENTS

A3 - DURNACOL FACTORIAL DESIGN - STATISTICAL ANALYSES

A4 - GENSTAT INPUT/OUTPUT LISTINGS

APPENDIX A1

CONSTRUCTION OF FACTORIAL DESIGNS

A1.1 Terminology

Before proceeding to develop the concepts utilised in factorial experiments it is necessary to introduce a few definitions.

A **response** is defined as the outcome of an experimental trial (test run). A **factor** is an experimental variable being investigated to determine its effect on a response. A *factor* is considered controllable, i.e. the experimenter can *choose* values (*levels*) of the experimental variable prior to the start of the test programme. Input variables which influence a process response but which cannot be controlled are called **covariates**. A *test run* (trial) is a single factor-level combination from which an experimental observation (*response*) is *obtained*. An **effect** is defined as a change in average response between two or more factor-level combinations. For clarity, main and interaction effects are defined section A1.2 below, within the context of an example of a factorial design experiment.

Repeat tests are two or more observations taken for a particular test run. **Replications** are repetitions of test runs (or the entire experiment).

Experimental responses are only comparable when they are taken from **homogeneous experimental units**. The only differences between such groups is due to inherent random variation. A **block** is defined as a group of homogeneous experimental units.

Confounding occurs when changes in effects cannot unambiguously be attributed to a single factor or interaction. Confounding effects are further discussed in the section on fractional factorial designs (A1.3) below.

When relatively few factors and factor-levels are tested it is possible to conduct all the experimental trial runs within a single block. The

sequence in which the trial runs are conducted is entirely random. Such an experiment is known as a completely randomised design. A completely randomised design is required to counteract **bias** which may arise as the experiment progresses, for example, readings displayed by electronic instruments usually drift with time.

A1.2 Full Factorial Designs

In a full (complete) factorial design all possible factor-level combinations are included. Take the general case where there are n independent variables [x_1, x_2, ... x_n] affecting an output response y. Now suppose there are m levels of each factor i.e. (x_{11}, ... x_{1m}) ... (x_{n1}, ... x_{nm}) etc. This class of experiments where the number of *levels* of *each factor* in an experiment are the *same* is known as a *symmetrical* factorial experiment. The total number of possible combinations, N, is equal to m^n. Obviously N becomes large rather quickly, for example, m = 3 n = 3 N = 27; m = 2 n = 6 N = 64.

The most widely used factorial designs are symmetrical experiments conducted at two levels, i.e. the number of trial runs required for one complete replicate is $N = 2^n$.

The principles of designing and developing 2^n experiments are best illustrated by an example.

Consider a 2^3 design where 3 input variables (factors) A, B, C are each tested at two levels arbitrarily designated low (-) and high (+) respectively.

Let the high value of A be a, the high value of B be b and the high value of C be equal to c. Furthermore, let the test run for which A, B and C are low be designated (1). The 8 possible test combinations are given in Table A1.1.

Each row combination represents a particular test run. The algebraic and (-) (+) sign notation are equivalent; however, for reasons which will soon be apparent the sign notation is preferred.

Table A1.1 : Full 2^3 factorial design

Combination	A	B	C	Response	Average
(1)	-	-	-	y_{11}, y_{12}	$y_{1.}$
a	+	-	-	y_{21}, y_{22}	$y_{2.}$
b	-	+	-	y_{31}, y_{32}	$y_{3.}$
c	-	-	+	y_{41}, y_{42}	$y_{4.}$
ab	+	+	-	y_{51}, y_{52}	$y_{5.}$
ac	+	-	+	y_{61}, y_{62}	$y_{6.}$
bc	-	+	+	y_{71}, y_{72}	$y_{7.}$
abc	+	+	+	y_{81}, y_{82}	$y_{8.}$

Another important feature introduced above is the 8 pairs of responses obtained from the experiments. These pairs can represent either repeat observations or replicates. They are required to provide estimates of the sample error. It is possible to conduct a factorial experiment without taking any replicate or repeat samples; this is discussed shortly. The mean response from test run i is defined by

$$y_{i.} = (y_{i1} + y_{i2}) / 2 \qquad \text{(A1.1)}$$

or in general where r repeats/replicates are taken

$$y_{i.} = \Sigma_j \, y_{ij} / \sigma \qquad \text{(A1.2)}$$

The sample variance, s_i^2, is defined by

$$s_i^2 = \Sigma_j \, (y_{ij} - y_{i.})^2 / (r - 1) \qquad \text{(A1.3)}$$

Changes in response due to changes in the *levels* of the *individual* input variables (*factors*) are referred to as **main effects**. The effect of factor A on the process response can be seen to be the average of the differences in mean responses when A is changed between high and low levels, i.e.

$$A = 1/4 \, [(y_{2.} - y_{1.}) + (y_{5.} - y_{3.}) + (y_{6.} - y_{4.}) + (y_{8.} - y_{7.})] \qquad \text{(A1.4)}$$

Equation (A1.4) can be rewritten as

$$A = 1/4\ [-y_{1.} + y_{2.} - y_{3.} - y_{4.} + y_{5.} + y_{6.} - y_{7.} + y_{8.}] \qquad (A1.5)$$

The term in the square brackets is known as a **contrast** and the sign coefficients of the contrast correspond to those in the column identified by the heading A in Table A1.1. Thus the contrast l_A is defined as

$$l_A = [-y_{1.} + y_{2.} - y_{3.} - y_{4.} + y_{5.} + y_{6.} - y_{7.} + y_{8.}] \qquad (A1.6)$$

The main effects B and C are similarly defined, as are the contrasts l_B and l_C.

Refer to the sign coefficients listed under the columns A, B and C in Table A1.1. If one substitutes the values 0 and 1 for the negative and positive coefficients it can be seen that each column of *contrast sign coefficients* represents a *vector*. Furthermore, the three vectors represented in columns A, B and C are linearly independent (*mutually orthogonal*). Therefore each *main effect* is defined by a unique linear combination of (average) response observations, i.e. a *unique contrast*.

Typically there are many contrasts which one can define. For example, one could define the contrast $l_{A*} = -y_{1.} - y_{2.} + 2y_{3.}$. In general a contrast l is defined by

$$l = \Sigma_i^N C_i * y_{i.} \qquad (A1.7)$$

with the imposed restriction

$$\Sigma_i\ C_i = 0 \qquad (A1.8)$$

where C_i represents a negative (-) or positive (+) sign coefficient.

Consider now the **interaction effects**. The interaction effect AB can reasonably be defined as the difference between the (average) factor A effect when B is low (-) subtracted from the (average) factor A effect when B is high (+), i.e.

$$AB = 1/4\ l_{AB} \qquad (A1.9)$$

where the contrast l_{AB} is given by

$$l_{AB} = \{ - [(y_{2.} - y_{1.}) + (y_{6.} - y_{4.})] + [(y_{5.} - y_{3.}) + (y_{8.} - y_{7.})]\}$$

$$= [+ y_{1.} - y_{2.} - y_{3.} + y_{4.} + y_{5.} - y_{6.} - y_{7.} + y_{8.}] \qquad \text{(A1.10)}$$

If one transposes the sign coefficients in equation (A1.10) into a column vector an extremely interesting property can be discerned; the sign coefficient of each row element i in column AB is equal to the product of the sign coefficient of element i in column A multiplied by the sign coefficient of element i in column B, where the following three laws are obeyed : (-) * (-) = (+); (-) * (+) = (-); (+) * (+) = (+). Furthermore, these properties are commutative; their operation is more clearly distinguishable in Table A1.2.

Table A1.2 : Main effect and Interaction Contrasts in 2^3 factorials

Combination	Main Effects and Interactions							
	A	B	C	AB	AC	BC	ABC	I
(1)	-	-	-	+	+	+	-	+
a	+	-	-	-	-	+	+	+
b	-	+	-	-	+	-	+	+
c	-	-	+	+	-	-	+	+
ab	+	+	-	+	-	-	-	+
ac	+	-	+	-	+	-	-	+
bc	-	+	+	-	-	+	-	+
abc	+	+	+	+	+	+	+	+

The sign coefficients of the AC and BC contrasts are derived in an identical manner. The sign coefficients of higher order interaction contrasts are defined inductively from the two factor (AB, AC, BC) interaction contrasts. For example, the contrast which defines the ABC interaction effect is obtained by subtracting the average AB interaction effect when C is at the low (-) level from the average AB interaction effect when C is at the high (+) level, i.e.

$$ABC = 1/4\ l_{ABC} \qquad \text{(A1.11)}$$

where

$$l_{ABC} = \{ - [-(y_{2.} - y_{1.}) + (y_{5.} - y_{3.})] + [-(y_{6.} - y_{4.}) + (y_{8.} - y_{7.})]\}$$

$$l_{ABC} = [- y_{1.} + y_{2.} + y_{3.} + y_{4.} - y_{5.} - y_{6.} - y_{7.} + y_{8.}] \qquad (A1.12)$$

The contrast sign coefficients in row i of the column vector ABC are again equal to the product of the sign coefficients in row i of columns A, B and C respectively.

The four factor interaction ABCD in a 2^4 factorial experiment is then defined as the ABC interaction effect at D (-) subtracted from the ABC interaction effect at D (+), etc.

The column corresponding to I in Table A1.2 has only positive (+) signs. Therefore I represents the total number of (mean) observations or the average observation for the entire experiment and is known as the identity element. Furthermore, one can readily see that I * A = A, A * AB = B.

These types of arithmetic operations belong to the class of mathematics known as Modulus 2 arithmetic, which is based on the properties of finite fields (a brief review of which is given by Das and Giri (1979)).

A *two factor interaction* is known as a *first order* interaction. Similarly three and four factor interactions are known as interactions of the second and third order respectively. Often second and *higher order interactions* are of the order of the error and consequently the combination of their contrasts can be used to *estimate experimental error*. For example, in a 2^4 design one might assume that the ABCD interaction is negligible. Consequently $l_{ABCD} \approx 0$, the difference between the contrast and 0 being due to random error. However, it is still preferable to obtain an independent error estimate from replicates or repeat samples wherever possible because if some interactions are present the experimental error is inflated when inferred from interaction contrasts.

It can be seen from Table A1.2 that there are 7 independent columns of sign coefficients, i.e. *every* main and interaction *factor effect* is

defined by a *unique contrast* consisting of 8 terms. Furthermore, only 8 average observations were required to obtain 7 input variable effects; a remarkably efficient experiment.

In general $(2^n - 1)$ factor effects are associated with a 2^n factorial experiment. As each factor effect represents one degree of freedom (d.o.f.) there are $(2^n - 1)$ d.o.f. associated with a 2^n factorial experiment. Therefore a **minimum** of 2^n observations are required to obtain the $(2^n - 1)$ mutually orthogonal **contrasts** which **define every factor effect**. Specifically one replicate of such an experiment has n main effects (A, B, ..., N); n combination 2 two factor effects; n combination 3 three factor interaction effects, etc; and one n factor (n combination n) effect. Each average effect F is defined as

$$F = 2 * 1 / n \qquad \text{(A1.13)}$$

where 1 contains 2^n terms and therefore represents the (unique) contrast defining the F effect.

The methodology for quantifying factor effects and experimental errors is deferred to section A2 below which deals with the analysis of factorial designs.

A1.3 Fractional factorial designs

As the number of factors in a 2^n or 3^n factorial design increases, the number of runs required for one complete replicate rapidly outgrows the resources available for the conduction of the experiment. For example, 64 test runs are required for one replicate of a 2^6 factorial experiment. Of the 63 d.o.f. associated with this full factorial design only 6 d.o.f. are associated with main effects, 15 d.o.f. correspond to 2 factor interaction effects and the remaining 42 d.o.f. are associated with second and higher order interactions.

The latter statement provides the clue to reducing the number of test runs required for investigating n factors (input variables). Suppose a subset (**fraction**) of 2^a test runs are chosen from the 2^n tests required for the full factorial experiment.

The contrasts defining the factor effects are given by

$$1^* = \Sigma_{i=1}^{m} C_i * y_{i.} \qquad \text{(A1.14)}$$

$$m = 2^a \qquad \text{(A1.15)}$$

and the constraint equation (A1.8) still holds, i.e. $\Sigma_i C_i = 0$.

Now $2^a < 2^n$ and therefore $(2^a - 1) < (2^n - 1)$, i.e. only $(2^a - 1)$ independent contrasts exist and since there *remain* $(2^n - 1)$ factor effects, *different factor effects* are defined by the *same contrast*. In statistical terminology this is known as **confounding**. Factor effects which are confounded are called **aliases**.

Clearly the *factor aliases* which arise from a fractional experiment *depend* on which *test runs* are *selected*.

Before developing a formal methodology for choosing appropiate test run combinations the rationale underlying such methodology should be considered. It was previously stated that higher order interactions are often negligible. Consequently, if these higher order effects are aliased with factor effects of interest (typically main effects and two factor interactions) the defining contrast essentially reflects only the dominant factor effect(s).

For example, suppose a contrast, L^*, is chosen which defines both a main factor effect, A, and a five factor interaction effect, ABCDE. In fact L^* represents the algebraic sum of the A and ABCDE effects, i.e.

$$L^* = A \pm ABCDE \qquad \text{(A1.16)}$$
$$\approx A \text{ if } ABCDE \approx 0.$$

Now consider what happens if main effects and two factor interactions are aliased.

$$L^* = A \pm BC \qquad \text{(A1.17)}$$

Two factor interactions very often exert a strong influence on a process response, thus in the absence of any additional information, one cannot

assume that the defining contrast L^* reflects only a factor A effect. Therefore one would avoid confounding main effects and two factor interaction effects as far as possible. More generally it is apparent that the conclusions drawn from fractional experiments are subject to more uncertainty than full factorial designs essentially because confounding results in a loss of information.

In fractional factorial experimentation terminology, the concept of *design resolution* is employed to describe how main effects and interactions are confounded. For example, a resolution III fractional design is one where main effects are confounded with two-factor interactions and two-factor interactions are confounded with each other, a resolution IV design is one where main effects are confounded with three factor or higher interactions but two factor interactions remain confounded with each other, etc.

A formal definition of design resolution can be developed (Meyer et al, 1989) :

An experimental design is of resolution R if all effects containing s or fewer factors are unconfounded with any effects containing fewer than R - s factors.

Obviously it is desirable for a fractional experiment to have as high a resolution as possible; however, as one would intuitively expect, resolution is directly linked to the size of the fractional group. Thus a 1/4 fractional design of a 2^6 factorial experiment, which requires 16 runs (optimal resolution R = IV), has a lower resolution than a 1/2 fractional design (optimal resolution R = VI). In other words, the penalty incurred for running *smaller fractions* of the full factorial experiment is the *reduction* of the *resolution* of the design.

Methods of constructing fractional factorial designs are considered next.

A1.3.1 Half (2^{n-1}) fractions

Each factor effect in a complete 2^n factorial experiment has 2^n terms, half of which are at the low (-) level and half at the high (+) level, i.e 2^{n-1} (-) and 2^{n-1} (+) terms.

Now a **1/2** fractional *design* consists of 2^{n-1} terms. One way of selecting the 2^{n-1} test runs required is to set **any** *factor effect constant* (either high (+) or low (-)) and then select the 2^{n-1} test runs for which this factor effect is constant. The contrast corresponding to the constant factor effect is known as the *defining contrast*. Also, the defining contrast is evidently confounded with the average effect I.

Example : Consider running a half fraction of a 2^3 factorial design. All the factor effects are listed in Table A1.2.

Suppose ABC at a high (+) level is selected as the defining contrast. Mathematically we can write I = ABC. The corresponding test run combinations and contrast defining the factor effects are listed in Table A1.3a below.

Table A1.3a : Half fraction 2^3 factorial design

Test run	Factor effects							
combination	A	B	C	AB	AC	BC	ABC	I
a	+	-	-	-	-	+	+	+
b	-	+	-	-	+	-	+	+
c	-	-	+	+	-	-	+	+
abc	+	+	+	+	+	+	+	+

Table A1.3a indicates which factor effects are aliased; the main effect A is confounded with the BC interaction effect, the factor B effect is confounded with the AC interaction effect and the factor C effect is confounded with the AB interaction effect.

Once a defining contrast has been selected, factor aliases can be readily identified by applying Modulus 2 arithmetic. Thus the alias of factor A is identified by multiplying A by the Identity ABC, i.e.

I.A = A.ABC = BC
Similarly I.B = AC ; I.C = AB

Actually the contrast L defining both factor A and interaction BC effects represents the algebraic sum of the two effects, i.e.

$L_A \rightarrow A + BC$ (A1.18)

$L_B \rightarrow B + AC$ (A1.19)

$L_C \rightarrow C + AB$ (A1.20)

As main and 2 factor effects are aliased it is evidently a Resolution III class of design. Recall that the defining contrast is I = ABC which is composed of three letters, i.e. the *defining contrast* is a 3 letter *word*. As a *general rule* the *resolution* of a fractional design is equal to the *number of letters* in the smallest word of any of the defining *contrasts* (fractional designs smaller than a 1/2 fraction have more than one defining contrast - see following subsection).

If one ran the reverse design, i.e. I = - ABC, the test run combinations would be (1), ab, ac, and bc. These are listed in Table A1.3b.

Table A1.3b : Half fraction 2^3 factorial design

Test run	Factor effects							
combination	A	B	C	AB	AC	BC	ABC	I
(1)	-	-	-	+	+	+	-	+
ab	+	+	-	+	-	-	-	+
ac	+	-	+	-	+	-	-	+
bc	-	+	+	-	-	+	-	+

In this fractional design the contrast defining the factor A effect l_A is equal to the negative of the contrast defining the BC interaction effect, l_{BC}, i.e. $l_A = - l_{BC}$. Hence

$L^*_A \rightarrow A - BC$ (A1.21)

Identical relationships can be developed for B, C, AB and AC factor effects:

$$L^*_B \rightarrow B - AC \qquad (A1.22)$$

$$L^*_C \rightarrow C - AB \qquad (A1.23)$$

Now the full fractional design can be seen to be the sum of the two half fractions, i.e. the factor A effect is given by

$$A = 1/2\ [L_A + L^*_A] \qquad (A1.24)$$

and the BC interaction effect is given by

$$BC = 1/2\ [L_A - L^*_A] \qquad (A1.25)$$

The sum of two half-fractions is strictly not completely equivalent to performing the full factorial design as the defining contrast (in the above case ABC) remains confounded with the constant effect I and consequently information about this factor effect is lost.

Earlier, it was stated that any contrast could be selected as the defining contrast. Consider, for example, if factor B at the low level (-) is selected as the defining contrast, i.e. I = -B. The test runs for which B is low (-) are given in Table A1.4.

Table A1.4 : Half fraction 2^3 factorial design

Test run	Factor effects							
combination	A	B	C	AB	AC	BC	ABC	I
(1)	-	-	-	+	+	+	-	+
a	+	-	-	-	-	+	+	+
c	-	-	+	+	-	-	+	+
ac	+	-	+	-	+	-	-	+

Now I.A = -AB, i.e. the main effect A is aliased with the AB interaction effect. Similarly, I.C = -BC and I.ABC = - AC.

Tables A1.3a, A1.3b and A1.4 can be constructed by applying the following principles :

Construct the complete Table for the complete 2^{n-1} design, i.e. in this case 2^2 factorial design. Arbitrarily assign a main effect (provided it is not a defining contrast) to each column (contrast) of the 2^{n-1} design. In an adjacent column fill in the sign coefficients of the defining contrast. Identify factor aliases utilising Modulus 2 algebra and expand the Table to include all 2^{n-1} factor effects.

A1.3.2 One quarter (2^{n-2}) fractions

Quarter fractions of two-level complete factorial experiments are constructed similarly to half fractions, the major distinction being that **two** *defining contrasts* are needed to partition the factor-level combinations.

Adopting the notation used previously one can write

$$I = I_1 = P = I_2 = Q$$

where again P and Q can be any of the $(2^n - 1)$ factor effects from the full 2^n experiment. Any of four PQ combinations can be selected from a pair of defining contrasts ±P, ±Q. Again, the approach to constructing a 1/4 fraction factorial experiment is best illustrated by an example.

Example : Consider a 2^{6-2} fraction of a 6-factor factorial experiment (Mason et al, 1989; p 172).

Suppose I_1 = -ABCDEF and I_2 = ABC are chosen as the defining contrasts. The factor-level combinations for which I_1 and I_2 are satisfied are listed in Table A1.5.

All the factor-level combinations which satisfy the defining contrasts I_1 = -ABCDEF and I_2 = ABC also satisfy a *third implicit* defining contrast I_3 = -DEF which is the Modulus 2 product of the two defining contrasts, i.e. $I_3 = I_1 * I_2$. Also, since the smallest number of

letters in any of the defining contrast *words* is three, the fractional design is a Resolution III design.

Table A1.5 : One quarter fraction of 2^6 factorial design

Factor-level combination	Factor effects representation								
	A	B	C	D	E	F	ABCDEF	ABC	DEF
1	-	-	+	-	-	-	-	+	-
2	-	-	+	-	+	+	-	+	-
3	-	-	+	+	-	+	-	+	-
4	-	-	+	+	+	-	-	+	-
5	-	+	-	-	-	-	-	+	-
6	-	+	-	-	+	+	-	+	-
7	-	+	-	+	-	+	-	+	-
8	-	+	-	+	+	-	-	+	-
9	+	-	-	-	-	-	-	+	-
10	+	-	-	-	+	+	-	+	-
11	+	-	-	+	-	+	-	+	-
12	+	-	-	+	+	-	-	+	-
13	+	+	+	-	-	-	-	+	-
14	+	+	+	-	+	+	-	+	-
15	+	+	+	+	-	+	-	+	-
16	+	+	+	+	+	-	-	+	-

Table A1.5 is constructed as follows : Firstly draw up the complete 2^4 factorial design. Now I = ABC = -DEF = -ABCDEF, thus applying Modulus 2 arithmetic let C = AB and F = -DE. Thus the main factor effects A, B, D and E are confounded with three-factor and higher interactions whilst C and E are confounded with two-factor interactions.

Suppose instead, I_1 = ABCEDF and I_2 = ABCDE were chosen as defining contrasts. Then the implicit contrast I_3 = F and the design becomes Resolution V half fractional design of 5 factors. Upon reflection it is apparent that the highest resolution possible for a 1/4 fraction of a 2^6

factorial experiment is a Resolution IV design which can be constructed by taking appropriate contrasts representing 4 factor interactions as the defining contrasts. For example one could let I_1 = ABCE and I_2 = ACDF, then I_3 = BDEF.

A1.3.3 2^{n-p} fractional factorial designs

A 2^{n-p} (or equivalently $1/2^p$) fractional factorial design requires p independent defining contrasts. The defining relation for the design, I, consists of the p defining contrasts initially chosen and $(2^n - p - 1)$ implicit contrasts.

Each factor effect has $(2^p - 1)$ aliases. For moderately large values of n, higher order interactions (say third order and higher) are usually assumed to be negligible; this greatly simplifies the alias structure.

Mason et al (1989, pp 182 - 183) list a selection of defining equations for fractional factorial experiments of up to 11 factors; the lowest designs included are of Resolution III and the highest of Resolution V. An impressive collection of design "recipes" covering a broad spectrum of factorial and fractional designs has been produced by McLean and Anderson (1984).

A1.4 Blocking Fractional Factorials

When a fractional factorial design requires more runs than can be performed under homogeneous conditions the design may be confounded into blocks.

Consider the 2^{6-2}_{IV} design previously discussed. Suppose it is only possible to run the design in 2 blocks of 8 runs. The approach to this situation is identical to selecting defining contrasts for sequential fractional designs.

For convenience let (Montgomery, 1984; p 336) I_1 = ABCE and I_2 = ACDF, then I_3 = BDEF. The aliased factor effects are listed in the Table below.

Table A1.6 : Alias structure of 2^{6-2}_{IV} Design

Factor Effect	Alias		
A	BCE	CDF	ABDEF
B	ACE	DEF	ABCDF
C	ABE	ADF	BCDEF
D	ACF	BEF	ABCDE
E	ABC	BDF	ACDEF
F	ACD	BDE	ABCEF
AB	CE	BCDF	ADEF
AC	BE	DF	ABCDEF
AD	CF	BCDE	ABEF
AE	BC	CDEF	ABDF
AF	CD	BCEF	ABDE
BD	EF	ACDE	ABCF
BF	DE	ABCD	ACEF
ABF	CEF	BCD	ADE
CDE	ABD	AEF	CBF

In total there are $2^6 - 1$, i.e. 63 factor effects, three of which are represented as defining contrasts, the remainder are listed in Table A1.6.

An examination of Table A1.6 indicates that ±ABF or ± CDE would be the best defining contrasts to select, as these are aliased with other three factor interaction effects.

A1.5 Fractional Factorial Design for Durnacol Laboratory Column Runs

Each of the following seven factors were investigated at 2 levels :

A - Froth height (FH)
B - Frother concentration (FC)
C - Air flowrate (AF)
D - Slurry feedrate (QF)
E - Washwater rate (WW)
F - Sparger type (ST)

G - Column (collection zone) height (CH)

Initially seven (7) factors were investigated in eight (8) runs. This is a Resolution III design. Four defining equations were used (Montgomery, 1984; pp 345 - 346), namely, I = ABD = ACE = BCF = ABCG, thus the design was a Resolution III class, i.e a 2^{7-4}_{III} design.

The complete set (including implict) of contrasts associated with the above defining equations (words) is

I = ABD = ACE = BCF = ABCG = BCDE = ACDF = CDG = ABEF = BEG = AFG = DEF
= ADEG = CEFG = BDFG = ABCDEFG

The aliases of any factor effect can be obtained from Modulus 2 arithmetic. For example the aliases of A are

A = BD = CE = ABCF = BCG = ABCDE = CDF = ACDG = BEF = ABEG = FG = ADEF
= DEG = ACEFG = ABDFG = BCDEFG

If the effects of two and higher order interactions are assumed negligible then

$$L_A \rightarrow A + BD + CE + FG \qquad \text{(A1.26)}$$

The 8 test run combinations for this experiment are listed in Table A1.7 below.

As main effects and two factor interactions are aliased in this design, it was decided to run a second series of experiments using the negatives of all the defining contrasts, i.e. I = -ABD = -ACE = -BCF = -ABCG. The effect of this is to reverse the sign coefficients in columns D to G. As was the case with summing of the two 2^{3-1} fractional designs discussed above (section A1.3), combining the sets of defining contrasts enables main effects to be separated from two factor interactions; the combined design then becomes a Resolution IV design.

Table A1.7 : 2^{7-4}_{III} fractional factorial design

Test run combination	A	B	C	D = AB	E = AC	F = BC	G = ABC
1	-	-	-	+	+	+	-
2	+	-	-	-	-	+	+
3	-	+	-	-	+	-	+
4	+	+	-	+	-	-	-
5	-	-	+	+	-	-	+
6	+	-	+	-	+	-	-
7	-	+	+	-	-	+	-
8	+	+	+	+	+	+	+

For example, in the second fractional design the factor A effect is aliased with two factor interactions as follows

$$L^*_A \rightarrow A - BD - CE - FG \qquad (A1.27)$$

hence the factor A effect is given by

$$A \rightarrow 1/2\ [L_A + L^*_A] \qquad (A1.28)$$

and similarly the sum of the 2 factor interactions aliased with A is

$$BD + CD + FG \rightarrow 1/2\ [L_A - L^*_A] \qquad (A1.29)$$

All the sets of two factor aliases are listed in the Table below :

Three pulp tank batches were used to obtain the 16 test runs required for the fractional design. Statistical analysis of the variability within and between pulp batches was performed (Appendix A3). This was found to be within the limits of inherent block error; an estimate of which has been obtained by Breed (1992).

Table A1.8 : Two factor alias structure for a 2^{7-3}_{IV} design.

(Main Effect)	Aliases		
(A)	BD	CE	FG
(B)	AD	CF	EG
(C)	AE	BF	DG
(D)	AB	CG	EF
(E)	AC	BG	DF
(F)	BC	AG	DE
(G)	CD	BE	AF

At this point it is appropriate to address further the subject of randomisation within a block. It was stated earlier that all the *tests* performed within a block *should* be run completely *randomly*. Unfortunately, for the *column trials*, as is the case with many real life systems, it was not possible to conduct all the tests completely randomly, i.e. there were *restrictions* on *randomisation*. Specifically, unless for some reason the experiment was stopped and then restarted, it was not possible to change either sparger type or column height whilst the column cell was operational. Therefore run sequences were conducted as follows : For a given column height, CH (factor G) and sparger type, ST, the following factors were varied randomly : air flowrate, AF, froth height, FH, slurry feedrate, QF, and frother concentration, FC. After 4 such tests were performed, either the ST or CH parameter level was changed and the procedure repeated.

There are statistical techniques available to counter randomisation restrictions (e.g. split-plot designs); these essentially involve further blocking and consequently more tests must be performed or a lower design Resolution accepted. Fortuitously, for the system under investigation, an independent check could be used to infer whether randomisation has been satisfied. The column cell is a continuous flow system with an input and two output flow streams. As timed samples were taken from all three streams, mass balances (ash analyses on the samples were also performed) could be used to check for composition and steady state. If the feed composition value lay within an acceptable range the test run is accepted, otherwise the trial was replicated.

APPENDIX A2

ANALYSIS OF DESIGNED EXPERIMENTS

A2.1 Selection of a System Model

The general form of a linear statistical model, reproduced below, was introduced at the beginning of section 2.6 :

$$y = f(x_1 , x_2) = f_1(x_1) + f_2(x_2) + g(x_1 , x_2) \qquad (A2.1)$$

Broadly speaking, there are two classes of statistical models, the classification being based upon whether the input variables (factors) are chosen at specific levels or over continuous ranges of values.

A model in which each of the *input variables* can be *set* at a specified *level* for each test run is termed a **fixed effects** model. Here the only random response component is the system error. Models where all the *factors* are a *random sample selected* from a larger *population* are called **random effects** models. Mixed models are models where some factors are fixed and some factors are random.

The model of interest here is the linear fixed effects type of model.

Consider as an example, a linear model consisting of 3 input variables A, B and C. Now suppose a levels of factor A, b levels of factor B and c levels of factor C are tested. Assume that there are r repeat tests for each factor-level combination. The total number of trial runs, N, is therefore N = rabc.

The linear model for this system is

$$f = \mu + \alpha_i + \beta_j + \gamma_k + (\alpha\beta)_{ij} + (\alpha\gamma)_{ik} + (\beta\gamma)_{jk} + (\alpha\beta\gamma)_{ijk} \qquad (A2.2)$$

where

f = predicted response
μ = overall system mean
α_i = fixed effect due to factor A at level i

β_j = fixed effect due to factor B at level j
γ_k = fixed effect due to factor C at level k
$(\alpha\beta)_{ij}$ = fixed effect due to AB interaction at level ij, etc.

i = level of factor A; i = 1 to a
j = level of factor B, j = 1 to b
k = level of factor C; k = 1 to c

Now let

$$y_{ijkl} = f + e_{ijkl} \qquad \text{(A2.3)}$$

where

l = repeat test; l = 1 to r
y_{ijkl} = observed response for test run ijkl
e_{ijkl} = random error component

The system model as presented in equations (A2.2) and (A2.3) is capable of performing the following tasks :

(i) Main and interaction factor effects which affect the system response can be identified. This is done by partitioning the total sample variance into factor effect components and a single error component by a method formally known as the Analysis of Variance (ANOVA) technique.

(ii) Factor effects can be quantified, i.e. the factor constants α_i, $(\alpha\beta)_{ij}$, etc. can be determined by the method of minimisation of least squares, the details of which are available in standard texts, for example, Das and Giri (1979), Mason et al (1989), Montgomery (1984) and Scheffe (1959).

The linear model, like any mathematical equation describing a real system, has underlying requirements and assumptions which must be satisfied if the model is to provide a valid description of system behaviour. Some of the more important of these are :

Firstly, the model requires orthogonal data, i.e. unique contrasts (see section A1.3 for details), for every factor effect. Secondly, response data must be available for every factor-level combination; no responses must be "missing" from the test results. Experimental designs which meet these two criteria are known as *balanced* designs.

In order for equation (A2.2) to have a unique solution, the sum of each factor effect over its complete range of levels must equal zero, i.e.

$\Sigma_i \alpha_i = 0$, $\Sigma_j \beta_j = 0$, $\Sigma_i\Sigma_j (\alpha\beta)_{ij} = 0$, $\Sigma_i\Sigma_j\Sigma_k (\alpha\beta\gamma)_{ijk} = 0$, etc.

It is assumed that the error components, e_{ijkl} are normally and independently distributed. In practice, even if the *error* terms *deviate* somewhat from *normality*, the *statistical inferences* based on the linear model are *not* seriously *invalidated* (Scheffe, 1959 p 98). The normality assumption may also be checked by residual plots of repeat data.

It is assumed that *factor effects* are *additive*, and that the model is a *hierarchial* model where interaction effects are successively included in the model only when the main effects cannot account for the observed response, y_{ijkl} .

A rigorous treatise of Analysis of Variance techniques in which the assumptions underpinning the use of this method are examined has been undertaken by Scheffe (1959).

A2.2 ANOVA Method for Balanced Designs

A2.2.1 Partition of variance

Consider the 3 factor example cited earlier. The total system variability can be represented by the *total* sum of squares, designated TSS :

$$TSS = \Sigma_i\Sigma_j\Sigma_k\Sigma_l (y_{ijkl} - y_{....})^2 \qquad (A2.4)$$

where

$y_{....}$ = overall system average

$$y_{....} = \Sigma_i\Sigma_j\Sigma_k\Sigma_l\, y_{ijkl} / rabc$$

$$= \Sigma_i\Sigma_j\Sigma_k\Sigma_l\, y_{ijkl} / N \qquad \text{(A2.5)}$$

Now the bracketed term in equation (A2.4) can be expanded to include main and interaction contributions to the total system variance. This can be done as follows :

Let $\alpha_i = y_{i...} - y_{....}$ (A2.6)

where

$y_{i...}$ = average system response at level i of factor A.

$$y_{i...} = \Sigma_j\Sigma_k\Sigma_l\, y_{ijkl} / bcr \qquad \text{(A2.7)}$$

β_j and γ_k are similarly defined.

Interaction effects are defined inductively from the main factor effects (this procedure was discussed in section A1.3). Thus $(\alpha\beta)_{ij}$ is defined as

$$(\alpha\beta)_{ij} = (y_{ij..} - y_{.j..}) - (y_{i...} - y_{....}) \qquad \text{(A2.8)}$$

$$= y_{ij..} - y_{i...} - y_{.j..} + y_{....}$$

= (main effect for A at level j of B) - (main effect for A)

$$y_{ij..} = \Sigma_k\Sigma_l\, y_{ijkl} / cr \qquad \text{(A2.9)}$$

$y_{ij..}$ is a subset of $y_{.j..}$, thus $(y_{ij..} - y_{.j..})$ represents an average difference at level j of B arising from changes in the levels, i, of factor A or, if these are neglible, from random error. The difference between $(y_{ij..} - y_{.j..})$ and $(y_{i...} - y_{....})$ then represents the difference between the effect of factor A at level j of B and the effect of factor A at level i.

The three factor interaction $(\alpha\beta\gamma)_{ijk}$ is defined similarly. Thus the difference $[(y_{ijk.} - y_{.jk.}) - (y_{i.k.} - y_{..k.})]$ represents the average $(\alpha\beta)$ interaction effect at the k level of C. Subtracting $(\alpha\beta)_{ij}$ this from yields the $(\alpha\beta\gamma)_{ijk}$ interaction, i.e.

$$(\alpha\beta\gamma)_{ijk} = (y_{ijk.} - y_{.jk.} - y_{i.k.} + y_{..k.}) \qquad \text{(A2.10)}$$

$$- (y_{ij..} - y_{i...} - y_{.j..} - y_{...})$$

$$y_{ijk.} = \Sigma_l \, y_{ijkl} \, / \, r \qquad \text{(A2.11)}$$

and y_{ik}, y_{jk} are defined in the same manner as y_{ij}.

Lastly, the error term e_{ijkl} is given by

$$e_{ijkl} = (y_{ijkl} - y_{ijk.}) \qquad \text{(A2.12)}$$

$$y_{ijk.} = \Sigma_l \, y_{ijkl} \, / \, r \qquad \text{(A2.13)}$$

The complete set of terms defining each factor effect are listed as negative (-) and positive (+) sign coefficients in Table A2.1.

Table A2.1 : Partition of total variance into components

	y_{ijkl}	$y_{i...}$	$y_{.j..}$	$y_{..k.}$	$y_{ij..}$	$y_{i.k.}$	$y_{.jk.}$	$y_{ijk.}$	$y_{....}$
A		+							-
B			+						-
C				+					-
AB		-	-		+				+
AC		-		-		+			+
BC			-	-			+		+
ABC		+	+	+	-	-	-	+	-
e	+							-	
Sum	+								-

If the respective column coefficients in Table A2.1 are summed it is apparent that no net change has arisen as a result of expanding the total sum of squares, TSS, to include all factor effects.

For convenience let the symbol *A* denote $y_{i...} - y_{....}$ etc. Then the total sum of squares, TSS, can be written as

$$TSS = \Sigma_i \Sigma_j \Sigma_k \Sigma_l \, [A + B + C + AB + AC + BC + ABC + E]^2 \qquad \text{(A2.14)}$$

Now, it can be shown that all the internal *co-factors A*B*, *A*C*, *A*ABC*, etc. *each sum* to *zero*, because for every co-factor, at least one of the four summation steps involves adding the difference between an effect and its mean, i.e.

$$\Sigma_p (x_p - x_{avg}) = 0 \qquad \text{(A2.15)}$$

where

x_p = factor effect
x_{avg} = average of factor effect

Therefore the total sum of squares reduces to

$$TSS = bcr \Sigma_i A^2 + acr \Sigma_j B^2 + abr \Sigma_k C^2 + cr \Sigma_i\Sigma_j AB + br \Sigma_i\Sigma_k AC + ar \Sigma_j\Sigma_k BC + r \Sigma_i\Sigma_j\Sigma_k ABC + \Sigma_i\Sigma_j\Sigma_k\Sigma_l E^2 \qquad \text{(A2.16)}$$

where A takes on levels i = 1 to a, B takes on levels j = 1 to b, C takes on levels k = 1 to c and l consists of r repeat tests.

The more conventional notation is to write

$$TSS = SS_A + SS_B + SS_C + SS_{AB} + SS_{AC} + SS_{BC} + SS_{ABC} + SS_e \qquad \text{(A2.17)}$$

where

SS_A = the sum of the squares of main effect A

$$= bcr \Sigma_i (y_{i...} - y_{....})^2 = bcr \Sigma_i \alpha_i^2 \qquad \text{(A2.18)}$$

etc.

SS_A, SS_B, SS_C, SS_{AB}, etc. represent the individual contributions of all the factor (main and interaction) effects to the total system sum of squares.

The size of each of the variance terms above is evidently dependent on the number of levels and repeat tests selected; for comparative purposes it is more convenient to convert each term into a unit variance term, called a *mean square*. A mean square is defined as a variance divided by its number of degrees of freedom.

Thus the mean square of factor effect A is given by

$$MS_A = SS_A / (a - 1) \qquad \text{(A2.19)}$$

The mean square of the error (equal number of repeat tests) is given by

$$MS_e = SS_e / [abc(r - 1)] \qquad (A2.20)$$

A2.2.2 F-tests for factor effects

Recall equation (A2.18), i.e. $SS_A = bcr \Sigma_i \alpha_i^2$. SS_A is the contribution of the main factor effect A to the total system variance; the question of how large this relative contribution is needs to be resolved.

If factor A exerts no effect on the system response, then the SS_A (and by inference MS_A) term should be small since any value deviating from zero arises solely from random error. Furthermore one would expect that $MS_A \approx MS_e$ or equivalently, the ratio $MS_A / MS_e \approx 1$.

In section A2.1. it was stated that the error terms in the linear fixed effects model are assumed to be independently and normally distributed. Under these circumstances, an F test statistic (similar to the z- and t-test statistics) can be used to compare sample variances.

The basis for the use of this statistic as a test of sample variance is briefly related below. For details consult the sources listed in section A2.1 above.

Let a random sample $y_1, y_2, \ldots, y_n$ be taken from a normal population designated 1 which has a characteristic population variance σ_1^2. The sample variance s_1^2 is computed by the usual procedure (see section A3.1. for an example). The ratio s_1^2 / σ_1^2 follows a Chi-squared (χ_1^2) distribution with $\nu_1 = (n - 1)$ degrees of freedom. Now consider another (independent) random sample $x_1, x_2, \ldots, x_m$ taken from a normal population 2, this also follows a Chi-squared (χ_2^2) distribution with $\nu_2 = (m - 1)$ degrees of freedom. The sampling distribution

$$F = \frac{\chi_1^2 / \nu_1}{\chi_2^2 / \nu_2} \qquad (A2.21)$$

has ν_1 numerator degrees of freedom and ν_2 denominator degrees of freedom. It is evident that the mean square variances defined earlier

are just χ^2 distributions divided by their respective degrees of freedom.

The F-statistic enables hypothesis tests on sample variance (s^2) components of the linear model to be devised.

Take as an example, the main effect due to experimental factor A. Define as a null hypothesis the premise that the factor A effect does not influence the system response. Then the alternative hypothesis is that at least one factor-level i affects the system output. Mathematically one can write

$H_o : \alpha_1 = \alpha_2 = \ldots \alpha_a = 0$
$H_a : \alpha_i \neq 0$ for at least one factor-level i

The expected or repeated average value of MS_A is σ_A^2, where σ_A^2 is the normalised random variance associated with experimental factor A.

$$E[MS_A] = \sigma_A^2 \qquad \text{(A2.22)}$$

Similarly

$$E[MS_e) = \sigma_e^2 \qquad \text{(A2.23)}$$

σ_e^2 = normalised system random error

$$\text{Now } E[MS_A / MS_e] = E[F] = \sigma_A^2 / \sigma_e^2 \qquad \text{(A2.24)}$$

It is apparent that under the null hypothesis, H_o, the normalised random variance associated with A is due solely to random error, $\sigma_A^2 = \sigma_e^2$. Therefore the null and alternative hypotheses can be re-expressed as

$H_o : \sigma_A^2 = \sigma_e^2$
$H_a : \sigma_A^2 > \sigma_e^2$

A one-tailed F-test at a desired confidence level (typically 95 % , α = 0.05) is therefore appropriate. F_o is obtained from statistical tables.

$F_o = f(\alpha, \nu_1, \nu_2)$

If $F = MS_A / MS_e < F_o$ then accept H_o, H_o' otherwise H_a is true and the factor effect A exerts a significant effect on the system response.

A2.3 Contrasts and ANOVA

The factor effect sample variances defined for ANOVA analysis can be related to the **contrasts** of average responses discussed at some length in section A1.2. An example best illustrates the general method of relating what are essentially two measures of response variance.

Again use the variance due to main effect A as an example.

$$SS_A = \Sigma_i (y_{i...} - y_{....})^2 = \Sigma_i \alpha_i^2$$

Consider the specific case of 2^3 full factorial design. The test runs 1-8 are run in random sequence. The complete set of input variable combinations are reproduced below.

Table A2.2 : Full 2^3 factorial design

Test run number	Factor I	A	B	C	average response
1	+	-	-	-	$y_{1.}$
2	+	-	+	-	$y_{2.}$
3	+	-	-	+	$y_{3.}$
4	+	-	+	+	$y_{4.}$
5	+	+	-	-	$y_{5.}$
6	+	+	+	-	$y_{6.}$
7	+	+	-	+	$y_{7.}$
8	+	+	+	+	$y_{8.}$

The contrast defining the factor A effect is

$$C_A = -y_{1.} - y_{2.} - y_{3.} - y_{4.} + y_{5.} + y_{6.} + y_{7.} + y_{8.} \qquad (A2.25)$$

Now adopting the ANOVA approach, the factor A is tested at two levels, low (-) and high (+), i.e. m = 1, 2.

The average responses at the two levels are

$$y^*_1 = (y_{1.} + y_{2.} + y_{3.} + y_{4.}) / 4 \qquad m = 1 \qquad \text{(A2.26)}$$

$$y^*_2 = (y_{5.} + y_{6.} + y_{7.} + y_{8.}) / 4 \qquad m = 2 \qquad \text{(A2.27)}$$

The average system response is

$$y_{...} = \Sigma_i\, y_{i.} / 8 \; ; \; i = 1 \text{ to } 8 \qquad \text{(A2.28)}$$
$$= (y^*_1 + y^*_2) / 2$$

Equation (A2.25) can be rewritten as

$$C_A = 4\ (-y^*_1 + y^*_2) \qquad \text{(A2.29)}$$

The sum of squares due to main effect A is then

$$SS_A = \Sigma_m\, (y^*_m - y_{...})^2 \qquad \text{(A2.30)}$$
$$= [(y^*_1 - y_{...})^2 + (y^*_2 - y_{...})^2]$$

substituting eq. (A2.29)

$$= \{[(y^*_1 - y^*_2)/2]^2 + [(-y^*_1 + y^*_2)/2]^2\}$$
$$= 1/4\ [2\ (-y^*_1 + y^*_2)^2]$$
$$= 1/2 * C_A^2 / 16$$
$$= C_A^2 / 32$$

As there is only one degree of freedom the mean square of the factor effect variance is equal to the component variance sum of the squares, i.e. $MS_A = SS_A$.

For a set of averages, $y_{i.}$, with each level i consisting of n (repeat) observations, the general formula for a contrast C is

$$SS(C) = (\Sigma_i\, a_i y_{i.})^2 / n\, \Sigma_i\, a_i^2 \qquad \text{(A2.31)}$$

where the a_i's are the respective sign coefficients which obey the constraint

$$\Sigma_i \, a_i = 0 \qquad \text{(A2.32)}$$

A2.4 Analysis of Fractional Designs

Fractional designs are *unbalanced* as there are more factor effects than independent contrasts (section A1.3). The ANOVA technique can still be used to detect factor effects, however, the component variance calculated from the *square* of a *contrast* reflects the sum of the variances of *all* the *aliases* associated with that contrast. If one assumes however, that the variance associated with the higher order aliases are negligible then the factor effects of interest can still be identified.

In the case of a Resolution IV design main effects are aliased with three factor and higher interaction effects. If these are negligible (which is an acceptable assumption) the main effects are defined by unique contrasts. Also, the two factor contrasts are aliased with each other so the interaction sum of squares terms represent the *sum* of two factor interactions (see section A1.5).

Experiments which require *unbalanced designs* can be analysed more precisely by other statistical methods, whihh usually involve fitting of regression models; in statistical jargon known as *subset hierarchial models*. These models allow one to compare main effects and interactions by comparing error sums of squares from different model fits. For example, if the experimental data is fitted to two models M_1 and M_2 where the factor effect terms in M_2 are a subset of M_1, the difference in error sum of squares between the two models represents the factor effects in M_1 which are not in the subset M_2. Model fits are usually performed by computer software. Details of this procedure are available in Mason et al (1989, pp 310 - 314).

APPENDIX A3

DURNACOL FACTORIAL DESIGN - STATISTICAL ANALYSES

A3.1 Error Estimates

Take the duplicate factorial design response data. These are listed in Table A3.1. The method used to calculate the yield, recovery and ash content errors is described below.

(Mason et al; 1989, p 302)

For factor level i the associated error sample variance is

$$s_i^2 = \Sigma_j (y_{ij} - y_{iavg})^2 / (n_i - 1) \qquad (A3.1)$$

where

$n_i = \Sigma_j = 2$ = number of sample repeats

$\Sigma_i = 12$ = number of runs for which repeat samples available

The total variance is

$$SS_e = \Sigma_i s_i^2 \qquad (A3.2)$$

The degrees of freedom d.o.f. associated with the sample error is

$$\nu = \Sigma_i (n_i - 1) = 12 \qquad (A3.3)$$

The mean square of the error MS_e

$$MS_e = SS_e / \nu = SS_e / 12 \qquad (A3.4)$$

The complete error analysis is listed in Table A3.1.

Table A3.1 : Analysis of variance - Durnacol factorial design

Duplicate sample data

Run ID	Yield		Recovery		Concentrate ash	
Sample	1	2	1	2	1	2
5	79.01	83.82	92.65	93.80	14.62	14.78
7	81.11	82.15	92.26	93.04	20.41	19.51
3	38.23	33.32	45.30	40.05	11.83	11.88
8	81.01	81.40	93.97	94.10	17.27	17.41
9	78.21	78.67	92.11	92.17	16.70	16.62
10	36.34	28.80	46.57	38.91	10.08	8.65
11	80.33	83.43	93.93	95.53	18.63	19.03
12	23.52	24.92	29.77	32.31	10.27	10.27
13	71.83	62.95	84.77	79.52	16.45	14.65
14	21.40	24.53	24.57	28.30	8.07	8.03
15	6.52	5.27	7.65	6.21	8.52	8.38
16	18.04	17.94	22.86	22.96	7.41	6.52

Run ID	Yield error		Recovery error		% Ash error	
Sample	si^2	yiavg	si^2	yiavg	si^2	yiavg
5	11.57	81.42	0.66	93.23	0.01	14.70
7	0.54	81.63	0.30	92.65	0.40	19.96
3	12.05	35.78	13.78	42.68	0.00	11.86
8	0.08	81.21	0.01	94.04	0.01	17.34
9	0.11	78.44	0.00	92.14	0.00	16.66
10	28.43	32.57	29.34	42.74	1.02	9.37
11	4.80	81.88	1.28	94.73	0.08	18.83
12	0.98	24.22	3.23	31.04	0.00	10.27
13	39.43	67.39	13.78	82.15	1.62	15.55
14	4.90	22.97	6.96	26.44	0.00	8.05
15	0.78	5.90	1.04	6.93	0.01	8.45
16	0.00	17.99	0.01	22.91	0.40	6.97
	102.88		69.34		3.16	
d.o.f.	12		12		12	
MSe	8.57		5.78		0.26	
se	2.93		2.40		0.51	

A3.2 Analysis of Variance

F-tests were used to determine which factor effects (defined below) were statistically significant (Mason et al; 1989, p330)

A factor effect can defined by its contrast, l [equations (A1.8) and (A1.9) in Appendix A1] where

$$l = \Sigma_i C_i * y_{iavg} \quad (A3.5)$$

$$\Sigma_i C_i = 0 \quad i = 1 \text{ to } k \quad (A3.6)$$

C_i represents a sign coefficient (- or +)

For 2 level factorial experiments the contrast effect, E, is defined by

$$E = 2 * l / N \quad (A3.7)$$

where

N = total number of observations

The factorial design used on the Durnacol sample tests each factor at 8 low (-) and 8 high (+) levels. Thus for a given factor one is effectively repeating each level (- or +) 8 times, so each level has an average low (-) and high (+) effect, where

$$\Sigma i = N = 16 \quad (A3.8)$$

$$y_{(-)avg} = \Sigma_i y_{i(-)} / (N/2) \quad (A3.9)$$

$$y_{(+)avg} = \Sigma_i y_{i(+)} / (N/2) \quad (A3.10)$$

$$y_{(-+)avg} = [y_{(-)avg} + y_{(+)avg}] / N \quad (A3.11)$$

The standard variance due the factor effect(s) defined by the contrast l is then

$$SS(l) = \Sigma_\beta (y_{(\beta)avg} - y_{(-+)avg})^2 \quad (A3.12)$$

where β = - or +

Applying equation (A2.31) of section A2.3. one obtains

$SS(1) = 1^2 / 8 * 16 = 12 / 128$

The identical result could be obtained by calculating factor sums of squares for a full 2^4 factorial design applying the methods described in section A2.3.

It is apparent that SS(1) has only one degree of freedom hence it is a mean square, i.e.

$$MS(1) = SS(1) \qquad (A3.13)$$

For example, the effect of Froth height (FH) on yield was obtained as follows :

The sign coefficients for each test run and corresponding results for each test run are given below in Table A3.2.

Table A3.2 : FH main effect on average yield response

Test run ID	C_i	$y_{i.}$
15	-1	5.90
14	+1	22.97
7	-1	81.63
4	+1	58.34
2	-1	16.42
3	+1	35.77
5	-1	81.41
6	+1	74.63
8	+1	81.21
9	-1	78.44
10	+1	32.57
12	-1	24.22
11	+1	81.88
13	-1	67.39
16	+1	17.99
1	-1	15.66
Total	0	34.29

Therefore $SS(1) = SS(FH) = MS(FH) = 34.292 / 128 = 9.186$

The yield error $MS_e = 8.57$

Analysis of variance

Repeat sample values are reported as averages in the factorial design.

Number of experiments in factorial design n = 16

Contrast no of degrees of freedom d.o.f. = 1

MSe 12 degrees of freedom

F1,12 = 3.18 at a 10 % significance level

F1,12 = 4.75 at a 5 % significance level

Table A3.3 - Analysis of variance main effects

Parameter	Yield		Recovery		Ash	
MSe	8.57		5.78		0.26	
k	Contrast Effect lk	Mean Square MSlk	Contrast Effect lk	Mean Square MSlk	Contrast Effect lk	Mean Square MSlk
FH	34.29	9.19	47.66	17.75	-7.84	0.48
FC	433.43	1467.67	489.6	1872.72	55.94	24.45
AF	72.91	41.53	87.24	59.46	3.28	0.08
QF	-73.07	41.71	-68.26	36.40	-21.42	3.58
WW	24.49	4.69	17.94	2.51	9.00	0.63
ST	5.51	0.24	15.04	1.77	-4.02	0.13
CH	-3.51	0.10	0.46	0.00	-3.38	0.09

MSlk = SSlk^2/(8 * 16) = SSlk^2 /128

Ratios MSlk/MSe = Fk = effect of factor k

Table A3.4 - F tests main effects

Parameter	Yield Ratio	Recovery Ratio	Conc Ash Ratio
FH	1.07	3.07	1.85
FC	171.26	324.00	94.03
AF	4.85	10.29	0.32
QF	4.87	6.30	13.79
WW	0.55	0.44	2.43
ST	0.03	0.31	0.49
CH	0.01	0.00	0.34

Table A3.5 - Analysis of variance interaction effects

Parameter	Yield		Recovery		Ash	
MSe	8.57		5.78		0.26	
k	Contrast Effect lk	Mean Square MSlk	Contrast Effect lk	Mean Square MSlk	Contrast Effect lk	Mean Square MSlk
FH	-21.59	3.64	-10.68	0.89	-7.84	0.48
FC	-3.53	0.10	-1.98	0.03	-7.54	0.44
AF	5.87	0.27	6.74	0.35	-1.24	0.01
QF	-59.91	28.04	-67.4	35.49	-5.5	0.24
WW	13.09	1.34	13.96	1.52	8.2	0.53
ST	-20.01	3.13	-26.98	5.69	-9.98	0.78
CH	31.97	7.99	40.56	12.85	6.14	0.29

MSlk = SSlk^2/(8 * 16) = SSlk^2 /128

Ratios MSlk/MSe = Fk = effect of factor k

Table A3.6 - F-tests interaction effects

Parameter	Yield Ratio	Recovery Ratio	Conc Ash Ratio
FH	0.42	0.15	1.85
FC	0.01	0.01	1.71
AF	0.03	0.06	0.05
QF	3.27	6.14	0.91
WW	0.16	0.26	2.02
ST	0.37	0.98	2.99
CH	0.93	2.22	1.13

Hence the test F-factor is
$F = MS(FH) / MS_e = 9.186 / 8.57 = 1.07$

Now $F_o(0.05, 1, 12) = 4.75$ at a = 5 % significance level
$F_o(0.10, 1, 12) = 3.18$ at a = 10 % significance level

$1.07 < 3.18, 4.75$ therefore conclude FH did not affect flotation yield response.

Tables A3.3 and A3.5 list the contrasts and Mean Squares associated with main effect and (2 factor) interactions.

F ratios for main effects are indicated in Table A3.4 and those representing interactions are listed in Table A3.6.

The results were calculated on a QUATTRO spreadsheet programme; the calculations performed were based on the algorithm just described.

A3.3 Feed Ash Variability - Block and Covariate Effects

Three batches (blocks) of feed were required to generate the 16 trials needed to complete the 2^{7-3}_{IV} design. The effects of fluctuation in feed composition within each pulp tank batch (a **covariate** effect) and the possibility that different batches (blocks) had different feed compositions (**confounding** between **blocks**) had therefore to be considered. Bulk ash content was the parameter selected to represent feed composition.

Ash analyses of feed slurry samples taken for the individual experimental runs are given under the column heading "MF" in Table A3.7. No feed sample was taken for column run 2. Column trials 1-7 were run from the same batch of pulp feed identified by the acronym B1. A similar order applies to the runs performed from pulp batches B2 and B3. The averages and sample deviations of the individual sets of block feed samples are given in Table A3.8. The sample standard deviation, s, within each pulp batch (or block) represents the inherent sampling error in the pulp feed tank.

Table A3.7 - Bulk Feed composition data

Run ID		Feed % ash MF	Calculated Feed Ashes % ash CF1	% ash CF2	del CF
1	B1	28.66	30.40		
2			32.53		
3		28.50	25.59	26.70	1.11
4		24.38	27.75		
5		29.69	27.61	26.15	-1.46
6		31.99	28.22		
7		29.12	29.63	28.93	-0.70
8	B2	29.49	28.67	28.58	-0.09
9		29.82	29.27	29.05	-0.22
10		32.44	29.82	32.38	2.56
11		29.92	30.41	29.28	-1.13
12		24.75	29.12	29.95	0.83
13	B3	32.57	29.39	31.68	2.29
14		30.86	30.98	30.91	-0.07
15		32.91	32.95	31.17	-1.78
16		27.73	26.90	27.21	0.31
	Avg	29.52	29.33	29.33	0.14
	sample s	2.56	1.93	1.99	1.37

Table A3.8 - Measured Feed Compositions between batches

Batch	Avg	sample s	d.o.f.	Number of samples, N
B1	28.72	2.48	5	6.00
B2	29.28	2.80	4	5.00
B3	31.02	2.37	3	4.00

row	FASH	BATCH
1	28.66	B1
2	28.50	B1
3	24.38	B1
4	29.69	B1
5	31.99	B1
6	29.12	B1
7	29.49	B2
8	29.82	B2
9	32.44	B2
10	29.92	B2
11	24.75	B3
12	32.57	B3
13	30.86	B3
14	32.91	B3
15	27.73	B3

One-Way Analysis of Variance

Data: STATFASH.FASH

Level codes: STATFASH.BATCH

Labels:

Range test: Conf. Int. Confidence level: 95

Analysis of variance

Source of variation	Sum of Squares	d.f.	Mean square	F-ratio	Sig. level
Between groups	7.327712	2	3.6638558	.520	.6071
Within groups	84.486128	12	7.0405107		
Total (corrected)	91.813840	14			

0 missing value(s) have been excluded.

An ANOVA analysis was performed to check whether the differences in mean feed bulk grades between blocks were significantly different from the inherent sampling error within the feed tank. The analysis was executed on STATGRAPHICS. An input and output listing are given on page A-39 above.

$F_{(2,12)} = 3.89$ at $\alpha = 5$ % significance level

The F-ratio is ≈ 0.5, i.e. < 1, therefore *variability* between *pulp batch* compositions was *negligible* compared to the inherent *tank* sample composition *error*, i.e. the pulp batch *blocks* were *unconfounded*.

A normal probability plot performed on STATGRAPHICS demonstrates that the measured feed ashes can be regarded as being normally distributed.

A3.4 Slurry Feedrate and Residence Time Effects on Yield

Yield and recovery response data were clustered into two groups corresponding to low (-) and high (+) frother dosage levels. In Table A3.9 column run data are grouped according to frother dosage, FC, and slurry feedrate, QF, levels .

Two-sample t-tests were used to check the effect of QF on yield response at each frother level. The tests were performed on STATGRAPHICS, programme input and output listings are provided overleaf. The symbols "l" and "h" were substituted for "-" and "+" when the runs were grouped by the QF and FC criteria.

The average yield obtained at the high slurry feedrate/ low frother dosage level (DATA.QFhFCl) was not any worse than those at the low slurry feedrate/low frother dosage level (DATA.QFlFCl). However, comparision between DATA.QFhFCh and DATA.QFlFCh indicates that, at a 95 % confidence level, the higher slurry flowrates, QF (+), caused an average drop in yield at the high frother concentration , FC (+).

Table A3.9 - Effect of QF on Yield

Run ID	CH	QF	FC	Yield
1	-1	-1	-1	15.66
3	-1	-1	-1	35.77
12	1	-1	-1	24.22
14	1	-1	-1	22.97
15	-1	1	-1	5.90
10	-1	1	-1	32.57
16	1	1	-1	17.99
2	1	1	-1	16.42
8	1	-1	1	81.21
7	1	-1	1	81.63
11	-1	-1	1	81.88
5	-1	-1	1	81.41
4	-1	1	1	58.34
13	1	1	1	67.39
6	1	1	1	74.63
9	-1	1	1	78.44

Table A3.10 - Comparision residence time vs column height

Run ID	CH	QF	FC	QT l/min	Tavg min	Yield
4	-1	1	1	1.32	4.77	58.34
10	-1	1	-1	1.57	4.01	32.57
11	-1	-1	1	0.68	9.26	81.88
5	-1	-1	1	0.50	12.60	81.41
15	-1	1	-1	1.96	6.13	5.90
3	-1	-1	-1	0.70	9.00	35.77
1	-1	-1	-1	1.18	5.34	15.66
9	-1	1	1	1.32	4.77	78.44
6	1	1	1	1.28	9.39	74.63
13	1	1	1	1.15	10.45	67.39
16	1	1	-1	1.50	8.01	17.99
14	1	-1	-1	1.26	9.54	22.97
12	1	-1	-1	1.21	9.93	24.22
7	1	-1	1	0.94	12.79	81.63
8	1	-1	1	0.80	15.03	81.21
2	1	1	-1	1.40	8.59	16.42

Mean nominal slurry residence times, defined as the collection zone volume divided by the (net) tails rate, are listed in Table A3.10. Tails rates, QT, for column trials in which the USBM sparger was used are calculated by subtracting the water addition rate to the USBM sparger from the measured tails rate, i.e. it is assumed that all the sparger water short-circuits into the tailings stream.

A two-sample t-test, was also performed on STATGRAPHICS, to check whether slurry residence times were, on average, lower at the shorter column height, CH (-). Programme input and output listings are attached. At a 95 % confidence level, residence times are in fact shorter at CH (-).

Cursor at Row: 1 Data Editor Maximum Rows: 4
Column: 1 File: STATQF Number of Cols: 4

Row	QF1FC1	QFhFC1	QF1FCh	QFhFCh
1	15.66	5.90	81.21	58.34
2	35.77	32.57	81.63	67.39
3	24.22	17.99	81.88	74.63
4	22.97	16.42	81.41	78.44
5				
6				
7				
8				
9				
10				
11				
12				
13				
14				
Length	4	4	4	4
Typ/Wth	N/13	N/13	N/13	N/13

Two-Sample Analysis Results

		Sample 1	Sample 2	Pooled
Sample Statistics:	Number of Obs.	4	4	8
	Average	24.655	18.22	21.4375
	Variance	69.1606	120.333	94.7466
	Std. Deviation	8.31628	10.9696	9.73379
	Median	23.595	17.205	20.48

Difference between Means = 6.435

Conf. Interval For Diff. in Means:		95 Percent	
(Equal Vars.)	Sample 1 - Sample 2	-10.4118 23.2818	6 D.F.
(Unequal Vars.)	Sample 1 - Sample 2	-10.7142 23.5842	5.6 D.F.

Ratio of Variances = 0.574745

Conf. Interval for Ratio of Variances: 0 Percent
Sample 1 - Sample 2

Hypothesis Test for H0: Diff = 0 — Computed t statistic = 0.934936
vs Alt: NE — Sig. Level = 0.385905
at Alpha = 0.05 — so do not reject H0.

Two-Sample Analysis Results

		Sample 1	Sample 2	Pooled
Sample Statistics:	Number of Obs.	4	4	8
	Average	81.5325	69.7	75.6162
	Variance	0.0830917	78.3594	39.2212
	Std. Deviation	0.288256	8.85208	6.26269
	Median	81.52	71.01	79.825

Difference between Means = 11.8325

Conf. Interval For Diff. in Means:		95 Percent	
(Equal Vars.)	Sample 1 - Sample 2	0.993339 22.6717	6 D.F.
(Unequal Vars.)	Sample 1 - Sample 2	-2.24376 25.9088	3.0 D.F.

Ratio of Variances = 1.06039E-3

Conf. Interval for Ratio of Variances: 0 Percent
Sample 1 - Sample 2

Hypothesis Test for H0: Diff = 0 — Computed t statistic = 2.67197
vs Alt: NE — Sig. Level = 0.0369296
at Alpha = 0.05 — so reject H0.

Cursor at Row: 1 Data Editor Maximum Rows: 8
Column: 1 File: STATCHI Number of Cols: 2

Row	CHl	CHh
1	4.77	9.39
2	4.01	10.45
3	9.26	8.01
4	12.60	9.54
5	6.13	9.93
6	9.00	12.79
7	5.34	15.03
8	4.77	8.59
9		
10		
11		
12		
13		
14		
Length	8	8
Typ/Wth	N/13	N/13

Two-Sample Analysis Results

		STATCHI.CHl	STATCHI.CHh	Pooled
Sample Statistics:	Number of Obs.	8	8	16
	Average	6.985	10.4662	8.72562
	Variance	8.9806	5.44074	7.21067
	Std. Deviation	2.99676	2.33254	2.68527
	Median	5.735	9.735	9.13

Difference between Means = -3.48125

Conf. Interval For Diff. in Means:		95 Percent	
(Equal Vars.)	Sample 1 - Sample 2	-6.36164 -0.600858	14 D.F.
(Unequal Vars.)	Sample 1 - Sample 2	-6.37801 -0.584486	13.2 D.F.

Ratio of Variances = 1.65062

Conf. Interval for Ratio of Variances: 0 Percent
Sample 1 - Sample 2

Hypothesis Test for H0: Diff = 0 Computed t statistic = -2.59285
vs Alt: NE Sig. Level = 0.0212712
at Alpha = 0.05 so reject H0.

APPENDIX A4.1

GENSTAT INPUT LISTING

-1	-1	-1	1	1	1	-1	6.52	8.9	8.52	32.95	1
1	-1	-1	-1	-1	1	1	21.4	28.51	8.07	30.98	1
-1	1	-1	-1	1	-1	1	81.11	91.73	20.41	29.07	1
1	1	-1	1	-1	-1	-1	58.34	70.94	12.14	32.44	1
-1	-1	1	1	-1	-1	1	16.42	22.24	8.65	32.53	1
1	-1	1	-1	1	-1	-1	38.23	45.3	11.83	28.5	1
-1	1	1	-1	-1	1	-1	79.01	92.6	15.15	29.69	1
1	1	1	1	1	1	1	74.63	90.31	13.14	31.99	1
1	1	1	-1	-1	-1	1	81.01	93.97	17.27	29.49	1
-1	1	1	1	1	-1	-1	78.21	92.11	16.7	29.82	1
1	-1	1	1	-1	1	-1	36.34	46.57	10.08	24.66	1
-1	-1	1	-1	1	1	1	23.52	29.77	10.27	29.12	1
1	1	-1	-1	1	1	-1	80.33	93.93	18.63	29.92	1
-1	1	-1	1	-1	1	1	71.83	84.99	16.45	29.39	1
1	-1	-1	1	1	-1	1	18.04	22.86	7.41	26.92	1
-1	-1	-1	-1	-1	-1	-1	15.66	20.24	10.05	28.66	1
-1	-1	-1	1	1	1	-1	5.27	6.83	8.38	29.25	2
1	-1	-1	-1	-1	1	1	24.53	32.66	8.03	30.91	2
-1	1	-1	-1	1	-1	1	82.15	93.04	19.51	28.93	2
1	1	-1	1	-1	-1	-1	*	*	*	*	2
-1	-1	1	1	-1	-1	1	*	*	*	*	2
1	-1	1	-1	1	-1	-1	33.32	40.05	11.88	26.7	2
-1	1	1	-1	-1	1	-1	83.82	94.45	16.78	26.15	2
1	1	1	1	1	1	1	*	*	*	*	2
1	1	1	-1	-1	-1	1	81.4	94.1	17.44	28.58	2
-1	1	1	1	1	-1	-1	78.67	92.17	16.62	28.84	2
1	-1	1	1	-1	1	-1	28.8	38.91	8.65	32.38	2
-1	-1	1	-1	1	1	1	24.92	32.31	10.27	30.79	2
1	1	-1	-1	1	1	-1	83.43	95.53	19.03	29.28	2
-1	1	-1	1	-1	1	1	62.95	78.65	14.65	31.68	2
1	-1	-1	1	1	-1	1	17.94	22.96	6.52	26.96	2
-1	-1	-1	-1	-1	-1	-1	*	*	*	*	2

APPENDIX A4.2

GENSTAT OUTPUT LISTING

```
Genstat 5  Release 2.1  (Vax/VMS5)  23-AUG-1991 12:24:38.97
Copyright  1990,  Lawes  Agricultural  Trust  (Rothamsted  Experimental
Station)

   1  UNITS [NVALUES=32]
   2  FACTOR [LEVELS=1] BLK
   3  & [LEVELS=2] RUN
   4  & [LEVELS=16] WHPL
   5  GENERATE BLK,RUN,WHPL
   6  FACTOR [LEVELS=!(-1,1)] FH,FC,AF,QF,WW,ST,CH
   7  READ FH,FC,AF,QF,WW,ST,CH,YIELD,REC,ASH,COV,JUNK

    Identifier   Minimum      Mean   Maximum    Values   Missing
         YIELD      5.27     49.56     83.82        32         4
           REC      6.83     59.17     95.53        32         4
           ASH      6.52     12.95     20.41        32         4
           COV     24.66     29.52     32.95        32         4
          JUNK     1.000     1.500     2.000        32         0
  41  TREATMENTSTRUCTURE FH+FC+AF+QF+WW+ST+CH+QF.AF+QF.FC+QF.CH+FH.FC
  42  BLOCKSTRUCTURE   WHPL/RUN
  43  COVARIATE COV
  44  ANOVA [UPRINT=A,I,C,M,MI;FP=Y]YIELD,REC,ASH

44..............................

***** Analysis of variance *****

Variate: YIELD

Source of variation       d.f.(m.v.)      s.s.       m.s.     v.r.  F pr.

WHPL stratum
FH                                 1       146.930    146.930     4.35  0.105
FC                                 1     23483.203  23483.203   695.03  <.001
AF                                 1       664.756    664.756    19.67  0.011
QF                                 1       667.497    667.497    19.76  0.011
WW                                 1        74.999     74.999     2.22  0.211
ST                                 1         3.788      3.788     0.11  0.755
CH                                 1         1.553      1.553     0.05  0.841
AF.QF                              1       127.721    127.721     3.78  0.124
FC.QF                              1        58.240     58.240     1.72  0.259
QF.CH                              1         4.344      4.344     0.13  0.738
FH.FC                              1       448.874    448.874    13.29  0.022
Residual                           4       135.150     33.788     3.91

WHPL.RUN stratum              12(4)       103.667      8.639

Total                         27(4)     23001.871
* MESSAGE: the following units have large residuals.
```

```
WHPL 11   RUN 1          3.77   s.e. 1.80
WHPL 11   RUN 2         -3.77   s.e. 1.80
WHPL 14   RUN 1          4.44   s.e. 1.80
WHPL 14   RUN 2         -4.44   s.e. 1.80


***** Tables of contrasts *****

Variate: YIELD


***** Tables of means *****

Variate: YIELD

Grand mean  48.53

       FH    -1.00     1.00
             46.38    50.67

       FC    -1.00     1.00
             21.44    75.62

       AF    -1.00     1.00
             43.97    53.08

       QF    -1.00     1.00
             53.09    43.96

       WW    -1.00     1.00
             47.00    50.06

       ST    -1.00     1.00
             48.18    48.87

       CH    -1.00     1.00
             48.75    48.31

       AF        QF    -1.00     1.00
    -1.00              50.53    37.40
     1.00              55.65    50.52

       FC        QF    -1.00     1.00
    -1.00              24.66    18.22
     1.00              81.53    69.70

       QF        CH    -1.00     1.00
    -1.00              53.68    52.51
     1.00              43.81    44.11

       FH        FC    -1.00     1.00
    -1.00              15.55    77.22
     1.00              27.32    74.01
```

*** Standard errors of differences of means ***

Table	FH	FC	AF	QF	WW	ST	CH	AF QF
rep.	16	16	16	16	16	16	16	8
s.e.d.	2.055	2.055	2.055	2.055	2.055	2.055	2.055	2.906

Table	FC QF	QF CH	FH FC
rep.	8	8	8
s.e.d.	2.906	2.906	2.906

(Not adjusted for missing values)

***** Missing values *****

Variate: YIELD
Covariate: COV

Unit	estimate
20	58.34
21	16.42
24	74.63
32	15.66

Max. no. iterations 4

44.....

***** Analysis of variance (adjusted for covariate) *****

Variate: YIELD
Covariate: COV

Source of variation	d.f.(m.v.)	s.s.	m.s.	v.r.	cov.ef.	F pr.
WHPL stratum						
FH	1	127.253	127.253	3.42	0.98	0.161
FC	1	22250.645	22250.645	598.56	0.93	<.001
AF	1	602.518	602.518	16.21	0.97	0.028
QF	1	291.911	291.911	7.85	0.61	0.068
WW	1	40.375	40.375	1.09	0.87	0.374
ST	1	12.555	12.555	0.34	0.87	0.602
CH	1	0.629	0.629	0.02	0.84	0.905
AF.QF	1	151.078	151.078	4.06	0.87	0.137
FC.QF	1	20.877	20.877	0.56	0.79	0.508
QF.CH	1	0.155	0.155	0.00	0.89	0.953
FH.FC	1	114.524	114.524	3.08	0.45	0.177
Covariate	1	23.629	23.629	0.64		0.484
Residual	3	111.521	37.174	5.92	0.91	
WHPL.RUN stratum						
Covariate	1	34.622	34.622	5.52		0.039
Residual	11(4)	69.045	6.277		1.38	
Total	27(4)	23001.871				

* MESSAGE: the following units have large residuals.

WHPL 6	RUN 1	3.21	s.e. 1.47
WHPL 6	RUN 2	-3.21	s.e. 1.47
WHPL 14	RUN 1	3.48	s.e. 1.47
WHPL 14	RUN 2	-3.48	s.e. 1.47

***** Covariate regressions *****

Variate: YIELD

Covariate	coefficient	s.e.
WHPL stratum		
COV	-1.0	1.30
WHPL.RUN stratum		
COV	-0.83	0.356

***** Tables of means (adjusted for covariate) *****

Variate: YIELD
Covariate: COV

Grand mean 48.53

FH	-1.00	1.00
	46.51	50.54
FC	-1.00	1.00
	21.20	75.85
AF	-1.00	1.00
	44.12	52.93
QF	-1.00	1.00
	52.40	44.65
WW	-1.00	1.00
	47.32	49.73
ST	-1.00	1.00
	47.86	49.20
CH	-1.00	1.00
	48.37	48.68

AF	QF	-1.00	1.00
-1.00		50.32	37.92
1.00		54.48	51.38

FC	QF	-1.00	1.00
-1.00		24.17	18.24
1.00		80.63	71.07

QF	CH	-1.00	1.00
-1.00		52.32	52.48
1.00		44.42	44.88

FH	FC	-1.00	1.00
-1.00		16.38	76.64
1.00		26.02	75.06

*** Standard errors of differences of means ***

Table	FH	FC	AF	QF	WW	ST	CH	AF QF
rep.	16	16	16	16	16	16	16	8
s.e.d.	2.179	2.234	2.189	2.766	2.308	2.305	2.350	3.441

Table	FC QF	QF CH	FH FC
rep.	8	8	8
s.e.d.	3.513	3.499	3.647

(Not adjusted for missing values)

***** Missing values (adjusted for covariate) *****

Variate: YIELD
Covariate: COV

Unit	estimate
20	60.58
21	18.74
24	76.49
32	14.74

Max. no. iterations 4

44.....

***** Analysis of variance *****

Variate: REC

Source of variation	d.f.(m.v.)	s.s.	m.s.	v.r.	F pr.
WHPL stratum					
FH	1	284.049	284.049	5.12	0.086
FC	1	29962.252	29962.252	540.38	<.001
AF	1	951.133	951.133	17.15	0.014
QF	1	582.260	582.260	10.50	0.032
WW	1	40.184	40.184	0.72	0.443
ST	1	28.312	28.312	0.51	0.514
CH	1	0.028	0.028	0.00	0.983
AF.QF	1	205.641	205.641	3.71	0.126
FC.Q	1	14.258	14.258	0.26	0.639
QF.CH	1	5.645	5.645	0.10	0.766
FH.FC	1	567.507	567.507	10.24	0.033
Residual	4	221.786	55.447	8.21	
WHPL.RUN stratum	12(4)	81.061	6.755		
Total	27(4)	28990.758			

* MESSAGE: the following units have large residuals.

WHPL 11	RUN 1	3.83	s.e. 1.59
WHPL 11	RUN 2	-3.83	s.e. 1.59

***** Tables of contrasts *****

Variate: REC

***** Tables of means *****

Variate: REC

Grand mean 58.14

FH	-1.00	1.00
	55.16	61.12
FC	-1.00	1.00
	27.54	88.74
AF	-1.00	1.00
	52.68	63.59
QF	-1.00	1.00
	62.40	53.87

WW	-1.00	1.00
	57.02	59.26
ST	-1.00	1.00
	57.20	59.08
CH	-1.00	1.00
	58.11	58.17

AF	QF	-1.00	1.00
-1.00		59.49	45.88
1.00		65.32	61.86

FC	QF	-1.00	1.00
-1.00		31.14	23.94
1.00		93.67	83.80

QF	CH	-1.00	1.00
-1.00		62.79	62.01
1.00		53.42	54.32

FH	FC	-1.00	1.00
-1.00		20.35	89.97
1.00		34.73	87.50

*** Standard errors of differences of means ***

Table	FH	FC	AF	QF	WW	ST	CH	AF QF
rep.	16	16	16	16	16	16	16	8
s.e.d.	2.633	2.633	2.633	2.633	2.633	2.633	2.633	3.723

Table	FC QF	QF CH	FH FC
rep.	8	8	8
s.e.d.	3.723	3.723	3.723

(Not adjusted for missing values)

***** Missing values *****

Variate: REC
Covariate: COV

Unit	estimate
20	70.94
21	22.24
24	90.31
32	20.24

Max. no. iterations 4

44.....

***** Analysis of variance (adjusted for covariate) *****

Variate: REC
Covariate: COV

Source of variation	d.f.(m.v.)	s.s.	m.s.	v.r.	cov.ef.	F pr.
WHPL stratum						
FH	1	247.849	247.849	4.10	0.98	0.136
FC	1	28466.248	28466.248	470.88	0.93	<.001
AF	1	856.544	856.544	14.17	0.97	0.033
QF	1	219.565	219.565	3.63	0.61	0.153
WW	1	13.333	13.333	0.22	0.87	0.671
ST	1	52.267	52.267	0.86	0.87	0.421
CH	1	7.208	7.208	0.12	0.84	0.753
AF.QF	1	245.363	245.363	4.06	0.87	0.137
FC.QF	1	0.207	0.207	0.00	0.79	0.957
QF.CH	1	0.034	0.034	0.00	0.89	0.983
FH.FC	1	129.367	129.367	2.14	0.45	0.240
Covariate	1	40.428	40.428	0.67		0.473
Residual	3	181.358	60.453	10.62	0.92	
WHPL.RUN stratum						
Covariate	1	18.441	18.441	3.24		0.099
Residual	11(4)	62.620	5.693		1.19	
Total	27(4)	28990.758				

* MESSAGE: the following units have large residuals.

WHPL 6	RUN 1	3.17	s.e. 1.40
WHPL 6	RUN 2	-3.17	s.e. 1.40

***** Covariate regressions *****

Variate: REC

Covariate	coefficient	s.e.
WHPL stratum		
COV	-1.4	1.66
WHPL.RUN stratum		
COV	-0.61	0.339

***** Tables of means (adjusted for covariate) *****

Variate: REC
Covariate: COV

Grand mean 58.14

FH	-1.00	1.00
	55.32	60.95

FC	-1.00	1.00
	27.23	89.04
AF	-1.00	1.00
	52.88	63.39
QF	-1.00	1.00
	61.50	54.77
WW	-1.00	1.00
	57.45	58.83
ST	-1.00	1.00
	56.77	59.50
CH	-1.00	1.00
	57.62	58.65

AF	QF	-1.00	1.00
-1.00		59.21	46.56
1.00		63.79	62.99

FC	QF	-1.00	1.00
-1.00		30.50	23.96
1.00		92.49	85.59

QF	CH	-1.00	1.00
-1.00		61.01	61.98
1.00		54.22	55.33

FH	FC	-1.00	1.00
-1.00		21.44	89.21
1.00		33.03	88.87

*** Standard errors of differences of means ***

Table	FH	FC	AF	QF	WW	ST	CH	AF QF
rep.	16	16	16	16	16	16	16	8
s.e.d.	2.779	2.848	2.791	3.528	2.943	2.940	2.997	4.389

Table	FC QF	QF CH	FH FC
rep.	8	8	8
s.e.d.	4.480	4.463	4.651

(Not adjusted for missing values)

***** Missing values (adjusted for covariate) *****

Variate: REC
Covariate: COV

Unit	estimate
20	72.58
21	23.93
24	91.67
32	19.57

Max. no. iterations 4

44.....

***** Analysis of variance *****

Variate: ASH

Source of variation	d.f.(m.v.)	s.s.	m.s.	v.r.	F pr.
WHPL stratum					
FH	1	7.7127	7.7127	0.91	0.394
FC	1	91.2301	391.2301	46.28	0.002
AF	1	1.3325	1.3325	0.16	0.712
QF	1	57.3252	57.3252	6.78	0.060
WW	1	10.1362	10.1362	1.20	0.335
ST	1	2.0151	2.0151	0.24	0.651
CH	1	1.4238	1.4238	0.17	0.703
AF.QF	1	4.7355	4.7355	0.56	0.496
FC.QF	1	7.6538	7.6538	0.91	0.395
QF.CH	1	0.1937	0.1937	0.02	0.887
FH.FC	1	3.7606	3.7606	0.44	0.541
Residual	4	33.8128	8.4532	20.78	
WHPL.RUN stratum	12(4)	4.8815	0.4068		
Total	27(4)	500.5670			

* MESSAGE: the following units have large residuals.

WHPL 7	RUN 1	-0.82	s.e. 0.39
WHPL 7	RUN 2	0.82	s.e. 0.39
WHPL 14	RUN 1	0.90	s.e. 0.39
WHPL 14	RUN 2	-0.90	s.e. 0.39

***** Tables of contrasts *****

Variate: ASH

***** Tables of means *****

Variate: ASH

Grand mean 12.70

FH	-1.00	1.00
	13.19	12.21

FC	-1.00	1.00
	9.21	16.20
AF	-1.00	1.00
	12.50	12.91
QF	-1.00	1.00
	14.04	11.37
WW	-1.00	1.00
	12.14	13.27
ST	-1.00	1.00
	12.95	12.45
CH	-1.00	1.00
	12.91	12.49

AF	QF	-1.00	1.00
-1.00		14.22	10.78
1.00		13.86	11.95

FC	QF	-1.00	1.00
-1.00		10.06	8.36
1.00		18.03	14.37

QF	CH	-1.00	1.00
-1.00		14.18	13.91
1.00		11.65	11.08

FH	FC	-1.00	1.00
-1.00		9.36	17.03
1.00		9.06	15.37

*** Standard errors of differences of means ***

Table	FH	FC	AF	QF	WW	ST	CH	AF QF
rep.	16	16	16	16	16	16	16	8
s.e.d.	1.028	1:028	1.028	1.028	1.028	1.028	1.028	1.454

Table	FC QF	QF CH	FH FC
rep.	8	8	8
s.e.d.	1.454	1.454	1.454

(Not adjusted for missing values)

***** Missing values *****

Variate: ASH
Covariate: COV

Unit	estimate
20	12.14
21	8.65
24	13.14
32	10.05

Max. no. iterations 4

44.....

***** Analysis of variance (adjusted for covariate) *****

Variate: ASH
Covariate: COV

Source of variation	d.f.(m.v.)	s.s.	m.s.	v.r.	cov.ef.	F pr.
WHPL stratum						
FH	1	7.9618	7.9618	0.71	0.98	0.461
FC	1	369.4975	369.4975	33.04	0.93	0.010
AF	1	1.0992	1.0992	0.10	0.97	0.774
QF	1	31.1483	31.1483	2.78	0.61	0.194
WW	1	7.7975	7.7975	0.70	0.87	0.465
ST	1	1.3156	1.3156	0.12	0.87	0.754
CH	1	0.7956	0.7956	0.07	0.84	0.807
AF.QF	1	4.9047	4.9047	0.44	0.87	0.555
FC.QF	1	4.9682	4.9682	0.44	0.79	0.553
QF.CH	1	0.3380	0.3380	0.03	0.89	0.873
FH.FC	1	0.8697	0.8697	0.08	0.45	0.798
Covariate	1	0.2586	0.2586	0.02		0.889
Residual	3	33.5542	11.1847	45.31	0.76	
WHPL.RUN stratum						
Covariate	1	2.1661	2.1661	8.78		0.013
Residual	11(4)	2.7153	0.2468	1.65		
Total	27(4)	500.5670				

* MESSAGE: the following units have large residuals.

WHPL 14	RUN 1	0.661	s.e. 0.291
WHPL 14	RUN 2	-0.661	s.e. 0.291

***** Covariate regressions *****

Variate: ASH

Covariate	coefficient	s.e.
WHPL stratum		
COV	-0.11	0.713
WHPL.RUN stratum		
COV	-0.209	0.0705

***** Tables of means (adjusted for covariate) *****

Variate: ASH
Covariate: COV

Grand mean 12.703

FH	-1.00	1.00
	13.208	12.199
FC	-1.00	1.00
	9.182	16.224
AF	-1.00	1.00
	12.515	12.892
QF	-1.00	1.00
	13.970	11.437
WW	-1.00	1.00
	12.175	13.232
ST	-1.00	1.00
	12.920	12.487
CH	-1.00	1.00
	12.875	12.532

AF	QF	-1.00	1.00
-1.00		14.200	10.830
1.00		13.739	12.044

FC	QF	-1.00	1.00
-1.00		10.006	8.359
1.00		17.933	14.515

QF	CH	-1.00	1.00
-1.00		14.033	13.906
1.00		11.718	11.157

FH	FC	-1.00	1.00
-1.00		9.442	16.973
1.00		8.923	15.476

*** Standard errors of differences of means ***

Table	FH	FC	AF	QF	WW	ST	CH	AF QF
rep.	16	16	16	16	16	16	16	8
s.e.d.	1.1952	1.2252	1.2007	1.5174	1.2658	1.2646	1.2891	1.8877

Table	FC QF	QF CH	FH FC
rep.	8	8	8
s.e.d.	1.9270	1.9195	2.0005

(Not adjusted for missing values)

***** Missing values (adjusted for covariate) *****

Variate: ASH
Covariate: COV

Unit	estimate
20	12.700
21	9.229
24	13.606
32	9.821

Max. no. iterations 4

45 STOP

******** End of job. Maximum of 15132 data units used at line 44 (34582 left)

APPENDIX B

B1 - BUBBLE SIZE DATA

B2 - IDENTIFICATION OF CONDITIONING TEST RUNS AND FIGURES

APPENDIX B1

BUBBLE SIZE DATA

Key for Table B1 :

dbavg - mean bubble diameter, mm
s - standard bubble diameter deviation, mm
R - rotameter reading
Jg - equivalent superficial velocity (@ 1 atm), cm/s
FC - frother concentration in frother solution tank, ul/l
Jl - net downward liquid velocity, cm/s
Ql - net downward liquid flowrate, ml/min
Lc - distance between sparger and solution/froth interface, mm
delH - difference between level in water manometer and Lc, mm
% E - % fractional air holdup (volumetric basis)

Table B1 : Bubble size data

File ID	dbavg m	s mm	% Disc	R	Jg cm/s	FC ul/l	Ql ml/min	Jl cm/s	delH	Lc mm	% E
TEST2	2.940	0.081	0.06	1.0	0.5	0					
TEST3	2.924	0.087	0.08	1.7	0.8	0					
TEST4	3.088	0.100	2.59	1.7	0.8	0					
TEST5	2.938	0.088	0.09	1.7	0.8	0					
TEST6	2.888	0.090	0.23	1.7	0.8	0					
5DBK2	1.556	0.038	0.06	2.0	1.0	5	840	0.61	87		
5DBK3	1.530	0.038	0.06	2.0	1.0	5	880	0.64	94		
5DBK4	1.490	0.038	0.18	2.0	1.0	5	840	0.61	95		
5DBK5	1.716	0.040	0.06	3.2	1.7	5	840	0.61	174		
5DBK6	1.715	0.039	0.05	3.2	1.7	5	840	0.61	175		
5DBK7	1.680	0.040	0.06	3.2	1.7	5	840	0.61	175		
5DBK9	1.894	0.044	0.12	4.4	2.5	5	800	0.58	190		
5DBK10	1.907	0.045	0.06	4.4	2.5	5	800	0.58	191		
5AMIBC2	1.898	0.038	0.19	2.0	1.0	5	860	0.63	60		
5AMIBC3	1.908	0.037	0.09	2.0	1.0	5	840	0.61	65		
5AMIBC4	2.085	0.037	0.06	3.2	1.7	5	840	0.61	120		
5AMIBC5	2.096	0.040	0.06	3.2	1.7	5	840	0.61	120		
5AMIBC6	2.213	0.043	0.19	4.4	2.5	5	850	0.62	175		
5MIBC2	2.216	0.041	0.07	4.4	2.5	5	840	0.61	170		
5AHTEB2	1.713	0.034	0.06	2.0	1.0	5	840	0.61	85	895	9.50
5HTEB9	1.719	0.032	0.06	2.0	1.0	5	840	0.61	85	895	9.50
5HTEB7	1.884	0.036	0.06	3.2	1.7	5	840	0.61	130	880	14.77
5HTEB8	1.898	0.037	0.06	3.2	1.7	5	840	0.61	125	880	14.20
5AHTEB3	1.884	0.036	0.06	3.2	1.7	5	880	0.64	130	880	14.77
5HTEB3	2.051	0.037	0.06	4.4	2.5	5	830	0.60	162	825	19.64
5HTEB4	2.078	0.040	0.06	4.4	2.5	5	830	0.60	170	825	20.61
5HTEB6	2.089	0.039	0.06	4.4	2.5	5	840	0.61	166	825	20.12
10DIBK6	1.238	0.034	3.46	2.0	1.0	10	940	0.68	107	895	11.96
10DIBK7	1.255	0.035	3.56	2.0	1.0	10	940	0.68	107	895	11.96
10DIBK8	1.538	0.040	6.24	3.2	1.7	10	940	0.68	153	895	17.09
10DIBK9	1.522	0.045	1.10	3.2	1.7	10	950	0.69	150	895	16.76
10DIBK2	1.747	0.047	1.35	4.4	2.5	10	900	0.65	190	825	23.03
10DIBK3	1.732	0.049	1.30	4.4	2.5	10	900	0.65	193	825	23.39
10DIBK4	1.780	0.048	1.63	4.4	2.5	10	890	0.65	194	825	23.52
10DIBK5	1.759	0.049	1.50	4.4	2.5	10	890	0.65	204	835	24.43
10BMIBC2	1.272	0.035	13.51	3.2	1.7	10	930	0.68	135	885	15.25
10BMIBC3	1.151	0.035	13.96	3.2	1.7	10	930	0.68	135	885	15.25
10ZMIBC6	1.145	0.040	3.80	3.2	1.7	10	930	0.68	127	880	14.43

File ID	dbavg m	s mm	% Disc	R	Jg cm/s	FC ul/l	Ql ml/min	Jl cm/s	delH	Lc mm	% E
10ZMIBC7	1.310	0.044	3.19	3.2	1.7	10	920	0.67	127	880	14.43
10ZMIBC8	1.226	0.045	3.98	3.2	1.7	10	920	0.67	127	880	14.43
10AMIBC2	1.271	0.040	12.02	4.4	2.5	10	930	0.68	195		
10MIBC8	1.236	0.044	13.27	4.4	2.5	10	930	0.68	190	825	23.03
10MIBC9	1.279	0.040	12.27	4.4	2.5	10	930	0.68	200	880	22.73
10ZMIBC9	1.281	0.048	6.42	4.4	2.5	10	960	0.70	171	860	19.88
10BMIBC4	0.989	0.025	16.33	2.0	1.0	10	930	0.68	82	895	9.16
10BMIBC5	0.996	0.035	18.14	2.0	1.0	10	920	0.67	80	895	8.94
10BMIBC6	1.036	0.027	14.50	2.0	1.0	10	920	0.67	80	895	8.94
10BMIBC7	0.951	0.033	15.50	2.0	1.0	10	920	0.67	80	895	8.94
10BMIBC8	0.862	0.032	16.16	2.0	1.0	10	920	0.67	80	895	8.94
10AHTEB9	1.167	0.038	12.66	2.0	1.0	10	760	0.55	91	825	11.03
10BHTEB2	1.162	0.035	10.30	2.0	1.0	10	760	0.55	110	825	13.33
10BHTEB3	1.221	0.037	9.09	2.0	1.0	10	760	0.55	110	825	13.33
10HTEB4	1.479	0.044	7.42	3.2	1.7	10	810	0.59	146	825	17.70
10AHTEB2	1.482	0.046	6.84	3.2	1.7	10	800	0.58	147	825	17.82
10AHTEB3	1.473	0.045	6.07	3.2	1.7	10	810	0.59	147	825	17.82
10AHTEB4	1.737	0.047	3.01	4.4	2.5	10	790	0.57	226	825	27.39
10AHTEB5	1.710	0.046	2.64	4.4	2.5	10	760	0.55	197	825	23.88
15ADIBK3	1.150	0.042	2.49	3.2	1.7	15	1000	0.73	146	845	17.28
15ADIBK4	1.136	0.041	1.92	3.2	1.7	15	1000	0.73	145	845	17.16
15ADIBK5	1.139	0.043	1.98	3.2	1.7	15	1000	0.73	146	845	17.28
15ADIBK8	1.265	0.047	2.69	4.4	2.5	15	860	0.63	200	825	24.24
15ADIBK9	1.251	0.047	2.23	4.4	2.5	15	860	0.63	205	820	25.00
15AMIBC4	0.983	0.042	13.08	3.2	1.7	15	930	0.68	135	880	15.34
15AMIBC5	0.986	0.041	9.18	3.2	1.7	15	930	0.68	135	880	15.34
15AMIBC6	0.976	0.043	14.87	3.2	1.7	15	930	0.68	135	880	15.34
15YMIBC4	1.102	0.048	8.28	3.2	1.7	15	920	0.67	157	885	17.74
15YMIBC5	1.093	0.048	9.15	3.2	1.7	15	920	0.67	157	885	17.74
15BMIBC2	1.100	0.048	12.92	4.4	2.5	15	960	0.70	186	840	22.14
15DMIBC4	1.077	0.048	16.19	4.4	2.5	15	960	0.70	186	840	22.14
15YMIBC6	1.098	0.053	10.04	4.4	2.5	15	920	0.67	190	870	21.84
15YMIBC7	1.171	0.053	10.23	4.4	2.5	15	920	0.67	190	870	21.84
15AHTEB7	1.051	0.043	7.71	3.2	1.7	15	870	0.63	140	860	16.28
15AHTEB8	1.040	0.042	10.12	3.2	1.7	15	860	0.63	135	860	15.70
15BHTEB6	1.042	0.043	5.68	3.2	1.7	15	870	0.63	150	790	18.99
15BHTEB7	1.045	0.044	6.14	3.2	1.7	15	880	0.64	150	790	18.99
15BHTEB3	1.159	0.047	3.14	4.4	2.5	15	880	0.64	195	740	26.35
15BHTEB4	1.159	0.041	4.47	4.4	2.5	15	840	0.61	175	740	23.65
25DIBK3	1.089	0.041	2.90	3.2	1.7	25	940	0.68	150	845	17.75
25DIBK4	1.081	0.042	3.02	3.2	1.7	25	930	0.68	152	845	17.99
25DIBK5	1.083	0.042	3.27	3.2	1.7	25	930	0.68	152	845	17.99
25DIBK6	1.250	0.047	2.57	4.4	2.5	25	840	0.61	209	825	25.33
25DIBK7	1.220	0.048	2.68	4.4	2.5	25	840	0.61	195	805	24.22
25DIBK8	1.237	0.048	3.30	4.4	2.5	25	820	0.60	210	825	25.45

File ID	dbavg m	s mm	% Disc	R	Jg cm/s	FC ul/l	Ql ml/min	Jl cm/s	delH	Lc mm	% E
25ZHTEB2	0.815	0.036	10.31	2.0	1.0	25	960	0.70	100	865	11.56
25ZHTEB3	0.857	0.038	12.15	2.0	1.0	25	960	0.70	99	865	11.45
25ZHTEB4	0.869	0.039	11.03	2.0	1.0	25	930	0.68	102	865	11.79
25ZHTEB5	0.819	0.038	13.39	2.0	1.0	25	930	0.68	102	865	11.79
25YHTEB2	0.856	0.039	9.98	2.0	1.0	25	950	0.69	105	865	12.14
25XHTEB9	1.114	0.040	3.75	3.2	1.7	25	800	0.58	170	815	20.86
25XHTEB1	1.089	0.039	2.94	3.2	1.7	25	770	0.56	170	815	20.86
25XHTEB2	1.005	0.045	13.37	3.2	1.7	25	770	0.56	170	825	20.61

APPENDIX B2

IDENTIFICATION OF CONDITIONING TEST RUNS AND FIGURES

The flotation runs listed below can be found in Appendix C3.

Table B2 :

Figure No.	Flotation test identification
3.11	KK f1, KK f2, KK f7, KK f8
3.12	KK f3, KK f4, KK f8, KK f9
3.13	DC f1, DC f5
3.14	KK f4, KK f7, KK f16
3.15	KK f1, KK f2, KK f7, KK f10
3.16	KK f2. KK f10, KK f11, KK f12, KK f13
3.17	KK f10, KK f12, KK f14, KKf15
3.18	DC f2, DC f3, DC f6, DC f7
3.19	KK f5, KK f6, KK f17, KK f18
3.20	GH f1, GH f2, GH f3, GH f4
3.21	DC f1, DC f4, DC f10
3.22	ZAC f1, ZAC f2

APPENDIX C

C1 - FLOAT/SINK DATA

C2 - RELEASE FLOTATION DATA

C3 - BATCH FLOTATION DATA

APPENDIX C1

FLOAT/SINK DATA

Table C1 : Washability data for the Durnacol thickener underflow sample

Relative Density	Cumulative % Yield	Cumulative % Ash	Calculated % Feed Ash
1.30	21.10	3.07	27.81
1.33	29.46	3.64	28.58
1.40	44.12	5.10	28.63
1.45	53.19	6.67	28.46
1.50	59.98	8.16	27.21
1.55	63.53	9.39	28.65
1.60	68.07	11.98	28.59
1.70	77.76	16.84	28.78

Table C2 : Washability data for the Kleinkopje thickener underflow composite Laboratory sample

Relative Density	Cumulative % Yield	Cumulative % Ash	Calculated % Feed Ash
1.30	7.03	2.40	22.13
1.35	17.42	3.50	22.95
1.40	28.80	4.05	22.85
1.45	42.57	5.70	23.23
1.50	59.52	6.40	22.92
1.55	65.93	7.65	23.01
1.60	73.22	9.45	23.35
1.65	75.34	9.20	23.45
1.70	78.82	10.30	23.29
1.75	80.82	10.95	23.44
1.80	82.78	12.15	23.64

Table C3 : Washability data for the 95 % passing 45 μm milled Greenside thickener underflow sample

Relative Density	Cumulative % Yield	Cumulative % Ash
1.35	17.46	3.15
1.40	31.44	3.96
1.45	51.60	5.59
1.50	67.89	6.98
1.55	77.35	7.58
1.60	82.80	8.13
1.65	84.72	8.75
1.70	86.42	9.38
S1.70	100.00	19.57

APPENDIX C2

RELEASE FLOTATION DATA

Table C4 : Release Flotation Data for Durnacol Thickener Underflow Sample

C - concentrate; T - tails

Sample ID	Mass (g)	% ash	Cumulative % Yield	Cumulative % ash
C1	6.17	5.63	2.21	5.63
C2	7.48	5.66	4.89	5.64
C3	8.25	5.90	7.85	5.74
C4	5.83	5.96	9.94	5.78
C5	15.12	7.27	15.36	6.31
C6	21.21	7.50	22.97	6.70
C7	18.05	7.67	29.44	6.91
C8	9.26	7.92	32.76	7.02
C9	2.50	7.69	33.65	7.03
C10	7.52	8.58	36.35	7.15
C11	17.44	9.74	42.60	7.53
C12	8.33	9.83	45.59	7.68
C13	12.92	12.51	50.22	8.13
C14	4.45	11.76	51.81	8.24
C15	13.91	12.22	56.80	8.59
C16	9.91	12.06	60.35	8.79
C17	11.58	13.36	64.51	9.09
C18	8.16	15.34	67.43	9.36
T	90.85	66.50		
Total	278.94			

Calculated % Feed ash	27.97	Collector	n-dodecane
		Total Dosage	107 ul = 288 g/t
Pulp Density % m/v	9.30	Frother	MIBC
		Total Dosage	54 ul

Table C5 : Repeat Release Flotation Data for Durnacol Thickener Underflow Sample.

C - concentrate; T - tails

Run ID	DCRF2			
Sample ID	Mass (g)	% ash	Cumulative % Yield	Cumulative % ash
C1	8.90	5.91	3.38	5.91
C2	7.34	6.52	6.18	6.19
C3	18.80	6.71	13.32	6.47
C4	21.33	7.18	21.44	6.74
C5	13.27	7.50	26.48	6.88
C6	6.06	7.19	28.79	6.91
C7	1.38	7.33	29.31	6.91
C8	8.37	8.64	32.49	7.08
C9	2.89	8.45	33.59	7.13
C10	4.40	8.36	35.27	7.19
C11	14.08	10.67	40.62	7.65
C12	10.83	11.16	44.74	7.97
C13	10.92	11.59	48.89	8.28
C14	9.51	11.89	52.51	8.53
C15	4.31	12.26	54.14	8.64
C16	4.55	13.96	55.87	8.80
C17	4.65	13.07	57.64	8.93
C18	13.79	13.43	62.89	9.31
T	97.60	58.54		
Total	262.98			

Calculated % Feed ash	27.58	Collector	n-dodecane
		Total Dosage	67 ul = 191 g/t
Pulp Density % m/v	8.77	Frother	MIBC
		Total Dosage	62 ul

Table C6 : Release Flotation Data for Laboratory Kleinkopje Thickener Underflow Sample.

C - concentrate; T - tails

Sample ID	Mass (g)	% ash	Cumulative % Yield	Cumulative % ash
C1	4.26	4.35	3.06	4.35
C2	2.44	4.79	4.82	4.51
C3	1.08	4.70	5.59	4.54
C4	1.43	7.37	6.62	4.98
C5	0.89	4.66	7.26	4.95
C6	1.69	5.43	8.48	5.02
C7	0.79	5.26	9.05	5.03
C8	2.04	5.09	10.51	5.04
C9	8.27	8.44	16.46	6.27
C10	7.89	9.07	22.13	6.99
C11	8.27	8.17	28.08	7.24
C12	2.96	7.36	30.21	7.25
C13	1.70	7.21	31.43	7.24
C14	1.77	7.03	32.70	7.24
C15	1.70	7.35	33.93	7.24
C16	0.89	7.65	34.57	7.25
C17	1.44	7.52	35.60	7.26
C18	4.46	7.81	38.81	7.30
C19	6.22	9.12	43.28	7.49
C20	7.00	9.67	48.32	7.72
C21	3.27	9.86	50.67	7.82
C22	8.14	10.06	56.53	8.05
C23	3.21	10.73	58.83	8.15
C24	10.21	12.06	66.18	8.59
T	47.01	39.75		
Total	138.97			

Calculated % Feed ash	19.13	Collector Total Dosage	n-dodecane 100 ul = 540 g/t
Pulp Density % m/v	4.63	Frother Total Dosage	MIBC 66 ul

C3 - Batch flotation data

Samples tested :

a. composite Kleinkopje (KK) thickener underflow
b. Durnacol (DC) thickener underflow
c. Goedehoop (GH) thickener underflow
d. Zululand Anthracite Colliery (ZAC) thickener underflow
e. Greenside thickener (GRN) underflow
f. 95 % passing 45 μm milled Greenside (UFGRN) thickener underflow

Standard conditions (unless otherwise stated) :

conditioning cell : 3 l modified Leeds cell
impeller speed : 1200 rpm
method : mode 1.
collector : ShellsolA

flotation cell : 3l modified Leeds cell
impeller speed : 1200 rpm
air rate (@ 1 atm): 4 l/min
method : see Appendix G1
frother : HTEB
frother dosage : 12 μl/l

The flotation runs can be identified from the acronyms listed above and a corresponding flotation run number, e.g. KK f1, DC f3 etc.

Note : Many of the flotation batch tests presented were used exclusively for the comparative conditioning tests described in section 3.4. No ash data was collected for these tests.

Batch flotation data for Durnacol thickener underflow sample

C - concentrate; T - tails

Run ID : DC f1

Conditioning : mode 1.

Sample ID	Time (s)	Mass (g)	% ash	Cumulative % Yield	Cumulative % ash
C1	15	63.09		31.59	
C2	30	37.36		50.30	
C3	60	23.83		62.23	
C4	120	17.35		70.92	
C5	210	6.79		74.32	
C6	300	1.64		75.14	
C7	420	1.44		75.86	
C8	540				
T		48.20			
Total		199.70		75.86	

Calculated % Feed ash	0.00
Pulp Densit % m/v	6.66
Collector dosage g/t	1037

Run ID : DC f2

Conditioning : mode 1.

Sample ID	Time (s)	Mass (g)	% ash	Cumulative % Yield	Cumulative % ash
C1	15	63.55	13.54	22.28	13.54
C2	30	62.29	16.23	44.11	14.87
C3	60	57.10	15.70	64.13	15.13
C4	120	28.35	18.97	74.07	15.65
C5	210	11.94	26.12	78.25	16.21
C6	300	4.06	27.68	79.68	16.41
C7	420	3.72	21.52	80.98	16.49
C8	540	1.74	19.04	81.59	16.51
T		52.51	68.97		
Total		285.26		81.59	16.51

Calculated % Feed ash	26.17
Pulp Densit % m/v	9.51
Collector dosage g/t	1625

Batch flotation data for Durnacol thickener underflow sample

C - concentrate; T - tails

Run ID : DC f3

Conditioning : mode 1.

Sample ID	Time (s)	Mass (g)	% ash	Cumulative % Yield	Cumulative % ash
C1	15	53.79	15.13	18.38	15.13
C2	30	61.48	17.20	39.40	16.23
C3	60	60.95	16.90	60.23	16.46
C4	120	28.35	20.02	69.92	16.96
C5	210	8.48	28.69	72.82	17.42
C6	300	4.84	30.80	74.47	17.72
C7	420	9.13	21.83	77.59	17.89
C8	540	1.92	19.54	78.25	17.90
T		63.65	67.90		
Total		292.59		78.25	

Calculated % Feed ash	28.78
Pulp Densit % m/v	9.75
Collector dosage g/t	1410

Run ID : DC f4

Conditioning : mode 1.

Sample ID	Time (s)	Mass (g)	% ash	Cumulative % Yield	Cumulative % ash
C1	15	69.60		24.33	
C2	30	69.82		48.74	
C3	60	35.29		61.08	
C4	120	29.35		71.34	
C5	210	10.92		75.16	
C6	300	4.13		76.61	
C7	420	2.58		77.51	
C8	540	0.8		77.79	
T		63.53			
Total		286.02		77.79	

Calculated % Feed ash	0.00
Pulp Densit % m/v	9.53
Collector dosage g/t	878

Batch flotation data for Durnacol thickener underflow sample

C - concentrate; T - tails

Run ID : DC f5

Conditioning : mode 2.

Sample ID	Time (s)	Mass (g)	% ash	Cumulative % Yield	Cumulative % ash
C1	15	56.60		27.90	
C2	30	38.93		47.09	
C3	60	22.20		58.03	
C4	120	17.89		66.85	
C5	210	11.87		72.70	
C6	300	3.16		74.26	
C7	420	1.11		74.81	
C8	540	0.71		75.16	
T		50.40			
Total		202.87		75.16	

Calculated % Feed ash	0.00
Pulp Densit % m/v	6.76
Collector dosage g/t	1139

Run ID : DC f6

Conditioning : mode 3.

Sample ID	Time (s)	Mass (g)	% ash	Cumulative % Yield	Cumulative % ash
C1	15	44.09	11.38	14.61	11.38
C2	30	54.80	12.00	32.77	11.72
C3	60	52.73	14.18	50.24	12.58
C4	120	41.26	33.60	63.91	17.07
C5	210	18.46	24.25	70.02	17.70
C6	300	6.08	33.70	72.04	18.15
C7	420	3.94	40.91	73.34	18.55
C8	540	1.99	50.06	74.00	18.83
T		78.46	74.10		
Total		301.81		74.00	

Calculated % Feed ash	33.20				
Pulp Densit % m/v	10.06	Conditioning cell	Denver	Impeller rpm	1400
Collector dosage g/t	1480	Slurry feedrate QF l/min	1.0		

C - concentrate; T - tails

Run ID : DC f7

Conditioning : mode 3.

Sample ID	Time (s)	Mass (g)	% ash	Cumulative % Yield	Cumulative % ash
C1	15	42.93	10.78	14.21	10.78
C2	30	53.26	12.15	31.85	11.54
C3	60	53.85	13.59	49.68	12.27
C4	120	43.89	17.17	64.21	13.38
C5	210	19.42	24.61	70.64	14.40
C6	300	5.84	33.20	72.57	14.91
C7	420	3.45	41.82	73.72	15.32
C8	540	1.55	48.69	74.23	15.55
T		77.83	71.21		
Total		302.02		74.23	15.55

Calculated % Feed ash	29.90				
Pulp Densit % m/v	10.07	Conditioning cell	Denver	Impeller rpm	1400
Collector dosage g/t	1518	Slurry feedrate QF l/min	1.0		

Run ID : DC f8

Conditioning : mode 3.

Sample ID	Time (s)	Mass (g)	% ash	Cumulative % Yield	Cumulative % ash
C1	15	45.42	10.33	18.30	10.33
C2	30	52.47	11.49	39.43	10.95
C3	60	51.30	14.50	60.10	12.17
C4	120	30.71	18.77	72.47	13.30
C5	210	10.80	27.86	76.82	14.12
C6	300	4.13	41.09	78.48	14.69
C7	420	2.79	50.85	79.61	15.20
C8	540	1.42	59.08	80.18	15.52
T		49.21	80.22		
Total		248.25		80.18	15.52

Calculated % Feed ash	28.34				
Pulp Densit % m/v	8.28	Conditioning cell	Denver	Impeller rpm	1400
Collector dosage g/t	1343	Slurry feedrate QF l/min	0.5		

Batch flotation data for Durnacol thickener underflow sample

C - concentrate; T - tails

Run ID : DC f9

Conditioning : mode 3.

Sample ID	Time (s)	Mass (g)	% ash	Cumulative % Yield	Cumulative % ash
C1	15	38.23	10.58	14.90	10.58
C2	30	55.02	12.74	36.35	11.85
C3	60	54.54	14.69	57.62	12.90
C4	120	32.89	19.52	70.44	14.11
C5	210	12.30	26.25	75.23	14.88
C6	300	4.01	36.19	76.80	15.31
C7	420	2.52	45.91	77.78	15.70
C8	540	2.09	57.51	78.59	16.13
T		54.91	81.18		
Total		256.51		78.59	16.13

Calculated % Feed ash	30.06				
Pulp Densit % m/v	8.55	Conditioning cell	Denver	Impeller rpm	1400
Collector dosage g/t	1387	Slurry feedrate QF l/min	0.5		

Run ID : DC f10

Conditioning : mode 5.

Sample ID	Time (s)	Mass (g)	% ash	Cumulative % Yield	Cumulative % ash
C1	15	27.59		10.01	
C2	30	48.55		27.63	
C3	60	51.24		46.22	
C4	120	43.08		61.86	
C5	210	23.68		70.45	
C6	300	8.02		73.36	
C7	420	4.71		75.07	
C8	540	2.00		75.80	
T		66.70			
Total		275.57		75.80	

Calculated % Feed ash	0.00
Pulp Densit % m/v	9.19
Collector dosage g/t	872

Batch flotation data for Kleinkopje thickener underflow sample

C - concentrate; T - tails

Run ID : KK f1

Conditioning : mode 1.

Sample ID	Time (s)	Mass (g)	% ash	Cumulativ % Yield	Cumulativ % ash
C1	15	21.95		10.32	
C2	30	54.19		35.78	
C3	60	37.88		53.58	
C4	120	28.35		66.91	
C5	210	13.48		73.24	
C6	300	2.28		74.31	
C7	420				
C8	540				
T		54.66			
Total		212.79		74.31	

Calculated % Feed ash	0.00
Pulp Densit % m/v	7.09
Collector dosage g/t	1559

Run ID : KK f2

Conditioning : mode 1.

Sample ID	Time (s)	Mass (g)	% ash	Cumulativ % Yield	Cumulativ % ash
C1	15	32.46		20.97	
C2	30	26.72		38.24	
C3	60	22.65		52.87	
C4	120	23.43		68.01	
C5	210	12.74		76.24	
C6	300	2.93		78.14	
C7	420				
C8	540				
T		33.84			
Total		154.77		78.14	

Calculated % Feed ash	0.00
Pulp Densit % m/v	5.16
Collector dosage g/t	1971

C - concentrate; T - tails

Run ID : KK f3

Conditioning : mode 1.

Sample ID	Time (s)	Mass (g)	% ash	Cumulativ % Yield	Cumulativ % ash
C1	15	43.27		23.43	
C2	30	44.07		47.29	
C3	60	34.36		65.90	
C4	120	26.93		80.48	
C5	210	8.34		85.00	
C6	300	0.68		85.36	
C7	420				
C8	540				
T		27.03			
Total		184.68		85.36	

Calculated % Feed ash	0.00
Pulp Densit % m/v	6.16
Collector dosage g/t	3330

Run ID : KK f4

Conditioning : mode 1.

Sample ID	Time (s)	Mass (g)	% ash	Cumulativ % Yield	Cumulativ % ash
C1	15	32.77		16.58	
C2	30	32.94		33.25	
C3	60	25.94		46.37	
C4	120	24.26		58.65	
C5	210	17.70		67.61	
C6	300	6.38		70.83	
C7	420	2.01		71.85	
C8	540				
T		55.63			
Total		197.63		71.85	

Calculated % Feed ash	0.00
Pulp Densit % m/v	6.59
Collector dosage g/t	1558

C - concentrate; T - tails

Run ID : KK f5

Conditioning : mode 1.

Sample ID	Time (s)	Mass (g)	% ash	Cumulativ % Yield	Cumulativ % ash
C1	15	29.40	10.23	12.89	10.23
C2	30	38.57	10.45	29.79	10.35
C3	60	33.61	10.14	44.53	10.28
C4	120	33.82	10.26	59.35	10.28
C5	210	30.16	12.16	72.57	10.62
C6	300	9.24	13.45	76.62	10.77
C7	420	4.65	14.38	78.66	10.86
C8	540	2.13	14.65	79.59	10.91
T		46.55	52.06		
Total		228.13		79.59	10.91

Calculated % Feed ash	19.31
Pulp Densit % m/v	7.60
Collector dosage g/t	1520

Run ID : KK f6

Conditioning : mode 1.

Sample ID	Time (s)	Mass (g)	% ash	Cumulativ % Yield	Cumulativ % ash
C1	15	40.40	11.08	15.44	11.08
C2	30	48.63	11.44	34.02	11.28
C3	60	43.79	11.37	50.76	11.31
C4	120	35.92	11.55	64.49	11.36
C5	210	26.20	13.42	74.50	11.64
C6	300	8.28	14.58	77.66	11.76
C7	420	3.60	15.42	79.04	11.82
C8	540	1.24	15.00	79.51	11.84
T		53.61	52.04		
Total		261.67		79.51	11.84

Calculated % Feed ash	20.08
Pulp Densit % m/v	8.72
Collector dosage g/t	1382

C - concentrate; T - tails

Run ID : KK f7

Conditioning : mode 2.

Sample ID	Time (s)	Mass (g)	% ash	Cumulativ % Yield	Cumulativ % ash
C1	15	2.13		1.06	
C2	30	4.49		3.29	
C3	60	6.23		6.39	
C4	120	12.30		12.52	
C5	210	21.83		23.38	
C6	300	26.27		36.45	
C7	420	25.16		48.97	
C8	540	13.13		55.51	
T		89.40			
Total		200.94		55.51	

Calculated % Feed ash	0.00
Pulp Densit % m/v	6.70
Collector dosage g/t	1314

Run ID : KK f8

Conditioning : mode 2.

Sample ID	Time (s)	Mass (g)	% ash	Cumulativ % Yield	Cumulativ % ash
C1	15	3.34		1.79	
C2	30	4.77		4.34	
C3	60	7.72		8.48	
C4	120	13.84		15.89	
C5	210	21.44		27.37	
C6	300	21.38		38.82	
C7	420	19.13		49.06	
C8	540	11.42		55.18	
T		83.70			
Total		186.74		55.18	

Calculated % Feed ash	0.00
Pulp Densit % m/v	6.22
Collector dosage g/t	1602

C - concentrate; T - tails

Run ID : KK f9

Conditioning : mode 2.

Sample ID	Time (s)	Mass (g)	% ash	Cumulativ % Yield	Cumulativ % ash
C1	15	7.10		3.93	
C2	30	11.44		10.25	
C3	60	15.51		18.83	
C4	120	33.30		37.25	
C5	210	45.65		62.50	
C6	300	19.81		73.46	
C7	420	10.31		79.16	
C8	540	4.49		81.64	
T		33.19			
Total		180.80		81.64	

Calculated % Feed ash	0.00
Pulp Densit % m/v	6.03
Collector dosage g/t	4412

Run ID : KK f10

Conditioning : mode 3.

Sample ID	Time (s)	Mass (g)	% ash	Cumulativ % Yield	Cumulativ % ash
C1	15	2.28		1.43	
C2	30	1.54		2.40	
C3	60	3.40		4.54	
C4	120	6.25		8.46	
C5	210	6.32		12.44	
C6	300	7.52		17.16	
C7	420	6.96		21.54	
C8	540	5.25		24.84	
T		119.61			
Total		159.13		24.84	

Calculated % Feed ash	0.00				
Pulp Densit % m/v	5.30	Conditioning cell	Denver	Impeller rpm	1400
Collector dosage g/t	1414	Slurry feedrate QF l/min	0.58		

C - concentrate; T - tails

Run ID : KK f11

Conditioning : mode 3.

Sample ID	Time (s)	Mass (g)	% ash	Cumulativ % Yield	Cumulativ % ash
C1	15	1.24		0.75	
C2	30	2.48		2.25	
C3	60	4.01		4.67	
C4	120	6.51		8.60	
C5	210	8.40		13.67	
C6	300	6.47		17.58	
C7	420	7.76		22.26	
C8	540	6.57		26.23	
T		122.17			
Total		165.61		26.23	

Calculated % Feed ash	0.00				
Pulp Densit % m/v	5.52	Conditioning cell	Denver	Impeller rpm	2700
Collector dosage g/t	1746	Slurry feedrate QF l/min	0.54		

Run ID : KK f14

Conditioning : mode 3.

Sample ID	Time (s)	Mass (g)	% ash	Cumulativ % Yield	Cumulativ % ash
C1	15	6.24		4.25	
C2	30	10.88		11.67	
C3	60	17.02		23.26	
C4	120	33.19		45.88	
C5	210	32.18		67.81	
C6	300	12.48		76.31	
C7	420	5.85		80.30	
C8	540				
T		28.91			
Total		146.75		80.30	

Calculated % Feed ash	0.00				
Pulp Densit % m/v	4.89	Conditioning cell	Denver	Impeller rpm	2700
Collector dosage g/t	4293	Slurry feedrate QF l/min	0.50		

C - concentrate; T - tails

Run ID : KK f13

Conditioning : mode 3.

Sample ID	Time (s)	Mass (g)	% ash	Cumulativ % Yield	Cumulativ % ash
C1	15	16.49		10.61	
C2	30	20.26		23.65	
C3	60	21.65		37.58	
C4	120	29.97		56.86	
C5	210	24.20		72.43	
C6	300	6.82		76.82	
C7	420	1.97		78.09	
C8	540				
T		34.05			
Total		155.41		78.09	

Calculated % Feed ash	0.00				
Pulp Densit % m/v	5.18	Conditioning cell	Denver	Impeller rpm	1400
Collector dosage g/t	5185	Slurry feedrate QF l/min	0.42		

Run ID : KK f14

Conditioning : mode 3.

Sample ID	Time (s)	Mass (g)	% ash	Cumulativ % Yield	Cumulativ % ash
C1	15	1.78		1.07	
C2	30	3.09		2.93	
C3	60	4.78		5.81	
C4	120	9.29		11.40	
C5	210	13.07		19.26	
C6	300	11.70		26.31	
C7	420	12.88		34.06	
C8	540	10.94		40.64	
T		98.63			
Total		166.16		40.64	

Calculated % Feed ash	0.00				
Pulp Densit % m/v	5.54	Conditioning cell	Leeds	Impeller rpm	1200
Collector dosage g/t	1921	Slurry feedrate QF l/min	0.5		

C - concentrate; T - tails

Run ID : KK f15

Conditioning : mode 3.

Sample ID	Time (s)	Mass (g)	% ash	Cumulativ % Yield	Cumulativ % ash
C1	15	14.28		8.54	
C2	30	25.40		23.74	
C3	60	28.04		40.52	
C4	120	33.12		60.34	
C5	210	19.39		71.94	
C6	300	6.18		75.64	
C7	420	2.79		77.31	
C8	540				
T		37.93			
Total		167.13		77.31	

Calculated % Feed ash	0.00				
Pulp Densit % m/v	5.57	Conditioning cell	Leeds	Impeller rpm	2000
Collector dosage g/t	4155	Slurry feedrate QF l/min	0.44		

Run ID : KK f16

Conditioning : mode 4.

Sample ID	Time (s)	Mass (g)	% ash	Cumulativ % Yield	Cumulativ % ash
C1	15	3.29		1.68	
C2	30	3.83		3.63	
C3	60	5.64		6.51	
C4	120	8.93		11.07	
C5	210	11.42		16.90	
C6	300	10.93		22.48	
C7	420	16.29		30.80	
C8	540	14.5		38.20	
C9	660	11.32		43.98	
T		109.75			
Total		195.90		43.98	

Calculated % Feed ash	0.00
Pulp Densit % m/v	6.53
Collector dosage g/t	1586

C - concentrate; T - tails

Run ID : KK f17

Conditioning : mode 5.

Sample ID	Time (s)	Mass (g)	% ash	Cumulativ % Yield	Cumulativ % ash
C1	15	2.70		1.22	
C2	30	4.89		3.43	
C3	60	7.49		6.81	
C4	120	13.82		13.06	
C5	210	18.39		21.37	
C6	300	14.39		27.87	
C7	420	11.52		33.08	
C8	540	4.30		35.02	
T		143.78			
Total		221.28		35.02	

Calculated % Feed ash	0.00
Pulp Densit % m/v	7.38
Collector dosage g/t	1535

Run ID : KK f18

Conditioning : mode 5.

Sample ID	Time (s)	Mass (g)	% ash	Cumulativ % Yield	Cumulativ % ash
C1	15	2.63		1.04	
C2	30	4.86		2.96	
C3	60	7.46		5.92	
C4	120	14.17		11.52	
C5	210	17.04		18.27	
C6	300	13.02		23.42	
C7	420	8.72		26.87	
C8	540	3.73		28.34	
T		181.09			
Total		252.72		43.98	

Calculated % Feed ash	0.00
Pulp Densit % m/v	8.42
Collector dosage g/t	1437

C - concentrate; T - tails

Run ID : GRN f1

Conditioning : mode 1.

Sample ID	Time (s)	Mass (g)	% ash	Cumulativ % Yield	Cumulativ % ash
C1	15	6.08	9.67	2.23	9.67
C2	30	14.51	9.90	7.54	9.83
C3	60	22.11	10.23	15.63	10.04
C4	120	44.54	10.85	31.93	10.45
C5	210	56.22	12.82	52.50	11.38
C6	300	20.40	15.62	59.97	11.91
C7	420	8.46	19.17	63.06	12.26
C8	540	5.96	20.78	65.24	12.55
T		94.97	37.05		
Total		273.25		65.24	12.55

Calculated % Feed ash	21.07
Pulp Densit % m/v	9.11
Collector dosage g/t	541

Run ID : GRN f2

Conditioning : mode 1.

Sample ID	Time (s)	Mass (g)	% ash	Cumulativ % Yield	Cumulativ % ash
C1	15	11.45	9.30	4.31	9.30
C2	30	25.70	9.71	13.98	9.58
C3	60	36.80	9.45	27.82	9.52
C4	120	57.35	9.43	49.39	9.48
C5	210	53.45	12.20	69.50	10.27
C6	300	16.72	13.71	75.79	10.55
C7	420	5.29	15.03	77.78	10.67
C8	540	2.01	17.28	78.54	10.73
T		57.05	53.19		
Total		265.82		78.54	10.73

Calculated % Feed ash	19.84
Pulp Densit % m/v	8.86
Collector dosage g/t	1112

Run ID : UFGRN f1

Sample ID	Time (s)	Mass (g)	% ash	Cumulative % Yield	Cumulative % ash
C1	0	5.18	6.15	6.26	6.15
C2	15	9.11	6.16	17.27	6.16
C3	30	12.87	6.71	32.82	6.42
C4	60	2.10	6.93	35.36	6.46
C5	120				
C6	180				
T		53.49	25.97		
Total		82.75		35.36	6.46

Calculated % Feed ash	19.07	Measured % Feed ash	19.20
Pulp Densit % m/v	2.76	Frother	2-ethylhexanol
Collector dosage g/t	0	Frother dosage	150 ul/l pulp
		Dispersant	Calgon
		Dispersant dosage	55 mg/l pulp

Run ID : UFGRN f2

Sample ID	Time (s)	Mass (g)	% ash	Cumulative % Yield	Cumulative % ash
C1	0	4.83	6.52	5.74	6.52
C2	15	10.19	6.51	17.84	6.51
C3	30	12.97	6.80	33.24	6.65
C4	60	4.49	7.17	38.57	6.72
C5	120				
C6	180				
T		51.72	26.27		
Total		84.20		38.57	6.72

Calculated % Feed ash	18.73	Measured % Feed ash	19.20
Pulp Densit % m/v	2.81	Frother	2-ethylhexanol
Collector dosage g/t	0	Frother dosage	150 ul/l pulp
		Dispersant	Calgon
		Dispersant dosage	55 mg/l pulp

C - concentrate; T - tails

Run ID : GH f1

Conditioning : mode 1.

Sample ID	Time (s)	Mass (g)	% ash	Cumulative % Yield	Cumulative % ash
C1	15	63.33		23.51	
C2	30	85.11		55.10	
C3	60	35.30		68.21	
C4	120	20.86		75.95	
C5	210	6.89		78.51	
C6	300	2.51		79.44	
C7	420	1.95		80.17	
C8	540	1.23		80.62	
T		52.20			
Total		269.38		80.62	

Calculated % Feed ash	0.00
Pulp Densit % m/v	8.98
Collector dosage g/t	944

Run ID : GH f2

Conditioning : mode 1.

Sample ID	Time (s)	Mass (g)	% ash	Cumulative % Yield	Cumulative % ash
C1	15	54.85		20.15	
C2	30	85.95		51.73	
C3	60	36.53		65.15	
C4	120	24.61		74.20	
C5	210	6.31		76.51	
C6	300	2.28		77.35	
C7	420	2.48		78.26	
C8	540	1.74		78.90	
T		57.42			
Total		272.17		78.90	

Calculated % Feed ash	0.00
Pulp Densit % m/v	9.07
Collector dosage g/t	934

C - concentrate; T - tails

Run ID : GH f3

Conditioning : mode 5.

Sample ID	Time (s)	Mass (g)	% ash	Cumulative % Yield	Cumulative % ash
C1	15	5.04		1.79	
C2	30	18.36		8.33	
C3	60	46.23		24.78	
C4	120	34.05		36.89	
C5	210	28.15		46.91	
C6	300	9.56		50.31	
C7	420	5.18		52.16	
C8	540	2.84		53.17	
T		131.61			
Total		281.02		53.17	

Calculated % Feed ash	0.00
Pulp Densit % m/v	9.37
Collector dosage g/t	1002

Run ID : GH f4

Conditioning : mode 5.

Sample ID	Time (s)	Mass (g)	% ash	Cumulative % Yield	Cumulative % ash
C1	15	4.32		1.76	
C2	30	12.87		7.01	
C3	60	25.39		17.35	
C4	120	40.87		34.01	
C5	210	35.34		48.41	
C6	300	7.10		51.30	
C7	420	7.52		54.37	
C8	540	3.75		55.89	
T		108.23			
Total		245.39		55.89	

Calculated % Feed ash	0.00
Pulp Densit % m/v	8.18
Collector dosage g/t	934

Run ID : ZAC f1

Conditioning : mode 1.

Sample ID	Time (s)	Mass (g)	% ash	Cumulative % Yield	Cumulative % ash
C1	15	47.46		19.24	
C2	30	34.74		33.33	
C3	60	34.34		47.25	
C4	120	27.19		58.28	
C5	210	20.81		66.72	
C6	300	8.23		70.05	
C7	420	6.06		72.51	
C8	540	4.23		74.22	
T		63.57			
Total		246.63		74.22	

Calculated % Feed ash	0.00		
Pulp Densit % m/v	8.22		
Collector dosage g/t	1063	Frother dosage ul/l	36

Run ID : ZAC f2

Conditioning : mode 5.

Sample ID	Time (s)	Mass (g)	% ash	Cumulative % Yield	Cumulative % ash
C1	15	25.69		10.29	
C2	30	45.19		28.40	
C3	60	38.85		43.96	
C4	120	32.36		56.92	
C5	210	21.28		65.45	
C6	300	9.77		69.36	
C7	420	5.74		71.66	
C8	540	3.19		72.94	
T		67.55			
Total		249.62		72.94	

Calculated % Feed ash	0.00		
Pulp Densit % m/v	8.32		
Collector dosage g/t	1133	Frother dosage ul/l	36

APPENDIX D

DURNACOL TESTS - COLUMN DATA

Run ID 1

Reagents :

Collector	ShellsolA	Dosage g/t	1239
Frother	HTEB		
Hold tank dosage rate FCT* ul/min			4.32
Water tank concentration FCWW ul/l			5

Column operating parameters :

Slurry feedrate	QF (l/min)	0.76
Tails rate	QT (l/min)	1.18
Sparger type	ST	filter
Sparger water	SW (l/min)	
Net tails rate	(l/min)	1.18
Washwater rate	WW (l/min)	0.40
Air flowrate (@ 1 atm)	AF (l/min)	2.06
Froth height	FH (m)	0.35
Collection height	CH (m)	2.75
Feed point distance from top overflow lip	(m)	1.25

Collector/frother dispersion properties :

Oil dispersion conc	ml/l	9.00
Frother dispersion conc	ul/l	120.0
Oil/water dispersion flow rate Qd	ml/min	11.0
Collector dosage rate Qdc	ul/min	99.0
Frother dispersion flowrate Qd	ml/min	36.0
Frother dosage rate Qdf	ul/min	4.32

Remarks :

Column diameter Dc 54.00 mm

Column XSA 2.290E-03 m2 22.90 cm2

Sample Doornecal t/u

Sample masses and analyses :

Sample	Mass (g/min)	% Ash	Mass (g/min)	% Ash
Feed	70.30	28.66		
Conc	11.93	10.05		
Tails	64.25	34.18		

Calculated parameters :

Calc Feed Ash		30.40		
% Yield		15.66		
% Recovery		20.24		
Feed pulp density % m/v		9.25		
Feed rate t/hr.m2	Fa	2.00		
Conc rate t/hr.m2	Ca	0.31		
Jf	cm/s	0.55		
Jw	cm/s	0.29		
Jg	cm/s	1.50		
Jb	cm/s	0.31		
Frother rate Fcd ul/min		6.32		
Fcd	g/t	82.96		
T	min	5.34	Vc =	6.30

Run ID 2

Sample Doornecal t/u

Reagents :

Collector	ShellsolA	Dosage g/t	1722
Frother	HTEB		
Hold tank dosage rate			3.96
FCT* ul/min			
Water tank concentration			5
FCWW ul/l			

Sample masses and analyses :

Sample	Mass (g/min)	% Ash	Mass (g/min)	% Ash
Feed				
Conc	16.62	8.65		
Tails	84.57	37.22		

Column operating parameters :

Slurry feedrate	QF (l/min)	
Tails rate	QT (l/min)	1.40
Sparger type	ST	filter
Sparger water	SW (l/min)	
Net tails rate	(l/min)	1.40
Washwater rate	WW (l/min)	0.40
Air flowrate	AF (l/min)	3.04
(@ 1 atm)		
Froth height	FH (m)	0.35
Collection height	CH (m)	5.25
Feed point distance	(m)	1.25
from top overflow lip		

Calculated parameters :

Calc Feed Ash		32.53		
% Yield		16.42		
% Recovery		22.24		
Feed pulp density				
% m/v				
Feed rate	Fa	2.65		
t/hr.m2				
Conc rate	Ca	0.44		
t/hr.m2				
Jf	cm/s	0.00		
Jw	cm/s	0.29		
Jg	cm/s	2.21		
Jb	cm/s			
Frother rate Fcd		5.96		
ul/min				
Fcd	g/t	58.90		
T	min	8.59	Vc =	12.02

Collector/frother dispersion properties :

Oil dispersion conc	ml/l	9.00
Frother dispersion conc	ul/l	120.0
Oil/water dispersion	ml/min	22.0
flow rate Qd		
Collector dosage	ul/min	198.0
rate Qdc		
Frother dispersion	ml/min	33.0
flowrate Qd		
Frother dosage	ul/min	3.96
rate Qdf		

Remarks :

Column diameter Dc 54.00 mm

Column XSA 2.290E-03 m2 22.90 cm2

Run ID 3

Sample Doornecal t/u

Reagents :

Collector	ShellsolA	Dosage g/t	1670
Frother	HTEB		
Hold tank dosage rate FCT* ul/min			3.96
Water tank concentration FCWW ul/l			5

Column operating parameters :

Slurry feedrate	QF (l/min)	0.62
Tails rate	QT (l/min)	0.70
Sparger type	ST	filter
Sparger water	SW (l/min)	
Net tails rate	(l/min)	0.70
Washwater rate	WW (l/min)	0.60
Air flowrate (@ 1 atm)	AF (l/min)	3.04
Froth height	FH (m)	0.75
Collection height	CH (m)	2.75
Feed point distance from top overflow lip	(m)	1.25

Collector/frother dispersion properties :

Oil dispersion conc	ml/l	9.00
Frother dispersion conc	ul/l	120.0
Oil/water dispersion flow rate Qd	ml/min	11.5
Collector dosage rate Qdc	ul/min	103.5
Frother dispersion flowrate Qd	ml/min	33.0
Frother dosage rate Qdf	ul/min	3.96

Sample masses and analyses :

Sample	Mass (g/min)	% Ash	Mass (g/min)	% Ash	Avg
Feed			54.55	28.50	
Conc	20.28	11.83	16.37	11.88	11.86
Tails	32.76	34.11	32.76	34.11	34.11

Calculated parameters :

Calc Feed Ash		25.59	26.70		26.15
% Yield		38.23	33.32		35.77
% Recovery		45.30	40.05		42.68
Feed pulp density % m/v		8.80			
Feed rate t/hr.m2	Fa	1.39	1.29		1.34
Conc rate t/hr.m2	Ca	0.53	0.43		0.48
Jf	cm/s	0.45			
Jw	cm/s	0.44			
Jg	cm/s	2.21			
Jb	cm/s	0.06			
Frother rate Fcd ul/min		6.96			
Fcd	g/t	136.27		Mavg =	51.08 g/min
T	min	9.00		Vc =	6.30

Remarks :

Column diameter Dc 54.00 mm

Column XSA 2.290E-03 m2 22.90 cm2

Run ID 4

Sample Doornecal t/u

Reagents :

Collector	ShellsolA	Dosage g/t	1855
Frother	HTEB		
Hold tank dosage rate			28.00
FCT* ul/min			
Water tank concentration			20
FCWW ul/l			

Sample masses and analyses :

Sample	Mass (g/min)	% Ash	Mass (g/min)	% Ash
Feed	100.36	24.38		
Conc	49.01	12.14		
Tails	35.00	49.61		

Column operating parameters :

Slurry feedrate	QF (l/min)	1.24
Tails rate	QT (l/min)	1.32
Sparger type	ST	filter
Sparger water	SW (l/min)	
Net tails rate	(l/min)	1.32
Washwater rate	WW (l/min)	0.36
Air flowrate	AF (l/min)	2.06
(@ 1 atm)		
Froth height	FH (m)	0.75
Collection height	CH (m)	2.75
Feed point distance	(m)	1.25
from top overflow lip		

Calculated parameters :

Calc Feed Ash		27.75
% Yield		58.34
% Recovery		70.94
Feed pulp density		8.09
% m/v		
Feed rate	Fa	2.20
t/hr.m2		
Conc rate	Ca	1.28
t/hr.m2		
Jf	cm/s	0.90
Jw	cm/s	0.26
Jg	cm/s	1.50
Jb	cm/s	0.06
Frother rate Fcd		35.20
ul/min		
Fcd	g/t	419.00
T	min	4.77

Vc = 6.30

Collector/frother dispersion properties :

Oil dispersion conc	ml/l	9.00
Frother dispersion conc	ul/l	700.0
Oil/water dispersion flow rate Qd	ml/min	23.5
Collector dosage rate Qdc	ul/min	211.5
Frother dispersion flowrate Qd	ml/min	40.0
Frother dosage rate Qdf	ul/min	28.00

Remarks :

Column diameter Dc 54.00 mm

Column XSA 2.290E-03 m2 22.90 cm2

Run ID 5

Sample Doornecal t/u

Reagents :

Collector	ShellsolA	Dosage g/t	1773
Frother	HTEB		
Hold tank dosage rate FCT* ul/min			0.00
Water tank concentration FCWW ul/l			20

Column operating parameters :

Slurry feedrate	QF (l/min)	0.60
Tails rate	QT (l/min)	1.70
Sparger type	ST	USBM
Sparger water	SW (l/min)	1.20
Net tails rate	(l/min)	0.50
Washwater rate	WW (l/min)	0.40
Air flowrate (@ 1 atm)	AF (l/min)	3.44
Froth height	FH (m)	0.35
Collection height	CH (m)	2.75
Feed point distance from top overflow lip	(m)	1.25

Collector/frother dispersion properties :

Oil dispersion conc	ml/l	9.00
Frother dispersion conc	ul/l	
Oil/water dispersion flow rate Qd	ml/min	11.0
Collector dosage rate Qdc	ul/min	99.0
Frother dispersion flowrate Qd	ml/min	
Frother dosage rate Qdf	ul/min	0.00

Remarks :

Column diameter Dc 54.00 mm

Column XSA 2.290E-03 m2 22.90 cm2

Sample masses and analyses :

Sample	Mass (g/min)	% Ash	Mass (g/min)	% Ash	Avg
Feed			49.14	29.69	
Conc	34.47	15.15	45.17	16.78	15.97
Tails	9.16	74.50	8.72	74.67	74.59

Calculated parameters :

Calc Feed Ash		27.61	26.15		26.88
% Yield		79.01	83.82		81.41
% Recovery		92.60	94.45		93.53
Feed pulp density % m/v		8.19			
Feed rate t/hr.m2	Fa	1.14	1.41		1.28
Conc rate t/hr.m2	Ca	0.90	1.18		1.04
Jf	cm/s	0.44			
Jw	cm/s	0.29			
Jg	cm/s	2.50			
Jb	cm/s	-0.07			
Frother rate Fcd ul/min		32.00			
Fcd	g/t	656.28		Mavg =	48.76
T	min	12.60		Vc =	6.30

Run ID 6

Sample Doornecal t/u

Reagents :

Collector	ShellsolA	Dosage g/t	1569
Frother	HTEB		
Hold tank dosage rate FCT* ul/min			0.00
Water tank concentration FCWW ul/l			20

Sample masses and analyses :

Sample	Mass (g/min)	% Ash	Mass (g/min)	% Ash
Feed			101.37	31.99
Conc			62.65	13.14
Tails			21.30	72.59

Column operating parameters :

Slurry feedrate	QF (l/min)	1.36
Tails rate	QT (l/min)	2.48
Sparger type	ST	USBM
Sparger water	SW (l/min)	1.20
Net tails rate	(l/min)	1.28
Washwater rate	WW (l/min)	0.60
Air flowrate (@ 1 atm)	AF (l/min)	3.44
Froth height	FH (m)	0.75
Collection height	CH (m)	5.25
Feed point distance from top overflow lip	(m)	1.25

Calculated parameters :

Calc Feed Ash			28.22	
% Yield			74.63	
% Recovery			90.31	
Feed pulp density % m/v		7.45		
Feed rate t/hr.m2	Fa		2.20	
Conc rate t/hr.m2	Ca		1.64	
Jf	cm/s	0.99		
Jw	cm/s	0.44		
Jg	cm/s	2.50		
Jb	cm/s	-0.06		
Frother rate Fcd ul/min		36.00		
Fcd	g/t	428.83		
T	min	9.39	Vc =	12.02

Collector/frother dispersion properties :

Oil dispersion conc Frother dispersion conc ul/l	ml/l	7.86
Oil/water dispersion flow rate Qd	ml/min	23.0
Collector dosage rate Qdc	ul/min	180.7
Frother dispersion flowrate Qd	ml/min	
Frother dosage rate Qdf	ul/min	0.00

Remarks : REPEAT DCB2

Column diameter Dc 54.00 mm

Column XSA 2.290E-03 m2 22.90 cm2

Run ID 7

Sample Doornecal t/u

Reagents :

Collector	ShellsolA	Dosage g/t	2507
Frother	HTEB		
Hold tank dosage rate FCT* ul/min			35.00
Water tank concentration FCWW ul/l			5

Sample masses and analyses :

Sample	Mass (g/min)	% Ash	Mass (g/min)	% Ash	Avg
Feed			33.09	29.12	
Conc	38.29	20.41	35.48	19.51	19.96
Tails	8.92	69.21	7.71	72.29	70.75

Column operating parameters :

Slurry feedrate	QF (l/min)	0.50
Tails rate	QT (l/min)	0.94
Sparger type	ST	filter
Sparger water	SW (l/min)	
Net tails rate	(l/min)	0.94
Washwater rate	WW (l/min)	0.60
Air flowrate (@ 1 atm)	AF (l/min)	2.06
Froth height	FH (m)	0.35
Collection height	CH (m)	5.25
Feed point distance from top overflow lip	(m)	1.25

Calculated parameters :

Calc Feed Ash		29.63	28.93		29.28
% Yield		81.11	82.15		81.63
% Recovery		91.73	93.04		92.39
Feed pulp density % m/v		6.62			
Feed rate t/hr.m2	Fa	1.24	1.13		1.18
Conc rate t/hr.m2	Ca	1.00	0.93		0.97
Jf	cm/s	0.36			
Jw	cm/s	0.44			
Jg	cm/s	1.50			
Jb	cm/s	0.32			
Frother rate Fcd ul/min		38.00			
Fcd	g/t	840.71		Mavg =	45.20 g/min
T	min	12.79		Vc =	12.02 l

Collector/frother dispersion properties :

Oil dispersion conc	ml/l	7.86
Frother dispersion conc	ul/l	700.0
Oil/water dispersion flow rate Qd	ml/min	12.0
Collector dosage rate Qdc	ul/min	94.3
Frother dispersion flowrate Qd	ml/min	50.0
Frother dosage rate Qdf	ul/min	35.00

Remarks :

Column diameter Dc 54.00 mm

Column XSA 2.290E-03 m2 22.90 cm2

Run ID 8

Sample Doornecal t/u

Reagents :

Collector	ShellsolA	Dosage g/t	1290
Frother	HTEB		
Hold tank dosage rate FCT* ul/min			23.10
Water tank concentration FCWW ul/l			20

Sample masses and analyses :

Sample	Mass (g/min)	% Ash	Mass (g/min)	% Ash	Avg
Feed			63.16	29.49	
Conc	53.21	17.27	54.37	17.44	17.36
Tails	12.47	77.34	12.42	77.33	77.34

Column operating parameters :

Slurry feedrate	QF (l/min)	0.72
Tails rate	QT (l/min)	0.80
Sparger type	ST	filter
Sparger water	SW (l/min)	
Net tails rate	(l/min)	0.80
Washwater rate	WW (l/min)	0.40
Air flowrate (@ 1 atm)	AF (l/min)	3.44
Froth height	FH (m)	0.75
Collection height	CH (m)	5.25
Feed point distance from top overflow lip	(m)	1.25

Calculated parameters :

Calc Feed Ash		28.67	28.58		28.63
% Yield		81.01	81.40		81.21
% Recovery		93.97	94.10		94.03
Feed pulp density % m/v		8.77			
Feed rate t/hr.m2	Fa	1.72	1.75		1.74
Conc rate t/hr.m2	Ca	1.39	1.42		1.41
Jf	cm/s	0.52			
Jw	cm/s	0.29			
Jg	cm/s	2.50			
Jb	cm/s	0.06			
Frother rate Fcd ul/min		31.10			
Fcd	g/t	469.54		Mavg =	66.24
T	min	15.03		Vc =	12.02

Collector/frother dispersion properties :

Oil dispersion conc	ml/l	7.71
Frother dispersion conc	ul/l	700.0
Oil/water dispersion flow rate Qd	ml/min	12.0
Collector dosage rate Qdc	ul/min	92.6
Frother dispersion flowrate Qd	ml/min	33.0
Frother dosage rate Qdf	ul/min	23.10

Remarks :

Column diameter Dc 54.00 mm

Column XSA 2.290E-03 m2 22.90 cm2

Run ID 9

Sample Doornecal t/u

Reagents :

Collector	ShellsolA	Dosage g/t	1677
Frother	HTEB		
Hold tank dosage rate FCT* ul/min			22.75
Water tank concentration FCWW ul/l			20

Sample masses and analyses :

Sample	Mass (g/min)	% Ash	Mass (g/min)	% Ash	Avg
Feed			101.19	29.82	
Conc	80.89	16.70	83.44	16.62	16.66
Tails	22.54	74.39	22.63	73.88	74.14

Column operating parameters :

Slurry feedrate	QF (l/min)	1.16
Tails rate	QT (l/min)	1.32
Sparger type	ST	filter
Sparger water	SW (l/min)	
Net tails rate	(l/min)	1.32
Washwater rate	WW (l/min)	0.66
Air flowrate (@ 1 atm)	AF (l/min)	3.44
Froth height	FH (m)	0.35
Collection height	CH (m)	2.75
Feed point distance from top overflow lip	(m)	1.25

Calculated parameters :

Calc Feed Ash		29.27	28.84		29.05
% Yield		78.21	78.67		78.44
% Recovery		92.11	92.17		92.14
Feed pulp density % m/v		8.72			
Feed rate t/hr.m2	Fa	2.71	2.78		2.74
Conc rate t/hr.m2	Ca	2.12	2.19		2.15
Jf	cm/s	0.84			
Jw	cm/s	0.48			
Jg	cm/s	2.50			
Jb	cm/s	0.12			
Frother rate Fcd ul/min		35.95			
Fcd	g/t	343.20		Mavg =	104.75 g/min
T	min	4.77		Vc =	6.30

Collector/frother dispersion properties :

Oil dispersion conc	ml/l	7.71
Frother dispersion conc	ul/l	700.0
Oil/water dispersion flow rate Qd	ml/min	25.0
Collector dosage rate Qdc	ul/min	192.9
Frother dispersion flowrate Qd	ml/min	32.5
Frother dosage rate Qdf	ul/min	22.75

Remarks :

Column diameter Dc 54.00 mm

Column XSA 2.290E-03 m2 22.90 cm2

Run ID 10

Sample Doornecal t/u

Reagents :

Collector	ShellsolA	Dosage g/t	1589
Frother	HTEB		
Hold tank dosage rate			0.00
FCT* ul/min			
Water tank concentration			5
FCWW ul/l			

Sample masses and analyses :

Sample	Mass (g/min)	% Ash	Mass (g/min)	% Ash	Avg
Feed		24.10	106.80	32.44	28.27
Conc	35.75	10.08	26.48	8.65	9.37
Tails	62.62	41.09	65.46	41.98	41.54

Column operating parameters :

Slurry feedrate	QF (l/min)	1.18
Tails rate	QT (l/min)	2.92
Sparger type	ST	USBM
Sparger water	SW (l/min)	1.20
Net tails rate	(l/min)	1.72
Washwater rate	WW (l/min)	0.40
Air flowrate	AF (l/min)	3.44
(@ 1 atm)		
Froth height	FH (m)	0.75
Collection height	CH (m)	2.75
Feed point distance	(m)	1.25
from top overflow lip		

Calculated parameters :

Calc Feed Ash		29.82	32.38		31.10
% Yield		36.34	28.80		32.57
% Recovery		46.57	38.91		42.74
Feed pulp density % m/v		9.05			
Feed rate t/hr.m2	Fa	2.58	2.41		2.49
Conc rate t/hr.m2	Ca	0.94	0.69		0.82
Jf	cm/s	0.86			
Jw	cm/s	0.29			
Jg	cm/s	2.50			
Jb	cm/s	0.39			
Frother rate Fcd ul/min		8.00			
Fcd	g/t	84.07		Mavg =	95.16 g/min
T	min	3.66		Vc =	6.30 l

Collector/frother dispersion properties :

Oil dispersion conc	ml/l	7.71
Frother dispersion conc	ul/l	0.0
Oil/water dispersion flow rate Qd	ml/min	25.0
Collector dosage rate Qdc	ul/min	192.9
Frother dispersion flowrate Qd	ml/min	0.0
Frother dosage rate Qdf	ul/min	0.00

Remarks :

Column diameter Dc 54.00 mm

Column XSA 2.290E-03 m2 22.90 cm2

Run ID 11

Sample Doornecal t/u

Reagents :

Collector	ShellsolA	Dosage g/t	1583
Frother	HTEB		
Hold tank dosage rate FCT* ul/min			0.00
Water tank concentration FCWW ul/l			20

Sample masses and analyses :

Sample	Mass (g/min)	% Ash	Mass (g/min)	% Ash	Avg
Feed			53.60	29.92	
Conc	46.12	18.63	49.25	19.03	18.83
Tails	11.29	78.52	9.78	80.90	79.71

Column operating parameters :

Slurry feedrate	QF (l/min)	0.66
Tails rate	QT (l/min)	2.03
Sparger type	ST	USBM
Sparger water	SW (l/min)	1.20
Net tails rate	(l/min)	0.83
Washwater rate	WW (l/min)	0.66
Air flowrate (@ 1 atm)	AF (l/min)	2.06
Froth height	FH (m)	0.75
Collection height	CH (m)	2.75
Feed point distance from top overflow lip	(m)	1.25

Calculated parameters :

Calc Feed Ash		30.41	29.28		29.84
% Yield		80.33	83.43		81.88
% Recovery		93.93	95.53		94.73
Feed pulp density % m/v		8.12			
Feed rate t/hr.m2	Fa	1.50	1.55		1.53
Conc rate t/hr.m2	Ca	1.21	1.29		1.25
Jf	cm/s	0.48			
Jw	cm/s	0.48			
Jg	cm/s	1.50			
Jb	cm/s	0.12			
Frother rate Fcd ul/min		37.20			
Fcd	g/t	638.96		Mavg =	58.22 g/min
T	min	7.59		Vc =	6.30 l

Collector/frother dispersion properties :

Oil dispersion conc	ml/l	7.71
Frother dispersion conc	ul/l	0.0
Oil/water dispersion flow rate Qd	ml/min	12.5
Collector dosage rate Qdc	ul/min	96.4
Frother dispersion flowrate Qd	ml/min	0.0
Frother dosage rate Qdf	ul/min	0.00

Remarks :

Column diameter Dc 54.00 mm

Column XSA 2.290E-03 m2 22.90 cm2

Run ID 12

Sample Doornecal t/u

Reagents :

Collector	ShellsolA	Dosage g/t	1430
Frother	HTEB		
Hold tank dosage rate FCT* ul/min			0.00
Water tank concentration FCWW ul/l			5

Sample masses and analyses :

Sample	Mass (g/min)	% Ash	Mass (g/min)	% Ash	Avg
Feed			56.96	24.75	
Conc	14.27	10.27	14.50	10.27	10.27
Tails	46.41	34.91	43.69	37.60	36.26

Column operating parameters :

Slurry feedrate	QF (l/min)	0.66
Tails rate	QT (l/min)	2.56
Sparger type	ST	USBM
Sparger water	SW (l/min)	1.20
Net tails rate	(l/min)	1.36
Washwater rate	WW (l/min)	0.64
Air flowrate (@ 1 atm)	AF (l/min)	3.44
Froth height	FH (m)	0.35
Collection height	CH (m)	5.25
Feed point distance from top overflow lip	(m)	1.25

Calculated parameters :

Calc Feed Ash		29.12	30.79		29.95
% Yield		23.52	24.92		24.22
% Recovery		29.77	32.31		31.04
Feed pulp density % m/v		8.63			
Feed rate t/hr.m2	Fa	1.59	1.52		1.56
Conc rate t/hr.m2	Ca	0.37	0.38		0.38
Jf	cm/s	0.48			
Jw	cm/s	0.47			
Jg	cm/s	2.50			
Jb	cm/s	0.51			
Frother rate Fcd ul/min		9.20			
Fcd	g/t	154.79		Mavg =	59.44 g/min
T	min	8.84		Vc =	12.02 l

Collector/frother dispersion properties :

Oil dispersion conc	ml/l	7.71
Frother dispersion conc	ul/l	0.0
Oil/water dispersion flow rate Qd	ml/min	12.0
Collector dosage rate Qdc	ul/min	92.6
Frother dispersion flowrate Qd	ml/min	0.0
Frother dosage rate Qdf	ul/min	0.00

Remarks :

Column diameter Dc 54.00 mm

Column XSA 2.290E-03 m2 22.90 cm2

Run ID 13

Sample Doornecal t/u

Reagents :

Collector	ShellsolA	Dosage g/t	1902
Frother	HTEB		
Hold tank dosage rate			0.00
FCT* ul/min			
Water tank concentration			20
FCWW ul/l			

Sample masses and analyses :

Sample	Mass (g/min)	% Ash	Mass (g/min)	% Ash	Avg
Feed			89.23	32.57	
Conc	65.79	16.45	51.32	14.65	15.55
Tails	25.80	62.38	30.20	60.62	61.50

Column operating parameters :

Slurry feedrate	QF (l/min)	1.20
Tails rate	QT (l/min)	2.50
Sparger type	ST	USBM
Sparger water	SW (l/min)	1.20
Net tails rate	(l/min)	1.30
Washwater rate	WW (l/min)	0.42
Air flowrate (@ 1 atm)	AF (l/min)	2.06
Froth height	FH (m)	0.35
Collection height	CH (m)	5.25
Feed point distance from top overflow lip	(m)	1.25

Calculated parameters :

Calc Feed Ash		29.39	31.68		30.53	
% Yield		71.83	62.95		67.39	
% Recovery		84.99	78.65		81.82	
Feed pulp density % m/v		7.44				
Feed rate t/hr.m2	Fa	2.40	2.14		2.27	
Conc rate t/hr.m2	Ca	1.72	1.34		1.53	
Jf	cm/s	0.87				
Jw	cm/s	0.31				
Jg	cm/s	1.50				
Jb	cm/s	0.07				
Frother rate Fcd ul/min		32.40				
Fcd	g/t	374.33		Mavg =	86.56	g/min
T	min	9.25		Vc =	12.02	l

Collector/frother dispersion properties :

Oil dispersion conc	ml/l	7.71
Frother dispersion conc	ul/l	0.0
Oil/water dispersion flow rate Qd	ml/min	25.0
Collector dosage rate Qdc	ul/min	192.9
Frother dispersion flowrate Qd	ml/min	0.0
Frother dosage rate Qdf	ul/min	0.00

Remarks :

Column diameter Dc 54.00 mm

Column XSA 2.290E-03 m2 22.90 cm2

Run ID 14

Sample Doornecal t/u

Reagents :

Collector	ShellsolA	Dosage g/t	403
Frother	HTEB		
Hold tank dosage rate			0.00
FCT* ul/min			
Water tank concentration			5
FCWW ul/l			

Sample masses and analyses :

Sample	Mass (g/min)	% Ash	Mass (g/min)	% Ash	Avg
Feed			57.38	30.86	
Conc	13.71	8.07	16.27	8.03	8.05
Tails	50.35	37.22	50.05	38.35	37.79

Column operating parameters :

Slurry feedrate	QF (l/min)	0.69
Tails rate	QT (l/min)	2.46
Sparger type	ST	USBM
Sparger water	SW (l/min)	1.20
Net tails rate	(l/min)	1.26
Washwater rate	WW (l/min)	0.45
Air flowrate (@ 1 atm)	AF (l/min)	2.06
Froth height	FH (m)	0.75
Collection height	CH (m)	5.25
Feed point distance from top overflow lip	(m)	1.25

Calculated parameters :

Calc Feed Ash		30.98	30.91		30.95
% Yield		21.40	24.53		22.97
% Recovery		28.51	32.66		30.58
Feed pulp density % m/v		8.32			
Feed rate t/hr.m2	Fa	1.68	1.74		1.71
Conc rate t/hr.m2	Ca	0.36	0.43		0.39
Jf	cm/s	0.50			
Jw	cm/s	0.33			
Jg	cm/s	1.50			
Jb	cm/s	0.41			
Frother rate Fcd ul/min		8.25			
Fcd	g/t	143.78			

Collector/frother dispersion properties :

Oil dispersion conc	ml/l	2.29
Frother dispersion conc	ul/l	
Oil/water dispersion flow rate Qd	ml/min	11.5
Collector dosage rate Qdc	ul/min	26.3
Frother dispersion flowrate Qd	ml/min	
Frother dosage rate Qdf	ul/min	0.00

Remarks :

Column diameter Dc	54.00	mm		
Column XSA	2.290E-03	m2	22.90	cm2

Run ID 15

Sample Doornecal t/u

Reagents :

Collector	ShellsolA	Dosage g/t	387
Frother	HTEB		
Hold tank dosage rate			0.00
FCT* ul/min			
Water tank concentration			5
FCWW ul/l			

Sample masses and analyses :

Sample	Mass (g/min)	% Ash	Mass (g/min)	% Ash	Avg
Feed			104.65	32.91	
Conc	6.98	8.52	5.93	8.38	8.45
Tails	99.99	34.65	106.47	32.44	33.55

Column operating parameters :

Slurry feedrate	QF (l/min)	1.20
Tails rate	QT (l/min)	3.16
Sparger type	ST	USBM
Sparger water	SW (l/min)	1.20
Net tails rate	(l/min)	1.96
Washwater rate	WW (l/min)	0.68
Air flowrate	AF (l/min)	2.06
(@ 1 atm)		
Froth height	FH (m)	0.35
Collection height	CH (m)	2.75
Feed point distance	(m)	1.25
from top overflow lip		

Calculated parameters :

Calc Feed Ash		32.95	31.17		32.06
% Yield		6.52	5.27		5.90
% Recovery		8.90	7.02		7.96
Feed pulp density % m/v		8.72			
Feed rate t/hr.m2	Fa	2.80	2.94		2.87
Conc rate t/hr.m2	Ca	0.18	0.16		0.17
Jf	cm/s	0.87			
Jw	cm/s	0.49			
Jg	cm/s	1.50			
Jb	cm/s	0.55			
Frother rate Fcd ul/min		9.40			
Fcd	g/t	89.82			

Collector/frother dispersion properties :

Oil dispersion conc	ml/l	2.00
Frother dispersion conc	ul/l	
Oil/water dispersion flow rate Qd	ml/min	23.0
Collector dosage rate Qdc	ul/min	46.0
Frother dispersion flowrate Qd	ml/min	
Frother dosage rate Qdf	ul/min	0.00

Remarks :

Column diameter Dc	54.00	mm		
Column XSA	2.290E-03	m2	22.90	cm2

Run ID 16

Sample Doornecal t/u

Reagents :

Collector	ShellsolA	Dosage g/t	414
Frother	HTEB		
Hold tank dosage rate			3.72
FCT* ul/min			
Water tank concentration			5
FCWW ul/l			

Sample masses and analyses :

Sample	Mass (g/min)	% Ash	Mass (g/min)	% Ash	Avg
Feed			107.14	27.73	
Conc	19.25	7.41	19.41	6.52	6.97
Tails	87.46	31.19	88.79	31.73	31.46

Column operating parameters :

Slurry feedrate	QF (l/min)	1.24
Tails rate	QT (l/min)	1.50
Sparger type	ST	filter
Sparger water	SW (l/min)	
Net tails rate	(l/min)	1.50
Washwater rate	WW (l/min)	0.60
Air flowrate	AF (l/min)	2.06
(@ 1 atm)		
Froth height	FH (m)	0.35
Collection height	CH (m)	5.25
Feed point distance	(m)	2.75
from top overflow lip		

Calculated parameters :

Calc Feed Ash		26.90	27.21	27.05
% Yield		18.04	17.94	17.99
% Recovery		22.85	23.04	22.94
Feed pulp density % m/v		8.64		
Feed rate t/hr.m2	Fa	2.80	2.83	2.82
Conc rate t/hr.m2	Ca	0.50	0.51	0.51
Jf	cm/s	0.90		
Jw	cm/s	0.44		
Jg	cm/s	1.50		
Jb	cm/s	0.19		
Frother rate Fcd ul/min		6.72		
Fcd	g/t	62.72		

Collector/frother dispersion properties :

Oil dispersion conc	ml/l	2.14
Frother dispersion conc	ul/l	120.0
Oil/water dispersion flow rate Qd	ml/min	23.5
Collector dosage rate Qdc	ul/min	50.4
Frother dispersion flowrate Qd	ml/min	31.0
Frother dosage rate Qdf	ul/min	3.72

Remarks :

Column diameter Dc 54.00 mm

Column XSA 2.290E-03 m2 22.90 cm2

APPENDIX E

KLEINKOPJE PLANT TRIAL DATA

Table E1 - Kleinkopje feed size fraction data

* denotes corresponding concentrate size property data also available

			% mass / size fraction							
Sample ID	Figures 5.4 - 5.7 Trial no	Figures 5.11 - 5.15 Trial no	+150 um	-150+106 um	-106+75 um	-75+45 um	-45 um	-45+20 um	-20 um	Total
18/04 F21*	1	1	8.00	6.40	15.90	18.70	51.00			100.00
27/04 F11*	2	2	5.34	12.33	11.23	23.43	47.67	38.83	8.84	100.00
27/04 F12	3		7.16	11.95	16.14	29.05	35.70	3.37	32.33	100.00
27/04 F21*	4	3	8.28	14.90	18.38	23.07	35.36	31.64	3.72	99.99
27/04 F22	5		6.49	14.70	16.26	22.39	40.15	37.07	3.08	99.99
28/04 F11*	6	4	3.58	7.25	15.90	18.37	54.90	48.67	6.23	100.00
28/04 F12	7		4.65	10.46	13.47	22.26	49.15	11.07	38.08	99.99
28/04 F13	8		4.55	13.93	18.07	22.86	40.59	36.87	3.72	100.00
28/04 F21*	9	5	6.27	12.45	16.09	18.55	46.64	39.01	7.63	100.00
28/04 F22	10		7.09	13.35	15.32	23.52	40.71	26.72	13.99	99.99
28/04 F31*	11	6	6.39	12.88	15.20	19.51	46.02	21.18	24.84	100.00
28/04 F32	12		6.84	14.79	15.44	25.90	37.03	30.28	6.75	100.00
28/04 F41*	13	7	3.35	13.12	19.84	21.12	42.56	17.37	25.19	99.99
28/04 F42	14		3.73	13.47	15.35	19.92	47.53	39.32	8.21	100.00
03/05 F11*	15	8	5.16	13.53	13.06	29.00	39.25			100.00
04/05 F11*	16	9	6.09	13.73	14.47	16.45	49.27			100.01
07/05 F11*	17	10	5.58	10.24	15.75	22.07	46.35			99.99
07/05 F12*	18	11	4.16	11.75	17.55	23.15	43.38			99.99
08/05 F11*	19	12	9.12	11.13	18.07	22.09	39.58			99.99
08/05 F12*	20	12	7.71	10.59	15.13	30.16	36.41			100.00
08/05 F21*	21	14	5.65	6.47	8.80	20.30	58.78			100.00
08/05 F22*	22	15	5.32	7.10	10.60	19.66	57.32			100.00
08/05 F31*	23	16	11.72	10.66	11.15	21.54	44.93			100.00
08/05 F32*	24	17	12.22	10.93	10.93	18.57	47.34			99.99
10/05 F11*	25	18	11.05	6.62	9.90	15.83	56.60			100.00
10/05 F12*	26	19	11.48	6.10	8.80	15.94	57.68			100.00
15/05 F12	27		4.09	9.37	11.82	24.94	49.79			100.01
15/05 F22	28		6.23	14.90	10.06	29.23	39.58			100.00
17/05 F11*	29	20	4.04	8.36	15.43	26.66	45.51			100.00
18/05 F11*	30	21	4.28	6.54	12.22	32.99	43.96			99.99
19/05 F11*	31	22	0.00	14.29	6.28	26.57	52.86			100.00
21/05 F11*	32	23	5.47	7.90	16.07	24.59	45.97			100.00
22/05 F11*	33	24	12.11	16.96	17.75	18.97	34.21			100.00
23/05 F11*	34	25	9.40	8.98	11.32	26.05	44.25			100.00
23/05 F12*	35	26	9.22	10.18	14.76	25.41	40.44			100.01
24/05 F11*	36	27	7.40	9.34	16.19	20.62	46.46			100.01
24/05 F12*	37	28	7.32	7.21	13.46	25.17	46.84			100.00
Average			6.66	10.94	14.11	22.83	45.45	29.34	14.05	
Sample deviation s			2.75	3.02	3.15	4.14	6.52	12.92	11.91	

Table E2 - Feed Ash/size fraction data

* denotes corresponding concentrate size property data also available

Sample ID	Figures 5.4 - 5.7 Trial no	Figures 5.11 - 5.15 Trial no	% Ash size fraction i +150 um	-150+106 um	-106+75 um	-75+45 um	-45 um	-45+20 um	-20 um	Reconstituted Total
18/04 F21*	1	1	9.3	10.4	13.4	19.3	26.0			20.41
27/04 F11*	2	2	12.6	12.8	14.3	19.5	27.6	27.1	29.6	21.57
27/04 F12	3		14.2	14.1	17.0	22.0	29.6	27.8	29.8	22.41
27/04 F21*	4	3	13.9	14.8	17.6	21.6	27.5	27.2	29.8	21.29
27/04 F22	5		12.1	14.1	17.4	21.4	27.7	27.5	30.1	21.60
28/04 F11*	6	4	9.9	12.5	15.6	19.2	27.2	26.9	29.6	22.20
28/04 F12	7		9.9	11.2	14.0	19.2	28.9	26.5	29.6	22.00
28/04 F13	8		10.8	14.2	17.2	20.9	27.0	26.8	29.5	21.33
28/04 F21*	9	5	9.4	11.2	15.4	20.1	27.5	27.0	29.9	21.00
28/04 F22	10		9.6	12.0	15.4	20.1	27.8	26.4	30.4	20.68
28/04 F31*	11	6	10.6	13.2	15.8	19.4	26.3	23.8	28.5	20.68
28/04 F32	12		10.6	13.2	16.6	20.9	26.8	26.3	29.3	20.59
28/04 F41*	13	7	15.3	15.2	18.0	21.1	27.3	24.8	29.1	22.17
28/04 F42	14		14.6	14.7	16.7	20.0	27.5	27.0	29.7	22.13
03/05 F11*	15	8	11.2	14.2	18.0	24.3	28.9			23.24
04/05 F11*	16	9	11.8	14.9	18.7	21.9	27.5			22.62
07/05 F11*	17	10	10.8	14.3	19.1	24.6	29.0			23.95
07/05 F12*	18	11	9.8	16.3	19.7	25.7	29.6			24.57
08/05 F11*	19	12	11.2	16.6	19.4	28.2	33.6			25.90
08/05 F12*	20	12	10.7	13.9	16.5	27.1	33.1			25.02
08/05 F21*	21	14	8.6	11.8	14.4	22.4	30.3			24.87
08/05 F22*	22	15	8.6	12.7	16.6	21.8	30.1			24.66
08/05 F31*	23	16	10.1	12.8	17.9	25.5	31.4			24.14
08/05 F32*	24	17	9.9	13.1	17.6	23.4	31.4			23.78
10/05 F11*	25	18	14.6	14.7	17.4	21.5	28.8			24.01
10/05 F12*	26	19	14.7	16.0	17.8	21.0	28.7			24.13
15/05 F12	27		16.0	18.6	20.4	24.0	28.3			24.88
15/05 F22	28		20.0	20.9	20.2	25.7	29.8			25.70
17/05 F11*	29	20	18.5	17.8	19.7	24.5	29.4			25.19
18/05 F11*	30	21	16.1	14.6	16.6	21.3	25.0			21.69
19/05 F11*	31	22		16.8	15.0	17.6	24.1			20.76
21/05 F11*	32	23	14.8	18.6	20.3	21.9	27.0			23.34
22/05 F11*	33	24	21.3	19.0	20.8	21.9	26.0			22.54
23/05 F11*	34	25	16.9	18.9	20.6	24.2	28.3			24.44
23/05 F12*	35	26	16.9	19.6	21.9	25.3	28.8			24.86
24/05 F11*	36	27	20.8	20.7	21.7	24.1	27.6			24.78
24/05 F12*	37	28	22.3	21.0	21.7	24.0	27.7			25.08
Average			13.29	15.17	17.74	22.34	28.36	26.55	29.61	
Sample deviation s			3.85	2.90	2.29	2.47	1.98	1.10	0.47	

Table E3 - CV size fraction data

* denotes corresponding concentrate size property data also available

Sample ID	Figures 5.4 - 5.7 Trial no	Figures 5.11 - 5.15 Trial no	CV MJ/kg size fraction i +150 um	-150+106 um	-106+75 um	-75+45 um	-45 um	-45+20 um	-20 um	Reconstituted Total
18/04 F21*	1	1	29.19	29.94	29.55	28.31	25.67			27.34
27/04 F11*	2	2	28.12	27.83	27.13	25.12	21.92	22.14	20.98	24.32
27/04 F12	3		26.30	27.15	25.97	23.96	20.77	21.53	20.69	23.69
27/04 F21*	4	3	27.42	27.00	25.77	24.13	21.90	22.02	20.86	24.34
27/04 F22	5		29.72	27.05	25.80	24.10	21.55	21.67	20.06	24.15
28/04 F11*	6	4	28.61	27.71	26.51	25.06	21.78	21.91	20.75	23.81
28/04 F12	7		28.77	28.27	26.92	25.04	21.07	22.05	20.79	23.85
28/04 F13	8		28.06	26.89	25.61	24.19	21.70	21.81	20.59	23.99
28/04 F21*	9	5	28.74	28.43	26.78	24.76	21.69	21.90	20.64	24.36
28/04 F22	10		29.18	28.17	26.78	24.90	21.83	22.50	20.54	24.67
28/04 F31*	11	6	28.70	27.83	26.66	25.25	22.29	23.42	21.32	24.65
28/04 F32	12		28.68	27.85	26.31	24.54	22.17	22.45	20.93	24.71
28/04 F41*	13	7	26.20	26.73	25.39	24.30	21.78	22.77	21.09	23.82
28/04 F42	14		27.10	26.84	26.01	24.65	21.64	21.83	20.71	23.81
03/05 F11*	15	8	28.87	27.70	26.17	23.41	21.65			23.94
04/05 F11*	16	9	27.76	26.47	24.99	23.49	21.52			23.41
07/05 F11*	17	10	28.90	27.34	25.40	23.05	19.33			22.46
07/05 F12*	18	11	29.44	26.64	25.27	22.73	21.13			23.22
08/05 F11*	19	12	28.34	26.32	25.27	21.78	19.51			22.61
08/05 F12*	20	12	29.13	27.28	26.20	22.16	19.96			23.05
08/05 F21*	21	14	29.94	28.59	27.47	23.89	21.23			23.29
08/05 F22*	22	15	29.61	27.98	26.53	24.41	21.16			23.30
08/05 F31*	23	16	28.99	28.02	26.29	23.16	20.91			23.70
08/05 F32*	24	17	29.49	28.07	26.08	23.85	20.92			23.85
10/05 F11*	25	18	26.83	26.56	24.99	23.46	20.49			22.51
10/05 F12*	26	19	26.27	25.21	24.90	23.61	20.69			22.44
15/05 F12	27		26.05	25.43	25.05	23.38	21.77			23.08
15/05 F22	28		25.05	24.52	24.96	22.60	21.82			22.97
17/05 F11*	29	20	25.75	26.12	24.77	22.87	20.96			22.68
18/05 F11*	30	21	26.66	27.04	26.34	24.42	22.89			24.25
19/05 F11*	31	22		25.48	26.35	25.28	22.70			24.01
21/05 F11*	32	23	26.54	25.72	24.88	24.37	22.37			23.76
22/05 F11*	33	24	24.50	25.55	24.85	24.46	22.94			24.20
23/05 F11*	34	25	26.50	25.92	24.94	23.70	21.68			23.41
23/05 F12*	35	26	26.05	25.77	24.67	23.49	22.15			23.59
24/05 F11*	36	27	24.64	24.85	24.33	23.40	22.00			23.13
24/05 F12*	37	28	24.09	24.76	24.62	23.58	22.08			23.14
Average			27.62	26.89	25.85	24.02	21.61			23.72
Sample deviation s			1.65	1.23	1.02	1.12	1.07			0.88

Table E4 - Kleinkopje concentrate size fractions

* denotes corresponding feed size property data also available

Sample ID	Figures 5.13 - 5.16 Trial no	Figure 5.16 Trial no	% mass / size fraction +150 um	-150+106 um	-106+75 um	-75+45 um	-45 um	Reconstituted Total
18/04 C12		1	0.00	0.00	6.50	27.10	66.40	100.00
18/04 C21*	1	2	0.00	0.00	7.00	12.00	81.01	100.00
27/04 C11*	2	3	0.00	0.00	0.00	27.59	72.41	100.00
27/04 C21*	3	4	0.00	0.00	9.87	14.60	75.53	100.00
28/04 C11*	4	5	0.00	0.00	8.87	10.65	80.48	100.00
28/04 C21*	5	6	0.00	0.00	9.65	11.18	79.17	100.00
28/04 C31*	6	7	0.00	0.00	9.25	16.03	74.72	100.00
28/04 C41*	7	8	0.00	0.00	5.27	13.99	80.74	100.00
03/05 C11*	8	9	0.00	0.00	0.00	23.34	76.66	100.00
03/05 C12		10	0.00	0.00	18.98	21.49	59.53	100.00
04/05 C11*	9	11	0.00	17.57	15.34	17.83	49.26	100.00
04/05 C12		12	5.77	14.04	12.42	22.01	45.76	100.00
07/05 C11*	10	13	0.00	0.00	0.00	26.48	73.52	100.00
07/05 C12*	11	14	0.00	0.00	8.20	29.43	62.37	100.00
08/05 C11*	12	15	0.00	0.00	0.00	19.47	80.53	100.00
08/05 C12*	13	16	0.00	0.00	0.00	0.00	100.00	100.00
08/05 C21*	14	17	0.00	0.00	6.84	16.91	76.24	100.00
08/05 C22*	15	18	0.00	0.00	0.00	28.12	71.88	100.00
08/05 C31*	16	19	0.00	0.00	7.18	17.93	74.89	100.00
08/05 C32*	17	20	0.00	0.00	17.09	21.37	61.55	100.00
10/05 C11*	18	21	0.00	0.00	0.00	20.42	79.58	100.00
10/05 C12*	19	22	0.00	10.72	0.00	29.79	59.48	100.00
17/05 C11*	20	23	0.00	6.13	18.79	17.89	57.19	100.00
17/05 C12		24	0.00	0.00	0.00	18.17	81.83	100.00
18/05 C11*	21	25	0.00	9.08	13.71	22.98	54.23	100.00
18/05 C12		26	0.00	5.74	13.84	20.06	60.36	100.00
19/05 C11*	22	27	0.00	0.00	17.02	11.58	71.40	100.00
19/05 C12		28	0.00	0.00	0.00	12.24	87.76	100.00
21/05 C11*	23	29	0.00	0.00	8.00	20.50	71.50	100.00
21/05 C12		30	0.00	0.00	0.00	29.70	70.30	100.00
22/05 C11*	24	31	0.00	0.00	0.00	30.91	69.09	100.00
22/05 C12		32	0.00	0.00	0.00	21.54	78.46	100.00
23/05 C11*	25	33	0.00	0.00	6.45	18.47	75.07	100.00
23/05 C12*	26	34	0.00	0.00	0.00	48.38	51.62	100.00
24/05 C11*	27	35	0.00	0.00	0.00	18.45	81.55	100.00
24/05 C12*	28	36	0.00	0.00	0.00	10.88	89.12	100.00
Average			0.16	1.76	6.12	20.26	71.70	
Sample deviation s			0.96	4.35	6.46	8.29	11.82	

Table E4 - Kleinkopje concentrate size fractions

* denotes corresponding feed size property data also available

Sample ID	Figures 5.13 - 5.16 Trial no	Figure 5.16 Trial no	% mass / size fraction +150 um	-150+106 um	-106+75 um	-75+45 um	-45 um	Reconstituted Total
18/04 C12		1	0.00	0.00	6.50	27.10	66.40	100.00
18/04 C21*	1	2	0.00	0.00	7.00	12.00	81.01	100.00
27/04 C11*	2	3	0.00	0.00	0.00	27.59	72.41	100.00
27/04 C21*	3	4	0.00	0.00	9.87	14.60	75.53	100.00
28/04 C11*	4	5	0.00	0.00	8.87	10.65	80.48	100.00
28/04 C21*	5	6	0.00	0.00	9.65	11.18	79.17	100.00
28/04 C31*	6	7	0.00	0.00	9.25	16.03	74.72	100.00
28/04 C41*	7	8	0.00	0.00	5.27	13.99	80.74	100.00
03/05 C11*	8	9	0.00	0.00	0.00	23.34	76.66	100.00
03/05 C12		10	0.00	0.00	18.98	21.49	59.53	100.00
04/05 C11*	9	11	0.00	17.57	15.34	17.83	49.26	100.00
04/05 C12		12	5.77	14.04	12.42	22.01	45.76	100.00
07/05 C11*	10	13	0.00	0.00	0.00	26.48	73.52	100.00
07/05 C12*	11	14	0.00	0.00	8.20	29.43	62.37	100.00
08/05 C11*	12	15	0.00	0.00	0.00	19.47	80.53	100.00
08/05 C12*	13	16	0.00	0.00	0.00	0.00	100.00	100.00
08/05 C21*	14	17	0.00	0.00	6.84	16.91	76.24	100.00
08/05 C22*	15	18	0.00	0.00	0.00	28.12	71.88	100.00
08/05 C31*	16	19	0.00	0.00	7.18	17.93	74.89	100.00
08/05 C32*	17	20	0.00	0.00	17.09	21.37	61.55	100.00
10/05 C11*	18	21	0.00	0.00	0.00	20.42	79.58	100.00
10/05 C12*	19	22	0.00	10.72	0.00	29.79	59.48	100.00
17/05 C11*	20	23	0.00	6.13	18.79	17.89	57.19	100.00
17/05 C12		24	0.00	0.00	0.00	18.17	81.83	100.00
18/05 C11*	21	25	0.00	9.08	13.71	22.98	54.23	100.00
18/05 C12		26	0.00	5.74	13.84	20.06	60.36	100.00
19/05 C11*	22	27	0.00	0.00	17.02	11.58	71.40	100.00
19/05 C12		28	0.00	0.00	0.00	12.24	87.76	100.00
21/05 C11*	23	29	0.00	0.00	8.00	20.50	71.50	100.00
21/05 C12		30	0.00	0.00	0.00	29.70	70.30	100.00
22/05 C11*	24	31	0.00	0.00	0.00	30.91	69.09	100.00
22/05 C12		32	0.00	0.00	0.00	21.54	78.46	100.00
23/05 C11*	25	33	0.00	0.00	6.45	18.47	75.07	100.00
23/05 C12*	26	34	0.00	0.00	0.00	48.38	51.62	100.00
24/05 C11*	27	35	0.00	0.00	0.00	18.45	81.55	100.00
24/05 C12*	28	36	0.00	0.00	0.00	10.88	89.12	100.00
Average			0.16	1.76	6.12	20.26	71.70	
Sample deviation s			0.96	4.35	6.46	8.29	11.82	

Table E6 - Concentrate CV / size data

* denotes corresponding feed size property data also available

Sample ID	Figures 5.13 - 5.16 Trial no	Figure 5.16 Trial no	CV MJ/Kg size fraction I +150 um	-150+106 um	-106+75 um	-75+45 um	-45 um	Reconstituted Total
18/04 C12		1			29.64	28.73	29.34	29.19
18/04 C21*	1	2				28.07	28.98	26.84
27/04 C11*	2	3				28.31	28.14	28.18
27/04 C21*	3	4			27.47	27.26	27.03	27.11
28/04 C11*	4	5			28.13	28.08	28.19	28.17
28/04 C21*	5	6			28.23	28.03	27.76	27.84
28/04 C31*	6	7			28.24	28.07	27.86	27.93
28/04 C41*	7	8			27.13	27.07	26.41	26.54
03/05 C11*	8	9				28.17	27.76	27.86
03/05 C12		10			28.57	27.57	27.40	27.66
04/05 C11*	9	11		27.84	26.85	26.10	26.74	26.84
04/05 C12		12		28.00	27.08	24.82	26.87	25.05
07/05 C11*	10	13				27.54	27.55	27.55
07/05 C12*	11	14			28.10	27.43	27.89	27.77
08/05 C11*	12	15				28.74	28.89	28.86
08/05 C12*	13	16					28.84	28.84
08/05 C21*	14	17			28.37	28.51	28.76	28.69
08/05 C22*	15	18				29.35	29.72	29.62
08/05 C31*	16	19			28.29	28.40	28.55	28.50
08/05 C32*	17	20			29.45	29.70	31.03	30.48
10/05 C11*	18	21				27.57	27.39	27.43
10/05 C12*	19	22		** 25.98		27.02	27.41	27.14
17/05 C11*	20	23		28.75	27.60	26.60	26.58	26.91
17/05 C12		24				28.19	28.08	28.10
18/05 C11*	21	25		27.54	26.90	26.07	25.22	25.86
18/05 C12		26		28.75	27.55	26.89	26.22	26.68
19/05 C11*	22	27			28.38	27.88	28.55	28.44
19/05 C12		28				29.28	29.57	29.53
21/05 C11*	23	29			28.90	28.20	28.58	28.53
21/05 C12		30				28.97	29.26	29.17
22/05 C11*	24	31				29.16	29.45	29.36
22/05 C12		32				29.48	29.61	29.58
23/05 C11*	25	33			28.63	27.41	27.44	27.51
23/05 C12*	26	34				29.66	29.93	29.80
24/05 C11*	27	35				28.32	29.15	29.00
24/05 C12*	28	36				28.98	29.53	29.47
Average				28.18	28.08	27.99	28.21	28.11
sample deviation s				0.55	0.80	1.09	1.24	1.20

** outlier therefore exclude from sample statistical calculations

Table E7 - Kleinkopje Bulk analysis data

Run ID	Feed		Concentrate		Tails	
	% Ash	CV MJ/kg	% Ash	CV MJ/kg	% Ash	CV MJ/kg
17/04 R11	20.27	24.92	11.80	28.56	22.50	24.48
17/04 R12	21.10	25.18	11.50	28.34	22.50	24.47
17/04 R21	21.40	25.02	12.10	28.55	26.40	20.81
18/04 R11	21.70	25.23	10.30	29.54	30.10	22.42
18/04 R12			9.70	29.61	34.40	19.57
18/04 R21	22.80	24.18	10.40	29.31	40.10	16.51
			10.70	29.56	41.00	16.54
18/04 R22	20.70	25.40	11.30	29.23	41.70	16.32
19/04 R11	25.40	22.94	9.66	29.05	30.25	21.04
19/04 R12	26.60	22.82	9.60	29.20	30.90	20.82
19/04 R21	25.17	22.40	15.54	26.73	44.22	14.40
19/04 R21	25.30	23.14				
19/04 R22	25.38	23.09	14.20	27.43	37.00	17.51
			14.20			17.51
19/04 R31			13.00	28.28		
20/04 R11	21.77	24.75	13.28	28.27	60.10	2.67
20/04 R11			13.30	28.25		
20/04 R12	21.40	24.93	12.30	28.54		
20/04 R21	20.17	20.90	12.40	28.44	44.22	14.40
20/04 R21	20.60	21.15				
20/04 R22	20.60	24.99	12.50	28.44	30.50	20.76
20/04 R31	21.40	24.72	12.70	28.35		
20/04 R31	21.50	24.74	13.60	27.56		
20/04 R32					29.60	21.50
23/04 R11	19.60	25.23	12.90	28.12		
23/04 R12	20.10	25.11	12.20	28.51	27.40	22.24
23/04 R21	20.20	24.88	11.30	27.70	28.90	21.70
23/04 R22	21.10	24.82			23.50	24.04
24/04 R11	21.40	24.53	7.70	29.54	23.40	23.74
24/04 R12	21.30	24.46			22.20	24.27
24/04 R21	26.70	21.99				
24/04 R22	27.10	22.31			28.00	21.90
24/04 R31	27.20	21.84			28.00	21.90
24/04 R32	27.30	22.48			28.40	22.18
24/04 R41	25.30	23.02			26.30	22.96
27/04 R11					25.30	22.90
27/04 R12			12.10	27.20	26.30	22.43
27/04 R21					31.40	20.20
27/04 R22			11.50	27.75	24.00	23.23
28/04 R11					26.30	22.20
28/04 R12			10.50	27.82	26.20	22.09
28/04 R13			10.30	28.31	26.10	22.38
28/04 R21					28.10	21.24
28/04 R22			11.10	27.98	26.40	22.21

Table E7 continued

Run ID	Feed		Concentrate		Tails	
	% Ash	CV MJ/kg	% Ash	CV MJ/kg	% Ash	CV MJ/kg
28/04 R31					27.10	21.92
28/04 R32			10.20	28.47	26.00	22.58
28/04 R41					30.00	20.66
28/04 R42			14.10	27.05	28.70	21.23
03/05 R11					29.60	22.21
03/05 R12	23.20	23.78			37.90	17.92
04/05 R11					59.10	9.88
04/05 R12	22.70	23.37			67.60	5.20
07/05 R11					31.80	20.30
07/05 R12					35.00	19.24
08/05 R11					28.70	21.79
08/05 R12					30.90	20.99
08/05 R21					33.30	20.22
08/05 R22					27.50	22.29
08/05 R31					32.50	20.64
08/05 R32					27.30	22.51
10/05 R11					39.50	16.68
10/05 R12					38.70	17.01
15/05 R11	24.70	23.08	14.90	27.12	74.20	2.96
15/05 R12			15.00	27.10	72.50	3.60
15/05 R21	25.90	22.68	14.00	27.30	44.00	15.40
15/05 R22			11.30	28.32	33.70	17.38
17/05 R11					67.50	5.76
17/05 R12	25.60	22.53			40.40	16.60
18/05 R11					61.80	7.54
18/05 R12	24.00	23.24			57.00	9.56
19/05 R11					64.20	6.38
19/05 R12	21.50	23.82			25.40	22.36
21/05 R11					53.60	11.96
21/05 R12	23.90	23.62			31.60	20.71
22/05 R11					23.70	23.76
22/05 R12	22.30	24.22			25.40	23.27

Parameter effects - KK testwork

Tables E8 and E9 - parameter symbol identification

Parameter description	Symbol
Batch reproducibility	R
Collector type	CT
Collector dosage	CC g/t
Frother type	FT
Frother dosage	FC
Pulp tank dosage	FCT ul/l pulp
Water tank dosage ul/l	FCWW ul/l
Slurry feedrate	QF l/min
Slurry tailsrate	QT l/min
Pulp density	PD % mass/volume
Froth height	FH cm
Washwater rate	WW l/min
Air rate	AF l/min @ 0.82 atm
Sparger type	ST
Sparger water rate	SW l/min
"Select" coal	S
"Non-select" coal	NS

Tables E1 - E7 raw data tables - as received from RICHLAB, AMCOAL, KK labs

Ash, CV analyses on some samples were repeated - The arithmetic average of

repeat samples are reported in Tables E9 and E10

Table E8 - Column operating parameters

Run ID	Parameter value													
	CT	CC	ST	FT	FCT	FCW	QF	QT	PD	FH	WW	AF	SW	% Yield
17/04 R11	SHELLSOL	2501	USB	HTEB		25	3.12		7.35	55	1.74	6.57	1.00	8.09
17/04 R12	SHELLSOL	2501	USB	HTEB		25	3.12		7.35	55	1.74	6.57	1.00	7.30
17/04 R21	SHELLSOL	6903	USB	HTEB		25	3.12		7.97	55	1.74	6.57	1.00	31.21
18/04 R11	SHELLSOL	6527	Filter	HTEB	25	10	3.12		8.43	55	1.74	6.57		41.71
18/04 R12	SHELLSOL	6527	Filter	HTEB	25	10	3.12		8.43	55	1.74	9.24		45.89
18/04 R21	SHELLSOL	6796	Filter	HTEB	25	10	1.44		8.46	55	1.74	6.57		65.42
18/04 R22	SHELLSOL	6796	Filter	HTEB	25	10	1.44	2.34	7.76	55	1.74	9.24		68.25
19/04 R11	SHELLSOL	2975	Filter	HTEB	25	10	1.38	2.84	6.30	55	1.74	6.57		15.19
19/04 R12	SHELLSOL	2975	Filter	HTEB	25	10	1.38	2.66	6.03	55	1.74	9.24		23.24
19/04 R21	SHELLSOL	7716	Filter	HTEB	25	10	1.36	1.78	7.35	50	1.74	13.4		74.36
19/04 R22	SHELLSOL	7716	Filter	HTEB	25	10	1.32	1.31	6.92	50	1.08	13.4		56.88
19/04 R31	SHELLSOL	6768	USB	HTEB		25	1.42	3.16	8.13	50	1.74	9.24	1.00	75.03
20/04 R11	SHELLSOL	5817	USB	HTEB		20	1.39	3.28	9.39	50	1.74	9.24	1.00	82.42
20/04 R12	SHELLSOL	5817	USB	HTEB		20	1.34	3.36	9.52	50	2.00	9.24	1.00	46.00
20/04 R21	SHELLSOL	7144	USB	HTEB		15	1.24	3.40	7.68	50	1.74	13.4	1.00	63.93
20/04 R22	SHELLSOL	7144	USB	HTEB		15	1.25	3.08	7.72	50	2.00	17.4	1.00	55.59
20/04 R31	SHELLSOL	4601	Filter	HTEB	25	10	1.28	1.72	7.68	50	1.74	13.4		62.77
20/04 R32	SHELLSOL	4601	Filter	HTEB	25	10	1.20	1.44	8.28	50	1.16	13.4		52.81
23/04 R11	Paraffin	6567	Filter	HTEB	25	10	1.42	2.40	8.18	50	1.74	9.24		80.27
23/04 R12	Paraffin	6567	Filter	HTEB	25	10	2.80	2.88	8.58	50	1.74	9.24		72.27
23/04 R21	Paraffin	2127	Filter	HTEB	25	10	1.32	2.20	8.38	50	1.74	9.24		47.48
23/04 R22	Paraffin	2127	Filter	HTEB	25	10	3.02	3.56	8.87	50	1.74	9.24		21.35
24/04 R11	SHELLSOL	1867	Filter	T DIBK WW HTEB	25	10	1.33	2.54	10.46	50	1.74	9.24		15.85
24/04 R12	SHELLSOL	1867	Filter	T DIBK WW HTEB	25	10	2.80	4.38	10.51	50	1.74	9.24		4.73
24/02 R21	Paraffin	2102	Filter	MIBC	25	10	1.47	3.00	8.12	50	1.74	9.24		1.32
24/04 R22	Paraffin	2102	Filter	MIBC	25	10	2.74	3.20	9.42	50	1.74	9.24		1.10
24/04 R31	Paraffin	2183	Filter	MIBC	25	10	1.32	3.16	9.01	50	1.74	9.24		0.00
24/02 R32	Paraffin	2183	Filter	MIBC	25	10	1.24	2.76	8.93	50	1.74	9.24		0.00
24/04 R41	SHELLSOL	2042	Filter	HTEB	25	10	1.26	3.36	8.98	50	1.74	9.24		2.43
26/04 R11	Paraffin	3580	USB	MIBC		20	1.74	4.05	8.59	50	1.74	9.24	1.20	24.05
26/04 R12	Paraffin	3580	USB	MIBC		20	1.74	3.89	8.87	50	1.74	9.24	1.20	27.15
26/04 R21	SHELLSOL	3701	USB	MIBC		20	1.69	4.35	8.44	50	1.74	9.24	1.20	36.70
27/04 R11	SHELLSOL	4040	USB	HTEB		15	1.90	4.26	9.96	75	1.74	13.4	1.20	14.00
27/04 R12	SHELLSOL	4040	USB	HTEB		15	1.90		9.41	50	1.74	13.4	1.20	21.46
27/04 R21	SHELLSOL	5425	USB	HTEB		15	1.90	3.66	7.96	50	1.74	13.4	1.20	41.43
27/04 R22	SHELLSOL	5425	USB	HTEB		15	1.82	3.72	7.42	25	1.74	13.4	1.20	15.90
28/04 R11	SHELLSOL	4569	Filter	HTEB	25	5	1.88	2.52	8.12	75	1.74	13.4		26.93
28/04 R12	SHELLSOL	4569	Filter	HTEB	25	5	1.88	2.60	7.98	50	1.74	13.4		24.54
28/04 R13	SHELLSOL	4569	Filter	HTEB	25	5	1.88	2.56	7.97	25	1.74	13.4		22.47
28/04 R21	SHELLSOL	4315	Filter	HTEB	25	5	1.88	2.38	8.19	50	1.74	13.4		40.57
28/04 R22	SHELLSOL	4315	Filter	HTEB	25	5	2.88	2.88	8.82	50	1.74	13.4		25.37

Table E8 continued

Run ID	Parameter value													
	CT	CC	ST	FT	FCT	FCW	QF	QT	PD	FH	WW	AF	SW	% Yield
28/04 R31	SHELLSOL	6174	Filter	HTEB	15	0	1.84	2.60	8.14	50	1.74	13.4		36.32
28/04 R32	SHELLSOL	6174	Filter	HTEB	15	10	1.68	2.68	9.85	50	1.74	13.4		28.19
28/04 R41	SHELLSOL	5997	Filter	HTEB	25	0	1.76	2.16	9.55	50	1.74	13.4		44.18
28/04 R42	SHELLSOL	5997	Filter	HTEB	25	10	1.84	2.10	8.83	50	1.74	13.4		36.93
03/05 R11	SHELLSOL	3430	USB	HTEB		15	1.34	1.47	7.28	50	1.74	13.4	1.00	35.78
03/05 R12	SHELLSOL	3430	USB	HTEB		15	0.74	2.86	8.93	50	1.74	13.4	1.00	58.80
04/05 R11	SHELLSOL	2425	USB	HTEB		15	0.59	2.94	7.56	50	1.40	10.8	1.00	81.85
04/05 R12	SHELLSOL	4068	USB	HTEB		15	0.66	2.90	6.37	50	1.40	10.8	1.00	82.17
07/05 R11	SHELLSOL	1976	USB	HTEB		15	0.60	2.68	9.28	50	1.40	10.8	1.00	41.53
07/05 R12	SHELLSOL	3035	USB	HTEB		15	0.62	2.12	8.86	50	1.40	10.8	1.00	45.15
08/05 R11	SHELLSOL	2046	USB	HTEB		15	0.60	2.38	13.86	50	1.40	10.8	1.00	15.48
08/05 R12	SHELLSOL	2046	USB	HTEB		15	0.60	2.76	7.68	50	1.40	10.8	1.00	23.53
08/05 R21	SHELLSOL	1913	USB	HTEB		20	0.62	2.18	14.97	50	1.40	10.8	1.00	44.75
08/05 R22	SHELLSOL	1913	USB	HTEB		15	0.62	2.48	14.94	50	1.40	10.8	1.00	20.96
08/05 R31	SHELLSOL	1883	USB	HTEB		15	0.56	2.40	15.40	50	1.40	10.8	1.00	35.53
08/05 R32	SHELLSOL	1883	USB	HTEB		10	0.60	2.60	15.08	50	1.40	10.8	1.00	12.53
10/05 R11	SHELLSOL	1976	USB	HTEB		20	0.60	2.00	15.80	50	1.40	10.8	1.00	55.07
10/05 R12	SHELLSOL	1976	USB	HTEB		20	0.59	2.24	15.75	50	1.74	10.8	1.00	53.18
15/05 R11	SHELLSOL	7057	USB	HTEB		20	1.32	3.00	7.79	50	1.74	9.24	1.00	84.89
15/05 R12	SHELLSOL	7057	USB	HTEB		20	1.30	2.54	7.80	50	1.74	13.4	1.00	84.00
15/05 R21	SHELLSOL	2728	USB	HTEB		25	1.32	2.80	9.85	50	1.74	13.4	1.00	55.36
15/05 R22	SHELLSOL	2728	USB	HTEB		20	1.34	3.14	9.85	50	1.74	13.4	1.00	31.52
17/05 R11	SHELLSOL	2609	USB	HTEB		20	0.74	2.52	7.32	50	1.40	10.8	1.00	81.36
17/05 R12	SHELLSOL	2609	Filter	HTEB	40	0	0.75	1.64	6.75	50	1.40	10.8		49.05
18/05 R11	SHELLSOL	2221	USB	HTEB		20	0.65	2.24	7.99	50	1.40	9.24	1.00	89.94
18/05 R12	SHELLSOL	2221	USB	HTEB		20	0.64	2.38	8.52	75	1.40	9.24	1.00	82.74
19/05 R11	SHELLSOL	3670	USB	HTEB		20	1.80	3.88	5.03	50	1.74	9.24	1.00	80.06
19/05 R12	SHELLSOL	3670	USB	HTEB		20	3.44	4.86	4.96	50	1.74	9.24	1.00	22.38
21/05 R11	SHELLSOL	2920	USB	HTEB		20	1.90	2.88	6.24	50	1.74	9.24	1.00	63.63
21/05 R12	SHELLSOL	2920	USB	HTEB		20	1.88	3.96	6.32	50	1.74	10.8	1.00	34.31
22/05 R11	SHELLSOL	791	USB	HTEB		20	1.64	3.36	9.53	50	1.74	10.8	1.00	12.98
22/05 R12	SHELLSOL	791	USB	HTEB		20	1.62	3.66	9.02	50	1.74	10.8	1.20	16.74
23/05 R11	SHELLSOL	2439	USB	HTEB		20	0.98	2.64	6.15	50	1.40	9.24	1.00	57.41
23/05 R12	SHELLSOL	2439	Filter	HTEB	20	20	1.00	2.24	5.88	50	1.40	9.24		19.09
24/05 R11	SHELLSOL	1801	USB	HTEB		20	0.99	2.44	9.27	50	1.40	9.24	1.00	48.53
24/05 R12	SHELLSOL	1801	Filter	HTEB	75	10	0.96	2.00	8.53	50	1.40	9.24		30.69

Table E9 : Scale - up parameter values

		Parameter value								
Run ID	Parameters tested	Fcd ul/min	Jb cm/s	Jf cm/s	Jw cm/s	Jg cm/s	Jg* cm/s	Jb/Jf B.R.	Fa	Cp
17/04 R11	R1	68.5		0.66	0.37	1.39	1.29		1.75	0.14
17/04 R12	R1	68.5		0.66	0.37	1.39	1.29		1.75	0.13
17/04 R21		68.5		0.66	0.37	1.39	1.29		1.90	0.59
18/04 R11	AF1 RB1	95.4		0.66	0.37	1.39	1.29		2.01	0.84
18/04 R12	AF1 RB2	95.4		0.66	0.37	1.96	1.81		2.01	0.92
18/04 R21	AF2 RB1	53.4		0.31	0.37	1.39	1.29		0.93	0.61
18/04 R22	AF2 RB2	53.4	0.19	0.31	0.37	1.96	1.81	0.63	0.85	0.58
19/04 R11	AF3	51.9	0.31	0.29	0.37	1.39	1.29	1.06	0.66	0.10
19/04 R12	AF3	51.9	0.27	0.29	0.37	1.96	1.81	0.93	0.64	0.15
19/04 R21	WW1	51.4	0.09	0.29	0.37	2.84	2.62	0.31	0.76	0.57
19/04 R22	WW1	43.8	-0.00	0.28	0.23	2.84	2.62	-0.01	0.70	0.40
19/04 R31		68.5	0.16	0.30	0.37	1.96	1.81	0.52	0.88	0.66
20/04 R11	WW2	54.8	0.19	0.29	0.37	1.96	1.81	0.64	1.00	0.82
20/04 R12	WW2	60.0	0.22	0.28	0.42	1.96	1.81	0.76	0.97	0.45
20/04 R21	AF4 WW3	41.1	0.25	0.26	0.37	2.84	2.62	0.94	0.73	0.47
20/04 R22	AF4 WW3	45.0	0.18	0.27	0.42	3.69	3.40	0.66	0.74	0.41
20/04 R31	WW4 CT	49.4	0.09	0.27	0.37	2.84	2.62	0.34	0.75	0.47
20/04 R32	WW4 CT	41.6	0.05	0.25	0.25	2.84	2.62	0.20	0.76	0.40
23/04 R11	QF1 CT	52.9	0.21	0.30	0.37	1.96	1.81	0.69	0.89	0.71
23/04 R12	QF1 CT	87.4	0.02	0.59	0.37	1.96	1.81	0.03	1.84	1.33
23/04 R21	S QF2 CT	50.4	0.19	0.28	0.37	1.96	1.81	0.67	0.85	0.40
23/04 R22	S QF2 CT	92.9	0.11	0.64	0.37	1.96	1.81	0.18	2.05	0.44
24/04 R11	QF3 FT	50.7	0.26	0.28	0.37	1.96	1.81	0.91	1.06	0.17
24/04 R12	QF3 FT	87.4	0.34	0.59	0.37	1.96	1.81	0.56	2.25	0.11
24/04 R21	NS CT FT	54.2	0.32	0.31	0.37	1.96	1.81	1.04	0.91	0.01
24/04 R22	NS CT FT	85.9	0.10	0.58	0.37	1.96	1.81	0.17	1.97	0.02
24/04 R31	NS CT FT	50.4	0.39	0.28	0.37	1.96	1.81	1.39	0.91	0.00
24/02 R32	NS CT FT	48.4	0.32	0.26	0.37	1.96	1.81	1.23	0.85	0.00
24/04 R41	NS CT FT	48.9	0.45	0.27	0.37	1.96	1.81	1.67	0.86	0.02
26/04 R11	R2 CT FT	58.8	0.24	0.37	0.37	1.96	1.81	0.64	1.14	0.27
26/04 R12	R2 CT FT	58.8	0.20	0.37	0.37	1.96	1.81	0.54	1.18	0.32
26/04 R21	FT	58.8	0.31	0.36	0.37	1.96	1.81	0.86	1.09	0.40
27/04 R11	FH1	44.1	0.25	0.40	0.37	2.84	2.62	0.61	1.45	0.20
27/04 R12	FH1	44.1		0.40	0.37	2.84	2.62	0.00	1.37	0.29
27/04 R21		44.1	0.12	0.40	0.37	2.84	2.62	0.29	1.16	0.48
27/04 R22		44.1	0.15	0.39	0.37	2.84	2.62	0.38	1.03	0.16
28/04 R11	FH2	55.7	0.14	0.40	0.37	2.84	2.62	0.34	1.17	0.31
28/04 R12	FH2 RB3	55.7	0.15	0.40	0.37	2.84	2.62	0.38	1.15	0.28
28/04 R13	FH2	55.7	0.14	0.40	0.37	2.84	2.62	0.36	1.14	0.26
28/04 R21	QF4 RB3	55.7	0.11	0.40	0.37	2.84	2.62	0.27	1.18	0.48
28/04 R22	QF4	80.7	0.00	0.61	0.37	2.84	2.62	0.00	1.94	0.49

Table E9 continued

Run ID	Parameters tested	Fcd ul/min	Jb cm/s	Jf cm/s	Jw cm/s	Jg cm/s	Jg* cm/s	Jb/Jf B.R.	Fa	Cp
28/04 R31	FCWW	27.6	0.16	0.39	0.37	2.84	2.62	0.41	1.14	0.42
28/04 R32	FCWW	42.6	0.21	0.36	0.37	2.84	2.62	0.60	1.26	0.36
28/04 R41	FCWW	44.0	0.08	0.37	0.37	2.84	2.62	0.23	1.28	0.57
28/04 R42	FCWW	63.4	0.06	0.39	0.37	2.84	2.62	0.14	1.24	0.46
03/05 R11	QF5	41.1	-0.18	0.28	0.37	2.84	2.62	-0.65	0.75	0.27
03/05 R12	QF5	41.1	0.24	0.16	0.37	2.84	2.62	1.51	0.50	0.30
04/05 R11	CC	36.0	0.29	0.13	0.30	2.29	2.12	2.29	0.34	0.28
04/05 R12	CC	36.0	0.26	0.14	0.30	2.29	2.12	1.88	0.32	0.26
07/05 R11	CC	36.0	0.23	0.13	0.30	2.29	2.12	1.80	0.43	0.18
07/05 R12	CC	36.0	0.11	0.13	0.30	2.29	2.12	0.81	0.42	0.19
08/05 R11	PD	36.0	0.17	0.13	0.30	2.29	2.12	1.30	0.64	0.10
08/05 R12	PD	36.0	0.25	0.13	0.30	2.29	2.12	1.93	0.35	0.08
08/05 R21	FC1	48.0	0.12	0.13	0.30	2.29	2.12	0.90	0.71	0.32
08/05 R22	FC1	36.0	0.18	0.13	0.30	2.29	2.12	1.39	0.71	0.15
08/05 R31	FC2	36.0	0.18	0.12	0.30	2.29	2.12	1.50	0.66	0.23
08/05 R32	FC2	24.0	0.21	0.13	0.30	2.29	2.12	1.67	0.69	0.09
10/05 R11	RB4 WW5	48.0	0.08	0.13	0.30	2.29	2.12	0.67	0.72	0.40
10/05 R12	WW5	54.8	0.14	0.13	0.37	2.29	2.12	1.10	0.71	0.38
15/05 R11	AF5	54.8	0.14	0.28	0.37	1.96	1.81	0.52	0.79	0.67
15/05 R12	AF5	54.8	0.05	0.28	0.37	2.84	2.62	0.18	0.77	0.65
15/05 R21	FC3	68.5	0.10	0.28	0.37	2.84	2.62	0.36	0.99	0.55
15/05 R22	FC3	54.8	0.17	0.28	0.37	2.84	2.62	0.60	1.01	0.32
17/05 R11	ST1	48.0	0.17	0.16	0.30	2.29	2.12	1.05	0.41	0.34
17/05 R12	ST1	30.0	0.19	0.16	0.30	2.29	2.12	1.19	0.39	0.19
18/05 R11	FH3	48.0	0.13	0.14	0.30	1.96	1.81	0.91	0.40	0.36
18/05 R12	FH3	48.0	0.16	0.14	0.30	1.96	1.81	1.16	0.42	0.34
19/05 R11	QF6	54.8	0.23	0.38	0.37	1.96	1.81	0.60	0.69	0.55
19/05 R12	QF6	54.8	0.09	0.73	0.37	1.96	1.81	0.12	1.30	0.29
21/05 R11		54.8	-0.00	0.40	0.37	1.96	1.81	-0.01	0.91	0.58
21/05 R12		54.8	0.23	0.40	0.37	2.29	2.12	0.57	0.91	0.31
22/05 R11	SW	54.8	0.15	0.35	0.37	2.29	2.12	0.44	1.19	0.15
22/05 R12	SW	58.8	0.18	0.34	0.37	2.29	2.12	0.52	1.12	0.19
23/05 R11	ST2	48.0	0.14	0.21	0.30	1.96	1.81	0.67	0.46	0.26
23/05 R12	ST2	48.0	0.26	0.21	0.30	1.96	1.81	1.24	0.45	0.09
24/05 R11	ST3	48.0	0.10	0.21	0.30	1.96	1.81	0.45	0.70	0.34
24/05 R12	ST3	86.0	0.22	0.20	0.30	1.96	1.81	1.08	0.63	0.19

Table E10 - Kleinkopje Column results

Solids feedrate = sum of concentrate and tails solids rates
% Yield based on solids concentrates and tails rates
* denotes value an average of results listed in Tables E1 - E7

Run ID	Tails l/min	Solids Feed g/min	% Yield	Feed % ash	Conc % ash	Tails % ash	Feed CV MJ/kg	Conc CV MJ/kg	Tails MJ/kg	Calc Feed % ash
17/04 R11		252.20	8.09	20.27	11.80	22.50	24.92	28.56	24.48	21.63
17/04 R12		234.20	7.30	21.10	11.50	22.50	25.18	28.34	24.47	21.70
17/04 R21		208.80	31.21	21.40	12.10	26.40	25.02	28.55	20.81	21.94
18/04 R11		256.00	41.71	21.70	10.30	30.10	25.23	29.54	22.42	21.84
18/04 R12		246.20	45.89		* 10.09	34.40		* 29.40	19.57	23.24
18/04 R21		112.50	65.42	21.37	* 10.94	* 40.60	* 25.63	* 29.24	* 16.53	21.20
18/04 R22	2.34	109.60	68.25	20.70	11.30	41.70	25.40	29.23	16.32	20.95
19/04 R11	2.84	81.00	15.19	25.20	9.66	30.25	22.94	29.05	21.04	27.12
19/04 R12	2.66	85.20	23.24	26.60	9.60	30.90	22.82	* 29.13	20.82	25.95
19/04 R21	1.78	86.20	74.30	25.24	15.54	44.22	* 22.77	26.73	14.40	22.91
19/04 R22	1.31	92.30	56.88	25.38	* 14.20	37.00	23.09	27.43	* 17.51	24.03
19/04 R31	2.16	84.50	75.03		13.00			28.28		
20/04 R11	2.28	101.90	82.43	21.74	* 13.29	60.10	* 24.74	* 28.26	2.67	21.51
20/04 R12	2.36	128.80	46.00	21.40	12.30	27.40	24.93	28.54	22.24	20.45
20/04 R21	2.40	81.50	63.90	20.39	* 12.45	37.50	* 24.53	* 28.44	* 18.71	21.49
20/04 R22	2.08	89.40	55.59	20.60	12.50	30.50	24.99	28.44	20.76	20.49
20/04 R31	1.72	93.20	62.77	21.45	13.60	32.30	* 24.73	* 27.97		20.56
20/04 R32	1.44	90.90	52.81	21.80	12.20	29.60	25.24	28.47	21.50	20.41
23/04 R11	2.40	104.40	80.27	19.60	12.90	46.86	25.23	28.12		19.60
23/04 R12	2.88	247.40	72.27	20.10	12.20	31.30	25.11	28.51	22.24	17.50
23/04 R21	2.20	103.20	47.48	20.10	11.30	28.90	* 24.96	28.12	21.70	20.54
23/04 R22	3.56	237.50	21.35	21.25		* 23.75	* 24.82	28.54	* 23.80	
24/04 R11	2.54	136.20	15.85	21.40	7.70	23.40	24.53	29.54	23.74	20.91
24/04 R12	4.38	276.70	4.73	21.30		22.20	24.46		24.27	
24/02 R21	3.00	121.30	1.32	26.70			21.99			
24/04 R22	3.20	238.20	1.10	27.10		28.00	22.31		21.90	
24/04 R31	3.16	112.40	0.00	27.20		28.00	21.84		21.90	
24/02 R32	2.76	106.90	0.00	27.30		28.40	22.48		22.18	
24/04 R41	3.36	115.10	2.43	25.30		26.30	23.02		22.96	
26/04 R11	2.83	137.80	24.05							
26/04 R12	2.67	164.80	27.15							
26/04 R21	3.15	136.30	36.70							
27/04 R11	3.06	218.00	14.00	21.57	10.22	25.30	24.32	28.18	22.90	23.19
27/04 R12		204.60	21.46	22.41	12.10	26.30	23.69	27.20	22.43	23.25
27/04 R21	2.46	121.40	41.43	21.29	13.07	31.40	24.34	27.11	20.20	23.81
27/04 R22	2.52	166.70	15.90	21.60	11.50	24.00	24.15	27.75	23.23	22.01
28/04 R11	2.52	165.60	26.93	22.20	10.72	26.30	23.81	28.17	22.20	22.10
28/04 R12	2.60	162.20	24.54	22.00	10.50	26.20	23.85	27.82	22.09	22.35
28/04 R13	2.56	154.40	22.47	21.33	10.30	26.10	23.99	28.31	22.38	22.55
28/04 R21	2.38	161.70	40.57	21.00	12.12	28.10	24.36	27.84	21.24	21.62
28/04 R22	2.88	244.40	25.37	20.67	11.10	26.40	24.67	27.98	22.21	22.52

Table E10 continued

Run ID	Tails l/min	Solids Feed g/min	% Yield	Feed % ash	Conc % ash	Tails % ash	Feed CV MJ/kg	Conc CV MJ/kg	Tails MJ/kg	Calc Feed % ash
28/04 R31	2.60	177.60	36.32	20.68	11.65	27.10	24.65	27.93	21.92	21.49
28/04 R32	2.68	151.10	28.19	20.59	10.20	26.00	24.71	28.47	22.58	21.55
28/04 R41	2.16	177.90	44.18	22.17	15.03	30.00	23.82	26.54	20.66	23.39
28/04 R42	2.10	176.30	36.93	22.13	14.10	28.70	23.81	27.05	21.23	23.31
03/05 R11	1.76	102.60	35.78	23.24	* 13.34	29.60	23.94	* 28.14	22.21	23.78
03/05 R12	1.86	55.30	58.80	23.20	* 14.20	37.90	23.78	* 27.83	17.92	23.96
04/05 R11	1.94	37.75	81.85	22.62	* 14.71	59.10	23.41	* 26.94	9.88	22.77
04/05 R12	1.90	41.50	82.17	22.70	* 13.38	67.60	23.37	* 27.20	5.20	23.05
07/05 R11	1.68	62.60	41.53	23.95	13.82	31.80	22.46	27.55	20.30	24.33
07/05 R12	1.12	61.90	45.15	24.57	13.06	35.00	23.22	27.77	19.24	25.09
08/05 R11	1.38	86.90	15.48	25.90	9.88	28.70	22.62	28.86	21.79	25.79
08/05 R12	1.76	50.15	23.53	25.01	10.20	30.90	23.05	28.84	20.99	26.03
08/05 R21	1.18	95.20	44.75	24.87	11.16	33.30	23.29	28.69	20.22	23.39
08/05 R22	1.48	97.35	20.96	24.65	7.94	27.50	23.30	29.62	22.29	23.40
08/05 R31	1.40	90.20	35.53	24.14	11.55	32.50	23.70	28.50	20.64	25.06
08/05 R32	1.60	93.40	12.53	23.77	7.56	27.30	23.86	30.48	22.51	24.83
10/05 R11	1.00	103.50	55.07	24.01	11.34	39.50	22.51	27.43	16.68	23.99
10/05 R12	1.24	107.00	53.18	24.13	12.49	38.70	22.44	27.14	17.01	24.76
15/05 R11	2.00	117.80	84.89	24.70	14.90	74.20	23.08	27.12	2.96	23.86
15/05 R12	1.54	91.90	84.00	24.88	15.00	72.50	23.08	27.10	3.60	24.20
15/05 R21	1.80	132.40	55.36	25.90	14.00	44.00	22.68	27.30	15.40	27.39
15/05 R22	2.14	139.90	31.52	25.70	11.30	33.70	22.97	28.32	17.38	26.64
17/05 R11	1.52	50.15	81.36	25.19	14.87	67.50	22.68	26.90	5.76	24.68
17/05 R12	1.64	49.75	49.05	25.60	11.45	40.40	22.53	28.10	16.60	26.20
18/05 R11	1.24	51.20	89.94	21.69	16.23	61.80	24.25	25.86	7.54	20.81
18/05 R12	1.38	49.25	82.74		14.52	57.00	23.24	26.68	9.56	21.85
19/05 R11	1.88	66.20	80.06	20.76	10.16	64.20	24.01	28.44	6.38	20.94
19/05 R12	3.86	161.30	22.38	21.50	7.25	25.40	23.82	29.54	22.36	21.34
21/05 R11	1.88	98.70	63.63	23.34	11.20	53.60	23.76	28.53	11.96	26.62
21/05 R12	2.96	133.20	34.31	23.90	9.65	31.60	23.62	29.17	20.71	24.07
22/05 R11	2.36	159.50	12.98	22.54	8.69	23.70	24.20	29.36	23.76	21.75
22/05 R12	2.66	166.70	16.74	22.30	8.16	25.40	24.22	29.58	23.27	22.51
23/05 R11	1.64	51.30	57.41	24.44	13.41	42.30	23.41	27.51	16.64	25.71
23/05 R12	2.24	60.50	19.09	24.85	8.59	29.43	23.59	29.80	21.89	25.45
24/05 R11	1.44	78.00	48.53	24.78	11.84	41.63	23.13	29.00	16.49	27.17
24/05 R12	2.00	82.60	30.69	25.08	9.27	33.56	23.14	29.47	19.80	26.11

APPENDIX F

F1 - OIL DROPLET AND COAL PARTICLE POPULATION DISTRIBUTIONS

F2 - TANK DESIGN AND MIXING CHARACTERISTICS

F3 - KOLMOGOROV/SMIRNOV GOODNESS-OF-FIT-TEST

F4 - NORMAL DISTRIBUTION CURVE FITS TO KLEINKOPJE PLANT GLOBAL FEED % ASH AND CV DATA

F5 - ERROR ANALYSIS OF KLEINKOPJE PLANT DATA

APPENDIX F1

OIL DROPLET AND COAL PARTICLE POPULATION DISTRIBUTIONS

In section 2.4.4 collision between an oil droplet and a coal particle was identified as a conditioning sub-process. As particle aggregation or flocculation processes can reasonably be assumed negligible, one would infer that the droplet-particle collision-attachment process is a "once-only" event, i.e. once an oil droplet has adsorbed on a particle it makes no further contribution to conditioning other coal particles. Consequently, given that 60-80 % mass recoveries are typical of coal flotation, one would expect that the number of oil droplets, N_o, present is of the same order of magnitude as the number of particles, N_p, in the slurry.

As a first approximation solid population distributions can be calculated from available size fraction data; a discrete particle frequency distribution can be generated from the Sauter mean diameters representative of each size range.

Measurement of oil droplet sizes in a 3 phase slurry is difficult, if not impossible. Instead these can be measured in two-phase oil-water mixtures and the distributions obtained assumed to apply in coal slurries. For order of magnitude estimates this should be adequate.

The (volumetric) mean droplet size, d_o, and its related distribution functions are dependent on the tank and impeller geometry and the rate of energy dissipation near the impeller (i.e. power supplied by motor). In dilute dispersions (i.e. no coalescence) semi-empirical correlations relating d_o to the above properties take the form

$$d_o/L = AWe^{-3/5} \qquad (F1)$$

L is the impeller diameter
We is the tank Weber number
A is a constant dependent on system geometry

$$We = \rho_c . N^2 . L^3 / \sigma \qquad (F2)$$

ρ_c is the continuous phase (water) density
N is the impeller speed
σ is the oil-water interfacial tension

Chen and Middelman (1967) and Calabrese et al (1986) have independently investigated volume fraction distributions as a function of the dimensionless variable $D_j = d_j/d_o$ for various sizes of (turbine) impellers, L, and tank capacities, T. The dimensionless data was found to fit a normal volume frequency distribution function which was independent of the system geometry as represented by the parameter L/T. The distribution function is

$$f_v(d_j/d_o) = 1/[0.23*\sqrt{(2.\pi)}]*\exp[-9.2(d_j/d_o - 1.06)^2] \qquad (F3)$$

where
d_j = diameter of droplet in j th size interval

Anderson (1988a) measured oil drop sizes of dilute oil-water dispersions in a 3-liter Leeds type flotation cell. This cell is fitted with a 6 bladed turbine type impeller. The oil dosages used were typical for coal flotation and the oil-water dispersions were extremely dilute (ϕ < 0.0002). Laboratory and commercial grade aromatic and aliphatic oils were investigated. Mean droplet diameters of betwen 10 and 40 μm were reported.

In particular, Anderson's data for the commercial oil Shellsol AB (similar aromatic content and physical properties as ShellsolA) were

ϕ = 200 μl oil/ l H_2O = 0.0002
d_o = 22.17 μm
σ = 8.48 μm

Now consider the execution of a theoretical standard batch flotation experiment in this 3 l Leeds cell.

Suppose the slurry density is 300 g/3 l pulp

A typical coal flotation collector dosage is 1000 g/t, for ShellsolAB ρ=0.88 g/cm^3, this translates to a dosage volume v_o = 0.35 ml.

Thus the dispersed oil fraction ϕ = 0.35/3000 = 0.00017

Now, neglecting solids and mixing time effects, assume that droplet size distribution generated is the same as the equilibrium distribution obtained by Anderson, i.e. the volume Sauter mean diameter d_o = 22 μm.

The volume fraction distribution function can be calculated from (F3). Using this volume distribution and v_o it is possible to calculate a frequency function for the number of droplets in the dispersion, N_p. This is done for two mean droplet sizes, d_o = 10 and 22 μm, the frequency function is shown on the two attached graphs. An algorithm for generating the functions is given overleaf.

The feed distribution data used was the averaged size distibution of Kleinkopje thickener underflow measured during the on-line column flotation trials. These are reproduced in Table F1. The number of particles in each size fraction is calculated simply by dividing the volume of material present (assuming a bulk particle density ρ_p = 1.4 g/cm^3) by the Sauter mean diameter of that range. Both tabulated and graphical results are presented.

The number of particles present, (excluding the -20 μm fraction) is of the order of 100 million, i.e. 10^9. Now if the droplet frequency distributions are examined, it is apparent that only at colloidal size (< 1 μm) does the number of droplets approach 10^9.

The algorithm for the droplet frequency calculation is

1. convert oil dosage v_o to dimensionless volume $V_o = 6.v_o/\pi.d_o^3$
2. choose initial drop size $d_{j=0} = 0.1\ \mu m$
3. choose droplet size increment $\Delta d = 0.1\ \mu m$
   convert to dimensionless increment $\Delta D = \Delta d/d_o$
4. convert droplet size to dimensionless variable $D_j = d_j/d_o$
5. calculate volume fraction $f_v(D_j)$
6. calculate droplet size $d_{j+1} = d_j + \Delta d$
7. repeat steps 4. and 5. for droplet size d_{j+1}
8. calculate an average dimensionless droplet size, volume and frequency function for the interval $d_j \rightarrow d_{j+1}$
   $D_{avg} = (D_j + D_{j+1})/2$
   $v_{Djavg} = \pi.D_{javg}^3/6$
   $f_{avg} = (f_j + f_{j+1})/2$
9. calculate number of droplets between the j'th and j'th + 1 interval
   $n_{javg} = f_{avg}*V_o/v_{Djavg}$
10. $j = j + 1$, repeat steps 4. - 9.

Number of particles in 300 g of coal solids - Calculation

Basis : 300 g solids

particle density 1.4 g/cm3

Table F1 : Kleinkopje t/u size and particle frequency distributions

Size fraction um	Sauter mean diameter	f(x)	Mass (g)	vp cm3	Np
150	150.00	6.66	19.98	1.77E-06	8075976.541
106	126.10	10.94	32.82	1.05E-06	22331414.48
75	89.16	14.11	42.33	3.71E-07	81464972.92
45	58.09	22.83	68.49	1.03E-07	476529556.2
20	30.00	30.34	91.02	1.41E-08	4598819975
10	10.00	15.12	45.36	5.24E-10	61879441874
Total		100	300		67066663769
			excl <20 um		5.19E+09
			incl <20 um		6.71E+10

Figure F1 – Droplet frequency distribution function; do = 22 um

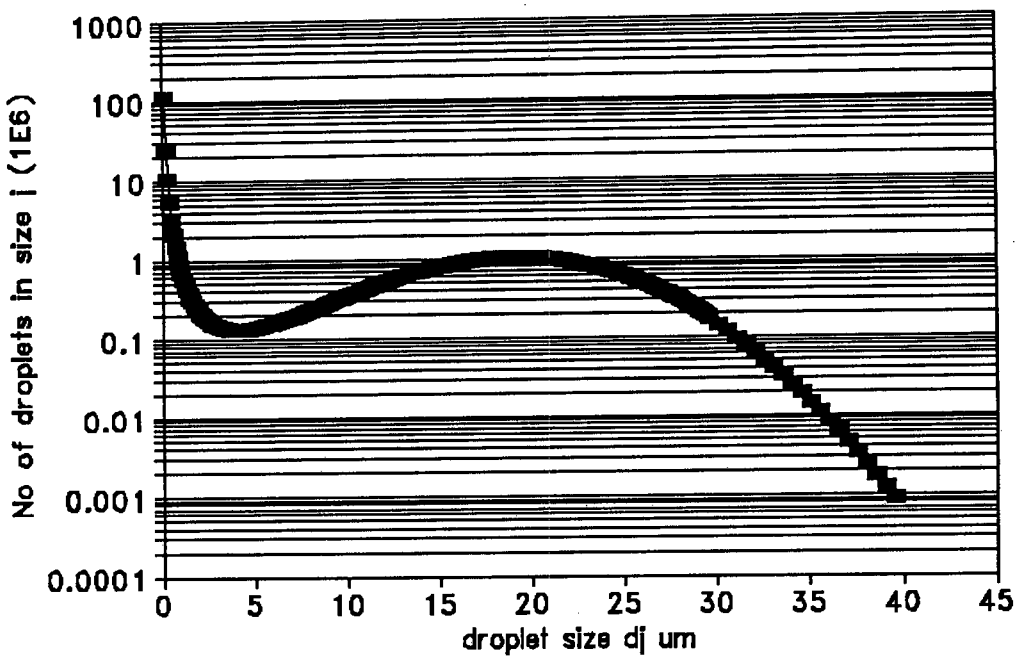

Figure F2 – Droplet frequency distribution function; do = 10 um

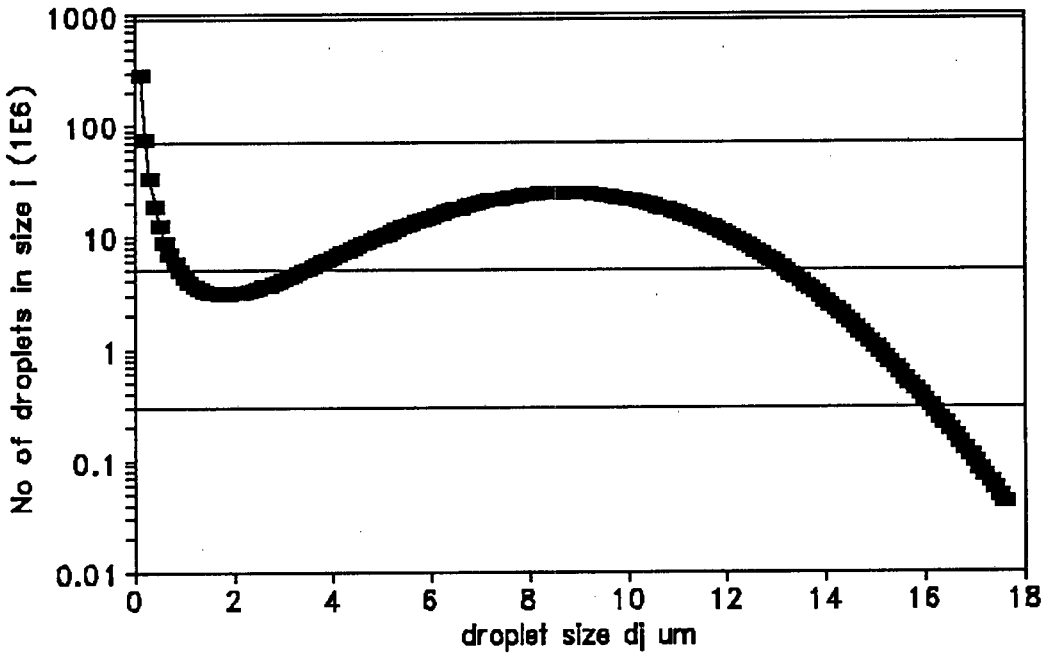

APPENDIX F2

TANK DESIGN AND MIXING CHARACTERISTICS

F2.1 400 l Laboratory Tank Design

There are geometric limitations if adequate mixing of water or water/solids suspensions (CSTR conditions) is to be approached.

Tank geometric configurations, performance and operating characteristics are supplied by Treybal (1982a).

Typical geometric configurations for cylindrical tanks are summarised below :

$Z/T \approx 0.75 - 1.5$
$d_i/T \approx 0.3$, maximum 0.6 (> 0.6 wall effects)
$C \approx d_i$, min $d_i/3$
$B \approx T/12$

where
Z = height of pulp in tank, m
T = tank diameter, m
d_i = impeller diameter, m
C = clearance, i.e height of impeller above tank base, m
B = baffle width, m (baffle height $B > Z$)

The dimensions of the 400 l laboratory tank used in the conditioning and laboratory column tests are shown on the schematic below. The following relations apply :

$Z/T = 0.67$
$d_i/T = 0.17$

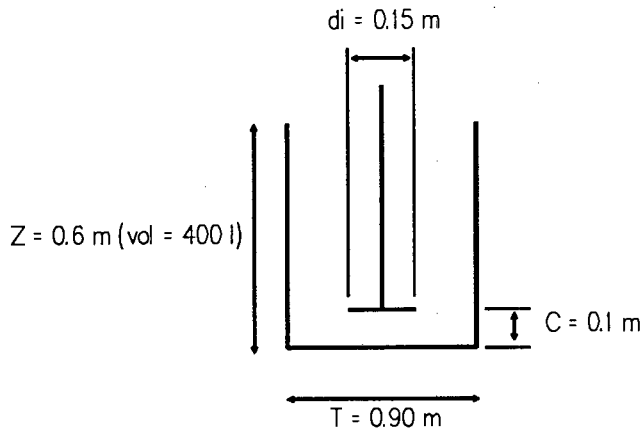

Figure F3 : Dimensions of 400 l Laboratory Rig Tank.

Two vertical baffles (180°) were used. Baffle width was 10 cm and height 100 cm. A clearance of 2 cm above the tank bottom was allowed. To prevent vortexing it was also necessary to install 3 horizontal baffles. These were joined across the pair of vertical baffles. They were each 80 cm long and 6 cm wide and were positioned a distance of 20 cm apart. The distance of the lowest baffle from the tank bottom was 13 cm.

For non-vortexing systems tank performance (single phase systems) is described by

$f(Re, Po) = 0$

i.e. $Po = f(Re)$

where Re, Po are dimensionless groups defined as follows

$$Re = N.d_i^2.\rho / \mu \qquad (F4)$$

$$Po = P.g_c / \rho.N^3.d_i^5 \qquad (F5)$$

where

Po is the Power number
Re is the impeller Reynolds number
N = impeller rotational speed, rev/s
ρ = fluid density, kg/m^3
μ = fluid viscosity, kg/m.s
g_c = gravitational constant (=1 in SI units)
P = power imparted to liquid by impeller, W
Q = fluid circulation rate, m^3/s or l/min
higher circulation rates gives better fluid mixing (pulp systems - more uniform solid dispersion)

For Re > 10000 fully turbulent flow exists in baffled tanks and Po is constant.

F2.2. Solids Suspension in 400 l Laboratory tank

A correlation developed by Weismann and Efferding (1960) and reproduced in Treybal (1982b) can be used to estimate at what height above the impeller the solids in a pulp are suspended for a given power input :

$$\frac{P.g_c}{g.n.\rho_m.v_m.V_{ts}} = \phi^{2/3}.(T/d_i)^{1/2}.\ \exp[4.35(Z'/T-0.1)] \qquad (F6)$$

$$\phi = S\ /\ (\rho_p * v_m) \qquad (F7)$$

$$\rho_m = \phi\ \rho_p+(1-\phi)\rho_l \qquad (F8)$$

$$\mu_m = \mu_l\ /\ (1\ -\ \phi/\phi_s) \qquad (F9)$$

Treybal recommends $\phi_s \approx 0.6$, and V_{ts} may be obtained from Stokes's Law and
Stokes law

$$V_{ts} = g.d_p^2.(\rho_p-\rho_l)\ /\ 18.\mu_l \qquad (F10)$$

where

$\varnothing$ = volume fraction solids
ρ_l = liquid density, kg/m^3
ρ_p = particle density, kg/m^3
ρ_m = slurry density, kg/m^3
μ_l = liquid viscosity, kg/m.s
μ_m = slurry viscosity kg/m.s
v_m = pulp volume to height Z'+ C, m^3

i.e. $v_m = f(Z') = \{\pi.T^2 / 4\} * (Z'+C)$ (F11)

V_{ts} = particle terminal velocity (estimated by Stokes law)
Z' = interface height above impeller to which particles are suspended
n = number of impellers = 1
d_p = particle size, m
g = 9.81 m/s^2
S = mass solids in pulp volume v_m, kg

The slurry/water interface is assumed to be on the verge of quiescence, so settling and suspension forces are taken as existing in equilibrium at height Z'.

For dilute solids suspensions it is assumed that Po, Re relationships developed for single phase fluids apply.

Flat-bladed turbine impellers were used in the study. However, Treybal states that equation (F6) is also reasonably applicable to disk type impellers. Equation (F6) also only applies for impeller Reynolds numbers greater than 1000.

Now consider the 400 l laboratory pulp tank :

From motor manufacturer specifications
Effective (i.e. supplied to impeller) maximum power output
P = 250 W
Impeller speed N = 1400 rpm = 23.33 rps
@ 8 % solids (m/v) in a 400 l tank S = 32 kg

T = 0.90 m

C = 0.10 m

For a solids suspension of similar size fractions (i.e essentially homogeneous), one can represent V_{ts} by a weighted average from size distribution properties. The size distribution of the laboratory sample of Kleinkopje thickener underflow given in Table 3.4 (section 3.2) was taken as representative and is reproduced in Table F2 below.

Table F2 : Average Feed size properties, Kleinkopje thickener underflow fines

Particle size	Average size	% passing	Weight %
+425 μm		97.39	2.61
+212 - 425 μm	300	88.23	9.16
+150 - 212 μm	178	80.00	8.23
+106 - 150 μm	126	71.57	8.43
+ 75 - 106 μm	89	62.52	9.05
+ 45 - 75 μm	58	49.85	12.67
- 45 μm	22		49.85
Total		100.00	23.75

The mean size for the + 425 μm fraction was conservatively estimated as 500 μm

Take $d_{avg} = \Sigma (d_i * W_i) / \Sigma W_i$ (F12)

$d_{avg} = 90$ μm

$\rho_p = 1450$ kg/m^3

$\rho_l = 1000$ kg/m^3

$\mu_l = 1.0 * 10^{-3}$ Pa.s ≡ kg/m.s

Then from Stokes law (F10)

$V_{ts} = 1.987 * 10^{-3}$ m/s

And substituting for S, T, ρ_p etc. into equations (F7) - (F11)

$v_m = \pi * 0.90^2 * (Z' + 0.1) / 4 = 6.362 * 10^{-1} * (Z' + 0.1)$

$\phi = 32 / (1450 * 6.362 * 10^{-1} * (Z' + 0.1))$

$= 3.469 * 10^{-2} / (Z'+0.1)$

hence

$\rho_m = \phi.\rho_p + (1 - \phi).\rho_l$

$= \phi * 1450 + (1 - \phi) * 1000$

$P.g_c / g.n.V_{ts} = 12829$

$(d_i/T)^{1/2} = (0.15 / 0.90)^{1/2} = 0.408$

Substitute above into (F6) and rearrange

$$f(Z') = (Z'/T-0.1)-0.23\ln[(P.g_c / g.n.\rho_m.v_m.V_{ts}) * \phi^{-2/3}(T/d_i)^{-1/2}]$$

and

$f(Z') = 0$

Solve iteratively start $Z' = 0.2$; increment $\Delta = 0.1$

$f(Z')$ vs Z' is plotted in Figure F4.

It can be seen that $f(Z') = 0$ for $Z' \approx 0.99$ m, i.e. $Z \approx 1.09$ m

Therefore based on a mean particle size of 90 μm there should be sufficient power to fully suspend the pulp.

Now let $d_p = 0.40$ mm

Solution is now $Z' \approx 0.42$ m, i.e. $Z = 0.52$ m (see Figure F5). Based on a total tank height of $Z = 0.6$ m, this should still be sufficient to fully suspend the coal solids since only 12 % of the Kleinkopje fines sample was coarser than 212 μm.

The impeller Reynolds number is approximately

at $Z = 0.6$; $T = 0.90$ m, $v_m = 0.44$ m^3, $N = 1440$ rpm

$\rho_m = 1022$ kg/m^3

$\mu_m = 1.08 * 10^{-3}$ kg/m.s

hence $Re = N d_i^2 \rho / \mu = 5 * 10^5$

$Re > 10^4$, therefore flow fully turbulent.

F2.3 Mechanical Design of and Suspension in the Pilot Rig Tank

The pilot rig tank dimensions are :

Z = 1.0 m (Vol = 240 l)

T = 0.55 m

C = 0.1 m

d_i = 0.15 m

Then

Z/T = 1.82

d_i/T = 0.22

C = 0.10 m

The maximum power supplied to the impeller is

P = 370 W

Impeller speed N = 1400 rpm = 23.33 rps

@ 10 % solids (m/v) in a 240 l tank S = 24 kg

T = 0.55 m

C = 0.10 m

Use the average size properties given in Table F2 as representative size properties, i.e. d_p = 0.090 mm. Figure F6 indicates that the solution for f('Z) = 0 is $\approx$ Z' = 0.75 m, i.e. Z = 0.85 m.

If the average feed size properties given in Table 5.1 (i.e. plant trial data) are taken as representative size properties then

Table F3 : Average Kleinkopje sample size distribution for plant trials.

Particle size	Average size d_i	% passing	Weight % W_i
+150 μm	200 μm		7
-150 + 106 μm	128 μm	93	11
-106 + 75 μm	91 μm	82	14
-75 + 45 μm	60 μm	68	23
-45 μm	22 μm	45	45

The mean size for the + 150 μm fraction was estimated as 200 μm. Then from equation (F12) the mean particle size, d_p, equals 65 μm. $f(Z')$ vs $F(Z)$ is plotted in Figure F7. The solution is $f(Z') \approx 0$ for $Z' \approx 0.83$. The maximum pilot tank height is $Z = 1.0$ m, i.e. $Z' = 0.90$m.

$0.83 \approx 0.90$ therefore sufficient power is available to suspend solids to the slurry surface.

Figure F4 – 400 l laboratory rig tank
Weisman's correlation

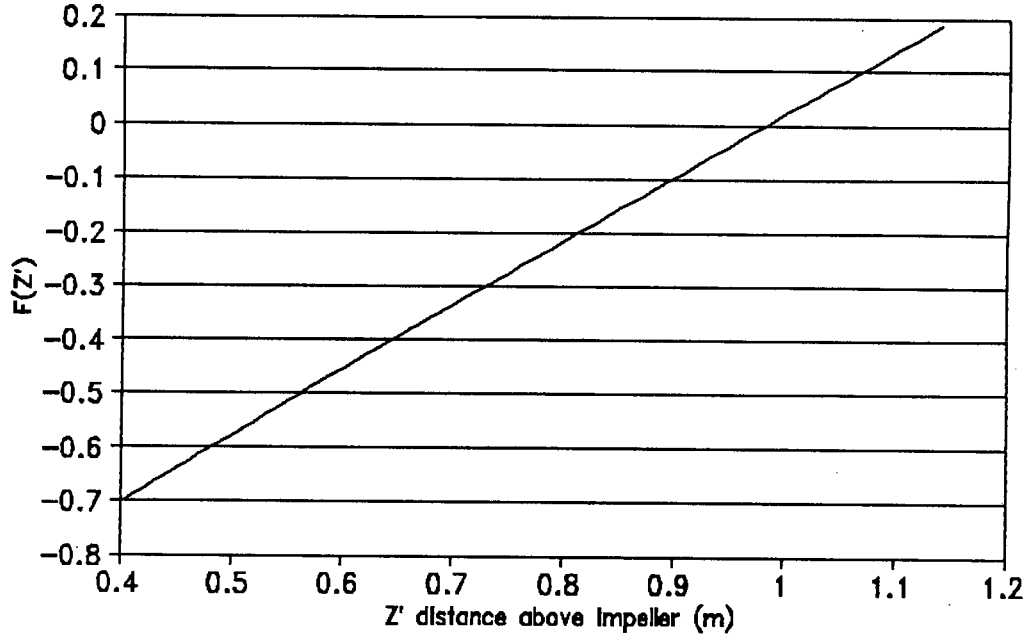

solution is Z' for F(Z') = 0; mean particle size, dp = 0.090 mm

Figure F5 – 400 l laboratory rig tank
Weisman's correlation

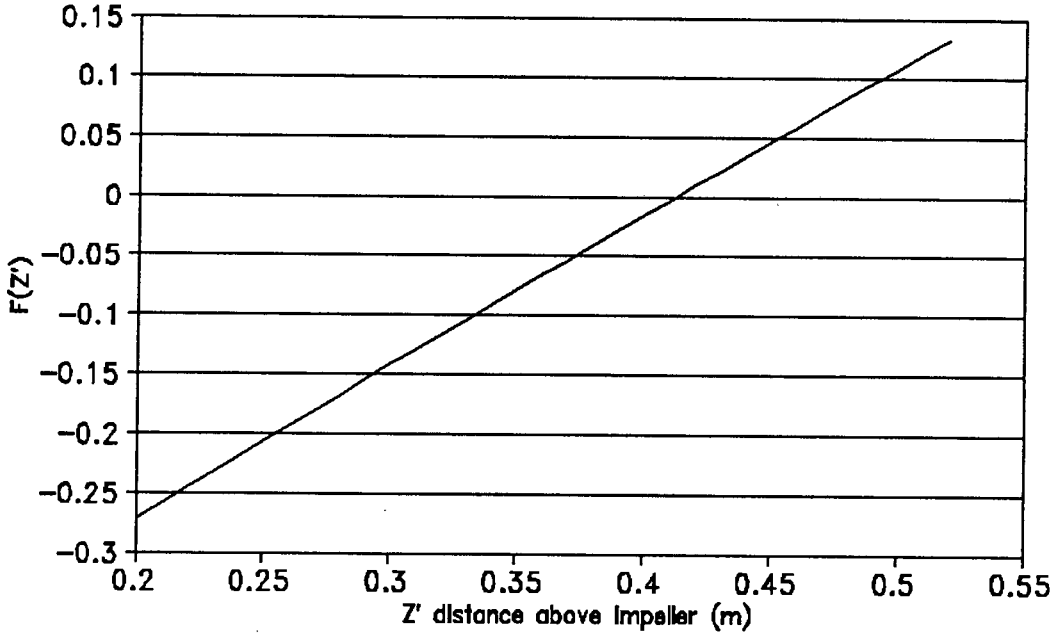

solution is Z' for F(Z') = 0; mean particle size, dp = 0.4 mm

Figure F6 – 240 l pilot rig tank
Weisman's correlation

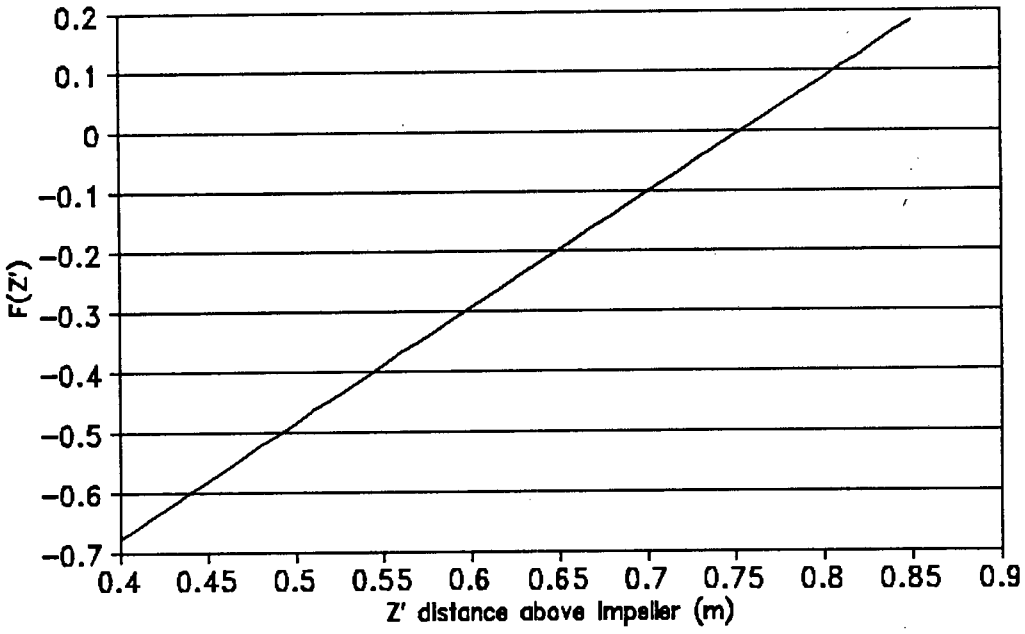

solution is Z' for F(Z') = 0; mean particle size, dp = 0.090 mm

Figure F7 – 240 l pilot rig tank
Weisman's correlation

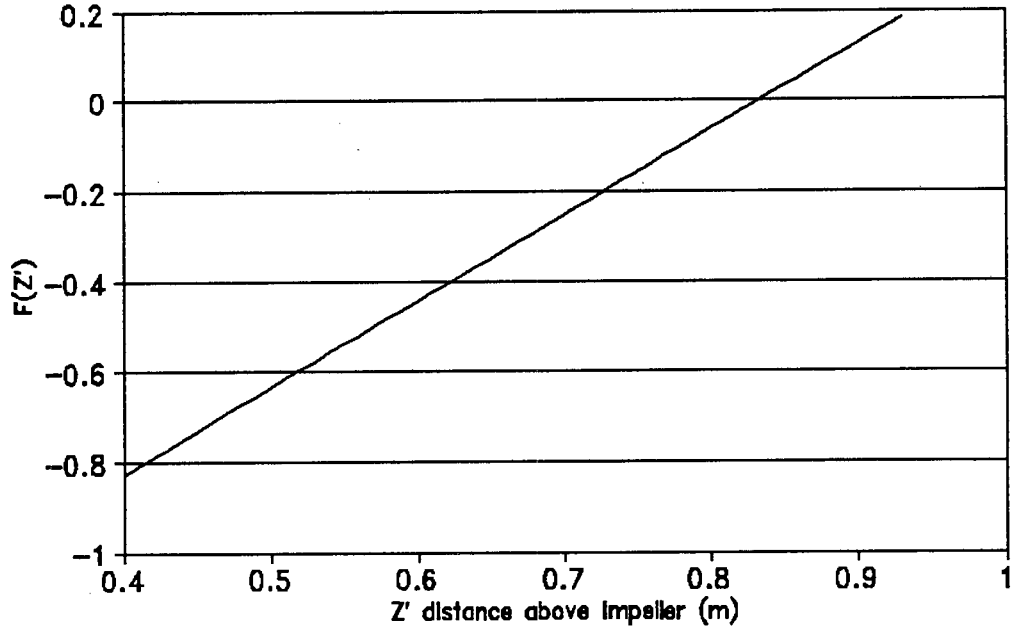

solution is Z' for F(Z') = 0; mean particle size, dp = 0.065 mm

APPENDIX F3

KOLMOGOROV/SMIRNOV GOODNESS-OF-FIT TEST

The algorithm for this test procedure was derived from Sachs (pp 330-332, 1982).

The Kolmogoroff-Smirnov (K/S) sample test checks how well an observed (sample) distribution $f_o(x)$ fits a theoretical statistical distribution function $f_e(x)$. The null hypothesis (H_o) is that the observed sample distribution, $f_o(x)$, comes from the known distribution function, $f_e(x)$, the alternative hypothesis (H_1) being that the population from which the sample was drawn does not fit $f_e(x)$. The K/S test statistic is computed as follows :

1. Divide the sample (parameter) interval into k classes. The parameter sample size is n. The minimum sample size and interval classes are $n \geq 10$, $k \geq 5$.
2. Calculate the observed and expected frequencies, $f_o(x)$ and $f_e(x)$ in each parameter interval. Then calculate the cumulative frequencies $F_o(x)$, $F_e(x)$ up to the k'th interval.
3. The test statistic is $D_k = |F_o - F_e| / n$ for the k'th interval
4. Choose the largest $D_k = D_{max} = \max|F_o - F_e| / n$
5. Compare D_{max} to the theoretical D, where $D = f(\alpha,n)$ is obtained from statistical tables.
   If $D_{max} < D$ then accept H_o
6. α is the significance level attached to the test. If α is increased then D becomes smaller and the more difficult it is for the test criteria $D_k = |F_o - F_e| / n$ to satisfy the null hypothesis, H_o. Consequently if H_o still remains true then the more confidently one can assert that the sample distribution tested represents the underlying theoretical distribution function.

Typically α is taken as 5 or 10 % (0.05, 0.10).

The K/S test does have a number of limitations, which must be borne in mind when applying this goodness-of-fit test. Firstly, the cumulative functions F_o, F_e represent the shape of the distribution functions and consequently if n is small, F_o can be distorted by a few unrepresentative sample points (outliers). Theoretically the test requires that k, $n \rightarrow \infty$ and Mason et al (pp 530, 1989) advise that the test be used for sample sizes, n, greater than 50.

APPENDIX F4

NORMAL DISTRIBUTION CURVE FITS TO KLEINKOPJE PLANT GLOBAL FEED % ASH AND CV DATA

Frequency distribution histograms of global feed % ash and CV data are displayed in Figures 5.2 and 5.3 of Chapter 5.

Here it is attempted to fit normal distribution curves to the experimental data displayed in these figures. There is no fundamental basis for this only the statistical observation Mason (pp 244, 1989) that large samples of independent observations, n, tend to be normally distributed.

Thus the hypothesis test can be considered as

Null hypothesis : H_o : Feed (ash or CV) data normally distributed
Alternative hypothesis : H_1 : Feed data not normally distributed

The Kolmogorov / Smirnov goodness-of-fit test was used to test for normality.

The global feed CV data can be summarised as:

Number of samples N = 72
sample mean y_m = 23.798
sample variance s^2 = 0.853
sample deviation s = 0.924

Detailed data are provided in Appendix E.

Assume that the sample mean and variance are adequate estimates of the normal population mean and variance (if H_o true). This is reasonable since the sample size, n, is large (n > 30).

The probability density of the normal distribution is given by Sachs (pp59, 1982)

$$f_e(y) = 1/\{\sigma \sqrt{(2\pi)}\} * \exp[-1/2\{(y - \mu)/\sigma\}^2] \quad \text{(F13)}$$

where $y, \mu, \sigma \in [-\infty, +\infty]$

the cumulative distribution function F_e is given by

$$F_e(y) = \int_{-\infty}^{y} f_e(y)dy \quad \text{(F14)}$$

F_e is the probability function
here $\mu = 23.798$, $\sigma = 0.924$

The theoretical normal CV distribution curve was generated as follows :

choose initial $y_o = 20.75$ (MJ/kg) $f_e = 0.0019 \approx 0$
select increment $dy = 0.05$
hence $y_j = y_o + j * dy$
calculate $f_e(y_j)$ for $y_j \in [20.75;26.75]$

The cumulative normal curve was then generated as follows :

the area under the curve $f_e(y)$ between y_{j-1} and y_j was calculated by Simpson's rule
$dA_j = (f_{j-1} + f_j) * dy / 2$
strictly $dA_j = dA_k$
where the midpoint $k = (y_{j-1} + y_j) / 2$ but the difference is negligible.

$$F_e = \Sigma^j A_j \quad \text{(F15)}$$

The experimental and theoretical frequency data are indicated in Table F4 below :

Table F4 : Observed vs theoretical cumulative CV distribution function

y range	Number samples	% fo	% Fo	% Fe	D
21.25	0	0	0	0.25	0.0034
21.75	0	0	0	1.29	0.0178
22.25	2	2.78	2.78	4.65	0.0259
22.75	9	12.50	15.28	12.79	0.0345
23.25	13	18.06	33.34	27.62	0.0794
23.75	9	12.50	45.84	47.90	0.0286
24.25	15	20.83	66.67	67.83	0.0162
24.75	11	15.28	81.95	84.83	0.0400
25.25	11	15.28	97.23	94.16	0.0425
25.75	2	2.78	100.00	98.23	0.0246
26.25	0	0	100.00	99.56	0.0061

The test statistics are Sachs (pp330, 1982) :

Table F5

α	D_{test}
0.2	0.1265
0.10	0.1442
0.01	0.1919

$D_{max} = 0.0794 < D_{test,\ \alpha=0.20} = 0.1265$

$D_{min} = 0.01624$

therefore take feed CV data to be normally distributed

A graph of F_o, F_e vs feed CV is plotted in Figure F8. It is apparent from the graph that the experimental data fits a normal distribution curve.

A similiar graph of F_o, F_e vs % feed ash is also plotted (Figure F9). The sample data does not appear to fit a normal distribution very well.

The global ash data can be summarised as :

Number of samples N = 71
sample mean y_m = 23.06
sample variance s^2 = 4.204
sample deviation s = 2.050

Detailed data is provided in Appendix E.

Repeating the procedure just outlined one obtains
D_{max} = 0.2218
D_{min} = 0.0139

The test statistics are

Table F6

α	D_{test}
0.20	0.1273
0.10	0.1453
0.01	0.1932
0.001	0.2313

$D_{max} < D_{test}$ only at 0.1 % significance level therefore conclude feed ash data not normally distributed.

Figure F8 : curve fit cumulative feed
CV's to cumulative normal distribution

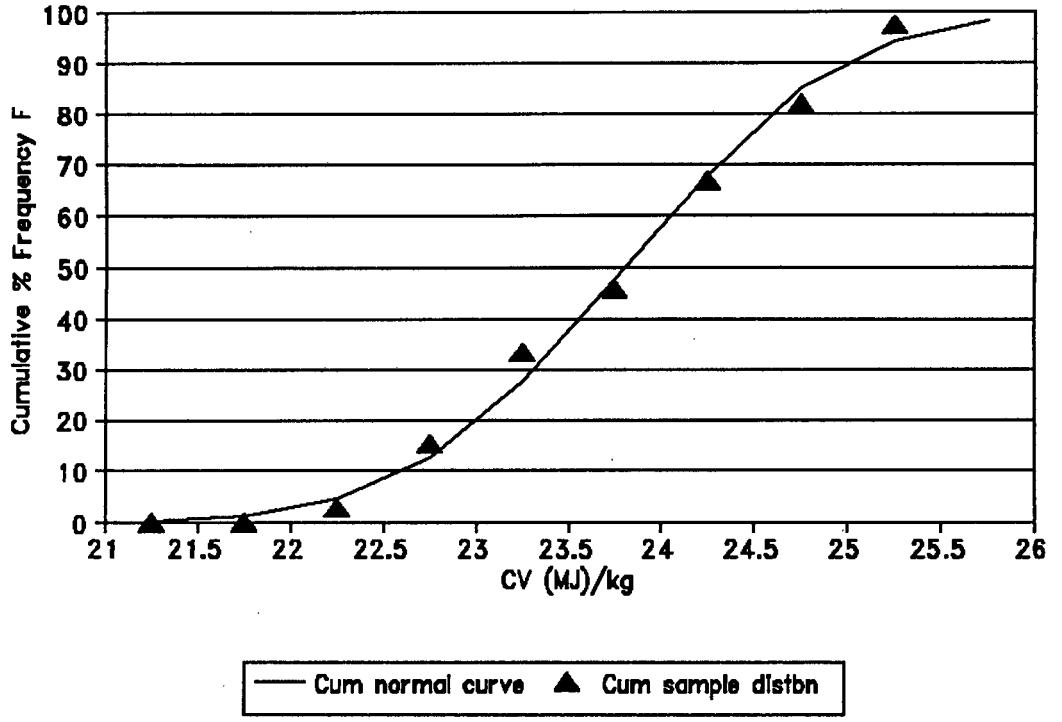

Figure F9 : curve fit cumulative feed
% ash to cumulative normal distribution

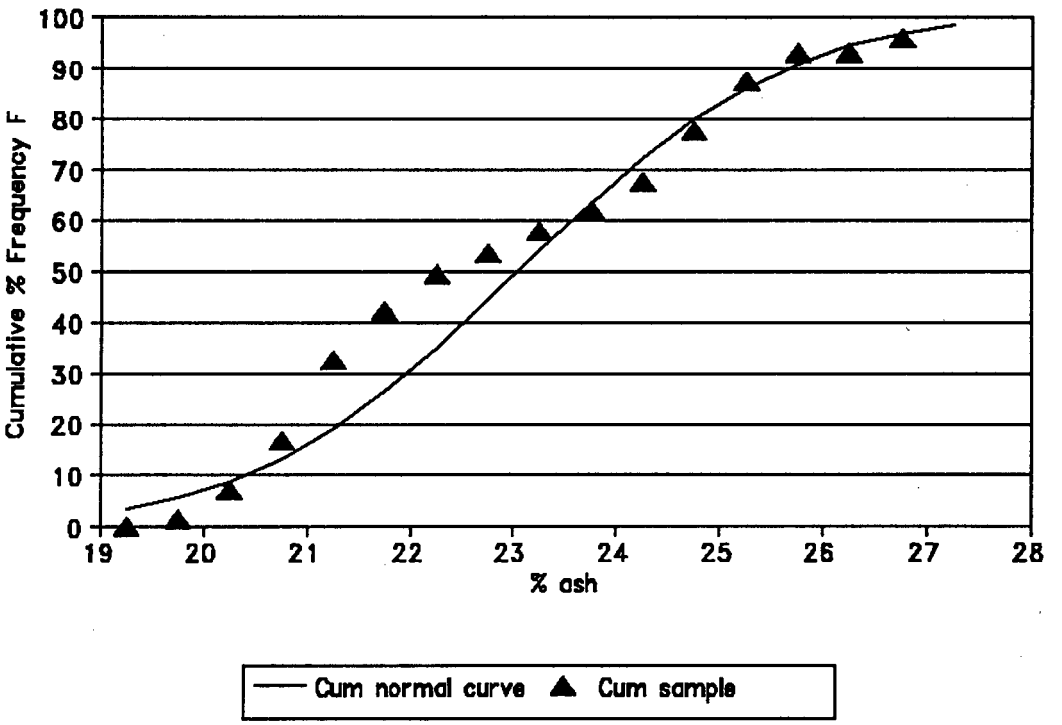

APPENDIX F5

ERROR ANALYSIS OF KLEINKOPJE PLANT DATA

Pairs of runs repeated within the same pulp batch are listed in Table F7. The runs can be identified by consulting Table E7 of Appendix E. The collector dosage was varied within the pairs of runs marked with asterisks. However, as this did not substantially alter the yields obtained, these are considered as repeat tests.

Error estimates were calculated using the procedures outlined in Appendix A3. For example, the standard sample error associated with the yield within a block was calculated as follows :

The number of repeat samples per test (pulp batch) , n_i, equals 2; the number of tests for which repeat samples (equivalently the number of levels i), Σi, is 5.

Applying equation (A3.1) to run pair 17/04 R11 (j=1) and 17/04 R12 (j=2) one obtains

$$s_{1.}^2 = \Sigma_{j=1}^{2} (y_{1j} - y_{1avg})^2 / (2 - 1) = 0.78$$

where $s_{1.}^2$ is the sample variance associated with repeat runs 17/04 R11 and 17/04 R12.

$s_{i.}^2$ is calculated similarly for run pairs 26/04 R1-; 04/05 R1-; 07/05R1- and 22/05 R1-.

$$SS_{eYld} = \Sigma_i \, s_{i.}^2 = 18.78$$

The degrees of freedom, ν, associated with the yield response error is (equation A3.3)

$$\nu = \Sigma_i \, (n_i - 1) = 5$$

Table F7 : Kleinkopje Plant Trials - Reproducibility within blocks - error estimates

RUN ID	% Yield	%Ash	CV	Yavg	Aavg	CVavg	del Y	del A	del CV	sum del Y	sum del A	sum del CV^2
17/04 R11	8.09	11.80	28.56	7.70	11.65	28.45	0.39	0.15	0.11	0,31	0.05	0.02
17/04 R12	7.30	11.50	28.34									
26/04 R11	24.05			25.60			-1.55			4.81		
26/04 R12	27.15											
04/05 R11*	81.85	14.71	26.94	82.01	14.05	27.07	-0.16	0.66	-0.13	0.05	0.88	0.03
04/05 R12*	82.17	13.38	27.20									
07/05 R11*	41.53	13.82	27.55	43.34	13.44	27.66	-1.81	0.38	-0.11	6.55	0.29	0.02
07/05 R12*	45.15	13.06	27.77									
22/05 R11	12.98	8.69	29.36	14.86	8.43	29.47	-1.88	0.26	-0.11	7.07	0.14	0.02
22/05 R12	16.74	8.16	29.58									

Total SS	18.79	1.36	0.11		
Se^2	3.76	0.34	0.03		
Se	1.94	0.58	0.16		
popsy^2	16.34	popsa^2=	1.91	popscv^2	0.15
popsy=	4.04	popsa=	1.38	popscv=	0.39

Chi-squared at n=5 d.o.f. and 95 % confidence level 1.15

Chi-squared at n=4 d.o.f. and 95 % confidence level 0.71

The mean square of the error, MS_e, is (equation (A3.4))

$s_{Yld}^2 = MS_e = SS_{eYld} / \nu = 18.78 / 5 = 3.76$

Hence the sample standard deviation associated with % yield within a pulp batch is $s_{Yld} = 1.94$ %.

Now the ratio $m.s_{Yld}^2 / \sigma_{Yld}^2$ follows a Chi-squared (χ^2) distribution with ν degrees of freedom (Mason et al; 1989; pp 243). σ_{Yld}^2 represents the true population (i.e. infinite) standard variance (represented as popsy^2 in Table F7). Values for χ^2 as a function of ν and the significance level, α, can be found from statistical tables.

If $\alpha = 0.05$, $\nu = 5$ then $\chi^2 = 1.15$ (Mason et al; 1989; pp 615).

$\chi^2 = \nu.s^2 / \sigma^2$

hence $\sigma_{Yld}^2 = \nu.s_{Yld}^2 / \chi^2 = 5 * 3.76 / 1.15 = 16.34$

For the ash and CV population standard deviations, σ_{ash} and σ_{CV}, a similar procedure is followed, however, now $\nu = 4$.

APPENDIX G

G1 - BATCH FLOTATION PROCEDURES

G2 - MASS BALANCE AND STEADY STATE CHECK CALCULATIONS

G3 - SAMPLE ASH, D.A.F. COAL CONTENT AND RECOVERY CALCULATIONS

APPENDIX G1

BATCH FLOTATION PROCEDURES

G1.1 Standard Flotation Procedure

Fill the 3 l modified Leeds cell to a volume of 2 l using Cape Town tapwater. Set the impeller speed to 1200 rpm. Add the desired quantity of coal solids (usually ≈ 150 g or 300 g on a dry basis). Fill the cell to 3 l with additional tapwater. The distance between the pulp-froth interface and the overflow weir (i.e. froth bed depth) is then 2.5 cm. Add the desired quantity of oily collector to the suspended pulp using a micropipette ensuring that the micropipette tip is below the pulp surface. After the pulp has been conditioned with collector for 3 minutes add the frother (again below the pulp surface) using a microsyringe. Allow 55 s for the frother to disperse through the pulp and then set the air rate to 6 l/min and open the air line.

Let time zero, t = 0, be 60 s after frother addition. Then concentrates are collected at varying intervals according to the sequence described below.

Conc no. 1 : t = 0-15 s, remove concentrate with scrapper paddle at 5 s intervals.

Conc no.2 : t = +15-30 s, remove concentrate with scrapper paddle at 5 s intervals.

Conc no. 3 : t = +30-60 s, remove concentrate with scrapper paddle at 10 s intervals.

Conc no. 4 : t = +60-120 s, remove concentrate with scrapper paddle at 10 s intervals.

Conc no. 5 : t = +120-210 s, remove concentrate with scrapper paddle at 10 s intervals.

Conc no. 6 : t = +210-300 s, remove concentrate with scrapper paddle at 10 s intervals.

Conc no. 7 : t = +300-420 s, remove concentrate with scrapper paddle at 10 s intervals.

Conc no. 8 : t = +420-540 s, remove concentrate with scrapper paddle at 10 s intervals.

Once no further concentrate can be removed as overflow from the weir, the flotation experiment is stopped. The cell is then drained into a bucket, this residual pulp constitutes the tailings sample. The concentrate and tails samples are then filtered, dried and weighed to determine the cumulative yield over the duration of the float. If ash analyses are performed on the samples, then cumulative concentrate ash contents and recoveries can also be determined.

G1.2 Differential ("release") Flotation Procedure

The procedure followed is similar to that described above, however, the flotation test is conducted at starvation collector and frother dosage levels. In addition, n-dodecane and MIBC are used as the standard collector and frother reagents respectively. Initially, no collector reagent is added, however, an initial frother concentration of 6 μl/l is used. Flotation is continued until no more concentrate can be recovered. Subsequently, a starvation dosage of collector reagent (equivalent to approximately 100 g/t) is added to the pulp and the float continued. If necessary, additional surfactant ($\approx$ 2 μl/l pulp) is added intermittently to regenerate the froth. The float is continued until the maximum possible coal recovery has been achieved, usually this corresponds to about 30 concentrate samples, some of which are subsequently recombined for ash analysis.

APPENDIX G2

MASS BALANCE AND STEADY STATE CHECK CALCULATIONS

Let the measured concentrate solids flowrate be M_c $(M.T^{-1})$
measured tailings solids flowrate be M_t $(M.T^{-1})$
measured feed solids flowrate be M_{fm} $(M.T^{-1})$

Similarly, let the measured % ash content of the coal concentrate be A_c
measured % ash content of the tailings be A_t
measured % ash content of the feed be A_{fm}

Then the calculated solids feedrate is

$$M_{fc} = M_c + M_t \qquad (G1)$$

and the reconstituted feed ash content is given by

$$A_{fc} = (M_c.A_c + M_t.A_t) / M_{fc} \qquad (G2)$$

Now let

$$\delta = | A_{fc} - A_{fm} | \qquad (G3)$$

δ can be used as a criterion to check whether sampling of the feed, concentrate and tailings was performed under steady state conditions.

Given a measured feed ash content, A_{fm}, and the standard sample deviation, s, associated with this measurement, one can calculate a tolerance interval, $A_{fm} \pm ks$. The parameter, k, is a function of sample size, n, significance level, α, and the parameters A_{fm} and s, obtained from sample measurements, which estimate the true population mean, μ, and standard deviation, s, with a $1-\gamma$ degree of confidence.

The standard sample deviation, s_{ash}, associated with a concentrate ash content is listed in Table F7 as ± 0.58 % ash. The number of samples used to obtain this estimate was n = 4. In Table 3.1 of Appendix A3.1 the sample standard deviation , s_{ash}, was estimated as 0.51 % ash; however, the number of samples, n, was 12. It is evident that these two estimates of the % ash variability are very similar. It is reasonable to assume that the standard % ash deviation associated with a feed sample is the same as that of the concentrate samples.

Therefore take s = 0.51 % ash and n = 12 sample observations as an estimate of the feed % ash deviation.

Choose significance level $\alpha = 0.05$
let $\gamma = 0.05$
$n = 12$

then from Mason et al (1989, pp 623) k = 3.39

Hence the tolerance interval associated with the feed ash content is
± k.s = ± 1.73 % ash

Thus applying equation (G3), for steady state the absolute difference between the calculated feed ash, A_{fc}, and measured feed ash content, A_{fm}, should be less than 3.46 ≈ 3.5 % ash.

Example :Take column tests on Durnacol thickener underflow, run 1 (Appendix D)

M_{fm} = 70.30 g/min; A_{fm} = 28.66 % ash
M_c = 11.93 g/min; A_c = 10.05 % ash
M_t = 64.25 g/min; A_t = 34.18 % ash

Applying equation (G1) M_c = 76.18 g/min
and applying equation (G2) A_{fc} = 30.40 % ash

hence δ = 1.74 % < 3.5 %; therefore steady state reached.

APPENDIX G3

SAMPLE ASH, D.A.F. COAL CONTENT AND RECOVERY CALCULATIONS

Consider Run 27/04 R11

Basis : 100 g Feed

From Tables E1 and E2 (Appendix E) the feed properties can be summarised as follows :

Table G1

size fraction (μm)	mass/size fraction (g)	% ash	g ash	g d.a.f. coal
+150	5.34	12.60	0.67	4.67
-150 + 106	12.33	12.80	1.58	10.75
-106 + 75	11.23	14.30	1.61	9.62
- 75 + 45	23.43	19.50	4.57	18.86
- 45	47.67	27.60	13.16	34.51
Total	100.00	21.58	21.58	78.42

Calculate g ash and g d.a.f. coal as follows :
consider +150 μm fraction

if assume that mass ash = mass uncombusted mineral then

g ash = 0.126 * 5.34 = 0.67 g

g d.a.f. coal = 5.34 - 0.67 = 4.67 g

repeat for -150 + 106, -106 + 75, -75 + 45, -45 μm fractions
results listed in Table G1 above

Now consider Run 27/04 R11 concentrate
From Table E10 (Appendix E) % Yield = 14.00 % ; therefore concentrate mass M_c = 14 g

From Tables E4 and E5 (Appendix E) the concentrate properties are :

Table G2

size fraction (μm)	% size	mass per size (g)	% ash	g ash	g d.a.f. coal
+150	0.00	0.00			
-150 + 106	0.00	0.00			
-106 + 75	0.00	0.00			
-75 + 45	27.59	3.86	10.30	0.40	3.46
- 45	72.41	10.14	10.19	1.03	9.11
Total	100.00	14.00	10.22	1.43	12.57

mass in -75 + 45 μm fraction = 0.2759 * 14 = 3.86 g ;
similarly -45 μm fraction g ash, g d.a.f. coal per size fraction as before
reconstituted concentrate ash content = 1.43 / 14 * 100 = 10.22 %

d.a.f. coal distributions are plotted in Figure 5.11 (Chapter 5), this example corresponds to trial N = 2.

Now compare feed, concentrate -75 μm total d.a.f. coal contents

Table G3

size fraction (μm)	g coal feed	g coal concentrate
-75	53.37	12.57
-45	34.51	9.11
Total	78.42	12.57

Recovery = mass d.a.f. coal concentrate / mass d.a.f. coal feed * 100
hence R_{tot} = 12.57 / 78.41 * 100 = 16.03
R_{-75} = 12.57 / 78.41 * 100 = 16.03
R_{-45} = 9.11 / 78.41 * 100 = 11.62

These recoveries correspond to trial N = 2 in Figure 5.12 (Chapter 5)

Rec size i = mass d.a.f. concentrate size i / mass d.a.f. feed size i

Table G4

size fraction (μm)	g coal Feed	concentrate	Rec size i
+150	4.67		0.00
-150 + 106	10.75		0.00
-106 + 75	9.62		0.00
-75 + 45	18.86	3.46	18.36
- 45	34.51	9.11	26.39